JOURNAL OF Metals

TECHNOLOGY · PRACTICE

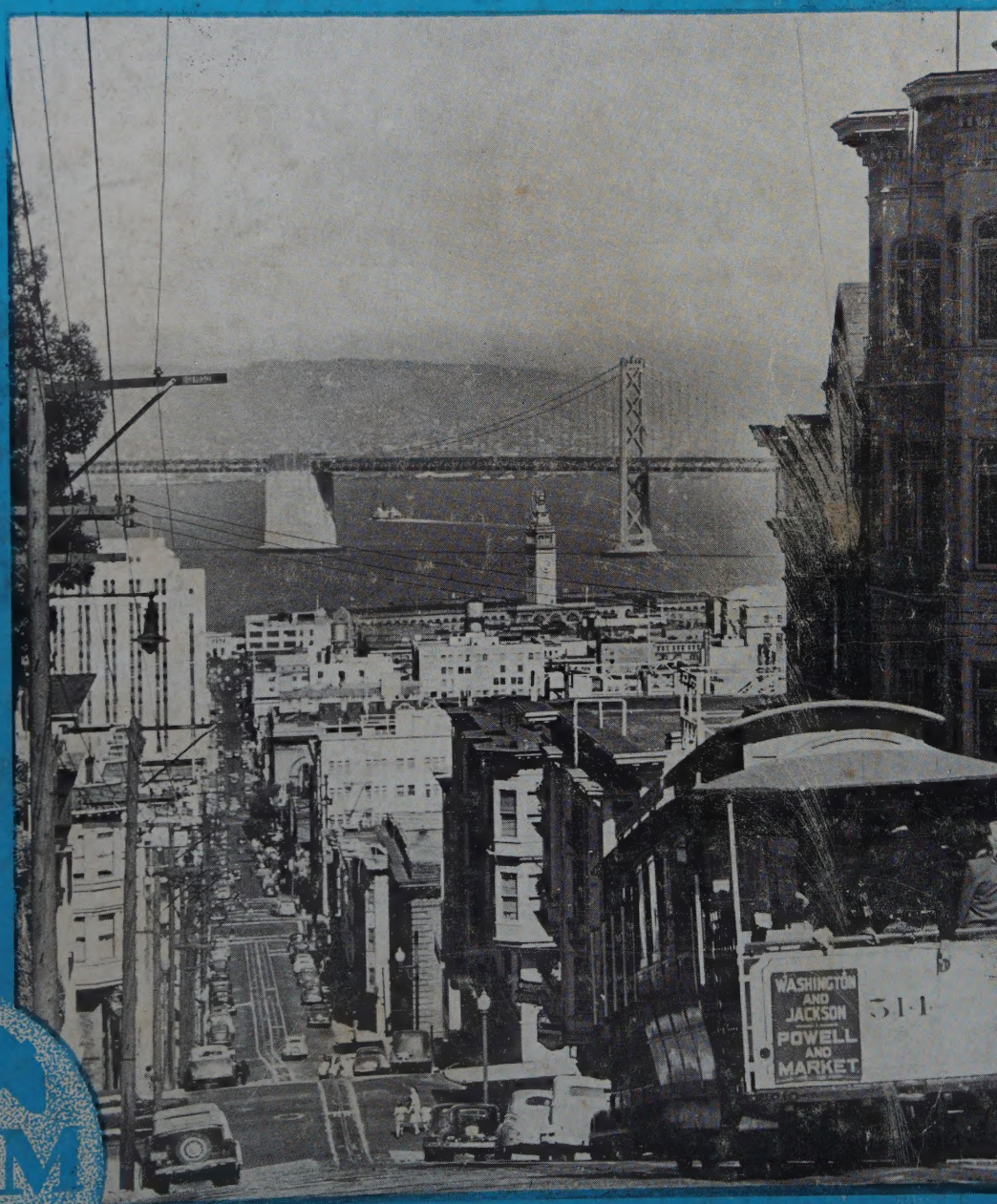

FEBRUARY 1949

Basing Points

•

East Coast Steel Plant

•

ıal Meeting Preprints

Powder Metallurgy

Lectures and Awards

A MONTHLY PUBLICATION OF THE
AMERICAN INSTITUTE OF MINING AND METALLURGICAL ENGINEERS
METALS BRANCH

FISHER *Unitized* Laboratory Furniture

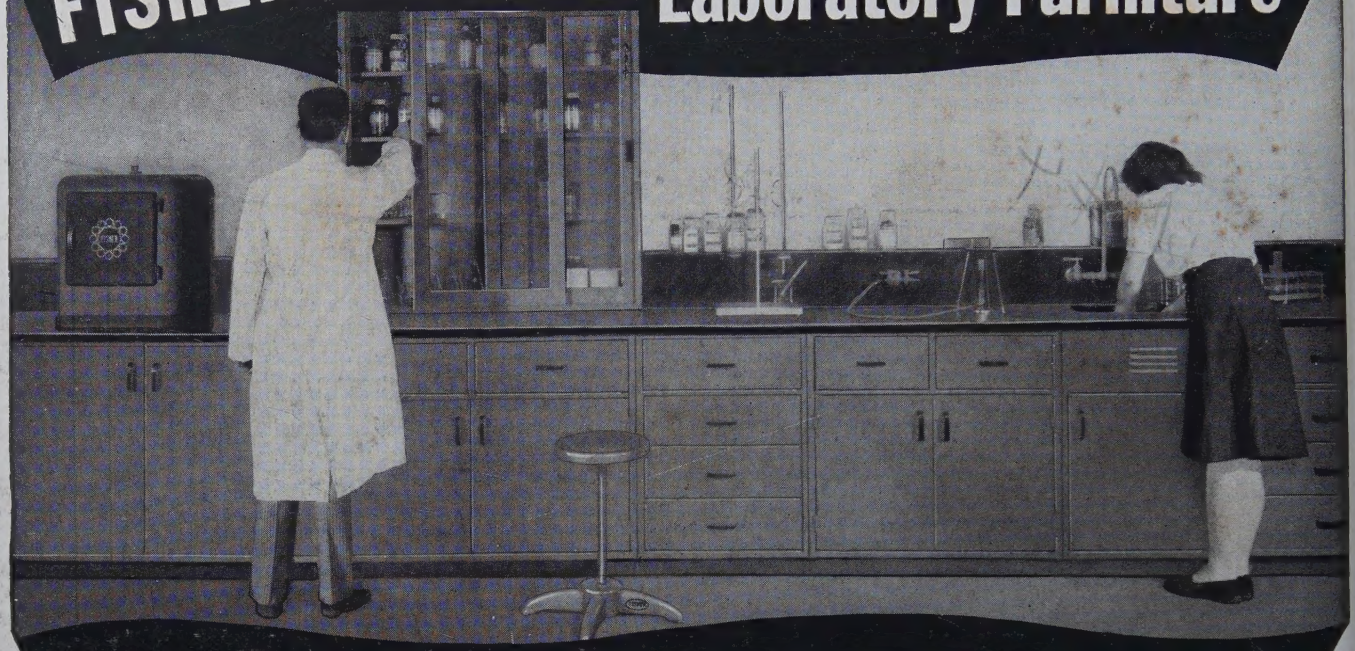

A completely *New System* for Equipping a Laboratory

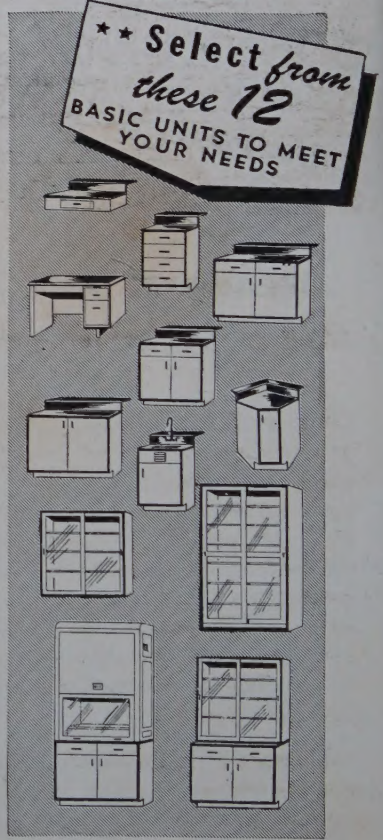

Available for Shipment from Stock

The unique Fisher Unitized Laboratory Furniture is adaptable to almost every need regardless of laboratory size or type of work to be done. It is featured by all-steel construction, Kemrock working surfaces, streamlined design and distinct advantages that eliminate engineering, manufacturing or installation delays.

Easy to Obtain and Install

Measure the space available—select the desired units—obtain from stock. Any handy man can assemble it.

Write for the free catalog describing and illustrating this new Fisher Unitized Laboratory Furniture.

Headquarters for Laboratory Supplies

FISHER SCIENTIFIC CO. | **EIMER AND AMEND**

717 Forbes St., **Pittsburgh (19), Pa.**
2109 Locust St., **St. Louis (3), Mo.**

Greenwich and Morton Streets
New York (14), New York

In Canada: Fisher Scientific Co., Ltd., 904 St. James Street, Montreal, Quebec

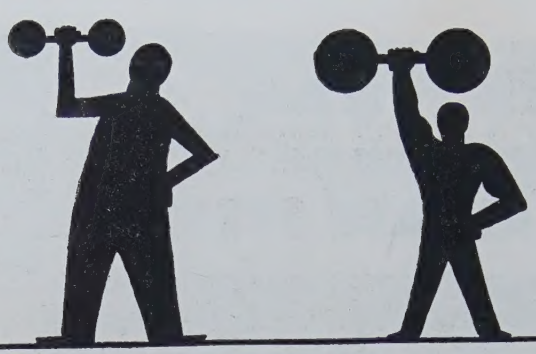

Add Load Capacity and Reduce Deadweight...

BY USING HIGH STRENGTH— LOW ALLOY STEELS Containing NICKEL

Many fabricated structures may be improved by redesigning to utilize the excellent mechanical properties of high strength low alloy steels containing nickel.

These steels provide:

1. **High strength in the as-rolled condition, permitting important weight reductions.**
2. **Excellent response to such fabricating operations as forming and welding.**
3. **Good resistance to corrosion, abrasion and impact.**

Sheet gages may be cold-formed into structural panels that assure maximum weight reductions without sacrifice of strength or safety.

These nickel alloyed steels have gained wide popularity by reducing maintenance, extending service life and eliminating thousands of tons of deadweight.

Produced under various trade names by leading steel companies, high strength low alloy steels containing nickel along with other alloying elements, have established notable performance records. Consult us on their use in your products or equipment.

* *

Over the years, International Nickel has accumulated a fund of useful information on the properties, treatment, fabrication and performance of engineering alloy steels, stainless steels, cast irons, brasses, bronzes, nickel silver, cupro-nickel and other alloys containing nickel. This information is yours for the asking. Write for "List A" of available publications.

EMBLEM OF INCO SERVICE

THE INTERNATIONAL NICKEL COMPANY, INC.

67 WALL STREET NEW YORK 5, N.Y.

JOURNAL OF Metals

TECHNOLOGY · PRACTICE

FEBRUARY 1949 Volume 1, No. 2

JOURNAL OF METALS Technology • Practice is on file in many public libraries and is indexed in Engineering Index, Industrial Arts Index, ASM Review and Chemical Abstracts.

Published monthly by the American Institute of Mining and Metallurgical Engineers, Inc., 29 West 39th St., New York 18, N. Y. Domestic subscription, North, South, and Central America, $8; foreign, $9. To AIME members, $6, or $4 in combination with a subscription to *Mining Engineering* or the *Journal of Petroleum Technology*. Single copies, 75 cents. Special issues, $1.50.

Entered as second class matter January 12, 1949, at the post office at New York, N. Y., under the Act of March 3, 1879. Registered cable address, AIME.

Printed in U. S. A.

COVER PHOTOGRAPH represents a typical scene in hilly San Francisco where the annual meeting of AIME is being held Feb. 14-17.

section one

section two . . . AIME

section three . . . metals transactions

(Continued on page 4)

AMERICAN INSTITUTE OF MINING AND METALLURGICAL ENGINEERS, INC.
Metals Branch
Editorial, Advertising and Business Office, 29 West 39th St., New York 18, N. Y.

AIME also publishes *Mining Engineering* and *Journal of Petroleum Technology*.

The deadline for Fall Meeting papers of IMD will be May 1, 1949.

CONTENTS

Continued from Page 3

JOURNAL OF Metals TECHNOLOGY • PRACTICE

GUEST EDITORIAL

J. L. BLOCK • VICE PRESIDENT, INLAND STEEL CO.

EFFECT OF CEMENT CASE DECISION ON THE STEEL INDUSTRY

On April 26, 1948, Mr. Justice Black delivered the opinion of the United States Supreme Court in what is commonly called the Cement Case and thereby set off a veritable economic chain reaction, the reverberations of which have shaken the business world to its very roots and the end of which is surely not in sight.

First of all, let us consider the question of just what there was in the Cement Case decision which made so many of our important corporations, including almost all of the leading steel producers, abandon their long-established practice of meeting competition by freight absorption or otherwise. All of us knew that the Clayton Act as amended by the Robinson-Patman Act made it "unlawful for any person engaged in commerce . . . to discriminate in price between different purchasers of commodities of like grade and quality . . . where the effect of such discrimination may be substantially to lessen competition or tend to create a monopoly . . ." But we also knew that the very next section provided that nothing in the act prevented "a seller rebutting the primafacia case . . . by showing that his lower price to any purchaser . . . was made in good faith to meet the equally low price of a competitor . . ." It was in full reliance on this provision of the act that the steel companies lowered their mill realizing prices, when it was necessary to meet the prices of competitors located more advantageously freight-wise in relation to the buyer.

But all this was changed by one brief sentence in the opinion handed down by Mr. Justice Black. After stating that Section 2 (b), the one just quoted, permitted a single company to sell a customer at a lower price to meet competition, he said: "But this does not mean that Section 2 (b) permits a seller to use a sales system which constantly results in his getting more money for like goods from some customers than he does from others." Now, the steel industry seeks to constantly sell our manufacturing and jobbing customers. We do not think it is good business for us to enter into such a relationship only occasionally or spasmodically.

The issue as I see it is a question of which of two alternatives is truly in the best interest of the public, the inflexible f.o.b. mill price on the one hand, and a mill price with, as so aptly put by a member of our industry, "the right to compete," on the other. Which of these alternatives will generate the most competition? The inflexible mill price in the steel industry leaves some territories as monopolies to single producers and in many others the buyers are at the mercy of but a handful of sellers. Surely this does not enhance competition; actually it stifles competition. On the other hand, the mill price with "the right to compete" leaves the competitive door open to everyone who elects to enter.

There are those who decry the variations in mill realizing prices as a result of meeting competition by absorbing freight. From a purely theoretical or emotional point of view one might object to the practice of having a higher mill net realizing price for the backyard customer than for the buyer in some distant territory. But, as a matter of fact, who is hurt? The local buyer gets as good a price as any other local buyer and the customer at the distant point already has the price which this seller is only meeting. How can it be argued that the effect of this discrimination "may be substantially to lessen competition or tend to create a monopoly . . ."?

Some of those who oppose this meeting of competition with varying mill nets ask why the seller will not give the same mill price to all his trade that he is willing to accept in certain instances. The answer is obvious. Manufacturers have aways been willing to accept some marginal business to help their volume, thereby giving better employment to their forces and in most cases absorbing a part or all of the applicable overhead charges. However, were they to take all of their business on the same basis, the enterprise in all likelihood would not provide a satisfactory return to justify its existence.

Our lawmakers should strive, not for some fantastic Utopia, but rather to strengthen competition under existing conditions and to make the best possible use of the marvelous producing facilities in this country. To my way of thinking a mill price with "the right to compete" is the answer. It abolishes "phantom" freight, promotes greater use of the highways and waterways and surely fosters competition. Such a method could be legalized by a simple amendment to the famous Section 2 (b) making it clear that the seller can be competitive *constantly* as well as occasionally.

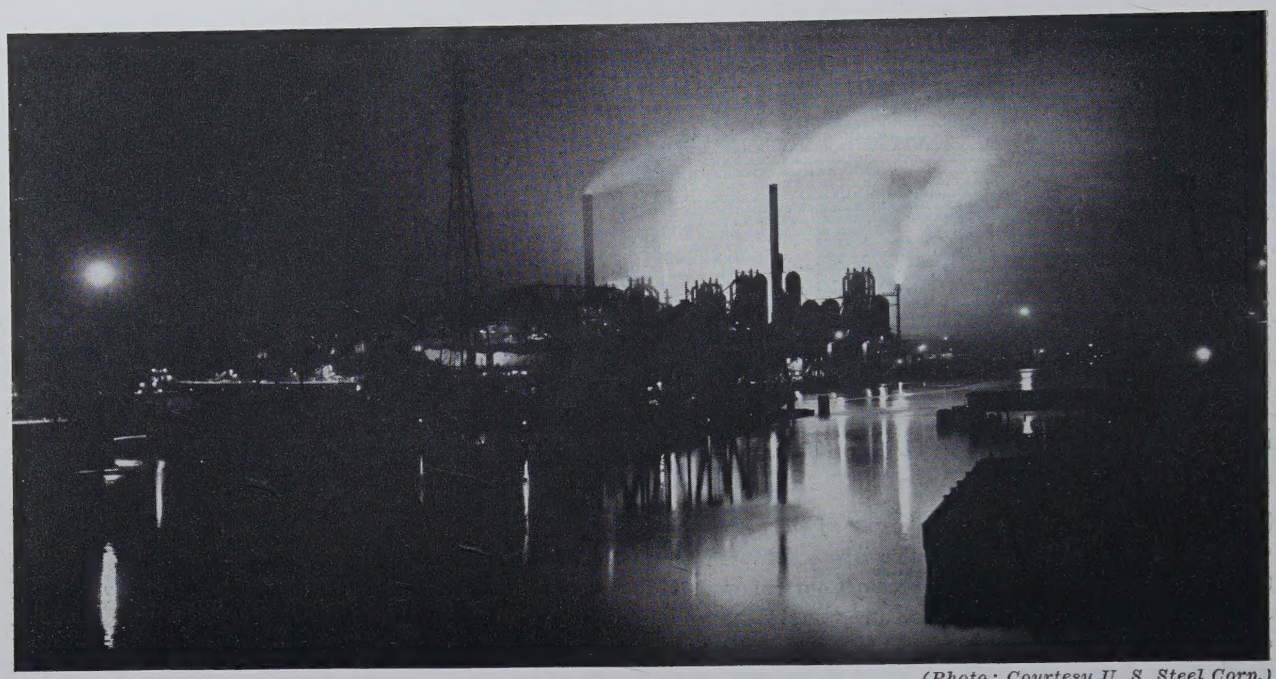

(Photo: Courtesy U. S. Steel Corp.)

Some plants work from sun to sun—a steel plant's work is never done.

Plan for East Coast Steel Plant

New York Area Has Potential 20,000,000 Customers

HAROLD A. KNIGHT, ASSISTANT EDITOR

SINCE the Federal Trade Commission ruled that the multiple basing point system for making sales in an industry, particularly cement and certain others, is illegal there has been much talk in steel circles of the possibility of a reshuffling of both steel plant sites and plant locations of steel consumers. The steel industry voluntarily abandoned the multiple basing point system shortly after the cement decision was made, seeing plainly the handwriting on furnace walls, and started selling on an f.o.b. mill basis, which immediately hurt steel consumers far from plants since the steel makers would no longer absorb freights. Several consumers have announced intention to move consuming plants to steel centers, particularly Pittsburgh, because of intolerable conditions developing.

Though the first apparent movement has been for consumers to move to producers, or "Mohamet to the mountain," there is evidence that there is the possibility that some movement may be the other way. Perhaps one of the most practical and up-to-date is a plan in the offices of H. A. Brassert & Co., consulting engineers for the iron and steel industries and builders of steel mills all over the world, to build a complete integrated steel plant in the Greater New York area—not exactly on Fifth Ave., near Tiffany's, but on Staten Island, or the New Jersey meadows where there is direct access to deep water. It is not a new idea, serious plans having been considered as long ago as 1906. Moreover, should construction of such a plant start soon it would appease the Washington Administration, who have agitated for expanded steel capacity again recently.

It is understood that several steel makers are considering these, or equivalent plans, one large company weighing the New York district as against Norfolk, Va. There is some talk, too, of the possibilities of a steel mill at some Connecticut point on Long Island Sound, such as Bridgeport, though such a point would be inferior from standpoints of water deliveries, warehousing and nearness to markets. Let it be said at the start that probably the one factor which prevents a rush of steel makers to build such a plant at tidewater on the northern Atlantic Coast is present day costs of construction, which conservatively figure $250 to $300 per ingot ton of steel produced, compared with $30 to $50 per ton when the majority of the older existing present steel mills were constructed, or even with $150, the cost of a very few years back.

traditional steel plant sites

For generations the site of a steel maker has easily been determined by that location where iron ore and coal are in close proximity, the ideal in this respect being the Birmingham area. Coal, inland waterways, and ore not too far away on the Great Lakes, were responsible for the great build-up at Pittsburgh where steel-making production today is much in excess of local consumption capacity. Relative nearness to ore abetted building of steel plants in Northernmost Ohio, on Lake Erie.

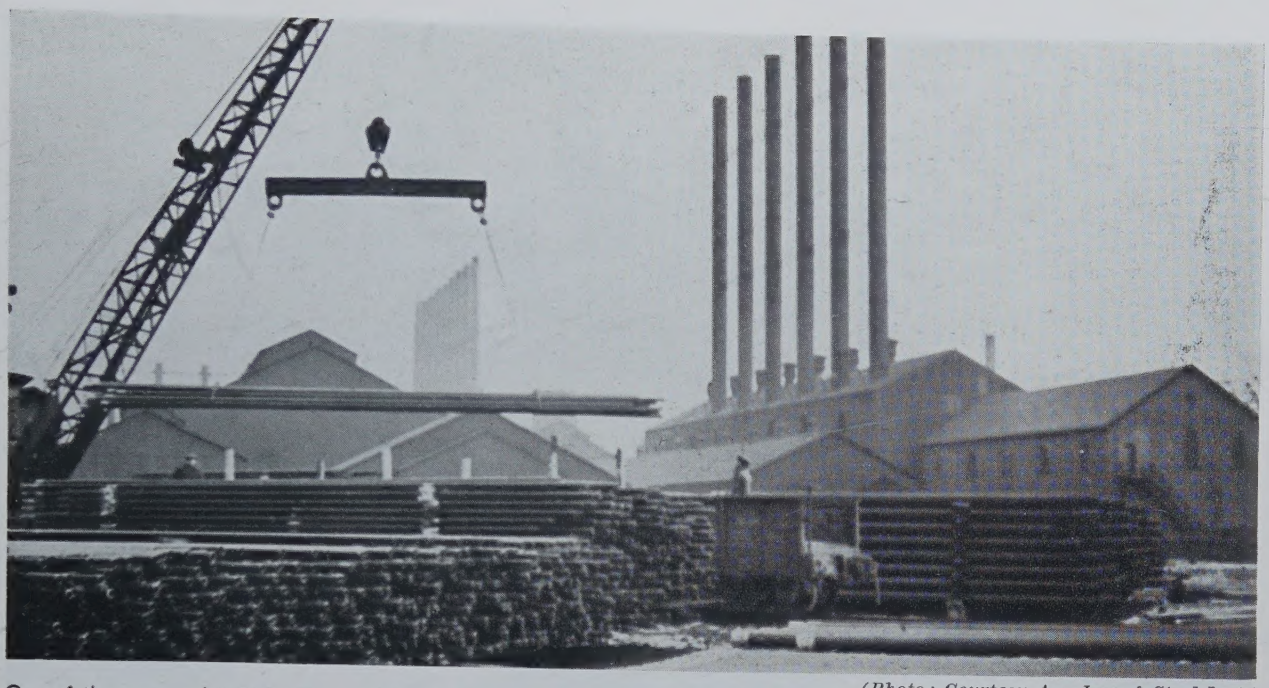

One of the proposed initial mills would be one for making pipe and tubing. *(Photo: Courtesy Am. Iron & Steel Inst.)*

In later years the concept of a good steel plant site was one on tidewater where ore and other raw materials could readily be brought in by freighter and barge and much of the finished product shipped by water, both for United States and foreign consumption. The Sparrows Point plant of the Bethlehem Steel Corp. first comes to mind in this category, it being understood that this company could ship finished steel via water, through the Panama Canal, to our own Pacific Coast, selling there, if the company willed, at $5 per ton cheaper than the nearest competitor before the present Kaiser company plant at Fontana, a plant that was built at around $140 per ton of annual plant capacity.

Now a new concept is springing up, to the effect that other factors being fairly satisfactory, a steel mill is well located when it is in the heart of a large steel consuming district, particularly if it is the only large mill there. Such a mill is envisioned by the Brassert planners, which factor, combined with site at tidewater and other favorable factors makes a New York steel maker no idle dream. With Mesabi iron ores rapidly becoming depleted there is not much point in locating near them.

Important among these factors is the large supply of ferrous industrial scrap that originates locally, in New Jersey, eastern Pennsylvania, Delaware, lower New York state, Connecticut and other near-by New England states. Brassert engineers propose to use 60 per cent scrap and 40 per cent pig iron in the open hearth furnace charges. Consult a steel trade journal, market news section, and observe that most districts' scrap market reports, involve prices delivered at mills. The New York report, however, is on a different basis. This market is based on dealers' buying prices, the scrap being shipped far afield and prices lower than in other markets. Thus the New York state barge canal carries much of it to the Buffalo steel makers. Bethlehem, Pa., is another important outlet for Greater New York scrap, while in many normal years much has been exported to Europe (though now the movement is reversed). Too, industrial scrap is the preferred kind, as compared with country scrap, which is variegated, dirty, analysis often unknown and more difficult to collect. In this enlightened metallurgical age industrial scrap is well segregated, tagged, in great abundance per analysis, often baled or briquetted—in fact the equal or superior of pig iron. Just now, too, in most locations steel scrap is much cheaper than pig iron.

variety of ores to choose from

Again, the proposed steel plant would have a wealth of iron ores to draw on. If such a plant could magically start work tomorrow it could draw upon Adirondack ores barged down the Hudson River. Or it could tap ores only 40 miles away in New Jersey, mines that have proven themselves for many years, such as those in Ringwood, Dover, Mt. Hope, N. J. Though these ores already are contracted for, in time they would tend to gravitate to the New York plant because of nearness. Or it can go farther afield with boats to Chile, where Bethlehem has secured ores for years; Brazil, whose wealth in iron is by now well known. It could use ore from Morocco, Algeria, Norway, Sweden, while purchased foreign ore at present, laid down on the eastern seaboard, is more expensive than Mesabi ore delivered to lower Lake ports. This is largely a shipping problem. In the past the price of foreign and domestic ores have always been competitive in normal times.

The use of high-phosphorus ores, so far turned down in this country, but employed extensively in Europe, could be adapted here, using the basic bessemer process, instead of the prevalent basic open hearth. One important advantage of the high phosphorus ores is the recovery of phosphorus in the slag for fertilizer, the sales of which

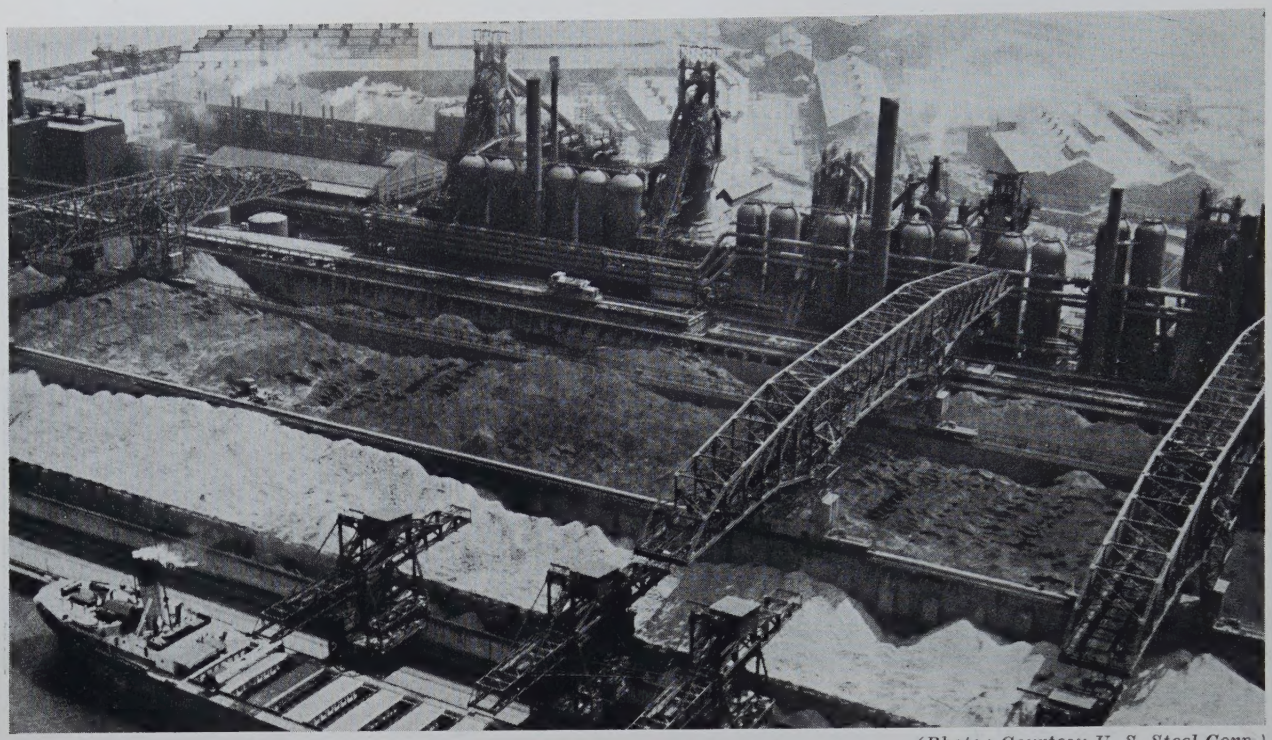

(Photo: Courtesy U. S. Steel Corp.)

A steel plant at tidewater facilitates receipt of raw materials such as iron ore.

offset the expense of the basic bessemer process. If high-phosphorus ore is decided upon the well known Wabana ores of Newfoundland or high-phosphorus Swedish ore may be used.

But since this steel plant can't emerge overnight like an Aladdin's Lamp project it will eventually draw upon other ores far afield perhaps. Thus within a year Bethlehem will be bringing ores from Venezuela while U. S. Steel is doing exploratory work there. The much publicized Labrador ores, with 300,000,000 tons virtually proven and comparing closely with Mesabi ores, are a likely possibility especially for a tide water plant.

Neither would the New York steel maker necessarily have to own its own fleet of ore carriers. Thus tramp steamers and other commercial carriers, taking American bulk goods down to South America, say, would be glad to load up with iron ore for the return trip. Nor would the commercial boats be bringing in much waste cargo when loaded with such ore as that from Venezuela which has a content of 65 to 68 per cent metallic richness.

Coals from Virginia and West Virginia, could be brought in from Norfolk and would probably cost only 30 to 40 cents per ton more than water borne coal would cost at Sparrows Point. Coke might be bought from some of the by-product coke makers located in the New York district particularly from Northern New Jersey. Should the steel maker produce its own coke, its by-product gas could undoubtedly be sold to some neighboring municipality. Limestone could be readily brought in from quarries on the lower Hudson, where several cement plants are already located, or from Pennsylvania quarries. In short, located on tidewater, its access to raw materials and even foreign markets for its finished products would be decidedly fluid and not as much a slave to local sources of supply and conditions as a plant situated farther inland.

plans as to size

As to initial plant size the engineers visualize a minimum size involving a yearly production of 550,000 tons of ingots and 400,000 tons of finished merchantable steel. As business progressed and the plant justified its existence, it could be expanded to produce 900,000 to 1,000,000 tons yearly. (For comparison, Bethlehem's Sparrows Point plant turns out 4,651,000 tons of ingots and steel castings yearly, of which 240,000 tons is Bessemer steel.)

The chief products at first would be bars, pipe and structurals, products which by experience are found to have the largest consumption in the Greater New York areas where, within a radius of 50 to 75 miles, 20,000,000 people live. In normal times bars and sheets enjoy the greatest versatility of uses and there are but very few lines of manufacture that utilize steel that do not consume some bars. Pipe would find its greatest use in building perhaps and is also a common raw material in many lines of manufacture. In a metropolitan area like New York a large consumption of structurals is obvious, both for housing, office and other large buildings and many kinds of manufacturing. Shipping to foreign markets would be extensive and profitable because demand is large.

In the bar classification concrete reinforcing bars and mesh would be one of the most important products in view of the many engineering enterprises in and surrounding a large city, such enterprises as superhighways, subways, bridges, water reservoirs, swimming pools and a host of others.

According to the Brassert plans for a small integrated

steel plant, equipment would be installed for an annual production of the following products:

	Tons
Pipe, ½ to 3 in., 40% black and 60% galvanized	120,000
Seamless pipe and tubing up to 6 in. to 7 in.	75,000
Thin wall mechanical tubing, ¼ to 2 in., electric-welded	15,000
Narrow cold-rolled strip, Nos. 12 to 30 gauge, rolled on a merchant bar mill	30,000
Cold-drawn screw stock	30,000
Cold-drawn carbon bars	60,000
Merchant bars, hot-rolled	70,000
	400,000

If and when the steel plan increased its output, its seamless capacity would be one of the first lines to be expanded by the addition of larger pipe, 8 to 14 in., for use in the petroleum and gas fields, a product which would doubtless be exported on a large scale. The pipe would be usable for both foreign and domestic petroleum and gas fields; also throughout the East for connecting the large 20 to 30 in. long distance lines to smaller communities. The added capacity would include more flat rolled material, especially sheets and strip, for which there is a good market now and probably in the future.

The chief items of equipment under the minimum initial plan would be the following: one 1200-ton blast furnace; dock facilities for receipt of all incoming raw materials; a basic Bessemer plant with a 25-ton converter and spare vessel; one 800-ton hot metal mixer; three 150-ton open hearth furnaces, being rebuilt, as the plant expands, to 200-ton furnaces; a 42 in. blooming mill, with soaking pits; a continuous billet mill; a combination bar and skelp mill; a 30 in. hot coil reversing strip mill; two 30 in. cold strip mills; one Fretz-Moon pipe mill; an electric-weld tube mill; a seamless pipe mill; a department for making cold-drawn bars.

Naturally the planners of this potential plant have constantly in mind the excessive cost of construction in these times. Some old-timers might shake their heads because it is not located next door to any essential raw material. The best factor on the credit side of the ledger is its contemplated location in one of the largest steel consuming areas of the world. Taking advantage of this fact the company managers would doubtless plan to sell about a third of their production on a warehouse basis, thus receiving around $20 per ton premium over mill prices for the jobbing service. The cost of warehousing at a mill runs $5 to $8 per ton, leaving $12 to $15 per ton profit. This would entail facilities for handling sales in extremely small quantities, with a fleet of delivery trucks and wide variety of sizes and descriptions ready for immediate delivery. This of course would not be the first time that a steel maker has turned jobber, as well, a notable case having been the purchase of the Joseph L. Ryerson Co. by the Inland Steel Co. If there proves to be a general movement in which steel makers build plants in large consuming areas there will be an increasing number of producer-warehouse set-ups.

This Metropolitan New York steel maker will depend on water haulage on a large scale for incoming raw materials and shipments of finished goods. As a matter of fact rail rates have been increasing so markedly that several steel makers had already ceased selling far afield because of burdensome freight rates which they were being forced to assume. Thus even had the Federal Trade Commission taken no action on multiple basing point selling of heavy commodities the tendency of steel makers would have continued toward greater local sales. Several consuming districts have been complaining for many months that they had been practically abandoned by old-time steel suppliers.

The theoretical cost of building the minimum plant would be $150,000,000 assuming that its capacity will be 550,000 tons of ingots yearly and the building cost is $270 per ingot ton. In view of the scarcity of steel there would be some problem to get the plates, etc., needed for building blast furnaces, stoves, etc. However several steel leaders predict a balance of supply and demand soon.

The engineers point out that they have not included plans for production of alloy steel, such as stainless steel, in the New York enterprise since this department of the steel industry of the United States tends to be over-built.

At first blush, labor might seem too expensive in a metropolitan district in the Northeast. In other years there has been an exodus of manufacturing enterprises from the cities to more rural districts. However here in 1949 under the influence of the unions, wage rates are quite uniform for the country as a whole. New Jersey, assuming the plant were built on the Jersey meadows, is the source of a great abundance of industrial labor, men who have had many years of experience with industrial enterprises including shipbuilding.

One might wonder if there is sufficient water suitable for a steel mill on either the Jersey meadows or Staten Island. The answer is that salt water will suffice for much of the plant, such as for condensers. All power stations located on tidewater habitually use salt water. Where fresh water is needed, such as for cooling rolls in action, fresh water can be reclaimed by standard practice and reused again and again. This combination of fresh water and salt is used by Sparrows Point, for instance. Kaiser Co., Fontana, Cal., using water supplied for irrigation, reclaims it constantly.

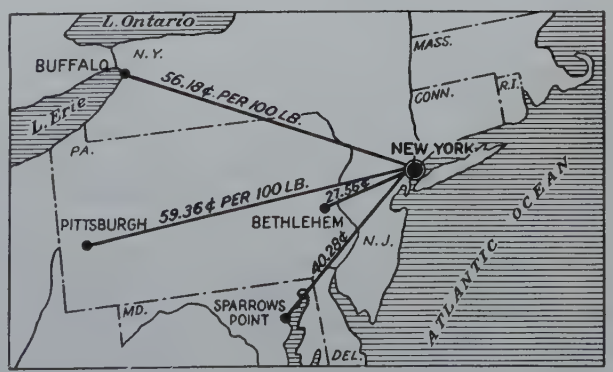

A plant at New York, with 20,000,000 population, would save much freight as the chart above on new rates on finished steel, Jan. 1, 1949, indicates.

Egon Orowan, Head, Metal Physics group, University of Cambridge, will give annual IMD lecture.

John Chipman, Head, Dept. of Metallurgy, M.I.T., will deliver the Howe Memorial lecture.

The late J. W. Hickman, Westinghouse Research Laboratories, is co-recipient of the annual Award Certificate of IMD.

Four Awarded at San Francisco

Egon Orowan and John Chipman Will Lecture

Two of the most popular activities at the AIME annual meeting at San Francisco Feb. 14-17 will be the special lectures and the tendering of awards and medals, features which usually attract large attendance and much interest. The IMD annual lecture this year will be delivered by Egon Orowan, head of the Metal Physics Group, University of Cambridge, England, who will talk at 11 a.m. Tuesday, Feb. 15. The subject he has chosen for his lecture is "The Structure of the Cold-worked Metal." The other special speaker will be John Chipman, head of the Department of Metallurgy at Massachusetts Institute of Technology, who will give the Howe Memorial Lecture at 11 a.m. Wednesday, Feb. 16, on the subject "What Is Metallurgy?"

Michael Tenenbaum, with the Metallurgical Department of the Inland Steel Co., has the unusual distinction of being the recipient of two awards, the Robert W. Hunt Medal and the Rossiter W. Raymond Memorial Award. John Daniel Saussaman, Blast Furnace Superintendent, Kaiser Co., Inc., will be given the J. E. Johnson, Jr., Award which involves creative work in the metallurgy or manufacture of pig iron.

The annual Award Certificate of the Institute of Metals Div. is being conferred jointly at the Wednesday night banquet to the late Joseph Weston Hickman, who was with the Westinghouse Research Laboratories, East Pittsburgh, Pa., and Earl A. Gulbransen, same company.

IMD annual lecture

The 1949 Institute of Metals Division Annual Lecture by Doctor Orowan will include a general survey of the present knowledge of structural changes due to plastic deformation. A brief discussion of how mosaic imperfections are revealed by X-ray methods will be followed by experimental evidence proving that such imperfections are not inherent in the crystal. Such imperfections, if present, are the consequence of growth defects or of plastic deformation.

Asterism, line broadening, and the change of lattice parameters after cold working will be treated. Asterism has recently been shown to be due to macroscopic bending and the limit to X-ray line broadening is related to yield stress. Internal stresses affect the lattice parameter. The spatial distribution of internal strains can be studied quite effectively with transparent non-metallic crystals using a polarizing microscope as well as by the Berg and Barrett methods.

Finally, the great amount of information about structural changes due to cold working that can be derived indirectly from features of strain hardening in combination with theoretical work on the elastic stresses around dislocations will be reviewed. A new field has opened up recently with the discovery of the polygonisation phenomenon which has led to the explanation, by Guinier, of the sub-grain structures observed by Lacombe and Beaujard.

Among the honors bestowed on Mr. Orowan have been the Thomas Hawksley Gold Medal of the Institution of Mechanical Engineers in 1945 and election as a Fellow of the Royal Society in 1947. He was born in Budapest, Hungary, in 1902, and received his diploma in Engineering and the Doctor of Engineering degree at the Technical University, Berlin-Charlottenburg. He continued there as teacher and research worker.

He returned to Budapest in 1933 and took charge of the Krypton Gas Works of the United Incandescent Lamp & Electric Co., the first plant in the world to produce krypton commercially from air as a main product. In 1937 he continued his research work on the mechanical properties of metals in the Physics Department of the University of Birmingham. Since 1939 he has been working in the Cavendish laboratory of the Physics Department of Cambridge University, his official position being that of reader in the Physics of Metals. The work ranges from mathematical investigations of the distribution of stress and strain in plastically deformed bodies, through physi-

Earl A. Gulbransen, Westinghouse Research Laboratories, receives the annual Award Certificate of IMD.

Michael Tenenbaum, Metallurgical Dept., Inland Steel Co., takes the Hunt Medal and Raymond Memorial Award.

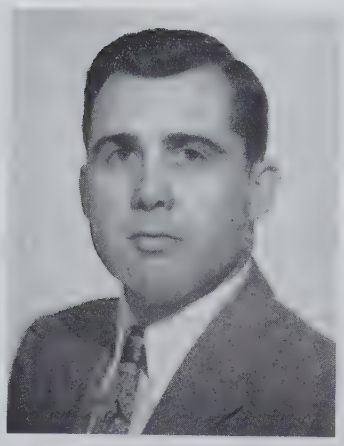

G. D. Saussaman, Blast Furnace Superintendent, Kaiser Co., Inc., is to receive the J. E. Johnson, Jr. Award.

cal investigations into plastic and strength properties of metallic and nonmetallic materials, including single crystals, to research on plastic working, in particular on rolling, cooperating with the British Iron and Steel Research Assn.

Howe memorial lecture

John Chipman, professor of Process Metallurgy at Massachusetts Institute of Technology since 1937, becoming head of the Department of Metallurgy in 1946, has for many years been engaged in teaching, research, in writing technical papers and related activities. During the late war he served as chief of the Metallurgy Section, University of Chicago's branch of the Manhattan Project. Born at Tallahassee, Fla., in 1897, his early education was received at the University of the South. He received his PhD from the University of California in 1926, while in 1940 he was awarded the honorary degree of Science Doctor by the University of the South. After several years of teaching he became associate director of research of the American Rolling Mill Co., joining M.I.T. in 1937. He has received awards and medals from AIME and ASM. He delivered the Campbell Memorial Lecture of ASM in 1942. He is a member of Sigma Xi and Phi Beta Kappa and is a foreign member of the Royal Swedish Academy of Science.

Hunt and Raymond honors

Michael Tenenbaum will receive the Robert W. Hunt Medal and Rossiter W. Raymond Memorial Award, both for the same paper, "Structure, Segregation and Solidification of Semikilled Steel Ingots," published in *Metals Technology*, September, 1947, Mr. Tenenbaum is with the Metallurgical Department of the Inland Steel Co. where he is concerned with problems involving metallurgical and operating phases of high temperature pyrometry, combustion, refractories, liquid steel reactions, various aspects of steel plant raw materials and product properties. He is a member of Physical Chemistry of Steelmaking Committee, Programs Committee and Chairman of the Iron and Steel Div. Auxiliary Publications Committee, AIME.

Mr. Tenenbaum was born July 23, 1914, at St. Paul and studied metallurgical engineering at the University of Minnesota, graduating in 1936 and obtaining an M.S. degree in 1937. He obtained a PhD degree from Minnesota in 1940, majoring in Metallurgy and minoring in Physical Chemistry. From 1936 to 1940 he was associated for limited periods with the Metallurgical Department, Inland Steel Co.; open hearth operations at Wisconsin Steel Works, and raw materials research for the Tennessee Coal, Iron & Railroad Co. He rejoined the Metallurgical Department of Inland in 1941.

J. E. Johnson, jr. award

John Daniel Saussaman won the J. E. Johnson, Jr., Award, for work done as described in his paper: "Sinter Practice, Kaiser Co., Inc., Fontana, Cal.," published in the 1948 Blast Furnace Proceedings, an abstract of which follows: During the first five years of blast furnace operation at Kaiser Co., Vulcan ore, from an open pit in the Mojave desert, made up the major portion of the furnace burden. The ore was satisfactory for a while but gradually the sulphur content increased until it could no longer be used economically. Excessive slag volumes needed for sulphur removal greatly reduced iron production and increased the coke rate. Since then the sintering plant has played an increasingly important part in the beneficiation of this ore.

The ore now contains 2.00 per cent sulphur. Crushing to minus $\frac{5}{8}$ in. prior to sintering has resulted in the removal of 95 per cent of the sulphur during sintering, converting it into an excellent furnace material, high in iron, low in phosphorous and sulphur and self-fluxing. The sinter is relatively soft and must be handled gently to avoid excessive fines. Important for physical properties is the rotary cooling table, designed and built by Kaiser, which eliminates need for quenching the sinter with large volumes of water. Furnace operations have definitely improved, the sinter being a better material physically, chemically and economically.

Mr. Saussaman, after serving as assistant blast furnace superintendent of Kaiser, was promoted to blast furnace superintendent in January, 1948. Originally planning to be a chemical engineer, he became interested in the production of iron and steel at Lehigh University. He was born at Harrisburg, Pa., in 1917 and was graduated from Lehigh in 1939 with a B.S. in Metallurgical Engineering. He was a member of the honorary engineering fraternity, Tau Beta Pi. He started as

an apprentice at the Duquesne plant, Carnegie-Illinois Steel Corp. and was promoted to other positions. After five years of military service he returned to Duquesne as special engineer, blast furnace department. Two months later he joined Kaiser Co., Inc.

award certificate of IMD

The award-winning paper of the late J. W. Hickman and Earl A. Gulbransen is entitled: "Electron Diffraction Study of Oxide Films on Iron, Cobalt, Nickel, Copper and Chromium," published in AIME Transactions, IMD, Vol. 171, 1947. The literature on the electron diffraction and X-ray diffraction studies of the oxidation of iron, cobalt, nickel, chromium and copper is reviewed, as is the prospective role of the electron diffraction reflection technique for the study of the reactions of gases with metals at high temperatures and *in situ* is presented. The apparatus, preparation of specimens, experimental procedures and the interpretation of the electron diffraction data are discussed.

The oxidation of pure iron shows the presence of three crystal structure transitions: (1) gamma Fe_2O_3 to alpha Fe_2O_3 at 225 C; (2) alpha Fe_2O_3 to Fe_3O_4 at 225 to 450 C, and (3) Fe_3O_4 to FeO at 450 to 550 C. The latter transition temperatures differ from the accepted value of 570 C from the iron-oxygen diagram. However, the deviation is a function of film thickness and the value approaches 570 C for thick films.

A study of the spot structure of the diffraction rings and the width of the diffraction line indicates crystal growth during the oxidation process, while the development of arcs in the diffraction diagram indicates preferred growth of certain crystal planes. Many of the crystal structure transitions and physical changes are reversible with temperature.

The oxidation of cobalt, nickel, chromium and copper are studied over a wide temperature range and for oxidation times up to one hour. The results are tabulated in existence diagrams. No unusual structures are observed for the oxides of these metals. One crystal structure transformation between Co_3O_4 and CoO is found to occur at 400 to 600 C while no changes are observed in crystal structures of the oxides formed on nickel, chromium and copper. However, crystal growth and orientation effects are noticed which indicate physical changes in the surface oxides of thin films.

The late Joseph Weston Hickman had been with Westinghouse Research Laboratories from 1944 until his untimely death on July 26, 1948. His latest work was supervising the expansion of his X-ray and electron diffraction laboratory. He was preparing to put into use some apparatus of his own design, with which this laboratory was to extend the scope of his work. He has been described as having "turned out a steady stream of scientific papers." Born at Philadelphia on May 5, 1908, he attended Bethany College, receiving his bachelor's degree in 1934. There he was as proficient with a football as with textbooks. After teaching at a local high school he entered the graduate school of Johns Hopkins University. He received his PhD degree in 1940 after research on the crystal structure of sulfamic acid. He remained there as a faculty member, rising to associate in chemistry, directing the X-ray laboratory. During the war he worked on an Army-Navy project dealing with application of the super-conducting phenomena to the detection of radiant energy.

Earl A. Gulbransen joined Westinghouse Research Laboratories in 1940, his principal project having been the establishment of a fundamental program on gas-metal reactions, including oxidation, reduction, degassing, decarburization and the vacuum behavior of oxides. For this purpose he developed a sensitive microbalance for the study of reaction kinetics and, in collaboration with Dr. J. Hickman, special electron diffraction and X-ray analyses for studying gas reactions on metals at high temperature. With co-workers he has developed electron microscope techniques for the study of chemical reactions on thick metal specimens, with over 40 publications on that subject.

Born on Jan. 20, 1909, in Seattle, Wash., he was graduated from the State College of Washington in 1931 in Chemical engineering. He received his PhD degree from the University of Pittsburgh in Physical Chemistry. In 1934 he accepted a National Research Council Fellowship at the University of California and the next two years continued work in the field of thermodynamics of solutions, especially non-aqueous; also in the low temperature laboratory determining data of state of gases. Then for four years he taught chemistry and chemical engineering at Tufts College, Medford, Mass., and pursued a research program on the abundance ratios of the carbon isotopes to natural processes using the mass spectrometer.

High Top Pressure Furnaces

The Republic Steel Corp. now has four blast furnaces operating on high top pressure and, according to E. M. Richards, vice president of Republic, operating results confirm expectations of higher productivity and greater economy, based on experimental operations begun in cooperation with Arthur D. Little, Inc. in 1944. Mechanical difficulties encountered in the early experiments have been reduced so that lost time on a pressure furnace is now no more than on a normal furnace, states Mr. Richards.

Erosion of the bell and hopper was one of the early problems, but the hard-surfaced, one-piece hopper and the hard-surfaced bell on the Cleveland furnace have been used continuously for 26 months and are still in excellent condition. The Chicago furnace has been on top pressure for three months only, but broke its tonnage record in August by producing 3000 tons more than in any previous month. The Cleveland pressure furnace has been operating on essentially a straight ore burden and has averaged 1250 tons daily for six months at a wet coke rate of 240 lbs. per ton of iron less than any other furnace in the Cleveland district. It has produced an average of only 117 lbs. of flue dust per ton of iron while being blown at a wind rate of 90,000 c.f.m.

The Youngstown No. 3 pressure furnace has produced an average of 170 tons more for a day at a coke rate 300 lbs. less per ton of iron than the Youngstown No. 1 furnace of exactly the same size and operating conditions. The furnace at Warren, Ohio, has been turning out over 1340 tons daily while operating at 6 lbs. per sq. in. top pressure and 92,000 c.f.m. with two old turbo blowers run in parallel.

Detroit AIME—Metal Powder Sintering

About one hundred members of the Detroit Section and their friends formed the enthusiastic audience at a lecture given by Dr. F. N. Rhines, Carnegie Institute of Technology, on Nov. 22. Using slides, Dr. Rhines discussed physical principles underlying the formation and spreading of bonds between powder particles during sintering. Mostly his lecture was devoted to an explanation of the expansion and contraction of residual pores associated with dimensional changes during the later stages of sintering, based on the hole-diffusion theory developed by himself and Birchenall in contrast to the viscous-flow theory of Wulff and Shaler.

Dr. Rhines discussed three factors which accelerate the sintering process without being essential to it: Pressing the powder, raising the temperature, and controlling the sintering atmosphere. Thus, upon storage even loose, unpressed powder tends to cake —the softer, cleaner, and finer the powder, the greater the caking. Pressing increases the number of points of metal-to-metal contact and hence would increase the rate of sintering, the latter also increased as the temperature is raised; which is to be expected, since sintering is essentially a process of diffusion. The effect of gaseous atmosphere depends somewhat upon the gas. All gases retard sintering to a certain extent; gases that do not diffuse readily retard the elimination of pores markedly. Hydrogen, having a high diffusion rate and serving as a reducing agent for the oxide films, provides good atmosphere.

The speaker described sintering as the sum of three overlapping steps. First, initial bonds or point-welds form at the points of contact between powder particles, the process being probably one of surface diffusion. After the initial welds are established, the bonds spread and the particles weld into a coherent body. The pores between the particles tend to spheroidize. Surface tension is the most important factor. In the final step there is a growth of some pores at the expense of others; however, the net result is a continual decrease in the number of pores.

Several theories have been advanced to account for the diminishing of porosity. One is the viscous-flow theory of Wulff and Shaler. From their equation governing the sintering process, it would follow that every pore would shrink continuously during sintering and that shrinkage would be independent of the mass of the powder. Rhines and Birchenall have demonstrated (by heating copper powder for various periods of time at 1000 F) that although the total amount of porosity decreases during sintering, some of the pores appear to grow at the expense of others. Their experimental work led Rhines and Birchenall to develop the hole-diffusion theory of sintering and to concentrate their attention on the pores rather than on metal particles. Forces of surface tension cause the pores to shrink, but movement of metal particles is purely by diffusion.

Vacant lattice sites are conceived as diffusing, so that while the smallest pores (because of greater surface tension) are shrinking, slightly larger, neighboring pores (having smaller surface tension) grow until the smallest pores disappear. This process continues, the pores of highest surface tension diminishing in size until they disappear. The net result is to increase the density of the sintered mass. The pores nearest the surface are lost to the system by movement into the "infinite" pore, the void surrounding the sintered mass. The assumption that the pore is spherical need cause no difficulty, for a change in the shape of the void merely introduces a "shape factor" into the mathematics describing the sintering.

Dr. Rhines' ability to treat a complex subject clearly but without undue simplification and the possibility of further development of his work in the fields of cast and wrought materials were responsible for the lively hour of discussion that followed.

—M. Semchyshen

SMELTS and SMILES

By Edgar Allen, Jr.

"Why did you order 'Killed' steel? We need very lively steel for springs!"

LETTERS TO THE EDITOR

Conference on Metallurgical Education

The following meeting report was placed in this department since it seemed to raise questions and expressed views upon which others might wish to comment.—Editors

Fifty members of the Yale Metallurgical Alumni met at Yale University for a panel discussion on Metallurgical Education. Chairman R. M. Brick asked Dr. C. H. Mathewson to introduce the subject. Dr. Mathewson emphasized that he considers that the purpose of the metallurgical department of a college is to teach "Scientific Metallurgy," whereas he felt in the early years of his profession that the curriculum should teach the "Reading, Writing and Arithmetic" of the metallurgist, and physical chemistry, as well. He would now, perhaps, place the emphasis on physics rather than physical chemistry.

A variety of viewpoints had been sought by asking both recent and older alumni from several fields of metallurgical activity to present their ideas. Brick stated that his purpose in planning the discussion was to see what suggestions could be made for improving the curricula of metallurgy departments so as to raise the professional standing of the graduates. He felt that metallurgists in general were held in rather low esteem among engineers, and that engineers in general were held in comparatively low esteem with respect to other professions. In support of this feeling he quoted published remarks derogatory of the metallurgist.

There was considerable difference of opinion as to whether this suspicion was justified, but the general tenor of the discussion concerned means for improving the metallurgical graduate's capacity for meeting the problems as a metallurgist. The suggestions:

1. Specific suggestions of the subject matter to be included in metallurgical curricula.

2. The relative emphasis on, or time devoted to, the various fields of subject matter.

3. The different preparation required by the research metallurgist and by the production metallurgist.

4. The need for training a man to prepare him for selling the value of metallurgy to management.

H. T. Green pleaded for the inclusion of a course on the purposes and the techniques of statistics, given on the graduate level, not in the form as taught in the mathematics department, but presenting the aspects which have direct application to metallurgical problems. Particular emphasis should be laid on making clear the purpose and desirability of the use of statistics. Approving the suggestion, E. A. Anderson said one direct benefit would be a greater realization by metallurgists that a point on a plot is really a center of scatter. There was some plea for the complete mathematical course in statistics so that the metallurgist would be a statistician as well, but it was concluded that, if the metallurgist knew the requirements of the statistician, he could ask the statistician to make interpretations of data for him. As a result, the metallurgist would not collect masses of data which could not be employed for statistical analysis.

On the basis of his experience, E. N. Skinner felt that metallurgical training had been somewhat lacking in familiarizing the graduate with knowledge of specific metals, and George Found indicated that he would like to see courses in techniques for analyzing production and complaint problems for all the commercial metals. The consensus, however, indicated that there would be little room for anything else should the metallurgical courses devote themselves in such detail to specific metals.

Kempton Roll's presentation opened the question of how much weight should be given to subjects other than metallurgy in the undergraduate and graduate curricula. He mentioned that, for advancement in the field, a metallurgist should have besides metallurgy:

1. An ability to express himself.

2. A curiosity about such subjects as economics, politics, and the social sciences.

3. A willingness to compromise perfection.

4. Knowledge of people.

Brick indicated the division of time in the undergraduate curriculum which he had concluded would best serve in his department at the University of Pennsylvania was as follows:

Metallurgy, 20 per cent; Physical Sciences, 40 per cent; General Engineering, 15 per cent; Social Sciences, 5 per cent; Humanities, 20 per cent.

Dr. Mathewson showed that the curriculum at Hammond Laboratory was quite comparable to this. John P. Nielsen had graded his development of a metallurgical curriculum by analyzing the fields of activity of an extensive list of members of the IMD of the AIME. His career distribution of metallurgists was as follows: Manufacturing (mill and plant), 40 per cent; Research and Development, 26 per cent; Executive, 17 per cent; Consulting, government, editing, 10 per cent; Teaching, 4 per cent; Sales, 3 per cent.

In discussion there was a considerable plea for greater emphasis in the undergraduate curriculum on the social sciences and humanities, and it was agreed that the embryo metallurgist should be given ample opportunity to develop his capacities for appreciation of these realms of thought. Skinner suggested there is too much metallurgy to be learned by any one man, and that perhaps it is time to divide the curriculum into courses for metallurgical engineers and for physical metallurgists. Extending this idea, F. N. Rhines

pointed out that a metallurgical graduate was asked by the public to do two things:

1. Develop new ideas and materials.
2. Employ existing knowledge in the operation of industries.

The physical metallurgist would be trained to handle the first, and the metallurgical engineer, the second. The curriculum for the metallurgical engineer would be quite similar to that of the chemical engineer, i.e., a basic mechanical engineering curriculum, modified to include metallurgy and the basic sciences. Present metallurgical curricula tend to develop the physical metallurgist although many enter the metallurgical engineering field. Anderson indicated that, while he was not yet ready to accept the idea of a curriculum in metallurgical engineering, he did feel that it was time to give the matter thought. He pointed out that the metallurgist in production work is generally underrated, the result of the present trend for the better men to go into research. Possibly, a specific course aimed at production work might attract men with better qualifications.

In an earlier presentation, Anderson made a strong plea that the methods of teaching be designed to develop habits of thinking which would provide a groundwork for continuing self-education after graduation. To this end, the curriculum should produce a graduate thoroughly versed in the basic sciences. He added a plea that the metallurgical department have more to say about the teaching of English, Mathematics, and Languages so that the student would be better versed in the application of these subjects to his own problems. Inclusion of humanities is very desirable. For those students who intend to take graduate work in metallurgy, it might even be possible to obtain a broader background at the expense of teaching metallurgy at the undergraduate level.

Citing metallurgy as an old art and a new science, Gerald Edmunds pointed out that there are some fields in which the artisan and the scientist have not developed mutual respect. Except for some prominent progressive concerns, he referred to the foundry industry as an example. In the field of melting and casting there are yet many problems to be solved by the physical metallurgist. Discussion brought out that the problem of mutual respect was one which involved the ability of the metallurgist to sell his product. Anderson mentioned the desirability for the employment of undergraduate metallurgists in the field during their summer vacations as a means for developing the metallurgist's respect for the artisan, and regrets were voiced by several that it was quite difficult for a student to find such employment.

To raise the standing of the graduate metallurgist, Nielsen felt that in addition to developing curricula that demand the most from the student, the metallurgy department should strive to attract the best students by publicity. This would be one means for meeting the basic problem pointed up by Professor Phillips that the extreme variation which is found in the "raw material" will always result in a fair proportion of mediocrity in the "product" regardless of what is done with the curricula.

The afternoon session was provocative in eliciting ideas which would be of use in modifying and improving metallurgical curricula. It was only indicative, however, of the many problems to which greater study could well be devoted for the purpose of improving the status of the graduate metallurgist. There was general agreement on two points: (1) that the type of curriculum established at Yale and Pennsylvania is quite satisfactory to the majority who prefer the strong background of the basic sciences to a more detailed engineering approach; and (2) that in the final analysis, the inherent qualities of the student are what really determine his ultimate success.

Franklin H. Wilson,
Secretary at Conference

Diffraction Table Available

A table has been computed to expedite the reduction of diffraction patterns obtained in the back reflection region and may be considered a continuation of Research Report R-94602-10-C. It is published by Westinghouse Research Lab., East Pittsburgh, Pa.

The table gives d values for Mo, Cu, Co, Fe and Cr targets for every tenth of a degree in 2θ, or five hundredth of θ, to four and five significant figures. The table is computed in Angstrom units for the $K\alpha_1$ radiation and factors are given for converting to $K\alpha_2$ and $K\alpha$ and to kx units.

BOOK REVIEWS

Metallurgical Materials and Processes. By John Elberfeld. Prentice-Hall Inc., New York City. 1948, 180 p. $5.

REVIEWED BY L. A. TWORK

THIS is a book on the fundamentals of metallurgy which would be suitable for students who wish some metallurgical background, but who do not wish to specialize in this field. The book surveys the entire ferrous and nonferrous fields briefly. The appendix contains several pages of elementary chemistry.

No previous knowledge of metallurgy is needed for the reader, but for more specific information on particular aspects of metallurgy a list of references appears at the end of the book.

The contents include information on grain structure, constitution diagrams, the effects of the various methods of fabrication upon the properties of metals, a brief discussion on welding and powder metallurgy, and an outline for a laboratory course in elementary metallurgy. About six to twelve essay-type quiz questions appear at the end of each chapter.

Refractories for Furnaces, Kilns, Retorts, etc. By A. B. Searle. 2 ed. Crosby Lockwood & Son, Ltd., 39 Thurloe Street, London, S.W. 7. 1948. 121 p., illus., charts, tables, diagrs., 7½ x 5 in., cloth, 7s.6d.

Describing the characteristics of the chief raw and manufactured refractory materials, this small volume also considers the processes and materials employed in their production. Refractory hollow ware is discussed, and the last section deals with the selection of refractory materials. A short bibliography of books and publications is included.

Report of a Conference on Strength of Solids held at the H. H. Wills Physical Laboratory, University of Bristol, on July 7-9, 1947. Published by The Physical Society, 1 Lowther Gardens, Prince Consort Road, London, S.W.7. 1948. 162 p., illus., diagrs., charts, tables, 10 x 7 in., paper, 25s. plus 8d. postage.

The nineteen papers reprinted from the conference are divided as follows: nine on creep and plastic flow; six on grain boundaries and recrystallization; three on precipitation; and one on fracture, dealing with size effects in steels and other metals.

Engineering Societies Personnel Service, Inc.

New York—8 West 40th St., Zone 18.
Detroit—100 Farnsworth Ave.
San Francisco—57 Post St.
Chicago—84 East Randolph St., Zone 1

These items are from information furnished by the Engineering Societies Personnel Service, Inc., which is under the joint management of the four Founder Societies. This Service is available to members and is operated on a co-operative, nonprofit basis.

In applying for positions advertised by the Service, the applicant agrees, if actually placed in a position through the Service as a result of these advertisements, to pay a placement fee in accordance with the rates as listed by the Service.

When making application for a position include six cents in stamps for forwarding application to the employer and for returning when necessary.

All replies should be addressed to the key numbers indicated and mailed to the New York Office.

A weekly bulletin of engineering positions open is available to members of the cooperating societies at a subscription of $3.50 per quarter or $12 per annum, payable in advance.

Positions Open

MILL SUPERINTENDENTS experienced in some particular phase or phases of mill operations in the manufacture of coke, pig iron, steel by the Bessemer and open hearth processes, blooming mill, bar mill, plate, sheet and tin plate mills, etc., to operate a steel mill and train personnel. Location, Chile. Y725.

METALLURGISTS OR METALLURGICAL ENGINEERS, for research work in field of powder metallurgy. Previous experience in field not necessary but some experience in metallurgy field desired. Salaries commensurate with background. Location, northern New Jersey. Y1128.

ASSISTANT METALLURGIST, graduate, with aluminum products experience for testing and development of aluminum and alloys. Salary, $3600-$4800 a year. Location, Long Island. Y1192.

PROCESS METALLURGIST for process development and semi-works production of metals by chemical or electro-furnace reduction. Write stating qualifications, experience and salary expected. Location, New Jersey. Y1646.

METALLURGIST, 25-30, graduate, with welding experience covering stainless steels, to analyze production difficulties, improve welding methods and procedures, and do general development work covering fabrication. Salary, $3640-$5200 a year. Location, New Jersey. Y1913.

RESEARCH METALLURGIST, 30-40, graduate, with non-ferrous smelting and refining experience, to supervise development of hydro-metallurgical pyro-metallurgical and electrolytic refining methods. Salary, $4200-$4800 a year. Location, northern New Jersey. Y1926.

METALLURGIST with minimum of five years' experience in specifications of materials for rocket construction. Salary, $3744-$4940 a year. Location, northern New Jersey. Y1963(b).

INSTRUCTOR, metallurgical, preferably on the application of mechanical engineering to metals. Will be permitted to carry full teaching assignment and at the same time prepare for advanced degree. Position open in January and March. Location, Midwest. Y1870-R-5368.

ENGINEERS. (a) Assistant to the Vice President, about 35, in charge of non-ferrous metals, scrap and residues, preferably with at least five years' experience in the non-ferrous metal and ore field. Must be able to buy and sell ores, be familiar with trade practices and have a good general knowledge of the various buyers and users of these products in this country. Reading knowledge of French desirable, but not essential. Salary dependent upon experience. (b) Engineer, who has specialized in aluminum and aluminum products. Should have a sound technical education and background experience in the industry. Should know production, fabrication and usage of aluminum products. Should be well acquainted with the technical processes involved and should also be able to sell the above products to domestic consumers. Salary dependent upon experience. Location, New York, Y1873.

ALL INSTITUTE SECTION

APPEARING IN:
- MINING ENGINEERING
- JOURNAL OF METALS
- JOURNAL OF PETROLEUM TECHNOLOGY

Mineral Economics Division Established—Board Sets Preliminary Budget for 1949

At its meeting on Dec. 15, President Wrather presiding, the AIME Board of Directors recognized the newly organized Mineral Economics Division, established the preliminary budget for 1949 in new form, and decided to discontinue the Junior Foreign Affiliate grade of membership at the end of 1949 provided the necessary change in the bylaws is effected.

Richard J. Lund presented the petition for the establishment of the Mineral Economics Division. The President of the AIME is to appoint the initial officers, consisting of a Chairman, three Vice-Chairmen, and a Secretary-Treasurer. Ten committees are specified in the bylaws, as follows: National Security, Conservation, Tariffs and Subsidies, Taxation and Finance, Foreign Mineral Policy, Statistics, Transportation, Marketing, Mineral Use and Substitution, and Management and Public Relations. The purpose of the Division "shall be to stimulate interest and promote progress in broad economic and political aspects concerned with the search for, finding, developing, producing, transporting, refining, marketing, and use of metals and minerals of all kinds, including mineral fuels; to hold meetings for social intercourse and the reading and discussion of papers on mineral economics; to encourage and assist in arranging for the inclusion of meritorious papers and discussions on mineral economics on programs of Regional, Divisional, and Annual Meetings of the Institute; and to arrange for the preparation of suitable economic and political papers dealing with minerals, having broad coverage of the industry—domestic and worldwide—for publication and distribution by the Institute." No conflict was seen by the Board in the professed aims of the Division with the Institute's policy on controversial matters as adopted by the Board at its Feb. 21, 1933, meeting, and printed in the current Directory on page 85. It was suggested that the papers of this Division might be published in Section 2—the All-Institute Section—of the monthly journals unless they covered only the specific field of one of the Branches.

The preliminary budget for 1949 as presented to the Board by Mr. Daveler, chairman of the Finance Committee, was, for the first time, arranged according to Branches, in line with suggestions made by the Petroleum Division that such an allocation be made so that it would be evident which fields of Institute activity were showing a profit, if any, and which a loss. The proper ratio of membership between the three Branches cannot yet be fixed, as many members have not yet indicated their primary choice of a monthly journal for the coming year, but the Mining Branch was estimated to have 52 per cent of the membership, and the Metals and Petroleum Branches each 24 per cent. These ratios will be changed, when more returns are in, for the final budget to be adopted later. This preliminary budget showed, for the Petroleum Branch, income of $90,476 and expenses of $118,018; for the Metals Branch, income of $78,330 and expenses of $112,403; and for the Mining Branch, income of $220,443 and expenses of $194,771. The over-all income budgeted for the year is $369,250, and expenditures, $425,192, or a prospective deficit of some $56,000. Two new staff members were provided for in the budget—an assistant editor for the petroleum journal, and another man to serve the Mining Branch as editor or field secretary or both.

An interim auxiliary publications committee of the Extractive Metallurgy Division was approved as follows: Carleton C. Long, chairman, Hugh M. Shepard and John D. Sullivan. Also the following auxiliary publications committee for the Petroleum Division was approved: Gordon H. Fisher, chairman; Owen F. Thornton, vice-chairman; J. Daviss Collett, K. C. Howard, Paschal Martin, and J. A. Slicker.

Appointments of AIME representatives on various committees and organizations were made as follows: Council of the American Association for the Advancement of Science, C. H. Mathewson and Donald H. McLaughlin; Seeley W. Mudd Memorial Fund, Wilber Judson; Engineering Societies Monographs, Reed W. Hyde; Engineering Index, Landon F. Strobel; Mining Standardization, ASA, Benjamin F. Tillson and Robert H. Morris; Pressure Piping, ASA, R. E. Crockett and Clarence M. Haight; American Year Book Corp., Bradley Stoughton.

Michael Tenenbaum was reported as having been selected to receive the Robert W. Raymond Memorial Award at the Annual Meeting.

THE DRIFT OF THINGS

. . . as followed by EDWARD H. ROBIE

Mining's Biggest Year

Mineral production in the United States reached an all-time peak again in 1948, according to data released at the end of the year by the Bureau of Mines. The tonnage of mineral fuels produced increased 4.8 per cent over 1947, other nonmetallic minerals 4.7 per cent, and metals 2.9 per cent. Expressed in value of output the figures were even more striking, of course, because of inflation, the total value of the mineral output being 15.6 billion dollars compared with 12.4 billion in 1947, an increase of 26 per cent.

The iron and steel industry operated at near-peak levels during most of the year and registered a 3½ per cent gain in output, at 88,000,000 tons of ingots and castings, but still this was only the third best year in the history of the steel industry. Strikes held back copper, lead, and zinc production so that output for the year was below that of 1947 by 1, 6, and 4 per cent respectively. Aluminum production achieved a new peacetime high but was a third below 1944. Gold output fell off 5 to 10 per cent because of higher costs and a fixed price for the product but the 90½-cent price of silver for the full year raised output of that metal by 5 per cent. Mercury production dropped sharply—to 13,950 flasks—because of imports at low prices, and at the end of the year only two companies were still operating.

Crude oil production gained 8 per cent, exceeding 2,000,000,000 barrels for the first time, at an average price of $2.59 per barrel. Ten per cent more natural gas was marketed. Bituminous coal and lignite output, at 596,000,000 tons, was down 5 per cent from the 1947 record because of a strike in March and April and reduced demand in the latter half of the year. Soft coal averaged $4.87 a ton at the mine. Anthracite, 57,000,000 tons, was about the same as in 1947, worth about $8 a ton.

Among the nonmetallics, all-time record shipments were made of sulphur, lime, salt, phosphate rock, potash, cement, gypsum, stone, kaolin, barite, talc, boron minerals, and vermiculite.

Many nonferrous metal mines, though enjoying high prices for their product, were prevented from setting new records in production during 1948, owing to strikes and a continued shortage of underground labor, but the Lake Superior iron mines, highly mechanized, were more fortunate. Vessel shipments down the Great Lakes totaled 82,937,291 long tons of ore (moisture included). This is a record for peacetime, and not greatly below the all-time high of 92,076,781 long tons reached in 1942. If high-grade iron ore reserves of the Lake Superior region are rapidly nearing exhaustion, that fact apparently has not yet acted as a brake on output.

Our Growing Institute

Along with its monthly bills, the telephone company sends little pamphlets concerning its service, and we are tempted to paraphrase the latest of these we have received, making it apply to the service the Institute gives:

There are lots of "hidden values" in your AIME service that can't be measured entirely in dollars and cents. There's the prestige of being a recognized member of your professional fraternity, the privilege of attending its meetings, of writing papers for its publications, or working with others on its committees. All these hidden values grow every time a new member is added to the roster. For it's pretty obvious that the more people that you can thus associate with, and who can associate with you, the more your membership is worth. So you'll be interested to know that, in the last fourteen years, more than 8000 members, net, have been added to the rolls, an increase of 118 per cent.

A New Commercial Metal?

Most of the metals commonly used were known and used hundreds, and some thousands, of years ago; a few, like aluminum, magnesium, and nickel, have achieved commercial importance only in the last 50 or 75 years. Is titanium destined to be the latest addition to the list of new and important metals?

The question is suggested by the expected early development of an immense body of titanium ore in Quebec, and of the good possibility that other deposits may be found, for the metal is supposed to be the seventh most common one in the earth's crust. Since the recent development of another large ore body in the Adirondack Mountains of New York State, titanium has been chiefly used in the oxide form as a white pigment, usually combined with zinc and lead in paint. It has also been on the market as ferrotitanium, but its use as a pure metal has been rare. The first such application that we can remember was as a filament in incandescent lamp

bulbs, a few such lamps being used about the time the carbon filaments were going out and the tungsten lamps coming into use.

The du Pont Company now has a pilot plant in operation with a capacity of 500 lb of titanium metal per day. The price is said to be $5 per pound, which would be excessive if the metal were made according to well-known production processes, but it is entirely within the realm of possibility that this figure could be shaded considerably if a new or improved process were developed, and commercial production on a large scale were carried on. Aluminum once sold for some such fancy price. Strength and corrosion resistance of titanium are comparable with stainless steel, under some conditions, at half the weight. It is less than twice as heavy as aluminum, but is about forty per cent stronger. It has a high melting point, and may find use in jet power plants and in the development of atomic power. A whole new family of titanium alloys is predicted.

News from Europe

Excerpts from a letter dated Nov. 16 from a friend who recently attended the Geological Congress in England, and has since traveled across the Continent to Italy:

Since arriving in Italy six weeks ago we have moved several times and I assure you that house-hunting in the smaller towns of this country is a bit of a problem though we've found fairly comfortable accommodations so far. We've been amazed at the recovery Italy has made. Factories are working and the railroads and highways carry a constant stream of freight. Out in the country the fields are teeming with people and everyone looks well. Some of the larger cities are a bit rugged, and there one sees some underfed and poorly clothed people. Food is plentiful and good although the Continental breakfast of coffee and a piece of bread makes us dream about hot cakes, bacon and eggs, etc. The highways are remarkably good, and a network of excellent secondary roads spreads out from the main trunk lines. However, don't take too much stock in all you hear about "sunny Italy." We're about to freeze to death most of the time, especially when we sit in an unheated room and look towards the snow-capped Apennines. All in all, Italy has been a pleasant surprise, but we'll be plenty ready to start home.

After the Geological Congress in London we took the two weeks' excursion to the Scottish Highlands. Up there we tried to keep up with Sir Edward Bailey, 67 years old, a rugged Scotch geologist who has spent his life in the Highlands and thinks nothing of taking a dip every frosty morning in the nearest loch. We managed to stay alive by huddling in wool shirts and raincoats. Stern, rocky mountains wreathed in almost perpetual mist, and pounded by howling gales with stinging rain thrown in your face while you climb 3000 ft to see some of the world's most complex geology—that's our impression of Scotland. And through all this stalked Sir Edward Bailey, bald head streaming with raindrops just about freezing, and clad only in shorts and a coat. It made me realize what fifteen years in the tropics does to your blood.

From England we crossed over to France, but only passed through. Had two weeks in Switzerland—our favorite of them all in every respect—food, people, and geology. From Zurich we drove through the Gothard Pass and so to Italy.

Let's Be Fair

That excellent weekly covering the Canadian mining industry, *The Northern Miner*, publishes the following editorial, based on ours in the December M&M:

Publications Should Stand On Own Feet

"Admission that the publication of *Mining and Metallurgy* has cost the AIME an average loss of $7,100 a year from 1920 to 1947 is made in announcing a reshuffle of the American institute's publications. The announcement confesses that the magazine when it sought greater advertising support met with opposition from the *Engineering and Mining Journal*. Now it is on the friendliest of terms with others papers in the mineral field, so it says, and adds that magazine publishing by professional societies has become 'generally accepted.'

"It is to be doubted whether such competition is truly accepted, except out of politeness. Mining journals that must appeal for subscriptions and advertising on their intrinsic usefulness to the public are able to assist the growth of their industry. The kind of competition which can afford large annual losses takes from commercial journals revenue which could be applied to enlarging the field of employment and advancement of professional men."

The writer of the above makes no mention of the fact, as plainly stated in the editorial on which he comments, that the average annual "loss" of $7,100 on M&M was incurred without any credit for subscription fees from members. If something like one dollar per year were allowed for a subscription fee, the magazine would have about broken even, and at the $1.50 rate nominally allowed for members' subscription fee to M&M through most of its history, a substantial profit would have been made. We wonder if *The Northern Miner* and other publications in the mining field would not also show a "loss" if they received no income from subscriptions.

Also, the implication is made in the above editorial comment that the publications of the AIME are not intrinsically useful and do not assist the growth of the industry they serve; that only "commercial" journals "enlarge the field of employment and advancement of professional men." We simply do not think this is so. We believe both professional society and privately published papers and magazines promote the advancement and the good of the professional men and the companies engaged in the industries they serve. One difference is that in the case of the professional societies no outside stockholders get any part of the profits that may be derived from such service. Certainly a part of the increased profit that private publications would make if they had no competition from society publications would go to their stockholders, whereas all the income received by the publications of the professional societies is a credit against their cost of operation, either acting as a brake on increases of dues, or making it possible for the members to get more for their money.

RICHARD J. ENNIS

Director, AIME

With but two geographical hops and one professional stint, Richard J. Ennis landed in the Porcupine district of Ontario. And although he remained stationary after this seven-league-boot sprint of 38 years ago, he managed to build up an éclat that has spread his name round the world. This feat of repose was accomplished at his Schumacher retreat by doing the work of the vice-president and general manager of McIntyre Porcupine Mines, Ltd.; of a councillor, vice-president, and president, successively, of the Canadian Institute of Mining and Metallurgy; and of a leader in the research that led to a preventive of silicosis.

It all started in Sheffield, Ill., where he was born in 1881. The next stop was the Smuggler Mining Co. of Aspen, Colo., to spend six years learning, at first hand, the art of the miner and millman. Then, a lord in the industry of those days who was duly impressed by Mr. Ennis's show of competence and enthusiasm invited the self-made man to design, erect, and operate a ten-stamp mill for a prospect in the Porcupine wilderness. With his acceptance, in 1911, came the development of what today is recognized as McIntyre Porcupine Mines, Ltd.

The story that fills the intervening years is marked by Mr. Ennis's own personality. Under his leadership the company sank twelve shafts—one to a depth of 7025 ft; built a 2450-ton flotation and cyanidation plant; and established McIntyre Research, Ltd., through which aluminum therapy was developed as a silicosis preventive.

A more precise appraisal of Mr. Ennis would be that offered by an old colleague:

"Starting out on his own in early life, he has, through constant study and successful experience, acquired an extraordinary knowledge of all things pertaining to the mining industry. He can hold forth with authority on what are the essential characteristics of a good mine hoist, the proper way to plan a stope or float gold, and, in the same tempo, switch into a description of a human lung—how fine silica particles attack it and how aluminum dust prevents the formation of silicic acid, and thus, with the elimination of dust so far as is possible and the use of the aluminum powder, how silicosis may be controlled and probably eliminated.

"In character, he is the happy, buoyant, friendly type of man—the perfect host. He is the typical leader, with great vision and the courage and energy to evolve new methods and then follow them through to a successful conclusion. I would say he is an out-and-out Irishman with almost all the characteristics peculiar to one of that race, and which include, in addition to those above described, the qualities of modesty and warm sympathy for those in trouble or distress."—*H.K.*

Malcolm Pirnie Receives Hoover Medal

Malcolm Pirnie, consulting engineer and head of the firm of Malcolm Pirnie Engineers, New York, has been named 1948 winner of the Hoover Medal, jointly awarded by four national engineering societies. Scott Turner, chairman of the Hoover Medal Board of Award, has announced. The award, one of the outstanding honors of the engineering profession, is in special recognition of Mr. Pirnie's leadership in the formulation of a program, sponsored by the Engineers Joint Council, for the postwar industrial control of Germany and Japan.

The medal was conferred at the Hotel Commodore, New York, on Jan. 19, the opening day of the 96th annual meeting of the American Society of Civil Engineers, of which Mr. Pirnie is a past president. The citation read: Malcolm Pirnie, engineer, leader of engineers and servant of his fellow man, whose ideals and accomplishments in public life beyond the call of his profession have benefited men in his own and other countries of the world, is awarded by his fellow engineers the Hoover Medal for 1948.

The program for the industrial disarmament of the aggressor nations, in which Mr. Pirnie played a leading part, was a voluntary contribution of the engineering profession toward world peace. It was carried on by the EJC through its National Engineers Committee, with Mr. Pirnie as chairman. Five national engineering societies are represented on this council.

The program for Germany got under way in 1944. It stated one clear objective: "an effective industrial means to keep Germany from starting another war." Removal of the plant and source materials essential to war was advocated but "with the least disturbance to the normal economy of western Europe." The program opposed "any plan which would make postwar Germany a drag on the economy of all Europe, if not of the world, and a breeder of future wars."

Later a similar report was prepared on the industrial disarmament of Japan. These reports, with their factual and scientific approach to the world recovery program, were approved in principle and in their main essentials by the State Department and Allied Control Council.

Winners of Student Paper Contests Announced

A telegram has just reached us before we go to press from C. B. Carpenter, chairman of the Student Prize Paper Contest Committee, announcing the winners of the 1949 contest. Winning first place in the graduate paper contest is W. E. Ellis, University of Illinois, and second place goes to F. J. Radavich, Purdue University. Winners in the undergraduate contest are: D. W. Pettigrew, Jr., Carnegie Institute of Technology; J. B. Seabrook, MIT; and G. T. Horne, Montana School of Mines. All were invited to receive their awards at the Annual Meeting in San Francisco.

First Pan-American Engineering Congress Planned

In an effort to establish closer relations between engineers in the Americas for their mutual benefit, the South American Union of Engineering Associations has decided to hold, in co-operation with engineering associations throughout the Americas, the First Pan-American Engineering Congress, from July 15 to 24, 1949, in Rio de Janeiro. Members of the AIME are cordially invited to participate by presentation of papers and attendance.

Of particular interest to members of the AIME will be sessions on fuel, mining engineering, geology, and metallurgy. Papers must be submitted by April 30. Copies of the agenda may be obtained from the Engineers Joint Council, 29 West 39th St., New York 18.

Calendar of Coming Meetings

FEBRUARY

1 Society for Applied Spectroscopy, 63 Park Row, New York City, 8 p.m. F. Nolan, on fluorescence.
2 Chicago Section, AIME. S. J. Creswell, on the Bessemer process.
3 Reno Branch, Nevada Section, AIME.
4 Columbia Section, AIME.
7 Boston Section, AIME.
8 East Texas Section, AIME.
9 El Paso Metals Section, AIME.
11-12 Association of American State Geologists, San Francisco.
11-12 New Mexico Miners and Prospectors Assn., Santa Fe.
14 Mid-Continent Section, AIME.
14-17 Annual meeting, AIME, Fairmont Hotel, San Francisco.
15 Gulf Coast Section, AIME.
15 Washington, D. C., Section, AIME.
16 Southwest Texas Section, AIME.
17 Carlsbad Potash Section, AIME.
17 North Pacific Section, AIME.
17 Utah Section, AIME.
18 Oregon Section, AIME.
21 Detroit Section, AIME. C. Lipson, on stress analysis.
22 Montana Section, AIME.
28 Alaska Section, AIME.
Feb. 28-Mar. 4 ASTM, spring meeting and committee week, Hotel Edgewater Beach, Chicago.

MARCH

2 Chicago Section, AIME. J. R. Van Pelt, Jr., on mineral economics.
3 Reno Branch, Nevada Section, AIME.
3-5 Symposium on Southeast mineral resources, University of Tennessee, Knoxville.
4 Columbia Section, AIME.
7 Boston Section, AIME.
8 East Texas Section, AIME.
9 El Paso Metals Section, AIME.
9 San Francisco Section, AIME.
10-12 American Physical Society, Division of Solid State Physics, annual meeting, Hollenden Hotel, Cleveland.
14 Mid-Continent Section, AIME.
14-17 American Association of Petroleum Geologists, annual meeting, Hotel Jefferson, St. Louis.
15 Gulf Coast Section, AIME.
15 Washington, D. C., Section, AIME.
16 Southwest Texas Section, AIME.
17 Carlsbad Potash Section, AIME.
17 North Pacific Section, AIME.
17 Utah Section, AIME.
18 Oregon Section, AIME.
21 Detroit Section, AIME. R. K. Hopkins, on the Kellogg process.
22 Montana Section, AIME.
28 Alaska Section, AIME.
Mar. 29-Apr. 1 Annual Safety Convention and Exposition, Hotel Statler (Pennsylvania), New York City.

APRIL

5-6 Metal Powder Assn., 5th annual meeting and exhibit, Drake Hotel, Chicago.
11-14 National Assn. of Corrosion Engineers, 5th Annual Conference and Exhibition, Netherland-Plaza, Cincinnati.
18-20 Midwest Power Conference, Sherman Hotel, Chicago.
18-20 Open Hearth Conference, and Blast Furnace, Coke Oven and Raw Materials Conference, Palmer House, Chicago.
24-28 American Ceramic Society, national meeting, Netherland-Plaza, Cincinnati, Ohio.

MAY

2-5 American Foundrymen's Society, 53rd annual meeting, St. Louis.

SEPTEMBER

25-28 Regional Meeting, AIME, Neil House, Columbus, Ohio.

OCTOBER

17-19 Institute of Metals Division, AIME, fall meeting, Cleveland.

DECEMBER

8-10 Seventh Annual Conference, Electric Furnace Steel Committee, Iron and Steel Division, AIME, Hotel William Penn, Pittsburgh.

FEBRUARY 1950

12-16 Annual Meeting, AIME, Statler (Pennsylvania) Hotel, New York City.

APRIL 1950

10-12 Open Hearth Conference, and Blast Furnace, Coke Oven and Raw Materials Conference, Netherland-Plaza Hotel, Cincinnati.

DECEMBER 1950

7-9 Eighth Annual Conference, Electric Furnace Steel Committee, Iron and Steel Division, AIME, Hotel William Penn, Pittsburgh.

What Went on at Recent Local Section Meetings

SECTION	DATE	PLACE	PRESIDING OFFICER	ATTEND-ANCE	SPEAKER, AFFILIATION, AND SUBJECT
Arizona	Oct. 20	Pioneer Hotel, Tucson	.....	23	W. E. Wrather, President, AIME. Institute Affairs.
Black Hills	Dec. 9	South Dakota School o Mines, Rapid City	.....	.....	Business meeting.
Boston	Dec. 6	Metals Processing Laboratory, MIT	George P. Swift	55	Howard F. Taylor, associate professor of mechanical engineering, MIT. Renaissance of the foundry.
Carlsbad Potash	Dec. 14	Riverside Country Club	R. H. Allport	120	Social meeting.
Colorado	Dec. 17	University Club, Denver	M. I. Signer	57	Steve Arrick, Le Panto Consolidated Copper Co. Present conditions in the Philippines.
Columbia	Oct. 1	Spokane	J. W. Melrose	15	Field trip to Trentwood aluminum rolling mill Permanente Metals Corp.
Columbia	Nov. 5	Spokane	Harold Culver	20	Film, "An Ore Sample," American Cyanamid Co.
Delta	Dec. 7	Petroleum Club, New Orleans	J. C. Posgate	50	L. V. McConnell, Lane Wells Co. Engineering of well depth measurements.
Detroit	Nov. 22	Detroit	C.L. Raynor	100	F. N. Rhines. associate professor of metallurgy, Carnegie Institute of Technology. Sintering of metal powders.
El Paso Metals	Dec. 8	El Paso	.....	.....	L. J. Russel, Paul E. Ayers, and M. E. Alarcon USNR, El Paso district. U. S. Navy in World War II.
El Paso Metals	Dec. 17	Biltmore Hotel, El Paso	.....	70	Social meeting with Woman's Auxiliary.
Lehigh Valley	Dec. 6	Bethlehem	M. L. Fuller	125	W. E. Wrather, President, AIME. Recent trip to the Near East.
Mid-Continent	Dec. 13	Tulsa	John P. Hammond	117	P. P. Scott, Jr., Stanolind Oil and Gas Co. Factors to be considered in obtaining proper cementing of casing.
Montana	Dec. 8	Finlen Hotel, Butte	H. G. Satterthwaite	92	Business meeting.
North Pacific	Dec. 16	Rose's Highway Inn, Seattle	.....	60	E. N. Patty, president, Alluvial Gold, Inc. Placer prospecting as an aid to lode discovery.
Tri-State	Dec. 1	Tri-State Zinc and Lead Ore Producers Assn., Picher	O. W. Bilharz	6	Business meeting.
Tri-State	Dec. 8	Picher	O. W. Bilharz	55	Jack Pulliam, Allis-Chalmers Mfg. Co. Atomic bomb test at Bikini.
Wyoming	Dec. 11	Park Hotel, Rock Springs	H. C. Livingston	20	M. M. Fidlar, chief geologist, Mountain Fuel Supply Co. Church Buttes gas field.

New Local Section Officers

ALASKA SECTION . . .

Ted C. Mathews, Chairman; Patrick H. O'Neill, Vice-Chairman; Ralph B. Norris, Secretary-Treasurer; Leonard M. Berlin, Vice-Chairman for Juneau; Harold Strandberg, Vice-Chairman for Anchorage; Frank E. Love, Vice-Chairman for Nome.

BLACK HILLS SECTION . . .

Fremont Clarke, Chairman; Paul Gries, First Vice-Chairman; J. O. Harder, Second Vice-Chairman; A. L. Slaughter, Secretary-Treasurer; Renaldo Gallo, A. B. Needham, and Albro Ayres, Executive Committee.

CARLSBAD POTASH SECTION . . .

J. P. Smith, Chairman; G. E. Atwood, First Vice-Chairman; E. W. Douglass, Second Vice-Chairman; John Nutt, Secretary-Treasurer.

COLORADO SECTION . . .

M. I. Signer, Chairman; J. W. Vanderwilt, Vice-Chairman; J. Paul Harrison, Secretary-Treasurer; E. D. Dickerman, C. E. Dobbin, M. H. Robineau, E. J. Eisenach (Climax Subsection), and H. S. Worcester (San Juan Subsection), Directors.

DELTA SECTION . . .

E. N. Dunlap, Chairman; H. M. Krause, Jr., and C. R. Blomberg, Vice-Chairmen; Fred E. Simmons, Secretary-Treasurer; Paul Ratliff, Junior Secretary; B. C. Craft and H. C. Petersen, Directors.

LEHIGH VALLEY SECTION . . .

F. E. VanVoris, Chairman; R. T. Gallagher, B. J. Larpenteur, and Robert B. Hoy, Vice-Chairmen; W. S. Cumings, James Guider, and M. L. Fuller, Managers.

MONTANA SECTION . . .

J. Hollis McCrea, Chairman; J. P. Spielman, Vice-Chairman; F. W. Strandberg, Secretary-Treasurer; Kuno Doerr, Jr., and E. C. Van Blarcom, Executive Committee.

NORTH PACIFIC SECTION . . .

Kenneth H. Anderson, Chairman; L. W. Heinzinger, Vice-Chairman; W. C. Leonard, Secretary-Tréasurer.

TRI-STATE SECTION . . .

Harold A. Krueger, Chairman; Ernest Blessing, Vice-Chairman; J. C. Stipe, Secretary-Treasurer; Ernest Blessing, F. J. Cuddeback, O. W. Bilharz, H. A. Krueger, C. Y. Thomas, G. M. Fowler, Elmer Isern, and J. P. Lyden, Directors; S. S. Clarke, Chairman, O. W. Bilharz, G. M. Fowler, and Dan Stewart, Program Committee; Ernest Blessing, Chairman, Curtis Stover, E. H. Crabtree, and R. K. Stroup, Membership Committee.

UTAH SECTION . . .

J. C. Landenberger, Jr., Chairman; Byron E. Grant, Vice-Chairman; R. C. Cole, Secretary-Treasurer.

News of AIME Members

Oliver Bowles

© Erica C. Anderson

John Van Nostrand Dorr

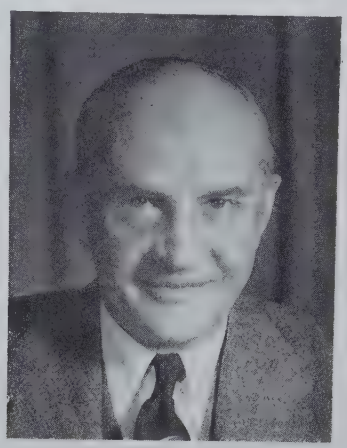

© Erica C. Anderson

Elmer R. Ramsey

Oliver Bowles was presented with the Gold Medal of the Department of the Interior on Dec. 15. The citation for distinguished service upon completion of 33 years of continuous service with the Federal Government reads: During his 33 years with the Bureau of Mines, he strongly influenced the growth of its work in the technology and economics of nonmetallic minerals. Author of more than 250 publications, 153 of them official publications of the Bureau, covering the broad field of nonmetallic minerals, and of a standard textbook, "The Stone Industries," he won international recognition as an authority on mining and quarrying. By introducing the wire saw, he enabled the American slate industry to expedite production, reduce waste, and cut costs. During the war, his opinion and advice on many problems involving nonmetallic minerals were eagerly sought by and freely given to the Government's war agencies. From 1914, when he became the Bureau's first quarry technologist, to Jan. 31, 1947, when he retired as chief of the nonmetallic minerals economics branch, Dr. Bowles served the nation with zeal, integrity, and distinction that entitle him to the highest commendation of this Department.—*J. A. Krug, Secretary of the Interior.*

John Van Nostrand Dorr, chemical, metallurgical, and industrial engineer, prolific inventor and founder of The Dorr Co., New York City, and five associated companies in Europe, has been elected to the newly created office of chairman of the board. **Elmer R. Ramsey,** who has been connected with the Company for 34 years, filling various positions, and more recently operating vice-president, became president. These changes became effective Jan. 20. He continues as chairman of the board of directors of Dorr-Oliver Co., London.

The Dorr Co. was started some forty years ago, literally as a 'one-man' organization, to apply a succession of inventions made by Dr. Dorr in plant operation in the Black Hills of South Dakota. The rest of the story is familiar—the 'one-man' organization gradually becoming an expanding engineering group. The Company's new inventions and new applications of the old carried it from its original metallurgical field through sugar and sanitary engineering and into the chemical industries and geographically pretty well around the globe. The present step in the development of its management is another step in the company's expansion and development.

Dr. Dorr's life has been one of engineering alertness, prolific inventiveness, and originality, in not one field but many, leading to industrial success, as well as full professional and academic recognition for his many and varied technical achievements. His own 26 inventions, notably the Dorr classifier, Dorr thickener, and Dorr agitator and modifications thereof, plus those of his staff, have been applied successfully in over a hundred separate and distinct processing industries. They have made it possible to convert intermittent chemical processes to continuous ones; they have contributed to the large-scale, low-cost exploitation of low-grade ore deposits; they have contributed to placing municipal and industrial sewage and water treatment on a sound engineering basis, to the benefit of the public health at home and abroad.

Mr. Ramsey became associated with Dr. Dorr in 1913, soon after graduation from the Colorado School of Mines. He started on design and test work in the Black Hills, and then took the job of junior engineer at the Denver plant. By 1927 he was in New York, where he became, consecutively, assistant general sales manager, executive assistant to the president, vice-president in charge of engineering department, operating vice-president, and now president.

Howard O. Gray resigned as mining editor of the *Joplin Globe* and *News Herald* and as secretary of the Tri-State Zinc and Lead Ore Producers Assn. on Dec. 1. He plans to engage in private business.

Robert B. Hall, geologist with the U. S. Geological Survey, has been transferred from Spread Eagle, Wis., to Grand Junction, Colo., P. O. Box 337.

R. J. Horsman is chief engineer for Day Mines Inc., Wallace, Idaho. His mail address there is 305 3rd St.

Donald C. Howe, former field supervisor for the Cardox Corp., has been made assistant mine foreman of the Vesta coal division of the Jones and Laughlin Steel Corp., California, Pa.

Carlton D. Hulin visited Institute headquarters during December while in New York on business for the Tungsten Mining Corp. for whom he is consulting geologist.

Danforth Jackson has a job in the geology department of the Republic Steel Corp., Port Henry, N. Y.

L. R. Jackson, who has been general manager of Ariston Gold Mines (1921) Ltd., is chairman and general manager of the Cyprus Sulphur and Copper Co., Limni Mines, Polis, Cyprus; the Company is engaged in reopening a mine formerly worked by the Phoenicians and Romans for copper.

William Karsten is mine shift boss for Cia. Huanchaca de Bolivia, Pulacayo, Bolivia.

Harry W. Kemery is assistant to the superintendent of the Tamaqua district of the Lehigh Navigation Coal Co., Lansford, Pa.

M. H. Kline for the past three years has been working with the Bureau of Mines. He is chief of the special minerals investigation branch at Mt. Weather, Bluemont, Va.

Simon Lake, III, has returned from Felton, Oriente, Cuba, where he was with the Juragua Iron Co., and can be reached at 1313 Fairmont Ave., Fairmont, W. Va.

T. F. Maddick, formerly with the St. Joseph Lead Co., is now employed by the Anaconda Copper Co., Butte, Mont., in the mechanical engineering department.

Samuel A. Madrid is vice-president and manager of the Hamilton Equipment Co., 257 Rio Grande St., Salt Lake City. He was with the Smith Engineering Works in Milwaukee.

Burt C. Mariacher, who was addressed in care of the Consolidated Feldspar Corp., Parkdale, Colo., is now reached in care of the Western-Knapp Engineering Co., 50 Church St., New York City 7.

Ernest N. Patty

Ernest N. Patty, president and general manager of Alluvial Golds Inc. and Gold Placers Inc., returned to his Seattle office last fall after spending the summer in Alaska and the Yukon Territory supervising gold dredging operations there.

Elmer Isern

Elmer Isern, who has been active in mining operations in the Tri-State district for more than twenty years, has been elected president of the Eagle-Picher Mining and Smelting Co., a subsidiary of the Eagle-Picher Co. Mr. Isern, a native of Ellinwood, Kans., and a graduate of Kansas University, worked for several years in Montana and California before going to Miami, Okla., as metallurgist and general milling superintendent for the Commerce Mining and Royalty Co. In 1939 he joined Eagle-Picher as metallurgist and general milling superintendent.

George P. Lutjen joined the staff of the *E&MJ* as assistant editor on Feb. 1. He had been a mining engineer for the Freeport Sulphur Co. since 1943 except for two years which he served with the Marine Corps in China. Mr. Lutjen is a graduate of the Columbia School of Mines.

H. Eugene Mauck recently accepted the post of assistant to the president of the Olga Coal Co. He was formerly superintendent of the Westland mine of the Pittsburgh Coal Co. His headquarters are in Cleveland in the Union Commerce Bldg. and his work takes him to the operations in southern West Virginia. There are three mines operating near Welsh, two of which mine the Pocahontas No. 4 seam and one of which mines the War Creek of Beckley seam with a total annual production of about 2,500,000 tons. Upon graduation from Penn State in 1939, Mr. Mauck entered a training program with the Pittsburgh Coal Co. He served as mine superintendent for that company for about six years.

John D. McAuliffe has been made mine superintendent of Falconbridge Nickel Mines, Ltd., Falconbridge, Ont.

Francis J. McCavitt, formerly a student at the New Mexico School of Mines, is chief of party of a U. S. Geological Survey topographic branch, Box 2858, Lakewood, Colo.

Vernon L. McCutchan, formerly assistant general manager of the Cerro de Pasco Copper Corp., Oroya, Peru, is now addressed at 140 5th St. W., Dickinson, N. Dak.

A. R. McGuire is president of the Fresno Mining Co., 415 Brix Bldg., Fresno, Calif., which operates the Strawberry tungsten mine.

A. L. Minter has taken a job as chemical engineer for the Loceria Colombiana, Medellin, Colombia, and is also engaged in mining consulting work.

Harry W. Montz left for Shanghai, China, on Dec. 8 as a representative of the J. G. White Engineering Corp. in connection with development of China's resources. He expects to be gone from one to one and a half years.

William P. Morris is research engineer at the research laboratory of the Oliver Iron Mining Co., 4832 Grand Ave., Duluth 7, Minn.

Garrett A. Muilenburg, who has been professor of geology at the Missouri School of Mines, has joined the staff of the Missouri Geological Survey, Rolla.

Randall T. Murrill, who has been local superintendent for the Mine La Motte Corp., is now general mine superintendent for the St. Joseph Lead Co., Bonne Terre, Mo.

Kenneth W. Nickerson, Jr., after graduation from the Colorado School of Mines last July and a short vacation at his home in Riverside, Calif., reported to work as a geologist for the Kennecott Copper Corp., Ray mines division, Hayden, Ariz.

Edward S. O'Connor is vice-president of the Hi-Heat Coal Co., 1894 E. 39th St., Salt Lake City. He had been with the Columbia Steel Co.

W. T. Pettijohn resigned as mine superintendent with the Mufulira Copper Mines Ltd., Mufulira, N. Rhodesia, in September and returned to the States to take up employment with the New Jersey Zinc Co. at Austinville, Va.

Colwell A. Pierce has retired as general superintendent of the U. S. Potash Co., Carlsbad, N. Mex. **Henry H. Bruhn,** former refinery superintendent, has been made resident manager with general supervision of mining and refinery operations.

Leslie W. Pullen, who was with the Oliver Iron Mining Co., has gone to Holden, W. Va., to join the engineering department of the Island Creek Coal Co.

Mat Sample, who has been in Chuquicamata, Chile, with the Chile Exploration Co., can now be reached at East Moriches, L. I., N. Y.

Robert M. Shapiro is an instructor at Penn State Extension University, Dravosburg, Pa., and also a graduate student at the University of Pittsburgh. His address is 434 S. Graham St., Pittsburgh.

William Sharp has changed his address from Eureka, Nev., to 1073 E. 6th S St., Salt Lake City.

Paul L. Shields has resigned as president of the Sheridan-Wyoming Coal Co. and has accepted the presidency of three Utah coal companies, Spring Canyon Coal Co., Royal Coal Co., and Standard Coal, Inc. **Walter J. Johnson,** general superintendent of the Bell & Zoller Coal and Mining Co., succeeds Mr. Shields as president of Sheridan-Wyoming.

John F. Simpson, Jr., after graduation from Penn State, became employed by the Clearfield Bituminous Coal Corp. at Arcadia, Pa. His present address is 28 Herman St., Commodore, Pa.

J. D. Sperr has been made construction inspector for the City of Oakland, Calif. His address there is 3600 Victor Ave., Oakland 19.

Charles E. Stott, who was vice-president and general manager of Cia. Minera de Penoles, division of the American Metal Co., is engaged in consulting work in Monterrey, Mexico.

Guy C. Riddell

Guy C. Riddell returned to the States in October after a year in Korea where he acted as mining advisor to the National Economic Board, Military Government, and Korean Government. He is staying at his farm at Royal Oak, Md.

William D. Lord, Jr.

William D. Lord, Jr., is now mine superintendent for the International Mining Co., an enterprise of W. R. Grace & Co. of New York City, at its Chojilla mines.

Roy G. Stott has been transferred by the Bureau of Mines from the Duluth office to its district offices at Wilkes-Barre, Pa., in the anthracite coal mining area.

Lester S. Thompson returned several months ago from Germany, where he had been conducting special studies for the Department of the Army.

Thaddeus S. Ullmann is assistant manager of the export department of the Eimco Corp., manufacturers of mining equipment, New York and Salt Lake City. His home address is 68-49 Burns St., Forest Hills, N. Y.

H. van Arkel, prisoner of war in Sumatra, was repatriated to Holland in 1946, left that country for Dutch Guiana as an employe of the Billiton Co., and remained in Surinam for about a year as manager of the Billiton bauxite mines. He left Surinam in July 1948 for Celebes, Indonesia, where the Company was exploring nickel ore deposits. His address at present is Mijnbouw Mij "Celebes," Malili, South Celebes, Indonesia.

David L. Watts has been made smelter superintendent for the Calumet & Hecla Consolidated Copper Co.

Bleecker L. Wheeler, formerly senior engineer with Ford, Bacon & Davis Inc., has opened a consulting office at 217 Broadway, New York City 7, in mining and industrial engineering.

David White, former geologist with the Alcoa Mining Co., has joined the staff of the Oregon State Department of Geology and Mineral Industries.

John B. White, Jr., metallurgical engineer with the Galigher Co., has been transferred from Butte, Mont., to Salt Lake City, Utah.

Robert T. Williams, of the University of Arizona, has been awarded the $750 scholarship provided by the Kennecott Copper Corp. to a senior student at the College of Mines there who is majoring in mining engineering. The prize was awarded on the basis of character, scholarship, leadership, and initiative.

Frank R. Zachar is general superintendent of the Christopher Coal Co., Pursglove, W. Va. He had been with the Pursglove Coal Mining Co.

• In Petroleum Circles

Allen D. Acomb, petroleum engineer with The Texas Co., has been transferred to the Company's Erath cycling plant at Erath, La.

Charles D. Axelrod, of 2416 Fenwick Rd., University Heights, Cleveland 18, Ohio, is occupied chiefly by buying and selling aluminum flat stock for the Alloys and Chemicals Co., Cleveland.

Max W. Ball resigned as director of the oil and gas division of the Department of the Interior on Dec. 1, and returned to private consulting work with offices in Washington, D. C. He lives at 1648 Foxhall Rd. Mr. Ball has been director of the oil and gas division since December 1946 and has had active experience in nearly all phases of the oil and gas industries. He served as chairman of the oil board of the Geological Survey, as engineer and law officer of the Bureau of Mines, as manager of exploration in the

Rocky Mountain region for the Shell Oil Companies, as president of the Argo Oil Co. and affiliated producing and pipe line companies, and during the war was with the PAW as special assistant to the deputy administrator. He had been in consulting practice since 1928 when not in Government service.

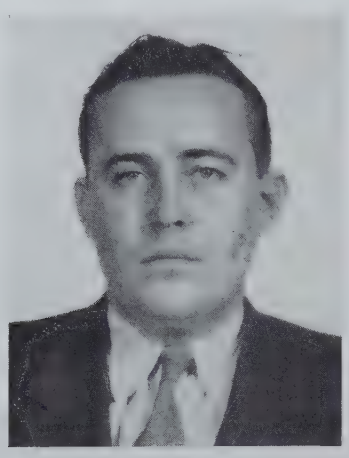

H. D. Spires

H. D. Spires has been transferred from the Tidewater Associated–Seaboard New Hope field in Franklin County, Texas, where he served as district petroleum engineer, to Kamay, where he has assumed his duties as district engineer and acting district foreman over the Tidewater Associated Oil Co. operations in the Wichita Falls area. His address is Box 204, Kamay, Texas.

Richard A. Barton, Jr., is a petroleum engineer trainee with The Texas Co. at Fort Worth, Texas. His mail goes to 836 N. Grand Ave., Gainesville, Texas.

Robert C. Beck is resident petroleum engineer for Michigan for the Superior Oil Co. He is staying at the Stearns Hotel, Ludington, Mich. He had been with the Michigan State Conservation Dept.

Gordon K. Bell, Jr., who is a researcher for the American Petroleum Institute, receives mail at 1155 Park Ave., New York City.

Eugene P. Bowler, who was chief of naval operations (OP-32), Mail and Dispatch Section, Navy Dept., Washington, is now addressed at P. O. Box 296, Shidler, Okla.

L. G. Chombart is manager of the Kansas division of the Schlumberger Well Surveying Corp., P. O. Box 1034, Wichita, Kans.

W. A. Clark, Jr., manager, foreign producing for The Texas Co., can be reached at 135 E. 42d St., New York City 17.

T. Dudley Cramer recently received his M. S. degree in petroleum engineering from Stanford University and is now employed by the producing department of the Standard Oil Co. of California at Taft, Calif.

Albert W. Dauer has the job of junior petroleum engineer with the Stanolind Oil and Gas Co. He is staying at the James Hotel, 219 NW 4th St., Oklahoma City, Okla.

Marshall Dayton, Jr., formerly of Norman, Okla., is now addressed at Drawer H., in care of the Sun Oil Co., Premont, Texas.

Robert H. Dickey has been employed as district geologist at Worland, Wyo., by the Pure Oil Co. since last July. He was a student at the University of Minnesota.

Robert E. Fearon is laboratory director for Well Surveys, Inc., Tulsa. He lives at 1430 S. Terrace Drive, Tulsa, Okla.

Thomas C. Frick, with the Atlantic Refining Co., has been transferred from Odessa, Texas, where he was district superintendent, to the post of division operations supervisor at Midland.

James H. Galloway, who was with the Humble Oil and Refining Co., Florey, Texas, is now addressed at Rm. 517, Hollingsworth Bldg., Los Angeles 14.

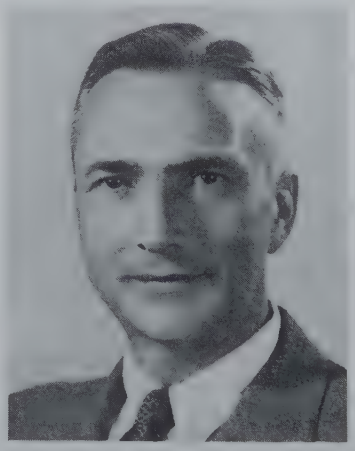

Joseph W. Walton

Joseph W. Walton, upon separation from the Army last summer, took some courses in real estate law and real estate brokerage at the University of Florida, and opened a real estate brokerage office in Vero Beach, Indian River County, Fla., on Dec. 1. He has made Vero Beach, Fla., his permanent residence and it is quite possible that he may add an engineering division to his present real estate activities sometime in the near future.

Howard K. Grant, home address 10524 Dorothy Ave., South Gate, Calif., is working for the Western Gulf Oil Co., Los Angeles, as a petroleum engineer.

Willard J. Larson, former manager of field operations for the Union Oil Co. of California, is now with the Yellowstone Oil Co., 629 S. Hill St., Los Angeles 14.

B. C. McRee, who is with the Union Producing Co., has been transferred from the Gulf Coast division to Shreveport, La.

Nace F. Mefford, Jr., Missouri School of Mines man, is working with the Ashland Oil and Refining Co., Ashland, Ky. His new address is 512 Center St., Henderson, Ky.

LeMoyne W. Myers, who has been addressed in care of the Creole Petroleum Corp., Maracaibo, Venezuela, is now reached in care of the Socony-Vacuum Oil Co. of Venezuela, Apartado 246, Caracas, Venezuela.

John A. Newman has been made division reservoir engineer for the Houston division of the Shell Oil Co. His new address is 4604½ S. Main, Houston.

Daniel B. Nolan, who has been studying at the University of California, Berkeley, is working as assistant geologist for the Capital Co., Los Angeles.

Sylvain J. Pirson, formerly associate professor of petroleum and natural gas engineering in the School of Mineral Industries at Penn State, joined the engineering department of the Stanolind Oil and Gas Co., Tulsa, Okla., as research reservoir engineer in January.

F. O. Prior, who has been president of the Stanolind Oil and Gas Co., Tulsa, is vice-president in charge of production of the Standard Oil Co. (Indiana), Chicago.

Michael R. Rector has a job as petroleum geologist with the Union Oil Co. of California, 702 Washington St., Olympia, Wash. He had been a student at the University of Washington.

Forest B. Rees is a geological trainee with the Carter Oil Co., P. O. Box 801, Tulsa, Okla.

Clarence W. Sanders, who was chief geologist for the Danciger Oil and Refining Co., is a consulting geologist in oil and gas exploration and development, with an address at 2413 Colonial Parkway, Fort Worth 4, Texas.

Douglas L. Saunders, who had been studying at the A&M College of Texas, is a petroleum engineer with the Sun Oil Co., Box 1312, Gladewater, Texas.

Herman E. Schaller has been made division sales manager of the Rocky Mountain-Mid Continent division of the Eastman Oil Well Survey Co., 1360 Speer Blvd., P. O. Box 1500, Denver.

Gene L. Scheirman, until recently a student at the University of Oklahoma, is a junior exploitation engineer with the Shell Oil Co., Houston. He gets his mail at 1423 N. W. 33rd St., Oklahoma City, Okla.

Albert T. Sindel, Jr., is division engineer for the Bay Petroleum Corp., and receives mail at Rt. 3, Seymour Rd., Wichita Falls, Texas.

Norman Soul is working as a geologist for the Pacific Western Oil Co. in Calgary, Alta. He had been with the McColl-Frontenac Oil Co.

J. Claire Sowers, Jr., former student at Penn State, is addressed in care of the Phillips Petroleum Co., City National Bank Bldg., Houston 2, Texas.

Charles E. Sturz is a paleontologist with the Tidewater Associated Oil Co., San Francisco. He receives mail at 915 College Ave., Menlo Park, Calif.

• In the Metals Branch

Robert E. Anderson has completed work for a B.S. degree in physical metallurgy at the University of California in Berkeley and is now employed by the University.

Mary Baeyertz has been named assistant chairman of the metals research department of Armour Research Foundation of Illinois Institute of Technology. Dr. Baeyertz, author of the recently published book, "Nonmetallic Inclusions in Steel," has been with the Foundation as a senior metallurgist since March 1, 1947. Previously she was supervisor of research at the South works of the Carnegie Steel Corporation. Dr. Baeyertz received her master's and doctor's degrees from Columbia University. She was awarded her bachelor's degree from Smith College. In her new position, Dr. Baeyertz will assist **W. E. Mahin,** chairman of the department, in general scientific supervision of numerous fundamental and applied research programs for industry and government agencies.

James L. Baker, who had been mill metallurgist for the Seymour Mfg. Co., Seymour, Conn., has become chief metallurgist with the Phosphor Bronze Corp., 2200 Washington Ave., Philadelphia, Pa.

Richard F. Baley is sales engineer for the Illinois Clay Products Co., Chicago. His mail reaches him at 20700 Ridgewood Ave., Cleveland 22, Ohio.

John H. Becque is night superintendent at the Tacoma smelter of the American Smelting and Refining Co., Tacoma, Wash. He had been a student at MIT.

R. L. Hallett

R. L. Hallett retired as chief chemist for the National Lead Co. and is now practicing as a consulting engineer with Arnold H. Miller. His office is at Rm. 2518, 120 Broadway, New York City 5.

Allan L. Brooks, who was a junior research engineer for the Air Reduction Co., is now working as metallurgical engineer in the standards engineering laboratory of the Sperry Gyroscope Co., Lake Success, N. Y.

A. Clemes is chief consulting metallurgist for New Consolidated Gold Fields Ltd. Mail reaches him at Box 1167, Johannesburg, S. Africa.

Dillon Evers, formerly on the staff of Michigan State College, is now on the staff of the school of chemical and metallurgical engineering at Purdue University, W. Lafayette, Ind.

Clarence T. Fletcher, who had been with the research division of the Mack Mfg. Corp., has gone to Braeburn, Pa., to work with the Braeburn Alloy Steel Corp.

Frank Foote, who was associate professor at the Columbia School of Mines, is now addressed at the Argonne National Laboratory, P. O. Box 5207, Chicago 80.

C. W. Hayes, formerly with the Sherwin F. Kelly Geophysical Services, is now with the Aluminum Co. of Canada, Arvida, Que.

Ray E. Huffaker, formerly a student at Purdue, is assistant lubrication engineer for the Ladish Co., manufacturer of forgings, at Cudahy, Wis. Mail reaches him at 1813 S. 28th St., Milwaukee 4, Wis.

Ivor Jenkins, with the research laboratories of the General Electric Co., Wembley, England, has been awarded the degree of Doctor of Science by the University of Wales for work in the field of metallurgy.

James G. Johnstone is now on the staff of Purdue University as an instructor in geology in the school of chemical and metallurgical engineering.

Herbert S. Kalish, formerly with the Electric Storage Battery Co., Philadelphia, is now working with Sylvania Electric Products Inc., Sylvania Center, P. O. Box 6, Bayside, L. I., N. Y.

Francis M. Krill is research metallographer for the Permanente Metals Corp., Spokane. His address is W. 1028 19th Ave., Spokane 9, Wash.

George E. Linnert works in the research laboratories of the Rustless division of the Armco Steel Corp., Baltimore, Md.

Robert T. Luedeman, formerly with the Braden Copper Co., Rancagua, Chile, has a job as metallurgist with the Weston Electrical Instrument Co., Newark, N. J. He receives mail at 192 Hillside Ave., Leonia, N. J.

H. Gerald Maiers

H. Gerald Maiers until last August was with the engineering department of the General Chemical Co. At that time he joined the development engineering department of the National Lead Company's Titanium division, where he is now employed. His address is 23 Park Ave., Cranford, N. J.

M. Merlub-Sobel has been appointed to the newly created post of associate professor of chemical engineering and metallurgy at the Hebrew Technical College, Haifa, Israel, the only engineering and technological school in Israel, and, for that matter, in that part of the Near East. His present work, that of manager of one of the divisions of Machleket Ha-Yitzur, will continue simultaneously with teaching and consultation in the fields of chemical and metallurgical engineering.

Gordon M. Miner is sales engineer for the Goodman Mfg. Co. His home is at 812 Baver Ave., Charleston, W. Va.

Ralph L. Nelson, Jr., resigned from the Tennessee Coal, Iron and Railroad Co. on Nov. 30 to enter the employ of Thomas Foundries, Birmingham, Ala., as a chemist.

M. N. Ornitz is assistant superintendent of National Alloy Steel, division of the Blaw-Knox Co., Blawnox, Pa.

F. A. Paciotti has a job with the Tin Processing Corp., Texas City, Texas, as a research engineer. His mail reaches him at 4801–R½, Galveston.

John W. Russell, who had been studying at Carnegie Institute of Technology, is working as apprentice engineer for the Mesta Machine Co., West Homestead, Pa. His home address there is 4723 Brierly Court West.

Ralph Sheppard is working as a research engineer for the St. Joseph Lead Co. of Monaca, Pa. He was a student at the South Dakota School of Mines.

George E. Sibbett, who has been a partner in the Coulter Sibbett Steel Co., is president of the Allen Fry Steel Co., Los Angeles. His home address is 1126 Greenwich St., San Francisco.

T. J. C. Smid, formerly chief engineer of the metallurgy department of the Billiton Co., is now working for a Bolivian tin company and is addressed at Fundicion de Estano, Oruro, Bolivia.

Austen J. Smith left the Lunkenheimer Co. as assistant director of research Nov. 1 to become connected with Michigan State College at East Lansing as associate professor of metallurgical engineering.

H. D. Stark has retired as assistant to the vice-president in charge of operations of the Jones & Laughlin Steel Corp. For many years he was general superintendent of the Pittsburgh works. Mr. Stark has completed 49 years of service with J&L. He started at the age of sixteen as a draftsman in the engineering department of the Pittsburgh works. After serving as superintendent of the machine shop, the steel works, and the blooming mill departments, he was appointed assistant general superintendent of the Pittsburgh works in 1927. He served as general superintendent from 1936 until August 1947, when he was appointed assistant to the vice-president in charge of operations.

Wilfred Sykes, president of the Inland Steel Co., Chicago, has been representing the U. S. Army on a one-way commission to report on organization by the American and British commission. He made a trip to Germany and other spots in Europe in December.

Robert M. Wagner returned to Stanford University in 1946 to obtain his doctorate in organic chemistry. He is now research chemist for the General Electric Co. at the Hanford engineering works, Richland, Wash.

Walter M. Weil, who has been general manager of the National Smelting Co., is general manager of the Enesco Corp., producers of magnesium alloys, Box 1791, Cleveland 5, Ohio.

Clarence Zener, professor of metallurgy at the Institute for the Study of Metals, University of Chicago, is serving as special lecturer and consultant in physical metallurgy in the department of mining and metallurgical engineering of the University of Illinois. He delivered his first lectures Nov. 18 and 19 on "The Problem of Fraction" and "The Acoustical Spectrum of Metals." Dr. Zener, a native of Indianapolis, received his undergraduate degree at Stanford University and his doctor's degree at Harvard, and was successively Sheldon traveling fellow, National research fellow, research fellow of Bristol University, and instructor in physics at Washington University and at CCNY before becoming principal physicist of the Watertown (Mass.) Arsenal in 1942.

Obituaries

H. Clarence Horwood

An Appreciation by C. C. Huston

In the sudden death of H. Clarence Horwood in Vancouver, B. C., on Oct. 30, his many friends and the mining industry have suffered a real and grievous loss. "Clare"—as he was invariably known—had been enjoying a holiday at the coast when he died.

Born in Ottawa in 1905, his career and progress in the field of mining geology had been direct and constant. He had won academic recognition with a B.A.Sc. in geological and mining engineering, at the University of British Columbia in 1930; an M.Sc. in geological engineering, at Queen's University in 1931; and a Ph.D. in geological and mining engineering, at MIT in 1934.

In 1936 he was appointed assistant geologist on the staff of the Ontario Department of Mines, after gathering experience in field work with the Geological Survey of Canada in Alberta, British Columbia, and Manitoba; and during an interval of private practice in Great Bear Lake. In addition, he also acted as assistant geologist in the Bureau of Economic Geology, in Ottawa. In 1943 Clare was appointed district geologist for Northwestern Ontario, residing at Port Arthur, and in 1947 was recalled to the headquarters staff of the Ontario Department of Mines in Toronto. In the course of his expanding career with the Department, he did work that took him into the Casummit Lake, Superior Junction, Red Lake, Little Long Lac, and Missanabie areas. He was very active during the war years in the strategic mineral field.

His report on the "Geology and Mineral Deposits of the Red Lake Area," a publication of the Ontario Department of Mines, is an outstanding contribution to Canadian geological knowledge. Although he was the author of more than thirty other papers and articles of great interest, the Red Lake report is the most outstanding, from every aspect, demonstrating as it does the basic knowledge of the writer, making a clear exposition of the information so meticulously gathered, and more particularly reflecting the calm confidence which the writer so obviously felt in his work and the future of this area and country.

His devotion to the interests of his profession is best demonstrated by briefly recounting his affiliation with the AIME, the Society of Economic Geologists, the Association of Professional Engineers of the Province of Ontario, and the Prospectors and Developers Association. In proper recognition of his contributions to geological knowledge, he was elected a Fellow of the Royal Society of Canada.

His wider humanities are only partially indicated by recalling that he found time in a busy professional life to be a member of the Junior Chamber of Commerce in Port Arthur where he originated and supervised a half-million dollar community center. He was also a director of the Rotary Club in that city and a member of the Masonic order.

A deserved and sincere tribute was recently paid to Clare by the Ontario minister of mines, Mr. Frost, speaking for his colleagues and fellows: his friends and associates will always remember his sincerity, vitality, warm heart, ready smile, and steady hand.

Walter Gifford Scott

An Appreciation by P. D. I. Honeyman

With the death of Walter Gifford Scott, superintendent of the Inspiration Cons. Copper Co. leaching plant, the metallurgical profession and all his associates have suffered a severe and shocking loss. Walter Scott, apparently well when he retired for the night, passed away in his sleep on Dec. 4, 1948.

Walter Scott was born on May 8, 1890,

Necrology

Date Elected	*Name*	*Date of Death*
1928	C. P. Barrett	Mar. 29, 1948
1907	George M. Colvocoresses	Dec. 14, 1948
1910	James S. Douglas	Jan. 2, 1949
1911	Charles Enzian	Dec. 7, 1948
1937	Chester H. Gibbons	Apr. 14, 1948
1917	Robert W. Handley	June 29, 1948
1886	David G. Kerr	Oct. 18, 1948
1920	Walter G. Scott	Dec. 4, 1948
1928	C. Wesley Smith	Feb. 10, 1948
1910	Frank M. Warren	Oct. 16, 1948
1944	Gordon T. Williams	Sept. 19, 1948
1908	Howard P. Zeller	Dec. 10, 1948

in Detroit, Mich. His early schooling was in Detroit, and his professional training in mining and metallurgy from the Michigan College of Mines in Houghton. Early in his career he went to work for the Anaconda Copper Mining Co. in Anaconda, Mont., where he was engaged in experimental and research work in extractive metallurgy. For a brief interlude during World War I, Scott, as assistant to the late Harold Aldrich, was loaned out to engage in the operation of a small smelting plant at Ladysmith on Vancouver Island, B. C. Following this, he returned to Anaconda and resumed his former work.

In 1918 the development of the ferric sulphate leaching process was being launched by Inspiration in Arizona. Mr. Scott joined the staff of the Company at that time and advanced steadily until he became superintendent of leaching, which position he occupied at the time of his death.

Walter Scott's name will always be associated with the successful development of this leaching process. In the early days he was foreman of the pilot plant in which the process was worked out. Following this early work he contributed greatly to the building of the commercial plant and, as assistant superintendent, guided its operation patiently and thoroughly through its early growing pains up to its present-day high state of efficiency.

In 1929, the late Harold Aldrich and Walter Scott jointly published a paper, on leaching and electrolytic precipitation of copper at Inspiration, which is a classic, constantly referred to by those interested in this phase of hydrometallurgy. In later years Walter Scott was always consulted on leaching problems, on which he was considered an outstanding authority.

Along with his accomplishments as a metallurgist, he was a good citizen, ever ready to do his part for the betterment of community life. He served several terms as president of the Cobre Valle Country Club, was a past president of the Globe Rotary Club, and also served as president of the Gila County Chamber of Commerce. He was a 32nd degree Scottish Rite Mason.

Walter Scott did his job and did it well. His death leaves a gap that will be hard to fill, but in his work he has established a foundation on which his associates can continue to build and expand the process of hydrometallurgy.

Proposed for Membership

Total AIME membership on December 31, 1948, was 15,580; in addition 4069 Student Associates were enrolled.

Admissions Committee

Albert J. Phillips, Chairman; James L. Head, Vice-Chairman; George B. Corless, T. B. Counselman, George C. Heikes, W. B. Plank, P. D. Wilson, E. M. Wise.

Institute members are urged to review this list as soon as the issue is received and immediately to wire the Secretary's office, night message collect, if objection is offered to the admission of any applicant. Details of the objection should follow by air mail. The Institute desires to extend its privileges to every person to whom it can be of service but does not desire to admit persons unless they are qualified.

In the following list C/S means change of status: R, reinstatement; M, member; J, Junior Member; A, Associate; S, Student Associate; F, Junior Foreign Affiliate.

ARIZONA

Ajo—TRAVIS, GEORGE ALBERT. (C/S—J-M). Engineer, Phelps Dodge Corp.

Bisbee—BUELL, LLOYD THOMAS. (R—M). Chief clerk, Copper Queen branch, Phelps Dodge Corp.

Douglas—FOARD, JAMES EDWIN. (J). Test engineer, Phelps Dodge Corp.

Humboldt — TOMKINSON, ELMER RAYMOND. (M). Mine superintendent, Iron King branch, Shattuck Denn Mining Corp.

Phoenix—MANNING, ROGER I. C. (R—M). Mining engineer, Arizona Dept. of Mineral Resources.

Tucson — WINTERS, VERNE WILLIAM. (M). Metallurgist, Eagle-Picher Mining and Smelting Co.

Willcox—COOPER, JOHN ROBERTS. (C/S—J-M). Geologist, U. S. Geological Survey.

ARKANSAS

Fort Smith—BOYD, BERNARD DEGEN. (R,C/S—JA-M). Vice-president and manager, Boyd Excelsior Fuel Co.

CALIFORNIA

Glendale—RHODES, JOSEPH RICHARD. (A). Vice-president and manager of refractories division, Gladding, McBean & Co.

Hammonton—HAAK, VINCENT ALFRED. (C/S—S-J). Sampler, research department, Yuba Cons. Gold Fields.

Lompoc — SCHUKNECHT, GEORGE G. (R,C/S—J-M). Superintendent of quarries and mines, Johns Manville Products Corp.

Los Angeles—DURGIN, LAURANCE IRA. (M). Geologist and petroleum engineer, self-employed. GLOVER, PATRICK NORMAN. (C/S—S-J). Exploitation engineer trainee, Shell Oil Co. HAWKINS, ROBERT RUSSELL. (M). Secondary recovery engineer, Signal Oil and Gas Co. RAY, HORATIO C. (R—M). Consulting engineer (retired).

Orinda — LINDSAY, JAMES EDWARD. (M). Reserves engineer, Standard Oil Co. of California.

Pasadena—DUWEZ, POL E. (M). Associate professor of mechanical engineering, California Institute of Technology. STOLZ, FRED C. (M). Petroleum engineer, Stanley & Stolz.

San Francisco—FARNOW, FREDERICK WILLIAM. (M). Manager, federated metals division, American Smelting and Refining Co. HEWITT, EDWARD THOMAS. (M). Manager, mining equipment division, Electric Steel Foundry Co. SELFRIDGE, JOHN SOLEY, Jr. (M). Plant superintendent, federated metals division, American Smelting and Refining Co.

COLORADO

Denver — AHLBORG, WILLIAM THOMAS. (M). Secretary, assistant to president, Denver Equipment Co. BARKER, CLAUDE L. (C/S—J-M). Assistant sales manager, E. I. du Pont de Nemours & Co. EMRICK, JOHN HOMER. (M). District manager, Joy Mfg. Co.

Idaho Springs — FAIRCHILD, GERARD LANHAM. (C/S—S-J). Geologist, American Smelting and Refining Co.

CONNECTICUT

Darien—KNAPP, THOMAS JULIAN. (A). Assistant vice-president, Freeport Sulphur Co.

Greenwich — MODEL, JEAN. (M). President and owner, Sonrisa Mining Co.

Old Greenwich—RUSSELL, JOHN C. (R,C/S—J-M). Senior process engineer, consulting engineering department, The Dorr Co.

DISTRICT OF COLUMBIA

Washington — NARTEN, PERRY FOOTE. (C/S—S-J). Geologist, U. S. Geological Survey. OLUND, HENNING EKSTROM. (R—M). Mining engineer, mining branch, Bureau of Mines.

FLORIDA

Bartow — CHILDS, WILLIAM BURTON. (M). Construction engineer, American Cyanamid Co. RAULERSON, JOHN DERIEUX, Jr. (J). Assistant mining superintendent, Florida phosphate division, International Minerals and Chemical Corp.

Pierce—ANDERSON, THOMAS JOHN, Jr. (M). Engineer, American Agricultural Chemical Co.

IDAHO

Burke—LINDSTROM, PHILIP MARTIN. (C/S—J-M). Mining engineer, Hecla Mining Co.

ILLINOIS

Glencoe—YOUNG, WILLIAM PEARCE. (R,C/S—JA-M). President, Bell & Zoller Coal and Mining Co.

Libertyville—CLAUSEN, CARL FREDERIK. (M). Manager of mfg. research, Portland Cement Assn.

Rockford—MILLER, LEE GEORGE. (M). Chief metallurgist, Greenlee Bros. & Co.

Wilmette—DICKEY, ROBERT McCULLOUGH. (R,C/S—J-M). Chief sales engineer, Bucyrus-Erie Co.

INDIANA

East Chicago—BAJOR, MENCESLAUS JOSEPH. (C/S—S-J). Metallurgical trainee, Inland Steel Co. HECHINGER, CARL JOSEPH. (C/S—S-J). Research and development metallurgist, Eagle-Picher Co.

Fort Wayne—CHEW, JOHN CARROLLTON. (C/S—S-J). Production engineer, Phelps Dodge Copper Products Corp.

Hammond—JONES, WILLIAM NORRIS. (M). Electric melter, Republic Steel Corp.

Terre Haute—MATTHEWS, MAX A. (M). President, Templeton-Matthews Corp.

KANSAS

Baxter Springs—SEXTON, KENNETH PAUL. (A). General manager, Consolidated Supply Co.

Ellinwood—MEYERS, JEAN WARREN. (J). Junior petroleum engineer, Stanolind Oil and Gas Co.

Eureka—CAWTHON, PETE W., Jr. (C/S—S-J). Trainee engineer, Phillips Petroleum Co.

Great Bend—PUGH, WILLIAM LEE. (J). Sales engineer, Lane-Wells Co.

McPherson—ZOLLER, JACQUES WILLIAM. (C/S—S-J). District exploitation engineer, Shell Oil Co.

Wichita—HOLLOW, WALTER BYRON. (M). Drilling superintendent, Bridgeport Oil Co. KOESTER, EDWARD ALBERT. (M). Consulting petroleum geologist. LUND, CARL I. (J). Sales representative, Moorlane Co. NATION, WILLIAM BENJAMIN. (R,C/S—S-M). Petroleum engineer, Co-operative Refinery Assn.

Zenith—MORGAN, JOHN VICTOR. (R,C/S—S-J). Field engineer, Stanolind Oil and Gas Co.

KENTUCKY

Jenkins—BERRY, JOHN KIRKMAN. (M). Chief production engineer, Consolidation Coal Co.

Louisville—ANDERSON, HARRY LeROY, Jr. (C/S—S-J). Ceramic engineer, Republic Steel Corp.

Wheelwright—PACE, EDWARD MINOR. (R,C/S—S-J). Engineer, Inland Steel Co.

LOUISIANA

New Orleans—KOKESH, FRANK PHILLIP. (M). Harvey district engineer, Schlumberger Well Surveying Corp.

MARYLAND

Silver Spring—LURIE, WILLIAM. (M). Metallurgist, U. S. Naval Gun Factory.

MASSACHUSETTS

Brookline—FITZPATRICK, JOHN McNEIL. (C/S—S-J). Research metallurgist, division of industrial co-operation, MIT.

Pittsfield—STONE, FRANCIS GILMAN. (C/S—J-M). Research metallurgist, Works laboratory, General Electric Co.

MICHIGAN

Detroit—GORTON, CLAIR ALLEN. (A). Metallurgical engineer, Hoskins Mfg. Co.

Marquette—DeHAAS, CLYDE TIFFANY. (A). Owner and manager, C. T. DeHaas Co. DREVDAHL, ELMER RANDOLPH. (C/S—S-J). Engineer, Vicar mine, Jones & Laughlin Ore Co.

MINNESOTA

Hibbing—STUART, JAMES REEVE. (R—M). Chief engineer, Meriden Iron Co.

Nashwauk—SWANSON, PAUL PETER. (R,C/S—A-M). Superintendent, Cleveland-Cliffs Iron Co.

MISSISSIPPI

Natchez—WHATLEY, ERROLL RENETH, Jr. (C/S—S-J). Petroleum engineer, California Co.

MISSOURI

Bonne Terre—OHLE, ERNEST LINWOOD. (C/S—J-M). Geologist, St. Joseph Lead Co.

Herculaneum—SHERMAN, JOHN WILLIAM. (R,C/S—J-M). General foreman, St. Joseph Lead Co.

Rolla—FUNK, CAMPBELL WILLIAM FLOYD. (C/S—S-J). Metallurgist, powder metallurgy section, Bureau of Mines. GORSKI, CHARLES HENRY. (M). Metallurgist, Bureau of Mines. WOODWARD, THEODORE. (J). Instructor in geology, Missouri School of Mines.

St. Louis—HAM, NEAL. (M). Branch manager, Ingersoll-Rand Co.

MONTANA

Butte—RENOUARD, EDWARD IGNATIUS, Jr. (M). Assistant general superintendent of mines, Anaconda Copper Mining Co.

NEVADA

Pioche—HYDE, DONALD EDWIN. (R,C/S—S-J). Junior engineer, Combined Metals Reduction Co.

Winnemucca—SPITZER, ROBERT BOWMAN. (M). Superintendent, Rossi mine, Merced mill, Baroid sales division, National Lead Co.

NEW JERSEY

Chatham—LIEBIG, EDWARD OTTO. (C/S—J-M). Production metallurgist, Baker & Co.

Franklin—McKECHNIE, DONALD. (M). Mill superintendent, New Jersey Zinc Co.

Morristown—ACKERMAN, DAVID HARTON. (J). Geologist, Jones & Laughlin Ore Co.

Netcong—FRANZ, HENRY WILLIAM. (C/S—J-M). Metallurgist, Singmaster & Breyer.

New Brunswick—WYATT, JAMES LUTHER. (C/S—S-J). Development engineer, titanium division, National Lead Co.

Passaic—MACIORA, JOSEPH GEORGE. (C/S—S-J). Metallurgist, Wright Aeronautical Corp.

Phillipsburg—SHEPHERD, BENJAMIN FRANKLIN. (R,C/S—A-M). Chief metallurgist, Ingersoll-Rand Co.

NEW MEXICO

Carlsbad—NELSON, RICHARD BENTON. (J). Junior mine engineer, Potash Co. of America.

Silver City—WALTON, MARSHALL RHODES. (M). President, M. R. Walton & Associates.

Vanadium—NEUMAN, JAMES VINCENT, Jr. (C/S—J-M). Assistant to manager, Bayard department, U. S. Smelting Refining and Mining Co.

NEW YORK

Brookhaven—COOK, HARRY CLARE. (J). Associate engineer, Brookhaven National Laboratories.

Brooklyn—BUGLIONE, VINCENT JOSEPH. (R,C/S—S-J). Metallurgist P-1, N. Y. Naval Shipyard. ROSS, EARL WARREN. (R,C/S—S-J). Metallurgist, N. Y. Naval Shipyard. YOKELSON, MARSHALL VICTOR. (M). Research metallurgist, General Cable Corp.

Flushing—NININGER, ROBERT D. (R,C/S—S-J). Geologist, assistant to the manager, raw materials operations, Atomic Energy Commission.

New York—DeKANSKI, LEON M. (R—M). Project engineer, The Dorr Co. MECHELYNCK, ANDRE L. (C/S—S-J). Trainee, American Radiator and Standard Sanitary Co. WEIDNER, PAUL NELSON. (M). Petroleum engineer, Standard Oil Co. (New Jersey).

New York Mills—WILLIAMS, GRIFFITH, Jr. (M). Supervisor of methods, Revere Copper and Brass Co.

Syracuse—CHUTE, NEWTON EARL. (M). Assistant professor of geology, Syracuse University.

OHIO

Cleveland—BURGESS, CHARLES OWEN. (R,C/S—JA-M). Technical director, Gray Iron Founders' Society. WILBUR, JOHN SMITH. (A). Sales representative, Cleveland-Cliffs Iron Co.

Gates Mills—POTTER, HORACE W. (C/S—J-M). Consultant (steel), Arthur G. McKee & Co.

Steubenville—McCABE, CHARLES GRIFFITH. (M). Foreman of open-hearth metallurgy, Wheeling Steel Co.

OKLAHOMA

Bartlesville—CARPENTER, ANDREW HOWLAND. (C/S—S-J). Junior engineer, Cities Service Oil Co. SMITH, SHOFNER. (J). Senior Reservoir engineer, Phillips Petroleum Co.

Oklahoma City—SEELY, DWIGHT H., Jr. (J). Junior process engineer, Sohio Petroleum Co. SNEED, ROBERT WHITE. (M). District sales manager, Eastman Oil Well Surveying Co.

Okmulgee—NEWMAN, ROBERT CLARK. (C/S—S-J). Petroleum engineer, Thomas S. Newman, Geologist and Civil Engineer.

Stillwater—SCHLEMMER, ALFRED EUGENE. (J). Instructor in mechanical engineering, Oklahoma Agricultural and Mechanical College.

Tulsa—BAUMAN, WILLARD EDWIN. (J). Production engineer, Gulf Oil Co. JARRELL, L. C. (C/S—S-J). Petroleum engineer trainee, The Texas Co. OCHELTREE, TEMPEST MATTHEWS. (R,C/S—S-M). Chief engineer, Devonian Co. WILDER, LAWRENCE BERNARD. (J). Junior research engineer, Stanolind Oil and Gas Co.

Webb City—DENNY, JACK PERSHING. (J). Engineer, Phillips Petroleum Co.

OREGON

Hillsboro—McWILLIAMS, JACK HUGH. (M). Geologist, Alcoa Mining Co.

PENNSYLVANIA

Beaver Falls—SUMMERFIELD, CHRISTIAN JOHN. (M). Research associate, Mellon Institute.

Bethlehem—SELLERS, PAUL EDWARD. (M). Quarry superintendent, Bethlehem Steel Co.

Exton—VON STROH, GERALD F. H. (M). Director, mining development program, Bituminous Coal Research.

Feasterville—SCHUCH, EDWARD ANTHONY. (M). Chief engineer, Aero Service Corp.

McKeesport—KELLER, RICHARD LATCHFORD. (M). Fellow, Mellon Institute.

Philadelphia—HESS, GEORGE L. (M). Sales engineer, Aero Service Corp.

Uniontown—HAMILTON, JAMES L. (M). Manager, safety and operating departments, Republic Steel Corp.

SOUTH DAKOTA

Belle Fourche—MIDDLETON, DAVID MAXWELL. (C/S—J-M). Plant superintendent, Aladdin Wyoming plant, National Lead Co.

Lead—WARREN, LYLE GEORGE. (M). Structural design, Homestake Mining Co.

TEXAS

Alice—BARB, GLEN WAYNE. (J). Petroleum engineer, Magnolia Petroleum Co.

Austin—CLARK, GLYNN ALDEN. (C/S—S-J). Research fellow, Texas petroleum research committee, University of Texas. PLAZ, LUIS. (M). Petroleum inspector, Venezuelan Government.

Beaumont—DUBLIN, JAMES ROLAND. (C/S—S-J). Junior petroleum engineer, Humble Oil and Refining Co.

Borger—DANA, PHILIP LYMAN. (M). Geologist, J. M. Huber Corp.

Dallas—BOCK, MORRIS. (M). Chief chemist, Southwest division, Sun Oil Co. LIPSON, LEONARD B. (J). Senior physicist, field research laboratories, Magnolia Petroleum Co. RENFRO, HAROLD BELL. (M). Geologist and petroleum engineer, Stodel Oil Co. SMITH, GERALD LLOYD. (J). Petroleum engineer, Magnolia Petroleum Co. STORMONT, DAVID HENRY. (M). District editor, *The Oil and Gas Journal*.

El Paso—DEISLER, PAUL F. (C/S—A-M). Management consultant, self-employed.

Fort Worth—WILSEY, LAWRENCE EARL. (C/S—S-J). Junior petroleum engineer, Stanolind Oil and Gas Co.

Freer—MURPHY, GORDON JOSEPH WARNER. (J). Petroleum field engineer, The Texas Co.

Houston—BEEZLEY, JOEL E. (C/S—S-J). Production engineer, Pure Oil Co. BEILHARZ, CARL FRICHOT. (M). Division reservoir engineer, Pure Oil Co. BERNHARD, WILLIAM E. (M). Petroleum engineer, Ginther, Warren & Ginther. GUEST, HENRY GRADY. (M). Senior engineer, Schlumberger Well Surveying Corp. LEGERON, ROBER AIME. (M). Manager of field operations, Schlumberger Well Surveying Corp. POYNER, HERBERT FLAKE, Jr. (C/S—S-J). Graduate student, University of Texas. SELIG, AUGUST LEWIS. (M). Consulting geologist.

McAllen—RIDGWAY, ROBERT JOSEPH. (C/S—S-M). Petroleum engineer, Sun Oil Co.

Midland—LITTLE, WILLIAM NORMAND. (M). Division engineer, Tide Water Associated Oil Co. MINTZ, JOHN MOORE. (J). Associate engineer, Tide Water Associated Oil Co.

Wichita Falls—REYNOLDS, JOHN CLIFFORD STANLEY. (C/S—S-J). Research assistant, department of petroleum engineering, University of Texas.

UTAH

Bingham Canyon—BARLOW, VINAL STOKER. (M). General mine foreman, Kennecott Copper Corp. McNEILIS, THOMAS ROSS. (M). Electrical foreman, Utah copper division, Kennecott Copper Corp. WILLEY, RICHARD HAVEN. (R,C/S—S-M). Assistant general drill and blast foreman, Utah copper division, Kennecott Copper Corp.

Lark—COFFEY, JAMES ARTHUR. (A). Chief clerk, Lark mine, U. S. Smelting Refining and Mining Co.

Salt Lake City—EARLY, LAWRENCE WILLIAM. (M). Sales service representative, Hercules Powder Co. RICHARD, FRED VINCENT. (M). Safety engineer, American Smelting and Refining Co.

VIRGINIA

Arlington—BRANDENBURGER, OSCAR LOUIS. (R—A). Chief, materials supply, Civil Aeronautics Administration.

WASHINGTON

Richland—CALLEN, ALFRED COPELAND, Jr. (J). Metallurgist, Hanford works, General Electric Co.

Seattle—STRANDBERG, THEODORE R. (A). Mining engineer, Strandberg & Sons.

Vancouver—JENSEN, JAMES HENRY. (M). Plant and chemical engineer, Pacific Carbide and Alloys.

WISCONSIN

Milwaukee—MAROLD, FRANK. (R,C/S—S-J). Application engineer, export sales department, Allis-Chalmers Mfg. Co.

WYOMING

Casper—ROBBINS, RAYMOND WILLIS. (M). District geologist, The Texas Co.

Cody—HAMMAR, HAROLD DAVID. (J). Junior petroleum engineer, Stanolind Oil and Gas Co. POLLOCK, CHARLES BERTRAND. (J). Junior petroleum engineer, Stanolind Oil and Gas Co.

Lusk—GALLIVAN, JOHN C. (C/S—J-M). Rocky Mountain division superintendent, Wood River Oil and Refining Co.

MANITOBA

Flin Flon—HUNT, EDWIN S. W. (M). Assistant mine superintendent and chief mining engineer, Hudson Bay Mining and Smelting Co.

ONTARIO

Ottawa—IGNATIEFF, ALEXIS. (M). Mining engineer, division of fuels, Bureau of Mines.

Toronto—DEAN, WILLIAM JOHN. (M). Manager, Kennex, Ltd.

ARGENTINA

Jujuy—RICCI, LUCIANO. (M). Chemical laboratory chief, Institute de Geologia y Mineria de la Universidad Nacional de Tucumun.

VENEZUELA

Caracas—STILLWELL, KENNETH LAWRENCE, Jr. (J). Trainee, The Texas Co. WILLIAMS, DAVID BOWEN. (M). Chief scout, Shell Caribbean Petroleum Co.

ENGLAND

London—LANCE, ALFRED EMERSON. (R—M). Principal control officer, ores and minerals, Germany section, British Foreign Office.

LIBERIA

Monrovia—REILINGH, ALBERT. (J). Geologist, Liberia Mining Co.

FEDERATED MALAY STATES

Perak—KENNEDY, ERROL MOSTYN. (C/S—S-J). Junior assistant, Gopeng Cons. Ltd.

INDIA

Bombay—MEHTA, PESI EDI. (C/S—S-M). Technical assistant, Tata Industries, Ltd.

Oorgaum—DAVID, JOSEPH PETER. (M). Inspector of mines, department of mines and explosives, Government of Mysore.

NEW SOUTH WALES

Broken Hill—FISHER, GEORGE READ. (R—M). General manager, Zinc Corp.

NEW CALEDONIA

Noumea—ROUTHIER, PIERRE JEAN. (M). Chief of the geological mission, Office de la Recherche Scientifique Coloniale.

Student Associates

Elected December 15, 1948

Thomas M. Anderson.....Univ. Ariz.
George H. Bailey.....Univ. Idaho
James H. Barnett....Colo. Sch. Mines
Lawrence E. Barrett..Colo. Sch. Mines
Boris J. Bermes.....Colo. Sch. Mines
Hubert E. Berninghausen
Colo. Sch. Mines
Billie L. Bessinger...Colo. Sch. Mines
Ervin G. Bilderback.....Texas A&M
Robert R. Blair.....Okla. A&M
John L. Bolles.....Colo. Sch. Mines
Ollen N. Bradford.....Okla. A&M
Tyler Brinker.....Colo. Sch. Mines
Richard S. Bryson....Colo. Sch. Mines
Floyd D. Burnside...Colo. Sch. Mines
David L. Caldwell....Colo. Sch. Mines
John W. Caldwell.....Colo. Sch. Mines
Walter M. Chapman..Colo. Sch. Mines
Chih Wen Chen.....Ill. Inst. Tech.
David C. Childers....Colo. Sch. Mines
Ben B. Chomick.....Colo. Sch. Mines
Charles C. Coenen....Colo. Sch. Mines
Robert H. Coleman.....Okla. A&M
Alva G. Comer.....Okla. A&M
Daniel M. Cooper.....Colo. Sch. Mines
William M. Denton.....Okla. A&M
William P. Donovan....Ill. Inst. Tech.
Joseph R. Driear.....Colo. Sch. Mines
Wilfried Drolet, Jr.....Univ. Ariz.
Joseph C. DuBois, Jr...Colo. Sch. Mines
Richard J. Durning....Colo. Sch. Mines
Arthur J. Dyson.....Colo. Sch. Mines
Aly A. El-Gazzar.....Okla. A&M
Burnett E. Ellis.....Univ. Mo.
Foster E. Endacott...Colo. Sch. Mines
Richard K. Epps.....Texas A&M
Hugh W. Evans.....Colo. Sch. Mines
Ernest C. Fitch, Jr.....Okla. A&M
Handren K. Fitzgibbons
Colo. Sch. Mines
Walter S. Forbes.....Colo. Sch. Mines
Martin S. French.....Colo. Sch. Mines
Richard H. Fulton....Colo. Sch. Mines
Jeremy V. Gluck.....Univ. Mich.
Dennis E. Gregg.....Colo. Sch. Mines
Niles E. Grosvenor...Colo. Sch. Mines
Alexander F. Halcrow.Colo. Sch. Mines
Harley H. Hartman....Colo. Sch. Mines
James S. Hastings....Colo. Sch. Mines
John A. Heffelfinger.....Okla. A&M
Robert N. Hendry....Colo. Sch. Mines
Donald C. Herron.....Colo. Sch. Mines
J. D. Hicks.....Okla. A&M
John C. Holden.....Okla. A&M
William R. Holman.....Univ. Calif.
Joseph P. Hopkins.....Okla. A&M
William E. Hopkins.....Univ. Mich.
Kenneth W. Hottinger.Colo. Sch. Mines
Donald L. Hovorka....Colo. Sch. Mines
Wei-pei Hu.....Univ. Utah
Shao-Chi Huang.....Ill. Inst. Tech.
Douglas O. Hukkanen.....Univ. Calif.
John B. Hundley, Jr....Stanford Univ.
John G. Jaka.....Colo. Sch. Mines
John F. Jarrell.....Queen's Univ.
Glen O. John.....Adelaide Univ.
Thomas C. Keating....Colo. Sch. Mines
Norman Korn .....Colo. Sch. Mines
Kenneth B. Larson....Colo. Sch. Mines
William A. Libby..Texas Mines & Met.
David R. Lohr.....Colo. Sch. Mines
Murrell D. Long.....Colo. Sch. Mines
David M. Mathews....Colo. Sch. Mines
William W. May.....Colo. Sch. Mines
Robert C. McCain....Colo. Sch. Mines
Sidney J. McDuff.....Univ. Ariz.
Ira E. McKeever, Jr...Colo. Sch. Mines
Donald T. Moore.....Colo. Sch. Mines
Edward A. Morrison...Colo. Sch. Mines
Robert H. Muench....Colo. Sch. Mines
Roger R. Nelson.....Colo. Sch. Mines
John D. Noll.....Colo. Sch. Mines
Hugh W. Olmstead....Colo. Sch. Mines
Homer C. Osborne.....Texas A&M
Harold B. Overstreet..Colo. Sch. Mines
Robert S. Padboy.....Colo. Sch. Mines
William L. Parker....Colo. Sch. Mines
Herbert L. Peel.....Okla. A&M
Eugene M. Pohoriles.....Okla. A&M
Fred F. Polizzano....Bklyn. Poly. Inst.
Dale A. Reagan.....Okla. A&M
Joseph C. Richardson, Jr...Texas A&M
Harold J. Riggott.....Colo. Sch. Mines
James A. Robertson.....Okla. A&M
Clovis E. Rodelander.....Okla. A&M
Charles W. Rohler....Colo. Sch. Mines
David A. Rowland....Colo. Sch. Mines
Leonard B. Saltzman....Ill. Inst. Tech.
Lawrence Sama.....Bklyn. Poly. Inst.
Norman Schapiro.....Bklyn. Coll.
Treadwell C. Schmitt.Texas Mines&Met.
Darrell G. Shurtliff....Colo. Sch. Mines
Richard C. Siegfried..Colo. Sch. Mines
John W. Stephens.....Colo. Sch. Mines
Harold W. Stouffer....Colo. Sch. Mines
Paul P. Sundback (C/S—J-S)....MIT
Roger W. Swindle.....Univ. Wis.
William P. Thornton.....Okla. A&M
Larry Toman, Jr.....Colo. Sch. Mines
Henry C. Wachtman, Jr....Okla. A&M
Arthur W. Wadman, Jr..Colo. Sch. Mines
James W. W. Walker....Stanford Univ.
Ralph Ward, Jr.....Okla. A&M
James W. Warfield....Colo. Sch. Mines
Jasper N. Warren....Colo. Sch. Mines
John R. Weeks, IV....Colo. Sch. Mines
Robert O. Wenzel.....Univ. Ariz.
John R. Weyler.....Colo. Sch. Mines
Robert D. Whitmer..Mo. Mines & Met.
Edward H. Whitlock.....Univ. Okla.
David B. Wilkie, Jr.....Kansas Univ.
Kimball M. Williams...Colo. Sch. Mines
Claud V. Winter.....CCNY
Russell L. Wood.....Colo. Sch. Mines
Shui Choh Yue.....Ill. Inst. Tech.

Elected January 19, 1949

Charles J. Adams....Mont. Sch. Mines
William E. Adkins..N. Mex. Sch. Mines
Richard A. Alexander
Mich. Min. & Tech.
Robert B. Anders....Mo. Mines & Met.
George M. Anderson..Mo. Mines & Met.
Richard C. Anderson (R—S)
N. Mex. Sch. Mines
Frank M. Antonioli..Mont. Sch. Mines
Charles Arentzen....Mont. Sch. Mines
John D. Aumen, Jr...N. Mex. Sch. Mines
John W. Bader (R—S)...Lehigh Univ.
Stephen S. Badzik....Univ. Pittsburgh
Walter E. Baily.....Mo. Mines & Met.
Emmett B. Ball, Jr.....Univ. Nev.
Dale G. Ballmer....N. Mex. Sch. Mines
Leo G. Barbee.....Okla. A&M
E. Crittenden Barker.....Univ. Ala.
Claude R. Barnes, Jr..Mont. Sch. Mines
John S. Benko.....Lafayette Coll.
Robert W. Berkhahn..Mich. Min. & Tech.
Irving G. Betz.....Mo. Mines & Met.
James R. Boyle.....Mo. Mines & Met.
George F. Braun.....Lafayette Coll.
Harold J. Braun...Mich. Min. & Tech.
Richard M. Brazier.....Univ. S. Calif.
Jack Brodsky.....N. Mex. Sch. Mines
Robert L. Bronnes.....Univ. Ala.
George G. Brown.....Univ. S. Calif.
Willow M. Burand..N. Mex. Sch. Mines
Henry J. Burnell.....Lafayette Coll.
Russell A. Calvin, II....Lafayette Coll.
Elton F. Carlile, Jr.....Univ. Nev.
Andrew T. Cassell, Jr.....Univ. Calif.
James H. Clement....Mont. Sch. Mines
Elbert E. Comstock..Mo. Mines & Met.
Birney S. Covell, Jr.....Univ. Wash.
Bill J. Cox.....Okla. A&M
William E. Coolbraugh.Mo. Mines&Met.
Richard G. Craddock
N. Mex. Sch. Mines
Worth B. Cunningham, Jr.
Rutgers Univ.
David Dalpini.....Mo. Mines & Met.
Gordon P. Daniells..N. Mex. Sch. Mines
Prodyot K. Das.....Mont. Sch. Mines
Donald H. Deibert..N. Mex. Sch. Mines
John P. Denny (R—S)....Univ. Utah
Buddy R. Dixon.....Okla. A&M
James J. Doherty..N. Mex. Sch. Mines
William L. Donovan..N. Mex. Sch. Mines
Richard R. Douglas..Mont. Sch. Mines
John T. Eastlick.....Mont. Sch. Mines
Thomas D. Edsall, III....Rutgers Univ.
Paul K. Edwards....Mo. Mines & Met.
Lewis B. Eubanks.....Univ. Ala.
Elwood Eutermoser.N. Mex. Sch. Mines
Robert E. Evenson...Mont. Sch. Mines
John A. Feeger.....Univ. Nev.
Robert J. Ferranti..N. Mex. Sch. Mines
Charles W. Fleming..N. Mex. Sch. Mines
Crawford E. Fritts..Mich. Min. & Tech.
Bill L. Gabelmann...Mo. Mines & Met.
Robert J. Ganley....Mo. Mines & Met.
John E. Gardner, Jr...Mo. Mines & Met.
Jack T. Gentry.....Mont. Sch. Mines.
Gustaf M. Granstrom.....Univ. Nev.
James O. Greenslade
Mich. Min. & Tech.
Darwin E. Gregory..N. Mex. Sch. Mines
John D. Grimsley..N. Mex. Sch. Mines
Robert O. Haas.....Univ. Pittsburgh
Robert J. Hand.....Texas A&M
Bobby J. Harrell.....Texas A&M
James V. Hastings.....Univ. Ala.
Kenneth G. Hatfield..Mich. Min. & Tech.
John F. Hildebrand, Jr.....RPI
William E. Hill.....Mo. Mines & Met.
Melvin C. Hockenbury
Mo. Mines & Met.
James S. Hopkins, Jr.
Mo. Mines & Met.
John E. Hopper....N. Mex. Sch. Mines
Arthur A. Huntzinger....Rutgers Univ.
Gordon B. Irvine, Jr.....Wash. State
Robert K. James.....Univ. S. Calif.
Sydney W. Jarvis.....Otago Univ.
Paul E. Jones.....Mich. Min. & Tech.
Vishwanath J. Joshi..Mont. Sch. Mines
James E. Kapteina..N. Mex. Sch. Mines
Allen D. Kennedy....Mont. Sch. Mines
Dale F. Kittel.....Mont. Sch. Mines
Max E. Kliewer.....Univ. Kans.
Albert M. Krainess..Mo. Mines & Met.
John A. Kruppenbach
N. Mex. Sch. Mines
Arthur W. Kruse, Jr...Univ. S. Calif.
Donald A. Lammers.....Univ. Calif.
Richard J. J. Lampson.....Univ. Wash.
John R. Land.....Okla. A&M
Louis L. Landers.....Colo. Sch. Mines
Frederic G. Layman....Lafayette Coll.
Donald W. Levandowski
Mont. Sch. Mines
Wallace C. Love.....Mont. Sch. Mines
James L. MacFarlane.....Texas A&M
Jack M. Mackenzie.....Univ. S. Calif.
Richard F. Marvin....Mont. Sch. Mines
Stewart H. McGaw.....Univ. Calif.
Paul McIlroy, Jr.....Mo. Mines & Met.
Jack E. McMahan....Mo. Mines & Met.
John S. McNabb, Jr.
Mich. Min. & Tech.
Russell H. Michel.....Rutgers Univ.
James T. Mikkola....Mont. Sch. Mines
Robert J. Misbeek.....Univ. S. Calif.
Charles E. Morgenthaler...Texas A&M
Walter A. Mourant.....Rutgers Univ.
Paul H. Nikoloff.....Rutgers Univ.
Daniel T. O'Brian...Mich. Min. & Tech.
John H. Osborne, Jr...Mo. Mines & Met.
Bobbie L. Perry.....Mo. Mines & Met.
Robert D. Perry.....Ohio State
Charles W. Phillips (R—S).Univ. Mich.
Salvatore F. Piperato....Lafayette Coll.
William L. Polglase..Mont. Sch. Mines
William R. Prindle.....Univ. Calif.
Robert W. Pullen....Mont. Sch. Mines
William E. Remmert..Mo. Mines & Met.
Linus J. Renner.....Mo. Mines & Met.
Earl W. Rogers (R—S)...Texas A&M
Harold B. Russell..N. Mex. Sch. Mines
John P. Russell.....Lafayette Coll.
Ronald E. Samples..N. Mex. Sch. Mines
Joseph A. Saplis....Mich. Min. & Tech.
Seymour O. Schlanger....Rutgers Univ.
Vernon B. Schneider.....Univ. Toronto
Eugene T. Schnieder..Mo. Mines & Met.
James B. Scott.....Univ. Nev.
Paul D. See.....Oreg. State Coll.
John W. Shannon.....Okla. A&M
Wright C. Sheldon..Mich. Min. & Tech.
Thomas A. Simpson .Mo. Mines & Met.
Richard W. Sippel..N. Mex. Sch. Mines
James E. Slosson.....Univ. S. Calif.
Donald R. K. Smith.....Otago Univ.
Harrison L. Staub.....Univ. S. Calif.
Paul M. Stevens....N. Mex. Sch. Mines
Lawrence H. Tate..N. Mex. Sch. Mines
Edwin M. Thomasson..Mo. Mines & Met.
Thomas E. Tietz.....Univ. Calif.
Joseph W. Tripp....Mont. Sch. Mines
Robert E. Turman....Mo. Mines & Met.
Dominic A. Verive....Mo. Mines & Met.
Albert Villarreal...Mich. Min. & Tech.
John W. Warren, Jr...Mont. Sch. Mines
William E. Watt.....Lafayette Coll.
Ronald J. White.....Mont. Sch. Mines
Robert W. Wilks....Mo. Mines & Met.
Richard V. Wyman.....Univ. Mich.
Francis M. Young....Mont. Sch. Mines
James R. Young, Jr..Mich. Min. & Tech.

Development of the Modern Zinc Retort in the United States

H. R. PAGE,* and A. E. LEE, JR.*

FROM the inception of zinc retorting on a commercial scale in the United States in 1890,[1] the retort employed has undergone wide variations in its composition and manufacture, facilitating in part equally remarkable improvements in furnace capacities. The early day hand made clay retort was charged with carbonates or silicates or with coarse dead roasted concentrates mixed with a large proportion of charge fuel resulting in a relatively low zinc burden and fired 24 hr in direct coal fired furnaces. Its modern counterpart is fabricated in hydraulic presses from clay mixtures containing sizeable amounts of either silicon carbide or silica flour, charged with sintered flotation concentrates to more than three times the early day zinc burden and fired 24 to 48 hr in gas fired furnaces.

This paper does not attempt to describe in detail the early day clay retort practice as it is well outlined in treatises by Ingalls,[2] Lodin,[3] Liebig,[4] Hofman[5] and others. A brief review of clay retort practice is presented together with a description of the major developments since 1912.

Clay Retorts

The Belgian type retort, both in the circular and elliptical forms, has been used almost exclusively. Typical dimensions of press made clay retorts around 1910 are shown in Table 1. Variations in these dimensions were used at different plants according to local conditions to a maximum inside diameter of 9 in. and inside length of 54 in. However, the effective heat penetration in a 24 hr firing cycle and the tendency of the retort to bend limited the retort size. Use of the elliptical vessel was an attempt to present a stronger cross-section resisting the tendency to bend and to increase the burden without increasing the depth of heat penetration.

Table 1 . . . Typical Dimensions of Press Made Clay Retorts around 1910

	Circular, In.	Elliptical, In.
Inside diameter	8	7.5 × 10.5
Inside length	50	50
Wall thickness	1¼	1¼
Butt thickness	2½	2½

One exception to the 48–54 in. length was the 60 in. retort used as early as 1905 at Palmerton by means of supporting the last 12 in. at the butt end with a specially designed furnace backwall. This backwall construction with the 60 in. retort had been developed and used at Bethlehem by G. G. Convers and A. B. DeSaulles. An attempt was made at Blende, Colo. to use even larger retorts of the Rhenish type based on European practice and requiring much higher furnace temperatures. Satisfactory plastic clays capable of withstanding these temperatures were not available, and the plant never operated successfully.

PREPARATION OF BATCH

Composition of the clay retort by weight was 40 to 50 pct raw clay and the balance "grog." Generally speaking the mix consisted of 7 parts plastic clay to 9 parts grog by volume. Principal source of the clay used was the Cheltenham vein—sometimes referred to as "St. Louis city clay." A typical analysis was Al_2O_3-31.0 pct, SiO_2-50.0 pct, Fe_2O_3-2.5 pct, MgO-0.3 pct, CaO-1.5 pct and loss on ignition 14.0 pct.

San Francisco Meeting, February 1949.

TP 2523 D. Discussion of this paper (2 copies) may be sent to *Transactions* AIME before May 15, 1949. Manuscript received September 29, 1948.

* Assistant Superintendent and Metallurgist, respectively, Blackwell Zinc Co., Blackwell, Okla.

[1] References are at the end of the paper.

At the smelter the clay was weathered whenever possible and then crushed to 0.08 in. or finer. Grog consisted of calcined adobies, cleaned retort scrap and cleaned refuse fire brick such as old furnace brick, blast furnace linings, and others. Saggers from ceramic plants and calcined flint clay were later used. The grog materials were ground to 0.12 in. or finer. Occasionally coke dust up to 10 pct of the mix was substituted for a part of the grog following European practice.[2]

Particle size of the grog has a major influence on the retort properties—the larger the grain, the better can the retort withstand thermal shocks, resist bending at furnace temperatures and resist corrosion from slag; the smaller the grain, the lower the loss of zinc vapor through the retort walls. Grog forms the skeleton of the retort, and the clay shrinks around its grains to act as a binder. In the drying process, the grog has a stabilizing effect on the drying rate, decreasing shrinkage and giving up previously absorbed water to the surrounding clay to minimize the danger of cracking or checking.[2]

Grog and clay were mixed through a horizontal pug mill with 10 to 20 pct water added, depending on whether the retort was to be formed by hand or mechanically, more water being required for the hand process. The batch or "mud" extruded from the pug mill was cut in convenient lengths for handling, stacked in piles or in special rooms, covered with wet burlap and allowed to "rot" or age from 1 to 8 weeks to increase plasticity.

HAND MOLDING

If the retort was to be molded by hand, the mud was repugged after the rotting period and given to the molders. Their molds consisted of 3 sheet iron or wood cylinders, each one third the retort length and defining the outer shape of the retort. Beginning with the bottom section, mud was placed in the form and tamped with a rammer

shaped to correspond with the retort interior. This formed a cup from which the retort walls were built up by winding a sort of rope of mud around the interior periphery of the mold. Each addition was tamped into place and the desired interior contour maintained by smoothing with a semicircular tool. Adjoining edges of the mud were roughened to secure a good bond. This process was continued, adding the remaining mold cylinders as required, until the retort was completed. After standing 48 hr the mold was removed and the retort air dried 1 to 3 weeks before being placed in the hot dry rooms.[5]

AUGUR MACHINE

Hand molding was superseded by use of the augur machine in forming retorts. The method of treating the mud between the rotting rooms and the machine varied at different plants. A few plants fed the mud directly to the machine; others repugged it first either in the mixing pug mill or in a larger more powerful mill extruding a 12 to 14 in. mud cylinder. The augur machine consisted essentially of a circular hopper to receive the mud, a series of blades on a central shaft to force the mud downward and a reduced section die and core representing the cross-section of the retort. The machine was arranged to discharge the retort downward in the form of a pipe which was received on a counterbalanced table passing through a temporary wooden mold. When the proper length cylinder had issued from the machine, the augur was stopped and the cylinder cut off, leaving it encased in the wooden mold. A ball of mud was thrown into the cylinder and tamped into place to form the retort butt. As in the case of the hand made vessel, the mold was left on for 48 hr, and the retort dried in the same manner.[5]

HYDRAULIC PRESS

Following the augur machine, a hydraulic press invented by a Belgian, E. Dor, and manufactured by C. Mehler, Aix-la-Chapelle, came into general use. Retorts made in the press, while more expensive than augur units, were denser and stronger. As a result, losses of zinc by absorption and penetration were reduced, a longer life and greater resistance to bending and corrosion were gained, and the charge could be forced longer at high temperatures to effect better zinc recoveries.[2] A further refinement in the Mehler press was effected in the unit made by C. A. Wettengel which formed retorts at higher pressures, was more durably constructed and incorporated a number of labor saving devices.[5]

For use in the press the mud had to be formed into ballots about 16 in. long, 14 in. in diam and weighing 200 lb. Initially this was accomplished by feeding mud from the rotting rooms to a hammering or "Schlag" machine. In time the Schlag machine was replaced by a powerful pug mill extruding a 14 in. diam ballot to be cut off in the proper lengths.

The ballot is placed in the receiver of the press and the die block and cover plate of the press closed and locked. Two rams, one a center punch corresponding to the retort interior and the other an annular ring between the receiver walls and the center punch, rise to compress the ballot. The center ram continues upward to a predetermined distance from the cover plate to form the retort butt while the ring retreats downward in corresponding displacement. After the desired pressure has been reached, the cover plate is swung open and the retort extruded upward between the die block and center ram by pressure from the ring ram. As the retort moves upward, it is guided by a sliding pipe framework with a plate fitting over the retort butt. After trimming to the desired length, the retort is placed in the drying room, no molds being required.

DRYING AND ANNEALING

Freshly made retorts were placed in rooms at atmospheric temperatures for 1 to 3 weeks. Then they were moved to hot rooms at 100 to 140°F for a period of 4 weeks to 6 months to be withdrawn as required by the furnaces. Some plants used a series of 2 or 3 hot rooms each at progressively higher temperatures. Prior to being used in the furnace, the dried retorts were sealed in small kilns and over a period of 15 to 20 hr gradually heated to 1500–1800°F. They were removed at this temperature and placed immediately in the furnace.

PERFORMANCE

The life and performance of clay retorts were materially improved by use of the hydraulic press. Life of a press made clay retort in a 24 hr furnace often averaged as high as 30 days with low iron ores such as coarse Joplin or Willemite. The M & H plant at La Salle is said to have had an outstanding record in this respect, achieving an average of 90 days with small diameter retorts and low burden of Joplin ore in the early 1900's. With western ores of higher iron content, however, the life was as low as 12 to 14 days in some cases. There was a sizeable loss of zinc vapor by absorption in the walls of the retort (7–9 pct of the retort weight) and by penetration through the walls into the laboratory of the furnace (estimated as high as 2 pct of the zinc in the charge by some operators). Retort failures were caused by excessive bending, build up of loam outside and "rock oxide" inside the retort mouth, cracking from thermal and physical shock, slag boring and corrosion. Among various attempted solutions to these difficulties were glazing[2] the exterior and/or interior of the retort to reduce vapor absorption and penetration, coating the interior with a noncorrosive basic lining[2] to resist slag corrosion from irony ores, making the retort bottom thicker than the other walls to give added strength and reduce boring losses, and making the retort in layers[5] of different materials—the interior to resist corrosion and the exterior to form the body of the retort.

Silicon Carbide Retorts

About 1912 the New Jersey Zinc Co. began experimenting with the use of silicon carbide in the retort mix in an effort to improve the life of the clay vessel. Although the higher cost of the retort was recognized at the outset, there were in addition to longer life and other potential advantages several attractive features at the Palmerton plant. These were the possibility of reducing the amount of St. Louis clay on which the freight charge was high, the nearby commercial electric furnace production of silicon carbide together with the producer's desire to find new uses, and the smelter's large scale use of Willemite ore.

The first retorts were cast units of very high silicon carbide content and failed as a result of thermal shock after a short time. Then followed a period of experimentation using carbide crushed and sized to the recommendation of the Carborundum Co., mixed with plastic clay, and processed in the conventional manner. About 1913 a batch consisting of 88 pct silicon carbide and 12 pct plastic clay by weight was prepared by hand mixing and working over a period of several weeks by Jake

Miller, a skillful potteryman. Ballots were prepared in a Schlag machine and passed through a Mehler press making 2 retorts. After drying and burning in the conventional manner, they were placed together in the middle of the second row of a 4 high Siemens regenerative furnace fired with producer gas made from anthracite coal. One of these retorts lasted 10 months and the other 355 days. A mix of 70 pct silicon carbide and 30 pct plastic clay was finally adopted as the composition which could best be worked with the then existing pottery equipment. Some years later this was changed to 65–35 pct. Under the conditions at Palmerton, the method of crushing the silicon carbide was found to be most important, and pan mill ground grain to produce a size distribution approximating Fuller's curve of minimum voids gave the best results.

The advantages realized at Palmerton in replacing clay retorts with carbide have combined to effect savings beyond the additional retort cost. These are: longer life—an average well over 100 days over the years—a more rigid piece of refractory permitting the use of a 5 ft retort without extra butt support, improved zinc recovery, smelting time saved in changing fewer retorts, better heat transfer with consequent fuel saving and better control of furnace.

There is a definite reaction between the silicon carbide and basic constituents of the charge, including zinc oxide, tending to decompose the carbide. The practice of salt additions in sintering is prohibited, and its use mixed with the charge is limited to a maximum of 0.25 pct because of the alkali reaction. Basic and alkali bearing dust carried in the producer gas used in firing attacks the exterior of the retort similarly. The highly acidic nature of the residue from the Willemite ore-anthracite coal charge undoubtedly contributes to the successful results at Palmerton.

Manufacture of silicon carbide retorts for use with sintered zinc sulphide charges has been described by E. J. Bruderlin[6] at the Amarillo plant of the American Smelting and Refining Co. Current retort size is 9¼ in. inside diameter, 62 in. inside length, 1⅛ in. wall, 2½ in. butt, weight burned 224 lb. Amarillo uses 2 classes of retorts—the No. 1 class made with clean, freshly produced silicon carbide and the No. 2 class made with about half new material and half reclaimed carbide. The average life in calendar days of these retorts for the period 1940 to 1947 inclusive was 228.6 days for the No. 1 retort and 123.1 for the No. 2. During this period 24, 28, 32, 36 and 48 hr cycles were used.

Silica Retorts

After the silicon carbide retort had been established successfully at Palmerton, several smelters experimented with the use of carbide in their retort mixes. However, the high cost, close process control required and relatively difficult furnace working conditions were prohibitive in most instances, and other methods of improving the clay vessel were sought.

During a visit to the Hillsboro plant of the American Zinc, Lead and Smelting Co. about 1915, a German engineer named Salzberg mentioned that German retort clays contained relatively high silica. In 1919 while experimenting with a wide variety of refractory materials mixed with the regular clay-grog mix in an effort to produce a longer retort which would resist bending, the Rose Lake smelter of the same company tested silica additions from 5 pct through 35 pct by volume of the mix. As a result of this work, the high silica retort mix became regular practice at Rose Lake in 1920, although the volume of silica was not standardized at 25 pct until 1929.

W. F. Rossman[7] of the American Zinc, Lead and Smelting Co. patented the high silica retort in 1922, specifying proportions by volume of 50 pct plastic clay, 25 pct grog and 25 pct silica flour of minus 140 mesh. Manufacture and performance of this retort at Rose Lake were described by G. L. Spencer, Jr.[8] in 1931. The first license under the patent was granted May 1, 1928 to the Hegeler Zinc Co., and within a few years the silica vessel was adopted universally by the other smelters not using silicon carbide.

From the information available, the 25 pct proportion of silica has been followed by the industry, although variations in the volumes of clay and grog have been made. For example, Dumas uses a mix of 45 pct plastic clay, 30 pct grog and 25 pct silica flour. The 5 pct additional grog is intended to further stiffen the retort, but no data are available to prove or disprove the benefits.

A further improvement in the practice of manufacturing both carbide and silica retorts was the use of the de-airing pug mill. This equipment was developed at the Donora Zinc Works in 1940 and has been described by M. M. Neale.[9] Greater density and strength of the retort wall are the principal advantages. Another recent innovation is controlled humidity or "quick" drying of retorts, introduced at Donora[10] on a commercial scale in 1947. Undoubtedly this process removes mechanical moisture much more rapidly and uniformly than is done during the first 15–45 days in the conventional drying room. However, the value of long aging in addition to drying is considered by some smelters to be of great importance to long retort life, and some believe that aging of quick dried retorts will materially improve them.

As an example of current manufacture of silica retorts, the practice of the Blackwell Zinc Co. is described. The retort is of circular cross-section and has the following dimensions burned: inside diameter 9 1/16 in., inside length 62 in., wall 1 1/16 in., butt 2 1/16 in., weight 171 lb.

MATERIALS

Materials used in fabricating the retort and their proportions by volume are 50 pct plastic clay, 25 pct grog and 25 pct silica flour. Wet weights per cu ft and average moisture content of the crushed materials as used are: clay, 78 lb per cu ft, 7.0 pct moisture; grog, 80 and 1.0 pct; silica flour, 68 and 0.5 pct. Missouri clay from the area about 100 miles northwest of St. Louis is used and has approximately the composition shown in Table 2. After weathering 6 to 12 months whenever possible, the clay is sized to minus 0.095 in. Grog is purchased de-aired setter slab material which has been used in making and burning fire brick. A typical analysis is given in Table 2. Grog is sized to minus 0.120 in. Silica flour is of high quality, assaying approximately 99.5 pct SiO_2, and is in the form of a fine flour, 95 pct through a 150 mesh sieve and 50 pct through 200 mesh.

Table 2 . . . Analysis of Clay and Grog Used in Blackwell Retorts

	Clay, Pct	Grog, Pct
Al_2O_3	30.5	38.9
SiO_2	58.0	56.0
Fe_2O_3	1.0	4.2
MgO	0.1	0.14
CaO	0.2	0.35
S	0.2	0.12
Loss on ignition	9.8	0.0

FORMING RETORTS

Desired quantities of clay, grog and silica are bucketed into a horizontal pug mill from adjacent storage bins. Sufficient water, usually 12.5 to 13.0 pct in the mix, is added to produce the desired stiffness. The mud is extruded through a round cornered $7\frac{3}{4} \times 10\frac{3}{4}$ in. opening from the mill, cut and stacked nearby. When approximately 23 tons (enough for 235 retorts) has been made, the feed of raw materials is stopped and the entire batch immediately repugged. It is recut and stacked in rotting rooms for 5 to 6 days. After the rotting period, the mud is fed into a Bonnot de-airing pug mill where it is repugged, shredded, de-aired under a vacuum of 25–27 in. of mercury, and compressed into an ejecting cylinder 15 in. in diam. The ballots are cut off in 17 in. lengths and made into retorts in a Mehler press. The butt is formed with a pressure on the mud of 1050–1100 psi and the walls extruded at 300–350 psi. After trimming to proper length, the retorts are wheeled individually on rubber tired trucks to the drying rooms.

DRYING

Drying rooms have brick walls and a gently sloping frame roof. The floor is made of wood 2×4's laid flat and spaced $\frac{1}{4}$ in. apart over the floor joists. To a height of 6 ft from the floor, a rough wood wainscoating separates the retorts from the brick walls by a 4 in. airspace. In the roof are constructed 2 ventilators with the outside openings shielded from possible entry of rain and containing dampers for varying the openings. Steam pipes are laid 6 in. below the floor and at the ceiling to effect drying. The average room holds about 1500 retorts.

Prior to using a room for drying, all steam is shut off, the ventilators are closed, and the walls and floor wet down. The retorts are carefully placed in rows beginning against the farthest wall from the door. Each retort is put as close as possible to its neighbors with each row interlocking the preceding row. At the end of each production shift, the exposed row is covered with damp burlap and the door closed. When the room is filled, boards are placed across the doorway to a height of 6 ft, the retorts in the doorway covered with burlap and the door closed.

Depending on outside conditions, the temperature in the room will average 80°F when filling is completed. Daily checking of the room is required, and its temperature at a regular time each day is recorded on a chart on the door. On the fifteenth day after closing, the ventilators are opened and steam is cracked on the floor coils. Steam additions are carefully controlled so that the temperature rises only 1 or 2° each day. When possible, all drying is effected with the floor coils only. However, after 30 days from start of heating, steam may be turned in the ceiling coils if necessary to maintain the temperature increase until 135°F is reached. Occasionally in cold weather it is necessary to use the top coils to prevent condensation drips from the ceiling.

The room is held at 130–135°F until opened for furnace use. Retorts are in the rooms 90 to 120 days. Loss in drying based on retorts used in the furnaces is quite low as evidenced by the following: 1945—0.12 pct, 1946—0.16 pct, 1947—0.11 pct.

PREHEATING

On the day preceding the prescribed furnace maneuver, the required number of retorts is taken from the oldest drying room and placed in conventional down draft gas-fired kilns. Doors are sealed and the kilns fired at 3 in the afternoon in anticipation of use the following morning between 6 and 9. Heating is gradual to a maximum of 1600–1800°F during the latter part of the period. When retorts are to be withdrawn, the gas is shut off and the doors opened. The retort must be placed immediately in the furnace when taken from the kiln as it is very sensitive to temperature change. During any pause in the removal of retorts over a few minutes duration, the kiln door is closed and the gas reapplied.

Retort loss at the kilns is 4 pct based on retorts used in the furnaces. 1 pct of this is due to errors in firing—primarily spalling from too rapid heating. 3 pct represents breakage from faulty handling on removal from the kiln. All retorts lost at the kilns are collected and returned to the pottery for use as grog. Retorts lost in drying are hard burned in a kiln and used in the same way.

PERFORMANCE

Performance of the silica retort at Blackwell for the period 1943 through August, 1948, is shown in Table 3. Ores used during this time were about one third low iron sulphide flotation concentrates of about 2.5 pct Fe in the green ore and two thirds containing about 7.0 pct Fe.

Table 3 . . . Performance of Silica Retort at Blackwell

	Life in Furnace Cycles*
1943	22.69
1944	28.54
1945	29.83
1946	31.59
1947	26.20
1948	29.34

* Furnace cycle 24 hr before June 1944 and 93 pct at 48 hr since.

Conclusion

The history of the horizontal zinc retort in the United States records a continual effort to enlarge the retort. The two most significant developments in this respect were the use of the hydraulic press in forming retorts and the use of silicon carbide and silica flour mixes. The 62–64 in. inside length employed today is not the limit at which the modern retort can effectively resist bending but is, rather, the supposed practical limit of effective manual charging. Extending the furnace cycle beyond 24 hr has permitted on a practical scale increasing diameter. However, even with the 48 hr cycle the maximum distance for heat penetration appears to be limited depending on the slagging characteristics of the ores charged. Longer life and improved wall density of modern retorts have made possible better zinc recoveries.

While the advantages of both the silicon carbide and silica retorts are easily discernible over the clay vessel, it is difficult to make any such distinction between the former. In the United States only the two primary zinc smelters previously mentioned use carbide retorts, and the balance use silica. In cost the carbide retort is 4 to 6 times as expensive, but correspondingly, its life is 3 to 4 times as long in terms of charge cycles dependent on the composition of ores used and character of the firing fuel.

Heat transfer within the furnace is much more effectively accomplished with the carbide than the silica. Carbide retorts can be and are fired to higher temperatures than silica retorts, resulting in lower zinc in the residue but greater demands on furnace linings. Special refractories are sometimes resorted to where carbide retorts are used. Because of the longer life, more attention must be given to

chiseling out loam build up and "rock oxide." For the same reason, use of carbide retorts in Hegeler furnaces is impractical because of build up of fusible fly ash fastening retorts to the shelves. The use of salt in sintering and in preparing the charge is restricted. Residual sinter sulphur must be held to a low figure, preferably 0.2 pct or lower. The silica retort is subject to boring and corrosion by fusible iron slags but is considerably easier to cut out and replace in the furnace. Thermal shock below furnace temperatures is much more damaging to the silica, even the old clay retort being superior in this respect. Because of the better heat transfer, heavier retort weight and greater difficulty in cutting out retorts, the working conditions are said to be less satisfactory on a silicon carbide retort furnace. On the other hand, changing less retorts per cycle at least partially offsets this. Practical burdens per retort are about the same for both vessels. Other things being equal, the longer life of carbide retorts should make possible higher recoveries of zinc. Choice of the retort is a matter depending on local conditions at the individual smelter.

Acknowledgment

The assistance of Mr. Francis P. Sinn of the American Metal Co. and Mr. Chester Skinner and the staff at Blackwell in preparing this paper is gratefully acknowledged. Thanks are extended to Mr. Henry Hardenbergh and Mr. L. S. Holstein of the New Jersey Zinc Co. for data on the early history of the silicon carbide retort and its use at Palmerton; to Mr. E. J. Bruderlin of the American Smelting and Refining Co. for data on the use of silicon carbide retorts at Amarillo; and to Mr. Robert Ammon and Mr. G. L. Spencer, Jr. of the American Zinc, Lead and Smelting Co. for the history of the silica flour retort.

References

1. W. R. Ingalls: Lead and Zinc in the United States. 313–315. 1908, New York. Hill Publishing Co.]
2. W. R. Ingalls: Metallurgy of Zinc and Cadmium. 216–256. 1903. New York. McGraw-Hill Book Co., Inc.
3. A. Lodin: Metallurgie du Zinc. 594–648. 1905. Paris.
4. R. G. Max Liebig: Zink und Cadmium. 324–373. 1913. Leipzig.
5. H. O. Hofman: Metallurgy of Zinc and Cadmium. New York. 131–154. 1922. McGraw-Hill Book Co., Inc.
6. E. J. Bruderlin: Manufacture of Silicon Carbide Retorts. *Trans.* AIME (1936) **121,** 441–444.
7. W. F. Rossman: U. S. Patent 1424120, July 25, 1922.
8. G. L. Spencer, Jr.: High-silica Retorts at the Rose Lake Smelter. *Trans.* AIME (1931) **96,** 119–124.
9. M. M. Neale: Deaeration in Manufacture of Zinc Retorts. *Trans.* AIME (1944) **159,** 127–129.
10. F. P. Sinn: Annual Review of Zinc Smelting. *Mining and Metallurgy,* (Feb. 1948) 97–98.

A view in an assaying laboratory (Ercker, 1574).

In the background are (left to right), a cementing furnace, a pot for reacting saltpeter and argol to make flux, a double wind furnace, and a muffle furnace for cupellation. The cylindrical tower furnace in the foreground is an Athanor and is making nitric acid for parting. The ring of fire heats silver granules in the pot with sulphur, forming silver sulphide which is subsequently melted to separate the contained gold. The man in the right foreground is smelting copper ore for assay directly in a little blast furnace, the air for which is provided by aeolipile acting as an injector. This is probably the earliest use of steam power for serious purposes.

(Courtesy Cyril S. Smith.)

The Effect of Strain-temperature History on the Flow and Fracture Characteristics of an Annealed Steel*

E. J. RIPLING† and G. SACHS,† Member AIME

Introduction

ALL ferrous alloys can be made brittle by straining at sufficiently low temperatures. However, the changes in mechanical properties for different ferrous materials with decreasing testing temperature do not appear to follow any universal law.

In particular, complex effects of testing temperature have been observed if cold worked steels were subjected to tensile tests at low temperatures.

EFFECTS OF PRESTRAINING AT A TEMPERATURE ABOVE THE TESTING TEMPERATURE ON THE FRACTURE CHARACTERISTICS‡

A considerable amount of data has been presented by a number of investigators on the fracture characteristics of various cold worked steels.[1] These data usually relate to a two-step procedure first used by Davidenkov,[2] consisting of stretching by tension to a certain strain or "prestraining" at room temperature and then completing the tensile test, or "testing" at the temperature of liquid air.

On the basis of data of this type made available to date, ferrous alloys can be classified into two groups with respect to their fracture characteristics observed on testing at a low temperature after prestraining at room temperature. Very complex phenomena have been observed for all annealed steels. On the other hand, some observations indicate that steels in certain other conditions represent a fundamentally simpler relation.

In considering the effect of prestraining at one temperature on the properties obtained at some lower temperature, it should be expected that any cold work reduces the ductility retained in proportion to the magnitude of the cold work. However, the test data presented to date indicate that only heat treated (quenched and tempered) steels appear to conform to this expectation, according to the very limited test data in Fig 1, presented by McAdam, Geil and Mebs. This series of tests, Fig 1, shows that the retained ductility became smaller the larger the prestrain. However, this decrease is less than the amount of prestrain or, in other words, less than the decrease in ductility at the prestraining temperature.

These effects of prestraining are fundamentally identical with those observed by Bridgman[3] when a steel was prestrained (in tension) under hydrostatic pressure and then subjected to a regular tension test. It appears, therefore, that the basic effect of prestraining under conditions which yield a higher ductility than the (subsequent) testing procedure, consists of gradually increasing the total ductility of the metal from the initial low value of testing to the higher value of prestraining.

On the other hand, all annealed steels, if cold worked by tension at room temperature and then tested at a lower temperature, provided that some ductility is retained, showed a far more complex behavior than that discussed above. This relationship is exemplified by Fig 2, for three pearlitic steels.[4,5] These particular steels were selected because of the various shapes of their ductility-prestrain curves. All three steels, and any other investigated so far, suffered a rapid decrease in retained (and consequently also in total) ductility when subjected to small prestrains. Then, after exceeding a certain prestrain it was generally observed that the ductility recovered.*

This rather complex behavior of annealed steels may be tentatively correlated with the presence of stretcher strains at small prestrains. Heat treated steels do not exhibit stretcher strains. This fact might possibly explain their simpler prestrain-retained ductility relationship.

The destructive effect of these stretcher strains may possibly be associated with the presence of triaxiality, which may occur in any highly nonuniform stress and strain state (and which is retained as residual stress after unloading). Even a small degree of triaxiality may then cause a reduction in ductility, or even embrittlement at a sufficiently low testing temperature.

The discussion presented above deals with the effects of cold working at a high temperature on the fracturing

San Francisco Meeting, February 1949.

TP 2514 E. Discussion of this paper (2 copies) may be sent to *Transactions* AIME before May 15, 1949. Manuscript received June 17, 1948; revision received Sept. 27, 1948.

*This paper is one of a series of reports in a research program conducted at the Research Laboratory for Mechanical Metallurgy, Case Institute of Technology, Cleveland, Ohio, in cooperation with the Office of Naval Research, U. S. Navy.

† Research Laboratory for Mechanical Metallurgy, Case Institute of Technology, Cleveland, Ohio.

‡ In most investigations in which the effect of some variable or variables on the fracturing characteristics is to be determined, it has been found that the ductility generally responds to the variables more simply and accurately than the fracture stress. Consequently, in this paper the main emphasis will be placed on ductility changes.

[1] References are at the end of the paper.

* This damaging effect of small tensile strains on the low temperature properties of annealed steels is further revealed by some tests made by Davidenkov and Sakharov[2] on a 0.20 to 0.25 pct carbon steel. The transition temperature of this steel was found to go through a maximum at small prestrains, as shown in Fig 3.

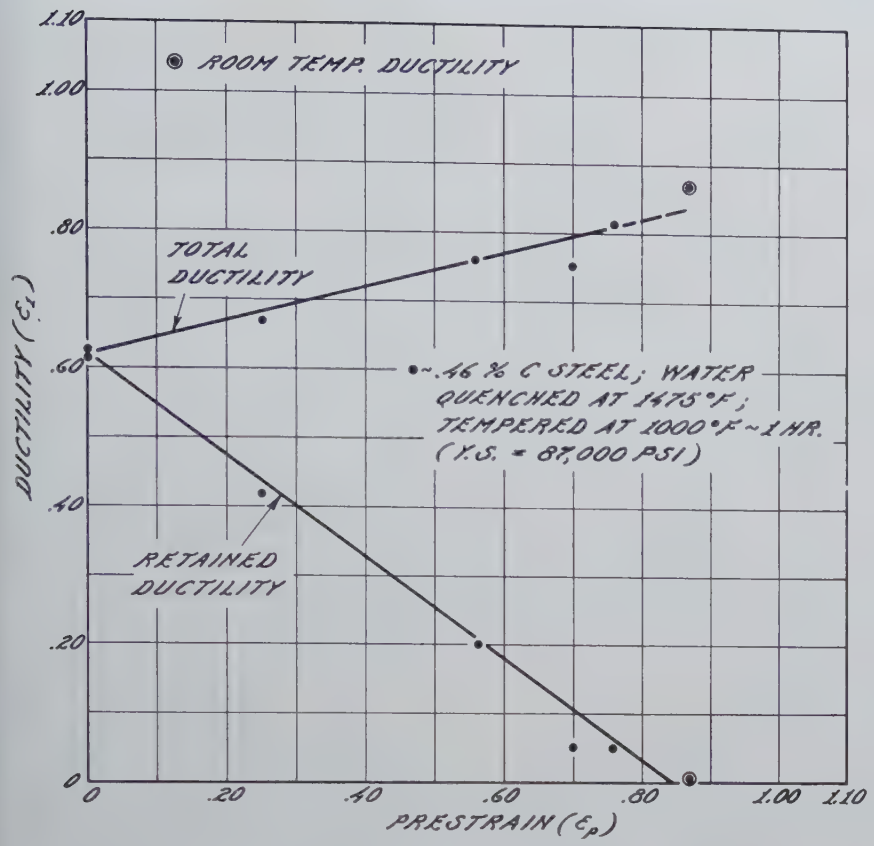

FIG 1—Effect of prestraining in tension at room temperature on the ductility at a low temperature (−190°C) obtained on a heat treated steel (McAdam, Geil, and Mebs).

characteristics at a lower temperature. Apparently, the reverse case, that is, prestraining at a low temperature and testing at a higher temperature to failure, has not yet attracted any attention.

EFFECT OF PRESTRAINING AT ONE TEMPERATURE ON THE FLOW CHARACTERISTICS AT A HIGHER AND A LOWER TESTING TEMPERATURE

The effect of two-step, cold work treatments has also been investigated on another metal characteristic, that is, strain hardening, as represented by the general shape of the stress-strain curve. The very limited data presented by Hollomon[6] obtained on a 1020 steel have been evaluated by him to prove that the temperature of prestraining has no effect on the strain hardening observed at a given temperature, Fig 4. In other words, the state of strain hardening is independent of the straining temperature, as long as the temperature is sufficiently low to prevent diffusion.

According to some data by Orowan,[7] however, obtained on copper which was strained in steps at room temperature and at the temperature of liquid nitrogen, Fig 5, the stress at any particular strain is very greatly affected by the temperature at which the strain was made. Furthermore, in some more recent tests, Dorn, Goldberg and Tietz[8] prestrained 2SO aluminum at various temperatures and then tested it at both a higher and a lower temperature than the prestraining temperature. Their results were in agreement with those of Orowan in that the flow stress at any particular strain depended greatly on the strain history. Furthermore, they found that prestraining at a high temperature had a greater effect on the flow stress at the low temperature than the reverse process of prestraining at a low temperature and testing at the high temperature. In addition to the work done on 2SO they also prestrained pure aluminum, copper, 65/35 brass, and 18/8 stainless steel at room temperature before testing at a low temperature. The flow stress of each of these materials also showed a great dependence on strain history.

PURPOSE OF PRESENT INVESTIGATION

This investigation was conducted in order to clarify some of the problems discussed above. A low carbon 2¾ pct silicon steel was selected for the investigation. Test series were conducted to determine the following:

1. Effect of testing temperature on the properties of the 2¾ pct silicon

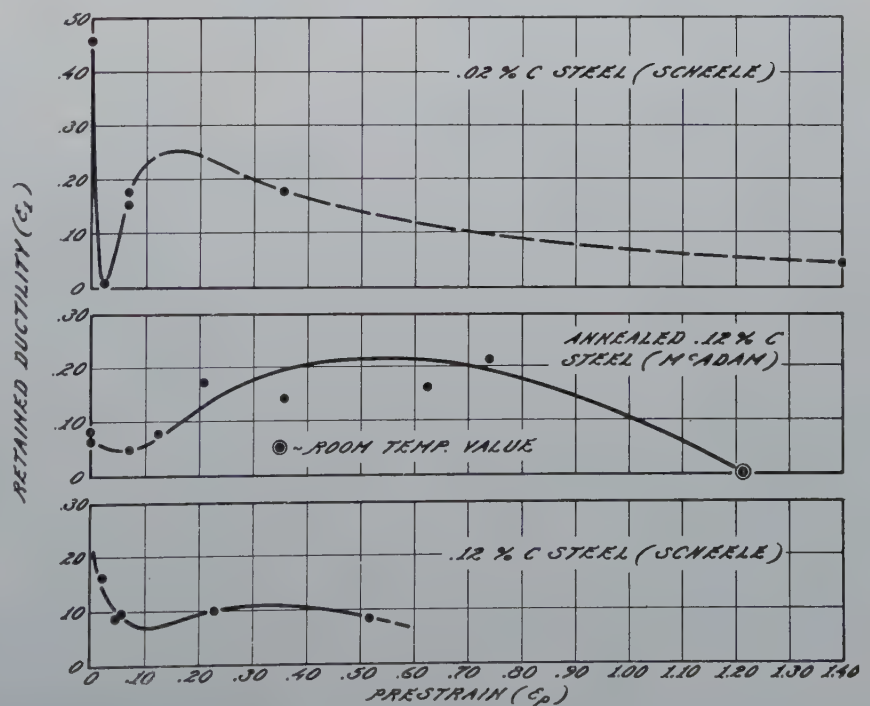

FIG 2—Effect of prestraining in tension at room temperature on the retained ductility at a low temperature (−190°C) obtained on annealed steels.

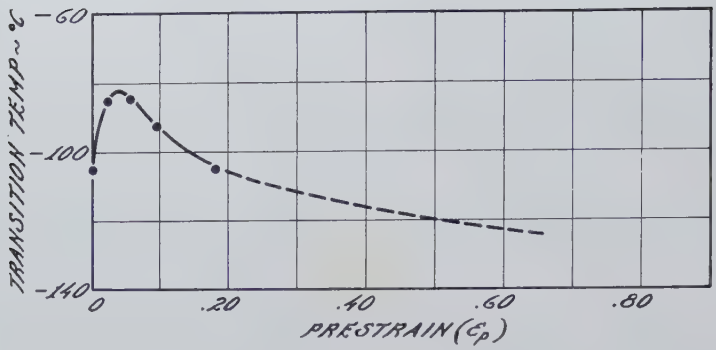

FIG 3—Effect of prestraining in tension at room temperature on the transition temperature of an annealed (coarse grained) 0.20 to 0.25 pct carbon steel (Davidenkov and Sakharov).

steel, to determine the basic effects of testing temperature on the mechanical properties of this metal.

2. Effect of prestraining at room temperature on the properties at various low temperatures.

3. Effect of prestraining at various temperatures on the properties at a constant low temperature.

4. Effect of prestraining at various low temperatures on the properties at room temperature.

Material and Equipment

MATERIAL

The mechanical properties of ordinary low and medium carbon steels behave in general quite peculiarly with varying temperature. As discussed in a later section, most steels, when the temperature of testing is reduced, become considerably stronger while their ductility is only slightly affected over wide limits. However, at some low temperature the ductility drops to very small values over a narrow temperature range. In an investigation of the type proposed here, a steel whose fracturing characteristics behaved in this complex manner would impose a considerable limitation on the results that could be obtained. Consequently, a 2¾ pct silicon steel was selected for this work. The steel, which approached a solid solution type alloy, had the following analysis: C, 0.031; Mn, 0.12; P, 0.011; S, 0.015; Si, 2.73; Ni, 0.098; Al, 0.23; Cu, 0.116; Sn, 0.008. This steel also possessed the advantages that its ductility at room temperature was quite high, while it decreased to a very low value at the lowest temperature obtainable. A high silicon steel of this type also possesses very uniform flow and fracture characteristics.

The steel which was supplied in the form of ¾ in. rods had been annealed at 1450–1500°F for 8 hr, so that it possessed quite a large grain size. The steel was used in this "as-received" condition.

EQUIPMENT

The prestraining and testing was done on a 10,000 lb Riehle tensile test machine. All room temperature strains were accomplished with the use of a specially designed loading fixture that yielded an eccentricity of loading of less than 0.001 in. and a radial strain gauge reading in 0.0001 in.[9] These same loading fixtures were adapted for the low temperature work under which condition the eccentricity was slightly higher. A remote reading mechanical gauge reading in 0.0001 in. was also developed to be used with this apparatus. A detailed description of this equipment is given in another report.[10]

Procedure and Method of Evaluation

PRESTRAINING AND TESTING PROCEDURE

All specimens used in this investigation were initially machined to a 2-in. contour radius at the reduced section, to enforce fracturing at a predetermined location and to facilitate measuring the strains at the neck. The other specimen dimensions are shown in Fig 6.

Specimens that were tested at temperatures less than −78°C (that is, −80, −100, −120, −150, and −196°C) were finished by polishing in such a manner that the scratches on these specimens were in the direction of the axis of the specimen. Specimens that were prestrained and then tested at temperatures less than −78°C were polished after prestraining. In this series of tests, specimens that were prestrained to less than approximately 30 pct were polished to a 2-in. radius. If the specimens were prestrained to

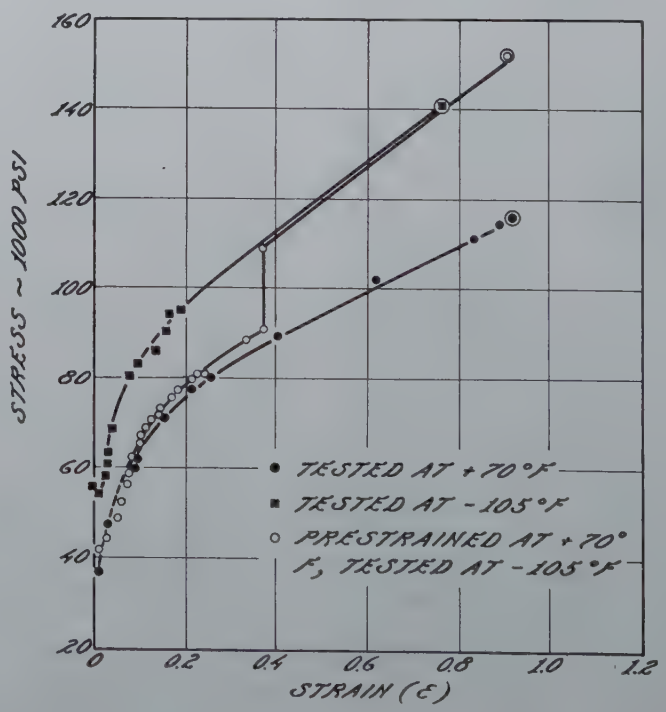

FIG 4—Stress-strain curves for 1020 steel at a high and a low temperature and for prestraining at a high temperature and testing at a low temperature (Hollomon).

more than 30 pct, the contour radius of the strained specimen was determined, and the specimen was polished to this radius. This procedure removed approximately 0.005 in. from the diameter.

All tests were made with the speed of the movable head of the tensile machine approximately 0.04 ipm so that for each specimen strained, a large number of gauge readings could be taken at different loads in order to enable point by point recording of the stress-strain curves. (This, of course, was not possible at temperatures at which the coolant was frozen.) These readings yielded values of the average or "true" stress,* and of the average decrease in diameter of the minimum section. The diameter reduction was converted into the natural maximum strain, ϵ_1, according to the equation:

$$\epsilon_1 = \frac{\text{Original area}}{\text{Instantaneous area}} = 2ln \frac{\text{Original diameter}}{\text{Instantaneous diameter}}$$

From these data a stress-strain curve was obtained for each specimen strained, showing the true stress as a function of the natural strain. In all instances these natural strains, therefore, relate to the dimensions of the specimen at the beginning of a particular straining operation. However, the use of natural strains made possible the addition of the prestrains and testing strains by the simple graphical operation of plotting the respective stress-strain curves side by side.

In the testing operation, particular care was exercised to observe the load at the moment of fracture so that the fracture stress† could be evaluated. The corresponding fracture strain or "retained ductility" was determined by diameter measurements made with a micro-comparator before and after straining.

METHOD OF EVALUATION

The evaluation of the test data was based primarily on the following two types of graphical representations:

1. A comparison of stress-strain curves obtained at a given temperature for various amounts of prestrains at several different temperatures, see Fig 16 to 21.

2. The dependence of the retained ductility at a given temperature upon the magnitude of prestrain, with the temperature of prestrain as parameter, see Fig 11 and 15.

These data were obtained, as mentioned before, on tensile test specimens having an initial longitudinal contour radius of two inches. This initial contour and the fact that the specimens developed necks on straining undoubtedly influenced the measured values of stress and ductility. However these effects of specimen shape are superimposed on the phenomena being discussed in this paper, and the measured average stresses and strains appear satisfactory. Furthermore, the principal conclusions derived relate to comparatively small strains and should, therefore, be only slightly influenced by the process of necking.

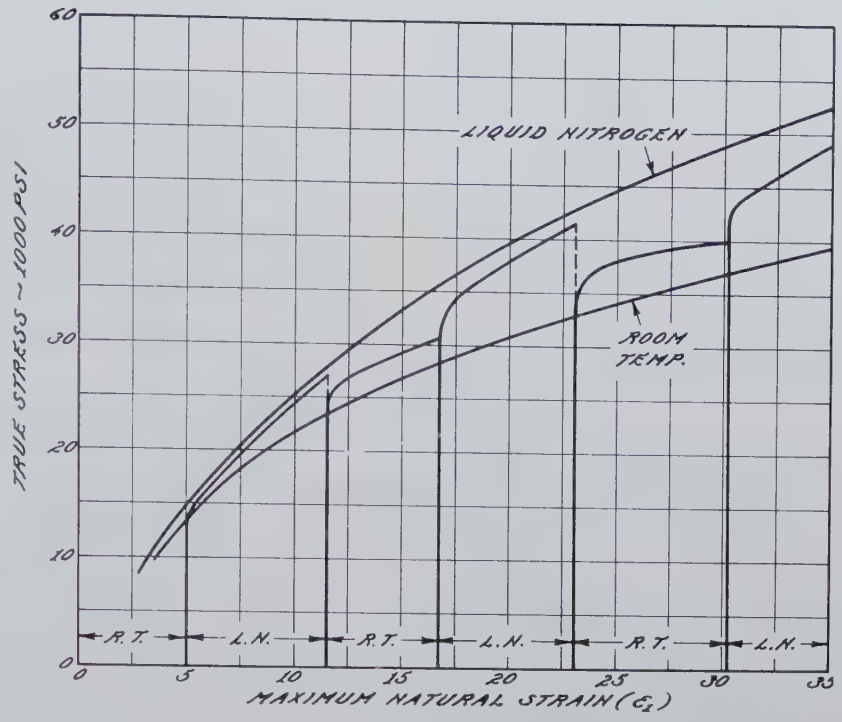

FIG 5—Effect of alternately straining at room temperature and at −196°C on the flow stress of a high conductivity copper (Orowan).

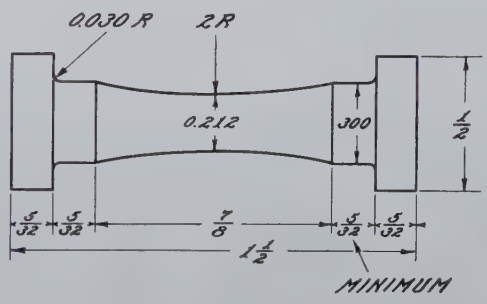

FIG 6—Tensile test specimen.

Discussion of Results

EFFECTS OF TESTING TEMPERATURE ON THE PROPERTIES OF THE UNSTRAINED MATERIAL

For the purpose of this investigation, it was first necessary to investigate the direct effect of testing temperature on the flow and fracture characteristics of the selected steel. Wherever possible, stress-strain curves were determined, which are plotted in Fig 7 and 8. The dependence of the yield strength (1 pct),* the tensile strength, and the

* The true stress was defined as the ratio of the load to the minimum area of the specimen at the instant at which the load was obtained.
† True stress at fracture.

* The yield strength was defined as the stress at 1 pct permanent set instead of the conventional value of 0.2 pct, since the strain gauge used at low temperatures yielded more reliable values at this higher strain.

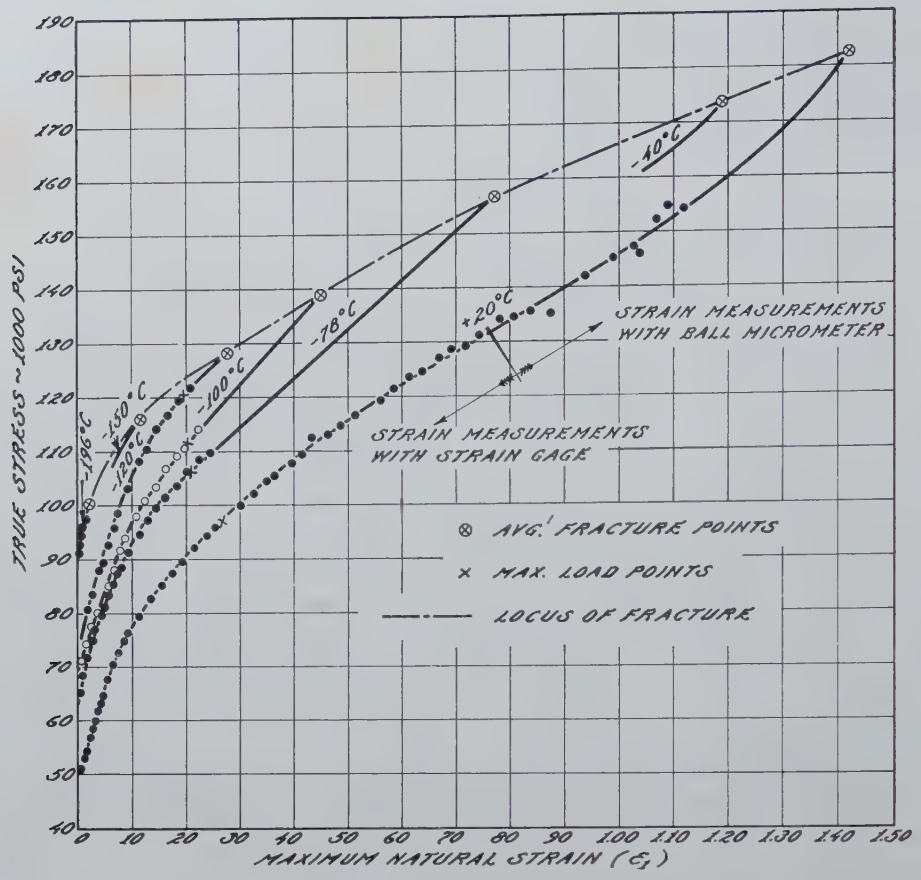

FIG 7—Effect of testing temperature on the stress-strain characteristics of a 2¾ pct Si steel.

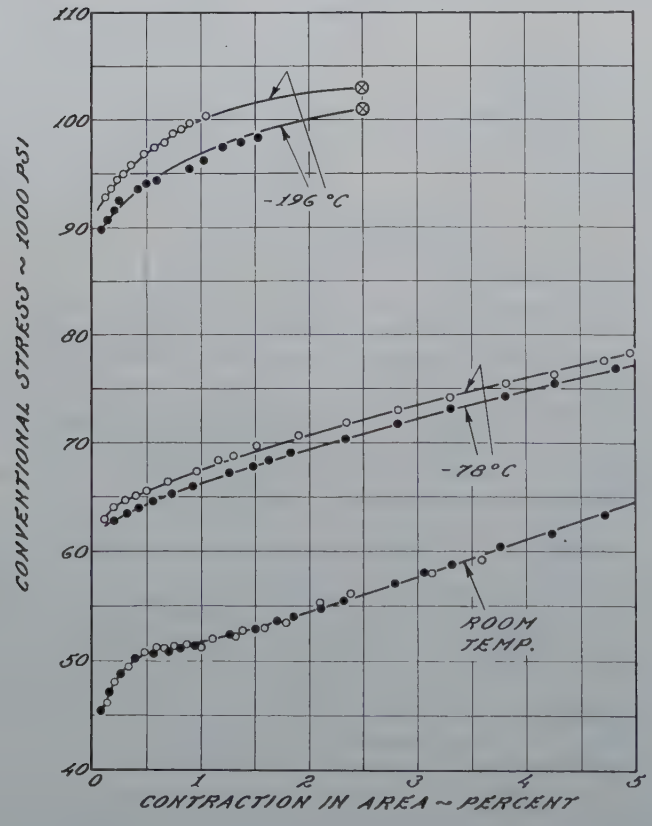

FIG 8—Effect of testing temperature on the stress-strain characteristics of a 2¾ pct Si steel.

fracture stress upon temperature is shown in Fig 9 and that of the ductility in Fig 10. In both Fig 7 and 10 approximate values of the maximum load strains are also indicated. It can be seen from the stress-strain curves in Fig 7 and from Fig 9 that the value of yield strength changed with temperature at an approximately constant rate over the entire range investigated. The general shapes of the various stress-strain curves in Fig 7 are rather similar. With decreasing temperature, the stress-strain curve moved to higher stresses, increasing its slope, $ds/d\epsilon_1$,* only very slightly. The maximum load strain (which depends upon the relative slope, $ds/sd\epsilon_1$) consequently decreased slightly with decreasing temperature. (See Fig 10.)

The tensile strength, like the yield strength, also changed with temperature at an approximately constant rate down to a temperature of −130°C. The tensile strength values then went through a maximum at about −150°C.

At room temperature the silicon steel curves exhibited a slight but dis-

* Where s = average tensile stress, and ϵ_1 = maximum natural strain.

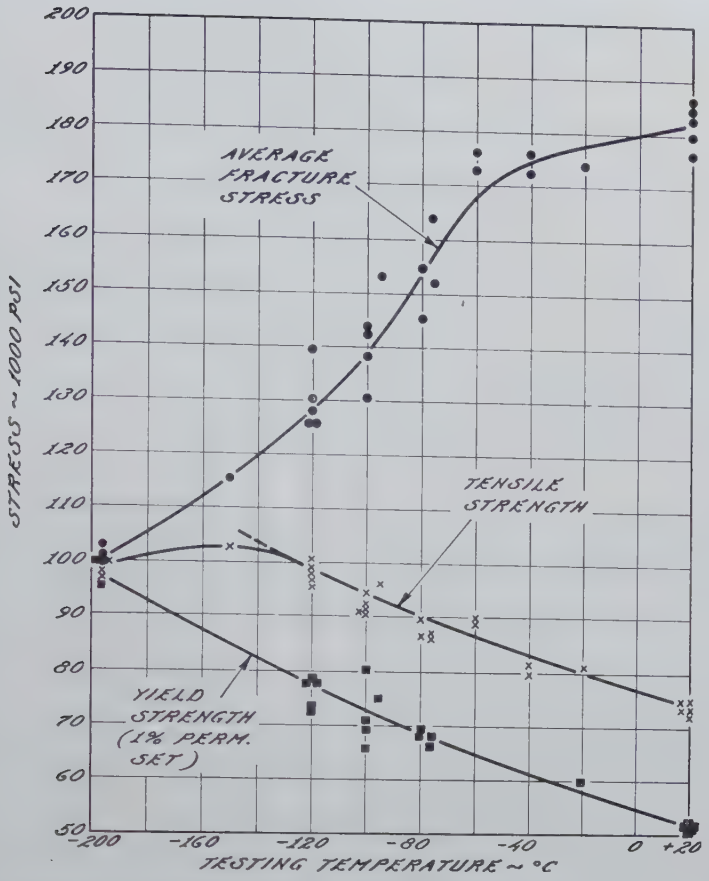

FIG 9—Effect of testing temperature on the strength properties of a 2¾ pct Si steel.

tinct yield point jog, or reversal in curvature at small strains, as apparent from the conventional stress-strain curves in Fig 8, which are plotted on an enlarged scale.* Fig 8 also includes several stress-strain curves taken at temperatures of −78 and −196°C. (These were the only low temperatures at which reliable small strain measurements were obtained.) The stress-strain curves for −196 and −78°C showed no indication of a yield point jog. It may be concluded, therefore, that the reversal in curvature of the stress-strain curves of the silicon steel decreases with decreasing temperature until it disappears somewhere before −80°C.

The ductility (contraction in area converted to natural strain) of the silicon steel decreased according to Fig 10 with decreasing temperature. At approximately −130°C the ductility became equal to the maximum load strain and at still lower temperatures it rather gradually approached very small values. At the lowest temperature used, −196°C, the steel was still distinctly ductile. (See Fig 8 and 10.)

The fracture stress changed with temperature in a manner which showed this property's dependence on both the flow stress (yield strength) and ductility. (See Fig 9 and 10.) This explains the rather slow decrease in fracture stress in the range below room temperature, where the relative change in ductility was also comparatively small. At lower temperatures the (average) fracture stress decreased at nearly a steady rate, to become slightly more than one half of the room temperature value at −196°C.

EFFECT OF PRESTRAINING AT ROOM TEMPERATURE ON THE FRACTURING CHARACTERISTICS AT VARIOUS LOW TEMPERATURES

Fig 11 shows the ductility values retained after specimens were prestrained various amounts in tension at room temperature and then tested to failure at various low temperatures.

The retained ductility values went through a minimum, the magnitude of which was proportionally larger the lower the testing temperature. Thus, for example, at −196°C the ductility dropped from 2½ pct with no prestrain to approximately 0.01 pct at

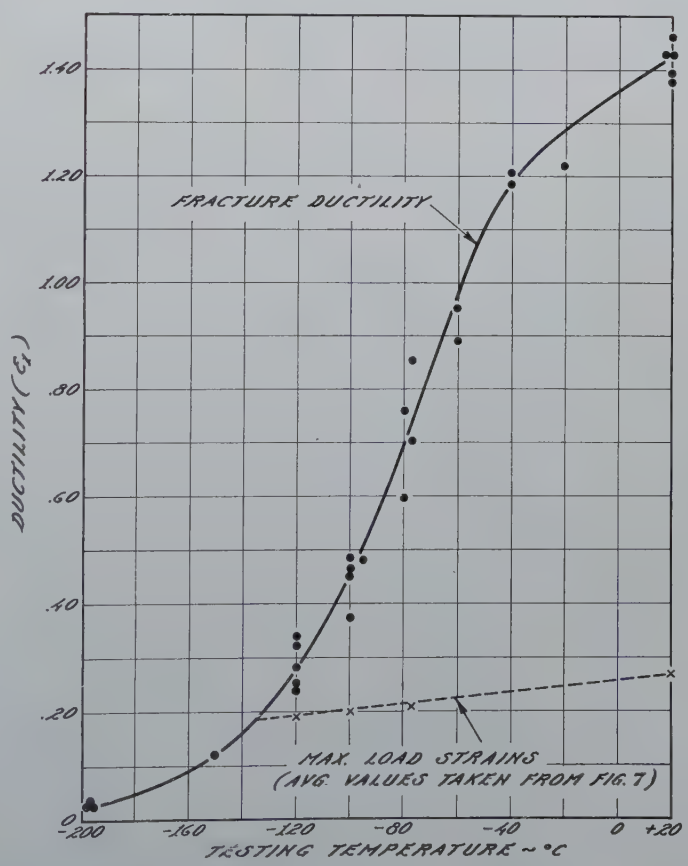

FIG 10—Effect of testing temperature on the ductility of a 2¾ pct Si steel.

* The pairs of stress-strain curves in Fig 8 represent tests obtained on pairs of randomly selected specimens at each temperature.

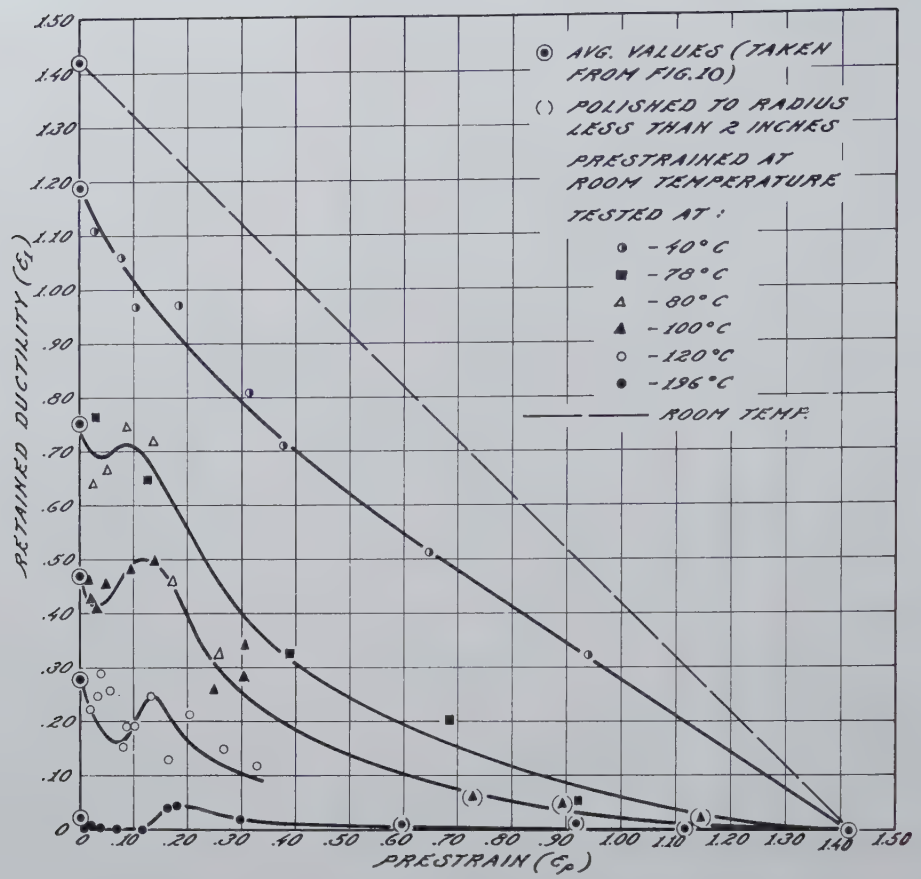

FIG 11—Effect of prestraining in tension at room temperature on the retained ductility at various low temperatures.

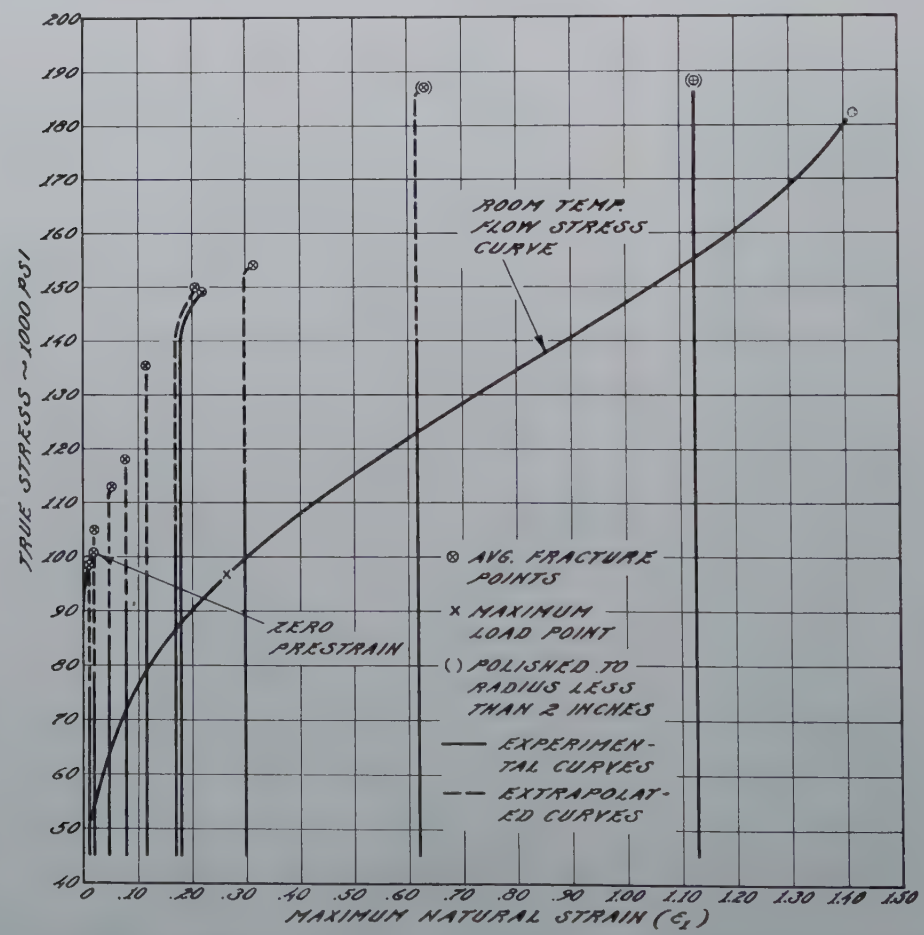

FIG 12—Effect of prestraining in tension at room temperature on the properties obtained at −196°C.

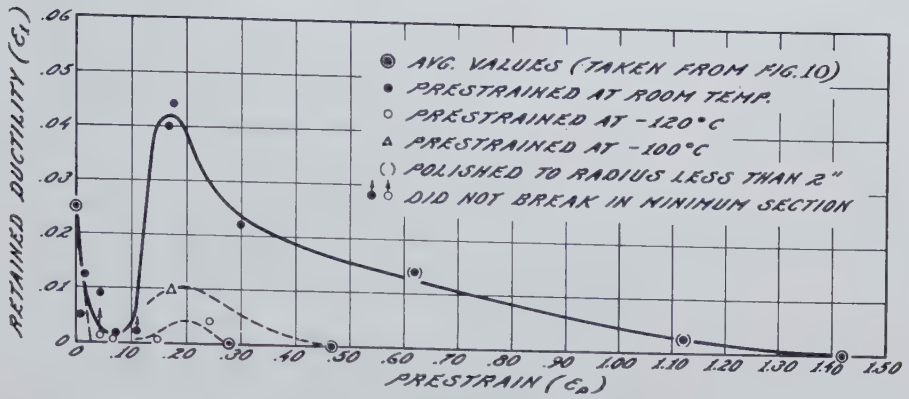

FIG 13—Effect of prestraining at various temperatures on the retained ductility at −196°C.

4 pct prestrain. At −100°C the ductility decreased from about 47 pct at zero prestrain to about 41 pct at a prestrain of 4 pct. At the highest temperature used in testing (−40°C), the minimum disappeared.

These curves also showed a maximum at the lower temperatures which gradually disappeared as the testing temperature was increased. At the lowest temperature used, −196°C, the maximum value of retained ductility (at 18 pct prestrain) was approximately 4 pct. This value was distinctly larger than the ductility of the unstrained metal which averaged only 2½ pct. It also appears that the prestrain value at which this maximum occurred moved to lower prestrains as the testing temperature was increased.

The data presented here confirmed previous test results in that a considerable ductility was generally retained at low testing temperatures even though the magnitude of the prestrains at the high temperature exceeded the total ductility of the steel at the (low) temperature of testing. Only when the prestrain approached its limiting value, that is, the ductility at room temperature, did the ductility retained at the testing temperature also approach zero. Thus, in the range of large prestrains the retained ductility decreased gradually from its maximum value to the value of zero at a prestrain equal to the room temperature ductility.

Fig 12 represents stress-strain curves obtained after prestraining at room temperature and testing at −196°C. These curves are plotted so that their position on the strain axis indicates the magnitude of prestrain. From these curves it can be seen that the points of fracture defined a smooth continuous function of the total strain. The considerable variations in retained ductility, therefore, affected the fracture stress only slightly. The decrease in fracture stress after small prestrains, frequently observed in previous investigations at −196°C, was therefore either absent or very small for the silicon steel. After prestrains larger than a few the percent, fracture stress increased rapidly with increasing prestrain up to a strain of $\epsilon_1 = 0.30$. After this value of prestrain, the increase in fracture stress became much slower. This can be explained by the increasing depth and sharpness of the neck beyond strains of $\epsilon_1 = 0.30$. Since the ductility retained at this temperature is quite small, the fracture stress should not only be a function of the strain, but also of contour (depth and sharpness) of the neck. Consequently, at high values of prestrain the specimen shape may account for the low fracture stress values.

EFFECT OF PRESTRAINING AT VARIOUS TEMPERATURES ON THE FRACTURE CHARACTERISTICS AT A CONSTANT LOWER TEMPERATURE

In Fig 13 the ductility retained at −196°C after prestraining at +20, −100, and −120°C, respectively, is plotted as a function of the prestrain. Small prestrains at any of these temperatures reduced the retained ductility to very small values which do not permit definite conclusions regarding any effect of the prestraining temperature. At larger prestrains, however, the ductility was found to be larger the

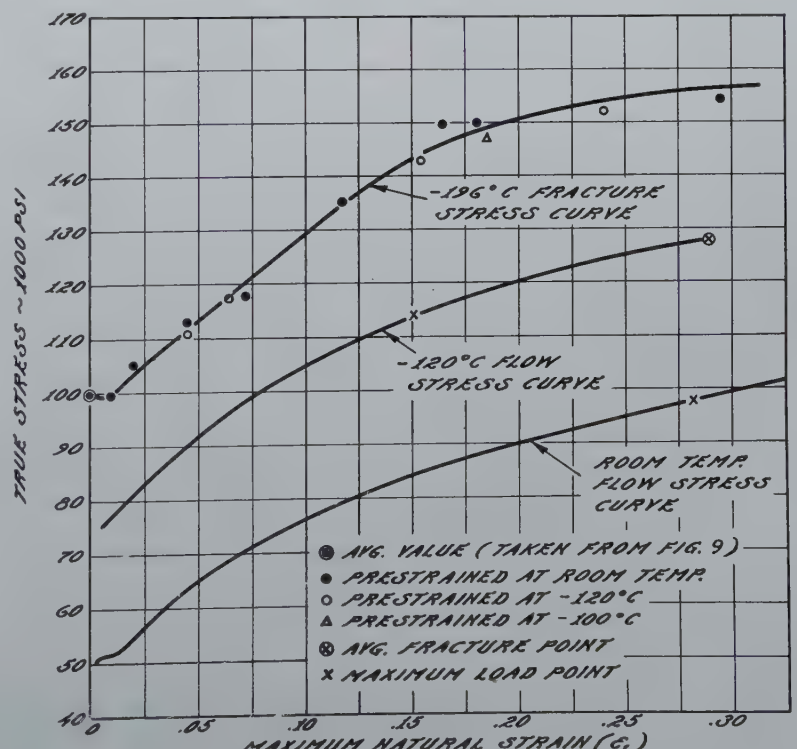

FIG 14—Effect of prestraining at various temperatures on the fracture stress at −196°C.

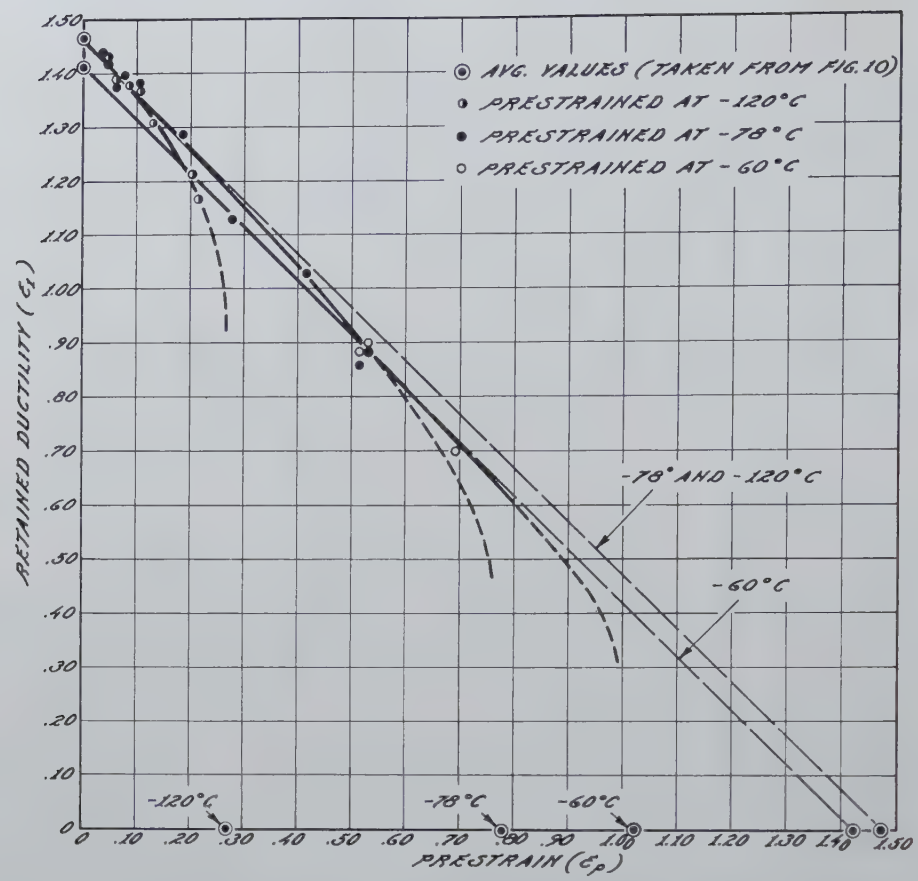

FIG 15—Effect of prestraining at various low temperatures on the retained ductility at room temperature.

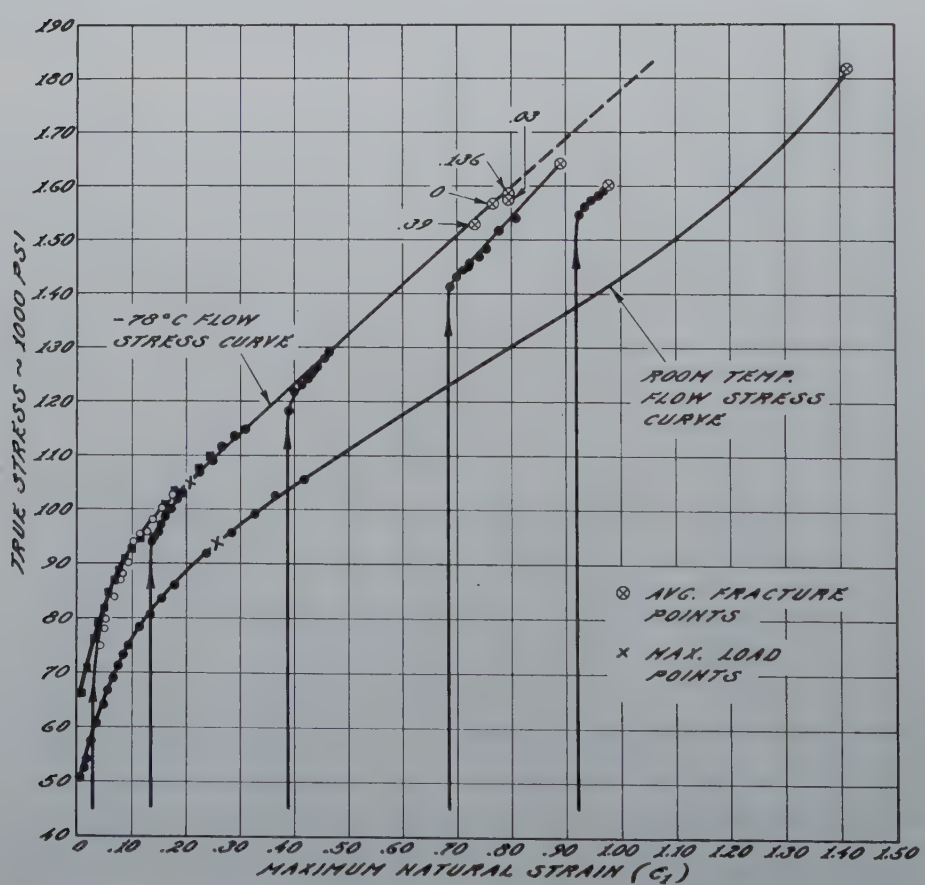

FIG 16—Effect of prestraining in tension at room temperature on the flow characteristics at —78°C.

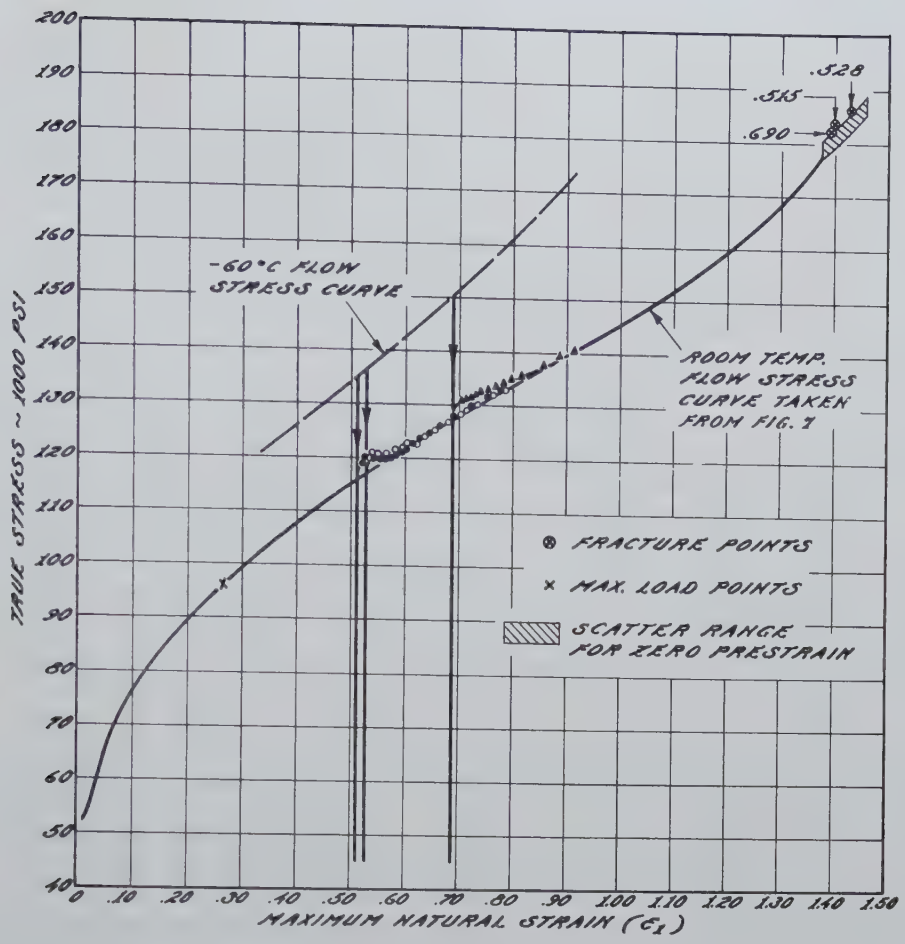

FIG 17—Effect of prestraining at −60°C on the flow characteristics at room temperature.

higher the prestraining temperature, as was to be expected from the results of the first group of tests discussed above.

Fig 14 shows the fracture stress values obtained in these three test series, at the temperature of −196°C. According to this graph, the fracture stress appears to be independent of the prestraining temperature, and only a function of the magnitude of strain. This would be in agreement with some data by Hollomon[11] in which a pearlitic steel was prestrained at various temperatures between −110 and +20°C and then tested at −190°C. However, from the fact that the ductility values appeared definitely dependent upon the temperature of prestraining, the conclusion must be drawn that this also applies to the fracture stress. On the other hand, these resulting differences in fracture stress would be very small for the small ductility values observed, assuming that the stress-strain curve is determined only by the magnitude of prestrain. As shown later, this assumption probably does not apply, and this may also cause differences in the fracture stress. Apparently, both these effects are of sufficiently small magnitude to be hidden in the general scattering of the test results.

EFFECT OF PRESTRAINING AT VARIOUS LOW TEMPERATURES ON THE FRACTURING CHARACTERISTICS AT A HIGH TEMPERATURE

The effects of prestraining at various low temperatures on the ductility retained at the high (room) temperature are shown in Fig 15. It appears that prestraining at any low temperature up to strains close to failure is no more damaging to the metal than if the same strain is accomplished at room temperature. The retained ductility values at room temperature decreased so that they were always equal to the total ductility in testing minus the prestrain. Only at high values of prestrain very close to the ductility of the steel at the temperature of prestraining did the straining appear slightly more harmful at the low temperature than the same strain would have been if the entire test had been conducted at room temperature. This applies to all three temperatures of prestraining.

Since the material used for the −60°C prestrains had slightly different properties than that used for the −78 and −120°C prestrains, two different 45° lines are given in Fig 15.

EFFECTS OF PRESTRAINING ON THE FLOW CHARACTERISTICS

The plastic flow characteristics of a metal are represented by the general shape of its stress-strain curve or, more specifically, by the initial value of the yield strength and the slope of the curve or strain-hardening rate. Consequently, an evaluation of the effect of prestraining on the flow characteristics was based on a determination of the effect of prestraining on these two characteristics. Furthermore, this analysis is based on the fact that straining at any single temperature simply uses up a portion of the initial stress-strain curve equivalent to the magnitude of the prestrain.

A number of stress-strain curves ob tained on the silicon steel after prestraining at a temperature higher than the testing temperature are given in Fig 16, and curves after prestraining at different temperatures lower than the testing temperature are presented in Fig 17 to 19. For reasons of clarity the fundamental changes in the stress-

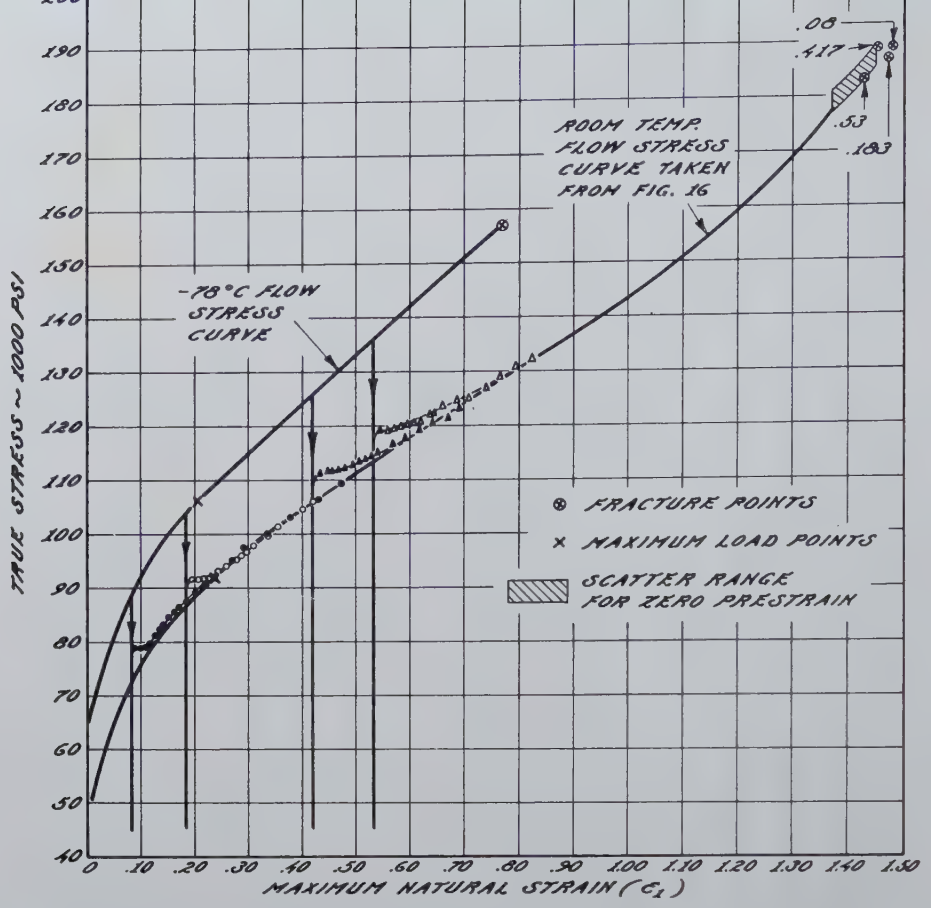

FIG 18—Effect of prestraining at −78°C on the flow characteristics at room temperature.

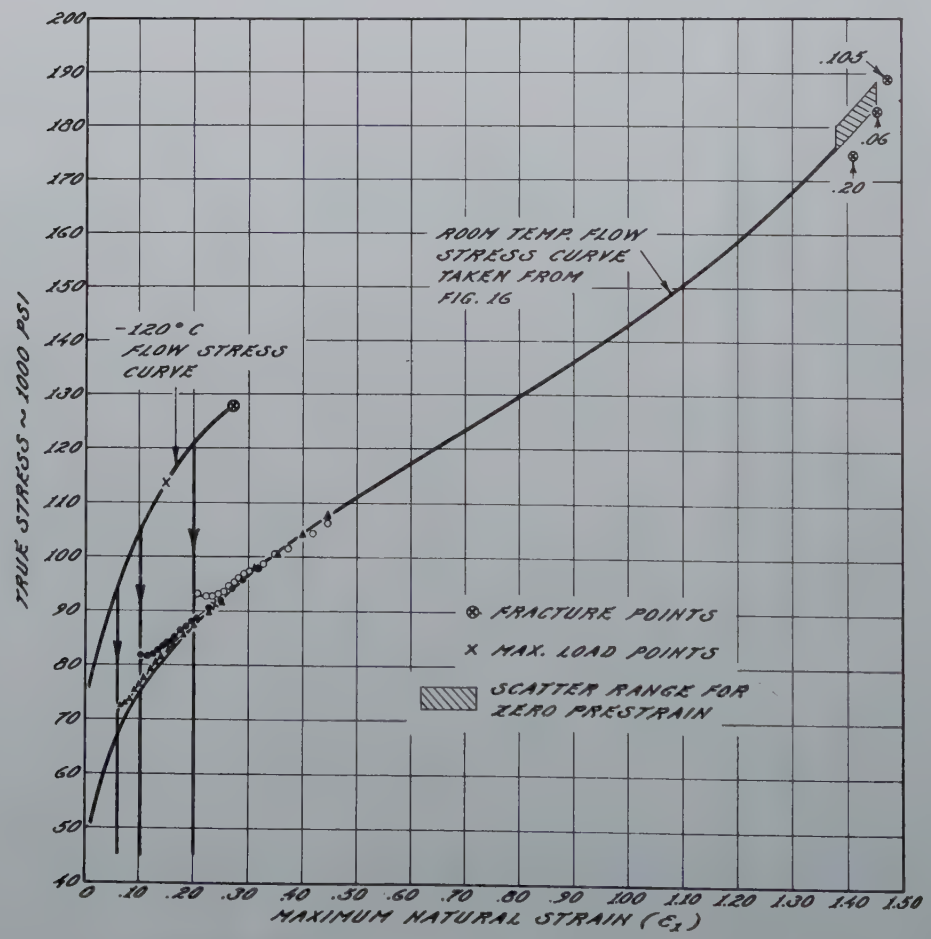

FIG 19—Effect of prestraining at −120°C on the flow characteristics at room temperature.

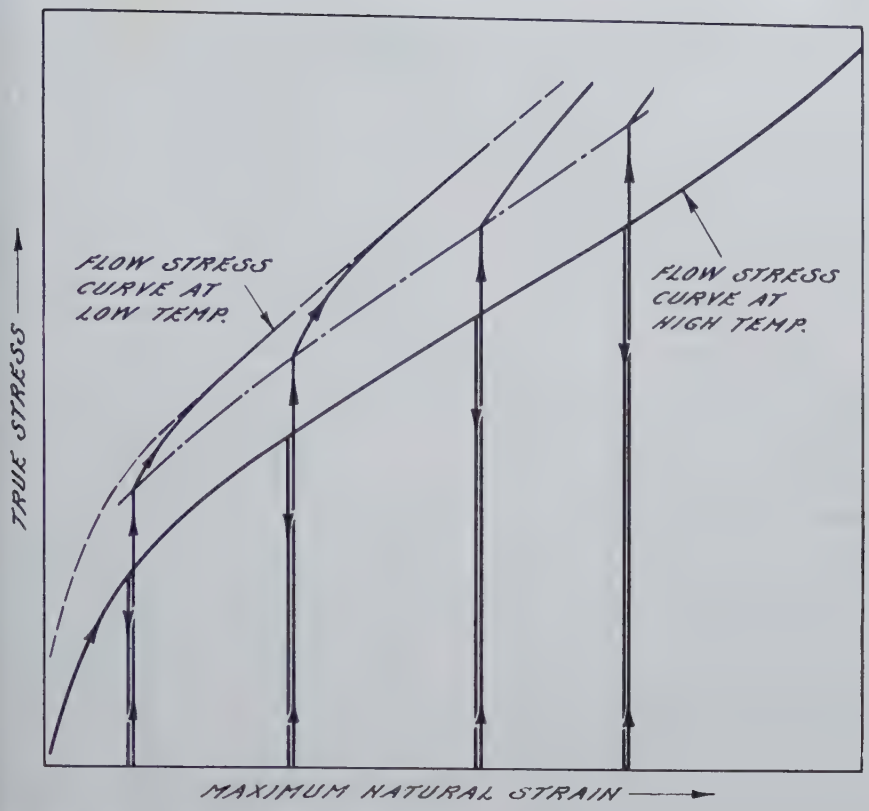

FIG 20—Schematic representation of the effect of prestraining at a high temperature on the flow characteristics at a lower temperature.

strain curves are also schematically shown in Fig 20 and 21. According to these graphs, prestraining at a temperature different from that of testing results in a stress-strain curve distinctly different from that obtained on straining at a constant temperature. These effects are in close qualitative agreement but possibly considerably smaller than those found in other metals.

It can be seen from Fig 16 and 20 that after prestraining at a relatively high temperature the yield strength at the low temperature is considerably reduced from the value that would have been obtained on straining at the low temperature. The subsequent rate of strain hardening, however, is larger after prestraining at the high temperature. Consequently, further straining in testing progressively reduces these deviations both in flow stress and in strain hardening. Both effects increase with increasing prestrain. Consequently, the deviations of the flow characteristics after high temperature prestraining from those after straining at the testing temperature disappear at comparatively small testing strains, if the prestrains are small.

According to Fig 17 to 19 and Fig 21, prestraining at a relatively low temperature causes effects diametrically opposite to those discussed above for prestraining at a relatively high temperature. The yield strength is raised and the rate of strain hardening is reduced.* Generally, however, these deviations disappear rather rapidly on further straining. It should be expected, furthermore, that the discussed effects increase with increasing difference between prestraining and testing temperature. The test results are not quite conclusive but, in general, in agreement with this expectation.

Conclusions

Based on the test data obtained on this silicon steel, certain conclusions can be drawn on the effect of straining a ferritic material at one temperature on the fracture and flow characteristics at some other temperature.

As far as the *fracturing characteristics after prestraining at a higher temperature than the testing temperature* are concerned, the phenomena observed in these tests are similar to those previously reported for annealed steels. Prestraining small amounts at room temperature caused the retained ductility values at a low testing temperature to pass through a minimum when

* This particular effect may result in a yield point jog which is illustrated more clearly in the conventional stress-strain diagrams in Fig 22, for the same tests illustrated by Fig 18.

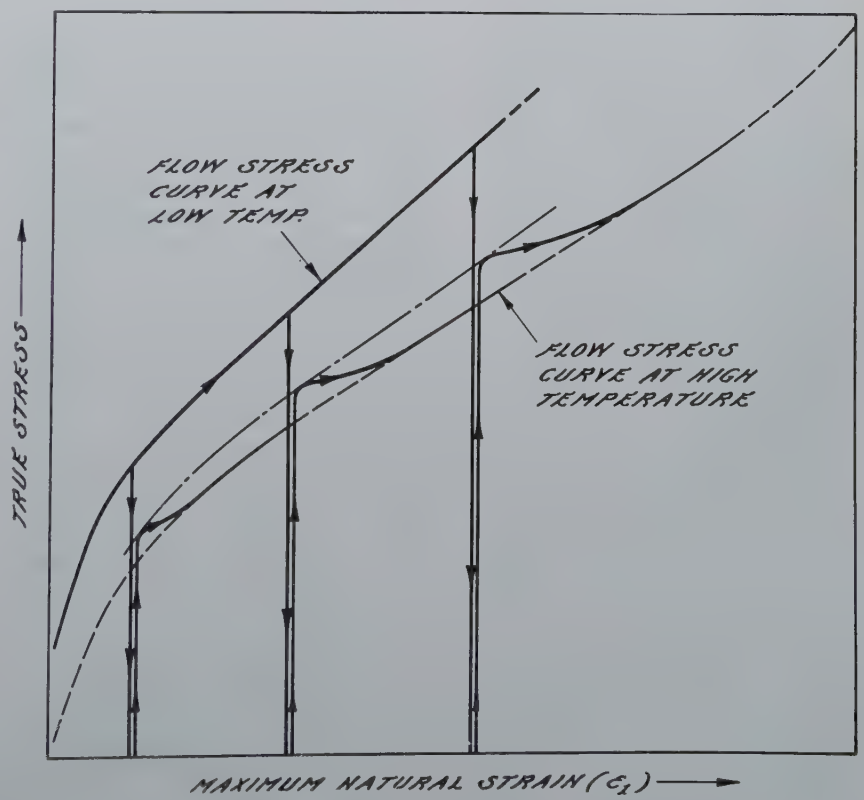

FIG 21—Schematic representation of the effect of prestraining at a low temperature on the flow characteristics at a high temperature.

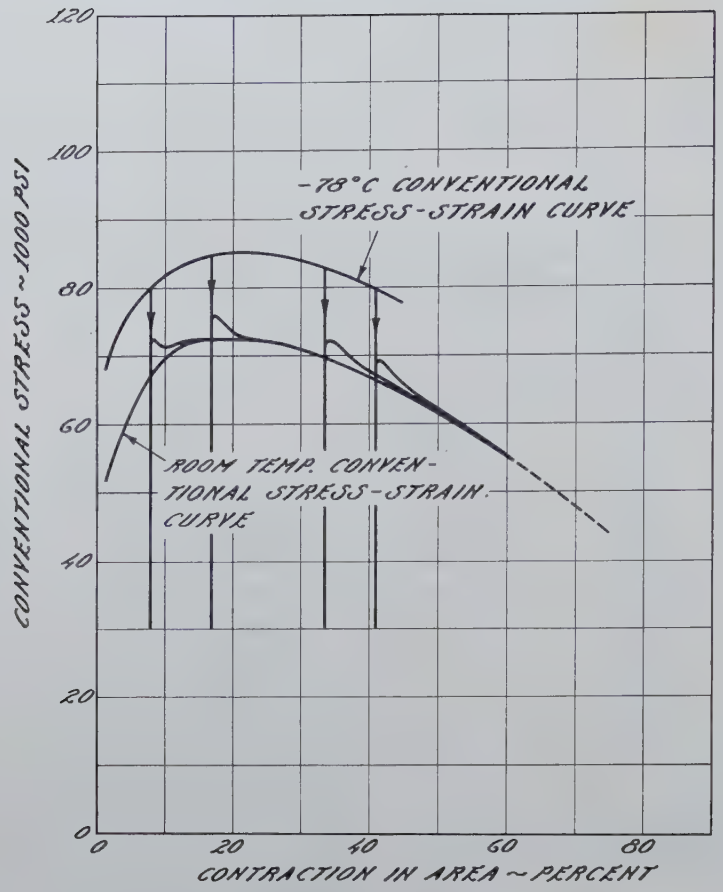

FIG 22—Effect of prestraining at −78°C on the conventional stress-strain characteristics at room temperature.

determined as a function of prestrain. The test data presented here further indicated that the magnitude of this minimum decreased as the temperature difference between the prestraining temperature and the testing temperature was decreased. This behavior of cold worked annealed steels was tentatively correlated with the phenomenon of an uneven yielding illustrated by the yield jog in a tensile test. The correlation was based on the assumption that plastic flow apparently becomes increasingly uniform (at small strains) with decreasing testing temperature.

At sufficiently large prestrains the retained ductility went through a maximum, after which it again decreased at a rate such that the retained ductility did not become zero until the ductility was completely exhausted in prestraining.

A few additional test data indicated that if cold worked material was tested at a low temperature at which the material was still ductile, the retained ductility at this temperature was found to be greater the greater the ductility under the conditions of prestraining.

The *fracturing characteristics after prestraining at a low temperature and testing at room temperature* appeared to obey a simpler law than that discussed above. It appeared that prestraining at any low temperature was no more harmful than the same magnitude of strain conducted at room temperature until the prestrain values were very close to failure, (Fig 15).

The effects of *prestraining at one temperature and testing at another temperature on the flow characteristics* for this annealed steel appeared to conform to the behavior of various other metals and alloys, which behavior was discussed in the Introduction. However, the magnitude of the effects was distinctly smaller for this ferritic material (body-centered cubic) than for other metals which crystallize in the face-centered cubic lattice. This can be tentatively correlated with the stress-strain curves, the general appearance of which is less changed with temperature for ferritic materials than for face-centered cubic metals.

The above investigation only reveals a small portion of the laws which govern the mechanical properties of a ferrous metal subjected to straining, under conditions where the temperature is not kept constant. So far, such practically important conditions have attracted little attention in the laboratory. The present investigation has shown clearly that no predictions can be made from any tests carried out at a constant temperature on the performance of the same metal when the strain-temperature history varies in a more general manner.

Acknowledgments

This work was conducted in cooperation with the Office of Naval Research to which the authors are indebted for permission to publish the report. The authors further wish to express their gratitude to Mr. L. J. Ebert for his suggestions, and to Mr. G. L. Tuer for his aid in the experimental work.

References

1. G. Sachs, et al: Mechanical Relations in Fracturing of Metals. In Cooperation with Office of Naval Research, U. S. Navy, N6ori-273, Task Order 1, Rep. No. 1, May 1947.
2. N. Davidenkov and P. Sakharov: On the Influence of Cold Working Upon the Brittleness of Steel. *Tech. Phys.*, USSR, (1938) **5**, 743–757.
3. P. W. Bridgman: Effects of High Hydrostatic Pressure on the Plastic Properties of Metals. *Rev. Mod. Phys.*, (1945) **7**, 3–14.
4. H. Scheele: Tensile Tests with Strain Restraint. *Arch. Eisenhuettenw.*, (1941) **14**, 513–519.
5. D. J. McAdam, Jr., G. W. Geil and R. W. Mebs: Influence of Plastic Deformation, Combined Stresses, and Low Temperatures on the Breaking Stress of Ferritic Steels. *Metals Tech.*, (Aug. 1947). TP 2220; *Trans.* AIME (1947) **172**.
6. J. H. Hollomon: The Mechanical Equation of State. *Metals Tech.*, (Sept. 1946). TP 2034; *Trans.* AIME (1947) **171**, 535.
7. E. Orowan: The Creep of Metals. West of Scotland Iron and Steel Inst. (Feb. 1947).
8. J. E. Dorn, A. Goldberg, T. E.Tietz: The Effect of Thermal-Mechanical History on the Strain Hardening of Metals. Univ. of Calif. In Cooperation with Office of Naval Research, U. S. Navy, Contract N7-onr-295, Task II, First Technical Rep.
9. G. Sachs, J. D. Lubahn and L. J. Ebert: Notched Bar Tensile Test Characteristics of Heat Treated Low Alloy Steels. *Trans.* Am. Soc. Metals, (1944) **33**, 340–395.
10. E. J. Ripling and G. Tuer: An Apparatus for Low Temperature Tensile Testing. *Products Eng.*, in print.
11. J. H. Hollomon: The Problem of Fracture. *Jnl.* Am. Welding Soc., Res. Suppl., (1946) **11**, 534–583.

Relation between Chromium and Carbon in Chromium Steel Refining

D. C. HILTY,* Member AIME

Introduction

It has long been known that in melting high-chromium steels, some of the carbon might be oxidized out of the melt without excessive simultaneous oxidation of chromium, and that higher temperatures favor retention of chromium. The advent of oxygen injection as a tool for rapid decarburization of a steel bath permits significantly higher bath temperatures, and it was quickly recognized that the use of oxygen injection facilitated the oxidation of carbon to low levels in the presence of relatively high residual chromium contents.

Up to the present time, however, specific data pertaining to the chromium-carbon-temperature relations in chromium steel refining have not been available. Individual steelmakers have evolved practices more or less empirically, but there has been very little real basis for predicting how effective any given practice can be in permitting maximum oxidation of carbon with minimum loss of chromium.

The current investigation, therefore, was undertaken in an effort to establish the fundamental carbon-chromium relationship in molten iron under oxidizing conditions. As reported below, the equilibrium constant and the influence of temperature on that constant have been derived for the iron-chromium-carbon-oxygen reaction in the range of chromium steel compositions with what appears to be a fair degree of precision. The practical application of the result will be obvious.

Experimental Procedure

The laboratory investigation was carried out on chromium steel heats melted in a magnesia crucible in a 100-lb capacity induction furnace at the Union Carbide and Carbon Research Laboratories. The charges for the heats consisted of Armco iron, low-carbon chromium metal, and high-carbon chromium metal, the relative proportions of which were calculated so that the various heats would contain from approximately 0.06 pct carbon and 8 pct chromium to 0.40 pct carbon and 30 pct chromium at melt-down. When the charges were melted, the bath temperatures were raised to the desired level, and the heats were then decarburized by successive injections of oxygen at the slag-metal interface through a ½-in. diam silica tube at a pressure of 30 psi. The duration of the oxygen injections was from 30 sec to 2 min. at intervals of approximately 5 to 30 min. It did not appear that length or frequency of the injection periods had any significant effect on the results; consequently, no effort was made to hold them constant and they were controlled only as was expedient to the general working of the heats. Between successive injections, the heats were sampled by means of a copper suction-tube sampler that yields a sound, rapidly-solidified sample representative of the composition of the molten metal at the temperature of sampling. This sampling device is a modification of the one described by Taylor and Chipman.[1]

An attempt was made to vary bath temperatures between samples, but it quickly became evident that, unless the variations were small or unless the new temperature was maintained for a minimum of 15 min. during which an injection of oxygen was made in order to accelerate the reactions, a very wide departure from equilibrium resulted. For most of the runs, therefore, temperature was maintained relatively constant at approximately 1750 or 1820°C. A few reliable observations at other temperatures, however, were obtained.

San Francisco Meeting, February 1949.

TP 2507 C. Discussion of this paper (2 copies) may be sent to *Transactions* AIME before April 1, 1949. Manuscript received-September 15, 1948.

* Research Metallurgist, Union Carbide and Carbon Research Laboratories, Inc., Niagara Falls, N. Y.

[1] References are at the end of the paper.

Temperature Measurement

The high temperatures involved in this investigation were measured by the radiation method, utilizing a Ray-O-Tube focused on the closed end of a refractory tube immersed in the metal bath. The immersion tubes employed were high-purity alumina tubes specially prepared by the Tonawanda Laboratory of The Linde Air Products Co. These tubes were quite sturdy under reasonable mechanical stress at high temperature. They were unusually resistant to thermal shock, and chemical attack on them by the melts was slow. With care, it was found possible to keep these tubes continuously immersed in a heat for as long as 5 hr at temperatures up to 1850°C, before failure by fluxing occurred.

The Ray-O-Tube—alumina tube assemblage was similar to those supplied commercially for lower temperature applications. In operation, the alumina tube was slowly immersed in the molten metal to a depth of approximately 5 in., and the device was then clamped solidly to a supporting jig where it remained for the duration of the run. A photograph of the equipment, in operation with Ray-O-Tube in place and oxygen injection in progress, is shown in Fig 1.

When in position in a heat, the instrument was calibrated by means of an immersion thermocouple and an optical pyrometer. For calibration through the range of temperatures from 1500 to 1650°C, a platinum — platinum + 10 pct rhodium thermocouple in a silica tube was immersed alongside the alumina tube. Output of the Ray-O-Tube in millivolts and the

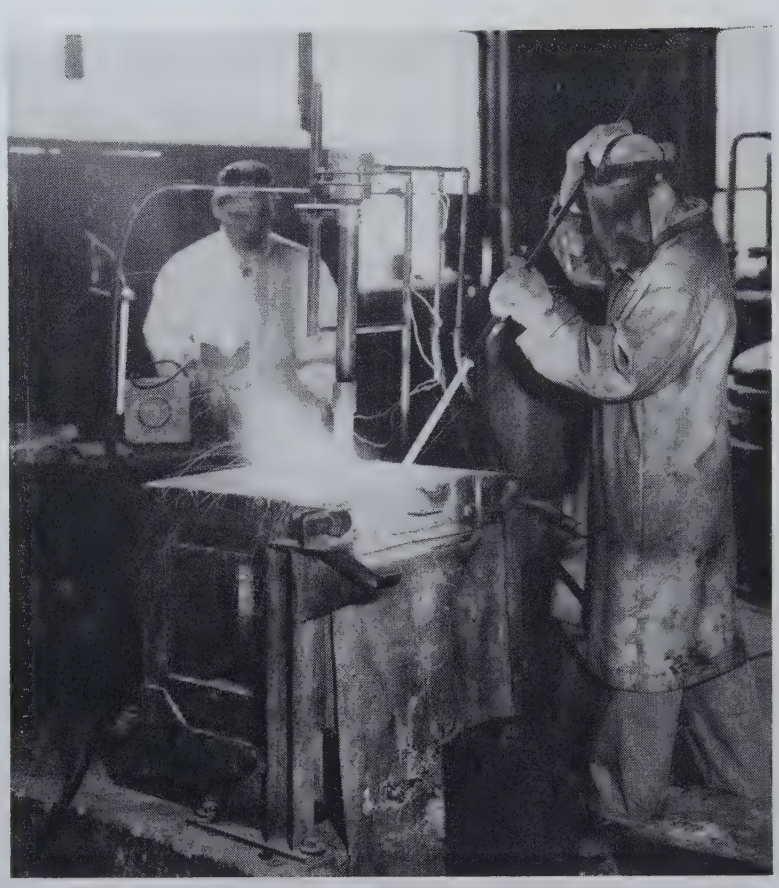

FIG 1—Experimental setup employed.

temperature indicated by the thermocouple were plotted logarithmically. At the same time, the optical pyrometer was standardized against the thermocouple by removing the Ray-O-Tube from its holder and sighting the optical pyrometer on the end of the alumina tube. The calibration was then extended to temperatures above 1650°C with the optical pyrometer.

It was observed that the depth of immersion of the alumina tube had a definite effect on the calibration of the Ray-O-Tube. This was probably at least partially due to the fact that the Ray-O-Tube was equipped with a lens that covered too large a field for the diameter of the alumina tube; but since the Ray-O-Tube was calibrated for each individual run, and the calibration was checked during the course of the runs, possible error due to the depth of immersion effect is considered to have been minimized.

A typical calibration curve is illustrated in Fig 2. It is evident that a fairly accurate calibration was obtained. From this and the calibration curves for the other heats, it appeared that most of the temperature measurements were within +10°C of the actual temperature.

Observations and Determination of Equilibrium Constant

The carbon and chromium contents and the temperatures of the samples obtained are listed in Table 1 and were plotted to give the equilibrium curves shown in Fig 3.

The oxidation of carbon from a steel bath containing chromium is limited by the simultaneous oxidation of the chromium. Whether decarburization is carried out by ore additions or by injection of gaseous oxygen, the oxygen content of the bath is limited by the formation of an oxide of chromium. Up to the present time, it has been assumed that this oxide is either Cr_2O_3 or $FeO{\cdot}Cr_2O_3$, and that at one atmosphere pressure of carbon monoxide the limiting reaction is

$$Cr_2O_3 \text{ (solid)} + 3\underline{C}^* = 2\underline{Cr}^* + 3CO_{(g)} \quad [1]$$

or

$$FeO\ Cr{\cdot}O_3 \text{ (solid)} + 4\underline{C} = 2\underline{Cr} + 4CO_{(g)} + Fe, \quad [2]$$

so that the equilibrium constant would be approximately defined as

$$K_1 = \frac{\text{pct Cr}^2}{\text{pct C}^3} \quad [1a]$$

* Conventionally, underlining of the symbols in a steelmaking reaction indicates that those substances are dissolved in the iron.

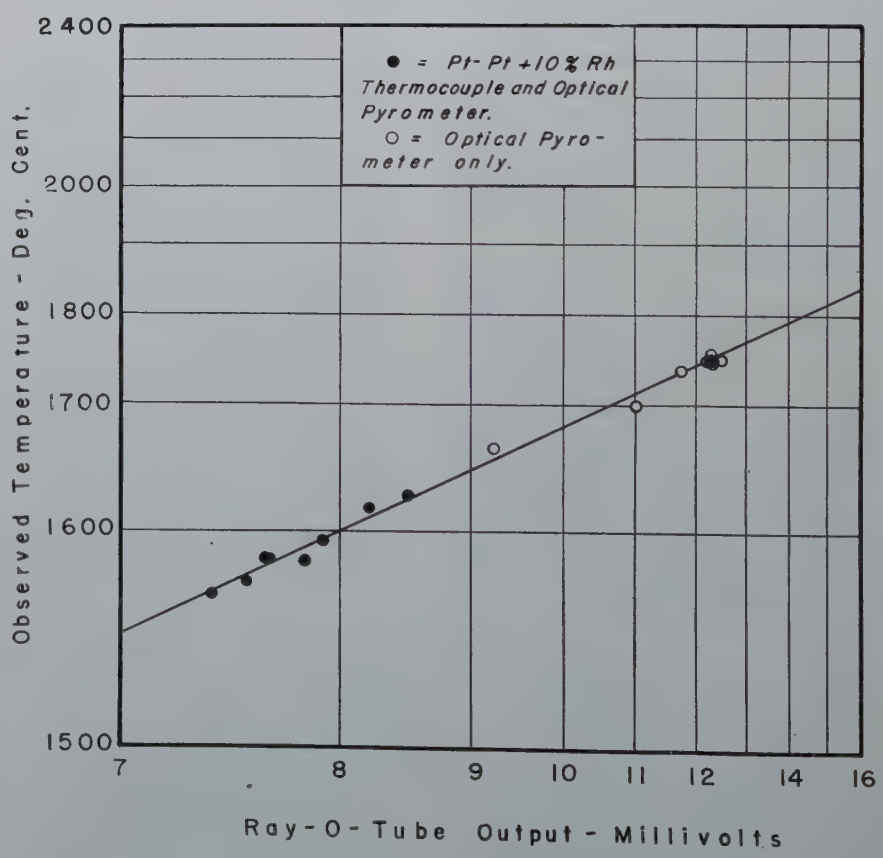

FIG 2—Typical Ray-O-Tube calibration curve.

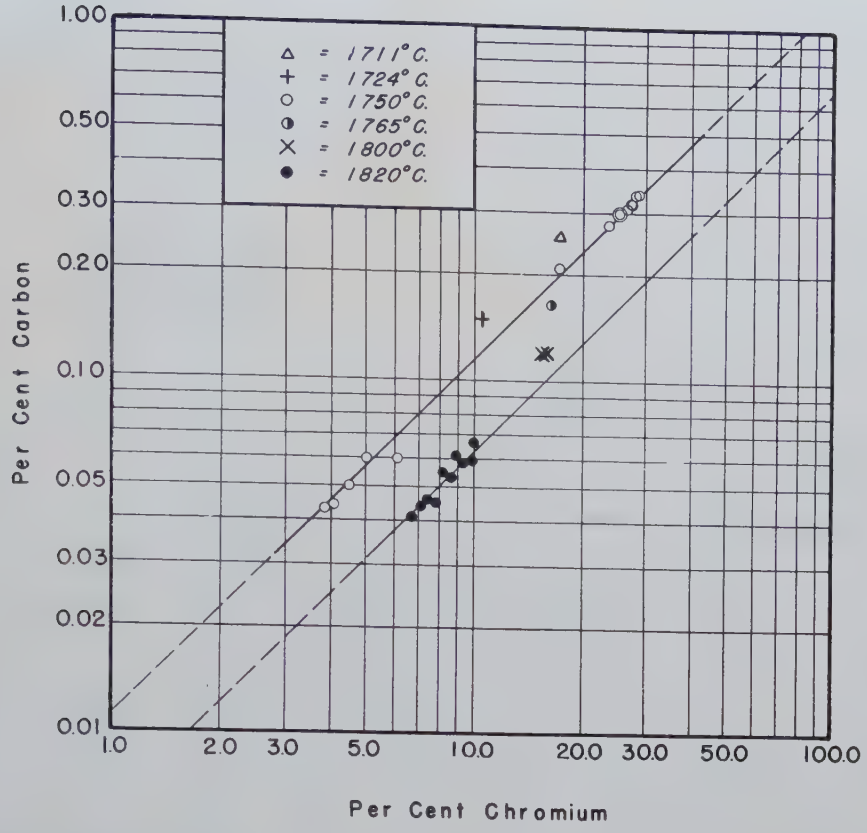

FIG 3—Relation of chromium to carbon in molten chromium steel at constant temperature.

Table 1 . . . Carbon and Chromium Contents and Temperature

Heat No.	Sample No.	Temperature °C	Carbon Per Cent	Chromium Per Cent	$K = \frac{\text{Pct Cr}}{\text{Pct C}}$
C-1	1	1711	0.26	17.19	6.62×10^1
	2	1750	0.21	17.19	8.19×10^1
	3	1765	0.17	16.37	9.63×10^1
	4	1802	0.12	15.79	1.31×10^2
	5	1800	0.12	15.40	1.28×10^2
C-2	1	1724	0.15	10.42	6.96×10^1
	2	1820	0.067	9.94	1.48×10^2
	3	1822	0.059	9.86	1.67×10^2
	4	1826	0.058	9.28	1.60×10^2
	5	1822	0.061	8.90	1.46×10^2
	6	1822	0.053	8.61	1.62×10^2
	7	1822	0.055	8.19	1.49×10^2
	8	1822	0.045	7.83	1.74×10^2
	9	1822	0.046	7.40	1.61×10^2
	10	1822	0.044	7.13	1.62×10^2
	11	1822	0.041	6.72	1.64×10^2
C-3	1	1746	0.060	6.12	1.02×10^2
	2	1748	0.060	5.00	8.34×10^1
	3	1750	0.050	4.50	9.00×10^1
	4	1749	0.044	4.09	9.28×10^1
	5	1749	0.043	3.85	8.96×10^1
C-4	1	1744	0.34	28.12	8.26×10^1
	2	1747	0.34	27.74	8.16×10^1
	3	1751	0.32	27.33	8.54×10^1
	4	1748	0.32	27.17	8.48×10^1
	5	1748	0.31	26.45	8.52×10^1
	6	1748	0.30	25.37	8.46×10^1
	7	1748	0.30	25.31	8.45×10^1
	8	1752	0.29	24.60	8.48×10^1
	9	1752	0.28	23.61	8.45×10^1

or $$K_2 = \frac{\text{pct Cr}^2}{\text{pct C}^4} \qquad [2a]$$

These assumptions, however, are not supported by the present experimental evidence. The slope of the curves in Fig 3 is approximately unity, a fact which strongly indicates that the actual constant is expressed by the equation,

$$K = \frac{\text{pct Cr}}{\text{pct C}} \qquad [3a]$$

Equilibrium constants calculated according to Eq 3a are given in the last column of Table 1. It is evident that at constant temperature these K's are truly constant well within the limits of experimental error.

Two explanations for this departure from the previously accepted hypothesis described by reactions 1 or 2 are suggested. The first is that reactions 1 or 2 do actually represent the equilibrium involved, but that the activity of carbon dissolved in the melt is greatly reduced by the presence of chromium so that it is not proportional to the concentration. This, of course, is possible and is in accordance with the principles of classical thermodynamics; but it seems somewhat improbable in a system that is in reality very far from being saturated with chromium carbides, in view of the magnitude of the effect at moderate chromium concentrations.

The second explanation presumes that the oxide of chromium directly involved is not Cr_2O_3 but CrO, so that the reaction is

$$CrO + \underline{C} = \underline{Cr} + CO_{(g)}, \qquad [3]$$

the nonmetallic phase being saturated with CrO and the CO pressure being approximately one atmosphere. At the temperatures of the experiments, the postulation of chromium monoxide does not appear to be unreasonable; it has previously been employed by Chen and Chipman[2] to account for some of the discrepancies observed in a study of the iron-chromium-oxygen system; CrO was suggested by Clark[3] as the oxide of chromium formed during the decarburization of chromium steel heats by magnetite ore; and according to Körber and Oelsen,[4] chromous oxide is the chief oxide of chromium occurring in acid slags in contact with molten iron-chromium alloys. Moreover, reaction 3 fits the observations without any complications regarding the activities of carbon or chromium. It is, therefore, considered that reaction 3 and Eq 3a are the most probable representations of the limiting equilibrium in the refining of chromium steels.

Effect of Temperature

The equilibrium constants calculated by Eq 3a were plotted logarith-

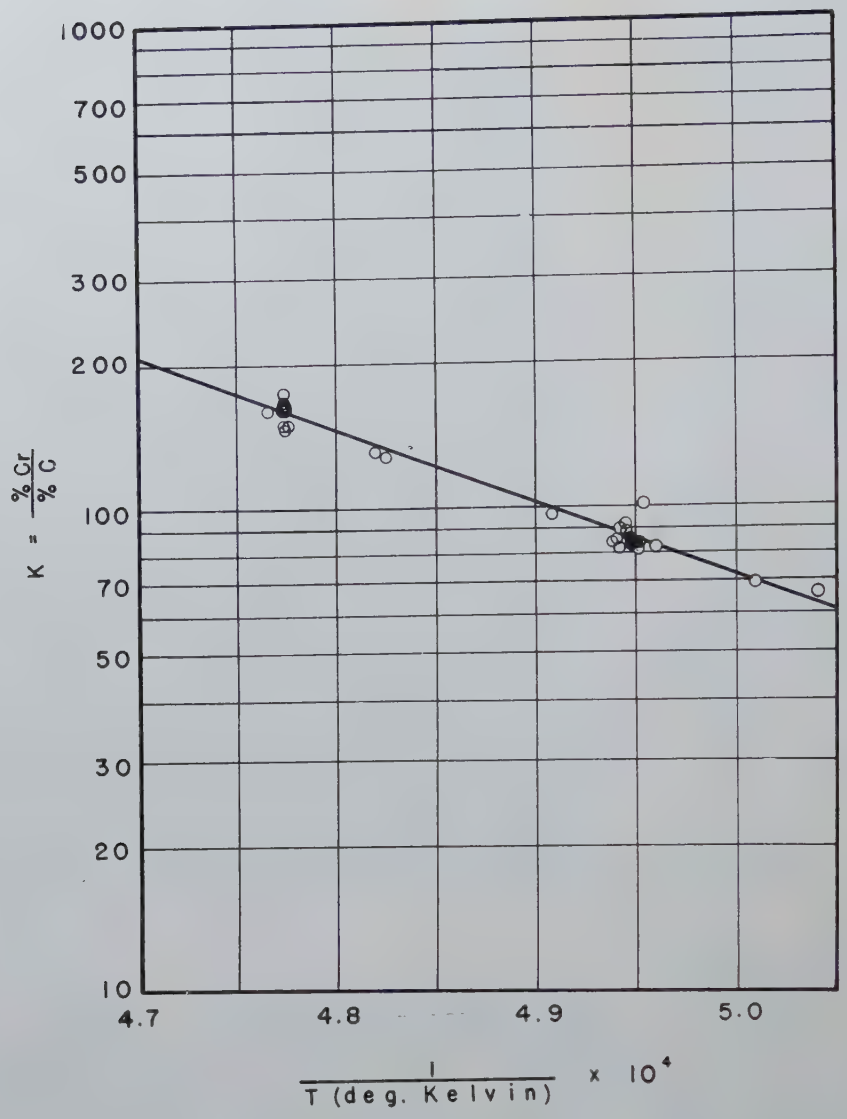

FIG 4—Effect of temperature on the equilibrium constant, $K = \frac{\text{Pct Cr}}{\text{Pct C}}$.

mically against the reciprocal of the absolute temperature as illustrated in Fig 4.

The equation of the resulting curve is calculated to be

$$\text{Log } K = -\frac{15{,}200}{T} + 9.46, \quad [4]$$

in which T is the absolute temperature in degrees Kelvin.

If published[5] thermal data for the carbon-oxygen reaction and the solution of chromium in molten iron be combined with the heat of reaction 3 calculated from Eq 4, a value of −106,750 cal per g mol is obtained for the heat of formation of CrO from the elements. This heat of formation, of course, is subject to considerable uncertainty, but it appears to be quite reasonable; it is of the same order of magnitude as the heat of formation of manganous oxide, MnO, as, presumably, it should be. Therefore, it seems to be additional evidence in support of the hypothesis stated by reaction 3.

With Eq 4, the carbon-chromium relationship in liquid chromium steel under oxidizing conditions can be calculated for any temperature. This was done for what was believed to be the probable range of steelmaking temperatures as shown in Fig 5. For convenience, the temperatures appearing in Fig 5, and subsequently in this paper, have been converted to Fahrenheit scale in accordance with accepted commercial usage. ??

Several random observations of chromium and carbon contents at the end of the oxidizing period in commercial arc-furnace heats were available and these were superimposed on the curves of Fig 5 in order to estimate the temperatures attained in commercial practice. Fig 6 illustrates the result.

From Fig 6, it is evident that the heats refined by conventional oreing methods attained temperatures averaging approximately 3025°F. As would be expected, heats made by oxygen practice were considerably hotter—large heats averaging 3275°F and small heats (less than 12 tons) about 3375°F. The maximum temperature appears to be on the order of 3400°F. In this connection, it is notable that in two of the heats, shown in Fig 6 as attaining temperatures close to 3400°F, serious damage to the furnace refractories occurred.

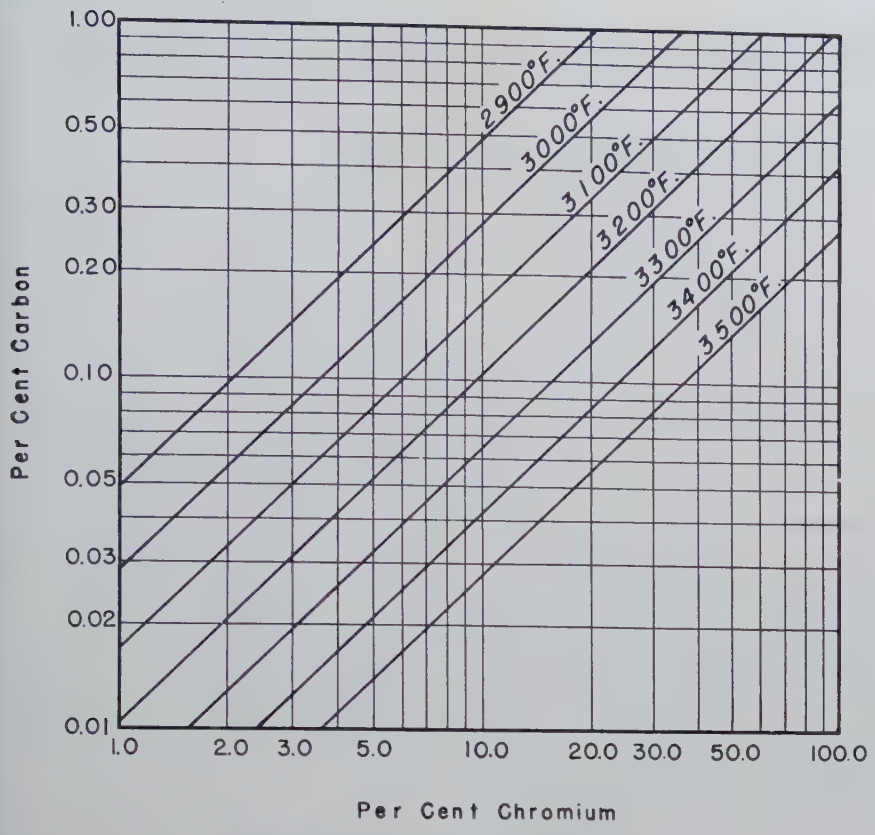

FIG 5—Chromium-carbon relation in chromium steel refining.

Conclusions

The conclusions drawn from this investigation are as follows:

1. It has been found that at constant temperature the relation between carbon and chromium in chromium steel refining can be expressed by the equilibrium constant,

$$K = \frac{\text{pct Cr}}{\text{pct C}}$$

2. The probable reaction is believed to be:

$$CrO_{(sat.)} + \underline{C} = \underline{Cr} + CO_{(g)}$$

3. The effect of temperature on the relation has been derived and may be defined by the equation:

$$\text{Log } K = -\frac{15{,}200}{T} + 9.46$$

Acknowledgments

The author is indebted to Walter Crafts, Chief Metallurgist of the Union Carbide and Carbon Research Laboratories, Inc., and to John Chipman, Professor of Metallurgy, Massachusetts Institute of Technology, who contributed many helpful suggestions and reviewed the data and manuscript.

Appreciation is also extended to J. J. Darby and J. J. Mikula who assisted in securing the data from the experimental melts.

References

1. C. R. Taylor and John Chipman: Equilibria of Liquid Iron and Simple Basic and Acid Slags in a Rotating Induction Furnace. *Trans.* AIME (1943), **154**, 228–245.
2. Hsin-Min Chen and John Chipman: The Chromium-oxygen Equilibrium in Liquid Iron. *Trans.* A.S.M. (1947), **38**, 70–112.
3. Donald Clark: Reduction of Carbon in Presence of Chromium. *Proc.* Elect. Furnace Steel Conf. (1946), **4**, 134–135.
4. F. Körber and W. Oelsen: Reactions of Chromium with Acid Slags. *Mitt. k. w. Inst. f. Eisenforshung.* (1935) **17**, 231–245. Düsseldorf.
5. Basic Open Hearth Steelmaking. Chap. 13 and 16. (1944) AIME.

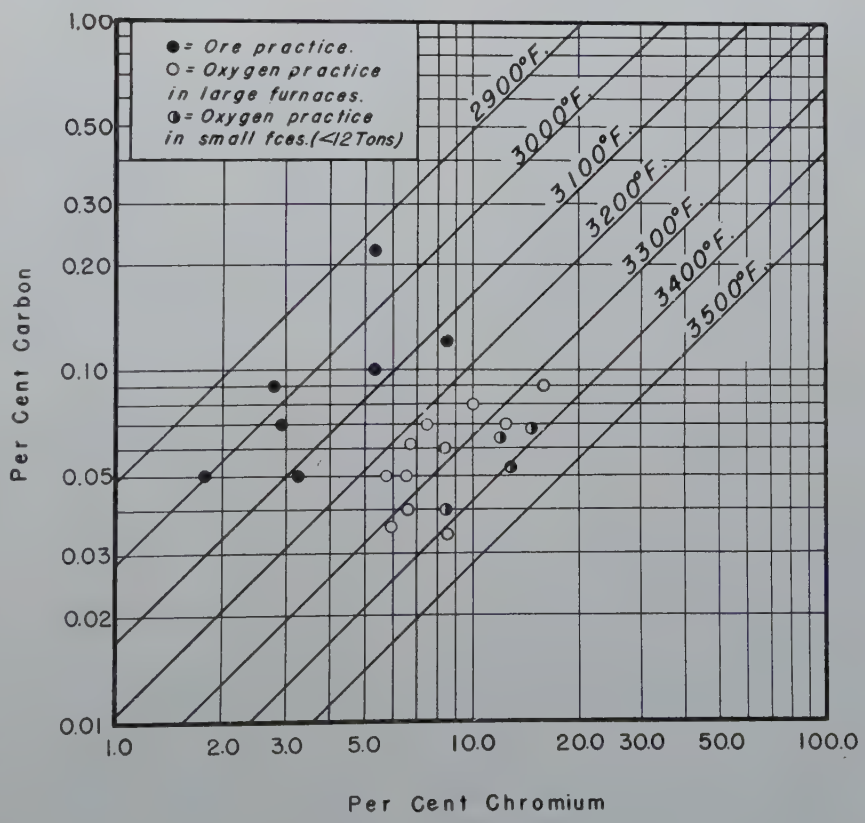

FIG 6—Indicated temperatures at end of oxidizing period in commercial heats made by ore and by oxygen practices.

The Densification of Copper Powder Compacts in Hydrogen and in Vacuum

CHARLES B. JORDAN* and POL DUWEZ*

Introduction

THE phenomenon of the change of volume of pressed powder compacts upon sintering is well known in the field of powder metallurgy. Depending upon the metal or metals involved and the pressure used in forming, a compact may, in the course of time of sintering at a given temperature, expand monotonically, contract monotonically, or first show a volume change of one sign followed by a change of the opposite sign. It is clearly desirable to have accurate knowledge of the magnitude and sign of the change in dimensions to be expected in any given case, both from the point of view of direct usefulness in the fabrication of parts by powder metallurgy, and from the longer range viewpoint of elucidating the fundamental mechanism of metallic sintering.

The present study was therefore undertaken as a first step in acquiring systematic and reasonably quantitative knowledge of the change in density of metal powder compacts during sintering. For practical reasons, copper was selected as the material to be studied first, and its densification followed as a function of temperature and time of sintering in hydrogen and in vacuum.

Experimental Procedure

The copper powder used was that designated by the manufacturer (Metals Disintegrating Co., Elizabeth, N. J.) as MD-151. This powder was sifted through Tyler standard screens to separate the fraction having particle size range between 200 mesh and 325 mesh, and this fraction was used in all the subsequent work. Compacts weighing about 10 g were then pressed in a 1 in. diam round die, using a pressure of 20,000 psi throughout.

Sintering was carried out in commercially built electric furnaces in which the resistance windings are so disposed as to produce a nearly uniform temperature along the axis of the furnace for a length of about 18 in. centrally located. In order to be able to sinter in a controlled atmosphere, a 2 in. stainless steel tubing was inserted in the furnace. Each end of the tube was cooled by a water jacket about 7 in. long, and closed with a rubber stopper. The hydrogen used for one series of specimens was purified as described in Ref. 1. For the other set, a pressure of about 0.5 mm Hg was maintained during sintering by a Welch Duo-Seal pump.

The specimens were heated on square trays made of stainless steel. In placing specimens in the trays, a thin even layer of powdered aluminum oxide was first sprinkled on the bottom of the tray. A copper guard disk about half the thickness of the specimen was then placed in the tray and covered with a second layer of alumina. The actual specimen was then set on the guard disk, and a final coat of alumina sprinkled over the specimen.

This technique was evolved for sintering the specimens in such a way as to reduce the influence of unknown extraneous factors to a minimum. If the specimen is placed directly on the tray and sintered, it is found that the resulting shape is that of a frustum of a cone, rather than a section of a right circular cylinder, since friction with the tray prevents the bottom of the specimen from contracting at the same rate as the top. In the arrangement used in these experiments, the guard disk provided a support which shrank at the same rate as the specimen, and the alumina powder reduced to a minimum friction between guard disk and tray, and between specimen and guard disk.

The procedure followed in sintering consisted of bringing the furnace to the required temperature, and then inserting the specimen into the central heated portion of the furnace tube in one of the two atmospheres used. At the end of the heating period, the specimen was cooled by bringing it into a portion of the furnace surrounded by a water jacket. These manipulations were carried out without opening the furnace, by means of rods which were attached to the trays and operated through a sliding seal in the rubber stopper.

The progress of densification of the copper compacts was studied at 1300, 1400, 1500, 1600, 1700, and 1800°F. At each of these temperatures, a specimen was allowed to sinter for each of the following time intervals: ½, 1, 2, 4, 8, 16, 32, and 64 hr. The thickness and diameter of each specimen were measured with micrometers before and after sintering, and each was weighed on an analytical balance after sintering.

Results

The techniques described in the preceding section were found to give satisfactory results. The specimens were not detectibly warped after sintering, and were usually of uniform diameter (that is, truly round) to within ±0.001 in., a very few showing a variation in diameter of ±0.002 in. All specimens were found to have the same diameter

San Francisco Meeting, February 1949.

TP 2516 E. Discussion of this paper (2 copies) may be sent to *Transactions* AIME before May 15, 1949. Manuscript received November 3, 1948.

* Research Engineer and Associate Professor of Mechanical Engineering and Chief of the Materials Section, respectively, Jet Propulsion Laboratory, California Institute of Technology, Pasadena, Calif.

References are at the end of the paper.

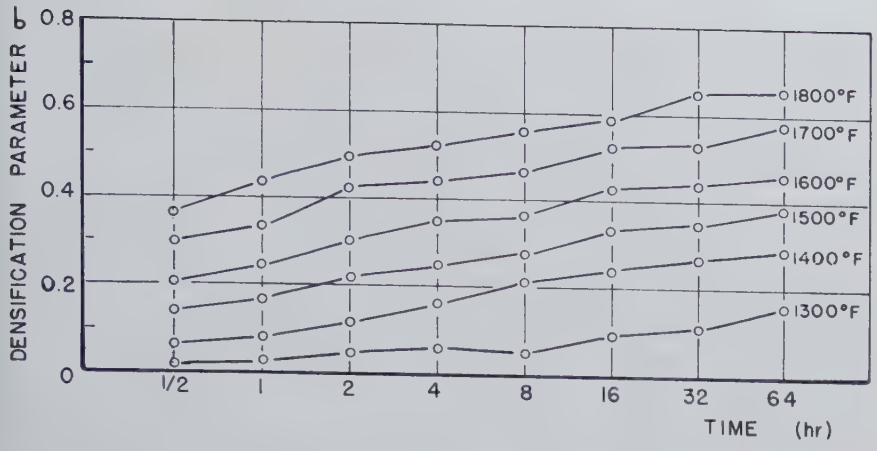

FIG 1—Densification parameter vs. sintering time in hydrogen.

before sintering (namely, 1.039 in.) as was to be expected, since all were pressed in the same die. It was not possible to maintain the same uniformity in thickness, because of slight variations in the amount of powder weighed out, and because of friction in the die during pressing. However, the variation in thickness at various points on a given specimen did not exceed ± 0.004 in., and variations from one specimen to another were of no importance, since the change in dimensions of each was followed separately.

From the measured values of mass, thickness, and diameter of each specimen before and after sintering, the value of the "densification parameter" (defined and explained in the next section of this paper) was calculated. The values of this parameter are plotted as a function of time for the various temperatures used in Fig 1 and 2.

The error introduced by filing the edges of the specimen also requires some consideration. In computing the density, the volume of each specimen was calculated from the measured thickness and diameter, assuming the specimen to be a right circular cylinder. Because of the chamfered edges, the calculated volume will obviously be larger than the true volume, and when used in conjunction with the true mass will give too low a value for the density. In order to estimate this error, several specimens were weighed before and after chamfering. It was found that the specimens which were filed lightly (duplicating conditions of the actual test specimens on which densification measurements were made) lost about 0.5 pct of their mass, while a specimen which was deliberately filed much more heavily than any of those used in the actual tests lost about 1 pct of its mass. This error was therefore considered negligible.

Interpretation of Results

Although the work described in this report was primarily undertaken as an investigation of the sintering of metals, it is important to note that the process actually observed is not one of pure sintering. When a powdered metal compact is heated, not only do the particles gradually bond together, but also the overall volume changes. In the case of the present work on copper, a monotonic shrinkage is observed, the porosity progressively decreasing and the voids becoming smaller and fewer. Evidently this process involves mechanisms other than those of sintering; for example, the overcoming of pressure in the voids due either to gas trapped during pressing, or to volatile impurities present. For this reason, it is more accurate to refer to the progressive shrinkage of copper compacts studied in this work as "densification" rather than as "sintering," since sintering is not the only process taking place. Nevertheless, it is possible to obtain information about sintering by this type of experiment, and it is moreover of practical importance to study sintering under the conditions which exist in the case of powdered metals.

The maximum density which a powder compact can attain is obviously that of the solid metal. This circumstance provides a natural scale on which the progress of densification can be measured. By comparing the observed change in density with the maximum possible change, a convenient dimensionless parameter is obtained, the value of which is initially zero and which becomes unity if the compact attains its maximum possible density.

Discussion of Technique

The method of cooling used may appear inadequate in view of the precautions commonly taken in metallurgical work to obtain a very rapid quench. It must be remembered, however, that there is no question of retaining a high temperature structure in the experiments described in this report, and that the only reason for quenching is to define the time of sintering. The water-jacket cooling used certainly accomplishes this end with no greater error than that necessarily introduced at the start of sintering by the time required for the specimen to heat to the required temperature, and possesses the great advantage of keeping the specimen flat and round.

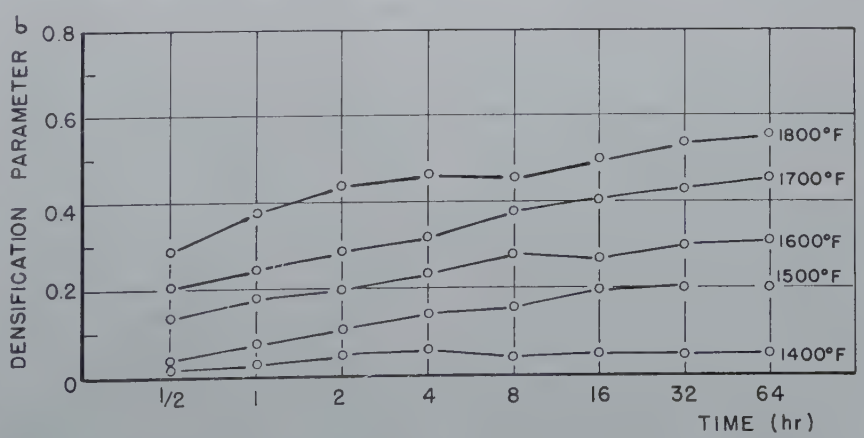

FIG 2—Densification parameter vs. sintering time in vacuum.

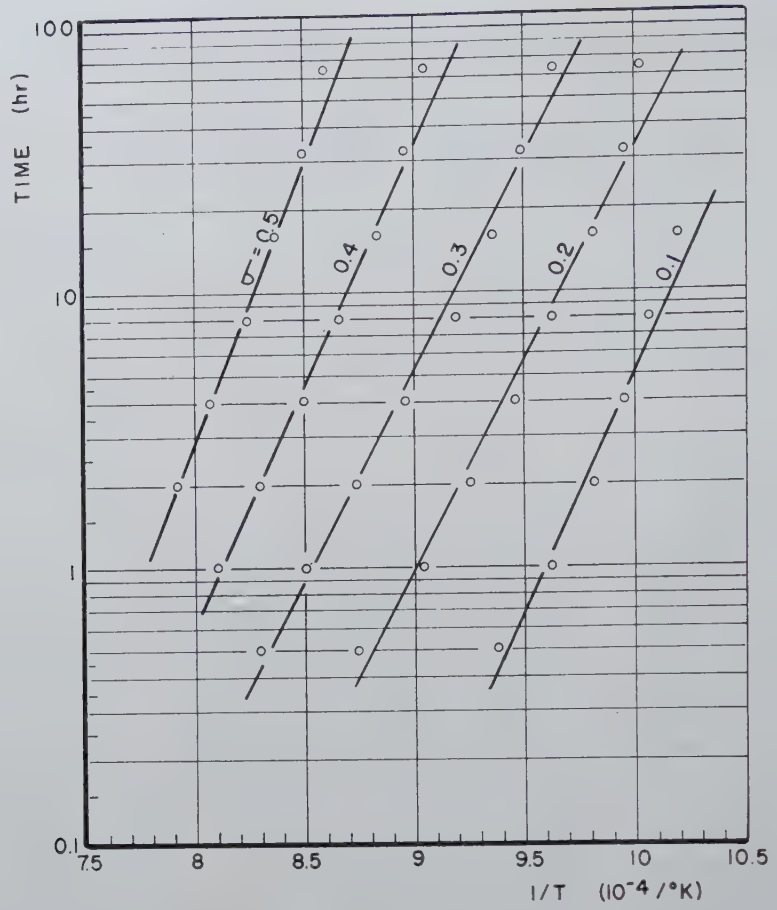

FIG 3—Relation between time and reciprocal of temperature for various values of densification parameter, hydrogen sintering.

Specifically, the "densification parameter" σ is defined as follows:

$$\sigma = \frac{\rho - \rho_0}{\rho_\infty - \rho_0} \qquad [1]$$

where ρ = density after partial sintering

ρ_0 = initial density (before sintering)

ρ_∞ = maximum possible density, that is, density of the solid metal.

It is in terms of this parameter that the experimental results are plotted in Fig 3 and 4.

The ultimate goal of the investigation, of which the experiments described in this paper are the first step, is to elucidate the mechanism by which metals bond or sinter together as a result of the application of pressure and heat at temperatures below the melting point. Several hypotheses as to the nature of this mechanism have been advanced (see, for example, Ref. 2, 3, and 4). While no such fundamental theory is developed in this paper, it will be shown that the results of the experiments described may be given a simple interpretation which may serve as a useful guide to future theoretical and experimental investigations.

Briefly stated, it appears possible that densification can be interpreted as a rate process such as that involved, for example, in chemical reactions. Such processes are characterized (see, for example, Ref. 5) by the fact that if a given state is attained in a time t_1 at absolute temperature T_1, and in time t_2 at some different absolute temperature T_2, then these four quantities are connected by the relation

$$\log_e \left(\frac{t_1}{t_2}\right) = \frac{Q}{R}\left(\frac{1}{T_1} - \frac{1}{T_2}\right) \qquad [2]$$

where R is the gas constant (1.99 cal per mol-°C), and the constant Q is the molal "heat of activation" or "activation energy." As applied to chemical reactions, for example, Q is proportional to the minimum energy which a molecule must have in order to take part in the reaction (see Ref. 5 for details). In the present case, the progress of the densification "reaction" is measured by the value of the parameter σ. Consequently, to see whether densification may be regarded as a rate process, it is necessary to plot curves of constant σ on a graph of log t vs. $1/T$, when, if the above relation is to be satisfied, straight lines must result. Fig 3 and 4 show curves of constant σ plotted in this fashion with the best-fitting straight line drawn through each set of points for comparison. These lines form an approximately parallel set for each of the two sintering atmospheres used, the set representing sintering in vacuum having a larger slope than the set for sintering in hydrogen. The two slopes correspond to values of Q of about 128,000 cal per mol for vacuum sintering, and 80,000 cal per mol for hydrogen sintering, corresponding to the fact (see Fig 1 and 2) that a given time and temperature produce a lower value of σ in vacuum than in hydrogen. A possible explanation of this result is that the hydrogen atmosphere cleans the oxide film from the surface of the particles by reduction, thus making it easier for the clean surfaces to bond together.

It should be noted that there appears to be a systematic deviation of the points from the straight lines drawn in Fig 3 and 4, and that therefore the present results are certainly not conclusive proof that densification is a rate process. It seems plausible, in fact, that densification is the result of superposition of several more fundamental proc-

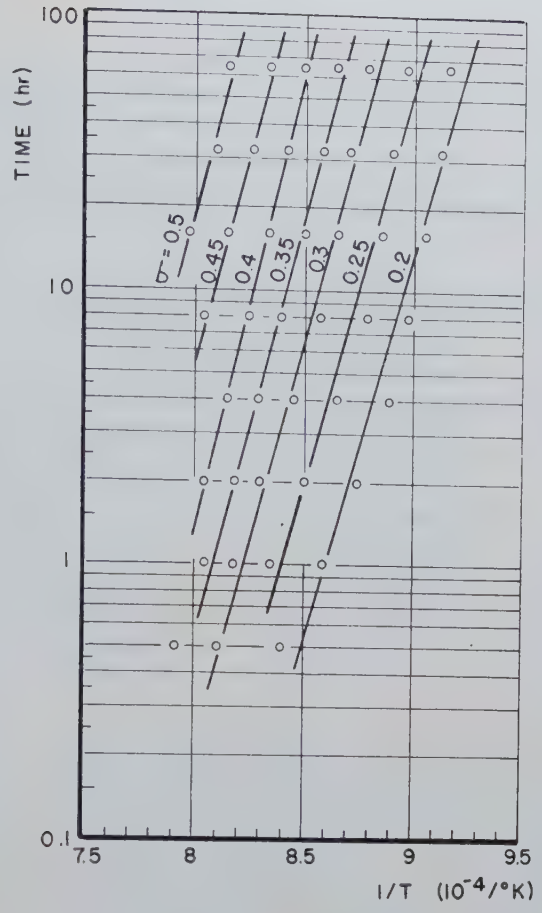

FIG 4—Relation between time and reciprocal of temperature for various values of densification parameter; vacuum sintering.

esses, each of which may be a rate process governed by a different energy of activation. The fact that the overall result may be approximately described as a single rate process would then seem to indicate that one of the fundamental processes predominates over the others.

Summary and Conclusions

From the results of the experimental work described in this paper, it appears that the densification of copper powder compacts in hydrogen and in vacuum may be approximately described as a rate process governed by a heat of activation. The agreement of such a description with the data, however, is not sufficiently good to permit a definite assertion of its validity, and it is suggested only as an hypothesis which may be a useful guide to further work.

The fact that copper powder compacts densify more slowly in vacuum than in hydrogen indicates that the oxide film on the surface of the particles influences the rate of densification. Accordingly, the next step in the experimental investigation will be to study the densification of compacts pressed from powder which has been cleaned of oxide by reduction in hydrogen. It would also be very desirable to investigate the densification of compacts made from powder of more closely controlled particle size, and it is hoped that the practical difficulties involved in obtaining such powder may be overcome sufficiently to permit some work along this line.

Acknowledgment

This work was done at the Jet Propulsion Laboratory, California Institute of Technology, under contract with the Army Ordnance Department, Washington, D. C. The authors wish to thank this agency for the permission to publish the results of this investigation.

References

1. P. Duwez and H. E. Martens: The Powder Metallurgy of Porous Metals and Alloys Having a Controlled Porosity. AIME *Metals Tech.* Apr. 1948, TP 2343.

2. W. D. Jones: Principles of Powder Metallurgy. Edward Arnold and Co., London (1937).

3. F. N. Rhines: *Metals Tech.* Aug. 1946, TP 2043; *Trans.* AIME (1946) **166,** 474.

4. A. J. Shaler and J. Wulff: *Ind. Eng. Chem.* (May 1948) **40,** 838.

5. A. A. Noyes and M. S. Sherrill: A Course of Study in Chemical Principles. 1938. New York. The Macmillan Co.

Influence of Composition on the Stress-corrosion Cracking of Some Copper-base Alloys

D. H. THOMPSON* and A. W. TRACY,* Members AIME

SEASON-CRACKING is a type of failure of brass that results from the simultaneous effect of stress and certain corrodants. The object of this paper is to present data that will aid in a more complete understanding of the mechanism of season-cracking and related phenomena. Results presented show that certain high copper alloys are susceptible to season-cracking or stress-corrosion cracking, and possible explanations are discussed. Starting at least as far back as 1906, many papers have been devoted to this subject but the symposium[1] held in Philadelphia in 1944 is the richest source of information.

In order to study season-cracking, several of the many variables were held constant so as to learn the effects of others. Season-cracking is generally understood to refer to the corrosion cracking of brass having internal stresses;[2,3] it is a special case of the general stress-corrosion cracking. Inasmuch as applied stresses are more readily produced and controlled, they were used exclusively in this research and the resulting phenomenon must be called stress-corrosion cracking.[2,3] Only constant tensile stresses were used. The agents believed to be most frequently responsible for season-cracking are ammonia, amines and compounds containing them. Both moisture and oxygen also appear to be necessary. Therefore, an atmosphere containing ammonia, water-vapor and air was selected for these tests.

Briefly, the work consisted of exposing sheet metal specimens, having a reduced section ¼ by 0.050 in., of copper-base alloys to the effect of static tensile stresses between 5,000 and 20,000 psi and simultaneous contact with a continuously renewed atmosphere containing 80 pct air, 16 pct ammonia and 4 pct water vapor at 35°C. The gas mixture and the specimens were maintained above the dew-point. The time-to-failure in minutes was the primary measure of results. In order to limit the experiment to finite time, it was considered that a specimen which had neither failed nor undergone microscopically detectable cracking in 40,000 min. (4 weeks) while under a stress of 10,000 psi or more could be considered immune to cracking. This is merely a convenient limit and is not to be considered proof of immunity. Supplementary tests in the absence of stress using weight loss or microscopical appearance as measures of attack were made.

Apparatus

The apparatus used in this research is shown in Fig 1. To facilitate the description it may conveniently be divided into six parts: stress-producing units, test chamber, gas train, electrical controls, timers and gas analysis device.

A stress-producing unit is shown in an exploded view at the left in Fig 2. At the right is an assembled unit with a specimen in place in the lower portion; it is this part that remains in the ammonia atmosphere during a test. The upper part contains a spring, a central threaded rod, a large nut and necessary washers, pins, and so forth. Stress is produced in the specimen by screwing down the top nut against the spring, thus putting a tensile load on the central rod and so on the specimen. The wrench that turns the nut by extending through the upper cap, is seen at the upper right of the figure. The magnitude of the load is gauged by measuring from the pin that extends through the side of the tube, to a fixed point on the large flange. Measurement is made with a vernier beam caliper, shown at the right of the figure. The necessary spring compression to give a desired stress is calculated from the calibration curve of the spring and the dimensions of the specimen.

The test chamber, center Fig 1, consists of a thermally insulated steel box 32 in. long by 10 in. high by 7 in. wide. A horizontal baffle reaching nearly to each end divides the chamber equally. Below this baffle are inlets for air and ammonia, a heating coil and a fan. Thus the gases are warmed and mixed in the lower level and flow past the specimens in the upper level. A thermoregulator and thermometer project into the upper space. The top is pierced by 12 ports flanked by ⅜ in. threaded studs. A test starts when a port is opened and a unit containing a stressed specimen is thrust through it and bolted down against a neoprene gasket. The test chamber is held at 35°C.

The gas train, right rear Fig 1, carries ammonia and air continuously to the test chamber. Tank ammonia passes through two reducing valves, a needle valve, a flow meter and into the test chamber. The air from either the plant compressor or a small laboratory compressor passes through wool towers and flow controls to the flow-meter. It then bubbles through water at 34°C and through a heated line to the test chamber.

Electrical controls, left rear, Fig 1, provide rectifiers and mercury relays for the test-chamber and humidifier-heating-control circuits and outlets for

San Francisco Meeting, February 1949.

TP 2518 E. Discussion of this paper (2 copies) may be sent to *Transactions* AIME before May 15, 1949. Manuscript received October 25, 1948.

* Research Assistant and Assistant Metallurgist respectively, The American Brass Co., Waterbury, Connecticut.

[1] Reference are at the end of the paper.

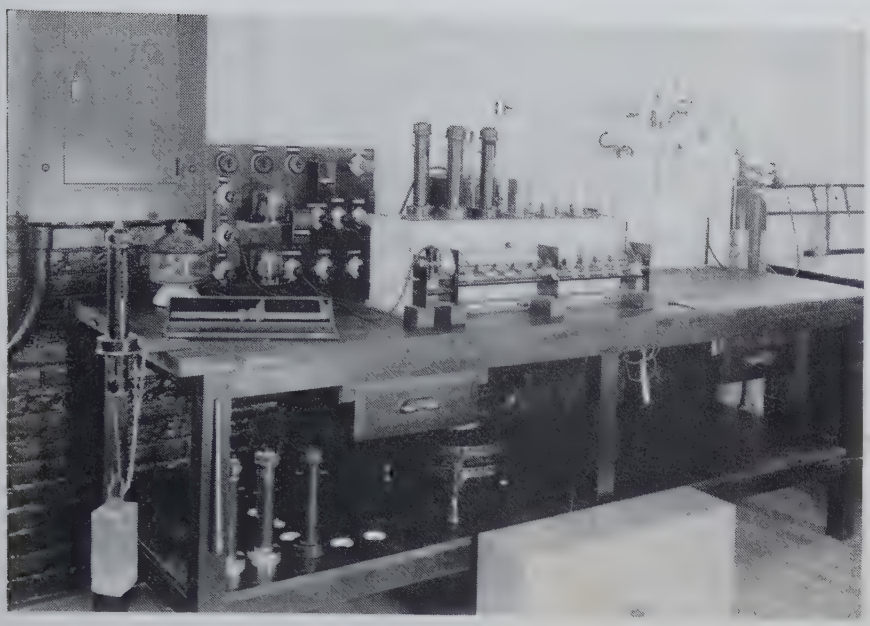

FIG 1—Apparatus for stress-corrosion cracking in moist ammoniacal atmosphere.

gas-line heaters, cover heater, fan and timers.

Timers occupy the space in front of the test chamber. They comprise 12 Veeder-Root counters operated by cams on a shaft driven by a 1 rpm Telechron motor. When a specimen breaks it releases a string which drops a weight stopping a counter. The life of that specimen in minutes is then directly available.

Analysis of the gases contained in the test chamber is performed at the outlet at the right-hand end. The mixed gases are drawn through an absorption train. In the first absorber a known amount of sulphuric acid neutralizes and removes ammonia from the mixture. The moisture is then absorbed in the second tube, which contains silica gel. The volume of air remaining is measured with an aspirator. The gain in weight of both absorption tubes less the known weight of ammonia gives the weight of water. Both ammonia and water are recorded as ml per 500 ml of air, which is the volume per minute delivered to the chamber.

Preparation of Specimens

The following metals and alloys were tested:

Oxygen-free high-conductivity copper
Tough-pitch copper
Copper-zinc alloys containing 0–40 pct zinc
Copper-phosphorus alloys containing 0–0.9 pct phosphorus
Copper-arsenic alloys containing 0–1.2 pct arsenic
Copper-antimony alloys containing 0–1.0 pct antimony
Copper-silicon alloys containing 0–4 pct silicon
Copper-nickel alloys containing 0–30 pct nickel
Copper-aluminum alloys containing 0–8 pct aluminum

Analyses of these alloys are given in Table 1.

The alloys were cast and rolled in the laboratory or obtained from mill production. When possible they were finished with a 50 pct reduction by cold rolling to 0.050 in. gauge. They were sheared to ⅜ in. by 5 in. and the reduced section filed by the use of a hardened-steel jig to ¼ in. by 0.050 in. Holes were drilled near the ends. The specimens were then annealed, usually at 500°C for one hour. Annealing scale was removed by suitable pickles, usually dilute nitric acid, but in every case

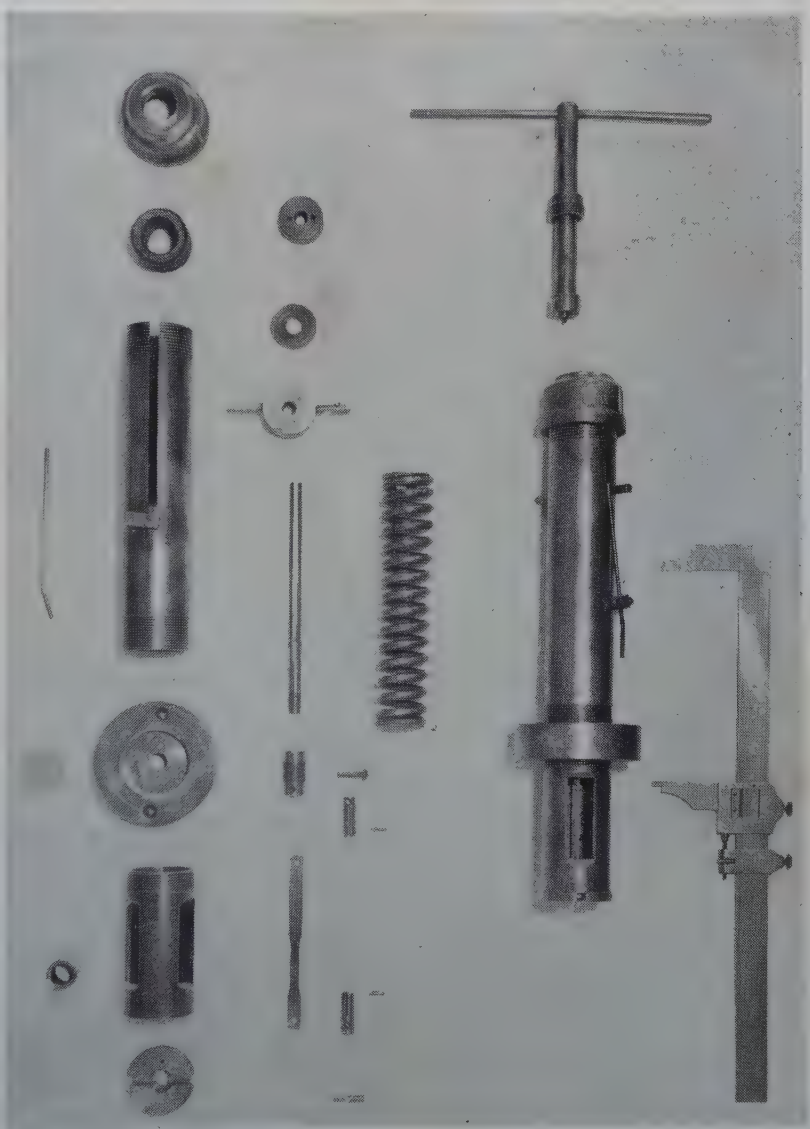

FIG 2—Stress-producing unit.

Table 1 . . . Analyses of Metals Tested

Alloy No.	Copper + Silver Pct	Oxygen Pct	Sulphur Pct	
1*M*	99.962	0.0344	0.0016	
2*M*	99.950	0.038	0.003	
3*M*	99.982	0.000		
			Iron	
4*	100.000	0.000	0.006	
5*		Zinc		
6	99.861	0.12	0.006	
7	99.52	0.50	0.005	
8	99.02	0.98	0.004	
9	94.81	5.18†	0.005	
10	89.99	10.00†	0.005	
11	79.89	20.01†	0.005	
12	70.16	29.82†	0.010	
13*M*	69.50	30.46†	0.021	Lead 0.016
14	60.12	29.88	0.004	
		Phosphorus		
15	99.996	0.001	0.006	
16	99.998	0.002	0.006	
17	99.998	0.004	0.006	
18	99.998	0.007	0.006	
19	99.992	0.014	0.006	
20	99.940	0.028	0.004	
21	99.942	0.056	0.004	
22	99.88	0.10	0.02	
23	99.78	0.24	0.01	
24	99.54	0.46	0.01	
25	99.07	0.93	0.01	
		Arsenic		
26	99.935	0.052	0.001	
27	99.858	0.126	0.002	
28	99.792	0.19	0.02	
29	99.670	0.305	0.002	
30	99.592	0.36	0.004	
31	99.360	0.607	0.003	
32	98.743	1.22	0.004	

Table 1 . . . (Continued)

Alloy No.	Copper + Silver Pct	Antimony Pct	Iron Pct			
33	99.968	0.010	0.014			
34	99.889	0.109	0.004			
35	99.74	0.25	0.02			
36	99.52	0.47	0.01			
37	98.94	0.95	0.02			
		Silicon				
38	99.86	0.11	0.03			
39	99.70	0.27	0.03			
40	99.48	0.46	0.02			
41	98.93	0.98	0.03			
42	97.97	1.97	0.02			
43	97.00	2.96	0.04			
44	96.07	3.92	0.04			
		Nickel		Manganese		
45	97.93	1.98	0.005	0.08		
46	95.17	4.78	0.005	0.077		
47	90.00	9.84	0.005	0.21		
48	79.69	20.16	0.004	0.28		
49	69.28	30.06	0.005	0.64		
		Aluminum				
50	99.897	0.09	0.007			
51	99.74	0.24	0.009			
52	99.53	0.51	0.010			
53	98.97	1.03	0.012			
54	98.00	1.98	0.012			
				Zinc	Nickel	
55*M*	94.94	4.85	0.06	0.10	0.05	
56*M*	92.00	7.96	0.04	0.0	0.00	
		Phosphorus				
57	99.966	0.024	0.002			
58	99.961	0.024	0.006			
		Zinc		Tin	Lead	Arsenic
59*M*	71.39	27.46†	0.01	1.10	0.006	0.034
60*M*	70.78	29.20†	0.01		0.006	
		Silicon		Manganese		
61	97.48	1.44	0.04	1.06		
		Zinc				
62*M*	63.78	36.22†				

M Mill stock. All others cast and rolled in laboratory.
* Chile cathode melted under charcoal. Spectrum shows lead, manganese and iron as traces. Microscope shows no cuprous oxide.
† By difference.

the final dip was cold 20 pct sulphuric acid. After a thorough water rinse the specimens were dipped in alcohol and dried in a blast of hot air. After being measured, they were inserted in units and loaded to the desired stresses. The upper end of each specimen passed out of the test chamber and the opening around it was sealed with wax; the lower end was held with a pin, which was also imbedded in wax to prevent attack of the specimen at this highly stressed point. Before exposure the whole unit, including the specimen, was warmed to prevent thermal condensation. As each unit was lowered into the test chamber, the appropriate counter was started.

Results

COPPER

Three types of substantially pure copper were subjected to stress-corrosion in the moist ammoniacal atmosphere without the occurrence of cracks. These were tough pitch, OFHC and copper prepared in the laboratory by melting Chile cathode copper under charcoal and pouring through city gas. The magnitude of applied stresses and the length of the exposures are given in Table 2. The column headed "Penetration" describes the result of microscopical examination of a longitudinal section up to an exposed surface. In only one case had any localized corrosion taken place, and in no case was there any evidence of cracking or intergranular penetration.

Table 2 . . . Copper in Moist Ammoniacal Atmosphere Did Not Break Under Stress Within Time Indicated

	Alloy No.	Stress PSI	Time Min.	Penetration
Tough Pitch Copper	1	5,000	50,000	None
Touch Pitch Copper	1	10,000	50,000	One Pit
Tough Pitch Copper	2	10,000	40,000	None
OFHC Copper	3	10,000	40,000	None
Copper	4	10,000	40,000	None
Copper (4 specimens)	5	15,000	50,000	None

COPPER-ZINC ALLOYS

Results obtained from copper-zinc alloys are presented graphically in Fig 3. The breaking times of specimens stressed at 5,000, 10,000 and 15,000 psi are plotted against the zinc content in per cent. The corrosion rate in inch per year (ipy) is also plotted against zinc content. Corrosion rate figures were computed from weight loss data on specimens exposed without stress to the same moist ammoniacal atmosphere. It is obvious that the resistance to cracking decreases rapidly as the zinc content increases. The corrosion rate, while relatively stable, does drop slightly with the cracking time, suggesting that the alloys which crack more rapidly are those that corrode less rapidly. Table 3 includes these data and also gives the microscopically observed intergranular penetration that occurred in the unstressed specimens.

Two things should be noted especially: the lack of correlation between cracking rate and corrosion rate, with the suggestion of negative correlation,

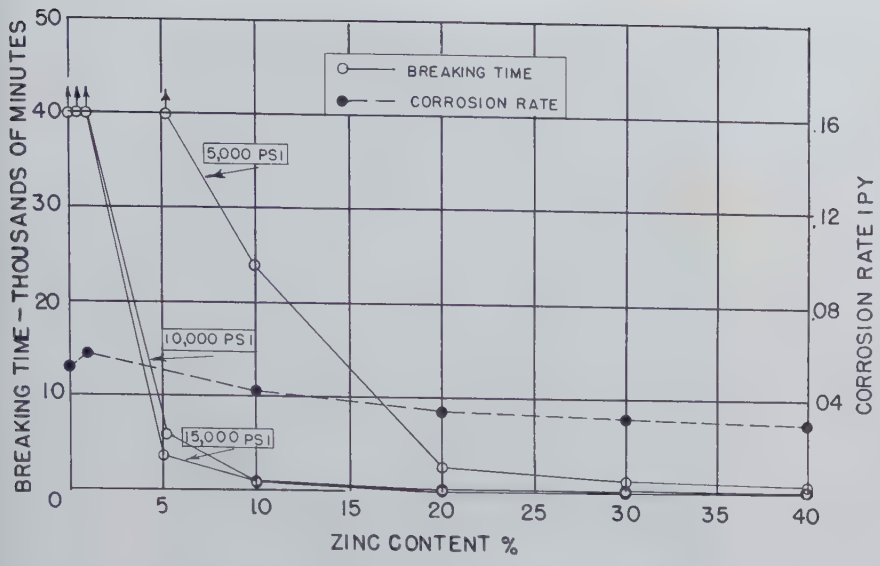

FIG 3—Copper-zinc alloys in moist ammoniacal atmosphere. Breaking time under various stresses vs. zinc content; corrosion rate, no stress, vs. zinc content.

Table 3 . . . Copper-zinc Alloys in Moist Ammoniacal Atmosphere

Breaking Time under Stress
Corrosion Rate and Intergranular Penetration in the Absence of Stress

Alloy No.	Zinc Pct	Breaking Time-minutes-at 5,000 PSI	Breaking Time-minutes-at 10,000 PSI	Breaking Time-minutes-at 15,000 PSI	Corrosion Rate—IPY	Penetration Grains in 1 Week
4	00	40,000†	40,000†	40,000†	0.052	None
6	0.12	40,000†	40,000†			
7	0.50	40,000†	40,000†	40,000†		
8	0.98	40,000†	40,000†	40,000†	0.058	None
9	5.18	40,000†	5,914	3,522		
10	10.03	24,070	973	757	0.042	3–4
11	20.01	2,689	258	161	0.036	1–2
12	29.82		254	102	0.032	*
13	30.45	1,379				
14	39.88	943	232	106	0.030	1

* Several grains at only one region.
† Did not break.
All samples annealed at 500°C for one hour. All metal cast and processed in the laboratory except 13, which was cast and processed to 0.400 in. ga in the mill and finished in the laboratory.

and the occurrence of intergranula penetration in the absence of stress.

COPPER-PHOSPHORUS ALLOYS

Similar results are shown in Fig 4 for copper-phosphorus alloys, although at only one applied stress, 10,000 psi. Comparison of Fig 4 with Fig 3 shows that the curves are similar in shape; the breaking time decreases sharply when either phosphorus or zinc is added to copper. An impressive difference is the extreme rapidity with which the breaking time drops as phosphorus is added. For instance, Table 4 gives 274 min. as the breaking time for the 0.1 pct phosphorus alloy (Alloy No. 22) under 10,000 psi stress in the moist ammoniacal atmosphere, while copper with no phosphorus does not break in 50,000 min. even at higher stresses. Comparison with Table 3 shows that this 0.1 pct phosphorus alloy breaks nearly as rapidly as 80–20 brass under the same conditions.

Table 4 also reveals the rapid attack of the moist ammoniacal atmosphere on annealed copper-phosphorus alloys without stress. A sample containing 0.24 pct phosphorus (Alloy No. 23) was annealed at 800°C for one hour and exposed to the moist ammoniacal atmosphere without stress. After 40,000 min. (1 month) it was found that the intergranular penetration had completely penetrated the 0.050 in. gauge sheet. The specimen could be broken apart into individual grains with the fingers. Some of the grains are shown in Fig 5, a micrograph taken at 30×. Fig 6 is a micrograph taken at 75× of a piece of 0.1 pct phosphorus alloy (Alloy No. 22) that was annealed at 800°C and exposed without stress to the

Table 4 . . . Copper-phosphorus Alloys in Moist Ammoniacal Atmosphere

Breaking Time under Stress
Corrosion Rate and Intergranular Penetration in the Absence of Stress

Alloy No.	Phosphorus Pct	Breaking Time at 10,000 PSI Min.	Corrosion Rate IPY	Penetration Grains in 1 Week
4	00	40,000*	0.033	None
15	0.001	40,000*		None
16	0.002	40,000*		None
17	0.004	39,459		1–2
18	0.006	18,417		4–5
19	0.014	6,298	0.038	4–5
20	0.028	642	0.027	4–8
21	0.056	428	0.016	4–5
22	0.10	274		6
23	0.24	262	0.013	6
24	0.46	314	0.030	3–4
25	0.92	14,740	0.022	Slight

* Did not break.
All alloys cast and processed in the laboratory.
All samples annealed finally at 500°C for 1 hour.

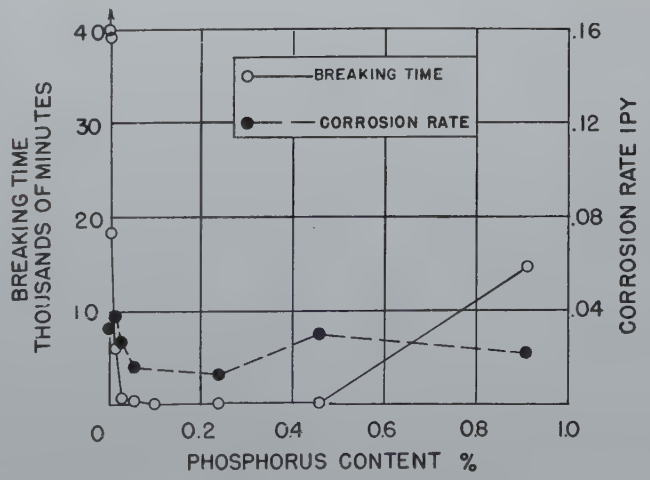

FIG 4—Copper-phosphorus alloys in moist ammoniacal atmosphere. Breaking time under 10,000 psi stress vs. phosphorus content; corrosion rate, no stress, vs. phosphorus content.

moist ammoniacal atmosphere for one week. The depth of penetration is obvious.

The results on the phosphorus alloys are extremely interesting. The addition of phosphorus to copper has a profound effect on the rapidity of stress-corrosion cracking and also on the rate of intergranular penetration in moist ammoniacal atmosphere in the absence of stress. The effect cannot be explained by the removal of oxygen from the copper since OFHC and copper deoxidized with some other elements do not crack. The changes in mechanical and physical properties are negligible except in the case of conductivity and the overall corrosion rate is but slightly affected.

Alloy No. 25 (0.92 pct phosphorus) broke less rapidly than alloys with intermediate phosphorus contents; it is beyond the solid solubility limit of phosphorus in copper. This upswing will be observed in other alloy systems, to be described.

In Fig 3 and 4, points are very close to the axes, but Tables 3 and 4 give the actual values that the points represent. No change in scale was adopted because of the advantage of having all the graphs use the same vertical scale.

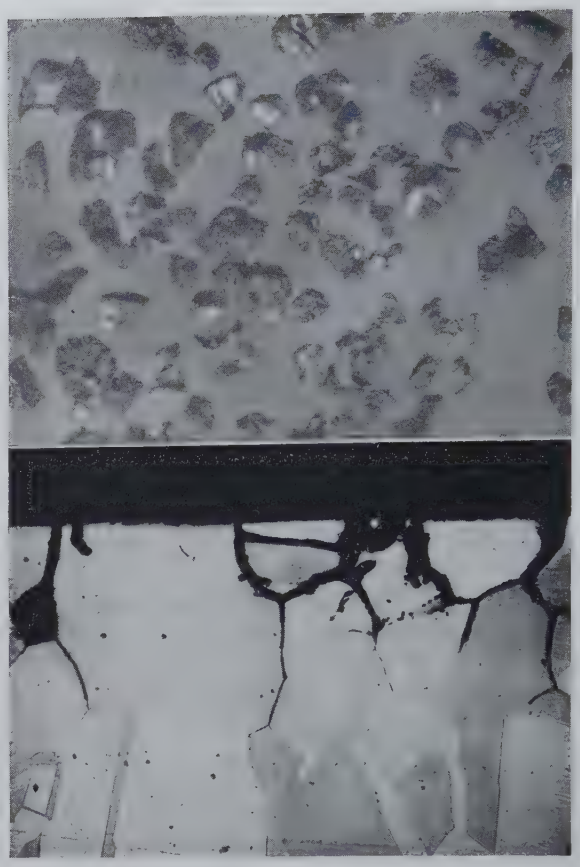

FIG 5 and 6—Copper-phosphorus alloys after exposure to moist ammoniacal atmosphere.
FIG 5 (Above)—Alloy No. 23, 0.24 pct phosphorus, 40,000 min., 30 ×.
FIG 6 (Below)—Alloy No. 22 0.1 pct phosphorus, 10,000 min., 75 ×. Potassium bichromate-sulphuric acid etch.

COPPER-ARSENIC ALLOYS

Stress-corrosion cracking and corrosion rate curves from data on copper-arsenic alloys in moist ammoniacal atmosphere are shown in Fig 7. These curves are quite different from those presented for copper-phosphorus and copper-zinc in that there is a pronounced minimum in the cracking curves at 0.2 pct arsenic and a maximum in the corrosion-rate curve at 0.05 pct arsenic. The 1.2 pct arsenic alloy is immune to cracking within the prescribed limits. Table 5 shows that intergranular penetration is appreciable after four weeks in the lower arsenic alloys. The effect of arsenic content on

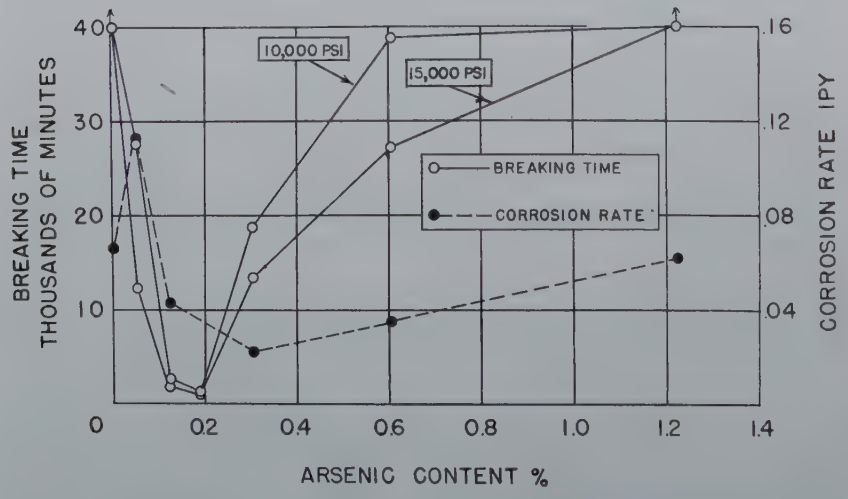

FIG 7—Copper-arsenic alloys in moist ammoniacal atmosphere. Breaking time under various stresses vs. arsenic content; corrosion rate, no stress, vs. arsenic content.

Table 5 . . . Copper-arsenic Alloys in Moist Ammoniacal Atmosphere

Breaking Time under Stress
Corrosion Rate and Intergranular Penetration in the Absence of Stress

Alloy No.	Arsenic Pct	Breaking Time at 10,000 PSI Minutes	Breaking Time at 15,000 PSI Minutes	Corrosion Rate IPY	Penetration Grains in 4 Weeks
4	00	40,000†	40,000†	0.066	0
26	0.052	27,609	12,342	0.113	Several
27	0.126	2,674	1,899	0.043	Several
28	0.19	1,417	1,093		
29	0.305	18,720	13,439	0.022	1
30*	0.365	16,905	16,484		
31	0.606	38,842	27,339	0.035	None
32	1.225	40,000†	40,000†	0.062	None

* Cuprous oxide present.
† Did not break.
All alloys cast and processed in the laboratory.
All specimens annealed finally at 500°C for 1 hour.

Table 6 . . . Copper-antimony Alloys in Moist Ammoniacal Atmosphere

Breaking Time under Stress
Corrosion Rate and Intergranular Penetration in the Absence of Stress

Alloy No.	Antimony Pct	Breaking Time, Min. at			Corrosion Rate IPY	Penetration Grains in 1 Week
		5,000 PSI	10,000 PSI	15,000 PSI		
4	00	40,000*	40,000*	40,000*	0.058	0
33	0.01		40,000*	36,665	0.080	1–3
34	0.109	15,012	6,882	2,894	0.160	5–7
35	0.25	6,412	4,602	2,232	0.137	10–12
36	0.47	15,565	2,197	2,635	0.139	3–4
37	0.95	21,997	3,373	2,217	0.055	2–3

* Did not break.
All alloys cast and processed in the laboratory.
All specimens annealed finally at 500°C for 1 hour.

Table 7 . . . Copper-silicon Alloy in Moist Ammoniacal Atmosphere

Breaking Time under Stress
Corrosion Rate and Intergranular Penetration in the Absence of Stress

Alloy No.	Silicon Pct	Breaking Time, Min., at		Corrosion Rate IPY	Penetration Grains in 4 Weeks
		10,000 PSI	15,000 PSI		
4	0	40,000*	40,000*	0.052	None
38	0.11	23,340	13,201	0.072	2–3
39	0.27		5,178	0.034	2–3
40	0.46	5,250	2,881	0.024	3–4
41	0.97	2,537	1,972	0.034	Doubtful
42	1.96	15,735	6,280	0.047	
43	2.97	49,000	28,005	0.053	
44	3.91		50,000*	0.082	None

* Did not break.
All alloys cast and processed in the laboratory.
All specimens annealed finally at 500°C for 1 hour.

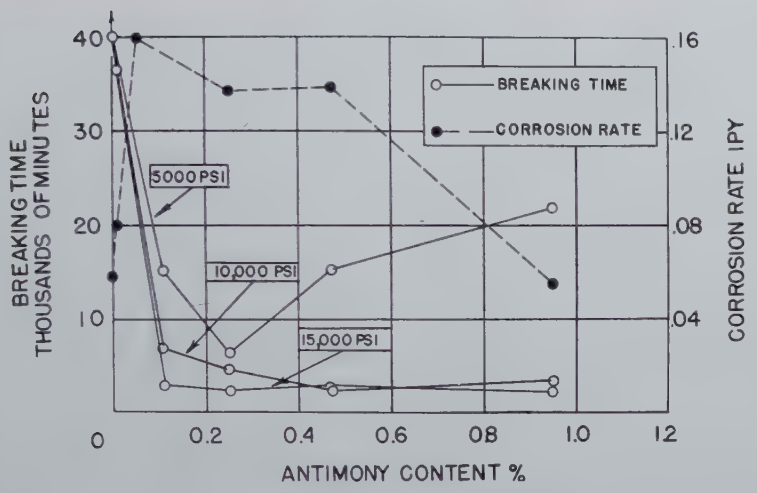

FIG 8—Copper-antimony alloys in moist ammoniacal atmosphere. Breaking time under various stresses vs. antimony content; corrosion rate, no stress, vs. antimony content.

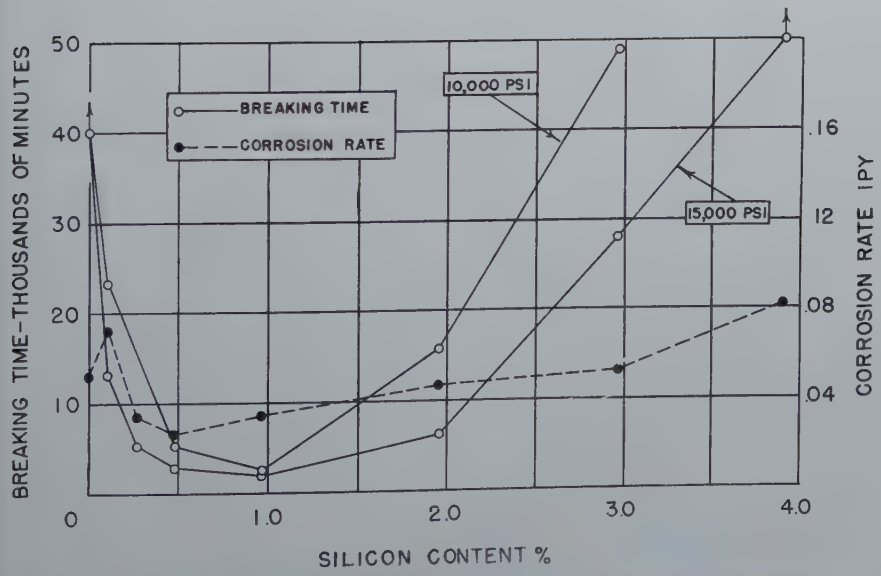

FIG 9—Copper-silicon alloys in moist ammoniacal atmosphere. Breaking time under various stresses vs. silicon content; corrosion rate, no stress, vs. silicon content.

cracking time is not nearly as pronounced as in the case of phosphorus and zinc and it extends over only a very narrow range.

COPPER-ANTIMONY ALLOYS

Fig 8 gives the results for copper-antimony alloys. The minimum cracking time is greater than with the alloy systems previously considered. There is some evidence of a minimum in the antimony per cent versus cracking-time curve. There is a maximum in the corrosion-rate curve. Intergranular penetration is shown by Table 6 to be appreciable in one week.

COPPER-SILICON ALLOYS

Results are given in Fig 9. There is a distinct minimum cracking time at 1 pct silicon, which is a higher percentage than in the case of arsenic. Immunity appears at 4 pct silicon. The corrosion rate is fairly constant. Intergranular penetration given in Table 7 is definite but only after four weeks.

COPPER-NICKEL ALLOYS

Fig 10 gives test results. The minimum in the cracking time is pronounced but the required exposure is long. With this system, as with others, a maximum appears in the corrosion rate curve at a more dilute composition than the minimum in the breaking curve. At 30 pct nickel, the corrosion rate is very small; the samples were hardly tarnished at the end of a week. Table 8 shows that intergranular penetration is almost absent, but it does occur.

Table 8 . . . Copper-nickel Alloys in Moist Ammoniacal Atmosphere

Breaking Time under Stress
Corrosion Rate and Intergranular Penetration in the Absence of Stress

Alloy No.	Nickel Pct	Breaking Time, Min., at 10,000 PSI	Corrosion Rate IPY	Penetration Grains in 1 Week	Final Anneal °C
4	00	40,000*	0.043	None	500
45	1.98	9,426	0.070	½	500
46	4.78	4,730	0.055	½	500
47	9.84	9,552	0.046	None	700
48	20.16	13,527	0.029	None	700
49	30.06	40,000*	0.0006	None	750

* Did not break.
All samples cast and processed in the laboratory.

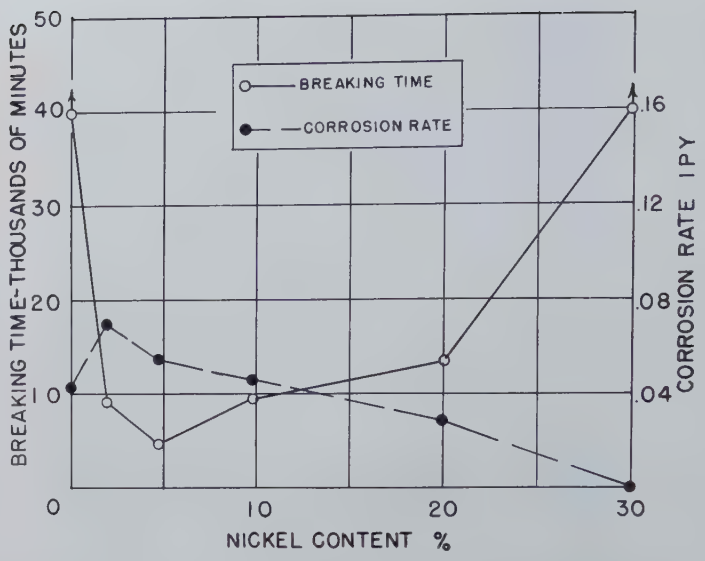

FIG 10—Copper-nickel alloys in moist ammoniacal atmosphere. Breaking time under 10,000 psi stress vs. nickel content; corrosion rate, no stress, vs. nickel content.

COPPER-ALUMINUM ALLOYS

Fig 11 shows a minimum breaking time at 1 pct aluminum. The corrosion-rate curve is relatively constant with only a slight maximum. Intergranular penetration is small in one week as given in Table 9.

OTHER TESTS

In line with Dix's[4] theories on the role of grain-boundary precipitates in rendering an alloy subject to stress-corrosion cracking, some tests were made to try to show whether the effect is important in copper-phosphorus alloys. About 0.5 pct phosphorus is soluble in copper, but iron phosphide is believed to be only slightly soluble in copper. Therefore, the attempt was made to precipitate iron phosphide and study its effect on cracking. Two alloys were cast; each contained 0.024 pct phosphorus. One contained 0.002 pct iron and the other contained 0.006 pct iron (alloy Nos. 57 and 58). Thermal treatments were designed to produce precipitation in the grain bodies, in the grain boundaries and to maintain solution. Microscopical examination of these specimens at 1000 diam revealed scattered spheres of some precipitate in all of them in about equal amount. The results of stress-corrosion cracking tests in moist ammonia vapor are given in Table 10. While there is apparently a trend indicating that metal treated to produce precipitation in the grain bodies is most resistant to cracking, followed by material with maximum solution and then that treated to produce grain-boundary pre-

Table 9 . . . Copper-aluminum Alloys in Moist Ammoniacal Atmosphere

Breaking Time under Stress
Corrosion Rate and Intergranular Penetration in the Absence of Stress

Alloy No.	Aluminum Pct	Breaking Time at 10,000 PSI Min.	Corrosion Rate IPY	Penetration Grains in 1 Week
4	00	40,000†	0.042	None
50	0.09	40,000†	0.042	None
51	0.24	40,000†	0.051	None
52	0.51	25,583	0.043	1
53	1.03	10,838	0.030	1
54	1.98	13,323	0.040	None
55*	4.85	50,000†	0.043	
56*	7.96		0.046	

All alloys cast and processed in the laboratory except
* which were cut from annealed mill stock.
All specimens annealed finally at 500°C for 1 hour.
† Did not break.

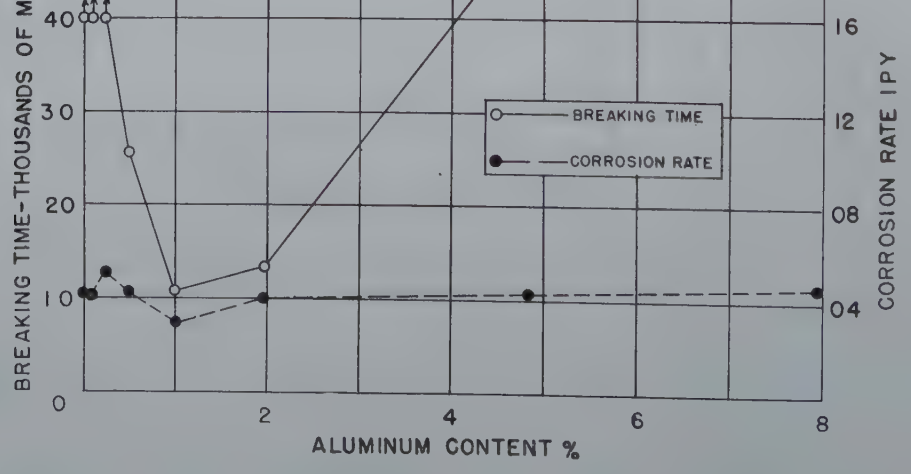

FIG 11—Copper-aluminum alloys in moist ammoniacal atmosphere. Breaking time under 10,000 psi stress vs. aluminum content; corrosion rate, no stress, vs. aluminum content.

Table 10 . . . Stress-corrosion Cracking of Copper Containing 0.024 Pct Phosphorus in Moist Ammoniacal Atmosphere

Alloy No.	Iron Pct	Ready-to-finish Anneal °C	Cooling	Rolled Pct	Final Anneal °C	Cooling	Breaking Time Min.
			Stressed at 5,000 PSI				
57	0.002	500	Air	50	400	Air	5,980
		800	Quenched	50	400	Air	2,380
		800	Quenched	50	800	Quenched	3,136
58	0.006	500	Air	50	400	Air	5,049
		800	Quenched	50	400	Air	2,244
		800	Quenched	50	800	Quenched	4,080
			Stressed at 10,000 PSI				
57	0.002	500	Air	50	400	Air	1,576
		800	Quenched	50	400	Air	1,011
		800	Quenched	50	800	Quenched	1,452
58	0.006	500	Air	50	400	Air	1,649
		800	Quenched	50	400	Air	821
		800	Quenched	50	800	Quenched	1,610

Table 11 . . . Effect of Heat-treatment on the Season-cracking of Copper Containing 0.1 Pct Phosphorus in Moist Ammoniacal Atmosphere

Alloy No. 22

	500°C Anneal	500°C Anneal Followed by 64 Hr at 350°C
Breaking time.....	491	316
Under 10,000 psi.....	299	286
Average.....	395	301

cipitation, there is no difference between the alloy having 0.002 pct iron and the one containing 0.006 pct iron. The statistical procedure, analysis of variance, has been applied to these data and the conclusion is reached that no significant difference exists among them. Either the thermal treatment produced no precipitation, or the submicroscopic precipitate had no large effect on the breaking time.

Another experiment was performed to show the effect of long-time anneals on the stress-corrosion cracking rate. The results are given in Table 11. The alloy contained 0.1 pct phosphorus, balance copper (alloy No. 22). Four samples were annealed at 500°C for one hour and in addition two of them were held for 64 hr at 350°C. While the long anneal produced a somewhat shorter cracking time, the difference is not significant in the face of the variation among supposedly identical specimens. At 1000 diam these samples also showed tiny, randomly distributed spheres of precipitate, the number of which was not greatly affected by the low temperature anneal. It is believed that such material has not been absorbed from segregation occurring in the casting, because of the relatively small amount of working and annealing of small laboratory castings. More work should be done in connection with the effect of heat treatment on the stress-corrosion cracking of this type of alloy.

PATH OF CRACKS

Although ammonia cracking in brass is usually largely intergranular, there are exceptions in alpha brass as well as in other alloys. Fig 12 at 500 diam shows typical intergranular cracking in ⅛ in. diam 70-30 brass rod (alloy No. 60) that failed under 5,000 psi in moist ammoniacal atmosphere. Radically different is Fig 13 at 500 diam, which shows cracking in arsenical admiralty (alloy No. 59) after the same preparation and exposure as the brass. It is difficult to find cracks that are intergranular in this micrograph. The 70-30 brass was annealed at 500°C and the admiralty brass at 550°C for one hour. Similar transcrystalline cracking has been observed in arsenical and nonarsenical admiralty and aluminum brass. Fig 14 is a micrograph at 250 diam of a 65-35 brass gear (alloy No. 62) that was sheared from ¼ in. wrought stock and then exposed to moist ammoniacal atmosphere for 48 hr. The cracks have a strong tendency to pass through the grains.

Fig 15 taken at 500 diam shows cracks in an alloy containing 1.5 pct silicon, 1 pct manganese (alloy No. 61) which failed under 20,000 psi stress in moist ammoniacal atmosphere. Cracks, besides being intergranular, have a tendency to follow twin boundaries, or slip planes.

Discussion of Results

In 1930, Bassett[5] stated that he had seen copper season-crack, while in 1944 Edmunds[6] reported that copper is immune to mercury and ammonia stress-cracking. These statements are not necessarily contradictory. Bassett referred to service failures of copper tubes, which are usually deoxidized with phosphorus. Such failures are not frequent but the authors have observed a number of them. One such tube is shown in Fig 16. It is a 1½ in. od by 0.082 in. ga wall, hard copper tube containing 0.019 pct phosphorus. In service, presumably a refrigeration plant, it was wrapped in tar paper, twine and two layers of hair felt. The line of the edge of the tar paper is shown as a helical row of pits, and the cracks are obvious. The present paper indicates that phosphorus-deoxidized copper cracks readily under the test conditions. Presumably the paucity of service failures of phosphorus-deoxidized copper is due to the low yield point of copper, which makes the occurrence of high internal stresses impossible. The authors have found no evidence that tough pitch or OFHC copper is subject to season-cracking or to stress-corrosion cracking in moist ammoniacal atmosphere and they therefore agree with Edmunds's statement.

As mentioned above, Dix[4] suggested that season-cracking is due to corrosion that is accelerated by the potential between grain boundaries and grain bodies and that this difference is caused by the precipitation of an insoluble phase at the grain boundaries and the depletion of the solute atoms surrounding the grain boundary. There seems to be no evidence to support the existence of a precipitated phase in brass. Nor is there evidence of a change in the breaking time curve when the solid solubility of zinc in copper is exceeded. Read, Reed and Rosenthal[7] attribute this potential difference rather to the high free energy of regions of lattice imperfection such as grain boundaries.

The behavior of phosphorus-deoxidized copper described in the present paper suggested that these theories be reconsidered. It will be recalled that 0.1 pct phosphorus is sufficient to allow rapid cracking of copper with which it is alloyed. Further, this alloy is subject to quite rapid intergranular corrosion in moist ammonia vapor in the ab-

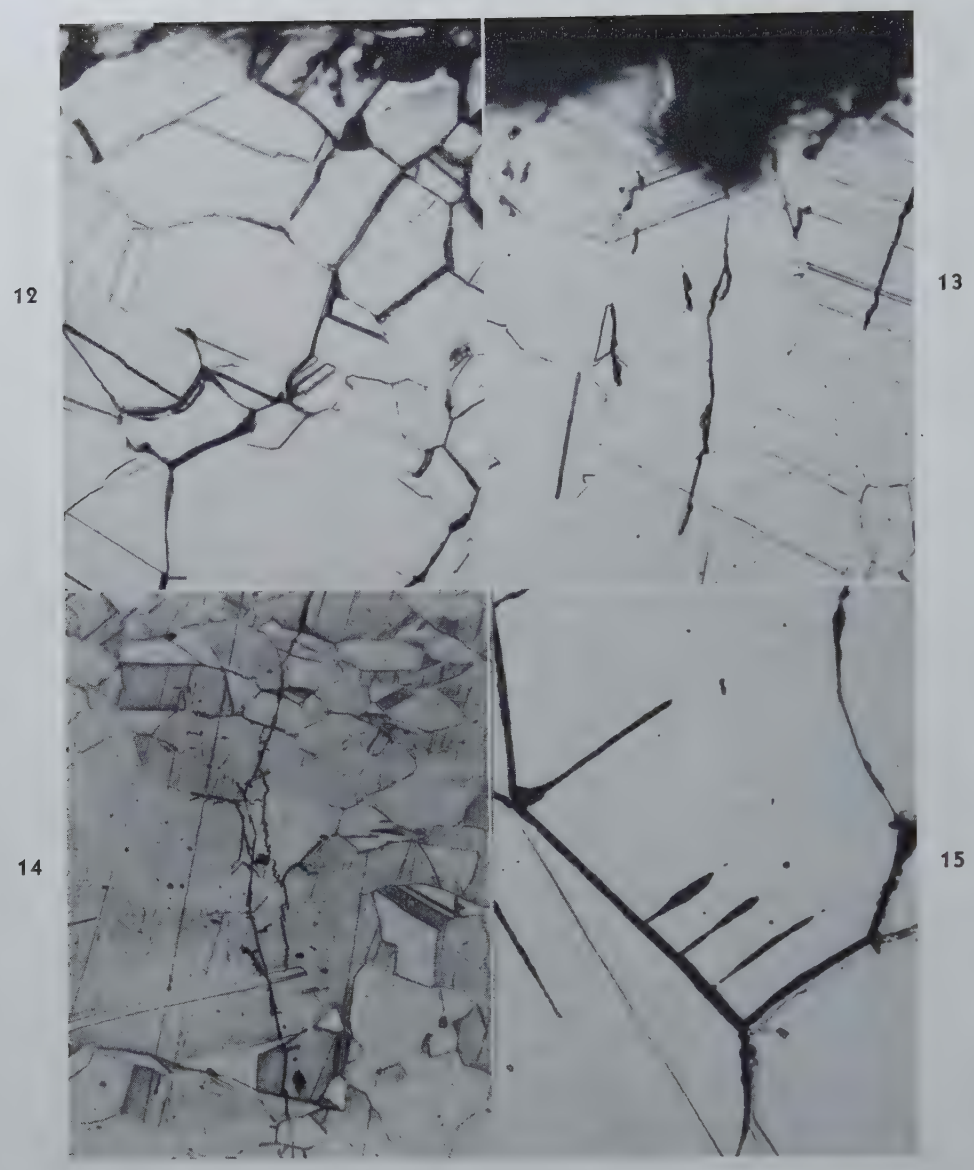

FIG 12 to 15—Types of ammonia cracking.
Fig 12—70-30 brass, alloy No. 60, 5,000 psi stress, 500 ×.
Fig 13—Arsenical admiralty, alloy 59, 5,000 psi stress, 500 ×.
Fig 14—65-35 brass gear, alloy 62, internal stress, 250 ×.
Fig 15—Copper-silicon-manganese, alloy No. 61, 20,000 psi stress, 500 ×.
Etchants: Fig 12 and 14—Ammonium hydroxide and hydrogen peroxide.
Fig 13 and 15—Potassium bichromate and sulphuric acid.

sence of stress either internal or external. Thus grain boundaries are open avenues for corrosion by moist ammonia vapor when a little phosphorus is present, but they are closed to traffic when only copper is present. This behavior suggests to the authors that phosphorus is concentrated at the grain boundaries and whether within or beyond the solid solubility limit, the alloy in this region is anodic to the higher-copper grain-bodies. This potential may be the result of lattice dislocation; not that caused by the abutting of adjacent differently-oriented grains at the boundaries but rather distortion around solute atoms of phosphorus. Such distortion is one of the causes for the large effect phosphorus has on the conductivity of copper.

The behavior of this alloy, if it be typical of season-cracking in general, allows some other conclusions to be drawn. Since intergranular penetration occurs in the absence of stress, it appears that stress merely accelerates the corrosive action of the ammonia, keeping the crack open and a fresh notch available for its action. Another possibility is the formation of protective films. It is conceivable that such films would form first on the exposed surfaces of the grain bodies, leaving the boundaries highly anodic. In more concentrated alloys the film might cover the *whole* surface and stifle boundary attack. In all the systems studied, except copper-zinc, up to 40 pct zinc, there is at least an indication that the cracking rate decreases as the per cent of alloying element is increased.

The presence of 0.1 pct phosphorus in copper changes the mechanical properties only negligibly and it is impossible to correlate the cracking tendency with yield strength, propor-

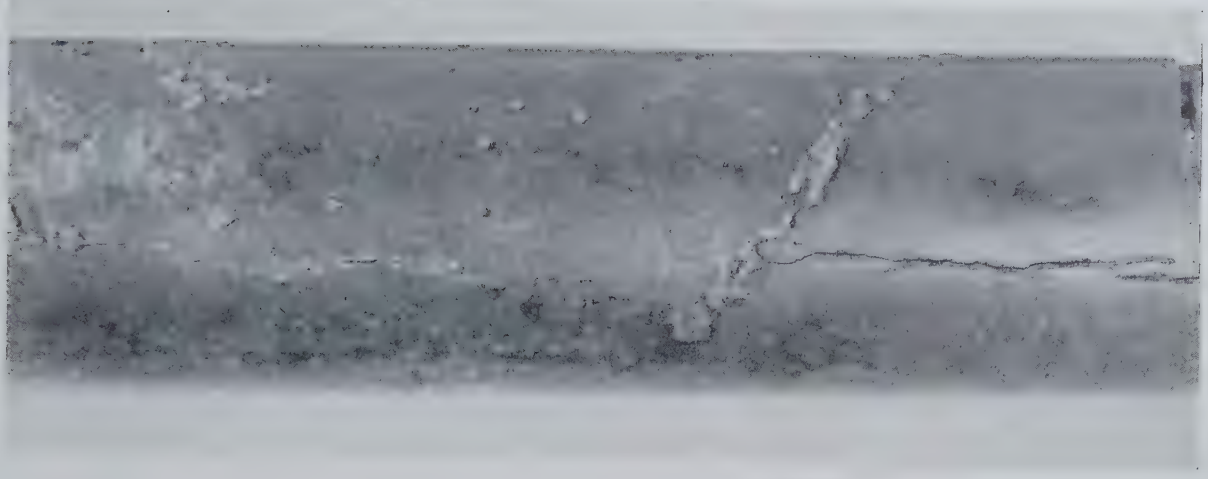

FIG 16—1½ in. od by 0.082 in. gauge hard copper tube containing 0.019 pct phosphorus. Cracked in service.

tional limit or the like.

It should be emphasized that these tests cannot be used as a basis for predicting service failures by season-cracking. The failures were produced under artificial laboratory conditions and should not arouse fears that phosphorized or arsenical copper tubes will crack in service except in rare instances.

Summary

These tests show that the addition of zinc, phosphorus, arsenic, antimony, silicon, nickel or aluminum to copper forms alloys that are subject to stress-corrosion cracking in moist ammoniacal atmosphere in some composition ranges.

The product of the cracking time and the per cent of the added element is an inverse measure of the cracking tendency per one per cent. From these figures the alloying elements may be formed into a rank of decreasing unit cracking tendency. This order follows: phosphorus, arsenic, antimony, silicon, zinc, aluminum, nickel. Brass cracks more rapidly than any of the other systems mentioned; but zinc is low on the list because so much of it must be added to give a rapid cracking rate.

Another observation is the appearance of a minimum in the per cent of alloying element versus breaking-time curve. This minimum breaking time is distinct in copper-nickel, copper-silicon, copper-arsenic, and copper-aluminum systems; is indicated in copper-antimony and copper-phosphorus and is absent in copper-zinc.

The curves relating per cent of added element to corrosion rate in the absence of stress have a maximum in all systems for one of the more dilute alloys. This maximum is distinct in the copper-arsenic and copper-antimony systems and fairly distinct in copper-nickel, but only slight in the others. The same three, copper-arsenic, copper-antimony and copper-nickel, may be said to exhibit positive correlation between cracking tendency and corrosion rate.

Intergranular penetration in the absence of stress in moist ammoniacal atmosphere places the elements in the following rank in order of decreasing penetration: phosphorus, antimony, zinc, arsenic, silicon, aluminum, nickel. The extent of this phenomenon is very greatly dependent on grain size and the rank is subject to so many variables, that it may be assumed to be nearly enough like the breaking-time rank to support the belief of a common cause.

Conclusion

The data presented are insufficient for a concrete conclusion, but the following are offered for consideration:

The addition of a soluble element to copper produces a concentration of the solute at grain boundaries. This concentration either forms a submicroscopic precipitate, a richer solid solution, or lattice disturbances. Any of these conditions makes the grain boundary region anodic to the grain bodies. Localized corrosion is accelerated and grain boundary penetration ensues. The presence of a tensile stress still further accelerates penetration by opening cracks and forming highly stressed notches.

Work is being continued on this research.

Acknowledgments

The authors are grateful to Mr. John R. Freeman, Jr., Technical Manager of The American Brass Co. for his encouragement during the experimental work and for permission to publish the results. They also wish to acknowledge the advice of Mr. E. W. Palmer and the assistance of many members of the technical staff of The American Brass Co.

References

1. Symposium on Stress-corrosion Cracking of Metals. ASTM-AIME (1944).
2. H. H. Uhlig (Editor): Corrosion Handbook. 30. 1948. New York. John Wiley and Sons.
3. ASTM Standards (1946), pt. IB, 134.
4. E. H. Dix, Jr.: *Trans.* AIME (1940). 137, 2.
5. W. H. Bassett: In discussion of Alan Morris, *Trans.* AIME (1930) 273.
6. G. Edmunds: Ref. 1, 87.
7. T. A. Read, J. B. Reed and H. Rosenthal: Ref 1, 108.

Cadmium Recovery Practice in Lead Smelting

P. C. FEDDERSEN,* Member AIME, and HAROLD E. LEE*

Introductory Review

GREENOCKITE is the only known cadmium mineral of importance. It occurs rather universally, in minor concentrations, as a secondary mineral in sphalerite deposits. The world's cadmium output is obtained through the processing of metallurgical by-products, largely from the treatment of residues from electrolytic zinc, retort zinc and lithopone plants. These sources are supplemented by the processing of fumes from lead and copper smelting operations. The development of modern selective flotation practice in the decade 1920–1930, which permitted the economical mining of complex lead-zinc ores, resulted in significant increases in the quantities of cadmium entering lead smelting systems.

Being closely related to zinc as to occurrence, properties and production, most detailed description of cadmium recovery methods are to be found recorded in connection with zinc metallurgy. Other than occasional articles pertaining to particular operational procedures, literature offers but little in the nature of a balanced survey of lead smelter cadmium recovery practices. While many of the basic operations described for the recovery of cadmium from zinc by-products are applicable to the treatment of lead plant products, the inherent problems involved differ widely. In general the cadmium content of related by-products from routine lead smelting operations is present in lower concentrations, exists in a less soluble state and is associated with both a greater quantity and a greater variety of detrimental impurities. To cope with these problems, lead smelter practices are found to follow the general outline:

Preparatory Processing

1. Concentration operations
2. Sulphation operations

Cadmium Plant Processing

1. Leaching operations
2. Purification operations
3. Sponge precipitation operations
4. Metal recovery operations
5. Refining and casting operations

As in the case of related zinc plant operations, cadmium recovery practices at lead smelters are not standardized. They not only vary as to type, but also extent. Depending upon prevailing conditions, lead smelter cadmium operations range from simple concentration campaigns, for the purpose of sufficiently "up-grading" products for shipment elsewhere, to complete processing steps for the production of refined metal.

Preparatory Processing

The cadmium content of lead smelter receipts is low and, as a rule, proportionate to the zinc content; the usual range of cadmium contained being of the order of 0.01–0.05 pct. Were it not for the low boiling point of cadmium, such small concentrations would, no doubt, be lost in the large tonnages of slag, metal and other smelter end products. However, the ready volatility of cadmium and its compounds at prevailing lead smelting temperatures results in its concentration in fractional portions of fume collected. This collected fume comprises a circulating load within the smelter system.

Thus, the cadmium content of blast furnace fume* increases with each successive circulation until an equilibrium value is reached when the sum of the cadmium losses, due to handling and in slag, waste gases and other end products, becomes equal to the intake as ore. With ore receipts averaging, say 0.03 pct cadmium, the concentration value obtainable, through fume circulation in a routine manner, approaches 10–12 pct. In such operations, cadmium concentrations in blast furnace fume of from 3–5 pct are readily attainable. However, the concentration gain beyond this range, with each additional circulation, is progressively decreased as a result of mounting losses occurring through handling and in end products. Therefore, to avoid excessive cadmium loss and to enhance the ultimate concentration attainable, it is customary practice to isolate blast furnace fume at some intermediate cadmium content for special concentration procedure.

The most common type cadmium concentration "campaign" involves special smelting operations wherein a relatively high portion of blast furnace fume at 3–6 pct cadmium is incorporated into the sinter charge. This type practice is roughly illustrated by the diagram on p. 111.

Cadmium fume collected from lead blast furnace operations is not amen-

San Francisco Meeting, February 1949.

TP 2509D. Discussion of this paper (2 copies) may be sent to *Transactions* AIME before April 1, 1949. Manuscript received Sept. 20, 1948.

* General Superintendent and Metallurgist, respectively, Bunker Hill Smelter, Kellogg, Idaho.

[1] References are at the end of the paper.

* The relatively low temperature and contact time which prevails during sintering operations is not conducive to cadmium volatilization. Practically all cadmium elimination occurs during blast furnace smelting operations.

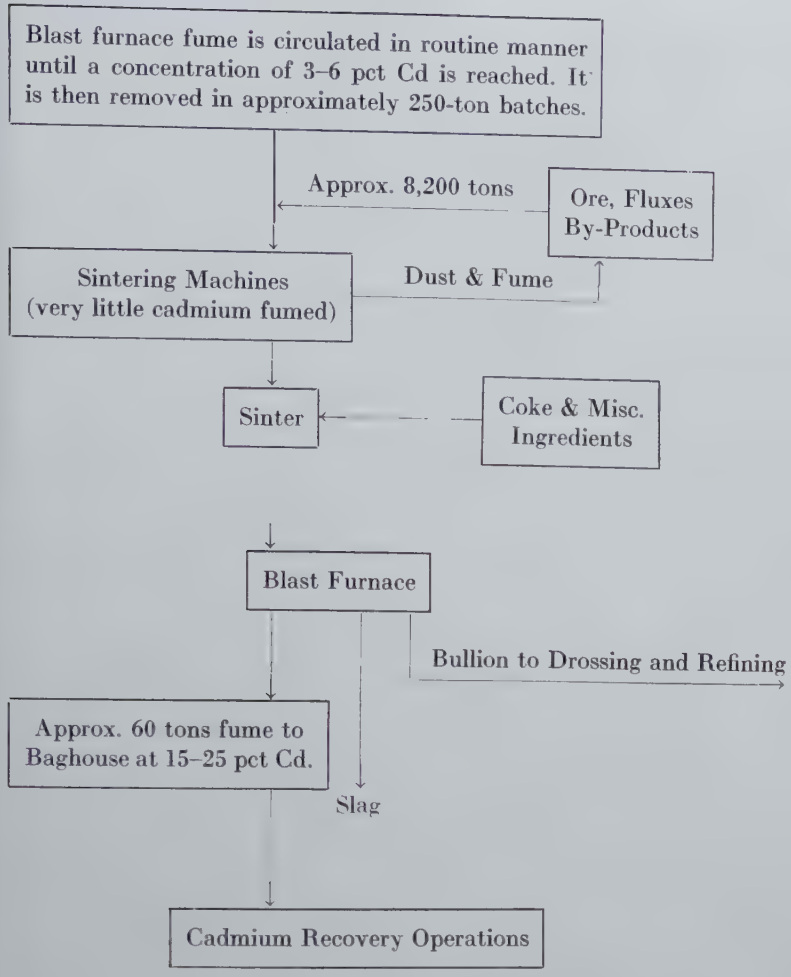

able to direct acid leaching. The cadmium contained is only partially soluble and the fume possesses a sort of "buffer" action which often limits the concentration of dissolved cadmium attainable. It is general practice in the processing of blast furnace fume to "precondition" by pugging with large portions of concentrated sulphuric acid, followed by heat treatment for elongated periods. While this sulphation step effects a high degree of solubility and greatly aids in impurity control, the attendant acid requirement is high and the physical aspects of the operation are not too desirable. At Kellogg, where acid is expensive, the Bunker Hill Smelter developed an alternative concentration procedure whereby a product of high cadmium concentration, amenable to direct acid leaching, is obtained by the fusion of blast furnace fume with silica.

In the fusion process, as in the more common method described above, blast furnace fume is circulated in the regular lead smelting system until a cadmium concentration of 4–6 pct is reached. It is then removed, mixed with a siliceous flux and fused in a special reverberatory operation. During the fusion, the bulk of the cadmium is distilled and the bulk of the lead retained as a silicate slag. Lead silicate slag is tapped and returned to the blast furnace; the cadmium fume is bag filtered, then sacked for delivery to a cadmium leach plant. In reverberatory melting, the grade of cadmium fume produced is limited by the necessity of excessive temperature in the upper bath layer. However, by limiting the proportion of silica used, and with reasonable care to avoid over-firing, blast furnace fume of 4–6 pct cadmium content may be raised to a product of 30 pct grade.*

At this point in our presentation of cadmium recovery procedures, it should be stated that descriptive terms such as "common," "customary," and so forth, are only used in their most limited sense; departures from the practices featured are many. Some of these diversions are itemized below:

* In experimental tests under closely controlled temperature conditions such as are readily attainable in an electric furnace, cadmium fume of 60 pct grade has been produced from blast furnace fume containing 6–8 pct cadmium.

TRAIL SMELTER—CONSOLIDATED MINING AND SMELTING CO. OF CANADA, LTD., TRAIL, B. C.

Cadmium-bearing fume from routine lead smelting operations, of 3–5 pct Cd. grade, is periodically forwarded to the zinc oxide leach plant and processed in conjunction with zinc fume from slag treatment operations. The insoluble lead-rich residue is subsequently returned to the lead smelting circuit.

FEDERAL PLANT—AMERICAN SMELTING AND REFINING CO. ALTON, ILL.

Up until 1941, at least, no special concentration campaigns were utilized. Blast furnace fume at about 5 pct cadmium was sulphated directly with concentrated sulphuric acid in preparation for subsequent leaching.

Some of the American Smelting and Refining Co. plants no doubt, practice cadmium concentration in accordance with an assigned patent[2] granted to R. Teats in 1930. This patent specifies the treating of a finely divided mixture of lead fluedust, carbonaceous material and limestone at 825–850°C to boil off cadmium which is oxidized and collected. The limestone, it is claimed, hinders the volatilization of lead and zinc.

PORT PIRIE WORKS—BROKEN HILL ASSOCIATED PTY., LTD., PORT PIRIE, AUSTRALIA[1]

Blast furnace fume from routine lead smelting operations is continuously advanced to a central sump and agitated with water for the solution of fractional portions of the cadmium present. The pulp is then subjected to vacuum filtration, giving two products: (1) Residue, which is returned to the blast furnace and (2) Filtrate, which is treated with sodium carbonate for the precipitation of dissolved cadmium. The cadmium carbonate precipitate is filtered, dried and shipped to the Electrolytic Zinc Co. of Australasia, Ltd., at Risdon.

Survey of Cadmium Production Methods at Lead Smelters

As already indicated, lead smelter

Table 1 . . . Outline of Representative Processes for the Production of Cadmium from Lead Smelter Fume

Plant and Location	U. S. Smelting, Refining and Mining Co. Midvale, Utah	St. Joseph Lead Co. Herculaneum, Mo.	Bunker Hill and Sullivan Mining and Conct. Co., Kellogg, Idaho
Preparatory processing Concentration	Blast furnace fume is circulated in routine manner until reaching cadmium content of 3–6 pct. It is then removed and incorporated in relatively high proportions in sinter charge. Blast furnace smelting of resultant sinter gives a fume product containing 15–25 pct cadmium	Similar to Midvale practice	Blast furnace fume is removed from regular circuit at 4–6 pct Cd., then mixed with siliceous flux and fused in a reverberatory furnace. Furnace products consist of lead silicate slag (returned to blast furnace) and cadmium fume at 25–30 pct Cd.
Sulphation	Above fume is pugged with 60° Be H_2SO_4 in batches (400 lb acid per 800 lb fume). After digestion period mixture is charged to furnace and baked 24 hr at low red heat, discharged, cooled and dry ground to 20-mesh in a 3 ft ball mill.	Fume at about 20 pct Cd. Pugged in batches with about 210 lb, 60° Be H_2SO_4 per 500 lb fume. Mixture is charged in 2,000 lb batches to a pan mounted on wheels. Charged pan is rolled on tracks into furnace and baked (no rabbling) for 8 hr at 850°F, then discharged, cooled and broken, and pulverized to −100 mesh.	None
Cadmium plant processing Leach Purification	Joint leach and purification practiced. Minus 20-mesh sulphated product is leached with spent electrolyte for 2 hr in a 4 × 8 ft Pachuca tank. Na_2S is added to ppt, Cu and final slurry is neutralized with hydrated lime, then filtered and washed in a 2-ft sq. Shriver press. Washed cake is returned to lead smelting circuit.	Pulverized sulphated product is leached in a mechanical agitated, 2,000 gal capacity steel tank with wash water from previous filter operations, then filtered and washed in 3-ft sq. Shriver press. Washed cake returned to lead circuit. Filtrate is treated with a limited quantity of zinc dust for ppt. of Cu and then passed through a clarifier.	Joint leach and purification practiced. Concentrated fume is subjected to a direct dilute H_2SO_4 leach, 800 lb H_2SO_4 being consumed per 6,000 lb of 27 pct cadmium fume. Fe, Sb, As, etc., purification effected by the addition of copperas and oxidizer in conjunction with pH control. Slurry is filtered and washed in a 65 cf capacity Shriver press. Washed cake is returned to lead smelting circuit.
Sponge precipitation	None	Pregnant Cd filtrate is drawn from storage tanks through two 4 ft × 2½ ft × 30 ft deposition tanks—each tank containing 96 − 21 × 12 × 2 in. plates. Cadmium ppt. as metallic sponge on zinc plate surfaces. Sponge is removed from tank, dewatered by a rough initial press, then briquetted at high pressure into 8 in. diam × 1 in. thick cakes which are stored under kerosene.	Pregnant solution is drawn from storage tanks in 800 gal batches to a conical-bottomed, high-speed agitation tank. The solution is acidified and treated with zinc dust for Cd sponge precipitation. Initial sponge washing is carried out by decantation and the final dewatering and wash in a Shriver press. Cd sponge is briquetted directly with a Stokes machine.
Metal recovery	Pregnant cadmium solution at 120 gpl electrolyzed down to 35 gpl in a cascade, side circulation, cell circuit. Five aluminum cathodes and six durion anodes used in each of 10–30 in. sq. × 40 in. deep California redwood cells. Cathode trees removed each shift. cathodes stripped each 24 hr 78–80 pct Ce at 12 amp per sq ft. Plant capacity = 450 lb cathode cadmium per day.	Cadmium briquettes retorted. Graphite bottles and cast iron condensers used. 3 retorts utilized per 2,000 lb Cd per day. 12 hr retorting time consumed per 500 lb charge.	Cadmium briquettes are retorted, using similar bottles and condensers as employed at Herculaneum plant. Four retorts are used per 1,500 lb of cadmium per day. Retorting time per 600 lb charge variable, depending upon life of bottle and grade of briquettes. Retort residue returned to leach.
Refining and casting	No additional refining practiced. Cathodes are rolled and rough melted under cylinder oil and cast into bars. These bars are then melted under a light caustic cover for casting into shapes for market.	Crude retort metal is subjected to two treatments; the first with $ZNCl_2$ for the removal of thallium. The Tl-bearing $ZnCl_2$ is marketed and the metal then treated with NaOH prior to casting into shapes for market.	Crude retort metal is melted under a caustic cover residual from a previous melt. This cover is then drossed and the bath agitated with NH_4Cl for thallium removal. The chloride dross is skimmed and stored. New caustic is then added and melted, followed by a brief period of agitation prior to casting into shapes for market.
Grade metal produced			
Copper	0.0128	Nil	0.0002
Lead	0.0595	0.02	0.0130
Iron	0.0048		0.0012
Zinc	0.0028	0.10	0.0150
Thallium		0.02	0.0060
Antimony, arsenic			Tr
Cadmium			99.9646

cadmium operations vary, both as to type and extent. The tonnage intake is low and few smelters pursue operations beyond the concentration stage. Markets for resultant cadmium products of reasonable grade may be found in zinc and chemical industries, and the American Smelting and Refining Co. operate a custom cadmium plant at Denver, Colo. Cadmium bearing products from the various A. S. and R. smelting operations are shipped for treatment at the Globe Plant. Prominent among other lead smelters equipped for cadmium production are the U. S. Smelting, Refining and Mining Co. at Midvale, Utah,* the St. Joseph Lead Co. at Herculaneum, Mo., and the Bunker Hill and Sullivan Mining and Concentrating Co. at Kellogg, Idaho. To a limited extent, in the past few years, the Bunker Hill plant has been operated on a custom basis.

Table 1 presents an outline of the essential processing steps employed in the three latter plants recorded above. This summary depicts a more or less representative composite of lead smelter practices. Among the component operations outlined may be found most processing steps employed for the recovery of cadmium from lead smelter fume. Though little information regarding recent practices at the Globe plant are available, earlier descriptions of H. R. Hanley[3] and T. P. Campbell[4] indicate no marked departures from the practices summarized in Table 1. Since an intelligent discussion of a process requires intimate plant knowledge and an appreciation of prevailing plant conditions, any detailed considerations of the practices outlined must be limited to Bunker Hill operations. It is interesting to note, however, that the Midvale process, developed by R. H. Stevens,[5] was placed in operation in 1915. This plant can probably be credited with the first production of electrolytic cadmium on a commercial scale.

* The Midvale Plant has not been operated since 1944.

[†] Flow-sheet, Fig 1, was drawn from information supplied by the Bunker Hill Smelter and appeared in an article by John B. Huttle, "Bunker Hill Plant Recovers Metallic Cadmium from Fume," *Eng. and Min. Jnl.*, Apr. 1946, 174 No. 4, 82–85. It is reproduced by permission of *Eng. and Min. Jnl.*

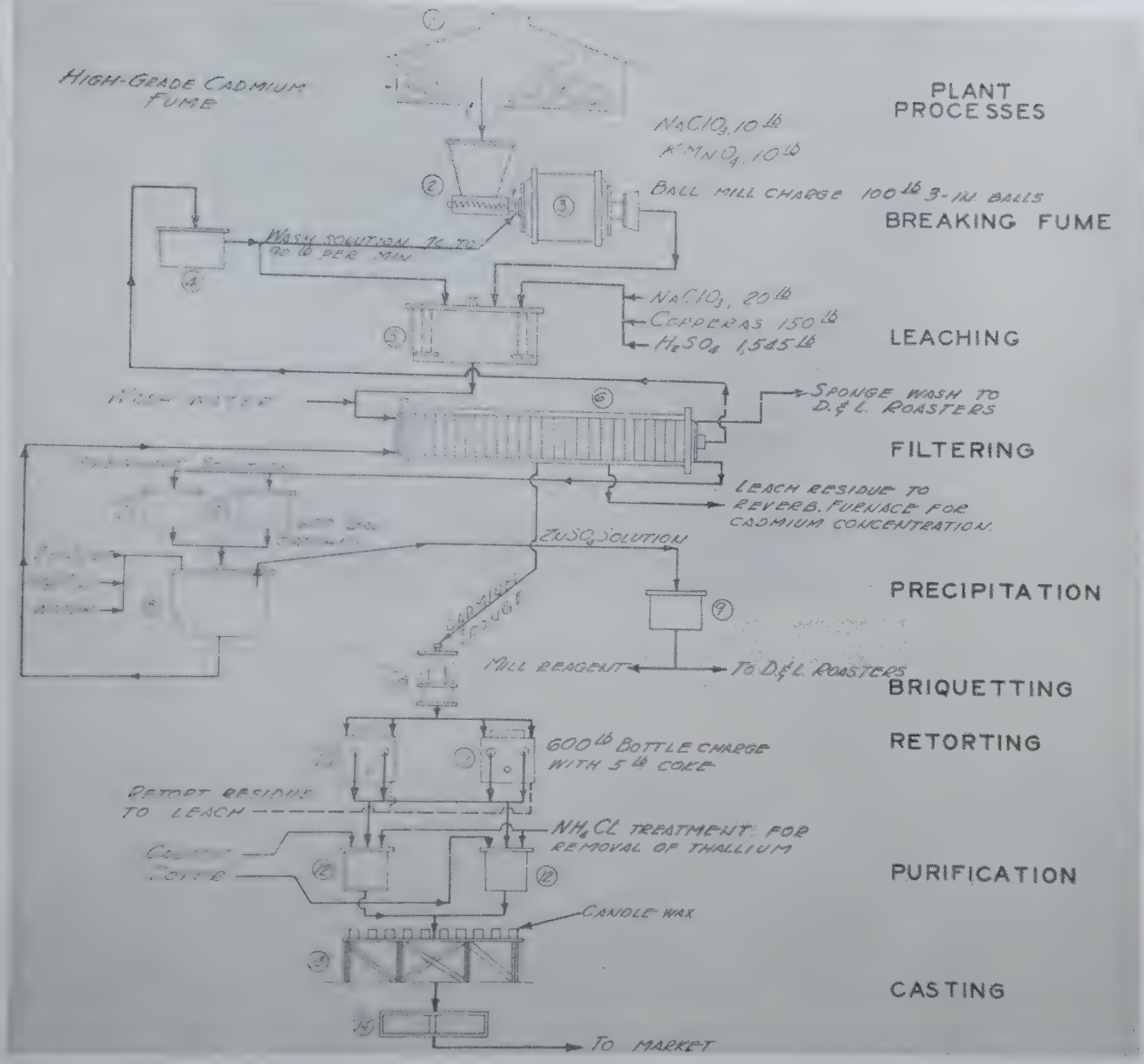

FIG 1—Flow sheet of Bunker Hill cadmium recovery plant.

1. Storage shed.
2. 6000 lb batch leach with screw feeder.
3. 3 × 3 ft ball mill.
4. Wash solution storage tank.
5. 8 × 8 ft lead-lined leach tank.
6. Shriver press, 42 2-in. × 3-ft × 3-ft frames.
7. 5000 gal pregnant solution storage tank.
8. 8 × 8 ft lead-lined precipitation tanks.
9. Zinc sulphate storage tank.
10. Briquette machine.
11. Two-bottle oil-fired retorts.
12. Holding pots, 3000-lb capacity.
13. Ten 4 × 16 × ¾-in. molds.
14. Cleaning & boxing section.

Bunker Hill Cadmium Recovery Operations

GENERAL DISCUSSION

As already described under "Preparatory Processing" Bunker Hill Cadmium Plant feed consists of fume concentrated by a special reverberatory fusion of a mixture of blast furnace fume and siliceous flux. This product, produced under more favorable oxidizing conditions than practically attainable in a blast furnace, contains very little sulphide and is amenable to direct leaching in dilute sulphuric acid. As is illustrated by the accompanying flow-sheet, Fig 1, the process employed utilizes a combined leaching and purification operation, followed by sponge precipitation with zinc dust and final metal recovery by retorting. The particular type and sequence of methods depicted were selected after a long experimental period during which many alternative practices were investigated.

Cadmium recovery obviously involves low tonnage operations wherein efficient processing is most essential to economic production. Processing efficiency is particularly important in the treatment of lead smelter fumes which generally contain high and variable percentages of troublesome impurities. In certain instances primary extraction becomes secondary to flow simplicity

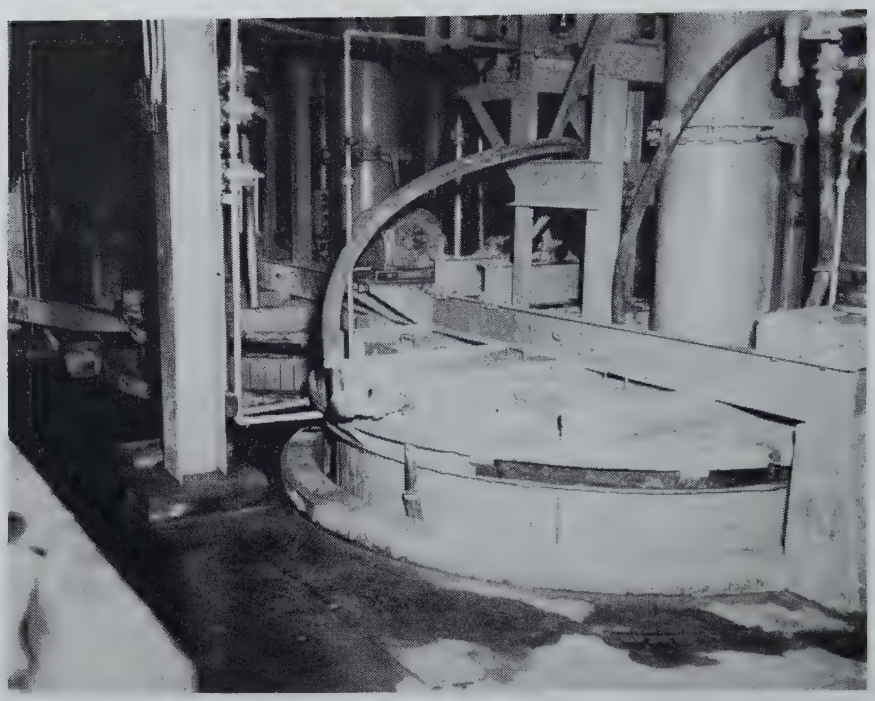

FIG 2—Cadmium leach and precipitation tanks—showing hodding and ventilation system.

and flexibility. In the development of Bunker Hill practice for example, experimental experience indicated that the increased primary extraction attainable by means of separate leaching and purification steps, would not justify the attendant complications of plant flow and the associated increased treatment and capital costs. Similar evaluations resulted in the choice of distillation procedure over electrolysis and sponge precipitation with zinc dust rather than on slab zinc as practiced at Herculaneum. For the processing of Bunker Hill fume, the degree of impurity control necessary for successful electrolytic operations would require re-solution of a thoroughly washed sponge in a separate electrolyte circuit. Retorting procedure not only avoided this extra treatment, but also provided operations more readily adjustable to variable capacity conditions. Although the Herculaneum type precipitation practice produces sponge of superior retorting grade, such a system would be very cumbersome in the processing of arsenic-bearing products where venting is necessary and every precaution to avoid arsine poisoning must be taken.

GENERAL PLANT DESIGN

The Bunker Hill Cadmium Plant represents a modern installation for the processing of lead fume, having been placed in operation in June, 1945. It is a compact steel and concrete structure, constructed for the production of 1000 lb of cadmium per day when treating fume of 25 pct grade. Into its design were incorporated all practical facilities to provide both operational ease and favorable working conditions. Equipment units are conveniently located and served by an excellent ventilation system. Solution levels in tanks are observable from strategic points by means of electronic level indicators. Retort temperatures are automatically indicated and recorded, and semiautomatic temperature control with a fuel-air ratio controller, is provided. Both the upper floor, utilized for the receipt and storage of fume and reagents, and the lower floor from which end products emerge, are readily served by truck. Material passes by gravity flow through the leaching, precipitation and metal recovery operations conducted on intermediate levels.

LEACHING AND PURIFICATION PRACTICE

Referring to the accompanying flow-sheet (Fig 1), sacked cadmium fume is weighed and dumped into a steel bin which is screw-discharged into a 3 × 3 ft pulping ball mill located on the leach floor. Circulating wash solution meets and carries the screw-discharged fume into the scoop box of the pulping mill from which it flows by gravity into a vented, lead-lined, 8 × 8 ft agitator tank. (Fig 2.)

Prior to the flow of ball mill slurry, a predetermined weight of concentrated H_2SO_4 is drawn into the leach-tank along with a small volume of wash water and the agitator started. To this strong acid mixture is then added copperas and sufficient sodium chlorate to oxidize the iron to the ferric state. About mid-run, to offset the reducing effects of fume ingredients, additional chlorate is added at the ball mill and at the close of the run, some potassium permanganate.

While reagent consumption varies widely with changes in fume character, the consumption when treating 6000 lb of 26 pct cadmium grade fume* may be roughly recorded in the range of:

Reagent	Pounds
60° Be H_2SO_4	800
Copperas	200
Sodium Chlorate	30
$KMnO_4$	10

About two hours is required to pulp 6000 lb of fume. Then, after a short period of additional agitation, the slurry is sampled for acidity. If its pH value runs much lower than 5.3, as shown by a Coleman pH tester, addi-

* Reagent proportions shown on the flow-sheet are for the treatment of high-grade cadmium fume (approx. 45 pct Cd).

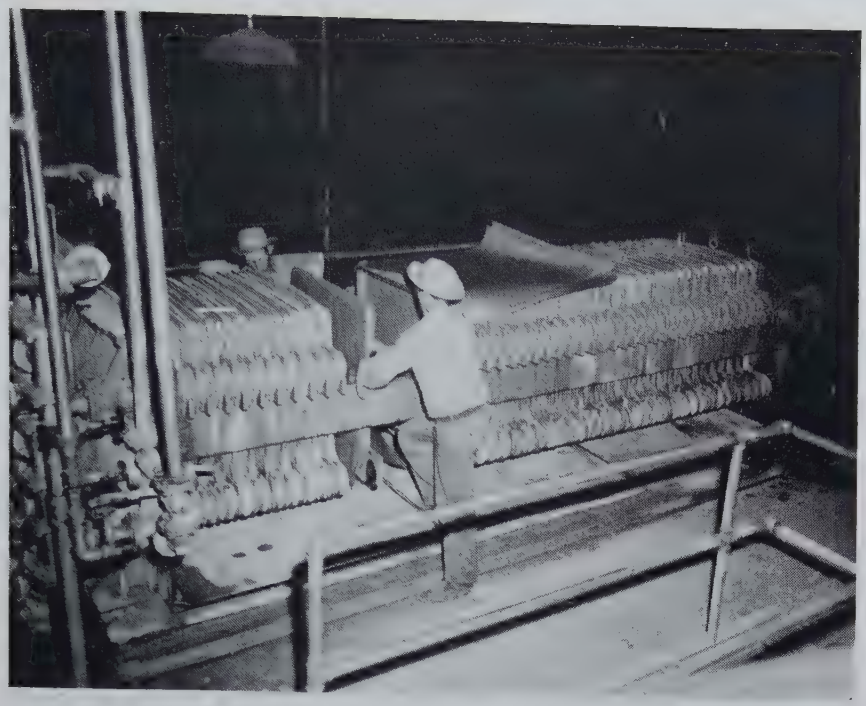

FIG 3—Sixty-five cubic foot capacity Shriver press—utilized for both cadmium leaching and precipitation operations.

tional fume is added. Upon reaching the required acidity range, a filtrate sample is assayed for arsenic. When the arsenic assay shows the presence of less than 10 mg per liter, the slurry is diluted to about 1700 gal and pumped through a 65 cf capacity, closed delivery Shriver press, (forty-two 2 in. × 3 ft square frames used), to one of two 5000 gal lead-lined, pregnant solution storage tanks. Seventeen hundred gallons of slurry results in about 1500 gal of pregnant solution. One leach cycle is completed per 2-man shift and about 10,000 gal of pregnant solution is obtained in six shifts' operation.

Purification is accomplished through the use of oxidizers and by pH control. Though copperas aids in arsenic removal, considerable arsenic precipitates as a cadmium compound, and the primary extraction attainable varies as the cadmium arsenic ratio; this ranges from a low of about 75 pct for products containing about 6–7 pct As to around 90 pct for products down to 3 pct As. Neutralization to a pH of 5.3 permits practically complete arsenic precipitation. While operations in a higher acidity range allow higher primary extraction, the arsenic purification problem is greatly complicated.

The leach residue is washed in the filter press with about 1500 gal of water which is pumped to an 8 × 8 ft lead-lined storage tank for use as make-up solution in a succeeding leach. Upon breaking the filter-press, the washed and blown residue is dropped through a chute to a concrete storage bin on the lowest plant level. From this bin it is conveyed back to the lead smelting circuit, wherein lead is recovered and the cadmium returned to the circulating fume load. (Fig 3.)

SPONGE PRECIPITATION PRACTICE

After two leach days, during which the solution of 8000 to 10,000 lb of cadmium is effected, the crew turns to precipitation operations. Stored pregnant solution, now of known cadmium content, is drawn in 600–800 gal batches into a lead-lined, conical-bottomed precipitation tank served by a high-speed agitator. As in the leach system, this tank is hooded and positively vented by means of a 6400 cfm fan. The vented tank atmosphere is conveyed and discharged into the blast furnace flue system. In this manner, possible hazardous concentrations of arsine are speedily removed and diluted to harmless proportions with 150,000 cfm of blast furnace gas.

Each batch of solution for precipitation is acidified by the addition of H_2SO_4, to about 4.5 grams acid per liter. Then, zinc dust is charged in the proportion of about 0.62 lb zinc per lb of cadmium contained. Electro-positive zinc displaces cadmium from solution with the production of cadmium sponge. The action, induced by high-speed agitation, breaks and rolls the sponge masses into dense pellets favorable to washing by decantation. To prevent the precipitation of basic sulphate salts, the solution acidity is not allowed to fall below 2.0 grams per liter and zinc additions are terminated when the solution assay shows a cadmium content below 0.5 grams per liter. At this point, the agitator is shut off, the pellets allowed to settle, and the clarified $ZnSO_4$ solution decanted and pumped to a strong zinc solution storage tank for marketing to the flotation mills of the district. The settled cadmium is then washed by dilution with water and agitation before being pumped to the Shriver press; the filtrate going to a weak $ZnSO_4$ storage tank for delivery to D and L sintering operations.

About 9 similarly treated precipitation batches are accumulated in the filter press prior to a final wash with water. The press is then blown with air until warm, broken, and the contents discharged to a steel storage bin on the retort floor below. To avoid excessive cadmium oxidation, briquetting op-

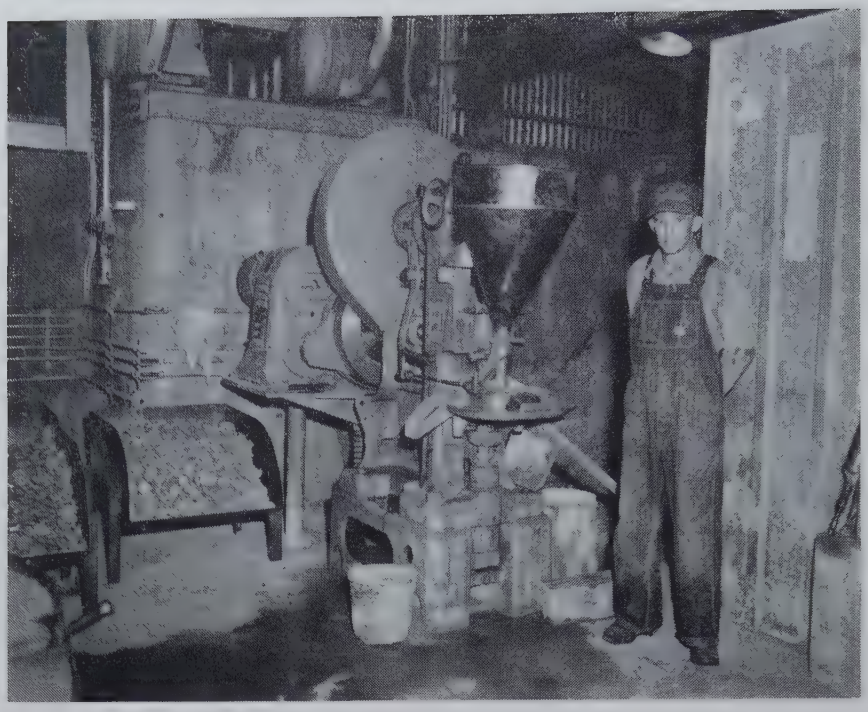

FIG 4—Stokes briquetting machine showing cadmium briquette storage pans.

erations are started soon after a press discharge.

METAL RECOVERY OPERATIONS

Sponge briquetting, with no additive agents and no prior treatment other than granulation through an 8-mesh screen, is practiced. The screened sponge is charged to the hopper of a Model R Stokes machine. The sponge is dewatered and its density increased about three times, by compression under 17 tons pressure, into 2 in. diam by ½ in. thick briquettes. The compressed discs discharge into steel storage pans at the rate of about 1000 lb per hr. Each storage pan has a capacity equivalent to that of a retort bottle. They stand off the floor on legs to permit ready transfer to the retorts by lift truck. (Fig 4.)

Two oil fired retort units are employed for cadmium distillation from briquetted sponge. Each retort unit is of firebrick construction and contains two No. 11 American Crucible Co. graphite bottles set on piers above a brick checker-work arch, which distributes the heat from the firebox below. The retort bottles are manually charged, 600 lb per bottle, 1200 lb per retort unit.

After being charged, portable, partially insulated, cast iron condensers, which fit about the extended neck of the retort bottles, are rolled into place and the bottle-condenser junction sealed with fireclay. The closed, outer ends of the cylindrical condensers have two ½-in., holes. The bottom hole is immediately sealed with clay and only opened when tapping metal. The upper hole is kept open for an hour or so after the start of a run to permit the escape of moisture and other gases noncondensible at elevated temperatures. When cadmium vapor is evidenced, the upper hole is sealed.

While the retorting cycle is a variable depending upon the bottle life and briquette character, the average time consumed approaches 20 hr. A description of Bunker Hill retorting practice is as follows:

With the condensers pulled aside, the briquette storage pans are moved to the retorts and the contents shovelled into the bottles. The condensers are then rolled into place and the junctions sealed with clay. Next, the firing is stepped up and the firebox temperature brought to, and maintained at, 2100°F. After about 1½ hr heating, cadmium starts to distill and the upper vent holes are sealed. From then on, at three-hour intervals, the condensers are tapped and the condensed, molten cadmium drawn into steel pans. When the charge is "cooked" as evidenced from the quantity of metal drawn, the condensers are pulled away and the bottles raked clean for the receipt of the succeeding charge.

Retort residue is returned to the leach circuit and the crude metal is charged to one of two pots utilized for refining and casting. Depending upon bottle life and the grade of briquettes, the operation of two retort units (four bottles) allows a crude metal production of from 1400 to 2000 lb of cadmium per day. (Fig 5.)

REFINING AND CASTING PRACTICE

Two 3000-lb capacity, electrically heated kettles are used for both refining and casting. One pot is being either held or used for casting while the other is being charged for refining. Refining operations are chiefly concerned with thallium removal. The crude retort metal produced meets all impurity specifications except for lead and thallium. All metal is treated for thallium removal; occasional lots destined for sale to bearing manufacturers must be redistilled to meet lead specifications.

Crude retort metal is charged to one of the two kettles and melted under a thin caustic cover. When the kettle is full, the caustic cover is skimmed and 30 lb of ammonium chloride is agitated into the bath over a ¾-hr period. The chloride dross is then removed and 20 lb of new caustic added. About 15 min. additional agitation is given as a precaution against zinc contamination. At this point the agitator is removed and the metal ready for casting.

Refined metal is drawn, by means of a screw-operated valve, through an outlet in the kettle bottom into a casting ladle that is heated by means of a kerosene torch. It is cast into shapes

FIG 5—Bunker Hill cadmium retort installation—showing condenser in place and tapping operations.

for marketing in vertical, air-operated molds. The solidified shapes (slabs, balls, sticks) are given a dilute hydrochloric acid dip and wiped dry before weighing and boxing for shipment.

Cadmium Metal Marketing

There are no A. S. T. M. Cadmium specifications. Although attempts have been made in recent years to establish market requirements of more restricted and uniform nature, standardization has not yet been realized. In general, platers are rather lenient with regard to lead (0.05 pct max.) but are insistent on limiting the thallium content to 0.005 pct. The bearing manufacturers, on the other hand, are willing to accept up to 0.05 pct thallium but limit the lead content to 0.02 pct. Some of the diversified marketing specifications are illustrated in Table 2.

As pointed out by John L. Bray,[6] cadmium is technically one of the younger metals. Although known since 1818, until comparatively recent times there have been but few uses for cadmium. Prior to 1925, the bulk of the world's cadmium was produced in Germany. Production in the United States, at that time, ranged between 25 and 100 tons per year. Concurrent with the use of cadmium as a plating medium, principally in the automotive industry, a marked growth occurred in U. S. production. By 1939, the United States became the world's largest producer.

While up-to-date statistics are unavailable at this writing, evidence points to a 1948 U. S. production approaching the 1947 total of 4,000 tons metallic cadmium. This production is somewhat under the war-time high of 4,300 tons, a decline that parallels a 10 pct decrease in zinc production from its war-time peak. At 4,000 tons per year, metallic cadmium production appears to be somewhat in excess of current domestic requirements. The pattern of current domestic consumption is of the following order:

	Pct
Electro-plating	75
Bearing alloys	15
Solder alloys	5
Pigments	2
Chemical	2
Miscellaneous	1

It is interesting to note that the foregoing pattern is not typical of foreign consumption. Abroad there is a more extensive use of cadmium in alloys and less in plating. About 10 pct of foreign consumption is also utilized in the manufacture of cadmium-nickel batteries for industrial and railroad units. This type battery has not been extensively used in this country, although within the past few years a small company in New England is reported to have started production.

Table 2 . . . Marketing Specifications

	Pct
Bureau of Federal Supply	
Cadmium	99.90 min.
Copper	0.01 max.
Iron	0.01 max.
Lead + silver + tin	0.05 max.
Zinc	0.05 max.
Antimony + Arsenic + Thallium	0.005 max.
Plating Industry	
Cadmium	99.90 min.
Lead + Silver + Tin	0.05 max.
Antimony + Arsenic + Thallium	0.005 max.
Bearing Manufacturer (A)	
Cadmium + Zinc	99.90 min.
Zinc	0.10 max.
Copper	0.02 max.
Lead	0.02 max.
Bismuth	0.01 max.
Antimony	0.01 max.
Tin	0.005 max.
(B)	
Cadmium	Remainder
Copper	0.40–0.60
Silver	0.60–0.80
Nickel	0.25 max.
Lead	0.05 max.
Zinc	0.05 max.
Tin	0.02 max.

Acknowledgments

The writers are indebted to Mr. Robert Wallace, Manager, Mr. W. M. Whitecotton, Asst. Smelter Supt., U. S. Smelting, Refining and Mining Co., Salt Lake City, Utah, and to Mr. W. T. Isbell, Supt., St. Joseph Lead Co., Herculaneum, Mo., for information used in references to their respective operations. Credit is also due Mr. C. R. Ince, Manager, Metal Sales Department, St. Joseph Lead Co., New York City, for the provision of cadmium production and marketing details.

References

1. *Proc.* Australasian Inst. of Mining and Metallurgy, (1932) 126.
2. U. S. Patent 1,727,492, Sept. 10, 1930.
3. H. R. Hanley: Mining and Sci. Press (1920) **121**, 795.
4. T. P. Campbell: Colo. School of Mines Mag. Oct. 1930, 26–27.
5. U. S. Patent 1,194,438, Aug. 15, 1916.
6. John L. Bray: Non-Ferrous Production Metallurgy. (1941), 64, New York, N. Y.—John Wiley and Sons, Inc.

Development of Muffle Furnaces for the Production of Zinc Oxide and Zinc at East Chicago, Indiana

GUNNARD E. JOHNSON*

Introduction

THE problem of efficient reclamation of zinc base die cast scrap became interesting early in 1930. Die Cast Metal, as referred to in this paper, is a zinc base alloy with various proportions of aluminum, copper, magnesium, antimony and tin.

Many attempts were made to work out some means of reclaiming the discarded die cast metal for re-use as new die cast metal. Difficulties in such reclamation were attributable to contamination by lead and tin from solder, chromium and nickel from electroplated coatings, and iron from iron inserts.

This paper relates the experiments that led to the development of a specialized muffle furnace for the treatment of zinc base die cast scrap for the production of zinc oxide and zinc, and describes the development of the muffle furnace and the equipment now used commercially for these purposes. The Eagle-Picher Co. acquired all patent rights[1] for these developments from the International Smelting and Refining Co. in connection with their purchase of the East Chicago Plant.

Zinc Base Scrap Situation

About 1935, the die cast scrap situation became increasingly acute for scrap dealers. This scrap was accumulating from dismantling automobiles and household appliances which contained die cast parts. Efforts to find an outlet for this type of scrap were intensified.

The International Smelting and Refining Co. began to study the possibilities of a commercial process for the recovery of values from die cast scrap. At that time most of the die cast metal reclaimed was melted down in small kettles of from one to five tons capacity, the iron inserts being removed by skimming. The dross was skimmed off and disposed of as a zinc dross. The drossed metal was cast into slabs and was given the trade name "die cast slabs." Distribution of the products produced by melting die cast scrap in kettles is shown in Table 1.

Table 1 . . . Distribution of Products Produced by Melting Die Cast Scrap

	Weight in Lb	Per Cent of Weight Charged	Per Cent Zinc	Lb Zinc	Per Cent of Zinc Charged
Charged					
Scrap as received	320,073	100.0	76.6	245,176	100.0
Products					
Die Cast Slabs	246,790	77.1	90.1	222,358	90.7
Melting Dross	35,620	11.1	55.1	19,627	8.0
Iron Rejects	36,491	11.4	10.0	3,649	1.5
Ignition Loss	1,172	0.4	0.0		
Unaccounted for Gain				−458	−0.2
	320,073	100.0		245,176	100.0

American Process Experiments

A method considered for the production of zinc oxide from die cast scrap was an adaption of the standard American Process of zinc oxide manufacture. Thus some die cast scrap was mixed with oxidized zinc materials and charged to Wetherill grates. The zinc oxidized to zinc oxide but, while the aluminum and copper largely remained in the residue, the color of the zinc oxide produced was impaired by copper contamination. As the proportion of die cast scrap was increased, liquation took place; that is, the metal trickled through the charge then solidified in the openings of the grates.

French Process Experiments

Several hundred tons of die cast scrap were purchased for test purposes and converted into die cast slabs. These slabs were charged into a French Process (horizontal retort) zinc oxide furnace with some electrolytic zinc. A satisfactory grade of zinc oxide was not produced.

Distillation in Belgian Retorts

It was then decided that, rather than attempt to use scrap die cast metal or scrap zinc for the production of zinc oxide, it would be advisable to redistill the die cast slab metal in a Belgian retort furnace.

The opportunity to do so was provided by the closing of the zinc smelter of the Illinois Zinc Co. at Peru, Ill. Arrangements were made for the operation of a Belgian retort furnace for such redistillation purposes. The results of this experiment are summarized in Table 2.

San Francisco Meeting, February 1949.

TP 2526 D. Discussion of this paper (2 copies) may be sent to *Transactions* AIME before May 15, 1949. Manuscript received October 4, 1948.

* General Manager—East Chicago, Indiana, Plant of the Eagle-Picher Co.

[1] References are at the end of the paper.

Table 2 . . . Results of Experiment

	Weight in Lb	Per Cent Charged
Metal Charged	2,778,541	100.0
Production		
Redistilled Metal	1,684,913	60.7
Metal from Blue Powder	518,711	18.6
Residue Metal	218,287	7.9
Loss	356,630	12.8

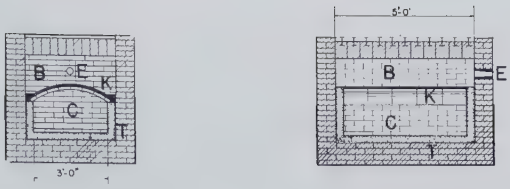

FIG 1—Experimental muffle furnace.

All of the zinc produced contained varying amounts of copper, tin and aluminum in sufficient quantities to make it unmarketable. The metals produced, however, were found satisfactory for use in making zinc oxide provided the quantities used were limited to a small fraction of the total metal charged.

Distillation in Graphite Retort Bottles

Some attempts were made to treat die cast scrap in graphite bottles to produce zinc. Very little success resulted from these attempts because graphite bottles had a short life. Also the relative position of the condenser with reference to the retort permitted the condensing metal to contact, and become contaminated with, aluminum and copper.

The next experiment was to produce zinc oxide from the die cast scrap charged to graphite retorts. The zinc oxide produced was conveyed directly to a baghouse by means of a fan and duct system. This zinc oxide was unsatisfactory because of the high copper content and very poor color. Further, contamination with lead and aluminum took place; these elements being mechanically carried into the baghouse when the mouth of the retort bottle was cleaned or when the charge of residue left in the bottle was poured into molds.

It was finally concluded that recognized processes for production of zinc or zinc oxide were not satisfactory for the treatment of die cast metal. Some new approach to the problem was needed.

Experimental Muffle Furnaces

Initial investigation began with the use of a laboratory muffle furnace. This was a rectangular muffle constructed of carborundum tile cemented at the joints. Attempts were made to hold the level of liquid metal at not over 2 in. in depth. Even with this small depth of metal, serious leakage occurred.

At about the same time, a pilot unit was constructed which provided means for heating the metal bath from above and below. Heat was introduced below the bath by means of a gas flame within a refractory tunnel. This furnace leaked badly after every effort had been made to make it tight enough to contain molten die cast metal.

Shortly afterward a larger experimental unit 5 ft long with a carborundum arch 3 ft wide was built and tested. This unit is illustrated in Fig 1 which shows cross-sectional and longitudinal-sectional views of the furnace.

This pilot unit established the fact that zinc could be vaporized, practically, by means of a large shallow bath and that such vaporizing is less violent and more easily controlled than in the more restricted areas of small retorts.

This furnace provided a monolithic hearth construction arranged within a steel shell to confine the molten metal against escape and loss. Also, operation of the furnace confirmed calculations that it was practical to apply heat to the bath, from above, through a carborundum arch. The zinc vapor did not seep through the carborundum arch.

The metal was charged into the furnace through two small openings in the vaporizing chamber just below the arch. Zinc vapors were conveyed by a short horizontal brick flue to a chamber. Oxidation of the metal vapor to zinc oxide took place at the brick chamber from which the zinc oxide was conducted to a baghouse through a steel flue. This furnace established operating characteristics of the larger furnaces later constructed and pointed out the need for a substantial arch anchorage and related construction problems.

Our experience with these furnaces indicated that satisfactory commercial operations would not be achieved until an integrated unit was produced, having a tight hearth, a tight arch, and adequate provisions for keeping the zinc or scrap metal heated to the desired temperature, in conjunction with a vaporizing unit from which zinc vapors would be discharged rapidly and at uniform rate. Analysis of experimental operations also led us to believe that commercial operations could proceed upon development of effective means for excluding air from the vaporizing chamber within which the molten bath was being heated. Any air entering this area would react with the vapors to form an oxide film or layer, which inhibits heat transfer to the bath of molten zinc, thus gradually impeding the liberation of zinc vapors from it. This factor was a principal cause of the decline in rate of oxide production soon after the start of operations in the experimental muffle units. It was recognized at the time that the results obtained in small scale equipment would not necessarily be predictive of those obtainable with a larger furnace. However, contemplation of a large scale unit introduced additional questions in respect to confinement of a large bath of molten zinc against escape. A further problem was the accommodation of expansion, under air-seal conditions, of a commensurately large arch capable of sustaining the relatively high temperatures involved.

To meet these requirements, the later design of our commercial furnaces at East Chicago was predicated upon the provision of a monolithic hearth construction arranged within a steel shell to confine the molten zinc against escape and loss. Above the hearth, the arch was sprung from skewbacks along the side walls longitudinally of the furnace whereby widthwise expansion of the arch could bow it without impairing the air-tight seals provided at the skewbacks. At the ends of the furnace, the arch extended into pockets or recesses of the end walls which in turn were filled with an elastic or yieldable cement capable of maintaining an air seal while allowing the expansion movements of the arch. Continued operations over a number of years have

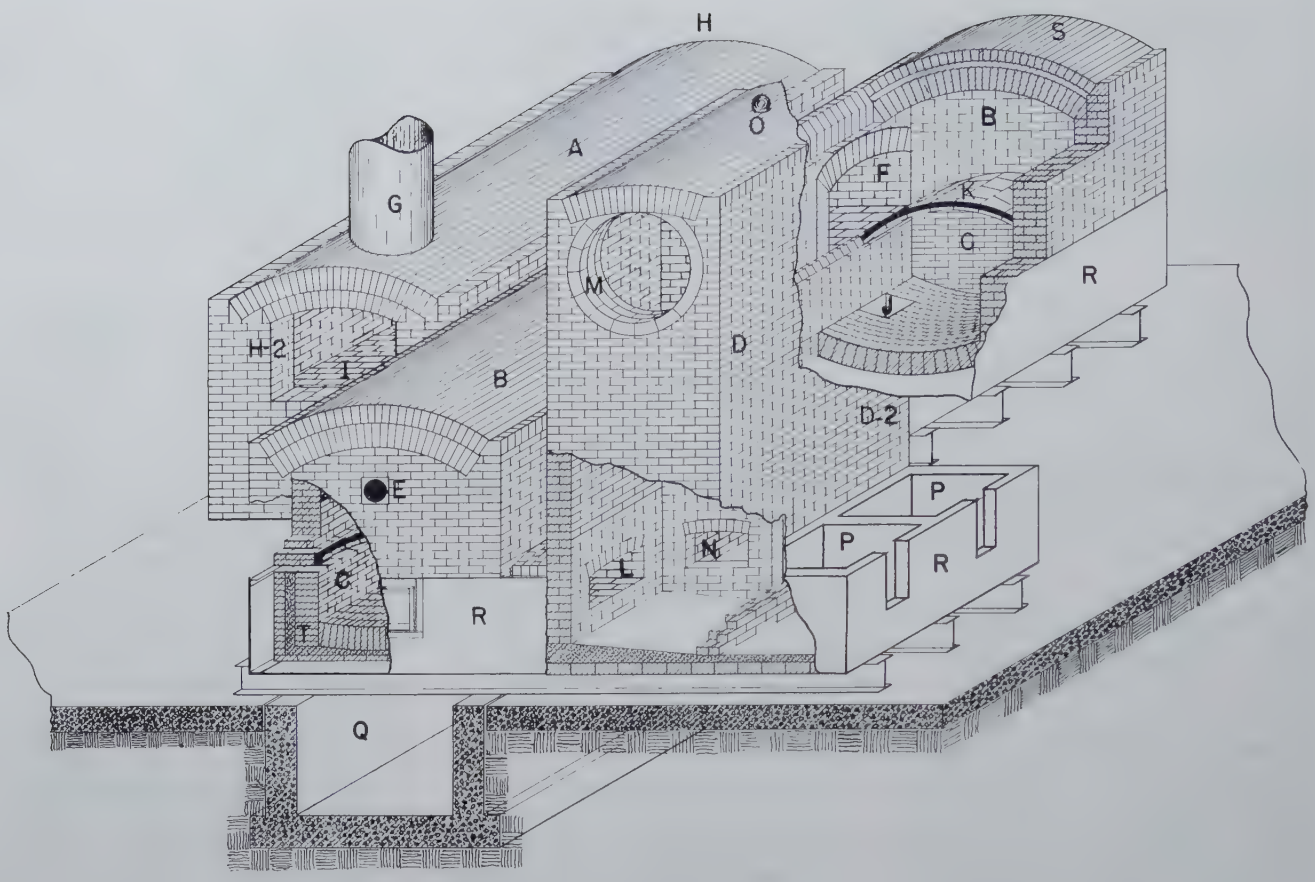

FIG 2—Improved muffle furnace.

Table 3 . . . Results Obtained with Melting Unit

	Weight in Lb	Per Cent of Weight Charged	Per Cent Zinc	Lb Zinc	Per Cent of Zinc Charged
Charged					
Die Cast Scrap as received	502,821	100.0	78.2	393,206	100.0
Produced					
Metal to Vaporizing Unit	398,235	79.2	88.2	351,243	89.3
Melting Dross	53,299	10.6	62.0	33,045	8.4
Iron Rejects	44,751	8.9	15.0	6,713	1.7
Unaccounted Loss	6,536	1.3		2,205	0.6
	502,821	100.0		393,206	100.0

proven these principles to be effective and reliable.

Commercial Muffle Furnace

The first commercial unit, producing 5 to 7 tons of zinc oxide per day, was equipped with a vertical riser. This brick riser received zinc vapors from the vaporizing chamber and provided for contact of zinc vapor and air to produce zinc oxide. The zinc oxide was conveyed through a steel duct into a baghouse.

In the operation of the first commercial furnace, the die cast scrap was first melted in kettles (heated by waste heat) to facilitate removal of unmeltables. These kettles were located in a manner that permitted the molten metal from the kettles to overflow into a sealed opening leading into the vaporizing unit. This practice was not satisfactory because of short kettle life.

Later furnaces embodied melting units consisting of a welded steel shell lined with fire brick to enable melting of the scrap continuously on a molten bath. The die cast scrap was charged onto this molten bath. This proved to be more efficient than kettle melting providing the temperature was adequately controlled.

The melting unit now in use consists of a sloping hearth inclined toward a central point, which discharges into a trough to the vaporizing unit. With controlled melting unit temperatures, the oxidation of zinc is maintained at a minimum. The results obtained with this melting unit are shown in Table 3.

Muffle Furnace

Assembly drawing Fig 2 and sectional views (Fig 4, 5 and 6) along planes as indicated in the plan as shown in Fig 3 may be helpful in a more detailed study of the furnace design. The letters apply to Fig 1 to 6 inclusive.

A—Melting Unit
B—Combustion Chamber
C—Vaporizing Chamber
D—Riser
*D*2—Condenser

The furnace is fired by oil burners at *E* into the combustion chamber *B* which connects through duct *F* with melting unit *A* and combustion gases are vented through stack *G*. The flow of metal through the furnace is countercurrent to the flow of gases. The zinc-bearing material is charged through door *H* (not shown) onto the melting

unit hearth *I* which is considerably above and to one side of the bottom of vaporizing chamber *C*. The molten charge drains from the hearth *I* of the melting unit which is pitched toward the center, through a duct entering the vaporizing chamber at point marked *J*. Means for drossing are provided between hearth *I* and outlet *J*. Unmeltables, such as iron inserts, and the like, are raked from the hearth of the melting unit through door *H2*. It will be noted that the combustion chamber *B* is separated from the vaporizing chamber *C* by a comparatively thin arch *K* to expedite the flow of heat from the combustion chamber into the vaporizing chamber. This arch is made up of standard commercial sizes of carborundum blocks. The arch extends into recesses of the end walls which are filled with an elastic material, forming a seal, and providing for expansion.

Under the proper conditions of temperature and pressure, zinc vapors are produced in chamber *C* which flow through opening *L* in the vaporizing chamber into the riser *D*. These vapors may be burned to zinc oxide as they escape from riser *D* through opening *M* to a zinc oxide collector. This assumes that opening *N* is closed. If it is desired to condense the vapors as metallic zinc, *N* is opened permitting the vapors to enter the condenser *D2*. The condenser may be laid up of carborundum brick which aids in condensing the zinc vapors to metallic zinc due to its high heat conductivity. Pressure, if it becomes excessive, is relieved by ball *O* resting on an opening into the condenser. Zinc wells marked *P* are used for tapping condensed metal.

Vaporizing chamber, condensers and zinc wells are all encased in a steel shell marked *R* which rests on supporting I-beams. The arch and side walls of combustion chamber *B* are constructed of a special high grade refractory. An insulating arch *S* covers the combustion chamber. Referring to the front of the vaporizing chamber *C* beneath the oil burner *E* it will be noted that the pan is first lined with a layer of fire brick, upon which is placed refractory concrete, designed to tighten the furnace against the flow of metallic zinc through brickwork *T*. The inverted arch and side walls of the vaporizing chamber *C* are constructed of high quality fire brick. The bottom arch of vaporizing chamber *C* pitches slightly to one end to assist in tapping metal from this chamber. Opening *Q* allows for atmospheric cooling of the furnace bottom

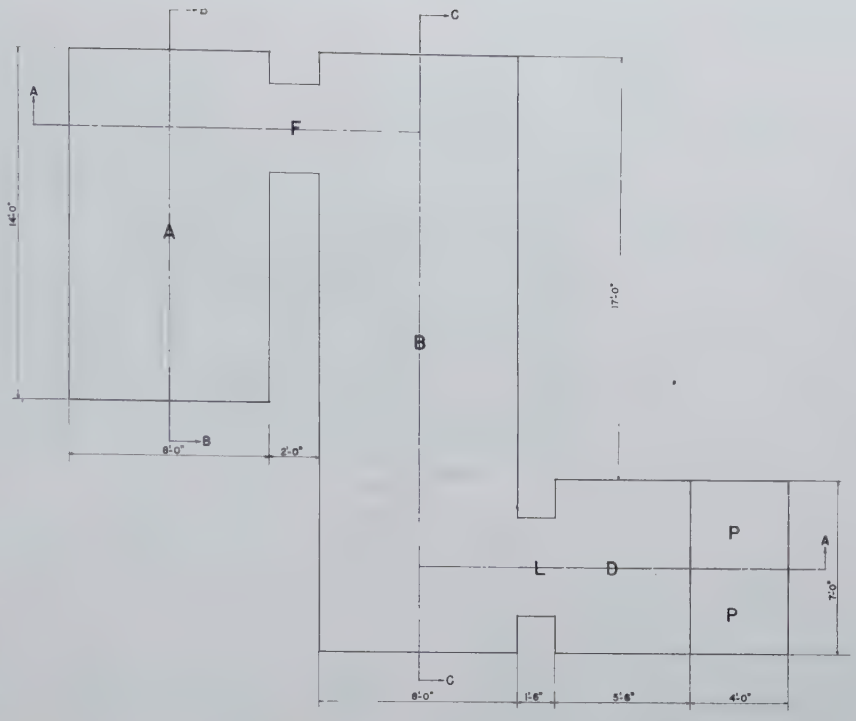

FIG 3—Plan of muffle furnace showing sections.

and provides for inspection of the bottom of the furnace pan.

Metallic Zinc is produced in the Muffle furnace by closing the opening *M*, used in producing oxide and open-communicating door *N* connecting condensers *D* and *D2*. Drains to zinc wells *P-P* are also opened.

This type of furnace construction provided for: Prevention of leakage of molten zinc by means of a monolithic hearth within a steel shell. Escape of vapors and infiltration of air by a tight arch fully sealed throughout its length and breadth and at the points where the arch joined the furnace. Pressure build up within the vaporizing chamber to permit the desired flow of zinc vapor to the riser and condenser. (Fig 7.)

Operating Procedure

The furnace is preheated with a gas flame, gradually raising the temperature to 1600°F. The oil burners are then started and the temperature of the combustion chamber elevated to 2400°F. Preheating requires about ten days.

Charging of metal is started at 2400°F and the production of zinc vapor begins almost at once. Charging is continued at as rapid a rate as possible until a depth of 5½ in. of metal has accumulated in the vaporizing unit. This accumulation of metal in the bath is exclusive of the metal vaporized during this period. Charging of die cast metal continues at a rate that will increase the depth of the metal in the vaporizing chamber about one inch for each 24 hr of operation until a total depth of 10 in. of metal is reached. This generally requires from six to ten days, depending on the zinc content of the metal charged. Where a high purity zinc is charged exclusively, the cycle may be extended to as much as 60 days without removal of residue metal.

Conditions which determine the end of the cycle are: The rate of zinc vapor production for economical operation of the furnace, a low zinc content in the residue metal, as tapped from the furnace, and a lead content low enough to meet the requirements of the particular zinc oxide being produced.

The cycle is ended by tapping residue metal from the vaporizing chamber, emptying it as far as possible. This metal is drained through a tap, not shown, into cast iron molds. The temperature of the furnace is held constant while it is being drained.

Furnaces have been operated for 72 cycles such as described above. This represents a continuous operation of approximately two years. The economical life of the furnace is determined by the heat transfer efficiency of the carborundum arch.

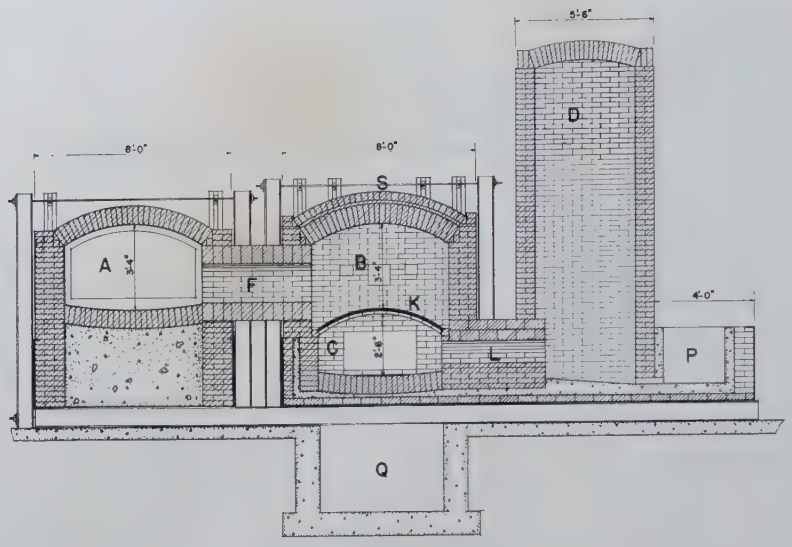

FIG 4—Muffle furnace section on line A-A.

The rate of heat transfer is reduced by: Accretions of zinc oxide which accumulate beneath the carborundum arch, an accumulation of slag on top of the arch and a gradual change in the composition of the arch.

Major furnace repairs are required every two years.

Table 4 . . . Typical Muffle Furnace Zinc Oxide

	Lead Free	Red Seal	Green Seal	White Seal	U.S.P.
Zinc Oxide—ZnO (Pct)	99.1	99.2	99.3	99.3	99.3
Lead—Pb (Pct)	0.25	0.10	0.07	0.07	0.02
Sulphur—S (Pct)	0.08	0.07	0.04	0.04	0.02
Insoluble—(Pct)	0.05	0.04	0.04	0.04	0.04
Ignition Loss—(Pct)	0.40	0.40	0.40	0.40	0.45
Cadmium—(Pct)	0.10	0.06	0.04	0.04	
Brightness*	83.5	86.0	90.0	91.0	92.0

* G. E. Recording Spectrophotometer.

Quality of Zinc Oxide

After the initial 20 ft muffle furnace was constructed and placed in operation a gradual improvement became apparent in the color and uniformity of the zinc oxide produced. Many changes in the furnace design improved the quality. The furnace, as now developed, can produce a wide range of zinc oxides including all grades of French Process zinc oxide and with minor modifications has produced acicular zinc oxides. Representative specifications for the French Process zinc oxides that are produced are shown in Table 4.

Production of Zinc

Of the various types of risers tried at East Chicago, several of them indicated the possibility that zinc metal could readily be produced from the muffle furnace. The relative position of the riser with respect to the molten bath of metal in the vaporizing unit seemed ideal to exclude or at least reduce contamination of the zinc metal by copper, aluminum and tin.

A simple design of riser was developed to permit zinc vapors condensed in the risers to be removed through a trapped opening into a zinc well from which the zinc metal could be removed at convenient intervals. A further development of this idea led to the design of a suitable condenser made of carborundum brick that would permit complete production of zinc metal from all of the vapors leaving the vaporizing units. For the purpose of controlling the rate of zinc condensation, by varying the heat loss, hinged steel frame doors lined with insulation brick were attached to the exterior of the condenser.

Zinc Produced from Secondary Metal

With this type of riser on the furnace, the distillation of zinc from secondary metals became a commercial possibility because the zinc produced in test runs was Prime Western, Brass Special or Intermediate grade. The results of such an experimental run are given in Table 5. In this run die cast slabs and die cast scrap were used as the source of zinc.

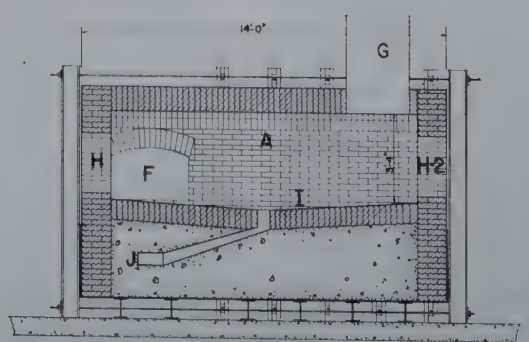

FIG 5—Melting unit section on line B-B.

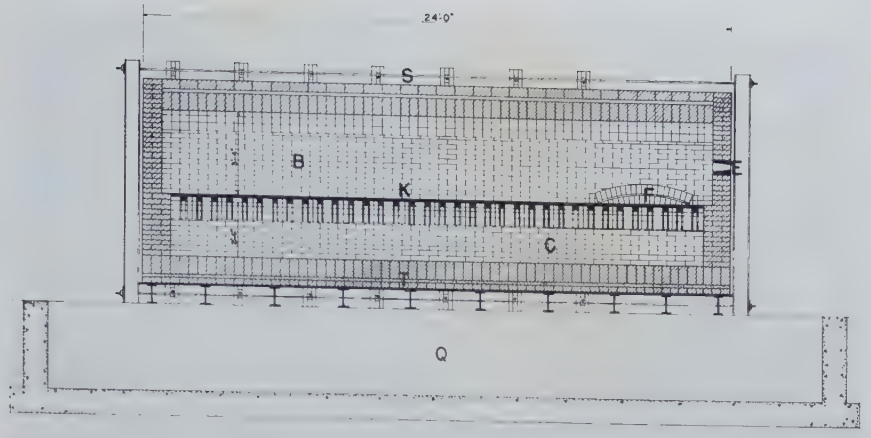

FIG 6—Vaporizing unit section on line C-C.

Table 5 . . . Zinc from Secondary Metals

	Lb	Per Cent of Metal Charged
Charged		
Die Cast Slabs	72,685	35
Die Cast Scrap	134,180	65
	206,865	100
Metal Production		
Condensed Metal	133,165	64.4
Residue Metal	11,515	5.6
By-products		
Muffle Dross	51,310	24.8*
Unmeltables	4,915	2.4
Unaccounted for Loss	5,960	2.8

* Dross production should approximate 14.0 pct.

Distillation of Prime Western Zinc

It was recognized that these furnaces could be used for redistillation of impure zinc into higher purity zinc. Results of a test made to determine the efficiency of the redistillation of Prime Western Zinc into higher purity zinc are shown in Table 6.

Table 6 . . . Redistillation of Prime Western Zinc into Higher Purity Zinc

	Lb	Grade Zinc	Pct of Metal Charged
Charged	300,095	Prime Western	100.0
Metal Production	269,554	Intermediate	89.8
	3,280	Brass Special	1.1
	10,246	Prime Western	3.4
By-products	9,238	Muffle Dross	3.1
	1,786	Blue Powder	0.6
	1,316	Residue Metal	0.4
	4,693	Loss	1.6

Distillation of High Grade Zinc

An experiment was conducted to determine the extent and economics of reducing the lead content of electrolytic high grade zinc in a muffle furnace. Table 7 summarizes the information obtained.

Table 7 . . . Reduction of Lead Content of Electrolytic High Grade Zinc in Muffle Furnace

	Pct Lead	Lb	Pct of Metal Charged
High Grade Zinc Charged	0.0081	366,085	
Condensed Metal Produced	0.0032	302,225	
Residue Metal		17,070	
Metal in Process		44,800	
Recovery			99.46

In this test the average production of metal per 24 hr was 29,257 lb. The oil consumption averaged 800 gal per 24 hr.

By-products

Several important by-products are produced in the conversion of die cast and zinc scrap into zinc or zinc oxide.

UNMELTABLES

The first by-product obtained is in the form of iron inserts or foreign material that is frequently associated with many forms of zinc scrap. The general term "unmeltables" is used to describe this form of by-product.

The following analysis as shown in Table 8 indicates the metals present in the unmeltables in addition to iron and zinc.

Table 8 . . . Metals in Unmeltables in Addition to Iron and Zinc
Per Cent

Pb	Cu	Sn	Ni	Cr	Al
4.39	3.61	0.80	0.36	0.11	10.0

MUFFLE DROSS

As the scrap is melted in the melting unit or in a kettle some of the zinc is oxidized. The partially oxidized zinc (muffle dross) is screened from the unmeltables and set aside for treatment or sale to zinc smelters. A representative analysis of muffle dross is shown in Table 9.

Table 9 . . . Analysis of Muffle Dross
Per Cent

Zn	Pb	Cu	Sn	Fe	Al	Insol.
69.7	5.1	4.0	2.3	8.5	10.0	0.4

RESIDUE METAL

The distillation of zinc from die cast metal concentrates the other metals (principally aluminum and copper) present in the original alloy. A representative analysis of residue metal is shown in Table 10.

Table 10 . . . Analysis of Residue Metal
Per Cent

Al	Cu	Zn	Sn	Fe	Pb
33.3	51.9	8.0	2.9	3.1	0.4

RECOVERY OF TIN-LEAD ALLOY FROM RESIDUE METAL

The residue metal is tapped from the furnace at between 5 and 10 per cent zinc content. This metal is remelted in a special liquation furnace in such a manner as to form a two-layer system. The lower layer which consists of a molten lead-tin alloy containing a small

FIG 7—No. 4 muffle furnace.

amount of zinc is tapped from beneath the solid upper layer. This crude lead-tin alloy is refined by removal of the zinc with chlorine and the final refining with caustic soda. It is used as a lead-tin alloy.

RECOVERY OF ALUMINUM FROM RESIDUE METAL

A number of studies were made of the best means of utilizing the aluminum and copper alloy which was left after the zinc, lead and tin had been removed from the residue metal. It was recognized that if the aluminum-copper alloy was freed of undesirable impurities it should be attractive to the die cast producer who could use it by adding electrolytic zinc to produce a high grade die casting alloy.

Extensive experiments were made to electrolyze residue metal in a fused salt cell. The cathode deposits were a high grade aluminum. As the aluminum was removed from the molten electrolyte the copper content of the residue metal increased and reached the point where the operating difficulties of such electrolysis became more and more complex and unattractive. The conclusion was reached that this sort of treatment to recover aluminum from residue metal might prove attractive if low cost power were available.

RECOVERY OF COPPER FROM RESIDUE METAL

The copper content of the residue metal is high enough to interest the copper smelters in its utilization. It has been treated in copper reverberatories along with the melting of scrap copper to produce electrolytic copper. In this treatment the aluminum values are lost in the reverberatory slag.

The residue metal can also be treated in copper converters where the aluminum is oxidized to Al_2O_3 and discarded in the converter slag. Great care, however, is necessary in this type of operation because the reaction between the copper sulphides and metallic aluminum is vigorously exothermic under certain conditions. Large quantities of this residue metal have been sold to manufacturers who find this alloy useful for their needs. It is obviously a secondary aluminum alloy that contains attractive values for many alloy specifications.

Acknowledgment

Acknowledgment is given to Messrs. George Anderson and R. S. Olsen for their early experimental contributions in the development of the muffle furnace. Appreciation is expressed for the valuable cooperation and assistance of Messrs. P. S. Toney, W. P. Ruemmler and E. F. Weaver of the East Chicago staff in the preparation of the manuscript.

References

1. U. S. Patent No. 2,156,420: Metal Vaporizing Furnace. George Anderson and R. S. Olsen.
   U. S. Patent No. 2,174,559: Vaporizing Furnace for Zinc and Other Metals. George Anderson and R. S. Olsen.

The Effect of Orientation Difference on Grain Boundary Energies

C. G. DUNN,* Member AIME, and F. LIONETTI†

The energy associated with grain boundaries in polycrystalline aggregates is believed to play a major role in grain growth processes and, when growth ceases, to determine the final equilibrium grain boundary angles. Further, the energy of grain boundaries of recrystallization nuclei is a factor in nucleation processes. It is important to know, therefore, how the energy per unit area of a grain boundary, that is, the grain boundary surface tension γ, depends on the difference in orientation of the two lattices of the grains producing the boundary. Although the problem is important, surprisingly little has been done toward a quantitative evaluation of the effect of orientation difference on grain boundary energies.

C. S. Smith[1] recently has discussed this problem and in addition to showing effects of orientation difference on equilibrium angles has shown a variety of interesting effects of surface tension on the appearance of microstructures. Fig 1 and the following relations expressed in Eq 1, which connect equilibrium grain boundary angles and surface tensions, illustrate equilibrium conditions which are believed to hold true in metals.

$$\frac{\gamma_{12}}{\sin \theta_3} = \frac{\gamma_{23}}{\sin \theta_1} = \frac{\gamma_{13}}{\sin \theta_2} \qquad [1]$$

Clearly any two of these surface tensions can be expressed in terms of the third when the equilibrium angles θ_1, θ_2, and θ_3 are known.

Applied to the present problem for solid state equilibrium of three grains, the angles θ_1, θ_2 and θ_3 must be measured in a plane perpendicular to the line of junction of the three grains. Normally a direct determination of these angles from random microsections is impossible. Consequently Harker and Parker[2] and Smith[1] (except for some measurements on flat specimens) resorted to a statistical method to determine equilibrium grain boundary angles. Smith reported that grain boundaries meet the surface of a piece of metal nearly perpendicularly. He reported also, in connection with direct angle measurements on flat specimens with grains extending through the thickness, that angles varied appreciably from 120° and concluded that there was a measurable effect of orientation difference on surface tension.

Another direct way of determining equilibrium angles and a method adaptable to studying particular configurations, recently suggested by Dunn,[3] is to use a three-grain flat specimen with orientations of grains so chosen that the junction line of the three grains will be straight throughout the thickness and perpendicular to the surface of the specimen. Choice of orientations is possible when individual grains of each group can be grown to predetermined orientations through the reorienting and growth of "seed crystals" as described.[3] Not only is it possible, for example, to have grains with the same crystallographic plane in the plane of the specimen, but a given orientation difference between two grains can be made a common factor to an unlimited number of three-grain groups while a series of orientation differences is investigated. Any effect of anisotropy of gas-solid surface tension due to grain orientation should be minimized by having all grains oriented the same with regard to crystallographic plane in the plane of the specimen.

Another feature of the three-grain group is the notched grain boundaries as shown in Fig 2 for one specimen (*S4*). The notches serve to anchor the end positions of the grain boundaries (especially at high temperatures) while the central and junction point of the grains moves toward an equilibrium position. Final equilibrium should produce straight grain boundaries if the notches are very narrow and if changes in orientation* of the grain boundary do not alter the surface tension.† If one assumes the straight line condition and no change of surface tension with small changes in grain boundary orientation and finds the equilibrium configuration by a minimization of the grain boundary energy, one obtains the relations given in Eq 1.

The approach to straight line boundaries or to minimum energy configurations in specimens containing large grains, such as those used in the present investigation, may be very slow compared with the approach to equilibrium conditions for the grain boundary angles. It may be desirable, as proved to be the case in the present investiga-

San Francisco Meeting, February 1949.

TP 2517 E. Discussion of this paper (2 copies) may be sent to *Transactions* AIME before May 15, 1949. Manuscript received Nov. 3, 1948.

* Research Physicist, General Electric Co., Pittsfield, Mass.

† Formerly Chemist, General Electric Co., Pittsfield, Mass. Now Assistant Professor of Chemistry at Union University, Albany, N. Y.

[1] References are at the end of the paper.

* Change in orientation of a grain boundary is not to be confused with difference in orientation between two grains.

† An effect of grain boundary orientation must exist for crystal orientations near the twinned position. A measurable effect may also exist for other crystal orientations. (See Ref. 1.)

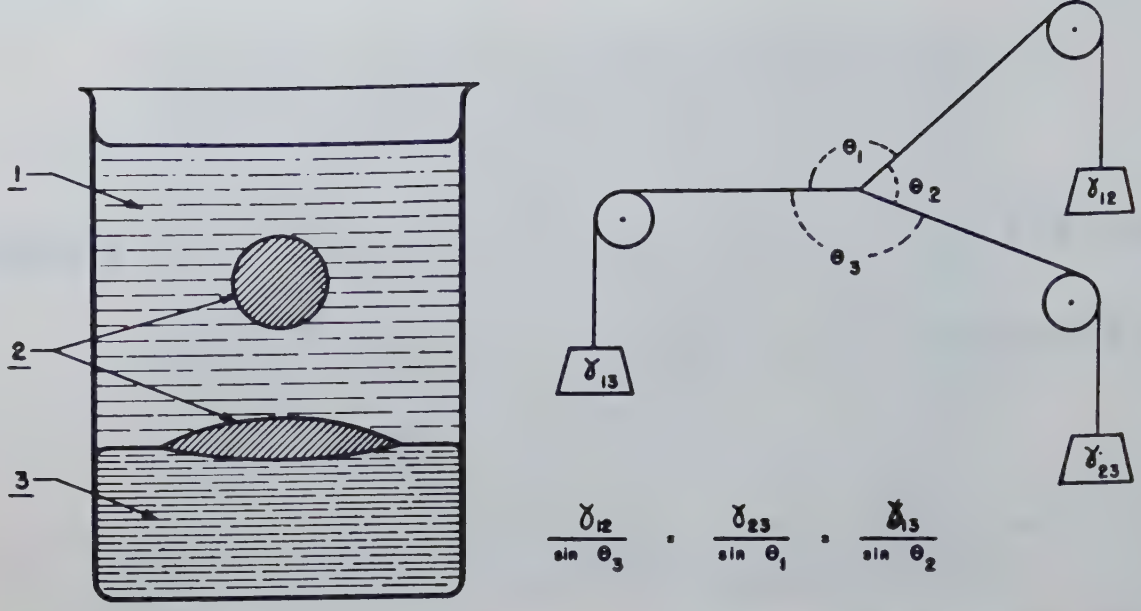

FIG 1—Interface equilibrium between three immiscible liquids and mechanical analogy with triangle of forces. (After Smith.)

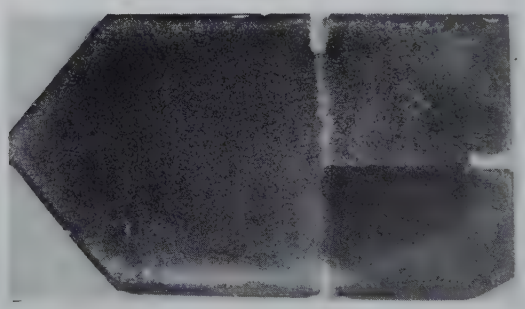

FIG 2—Photograph of $S4$ showing sample composed of three grains each having a {110} plane in the plane of the specimen. Approx. × 2. (After Dunn.)

tion, to observe relatively small changes in the boundaries near the junction point of the three grains rather than wait for large changes to occur in the grain boundaries prior to making accurate angle measurements.

In the present report a series of groups, each of three grains with the (110) plane in the plane of the specimen, are investigated. The difference in orientation between two grains i and j, with grain boundary surface tension γ_{ij}, is given in terms of an angle Δ_{ij}, which is the angle separating the [001] directions of the two grains. Each three-grain specimen, therefore, has three values of surface tension (γ_{12}, γ_{13}, γ_{23}) corresponding to the three grain boundaries where the differences in orientation of the grains are Δ_{12}, Δ_{13} and Δ_{23} respectively. Each three-grain group has one boundary where the difference in orientation of the grains is 15°, a value chosen somewhat arbitrarily. The purpose of the common value of Δ is to permit the calculation of surface tensions in terms of one surface tension (γ_c) which is assumed not to vary much with grain boundary orientation. Values of Δ_{ij} cover the range 5° to 90°.

If orientation of the grain boundary has little effect on the surface tension γ, then γ can be expressed as a simple function of Δ, the difference in orientation. However, even if the orientation of the grain boundary should prove to have little effect in general, the existence of twins with definite composition planes alone indicates an effect of grain boundary orientation when two lattices are near a twinned relation. McKeehan[4] and Preston[5] from considerations of the distances between atoms in a lattice and the distance between atoms at a twin boundary, showed that certain composition planes resulted in lower stress or lower boundary energy. On the basis of measured grain boundary angles, Smith[1] reported that the surface tension for a twin boundary in face-centered cubic metals must be relatively small.

In the present investigation no attempt was made to control the orientation of grain boundaries during the preparation of three-grain groups.

PREPARATION OF SPECIMENS

Silicon ferrite with about 3.5 pct silicon was selected for the investigation because the technique of growing three-grain specimens with each grain in a definite orientation had been previously developed. Furthermore, silicon ferrite remains a single phase even at high temperatures; so temperatures of 1300–1400°C, or near the melting point if desired, could be used to effect a more rapid approach to equilibrium.

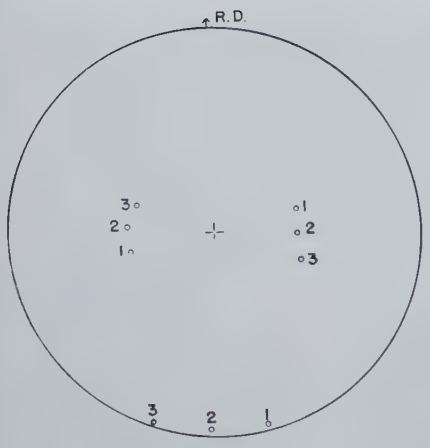

FIG 3—Stereographic projection of the {100} poles of the three grains in *S*2.

In the laboratory cold rolled strips of silicon steel of commercial grade were made in the form of sheets 0.025 in. thick. These had the property of supporting exaggerated grain growth. Upon lowering pieces of this material into a furnace with a high temperature gradient, large grains formed in the hot end. Two of these grains about one inch apart in each sample were then X rayed and analyzed for orientations. From the stereographic projection of the orientation of each grain, the two angle rotations necessary to bring a (110) plane into the plane of the specimen and a [001] direction into a predetermined azimuthal position could be read easily from a Wulff net. A small machine with angular scales was used to reorient each crystal, the neck part of the specimen (see Ref. 3 for illustration) being held at red heat during this operation to permit easy plastic flow of the metal.

Each specimen with its two reoriented seed crystals was then fed into a furnace with a high temperature gradient in order to grow two grains in one end. The speed of a specimen generally was about ½ cm per hr. In a similar manner, a third crystal was seeded, analyzed, reoriented, and grown from the opposite end. Eleven specimens were made, all but *S*8 by the exaggerated grain growth method. In the case of *S*8 where one Δ value reached 90°, a strain-anneal type of transformation was used. To facilitate identification, each sample was shaped differently. Also it will be noted that the three initial grain boundary angles obtained in specimens made in the manner previously described, if measured very roughly, will be near 90, 90, and 180° respectively (see Fig 2).

After preparation, the orientations of all grains were determined. Fig 3, which is illustrative of all specimens, shows a stereographic projection of the {100} poles of the three grains 1, 2, and 3 of *S*2. Tilt of the (110) plane did not exceed 2°. In general since the (110) planes were quite close to the plane of the specimen (within 3°), determining the [001] direction of each grain sufficed for a simple calculation of each orientation difference Δ. The plotting of stereographic projections, as shown in Fig 3, was not necessary since a direct reading analyzer could be used to find the direction of the zone axis of the [001] zone of Laue spots which were present in each Laue photograph. The tilt of the (110) plane could also be read directly from the film.

ANNEALING

On the assumption that well defined equilibrium angles with grain boundaries lacking or nearly lacking in curvature over appreciable distances could be obtained, it was decided to anneal each sample a number of times and observe the approach toward equilibrium. Temperatures near 1300 or 1400°C were considered necessary, and higher temperatures were avoided during long anneals since a failure of the furnace controls while the furnace was unattended could have been disastrous with samples too near the melting point. Furthermore, the higher temperatures favored the sticking of the specimens to supporting plates or surrounding material and this was undesirable. To prevent sticking at high temperatures, samples were separated from supporting and surrounding pieces of silicon iron by a thin layer of alumina powder.

A preliminary anneal of 48 hr at 1350°C with an atmosphere of pure dry hydrogen disclosed a serious desiliconization effect for some thin sheets of silicon iron and *S*3, *S*4, *S*5, and *S*7. Sufficient silicon was removed from the thin sheets of silicon iron to allow them to transform completely by a phase change. *S*7 and *S*4 had transformed sufficiently to require replacements. *S*9, *S*10 and *S*11, therefore, were immediately made. *S*3 and *S*5 showed some transformation along the edges but this was much less than the transformation in *S*4, a photograph of which is shown in Fig 4. The photographs of *S*4, shown before and after the 1350°C hydrogen anneal in Fig 2 and 4 respectively, clearly indicate a change in the grain boundaries near the common grain boundary point.

All samples were then annealed for about 70 hr at 1150°C in pure dry hydrogen. Although grain boundary changes were observable, it appeared expedient to anneal next in dry argon for 48 hr at 1300°C and then obtain some measure of the grain boundary angles. Measurements after the anneal were made at a magnification of 30 diam. Accuracy in the measurements proved difficult to obtain. Additional straightening of the boundaries, however, was anticipated; so the samples were given another anneal of 48 hr, this time at 1350°C in dry argon. Measurements on a number of specimens, especially *S*5, indicated a stabilizing condition of the angles. A comparison of photographs taken at different times also indicated a marked dropping off of grain boundary movement. A final anneal of 48 hr at 1400°C in an atmosphere of argon was then given the samples. Only minor further changes in grain boundaries occurred in this anneal. Long annealing, therefore, at these high temperatures had not produced the macrochanges sought for as an aid to the quantitative measure of the approach toward equilibrium

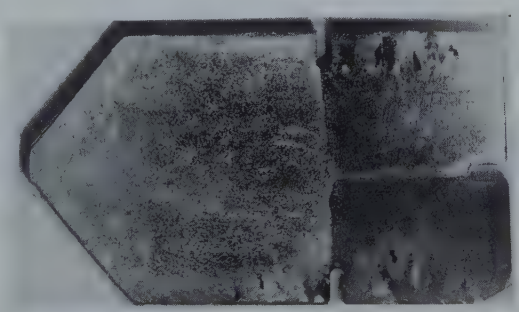

FIG 4—Photograph of *S*4 after a 48 hr anneal in pure dry hydrogen at 1350°C. Approx. × 2.

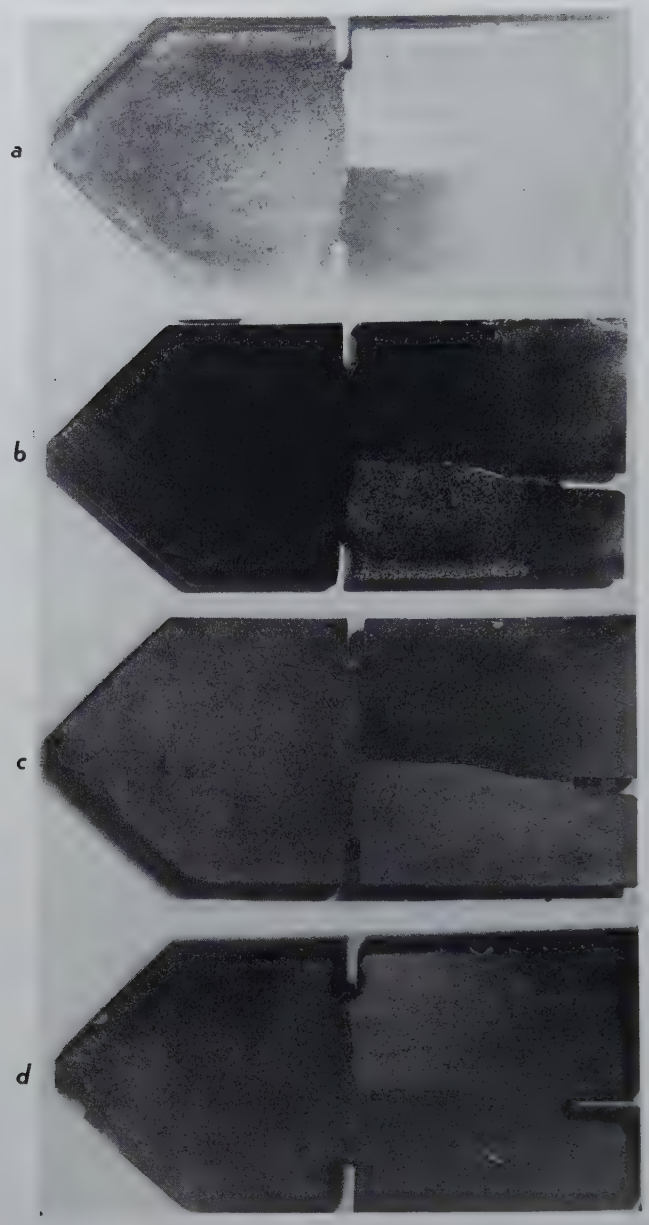

FIG 5—Photographs of $S5$. Approx. × 2.

a. Specimen as prepared

b. After 48 hr at 1350°C in pure dry hydrogen

c. After additional 70 hr at 1150°C in pure dry hydrogen and 48 hr at 1300°C in dry argon

d. After final 48 hr at 1400°C in dry argon

Table 1 . . . Orientation Differences, Initial (Gross) Angles, Final Angles after Annealing, Relative Surface Tensions, and Corrected Relative Surface Tensions for Eleven Specimens

Specimen No.	Orientation Difference			Initial Angles			Final Angles			Calculated Surface Tensions			Corrected Surface Tensions		
	Δ_{12}	Δ_{23}	Δ_{13}	θ_1	θ_2	θ_3	θ_1	θ_2	θ_3	$\frac{\gamma_{12}}{\gamma_e}$	$\frac{\gamma_{23}}{\gamma_e}$	$\frac{\gamma_{13}}{\gamma_e}$	$\frac{\gamma_{12}}{\gamma_e}$	$\frac{\gamma_{23}}{\gamma_e}$	$\frac{\gamma_{13}}{\gamma_e}$
1	15.	7	8	90	90	180	140	143	77	1	0.66	0.62	1	0.66	0.62
2	16.5	17	33.5	160	90	110	121.5	118.5	120	1	0.98	1.01	1.04	1.02	1.05
3	15.5	23	38.5	180	80	100	116.5	121	122.5	1	1.06	1.01	1.01	1.07	1.02
4	13.5	24	37.5	180	90	90	Sample ruined								
5	14	25	39	90	180	90	112	129	120	1	1.07	0.90	0.97	1.04	0.87
6	15.5	29.5	45	90	180	90	112	127.5	120.5	1	1.08	0.92	1.01	1.09	0.93
7	16.5	53	69.5	90	180	90	Sample ruined								
8	15.5	76.5	92	90	180	90	127.5	120	113.5	1	0.86	0.94	1.01	.87	0.95
9	14	26	40	180	90	90	115.5	117.5	127	1	1.13	1.12	0.97	1.10	1.09
10	14.5	56	70.5	90	180	90	120	133	107	1	0.91	0.76	0.98	0.89	0.74
11	14.5	57	71.5	90	180	90	105	134	121	1	1.13	0.84	0.98	1.11	0.82

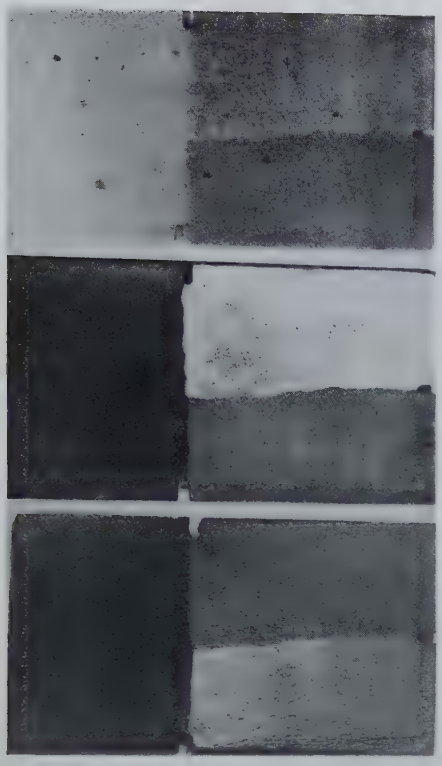

FIG 6—Photographs of *S*11. Approx. × 2.
a. Specimen as prepared
b. After 70 hr at 1150°C in pure dry hydrogen and 48 hr at 1300°C in dry argon.
c. After additional 48 hr at 1350°C and 48 hr at 1400°C in dry argon

conditions. The angle measurements in some cases agreed well with previous ones; in three cases it was clear that the specimens would first have to be mounted and polished metallographically so that a higher magnification could be used. Angles could be measured fairly accurately on some of the samples in the "as annealed" condition because the grain boundaries were clearly visible.

Experimental Results

STRUCTURE

Photographs of *S*4 shown in Fig 2 and 4 have already been discussed in connection with the changes produced by the removal of silicon.

Fig 5, showing a series of photographs at slightly less than double magnification of *S*5, illustrates well the early visible changes and the later stabilization of the boundary positions.

Photographs in Fig 6 likewise show the changes that occurred in *S*11. From the standpoint of macrochanges which were visible at no magnification, this specimen was the poorest of the nine used in the determination of grain boundary angles. Only slightly better in this respect was *S*9. Photographs of *S*9 are shown in Fig 7, one at about 2 diam magnifications, the other two at 5 diam. These photographs clearly show that grain boundary movement occurred in the 1150°C hydrogen anneal and also in subsequent anneals.

As mentioned previously three of the samples showed poor macroboundaries. These samples (*S*1, *S*9, and *S*3) were polished and the boundaries observed at 400 diam magnification. Fig 8 shows a photograph of the boundaries of *S*1, the specimen with the smallest differences in orientation. It is interesting to note that the boundary associated with largest difference in orientation, which stands out sharply in the photograph, is opposite an acute angle. *S*9,

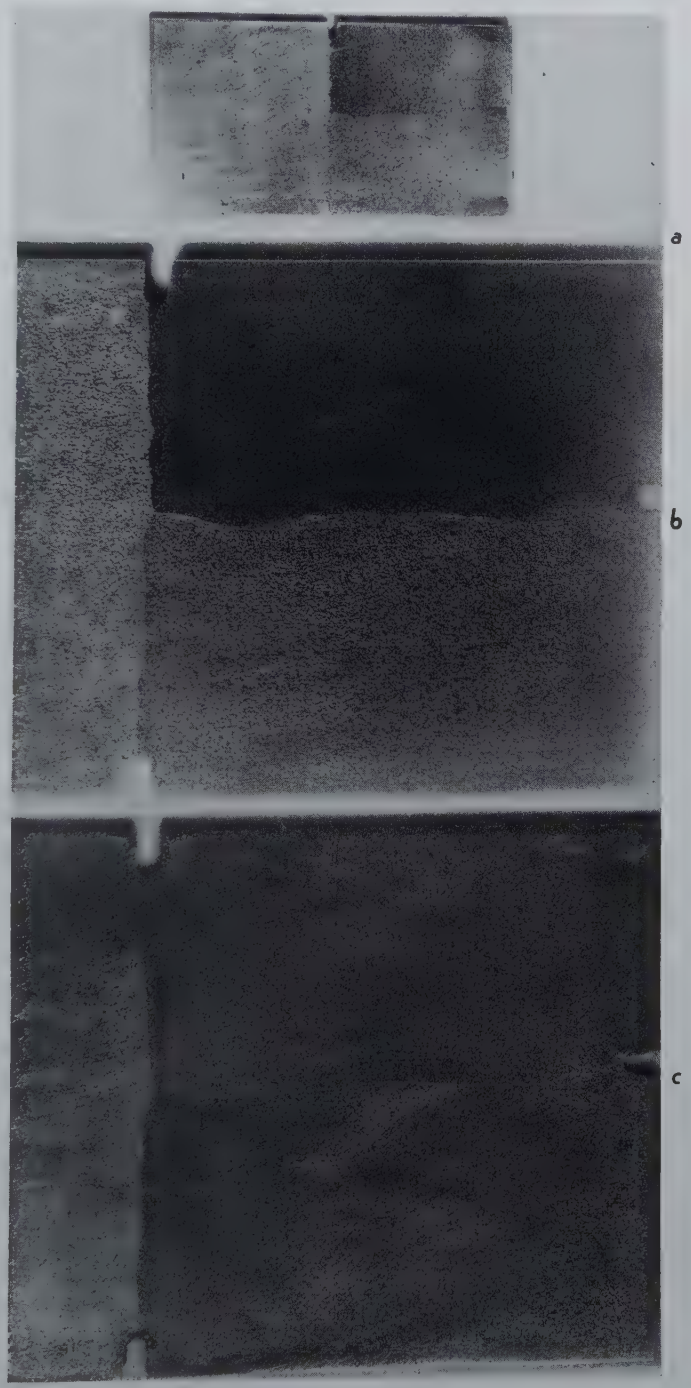

Fig 7—Photographs of *S*9.
a. Specimen as prepared. Approx. × 2.
b. After 70 hr at 1150°C in pure dry hydrogen × 5
c. After additional anneals in dry argon gas of 48 hr at 1300°C 48 hr at 1350°C, and 48 hr at 1400°C. × 5

FIG 8 (above)—Micrograph of $S1$ after annealing. Nital etch. × 400
FIG 9 (below)—Micrograph of $S9$ after annealing. Nital etch. × 400

which has already been discussed in connection with Fig 7, had one grain boundary that continuously curved near the common grain boundary point. This feature is apparent in the photograph shown in Fig 9. Angle measurements were made at 30 diam and then again from the photographic plate taken at 400 diam. One angle, defined by the straight grain boundaries, checked well in these two measurements. Readings from the plate were sufficiently accurate to permit checking the angles to within one degree. The angle measurements of $S3$ made at a magnification of 400 diam checked quite well with those taken at 30 diam.

Sections were made through a number of grain boundaries to determine how the boundaries passed through the specimen. Although the boundaries in general were close to the perpendicular position, there were some cases of departure from perpendicularity by as much as 5 to 10 degrees.

EQUILIBRIUM ANGLES AND CALCULATED RELATIVE SURFACE TENSIONS

Data for the nine specimens measured are given in Table 1. Following the columns of orientation differences under Δ_{12}, Δ_{23}, Δ_{13} are the gross initial grain boundary angles listed under initial angles. Referring to Fig 1 it will be noted that θ_3 is the angle opposite the grain boundary formed by grains 1 and 2 where the surface tension is γ_{12}. This is also the boundary where the orientation difference is Δ_{12}. The columns giving the second set of θ values are the final measured angles—the equilibrium angles. Using these angles and Eq 1, relative values of γ were calculated. Results appear in the table under the column headed "calculated surface tensions." A plot of γ against Δ indicated that γ was changing at an

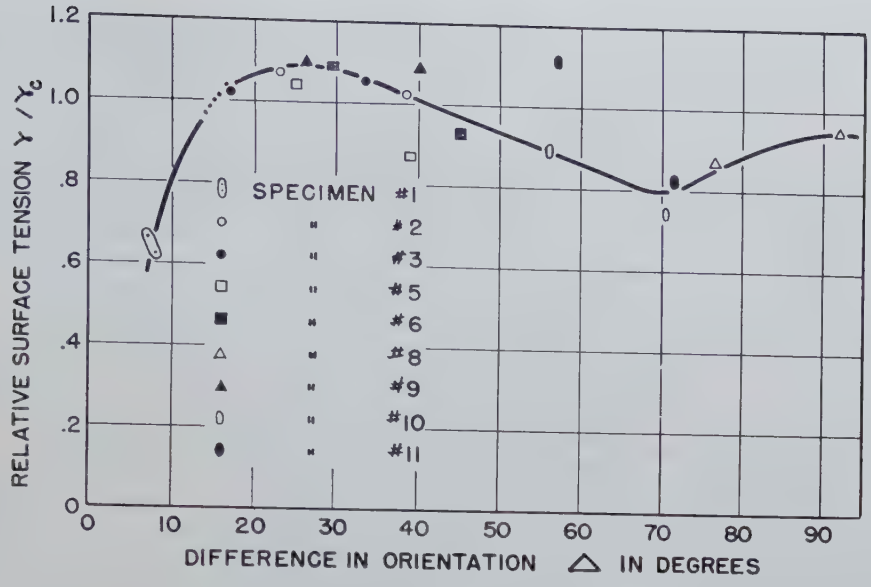

FIG 10—Plot showing variation of relative surface tension γ/γ_c (corrected) with difference in orientation Δ.

appreciable rate with Δ for values of Δ near 15°. Consequently γ for Δ equal to 16.5°, for example, should be slightly larger than γ for Δ equal to 15°, the approximate common value. From the shape of the curve a small correction could be made so that γ_c would apply only to Δ equal to 15°. This correction proved to be less than 4 pct in general. The same percentage change as that made in γ near 15° was also made for the remaining two γ values of each specimen. Results are listed under "corrected surface tensions." A plot of γ/γ_c versus Δ, using the corrected values given in the table, is shown in Fig 10.

Discussion of Results

The relationship between surface tension γ and orientation difference Δ shown by the curve in Fig 10 has three rather striking features: 1. A rapid decrease of surface tension with decreasing Δ for values of Δ less than 15°. 2. A maximum surface tension for orientation differences in the range of 20 to 30°. 3. A dip in the curve for orientation differences near 70°.

In regard to the first feature, one would expect some type of approach toward zero surface tension with decreasing Δ since the boundary must vanish at Δ equal to zero. The second point will be discussed later. In the case of the third point, however, one can speculate somewhat on the twin relation. If the boundary between grains 1 and 3 had been grown near a (112) plane, then approximate artificial (112) twins (grains 1 and 3) might have developed on annealing and a marked dip in the curve expected from the lower energy of a (112) twin boundary. Actually the 1–3 boundary in *S*10 and in *S*11 was grown much nearer a (111) plane, but the final configuration not only departed appreciably from the (111) plane but was different in the two specimens. The observed dip in the curve as well as the disagreement for *S*10 and *S*11 may reasonably be connected with an effect associated with the twin orientation even though the boundary is removed from a {112} plane. In the particular configuration involving two grains 1 and 3 with (110) planes in the plane of the specimen but differing in orientation by 70°32′, the more complete nature of this effect could be investigated by varying the orientation of the 1–3 boundary during the formation of each three-grain group.

*S*5 and *S*9, with orientations far removed from any twin position, actually illustrate the variation of grain boundary orientation in the initial samples for a constant set of Δ values. Referring to Table 1, the Δ values for both these specimens are seen to be roughly 15, 25, and 40°. The initial gross angles, however, are different except for angle θ_3 which was 90° for both specimens. (Other grain boundary directions and initial gross angles could have been formed by varying the direction of grain growth in each specimen.)

The purpose of making two angles is different in *S*5 and *S*9 was to have θ_1 increase from 90° in *S*5 and decrease in *S*9 (if the equilibrium angle was between these two values) until the two reached a common value, or the equilibrium angle. A converse relation would, of course, hold for θ_2. Lack of the anticipated large grain boundary movements prevented the measuring of the approach toward equilibrium in these samples. As far as angles measured on a small scale are concerned, which finally had to be done, in general the initial gross angles probably have little significance.

Lack of agreement for the final angles for *S*5 and *S*9, although possibly due in part to an effect of grain boundary orientation, may be due to failure to reach equilibrium. This view may seem unreasonable at first since long anneals at high temperatures were used in an attempt to reach equilibrium. There is one factor, however, which tends to prevent the reaching of equilibrium conditions as required in the application of Eq 1. Inclusions in a metal exert a constraining force to grain boundary movement, as Smith[1] (see Ref. 24) pointed out in connection with the work of Zener. It was further indicated that, under certain conditions, inclusions should completely stop boundary movement.

With regard to a maximum point on the surface tension curve, it can only be said that one should occur between zero and 70° if there is a marked dropping off of surface tension near 70°.

Considering all nine specimens, and the possibility of some effect of grain boundary orientation, the general consistency of the trend of variation of γ with Δ (especially in the range 15 to 45° where more points have been obtained) indicates that the effect of inclusions in general probably was not too serious. Nevertheless, it would be very desirable to use material of the highest possible purity to insure the attainment of better equilibrium conditions.

Although inclusions may stop a strongly curved grain boundary from moving further, the grain boundary orientation effect may also lead to a curved surface in order to produce a minimum energy configuration (this was also discussed by Smith[1]). With reference to the application of the present technique, consider a two-grain specimen with the grain boundary ends anchored and having grains with the same crystallographic plane in the plane of the sheet. If the grain boundary surface tension γ is high for the straight grain boundary compared to other directions, then a curved boundary could correspond to lower energy. We have here the case of minimizing the total energy obtained from the product of boundary area and surface tension, which may be expressed as follows:

Total grain boundary energy

$$= \int_\sigma \gamma \, d\sigma$$

where $d\sigma$ is an element of surface area and the integration is carried out over the entire boundary surface σ. The surface tension γ, of course, is considered to vary from point to point on the surface with orientation of the surface element $d\sigma$. A minimization of grain boundary energy would be valid only when relative sizes of the two grains produce no additional effect on total (internal plus surface) energy.

In any case, the nature of variation of surface tension with grain boundary orientation should be determined in order to obtain a clearer picture of the effect of orientation difference on surface tension. In the case of three-grain groups with common (110) planes, the curve for small values of Δ should be investigated more completely. Finally, three-grain groups with other crystallographic planes in the plane of the specimen should also be investigated and the results of surface tension measurements put on a common relative basis with those of the (110) series.

If relative surface tensions vary with particular orientation differences, as Fig 10 would indicate is actually the case, then some fundamental relationships may be found between surface tension data and recrystallization data involving orientation relationships. In this connection it is interesting to point out some possible correlations, using the shape of the curve in Fig 10 and published facts on recrystallization in silicon ferrite. Dunn[6] reported a rapid rise in the number of recrystallization nuclei with orientation difference for Δ in the range 10 to 20° and no nuclei with small Δ values. Referring to Fig 10 we note a similar rapid rise in the surface tension starting with small values of Δ. Secondly, the data on recrystallization nuclei show a maximum number of nuclei for Δ equal to approximately 25° with nuclei also having a {110} plane common with the original deformed grain (see Fig 8 of Ref. 6 for curve). The curve of surface tension versus Δ (Fig 10) has a maximum in this same region of orientation difference. However, until other crystallographic relationships are investigated and all values of surface tension are compared, the coincidence of maximum points probably should not be considered too significant. On the other hand some relationships involving either the ease of forming a nucleus or the ability of a nucleus to grow more rapidly in a deformed single crystal because of special orientation relationships is expected.

Experimental data on surface tensions are needed, of course, for application to the problem of grain growth following recrystallization, especially under conditions where recrystallization textures depart from random textures. Further, a strong texture material should have lower total grain boundary energy per unit volume than a random texture material provided both materials have the same grain size and provided the initial part of the curve of relative surface tension does not rise too rapidly to some approximate constant value. A curve of relative surface tension having the form shown in Fig 10 would indicate an appreciable dependence of energy on texture.

Summary

1. Eleven flat specimens of silicon ferrite each composed of three grains were prepared having (110) planes in the plane of the samples. The common grain boundary point of the three grains was centrally located.

2. Each sample was annealed for long periods of time in the temperature range 1300–1400°C until further change in grain boundaries seemed unlikely and equilibrium angles apparently had been obtained.

3. After annealing, the grain boundary angles were measured and the relative surface tensions calculated. Since each group of grains contained a similar type of boundary (one where the grains had a 15° difference in orientation) it was possible to calculate all surface tensions on a common basis.

4. A curve was obtained showing the variation of relative surface tension (relative energy in the grain boundary per unit area) with difference in crystal orientation.

Acknowledgments

The authors wish to express their appreciation to Drs. J. H. Hollomon and J. C. Fisher for valuable discussions on the problem of measuring surface tensions. Thanks are also extended to Mr. E. F. Welter for aid in the preparation of specimens and the making of X ray photograms and to Miss Mary Burdette for the micrographs appearing in the manuscript.

References

1. Cyril Stanley Smith: Grains, Phases and Interfaces: An Interpretation of Microstructures. AIME *Metals Tech.* TP 2387 (June 1948).

2. D. Harker and E. Parker: Grain Shape and Grain Growth. *Trans.* A.S.M. (1945) **34**, 156–195.

3. C. G. Dunn: Controlled Grain Growth Applied to the Problem of Grain Boundary Energy Measurements. *Trans.* AIME *Trans.* Jan. 1949, T.N. No. 9.

4. L. W. McKeehan: The Formation of Twin Metallic Crystals. *Nature* (1927) **119**, 120, 392.

5. G. D. Preston: The Formation of Twin Metallic Crystals. *Nature* (1927), **119**, 600.

6. C. G. Dunn: Effect of Original Orientation on Orientation Changes during Recrystallization in Silicon Ferrite. *Metals Tech.*, TP 1990 (Aug. 1946); *Trans.* AIME (1946). **167**, 357.

Solubility Relationships of the Refractory Monocarbides

JOHN T. NORTON* Member AIME and A. L. MOWRY*

THE monocarbides of the A subgroup elements in the fourth and fifth group of the periodic table in addition to being hard and refractory are of special interest in that they are isomorphous in crystalline structure. They are cubic with a sodium chloride type structure in which the metal atoms are essentially close packed in a face-centered cubic arrangement with the carbon atoms placed in the interstices between.

Interstitial structures of this close packed type were first investigated systematically by Hägg[1] and he gave the rule for their formation, stating that the radius ratio of the nonmetal to the metal atom should not exceed the value of 0.59. The carbides of interest are those of titanium and zirconium of the fourth group and vanadium, columbium and tantalum of the fifth group. Table 1 shows the radius ratio using the Goldschmidt radii for 12 coordination for the metal atoms and the diamond radius for the carbon atom.

It will be noted that while there is considerable variation in the size of the metal atom, in all cases the ratio is smaller than the limit of 0.59 placed by Hägg.

It has been known for some time that these cubic carbides are soluble in one another, at least to some extent or, in other words, the metal atoms can be replaced, one by another without destroying the stability of the structure. Since the stability of these close packed interstitial substances appears to depend more upon geometry than upon the exact chemical nature of the atoms involved, it is of interest to examine the possibilities of replacement in these carbides in some detail.

Hume-Rothery[2] has pointed out the importance of the difference in size of solute and solvent atom as a factor in limiting the solubility in simple binary solid solutions. Largely on an empirical basis, he states that if the difference in size between solvent and solute atom is more than 14–15 pct of the solvent atom, the range of solubility is very restricted. The atom size was based on the distance of closest approach in the elements involved. While there is some question as to how one should calculate the size of the metal atom in the carbide structures, reference to Table 1 will show that zirconium is the largest and vanadium the smallest of the group and that the difference is about 15 pct. The Ti-Zr difference is about 9 pct and the others are smaller. Thus one would predict that if the size factor controls the solubility, all of the pairs except VC-ZrC would have wide or complete solubility whereas this latter pair is on the border line and might have restricted solubility.

Table 1 . . . Radius Ratio for Metal Atoms and Diamond Radius for Carbon Atom

Metal	Radius, Metal, A.U.	Radius, Carbon, A.U.	Radius Ratio
V	1.35	0.76	0.56
Ti	1.46	0.76	0.52
Cb	1.47	0.76	0.52
Ta	1.47	0.76	0.52
Zr	1.60	0.76	0.48

The purpose of the present investigation was to examine the solubility of the several pairs of carbides by heating them together until equilibrium was established and then examining the product by X rays.

San Francisco Meeting, February 1949.

TP 2527 E. Discussion of this paper (2 copies) may be sent to *Transactions* AIME before May 15, 1949. Manuscript received November 1, 1948.

This investigation was sponsored by the Office of Naval Research, Contract No. N5ori-7817.

* Professor and Research Assistant, respectively, Department of Metallurgy, Massachusetts Institute of Technology.

[1] References are at the end of the paper.

Previous Work

Agte[3] and his associates prepared various transition metal carbides and determined the melting points of binary mixtures. He concluded from the shapes of the melting point curves that there was extensive solubility in the case of the cubic carbides.

Umanskii[4] and his colleagues made an investigation of a number of pairs of the cubic carbides, using X rays and plotted lattice parameter vs. composition curves for the systems TaC-TiC, CbC-TiC, TaC-ZrC and CbC-ZrC. All pairs showed a continuous series of solid solutions. The first two pairs gave a linear relation while the latter two showed a negative deviation from Vegard's law.

Kiefer and Nowotny,[5] in a paper which became available after the present work was well advanced, investigated the binary pairs of the five cubic carbides by means of X rays. Relatively few points were obtained and results indicated that in some cases, at least, equilibrium was not reached at the temperatures used. The results indicated that solubility in the VC-ZrC system was not complete. All of the results of previous investigations indicated the desirability of a more detailed study.

Materials

The raw materials used were monocarbides of titanium, zirconium, vanadium, columbium and tantalum and were the purest which could readily be obtained commercially. Spectrographic qualitative analysis showed that the CbC and TaC contained less than 1 pct

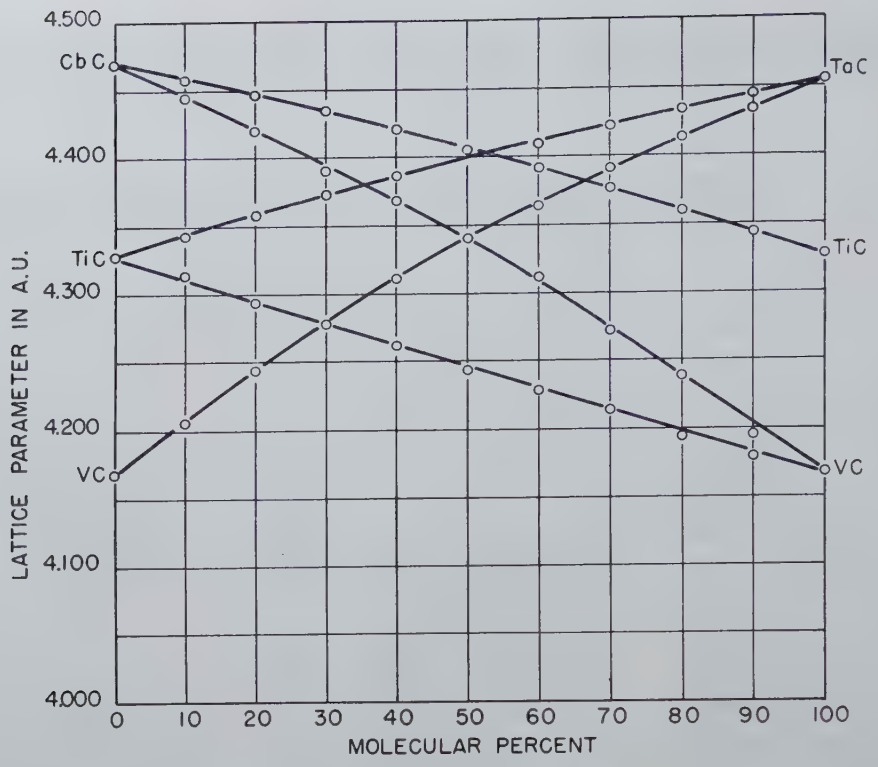

FIG 1—Lattice parameter vs. composition curve for the carbide pairs, CbC-TiC, Cb-VC, TiC-TaC, and VC-TaC.

of other metals. The TiC showed the presence of appreciable amounts of Cr, Fe, Si, V and Zr; the VC contained B, Cr, Fe, M and Si while the ZrC contained appreciable amounts of B, Fe and Ti. All were somewhat deficient in combined carbon content. The results of the investigation were such that the presence of these impurities does not influence the validity of the conclusions.

Experimental Procedure

Heating of the carbide mixtures was carried out in a high frequency vacuum furnace of conventional design, using a graphite crucible. Temperature was measured with a calibrated optical pyrometer sighting through a small tube in the crucible cover directly on the central specimen of the charge. Temperature was maintained by manual control during the heating runs within a limit of ± 20°C.

The individual carbides were mixed with additional carbon to correct the deficiency and heated in vacuum at 2100°C for 3 hr to recarburize and to volatilize some of the impurities. These carbides were then carefully weighed out and mixed in pairs at 10 molecular pct intervals. The mixing was done in a small stainless steel ball mill using benzene as a dispersing agent. Excess carbon powder was added as well as 1 pct of powdered cobalt to act as a diffusion aid during sintering. After mixing, the powders were pressed into small slugs and sintered.

The sintering was carried out at 2100°C in the vacuum furnace for a period of 3 hr in order to obtain an equilibrium state and then cooled in the furnace. During this treatment practically all of the cobalt was evaporated from the specimens. Equilibrium was judged from the appearance of the X ray diffraction lines which were sharp with well resolved alpha doublets after this treatment. A one hour treatment at temperature appeared to be sufficient in most cases but the longer treatment was used to make certain.

It was not possible to analyze all specimens after sintering but certain specimens selected at random and analyzed chemically for the metal content showed that the compositions as mixed and after sintering, did not differ by more than an amount corresponding to ± 2 molecular pct.

The X ray examination was carried out using radiation from a copper target and a Phragmen type focusing camera which covered the angular range from 45 to 83°. The powder specimens were prepared by crushing the sintered slugs, grinding in a mortar and mounting the fine powder on paper strips with adhesive. Some observations of relative line intensities were also made with the Norelco recording X ray spectrometer.

The X ray wavelength values used in calibrating the cameras and calculating the lattice constants were as follows:

Copper K beta —1.39217 A. U.
K alpha 1—1.54050 A. U.
K alpha 2—1.54434 A. U.

Thus the lattice constant values are in true Angstrom units. It must be remembered when comparing results with previous work that slightly different values of the wavelengths may have been used in the past.

X ray Results

The structures of the individual carbides were all of the NaCl type with metal atoms at coordinates 0, 0, 0; 0, ½, ½; ½, 0, ½; ½, ½, 0. The carbon atoms undoubtedly are at coordinates 0, 0, ½; 0, ½, 0; ½, 0, 0; ½, ½, ½; although no attempt was made to verify this conclusion in the present research.

The lattice parameters of the individual carbides are given in Table 2.

Table 2 . . . Lattice Parameters of Individual Carbides

Carbide	Parameter in A.U.
ZrC	4.689 ±0.001
CbC	4.470 0.001
TaC	4.457 0.001
TiC	4.329 0.001
VC	4.169 0.001

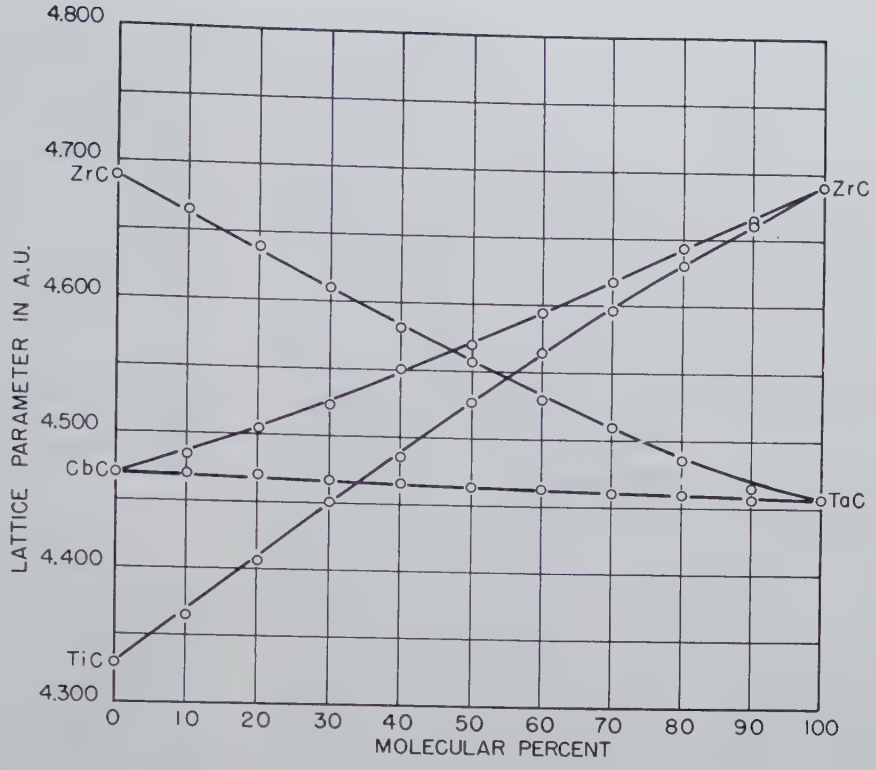

FIG 2—Lattice parameter composition curves for the carbide pairs, ZrC-TaC, CbC-ZrC, CbC-TaC, and TiC-ZrC.

A higher precision in the determination of the parameters of the individual carbides is not warranted in view of the small amounts of impurities present.

With the exception of the VC-ZrC series the X ray photograms of all of the other sintered binary pairs showed the presence of only a single phase having the same NaCl structure as the individual carbides but with varying lattice parameters. Fig 1 and 2 show graphically the variation of lattice parameter with composition of the carbides taken in pairs. It will be observed that the values lie on smooth continuous curves which depart only slightly from straight lines indicating uninterrupted series of solid solutions in each case.

The exception is the VC-ZrC system, the results of which are shown in Fig 3. Here all of the intermediate compositions between 10 and 90 molecular pct show two cubic phases of constant parameter having values close to the individual carbides. This indicates very limited solubility.

At the VC end of series, the lattice constants of the smaller cubic phase in the two-phase field is the same as that of VC, within experimental error. A specimen containing 4 molecular pct ZrC is definitely two-phase. Thus the solubility of ZrC in VC is certainly less than 4 pct and probably less than 1 pct.

At the ZrC end of the series, a definite but small solubility is indicated since in the two-phase region, the larger cubic phase has a parameter of 4.674 A. U. while that of ZrC is 4.689 A. U. An alloy containing 6 pct VC is two phase. If Vegard's law applies, the solubility would be 4 pct VC. One may conclude that the actual value of solubility of VC in ZrC at 2100°C is approximately 5 molecular pct. Carbides of higher purity would be necessary to obtain a more precise value.

Discussion of Results

The experimental results on the several pairs of carbides show clearly the limit placed on solubility by the size factor. A quantitative expression of the size factor depends upon the method of defining the atom size. One method is to employ the Goldschmidt atomic diameters, obtained from the distance of closest approach in the elements and corrected to a coordination number of 12. Another method is to assume that the metal and carbon atoms are in contact along the cube edge and that the carbon atom has a diameter which is constant for all of the carbides at a value equal to that in the diamond. The metal atom diameter is then calculated from the measured lattice parameter. Still a third method is to calculate the metal-to-metal atom distance in the carbide based on the measured lattice parameter. Table 3 shows a comparison of these methods of calculation.

Table 3 . . . Atomic Diameters of Metal Atoms in A.U.

Metal	D_1	D_2	D_3
V	2.69	2.66	2.95
Ti	2.93	2.82	3.06
Ta	2.94	2.95	3.15
Cb	2.94	2.96	3.16
Zr	3.19	3.18	3.31

D_1 = Diameter from element corrected to coordination number of 12.
D_2 = Diameter from carbide assuming carbon diameter of 1.511 A. U.
D_3 = Distance of closest approach of metal atoms in carbide.

A comparison of these values shows that in the carbides, the metal atoms have closely the same size as in the metals themselves and that in the carbides they are not quite closely packed but are pushed apart slightly by the carbon atoms. The exception is TiC where the diameter of the Ti atom in the carbide is definitely smaller than in the metal. No explanation suggests itself for this fact.

Using the value of D_2 in Table 3 one can calculate the percentage size differences for the several carbide pairs. The results are shown in Table 4.

Thus it can be seen that in this series of solid solutions in which the chemical properties of the elements are very similar but the size factor varies, extended solubility is possible if the

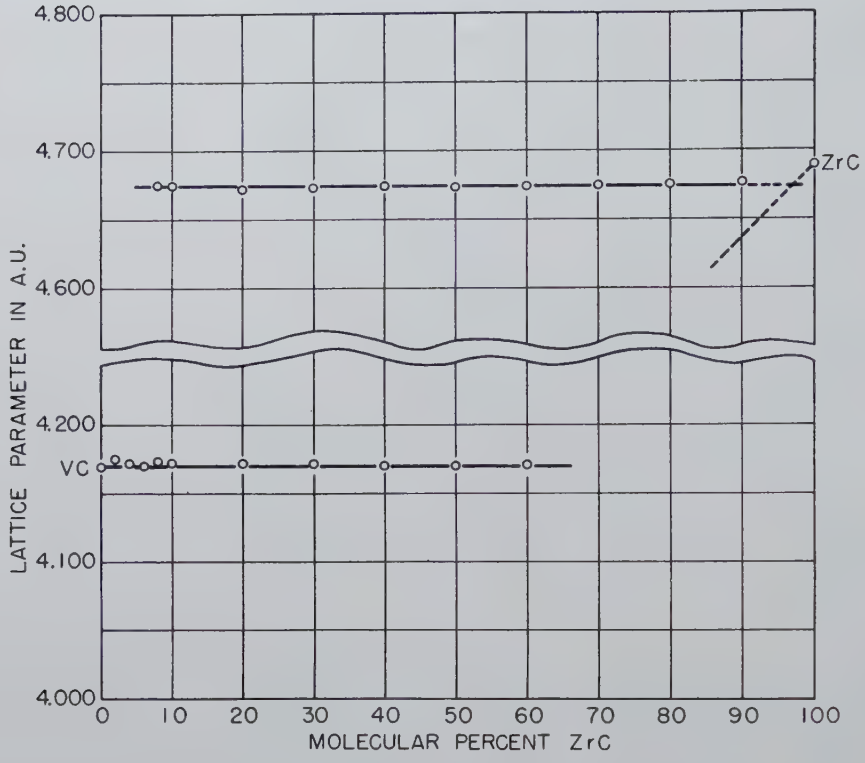

FIG 3—Lattice parameter composition curves for the carbide pair VC-ZrC.

Table 4 . . . Size Difference in Carbide Pairs

Carbide Pair	Difference in Pct Smaller as Solvent	Difference in Pct Larger as Solvent
VC-ZrC	21.1	16.3
TiC-ZrC	12.8	11.7
VC-CbC	11.3	10.0
VC-TaC	10.9	9.8
TaC-ZrC	7.8	7.2
CbC-ZrC	7.4	6.9
VC-TiC	6.0	5.7
TiC-CbC	5.0	4.7
TiC-TaC	4.6	4.4
TaC-CbC	0.34	0.34

difference in size of solute and solvent is 13 pct of the size of the solvent. If this figure increases to 16 pct the solubility is very restricted as in the zirconium-rich end of the VC-ZrC system and is practically zero at 21 pct which is the vanadium-rich end of this same system. This is in good agreement with the rule found for simple binary solid solution alloys.

The lattice parameter composition curves for the binary carbide pairs which form continuous series of solid solutions show slight variations from the linear relation required by Vegard's law. In the systems TiC-VC and CbC-TaC, the line is practically straight. Systems CbC-TiC, CbC-VC, TaC-TiC, TaC-VC and TiC-ZrC show a positive deviation. Systems CbC-ZrC and TaC-ZrC show a negative deviation. The maximum deviation occurs at a composition of about 50 molecular pct, the maximum positive value being 0.72 pct in the TaC-VC system and the maximum negative value being 0.40 pct in the TaC-ZrC system. At the present, no particular significance can be assigned to these small deviations.

There is no evidence in the sintered solid solution alloys that the distribution of the two kinds of metal atoms on the face-centered cubic lattice is other than random. Calculated and observed X ray line intensities are in good agreement on this basis and no superstructure lines have been observed. It is possible, however, that ordering might be induced by heating for long periods in the temperature range around 1500–1800°C. The system most likely to show ordering would be the TiC-ZrC system since this is the largest size difference for complete solubility. The composition ratios 3–1 and 1–3 should be examined since these compositions are favorable for the face-centered cubic lattice. The difference in atomic number should make it possible to recognize the existence of order in the structure by means of X rays.

The possibility other than ordering is that a solubility gap may exist at temperatures lower than 2100°C. Here again the TiC-ZrC system would be the most likely one. These two points are now under investigation.

Since the solubility of one carbide in another is limited by the change in lattice energy resulting from the strain produced by the misfit of the atoms, it is interesting to speculate about what would happen in the case of a ternary solid solution. For instance, suppose a mixture of equal parts of VC and ZrC, which are quite insoluble in one another were mixed with increasing amounts of TaC which has a metal atom size about halfway between the two and is capable of completely dissolving both. How much TaC would be required before a single homogeneous phase could be formed? Experiments to investigate this situation are in progress.

Conclusions

1. The monocarbides of the elements titanium, zirconium, vanadium, columbium and tantalum are isomorphous and have a sodium chloride type structure.

2. The binary carbide systems, TiC-ZrC, TiC-VC, TiC-CbC, TiC-TaC, ZrC-CbC, ZrC-TaC, VC-CbC, VC-TaC, CbC-TaC form continuous series of solid solutions.

3. The binary carbide system ZrC-VC shows very small solubility, the limits at 2100°C being 5 pct at the zirconium-rich end and less than 1 pct at the vanadium-rich end.

4. The parameter-composition curves show only slight deviations from Vegard's law but both positive and negative deviations are found.

5. The maximum size difference between atom diameters expressed in percent of the solvent atom diameter for extended solubility is 13 pct. The minimum value for very restricted solubility is 16 pct.

6. In the solid solution, the metal atoms are distributed at random on the points of the metal lattice.

Acknowledgment

The authors wish to acknowledge the services of Mr. Albert Mahfuz and Mr. Robert Bennett who assisted in carrying out these experiments.

References

1. G. Hagg: *Ztsch.* Physik. Chem., (1929); **6(B)**, 221 (1930); **7(B)**, 339 (1930) **8(B)**, 445.
2. Hume-Rothery: The Structure of Metals and Alloys. Inst. of Metals Monograph, p. 52. 1936. London.
3. Agte and Alterthum: *Ztsch.* Tech. Physik. (1930) **11**, 182.
4. Kovalskii and Unanskii: *Zhurnal* Fizicheskoi Khimii. (1946) **20**, 769.
5. Nowotny and Kieffer: *Metallforschung.* (1947) **2**, No. 9, 257.

Pressure Distribution in Compacting Metal Powders

POL DUWEZ* and LEO ZWELL*

Introduction

In recent years, the problem of pressing metal powder in a die has received much attention. The question has been the object of a Symposium held in New York in March 1947 under the sponsorship of the AIME; an excellent review of the subject may be found in Ref. 1. Various experimental techniques have been used to study the behavior of the powder in a die cavity. Two methods have been particularly successful; one consists of measuring the density distribution[2,3] and the other makes use of a lead grid in the powder during pressing.[4] In the present study, the pressure at various points on the bottom and the sides of a die 1.50 in. in diam was measured by means of small piston dynamometers and resistance sensitive strain gauges. In order to correlate the results with previous investigations, the pressure distribution inside the compact has also been determined by an indirect method based on density measurements

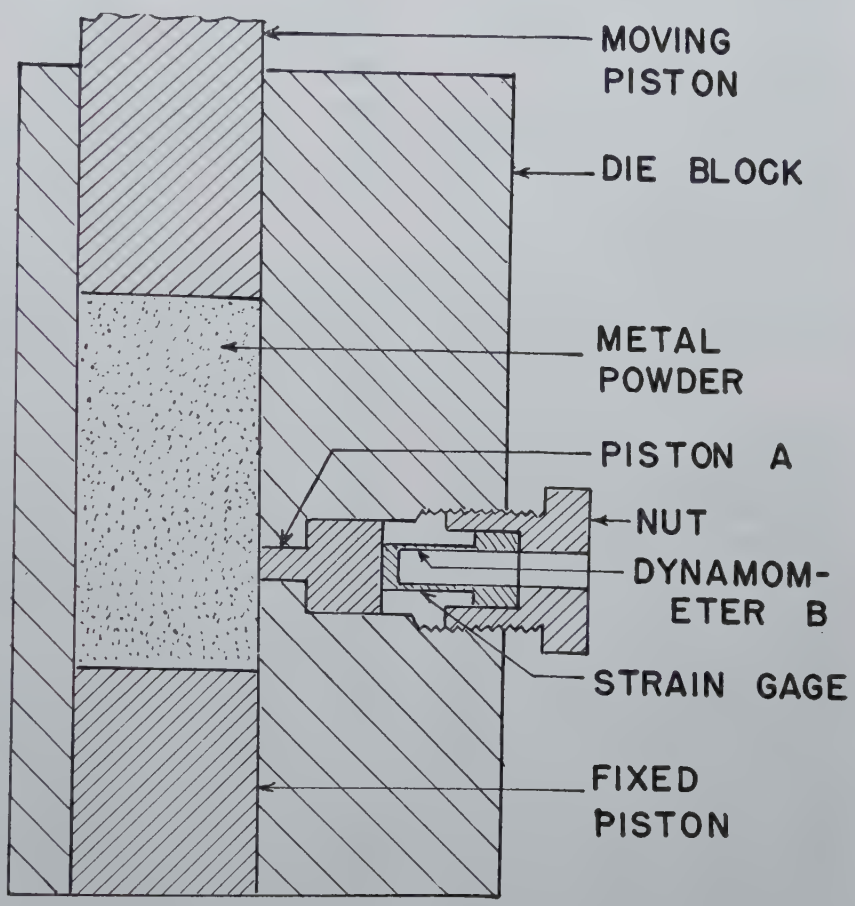

FIG 1—Experimental die for measuring side pressure.

Strain Gauge Measurements of Pressure on Side and Bottom of Die

A schematic drawing of the die used for measuring side pressures is shown in Fig 1. The pressure gauge consists of a 0.25-in. diam piston *A* which transmits the pressure to a dynamometer *B*, on which two Baldwin Southwark type A-14 strain gauges are fastened 180° apart. Because the installation of several dynamometer assemblies along the side of the die would have been difficult, the pressure distribution was obtained in successive tests in which the distance from the gauge to the bottom of the compact was adjusted to different values by changing the length of the bottom piston. The dynamometer, disassembled from the die, was calibrated under compressive loads and showed a 1.00 ohm change of resistance for every 15,300 psi change of pressure (750 lb load change).

All the strain gauge measurements were made with a null type Leeds and Northrup Wheatstone bridge. The sensitivity of the method was better than 1 pct and the accuracy was within 2 pct. These values were considered satisfactory in view of the rather large scatter in the measurements introduced by the random variation in packing the powder in the die. The stable ambient conditions and short time involved in the taking of observations made temperature compensation unnecessary.

The pressure distribution on the bot-

San Francisco Meeting, February 1949.

TP 2515 E. Discussion of this paper (2 copies) may be sent to *Transactions* AIME before May 15, 1949. Manuscript received Nov. 3, 1948.

* Associate Professor of Mechanical Engineering and Chief of the Materials Section, and Research Engineer, respectively, Jet Propulsion Laboratory, California Institute of Technology, Pasadena, Calif.

[1] References are at the end of the paper.

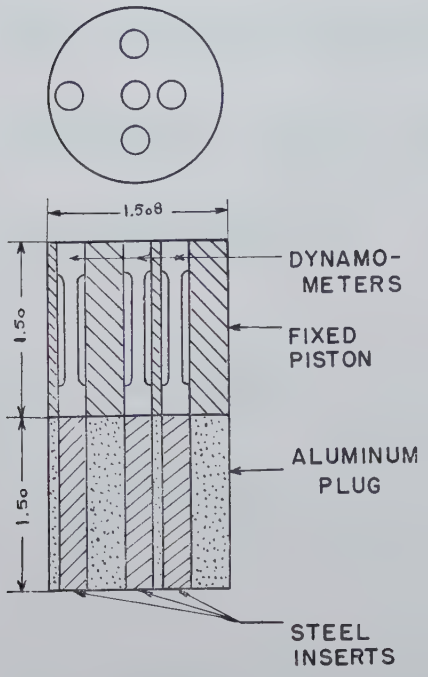

FIG 2—Pressure gauges on fixed piston.

tom of the die was determined with five dynamometers, as shown in Fig 2. The dynamometers were 0.25 in. in diam, 1.5 in. long, and had a 1 in. center length ground to 0.125 in. in diam. One Baldwin Southwark type C-7 strain gauge was pasted on each dynamometer. Under maximum loading, the elastic deformation of the dynamometers caused a relative displacement of about 0.0045 in. between the surface of the gauges and that of the bottom piston. In order to eliminate this source of error, an aluminum plug, 1.5 in. long, was placed under the piston with five steel inserts on which the dynamometers rested. Since the displacement of the aluminum plug with respect to the steel inserts compensated for the displacement of the dynamometers with respect to the bottom piston, the relative motion of the dynamometers to the bottom piston was negligible.

The average pressure acting on the fixed piston was measured by means of a strain gauge arrangement, shown in Fig 3. Four strain gauges, Baldwin Southwark type A-7, were attached around the dynamometer member of the piston. A calibration curve of gauge resistance with pressure was made by applying increasing loads with the moving piston acting directly on the fixed one.

PRESSURE ON THE SIDE OF A DIE

The copper powder used in the experiments was type MD-51 from Metals Disintegrating Co., Elizabeth, N. J. The stainless steel powder was the 18–8 standard grade made by Unexcelled Chemical Co., New York City. The particle size distribution of the powders is given in Table 1.

Table 1 . . . Particle Size Distributions of Metal Powders

Screen Size (mesh) Between	and	Weight of Particles in Each Size Fraction (per cent) Copper	18-8 Stainless Steel
35	60	0.8	
60	100	88.2	1.2
100	150	5.8	5.2
150	200	1.2	7.0
200	325	1.0	24.4
through	325	3.0	62.0

The pressure on the side of the die was measured for both powders. For each location of the gauge with respect to the fixed piston, the applied pressure was increased in steps of 10,000 psi up to a pressure of 60,000 psi and in steps of 5000 psi up to a pressure of 100,000 psi. A family of curves of side pressure vs. applied pressure was then obtained, each curve corresponding to a point at a certain distance from the fixed piston. Typical curves (only two of each family) are shown in Fig 4 for copper and in Fig 5 for stainless steel. Each point on the curve represents the average of at least three measurements.

The results of pressure measurements are more conveniently analyzed by tracing curves of side pressure vs. distance of the gauge from the fixed piston for a given compacting pressure. Such pressure distribution curves are shown in Fig 6 for copper powder and in Fig 7 for stainless steel powder. Although the experimental points are rather scattered, they seem to fall more or less on straight lines. Hence, it may be concluded that the pressure on the side of the die increases almost linearly from the bottom to the top of the compact.

It is significant to note that the side pressure measured for copper powder is about twice as large as for stainless steel. It is probable that the most important factor influencing the side pressure in a die is the plasticity of the powder. A soft powder is likely to flow sidewise and produce a higher lateral pressure than a hard powder. In order to substantiate this statement, side pressure measurements were made by replacing the powder with a cylinder of solid copper. With a fully annealed cylinder (Rockwell F30) the side pressure was about 50 pct greater than that measured with the powder. With a hard copper cylinder (Rockwell B47) the side pressure was 50 pct less than that observed with the powder. These results suggest that a systematic investigation of the effect of hardness of the powder on the side pressure would be very worthwhile.

PRESSURE DISTRIBUTION ON THE FIXED PISTON

A series of measurements was made with the five small gauges previously described in an attempt to determine the variation in pressure along two perpendicular diameters of the fixed piston. Numerous measurements were made with different thicknesses* of compact and at various compacting pressures. Only a typical set of curves is shown in Fig 8 for compacts of various thicknesses and a compacting pressure of 50,000 psi. The abscissa of the graph of Fig 8 is the distance from the center of the fixed piston expressed as a fraction of the radius of the piston. The results indicate clearly that the

* The word "thickness" refers to the dimension measured after the compact was ejected from the die.

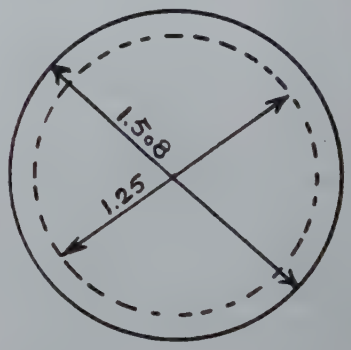

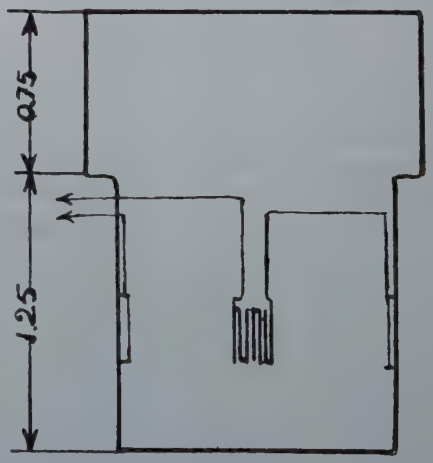

FIG 3—Fixed piston gauge for measuring average pressure.

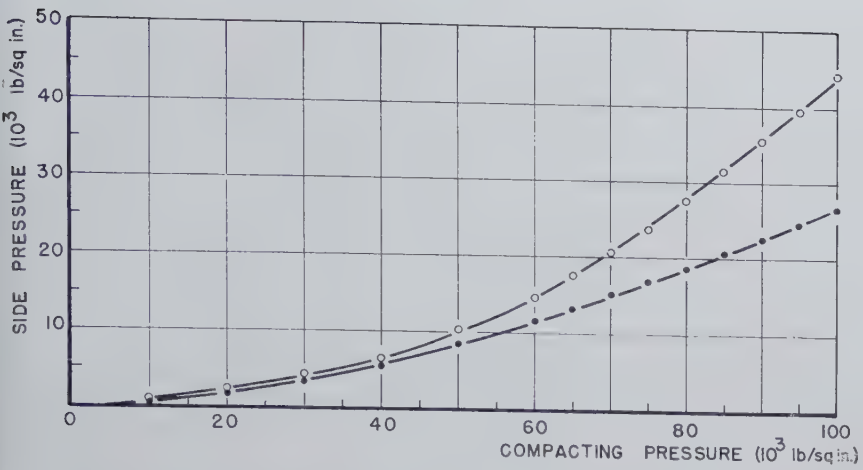

FIG 4—Variation of side pressure with compacting pressure for copper powder; compact thickness 1.15 in., compact diameter 1.51 in.
(⊙) 1.0 in. from fixed piston.
(●) 0.15 in. from fixed piston.

pressure on the fixed piston decreases steadily from the center to the periphery of the piston. Moreover, as the thickness of the compact increases, the average pressure on the fixed piston decreases, but the shape of the pressure distribution curve does not change appreciably, at least within the limits of thickness to diameter ratios considered in these measurements. It is also interesting to note that for a thin compact (ratio of thickness to diameter equal to 0.11 on Fig 8), the pressure at the center of the fixed piston is greater than the compacting pressure.

The results of this series of experiments were substantiated by the measurements of the density distribution within a compact (See "Pressure Distribution within a Compact").

AVERAGE PRESSURE ON THE FIXED PISTON

In spite of the fact that the pressure is not uniform on the fixed piston, the consideration of an average pressure is of interest because it introduces simplifications in both experimental technique and interpretation of the results. Experiments were therefore made with the purpose of relating the average pressure on the fixed piston with the thickness of the compact. The results of measurements are presented in Fig 9. In this diagram, the two variables are dimensionless, the ordinate being the ratio of base pressure to applied pressure and the abscissa the ratio of thickness of compact to diameter. These results were obtained with copper powder at compacting pressures of 40,000 and 100,000 psi. The scatter of the results is relatively large and may be attributed to the difficulty in obtaining a uniform packing of the powder during loading. In spite of the scatter, it seems reasonable to conclude that, in a first approximation at least, the ratio of bottom pressure to compacting pressure is a function of the ratio of thickness to diameter of compact and in the range of pressures from 40,000 to 100,000 psi does not depend upon the compacting pressure.

The variation of fixed piston pressure with the thickness of a compact is of great practical interest, since it shows what fraction of the compacting pressure is actually transmitted to the bottom of the compact. It is significant to note the rather rapid decrease in bottom pressure with increasing thickness of compact. For the copper powder used in the present experiments, and with a ratio of thickness to diameter equal to 1.0, only about 30 pct of the compacting pressure is acting on the bottom part of the compact.

The rather simple technique of measuring the average pressure on the fixed piston seems to be best suited to characterize the behavior of a powder during compacting. Its use should prove of great interest for studying quantitatively the effect of lubricants added to the powder or sprayed on the die walls.

Several investigators have proposed theoretical explanations for the decrease in fixed piston pressure with increasing compact thickness. The parabolic expression given by Unckel[5] does not give a satisfactory agreement with the results found in the present investigation. The exponential relation derived by Taylor[6] agrees with the results only for compacts having a thickness to diameter ratio less than one.

Pressure Distribution within a Compact

The pressure distribution within a compact was determined by an indirect method, based on the relation between the local density within the compact and the compacting pressure that would be required to obtain such a density. A calibration curve of density vs. compacting pressure was first obtained by pressing ⅛-in. thick compacts at various pressures and measuring their densities. In spite of the relatively small ratio of thickness to

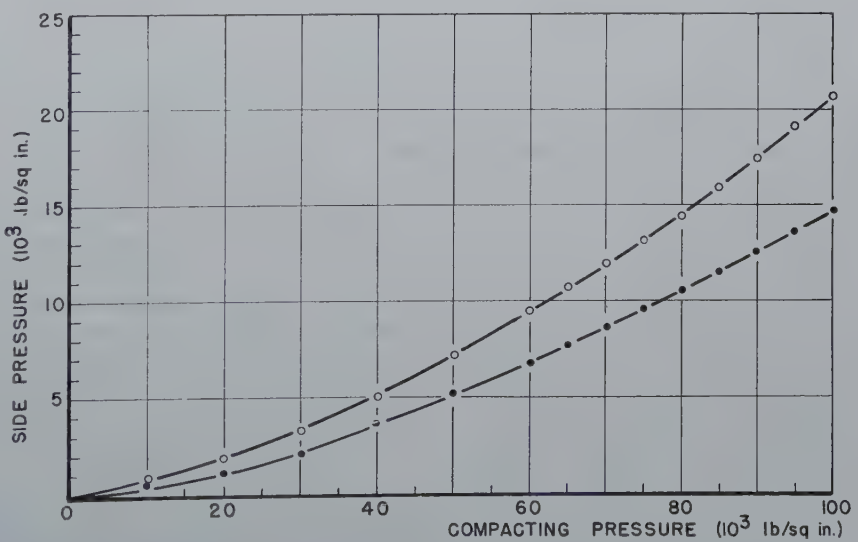

FIG 5—Variation of side pressure with compacting pressure for stainless steel powder; compact thickness 1.27 in., compact diameter 1.51 in.
(⊙) 1.0 in. from fixed piston.
(●) 0.15 in. from fixed piston.

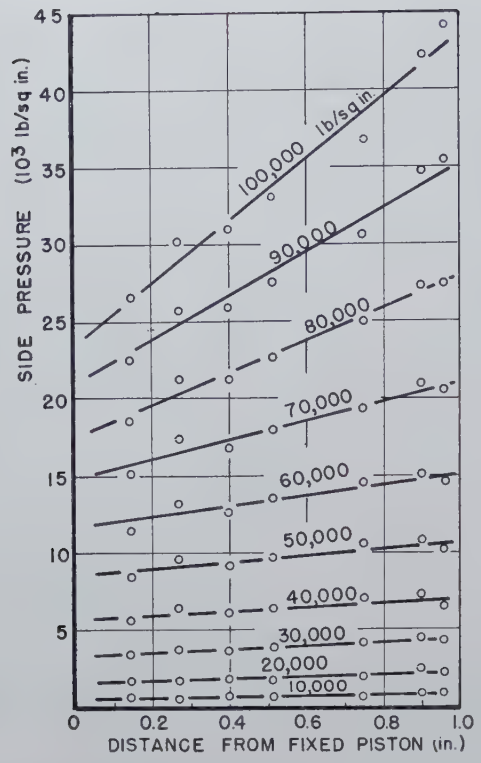

FIG 6—Pressure distribution on the side of a die for copper powder under various compacting pressures; compact thickness 1.15 in.

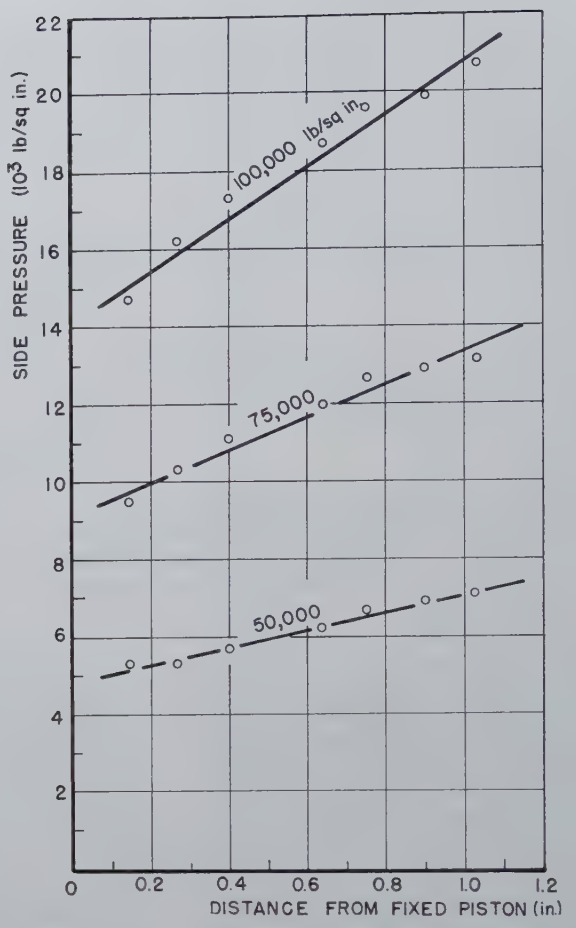

FIG 7—Pressure distribution on the side of a die for stainless steel powder under various compacting pressures; compact thickness 1.27 in.

diameter of these compacts (0.083), the strain gauge pressure measurements showed a base pressure about 6 pct smaller than the compacting pressure. An average pressure was then taken for tracing the calibration curve. Such a curve is shown in Fig 10 for copper powder. The densities of successive layers in a thick compact were obtained by facing off cross-sections of the compact and computing their densities from the dimensions and weights of the compacts before and after machining. In order to eliminate errors due to machining, some compacts were faced from top to bottom, others from bottom to top, and still others from both ends to the center.

The radial distribution of density was determined by turning down the diameter of compacts in steps of 0.20, 0.25, 0.35, and 0.70 in. for thicknesses varying from ¼ to ½ in. and computing the densities of these machined cylindrical sections. The densities of the compacts and sections were computed with an uncertainty of about 1 pct and the uncertainty in the pressure values was estimated to be about 6 pct.

The pressure distribution in the vertical direction is shown in Fig 11 for a series of compacts pressed at 100,000 psi. The different symbols used on this graph refer to specimens having various thicknesses after compacting. The ordinate of the diagram is the ratio of the average effective pressure in a given section of the compact to the applied compacting pressure. The abscissa is also a ratio, obtained by dividing the distance between a section of the compact and the moving piston by the diameter of the compact. This method of presenting the data has the advantage of dealing with dimensionless parameters. The rather large scatter in experimental results (See Fig 11) is probably due mostly to the nonuniform distribution of the powder in the die before pressing. In spite of the scatter, the results indicate that the pressure distribution is about the same for all compacts, regardless of thickness.

As expected, the average pressure decreases steadily from the top to the bottom of the compact. It is interesting to note, however, that for a ratio of thickness of compact to diameter greater than approximately 1.0, the pressure tends to decrease slowly, and approaches a value equal to about 20 pct of the applied pressure on the moving piston.

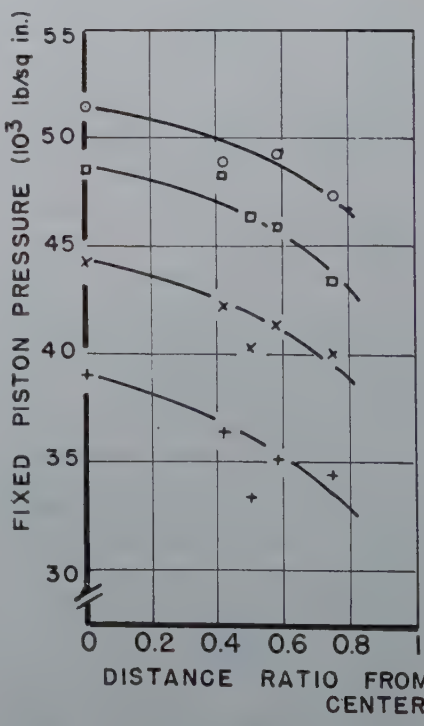

FIG 8—Pressure distribution on fixed piston for copper compacts of various thickness to diameter ratios.
(⊙) 0.11, (□) 0.35, (×) 0.61, (+) 0.88.

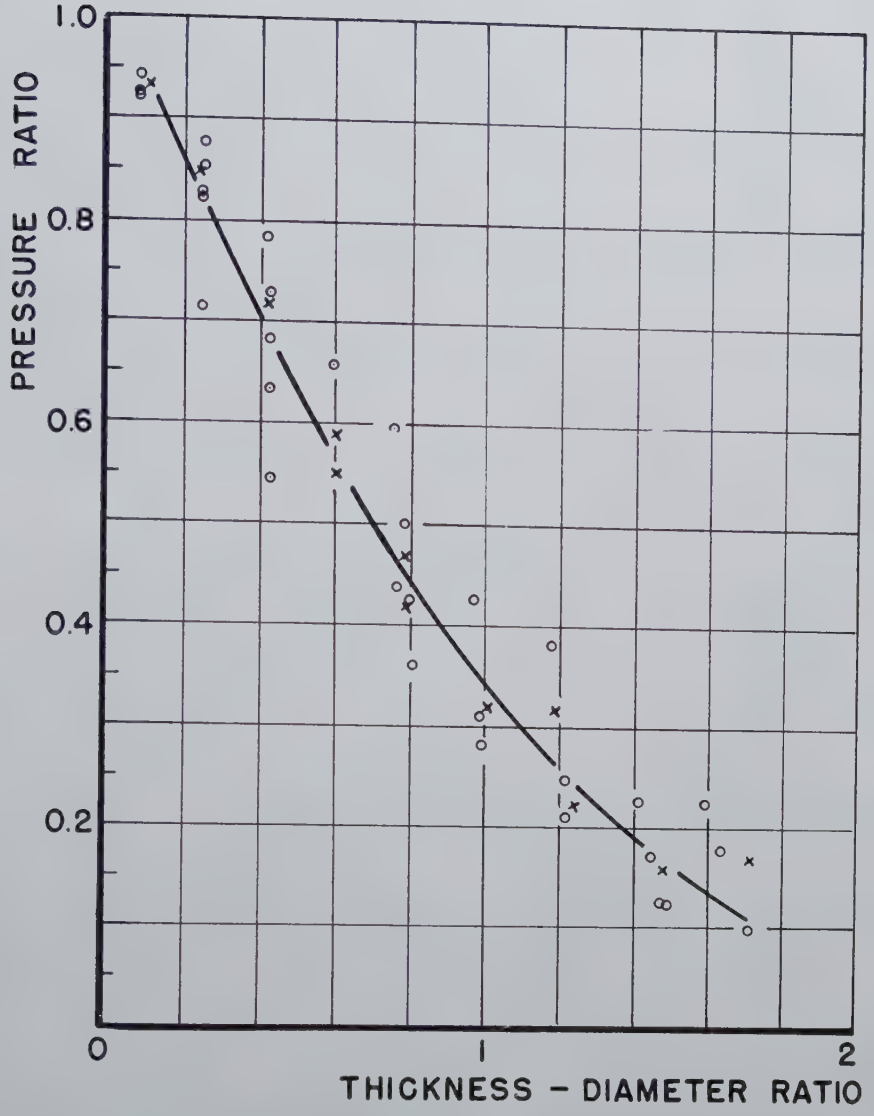

FIG 9—Ratio of average pressure on fixed piston to compacting pressure vs. ratio of thickness to diameter of copper compacts; compacting pressure 100,000 (⊙) and 40,000 (×) psi.

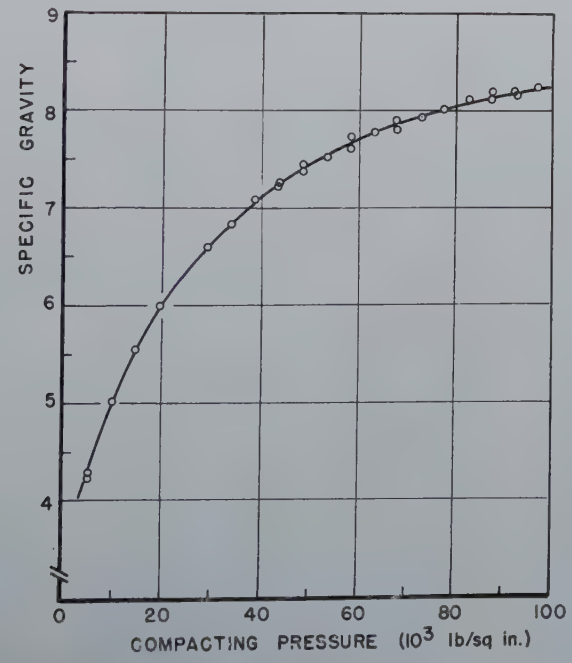

FIG 10—Calibration curve relating density and compacting pressure of copper powder.

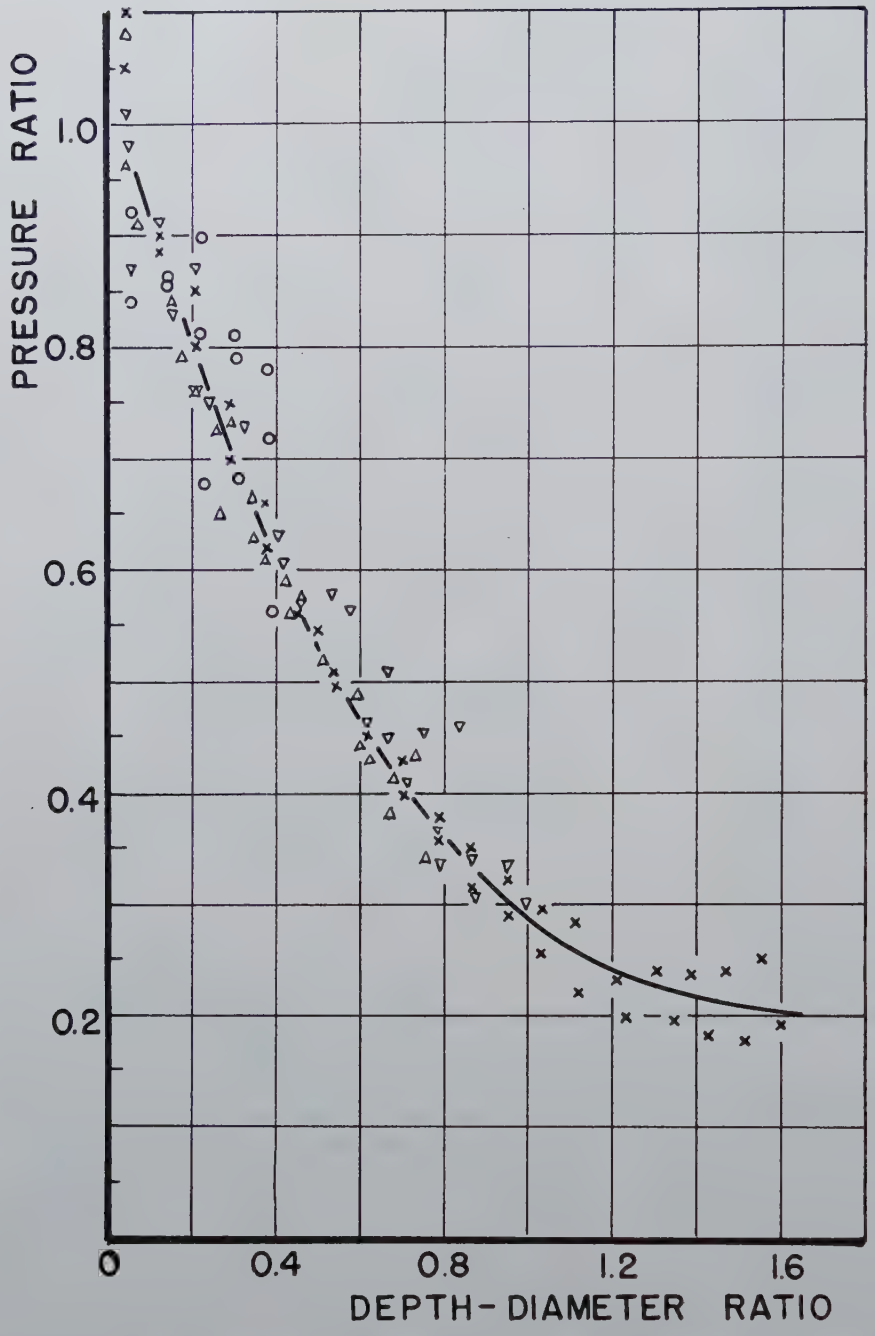

FIG 11—Pressure distribution in copper compacts of various thicknesses; compacting pressure 100,000 psi.
(⊙) 0.65 in., (△) 1.2 in., (▽) 1.5 in., (×) 2.4 in.

A comparison of the results in Fig 9 and 11 shows that there is satisfactory agreement between the values of the pressures on the fixed piston measured by strain gauges and the values of the pressures at equivalent depths of compacts determined from density measurements. The small difference observed in the two figures (the fixed piston measurements being slightly higher) may be due to the different radial pressure distributions in the two cases and to the different character of the contact layer; that is, at the fixed piston the powder is pressed against a solid support, while within the compact the powder is pressed against a soft support.

Additional results were obtained at pressures of 80,000 and 40,000 psi. In this case, it was possible to use longer compacts, for which the ratio of thickness to diameter was about 3.4. The results presented in Fig 12 indicate that the pressure distribution curves are reasonably close to the average curve obtained for 100,000 psi. The tendency for the pressure to level off in the bottom portion of long compacts, already mentioned in connection with the measurements made at 100,000 psi, is still more apparent from the graph of Fig 12. It seems reasonable to conclude that in the range of pressures of 40,000 to 100,000 psi, the pressure distributions in the die are similar. This result cannot be extrapolated to lower pressures. It was found, for example, that for a compacting pressure of 15,000 psi (See Fig 13), the pressure distribution curve does not fall as rapidly as for higher compacting pressures. This observation agrees with a generally recognized fact, that at low compacting pressures the uniformity of pressure (or density) in the longitudinal direction of a cylindrical compact, is relatively better than at high compacting pressures.

The pressure distribution in the radial direction and at various depths within a compact was also investigated by the density method. The results are rather complex, because the three dimensional pattern of pressure distribution depends on the thickness of the compact, and changes continuously as the compacting pressure increases. The results obtained with three compacts of different thicknesses and a compacting pressure of 100,000 psi are presented in Fig 14, 15, and 16. For all three specimens, the effective pressure near the moving piston is much higher at the outer circumference of the compact than at the center. This nonuniformity in pressure distribution decreases with the thickness of the compact and disappears at some distance from the top. In approaching the fixed piston, the situation is reversed, and the pressure decreases from center to periphery. This last observation is in agreement with the pressure measurements made with the five gauges on the fixed piston previously described. By comparing the graphs of Fig 14, 15, and 16, it is evident that the uniformity of pressure on the fixed piston is better for thicker compacts. This uniformity is obtained at the expense of the average pressure, which is, of course, very low on the bottom of a thick compact.

Additional measurements made with a compacting pressure of 50,000 psi did not alter essentially the shape of the pressure distribution curves obtained for 100,000 psi. It is probable that for low pressures of the order of 10,000 or 20,000 psi the distribution of pressure is more uniform. At low pressures, however, density measurements were difficult because of the lack of strength of the compacts.

An attempt was made to represent the distribution of pressure within a compact by tracing lines of equal pres-

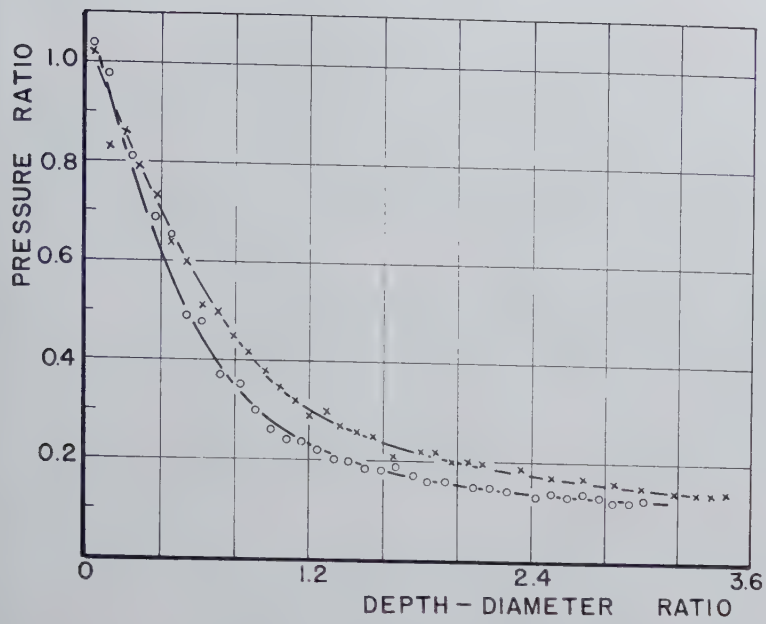

FIG 12—Pressure distribution in copper compacts pressed at 80,000 (⊙) and 40,000 (×) psi.

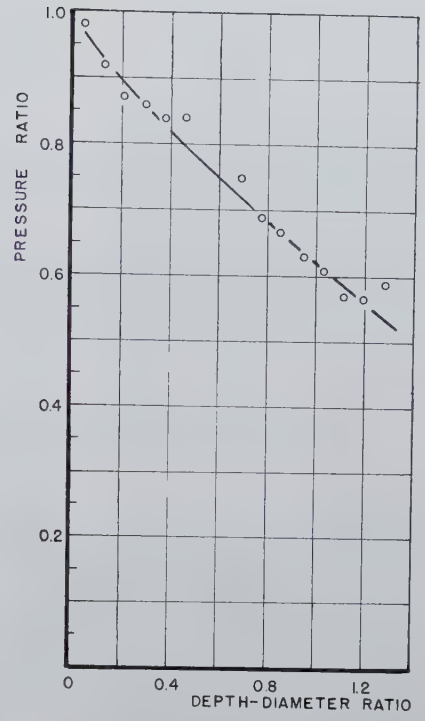

FIG 13—Pressure distribution in a copper compact pressed at 15,000 psi.

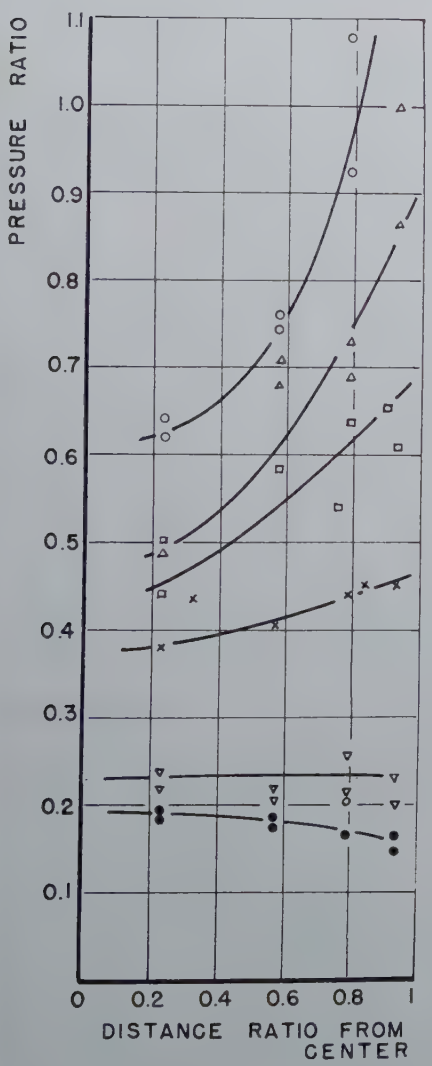

FIG 14—Radial pressure distribution in a copper compact 2.5 in. thick for a compacting pressure of 100,000 psi.

Distance from moving piston:
(○) 0.12 in. (□) 0.63 in. (▽) 1.72 in.
(△) 0.37 in. (×) 0.94 in. (●) 2.2 in.

sure in a longitudinal section. Three cases corresponding to compacts having a thickness to diameter ratio of 0.42, 0.79, and 1.66 are shown in Fig 17. Although these tracings should not be considered as very accurate, they provide a useful illustration of the results previously discussed.

The results of the present investigation of radial and longitudinal distributions of pressure agree in general with those obtained by Kamm, Steinberg and Wulff with the use of a lead grid in the powder during pressing.[4]

Summary and Conclusions

The experiments described in this paper have established the possibility of using resistance type strain gauges for measuring the pressure distribution on the walls and on the fixed piston of a die. The pressure on the walls in a cylindrical die varies almost linearly from the bottom to the top of the compact. On the fixed piston, the pressure decreases from the center to the periphery. The average pressure acting on the fixed piston or the die was also measured by a very simple strain gauge technique.

An interesting curve characterizing the behavior of the powder was obtained by plotting the ratio of the pressure on the fixed piston to the compacting pressure vs. the ratio of thickness to diameter of the compact.

The distance from the moving piston appears to be the basic factor determin-

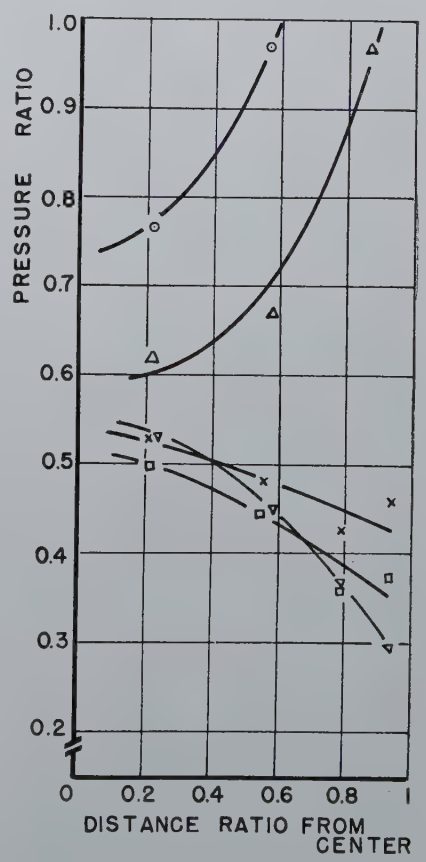

FIG 15—Radial pressure distribution in a copper compact 1.2 in. thick for a compacting pressure of 100,000 psi.

Distance from moving piston:
(⊙) 0.06 in. (△) 0.19 in. (×) 0.89 in.
(□) 1.01 in. (▽) 1.14 in.

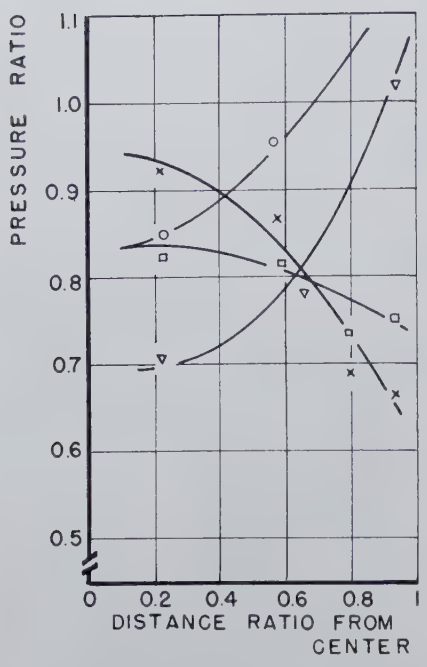

FIG 16—Radial pressure distribution in a copper compact 0.64 in. thick for a compacting pressure of 100,000 psi.
Distance from moving piston:
(○) 0.06 in. (▽) 0.16 in.
(□) 0.45 in. (×) 0.58 in.

ing the magnitude of effective pressure at any section of a compact; that is, variation of base pressure measurement with thickness of compact (distance from moving piston) agrees reasonably well with the variation of effective compacting pressure with depth of compact (distance from moving piston).

There is a radial distribution of pressure at the top and bottom of the compacts. Near the moving piston, the pressure is high at the outer edge and decreases towards the center. At the fixed piston, the pressure is higher at the center of the compact and decreases towards the outer edge. While the radial distribution at the top is always present, the radial distribution at the base of the compact decreases with increasing thickness of compact until it vanishes, in the case of copper, at a thickness to diameter ratio of about 1.5.

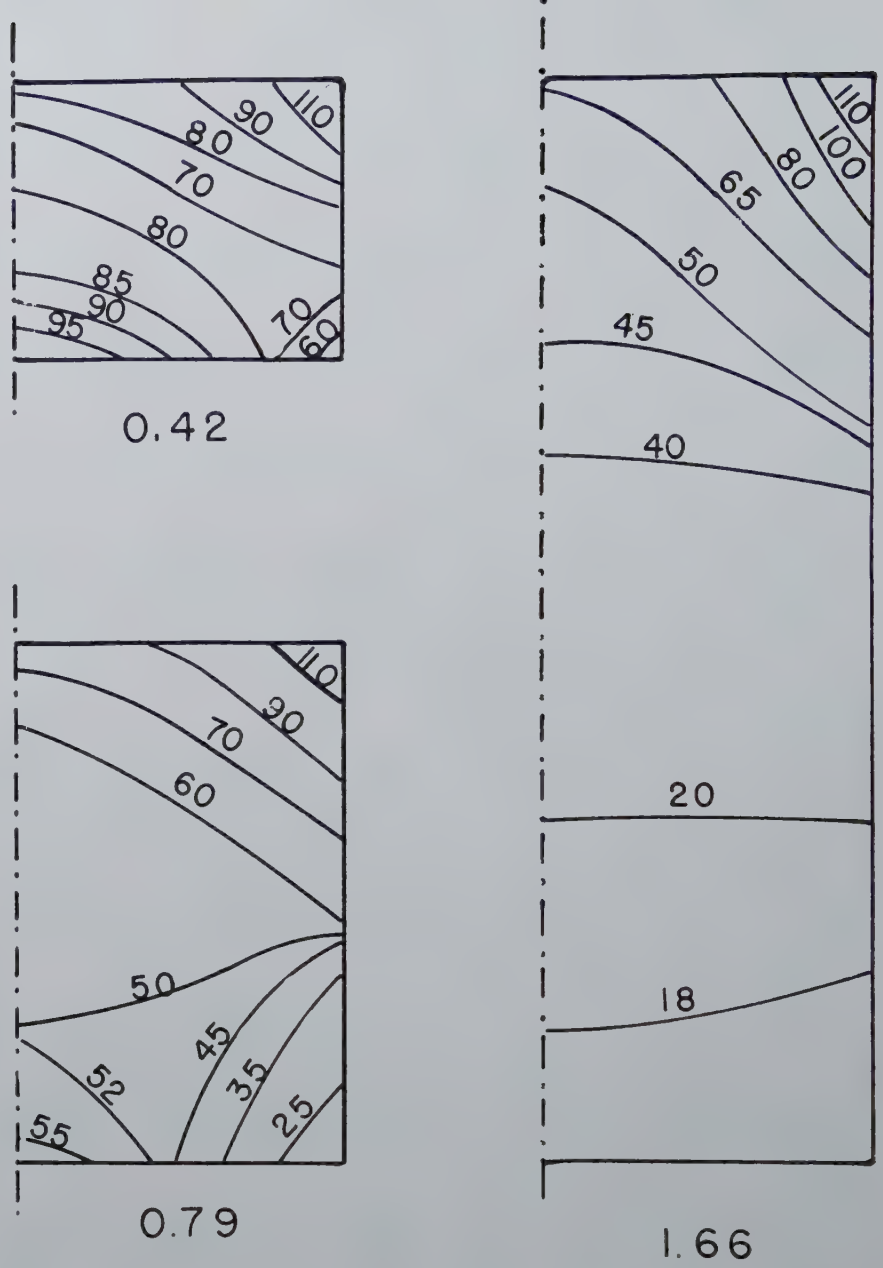

FIG 17—Approximate location of lines of equal pressure in copper compacts of 0.42, 0.79, and 1.66 thickness to diameter ratios; compacting pressure 100,000 psi.

Acknowledgment

This work was done at the Jet Propulsion Laboratory, California Institute of Technology, under contract with the Army Ordnance Department, Washington, D. C. The authors wish to thank this agency for the permission to publish the results of this investigation.

References

1. R. P. Seelig: Review of Literature on Pressing of Metal Powders. *Metals Tech.* TP 2236, Aug. 1947; *Trans.* AIME (1947) **171**, 506.
2. R. P. Seelig, and J. Wulff: The Pressing Operation in the Fabrication of Articles by Powder Metallurgy. *Metals Tech.*, TP 2044, Aug. 1946; *Trans.* AIME (1946) **166**, 492.
3. A. Squire: Density Relationships of Iron Powder Compacts. *Metals Tech.* TP 2165 (April 1947); *Trans.* AIME (1947) **171**, 485.
4. R. Kamm, M. Steinberg, and J. Wulff: Plastic Deformation in Metal Powder Compacts. *Metals Tech.* TP 2133 (Feb. 1947); *Trans.* AIME (1947) **171**, 439.
5. H. Unckel: *Archiv. Eisenhuttenwesen*, **18**, 161, (1945).
6. D. W. Taylor: Research on Consolidation of Clays. Prob. from Dept. of Civil and Sanitary Eng., Mass. Inst. of Tech., Ser. 82 (1942).

Preferred Orientation in Rolled and Recrystallized Beryllium

A. SMIGELSKAS* and C. S. BARRETT,† Member AIME

THERE have been no publications of the deformation and recrystallization orientations of the metal beryllium, yet pronounced textures would certainly be anticipated since it is close-packed hexagonal in structure. Having an axial ratio approximately that of magnesium, beryllium probably deforms by nearly the same slip and twinning mechanisms that operate in magnesium, and the textures are likely to be similar or but slightly different from the magnesium textures. In the tests reported below this is found to be the case; the textures are found to differ from those of magnesium only in the details of the scatter from the average orientation.

This report covers not only samples rolled at room temperature, but some rolled at elevated temperatures. Since magnesium has been suspected by some investigators of altering its crystallographic deformation mechanism at elevated temperatures, it was considered possible that beryllium might do so and alter its textures accordingly. No pronounced alterations were found, however. Unfortunately, the theory of deformation textures is not in a state of development that permits one to deduce the deformation mechanism from a knowledge of the textures, which means that the similarity of textures at different rolling temperatures, reported here, cannot be taken as definite evidence that the deformation mechanism is actually the same at all temperatures. The general similarity of the deformation textures of magnesium and beryllium also extend to the recrystallization textures of the two metals, judging by the pole figures for recrystallized sheet presented in this report.

Methods

Samples were prepared in the form of composite sheets made up of small pieces stacked in a pile. Each piece was trimmed with scissors so that an edge was parallel to the rolling direction, dipped in paraffin, and assembled into the pack by aligning it under the cross hair of a microscope. As the desired orientation was obtained on each piece it was secured in place by touching with a hot wire to melt the paraffin. A stack of ten or fifteen pieces was built up in this way, then trimmed to the shape of a T; the portion to be X rayed was then etched to the shape of a wire about 0.045 in. diam with 6N HCl. This method of shaping the sample is a modification of that used by Bakarian on magnesium.[1] The absorption of the rays in the sample was so slight that it caused no difficulty in interpreting the films.

Exposures were made with a 0.030 in. diam pinhole, using molybdenum radiation (40 kv, 25 ma. Type A film at 5 cm, 2 to 3 hr exposures). With the recrystallized specimens it was found necessary to oscillate the specimen so as to reduce the spottiness of the lines. A range of oscillation of 5° was sufficient to produce reasonably satisfactory patterns, though the quality was somewhat inferior to that of the deformation texture patterns, and only two degrees of intensity were read from the arcs on the films. Typical photograms for each of the deformation textures and the recrystallization texture are assembled in Fig 1.

The pole figures were plotted in the usual way with the intensity of the various portions of the diffraction rings estimated by eye. Seven to nine films were made of each sample and each was carefully read in plotting the pole figures.

Typical series included exposures with the beam normal to the rolling direction and at 11, 26, 41, 56 and 71° to the cross direction, plus two exposures with the beam normal to the cross direction, and at 11 and 79° respectively to the rolling direction.

The rolling was in each case considered sufficient to develop the final texture: the reduction by cold rolling was 84 pct (from 0.0045 to 0.0007 in. thickness), following prior hot rolling in longitudinal and transverse directions and recrystallization; the reduction by hot rolling at 800°C was 90 pct (0.010 to 0.001 in.), following similar prior treatment; the reduction by rolling at 350°C was 88 pct (from 0.005 to 0.0006 in.) after similar prior treatment. The recrystallization texture was determined on a sample rolled at 350° to a reduction of 88 pct (0.0165 to 0.002 in.) after similar prior treatment, then mounted between steel strips to keep it flat and annealed at 700° in an atmosphere of argon.

Discussion of Results

The results of the X ray determinations are assembled in the pole figures of Fig 2, 3, 4 and 5 for rolling at

San Francisco Meeting, February 1949.

TP 2522 E. Discussion of this paper (2 copies) may be sent to *Transactions* AIME before May 15, 1949. Manuscript received November 1, 1948.

* Argonne National Laboratory, Chicago, Illinois.

† Institute for the Study of Metals, University of Chicago; Consultant at Argonne National Laboratory.

[1] References are at the end of the paper.

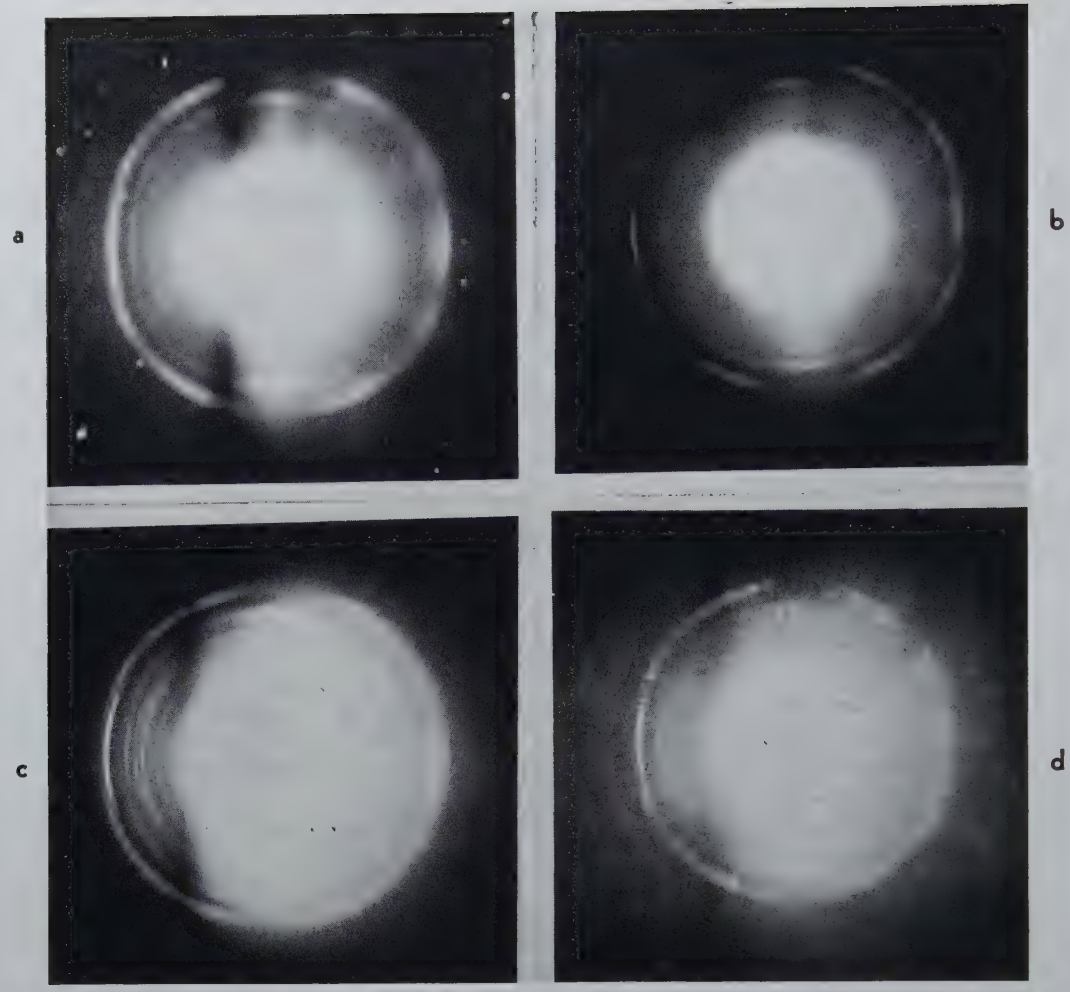

FIG 1—X ray photograms (a) room temperature rolled sheet (b) 350°C rolled sheet (c) 800°C rolled sheet (d) 350°C rolled sheet and recrystallized at 700°C.

Beam 11° to cross direction and 90° to rolling direction vertical. Outmost ring (101)[7]pyramidal planes show eight maxima; next ring (001) basal plane shows two maxima in 3 o'clock and 9 o'clock positions; the inner ring (100) planes show maxima at 6 o'clock and 12 o'clock positions.

25, 350 and 800°C and for 350°C rolled sheet after recrystallization, respectively. The plane of the sheet is parallel to the plane of the stereographic projection in all the figures, with the rolling direction vertical and the transverse direction horizontal. The densities of the arcs on the films are indicated by the closeness of the cross-hatching on the pole figures. The orientations of three different sets of planes are shown, the three with most marked evidence of orientation in the films, (0001), $(10\bar{1}0)$, and $(10\bar{1}1)$, that is, $(00\bar{0}1)$, (100), (101). The conclusions that are drawn from these data are consistent with the pole figures from all three sets of planes.

The texture is of the same type in all specimens. It may be described in terms of an ideal, or mean, orientation plus a scatter, the ideal orientation being (001) parallel to the plane of rolling and (100) perpendicular to the direction of rolling. This orientation is shown on each of the pole figures by small circles. Thus the basal plane is parallel to the plane of the sheet; two close-packed rows of atoms in this plane make an angle of 30° with the rolling direction, and the third close packed row is parallel to the transverse direction in the sheet.

The scatter from this mean position is such that the hexagonal axis tilts more toward the cross direction than toward the rolling direction. To state it differently, treating the rolling direction as an axis of rotation, the scatter around this axis extends as much as 50° each way from the mean orientation, while the scatter around the cross direction is only about 20° each way from the mean.

From the pole figures it appears that the scatter is greatest with room temperature rolling, is less with 350°C rolling, and still less with 800°C rolling and with recrystallization, the corresponding ranges of scatter around the rolling direction as an axis being about 65, 50, 40, and 40° from the mean orientation, respectively. Whether these different ranges are significant is problematical, however, for it must be noted that the grain size progressively increases throughout this sequence, hence the films are progressively less able to locate with certainty the exact limits of a pole figure area.

There is no evidence of an abrupt change in texture at an elevated temperature that would necessitate assuming that a different mechanism of deformation sets in above room temperature. But as mentioned earlier, it is not possible at the present time to definitely exclude this on the basis of the pole figure evidence, since a complete understanding of textures and their implications has not yet been reached.

The mean position of the basal plane in rolled beryllium (axial ratio $c/a = 1.568$) is the same as in magnesium, zirconium, and close-packed hexagonal

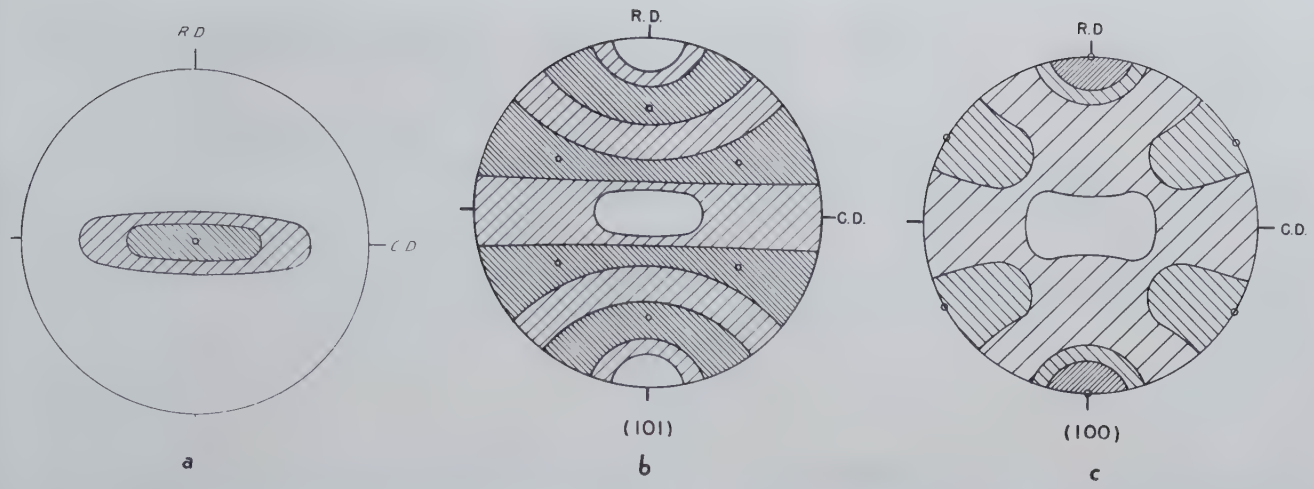

FIG 2—Pole Figures for Beryllium Rolled at Room Temperature (a) (001) Planes, (b) (100) Planes, (c) (101) Planes. Ideal texture indicated by small circles.

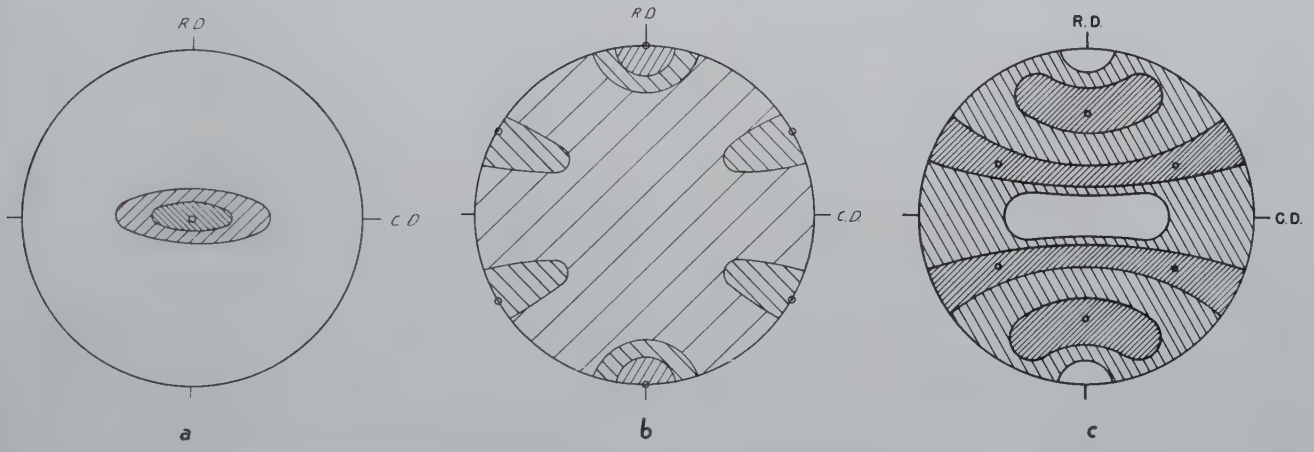

FIG 3—Pole Figures for Beryllium Rolled at 350°C. (a) (001) Planes; (b) (100) Planes; (c) (101) Planes.

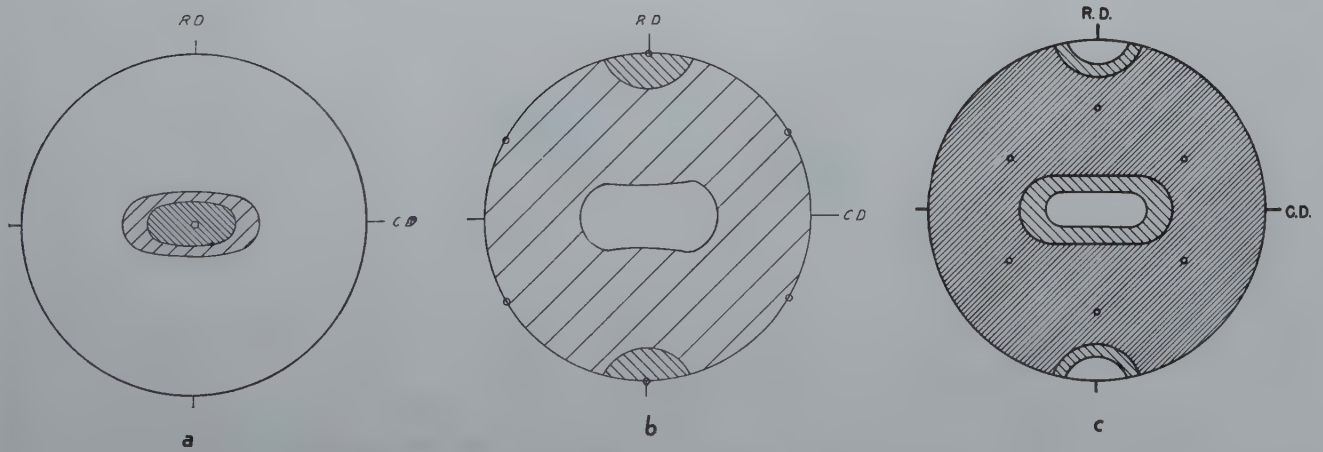

FIG 4—Pole Figures for Beryllium Rolled at 800°C. (a) (001) Planes; (b) (100) Planes; (c) (101) Planes.

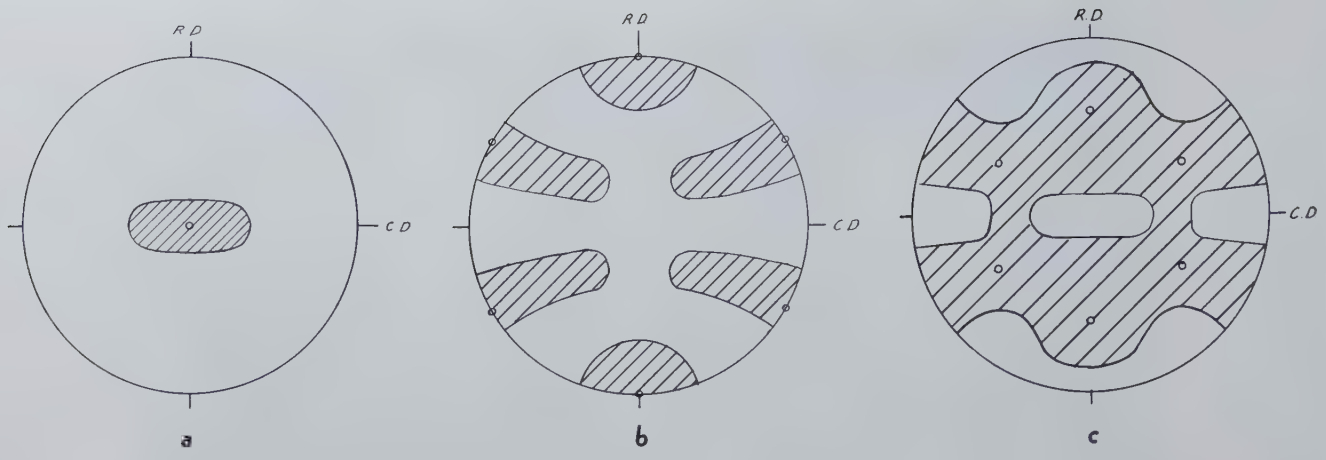

FIG 5—Pole Figures for Beryllium Rolled at 350°C and Recrystallized at 700°C. (a) (001) Planes; (b) (100) Planes; (c) (101) Planes.

cobalt, (c/a = 1.624, 1.589 and 1.624 respectively), but differs from that in zinc and cadmium, which have much greater axial ratios (1.85 and 1.88 respectively). Twinning is an important feature of the rolling process for zinc and cadmium and not for the metals of lower c/a ratio, and we now see that beryllium is no exception to this rule, for there is nothing in the texture of beryllium that suggests an appreciable amount of twinning in the final stages of deformation. There may be twinning, of course, in the early stages of deformation before the stable texture is reached.

It is not surprising that the recrystallization texture is the same as the rolling texture, for this is a common behavior in close-packed hexagonal metals.

There is no evidence for the double texture that is observed in certain alloys of magnesium,[1] in which the central spot of the (001) pole figure is double. The major axis of spread in beryllium is around the rolling direction of the sheet, which is similar to zirconium, rather than around the transverse direction as in magnesium.[2] Another interesting feature of the beryllium texture is the alignment of the [210] direction parallel to the rolling direction (that is, the alignment of the (100) plane normal to the rolling direction). In the usual textures reported for hexagonal metals there is no marked preference for any direction in the basal plane to be parallel to the rolling direction.

Summary

The rolling texture of beryllium is one in which the preferred position of the basal plane is parallel to the plane of the rolled sheet and close-packed rows of atoms in this plane lie 30° from the rolling direction. There is a scatter of from 40 to 65° in both directions from this orientation around the rolling direction as an axis, and a smaller scatter around the transverse direction in the sheet. The texture is approximately the same for rolling at room temperature, 350 and 800°C, and after recrystallization. There is no evidence of a change of slip mechanism with temperature.

Acknowledgments

We are indebted to Mr. James F. Schumar and Mr. S. Hugh Paine, Jr., for assistance in this work, and particularly to Mr. Robert E. Macherey for the difficult rolling of the samples. The work described in this article was performed under the auspices of the Atomic Energy Project.

References

1. P. W. Bakarian: *Trans.* AIME (1942) **147**, 266.
2. W. G. Burgers and F. M. Jacobs: *Metallwirtschaft*, (1935) **14**, 285.

Magnesium-lithium Base Alloys—Preparation, Fabrication, and General Characteristics

J. H. JACKSON,* P. D. FROST,* A. C. LOONAM,* L. W. EASTWOOD,* and C. H. LORIG,* Members AIME

Introduction

It is well known that for equal weights of material, thin sections of the lighter structural alloys are more resistant to buckling under a compressive stress than thin sections of more dense material. Therefore, structural parts having the same resistance to buckling stresses are generally lightest when they are made of magnesium alloys. Consequently, there is considerable interest in the development of strong alloys having densities equal to or lower than that of magnesium and strength-weight ratios equivalent to those of the strongest aluminum alloys.

The development of commercial magnesium-base alloys has been very successful, and their importance among materials in the structural field has been amply demonstrated. However, an even wider structural application of magnesium alloys might be effected if improvements could be made in the cold rollability and cold-forming characteristics. Such improvements, along with production of less directionality in properties, could be effected if the hexagonal close-packed lattice of present alloys could be replaced with a cubic lattice.

In 1942, a project, having as its objective the improvement of some of the characteristics of commercial magnesium-base alloys, was initiated at Battelle Memorial Institute under the sponsorship of the Mathieson Chemical Corporation. At that time, one of the authors,* then Chief Metallurgist for the Mathieson Chemical Corporation, postulated that the addition of lithium to magnesium in sufficient quantities to change the crystal structure of the resultant alloy from a hexagonal to a body-centered cubic lattice should produce a magnesium-rich alloy which would have the desired improvements in cold-working characteristics with less directionality in properties. To test this view, a series of alloys was made and was found to have many of the attributes that were predicted.

The view that magnesium-lithium alloys were of structural interest was also held by others. In 1943 and 1945, Dean and Anderson[1,2] obtained patents on magnesium-base alloys containing from about 1 to 10 pct lithium, from about 2 to about 10 pct manganese, and the balance substantially all magnesium; and on magnesium-base alloys containing from about 1 pct to about 10 pct lithium, from about 2 to about 10 pct manganese, from about 0.5 to 2 pct silver, and the balance substantially all magnesium. They noted that an alloy containing 83 pct magnesium, 10 pct manganese, 5 pct lithium, and 2 pct silver could be cold rolled by any of the usual methods and that this alloy was considerably harder and stronger than most other magnesium-base alloys heretofore available.

In 1945, Hume-Rothery, et al.,[3] predicted that magnesium-lithium base alloys should be soft and ductile and that such compositions, to which was added a third element for the purpose of producing a precipitation-hardening type of alloy, should be ductile, strong, and lighter than magnesium itself. Hume-Rothery investigated the binary magnesium-lithium and ternary magnesium-lithium-silver equilibrium relations and criticized the existing equilibrium diagrams. The binary magnesium-lithium equilibrium diagram has also been investigated by Grube, Von Zeppelin, and Bumm,[4] Henry and Cordiano,[5] Sal'dau and Shamrai,[6] Hofmann,[7] and Shamrai.[8] The work of most investigators agreed with that of Grube, whose constitution diagram is shown in Fig 1.

From the standpoint of development of structural alloys, the room-temperature equilibrium relations are of great interest. An examination of Fig 1 reveals that, from 0 to 5.7 pct lithium, the existing phase is alpha, which is a solution of lithium in hexagonal magnesium. The boundary between the alpha, and alpha plus beta regions, occurs at a Mg/Li of 16.5, corresponding to 5.7 pct lithium by weight. Between 5.7 pct and 10.3 pct lithium, there exists a mixture of the alpha phase (lithium dissolved in hexagonal magnesium) and the beta phase (magnesium dissolved in body-centered-cubic lithium). The boundary of the alpha plus beta and beta regions occurs at a Mg/Li of 8.7, corresponding to a lithium composition of 10.3 pct. Much of the work described here was directed toward obtaining an alloy made up of a large proportion, or entirely, of the body-centered-cubic beta structure.

In his early work, Loonam found that specimens of lithium-bearing alloys were very malleable. Ingots of alloys prepared at that time were extruded to ⅜-in. diam bars, and the mechanical properties and the effects of heat treatment were then determined. These data are given in Table 1. The outstanding ductility of the alloys, combined with their moderately high strength, evoked considerable interest.

San Francisco Meeting, February 1949.

TP 2534 E. Discussion of this paper (2 copies) may be sent to *Transactions* AIME before May 15, 1949. Manuscript received November 1, 1948; revision received November 26, 1948.

* Battelle Memorial Institute.

[1] References are at the end of the paper.

* A. C. Loonam

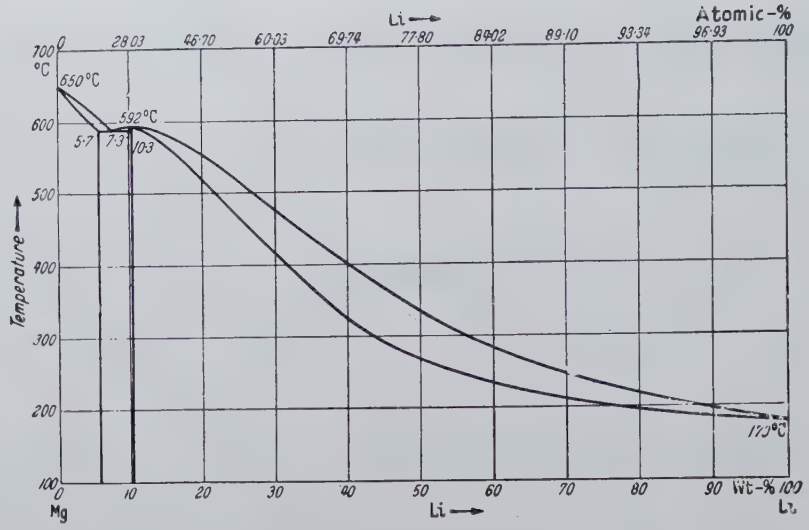

FIG 1—Magnesium-lithium equilibrium diagram (Grube).

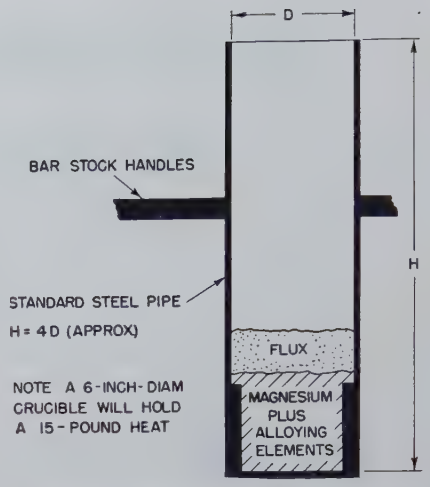

FIG 2—Melting crucible, showing relative positions of flux and metal before lithium addition.

Table 1 . . . Properties of Magnesium-lithium Alloys Prepared at Mathieson Chemical Corporation[1]

Heat No.	Mg/Li	Intended Composition, Pct					Chemical Analysis, Pct				As Extruded at 450°F[2]			Brinell Hardness		
		Mg	Li	Mn	Al	Zn	Li	Mn	Al	Zn	Tensile Strength, psi	Elongation, Pct in 1 In.	Reduction of Area, Pct	Extruded	Extruded and Air Cooled after 14 Hr at 500°F[3]	Extruded and Water Quenched after 18 Hr at 950°F[3]
2	7.6	86.9	11.5	1.6			12.1	0.74			19,000	40	42	39	36	40
4	11.3	90.4	8.0	1.6			9.2	1.24			21,200	32	43	43	42	44
5	11.2	90.0	8.0		2.0		8.5		2.05		31,600	21	27	65	55	77
6	11.0	88.0	8.0		4.0		8.3		4.15		34,400	9	11	67	57	78
7	10.7	86.0	8.0		6.0		8.4		6.20		37,100	11	13	72	61	85
8	11.4	91.0	8.0			1.0	8.8			1.12	23,900	25	50	47	44	44
9	11.2	90.0	8.0			2.0	9.6			2.27	26,000	32	42	51	46	50
10	11.0	88.0	8.0			4.0	8.8			4.03	28,000	46	58	58	57	53
12	9.0	88.2	9.8		2.0 Be		8.4		0.11 Be		20,800	29	36	43	39	40
13		98.0		2.0				1.53			45,600	2	6	48	47	36
Mg		Commercial magnesium metal									31,200	4	7	36	34	27

[1] Alloys were prepared at Mathieson and tested at Battelle.
[2] Extruded to ⅜-in.-diam rod. Reduction of 10 to 1.
[3] Protected from oxidation with argon atmosphere.

The fact that aluminum-bearing alloys, Nos. 5, 6, and 7, were hardened by water quenching from 950°F indicated that, by suitable heat treatment, higher strengths could be obtained. In order to explore completely the possibilities of magnesium-lithium alloys, an extensive project at Battelle was set up by the Mathieson Chemical Corporation. In 1945, when magnesium-lithium base alloys were found to be of military interest, the Navy Department, Bureau of Aeronautics, entered into a cooperative agreement with Mathieson for the sponsorship of further investigational work.

This paper summarizes the results obtained during the several years of investigation of the magnesium-lithium base alloys. These results are described under seven main topics covering melting technique, fabricating practice, density measurements, mechanical properties, work-hardening and stability characteristics, corrosion resistance, and metallographic structure.

Melting Techniques

Magnesium-lithium base alloys can be melted satisfactorily under a flux or under an inert atmosphere. The flux, when it is used, is comprised of lithium chloride and lithium fluoride in the proportions from 75/25 to 82/18, the choice of the composition depending to a great extent upon the alloy composition to be melted. In general, better separation of the metal from the flux is obtained when the salts are in the ratio of 75 to 25; hence, a flux of this composition is selected when a new type of alloy is melted for the first time. However, when this flux is used on certain alloys, especially those containing high percentages of cadmium, it tends to become very viscous. A change to the 82/18 composition will, in most instances, improve the fluidity, although the flux of higher lithium chloride content does not separate from the metal as well as does the flux of lower lithium chloride content.

In most of the experimental work, the quantity of flux used was equivalent to about 35 pct of the weight of the metallic charge. When "large" heats were made, that is, heats weighing 10 lb or more, it was possible to reduce the percentage of flux. The flux can be re-used, and if it becomes too thick for easy handling, the addition of unused material will increase its fluidity. To make certain, however, that the flux would be satisfactory on heats prepared for the experimental studies, fresh materials were used for each melt.

A crucible having a diameter about one-third its height is used in preparing the melts. The flux is melted first to eliminate all traces of water from the hygroscopic flux ingredients. The magnesium and alloying elements other than lithium are then added. In order to insure that the alloying elements dissolve, they are placed in a steel wire basket suspended in the molten magnesium. Before the lithium is added,

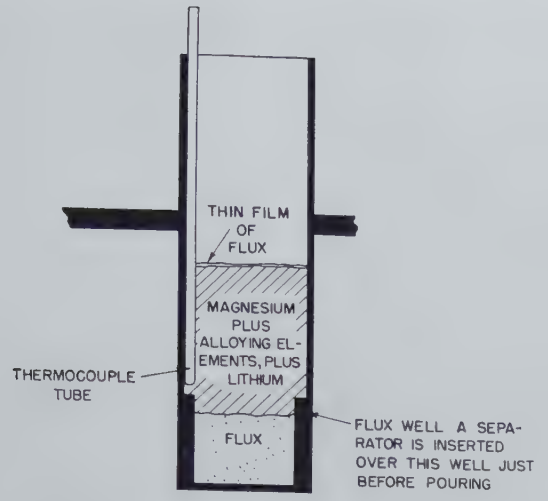

FIG 3—Melting crucible, showing relative positions of flux and metal after lithium addition.

the molten flux is lighter than the metal and provides an effective protective layer on the melt, as illustrated in Fig 2. Lithium, added by means of an inverted cup, is plunged below the surface of the metal bath. After the lithium dissolves, the cup is removed and the melt is thoroughly stirred.

The addition of lithium to the magnesium reduces the density of the alloy to a value lower than that of the flux, and the metal then floats on top of the flux, as shown in Fig 3. If the desired alloy contains elements which can be introduced into the metal more easily by the reduction of the salt of the element, such salt additions are made at this time. This addition can readily be introduced by melting the correct proportion of salt in a separate pot containing lithium chloride-lithium fluoride flux and then pouring the molten salt and flux mixture onto the metal bath. Should the element added in the form of salt not be soluble in molten magnesium alone but soluble in the magnesium-lithium melt, then the above procedure has various obvious advantages.

After all alloying additions are made, the flux is allowed to settle in the crucible. It is often desirable to make additions to the flux in order to increase its density and thus decrease the settling time. An addition of about 10 pct lithium bromide is especially effective.

It is desirable to equip the crucible with a sump in the bottom into which the flux may collect. A convenient method to avoid the mixing of metal and flux during pouring involves the insertion of a cover so that the cover rests on the sump and holds the flux in the sump while the metal is poured.

Although the flux is heavier than the metal after the lithium addition, a thin film of flux remains on the surface. The protection offered by this film, combined with the stack effect of the deep crucible, reduces the tendency toward burning or excessive oxidation of the metal. Magnesium-lithium base alloys are protected during pouring by a thin film of oxide which envelops the stream. The Durville method of pouring, or a slight modification of it, is necessary if turbulence and attendant inclusion of the oxide skin in the ingot are to be avoided. Therefore, the molds are tilted in such a way that the metal runs down the side with a minimum of turbulence. Ingot molds of either graphite or cast iron are satisfactory. When a cast iron ingot mold is used, a hot top either of graphite or of a refractory baked at high temperature is needed. The surfaces of cast iron molds are coated with acetylene soot. Before pouring, both graphite and cast iron molds are heated to about 250°F to drive off moisture. After pouring, any tendency toward burning on the surface of the ingot hot top is eliminated by the use of G-1 powder (a commercial graphite-base material) or paraffin, or by covering with an air-tight lid. By following the procedure described, the magnesium-lithium base alloys are less likely to burn during melting and pouring than are ordinary magnesium-base alloys.

Magnesium-lithium base alloys may be melted under argon in a capped crucible without the employment of a salt flux. To take full advantage of the inert atmosphere, it is desirable to place the entire charge, including the lithium, into a cold crucible. After purging the crucible with argon, the heat is melted and poured. Only a slight tendency toward burning during the pour is evident even though no salt flux is used.

A melting procedure combining the use of a flux and an argon atmosphere is also highly satisfactory, and by this technique the amount of flux required can be drastically reduced. The use of an argon atmosphere reduces oxidation and lessens the tendency for the flux to thicken.

Fabrication Practice

For the most part, the magnesium-lithium base alloys were cast into one or more of the various ingots described in Table 2. The ingots were fabricated to produce test material also described in Table 2.

The recrystallization temperature of many magnesium-lithium base alloys of the body-centered-cubic lattice type is about 375°F. The alloys can be hot worked readily by extruding, hammer forging, or hot rolling at temperatures between 400 and 700°F, depending on composition. Finishing temperatures at or just above the recrystallization temperature of 375 to 425°F were used in the experimental work in order to obtain a fine-grained product.

The reduction by hot rolling depended to some extent upon the alloy composition and, in general, was about 30 pct per pass. Hot rolling could be accomplished, however, at reductions as high as 50 pct per pass on most alloys. In order to prevent the magnesium-lithium alloy from adhering to the rolls, the latter were usually coated with kerosene for both hot and cold rolling.

The rolls during cold rolling were usually kept near room temperature. Practically all compositions could be cold rolled to total reductions of at least 15 pct immediately after hot rolling or after solution treating; in some instances, they could be cold rolled to total reductions of over 95 pct. Many of the alloys could be cold reduced as much as 50 to 75 pct per pass, although the general practice was to restrict cold-rolling reductions to 5 to 10 pct per pass.

The magnesium-lithium base alloys could be cold drawn to bar stock only with difficulty because of their tendency to seize on the die and because they

Table 2 . . . Typical Fabrication Procedures Used in Investigation of Magnesium-lithium Base Alloys

Weight of Heat	Cast Product	Machined Billets	Extruded Product	Disposition
1000 g	2½ ingots, 1⅛ in. in diam × 8 in. long.	3 pieces, 1 5/16 in. in diam × 3½ in. long. Balance of ingots saved.	3 rods, ⅜ in. in diam × 30 in. long.	4 tensile specimens, ¼-in. diam, 1-in. ga length, tested as extruded and as aged 48 hr at 150°F. 4 bend-deflection test specimens, tested as extruded and as aged 48 hr at 150°F. Balance of stock saved.
10 lb	6 ingots, 2½ in. in diam × 7 in. long.	6 pieces, 2 in. in diam × 5 in. long.	5 rods, ⅝ in. in diam × 36 in. long.[1] 2 strips, ⅞ in. × ¼ in. × 36 in.[2]	10 standard tensile specimens, 10 standard compression specimens, 10 unnotched Charpy impact and 10 notched Charpy impact specimens. These were tested as extruded, and as extruded and aged 48 hr at 150°F. Strips were corrosion test specimens; tested after aging 48 hr at 150°F.
10 lb	1 forging ingot, 4 × 4 × 12 in.			Forged to rolling slab, machined, and rolled to plate or sheet. (Total reduction effected: about 55 to 1.) Used in mechanical testing.
1500 g	2 ingots, 2½ in. in diam × 7 in. long.	2 pieces, 2 in. in diam × 5 in. long. Other ingot saved.	2 strips, 1⅛ in. × ¼ in. × 36 in.	One strip hot rolled to 0.053 in. and cold rolled 15 pct to 0.045 in. (Total reduction effected: about 55 to 1.) Used in mechanical testing. One strip hot rolled 1–30 pct pass and cold rolled 15 pct. Used in age hardening tests.

[1] Two billets were homogenized 48 hr at 600°F prior to extrusion.
[2] One billet was homogenized 48 hr at 600°F prior to extrusion.

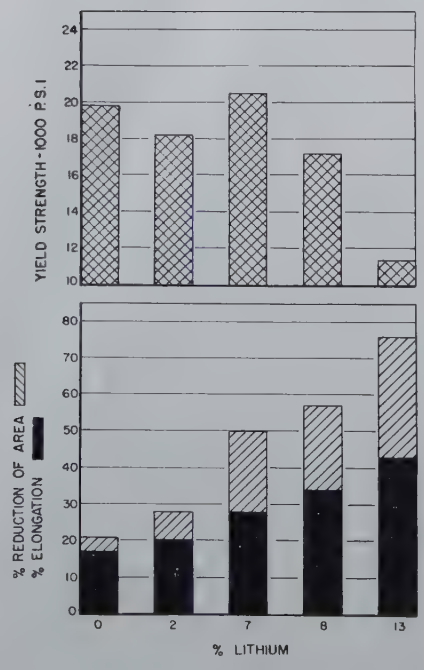

FIG 4—Effect of lithium on ductility and yield strength of extruded magnesium.

Density of Magnesium-lithium Alloys

One characteristic of great interest is the low density of the magnesium-lithium base alloys. A binary alloy containing 11.5 pct lithium has a density of approximately 1.4 g per cc; however, this binary alloy is so soft and ductile that it has little value from the structural standpoint, except where low strength is permissible and good formability is desired. If sufficient alloying additions of the heavier metals are made to this alloy to improve its strength, the density is often increased to about 1.45 to 1.65 g per cc. It is not difficult to formulate a magnesium-lithium alloy having mechanical properties superior to the commercial magnesium-base alloys and having a density considerably less than 1.8 g per cc, which is approximately the density of most commercial magnesium alloys.

Some Mechanical Properties of the Magnesium-lithium Alloys

MAGNESIUM-LITHIUM BINARY ALLOYS

Magnesium-lithium binary alloys have hardnesses of the order of 0 to 10 on the Rockwell E scale, which is equivalent to a Brinell hardness number of about 30 to 35. Magnesium-lithium base alloys having good mechanical properties have hardnesses of the order of 90 Rockwell E, which is equivalent to a Brinell hardness number of about 85.

One of the most important properties which lithium was found to bestow upon magnesium was increased ductility. Although the body-centered-cubic lattice structure does not exist below 5.3 pct lithium, as little as 2 pct lithium markedly enhanced the tensile ductility and formability of pure magnesium. The effect of lithium on tensile ductility is shown in Fig 4. It will be noted that a pronounced increase in reduction of area, accompanied by a marked decrease in yield strength, occurred as lithium was increased from 8 to 13 pct. This is explained by the transition, at 10.3 pct lithium, from the two-phase, hexagonal plus body-centered-cubic structure, to the single-phase, body-centered-cubic structure. Although the single-phase hexagonal and the two-phase alloys were by no means neglected in the experimental work, the greatest attention was paid to alloys with a body-centered-cubic structure.

The influence of lithium on the bend ductility of pure magnesium is shown in Fig 5. The increase in bend ductility of rolled alloys in going from the two-phase region to the region of 100 pct beta was very noticeable. For example, the 9 pct lithium, alpha- plus beta-

work harden only to a limited extent. The latter makes it difficult to strengthen the tip to resist fracture as the bar is started through the die. Various lubricants for cold-drawing operations were tried in an attempt to prevent die seizure. The only lubricating practice that has been successful involved the use of a flash coat of copper applied by dipping the magnesium-lithium bar in a solution of copper sulphate made slightly alkaline by the addition of ammonium hydroxide.

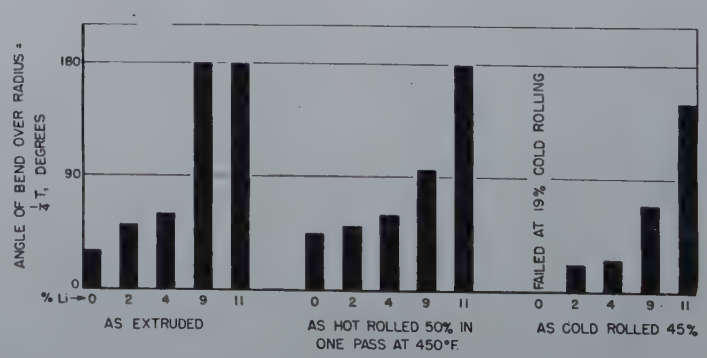

FIG 5—Effect of lithium on bend ductility of magnesium.

phase alloy could not be bent more than 90° while the 11 pct lithium, beta-phase alloy withstood a 180° bend. On the other hand, in the extruded condition, the 9 pct lithium, two-phase alloy, had bend ductility which was equal to that of the 11 pct lithium, beta-phase alloy. The superior bend ductility of the alpha- plus beta-phase alloy in the extruded state can be explained by the mode of occurrence of the alpha phase in the microstructure. The microstructure of the alloy in the extruded and hot-rolled states is shown in Fig 6. The alpha phase occurs in the form of more or less randomly oriented, short patches in the extruded material, whereas in the rolled material it occurs as long platelets, with the plane of the platelets parallel to the plane of the sheet. When the materials are bent, the long, brittle alpha platelets in the sheet are more prone to break and notch the beta material than are the short, brittle alpha patches in the extruded material.

The effect of lithium on the cold rollability of magnesium can be observed from data plotted in Fig 5. Whereas commercially pure magnesium failed in rolling after a cold reduction of 19 pct, the lithium-bearing alloys could be cold rolled at least 45 pct. In the cold-rolled state, the lithium-bearing alloys retained nearly the same bend ductility they possessed in the hot-rolled state.

FIG 6—Microstructure of extruded and hot-rolled two-phased Mg-Li alloy. Light areas are alpha and gray matrix is beta. (Etched in 2 pct HF.)
a. Hot-rolled longitudinal section. *b*. Hot-rolled transverse section. *c*. Extruded longitudinal section. *d*. Extruded transverse section. Reduced approximately one-third in reproduction.

MAGNESIUM-LITHIUM-BASE TERNARY ALLOYS

Among the original alloys prepared at the Mathieson Chemical Corporation were several which contained aluminum or zinc. The mechanical properties of the alloys with aluminum or zinc gave ample indication that these elements would be of importance in increasing the strength of the ductile magnesium-lithium base. In later work, effects of practically all of the metallic elements on the properties of the magnesium-lithium alloys were investigated by preparing and studying over 1800 individual heats.

The order of solid solubility of the elements in the beta phase at room or slightly elevated temperatures, as determined from the many experimental investigations, is roughly as follows:

Most Soluble Elements		
Ag	Cd	Al
	Hg	In
	Zn	Tl

Slightly Soluble Elements				
Ni	Cu	Ca	Si	Sb
Co		Sr	Ge	Bi
		Ba	Sn	
		Ce	Pb	

Relatively Insoluble Elements					
	Be	Cr	Ti	V	Mn
K	B	Mo	Zr	Cb	
		W	Th		
		U	Fe		

The elements which most effectively increased the mechanical strength of the magnesium-lithium base were aluminum, zinc, silver, and cadmium. An example of their effectiveness is shown in Fig 7. In this figure are plotted the maximum and minimum yield strengths obtained from a series of about 50 different ternary alloys of 8.1 Mg/Li base. At the extreme left, the yield strength of the 100 pct beta, 8.1 Mg/Li binary alloy is shown to be 12,000 psi. Antimony added in amounts of 1 to 4 pct and bismuth in amounts of 2 to 4 pct did not increase the yield strength. However, the recovery of these two elements in magnesium-lithium base alloys has consistently been very low. Copper increased the yield strength somewhat, but 1 pct copper was, for all practical purposes, equally as effective as 8 pct.

Substantial increases in yield strength were brought about by additions of silver, zinc, cadmium, and aluminum. In this series of alloys, 0.5 pct aluminum was as effective as 4 pct zinc, and was much more effective than either 2 pct cadmium or 4 pct silver. The elements which were most effective in alloys with a magnesium-lithium ratio of 8.1 were likewise very effective at other magnesium-lithium ratios.

Some interesting effects of aluminum and zinc on the properties of ternary alloys having various magnesium-lithium ratios are shown in Fig 8 and 9. The alloys with a magnesium-lithium ratio of 24 (24 Mg/Li) are of the hexagonal alpha phase, those with magnesium-lithium ratios of 13.3 and 9.7 consist of alpha plus beta, and those with a magnesium-lithium ratio of 8.1 consist of the body-centered-cubic

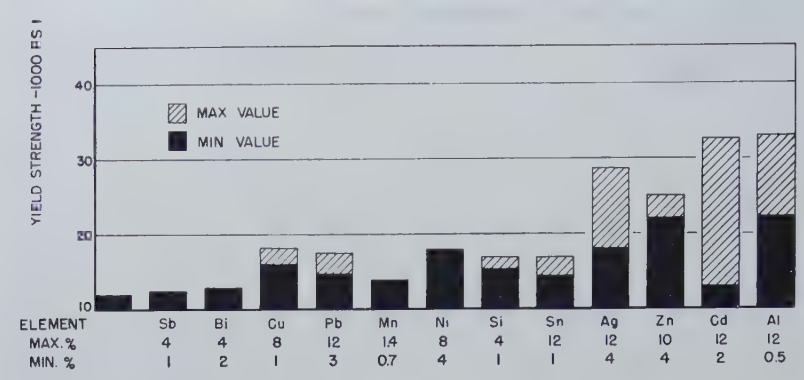

FIG 7—Effect of various elements on the yield strength of the 8.1 Mg/Li beta solid solution. All alloys tested in the as-extruded condition.

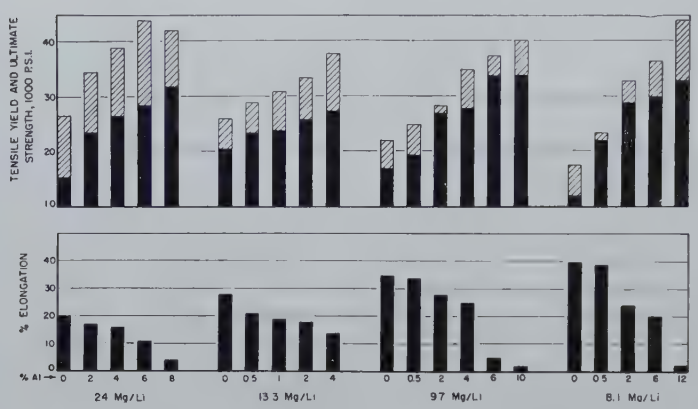

FIG 8—Effect of aluminum at different magnesium-lithium ratios on mechanical properties of extruded ternary alloys.

beta phase. The results plotted in these figures show that (1) several alloys possess rather good properties, a fact which offered an incentive for further investigation; (2) the elongation tends to increase as Mg/Li decreases; and (3) as Mg/Li decreases, there is an increase in the ratio of yield strength to tensile strength. In general, the yield strengths of the high-strength, magnesium-lithium alloys are proportionally high and are the same in tension and compression.

MAGNESIUM-LITHIUM BASE QUATERNARY AND QUINARY LOW-LITHIUM ALLOYS

The favorable properties observed for some of the ternary alloys proved an incentive to investigate quaternary and quinary alloys. The tensile properties of a 24 Mg/Li series of alloys having the hexagonal structure are shown in Fig 10. The average tensile strength of this series of alloys was about 45,000 psi.

MAGNESIUM-LITHIUM BASE QUATERNARY AND QUINARY HIGH-LITHIUM ALLOYS

The above data suggested the possibility of developing interesting alloys having the hexagonal structure or the two-phase, hexagonal plus body-centered-cubic structure. Of even greater interest have been the beta-phase, cubic lattice alloys, that is, alloys having magnesium-lithium ratios under 8.7. Alloys with magnesium-lithium ratios of 8.1, 7, 6, and 5 have been investigated in detail. A minor amount of work has also been done on 3.5 Mg/Li alloys.

In one series of 12 heats, the effects of variations in aluminum, cadmium, and silver in quinary alloys having a magnesium-lithium ratio of 6, with aluminum varying from 2 to 12 pct, silver varying from 0 to 4 pct, and cadmium varying from 0 to 4 pct were determined. The compositional levels were selected and the experiment performed as a factorial design. By means of this experimental technique, the individual effect of each of the three alloying additions, cadmium, silver, and aluminum, could be determined independent of the effects of the other two additions. The mechanical properties of the alloys are shown in Fig 11. In the as-extruded state, the tensile strength was improved by additions of the alloying elements. Increases in aluminum and cadmium contents caused decreases in mechanical properties in specimens aged at 150°F for 48 hr. The effect of an increase in silver from 0 to 4 pct stabilized the mechanical properties for the same aging treatment. This stabilizing effect of silver on mechanical properties was noteworthy throughout the work on magnesium-lithium base alloys.

The independent effects of variations in magnesium-lithium ratio, zinc, cadmium, and silver, were studied in 36 quinary magnesium-lithium-zinc-cadmium-silver alloys by means of the factorial design technique. In Fig 12

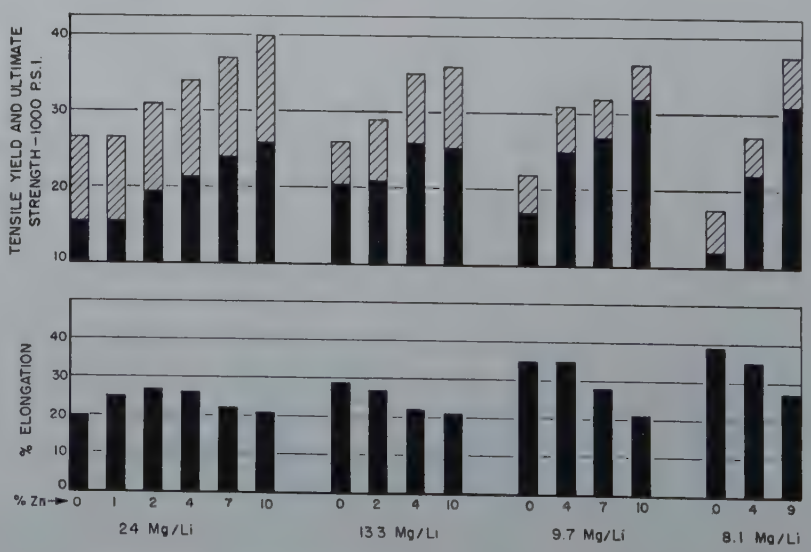

FIG 9—Effect of zinc at different magnesium-lithium ratios on mechanical properties of extruded ternary alloys.

the average yield strengths of the alloys in the as-extruded state and after aging at 150°F for 48 hr are plotted as functions of the composition.

The yield strength of the alloys increased in the as-extruded condition as Mg/Li increased. Aging increased the yield strength of 6 Mg/Li alloys but decreased the yield strength of alloys of higher magnesium-lithium ratio.

Cadmium was similar in its effect in this series of alloys as in the previous series. It increased the yield strength of the alloys in the extruded condition but did not prevent the loss of yield strength upon aging at 150°F. The effects of zinc additions were similar to those produced by cadmium. An increase in silver from 4 to 6 pct had a stabilizing influence as shown by the fact that there was no decrease in yield strength after aging for 48 hr at 150°F.

The effects of aluminum in two series of 6 Mg/Li-aluminum-cadmium-silver alloys are shown in Fig 13. Excellent mechanical properties were obtained with 1 and 2 pct of aluminum in the alloys containing 4 pct silver. The alloys with 4 pct silver were less adversely affected by the 150°F aging treatment than were the alloys with 2 pct silver. As a point of interest, the alloys with 2 pct aluminum were less stable than were the alloys with 0.5 and 1 pct aluminum.

From the results obtained on 36 magnesium-lithium-zinc-cadmium-silver alloys prepared according to a factorial design, it was possible to select a number of alloys whose tensile and yield strengths were increased by aging for 48 hr at 150°F. Their mechanical properties after the aging treatment are shown in Table 3. These results are indicative of the excellent mechanical properties which can be obtained in the magnesium-lithium base alloy system. It is noteworthy that these alloys, like all high-lithium, magnesium-lithium base alloys, have equal compressive and tensile yield strengths and have high elastic limits in both tension and compression. Their notched impact strength, on the other hand, is rather low. The 8.1 Mg/Li alloy is included in this table for comparison purposes. The high-strength alloys of the 8.1 Mg/Li type show a considerably greater loss in strength during the

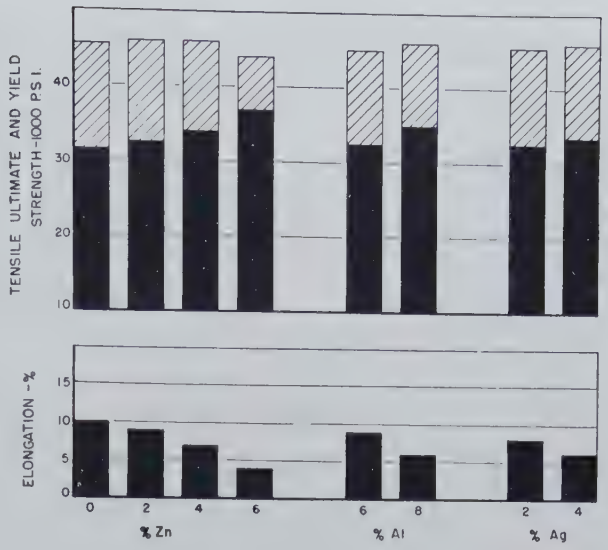

FIG 10—Effect of variations in zinc, aluminum, or silver contents on the tensile properties of extruded 24 Mg/Li-Zn-Al-Ag alloys.

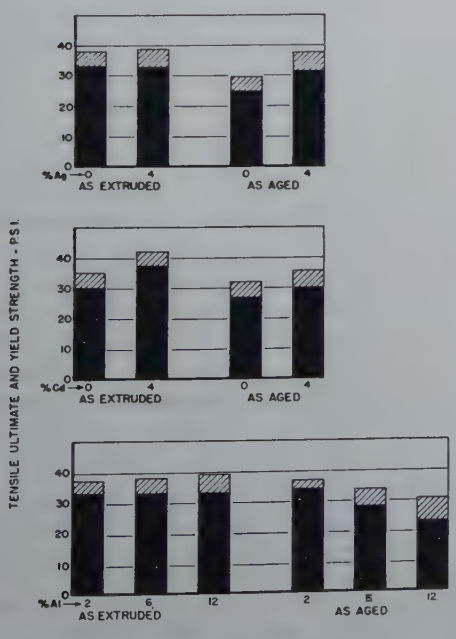

FIG 11—Effect of variation in aluminum, cadmium, or silver contents on the tensile properties of 6 Mg/Li-Al-Cd-Ag alloys as extruded and as aged at 150°F for 48 hours.

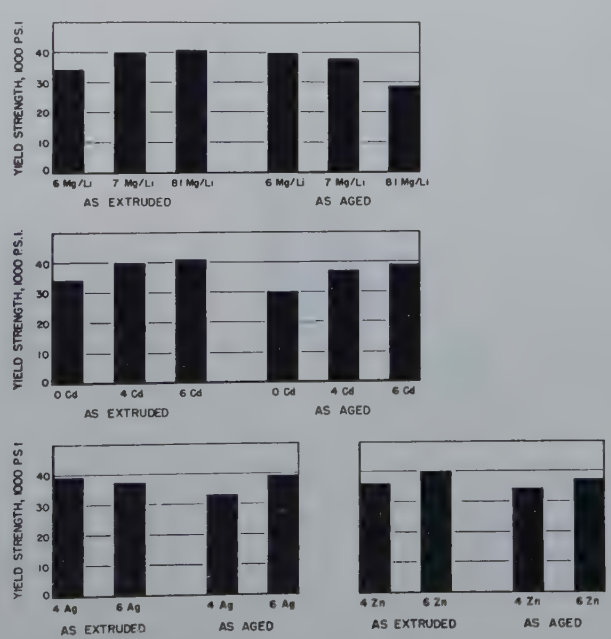

FIG 12—Effect of variation in Mg/Li, Zn, Cd, and Ag on the yield strength of 36 Mg-Li-Zn-Cd-Ag alloys, as extruded and as aged at 150°F for 48 hours.

Table 3 . . . Mechanical Properties of Ten-pound Heats of Selected Mg-Li-Zn-Cd-Ag Alloys after Aging at 150°F for 48 Hr

Heat No.	Intended Composition, Pct						Pre-extrusion Heat Treatment	Tensile Properties[1]						Compressive Properties[1]			
	Mg/Li	Mg	Li	Zn	Cd	Ag		Elastic Limit, psi	Yield Strength, psi	Ultimate Strength, psi	Elongation, Pct in 1 In.	Reduction of Area, Pct	Hardness, Rockwell E	Elastic Limit, psi	Yield Strength, psi	Charpy Impact Strength, Foot-pounds	
																Notched	Unnotched
1091	6	75.4	12.6	6	0	6	None	31,300	41,300	46,700	2	4.4	94.5	36,900	47,100	0.5	2.5
							600°F-16 hr	30,300	43,200	48,900	3	3.7	96	39,900	49,600	0	2
1095	6	73.7	12.3	6	4	4	None	34,200	48,500	53,100	1	1.9	96.5	47,700	54,900	0.5	2
							600°F-16 hr				0[2]	0	98.5	47,800	55,300	0.5	2
1075	6	72.0	12.0	6	4	6	None	33,200	49,100	53,200	1	1.1	98.5	42,800	55,200	0.5	1
							600°F-16 hr	40,400	50,300	48,000	0	0.4	88	45,100	53,200	0.5	1
1076	6	72.0	12.0	4	6	6	None	45,800	52,200	53,400	1	2.0	84.5	46,800	54,200	0.5	1
							600°F-16 hr	41,800	51,500	55,200	1	1.3	85	45,500	53,700	0.5	1
1092	7	76.1	10.9	4	4	5	None	32,200	39,200	43,200	20	30.1	93	36,300	44,000	1	5
							600°F-16 hr	31,000	38,400	43,100	20	35.2	92.5	35,400	43,700	1	5.5
1090	7	75.3	10.7	4	4	6	None	32,700	41,500	46,400	15	26.1	95.5	42,800	49,400	0.5	3
							600°F-16 hr	30,000	40,200	45,700	15	23.3	95	37,100	47,500	0.5	3.5
1077	7	75.3	10.7	4	6	4	None	31,100	39,200	43,300	19	34.5	88.5	36,300	43,900	1	4.5
							600°F-16 hr	31,500	40,800	44,400	14	19.7	88	36,000	44,200	0.5	4.5
1078	7	73.5	10.5	4	6	6	None	37,500	45,200	48,400	10	13.9	90.5	42,900	54,800	0.5	3.5
							600°F-16 hr	32,200	46,000	51,500	8	10.5	90.5	41,400	52,300	0.5	2.5
1093	7	72.6	10.4	5	6	6	None	31,000	41,900	49,300	9	13.5	97	37,500	50,800	0.5	3
							600°F-16 hr	30,800	40,500	49,100	6	7.4	97	38,300	48,300	0.5	3
1094	7	76.1	10.9	3	7	3	None	32,600	39,200	41,600	17	27.5	91	37,300	43,200	1	7
							600°F-16 hr	31,600	38,500	41,600	22	38.6	90	37,400	42,900	2	6.5
1079	8.1	73.0	9.0	6	6	6	None	19,700	25,600	35,000	41	60.9	87.5	25,200	30,300	1	4
							600°F-16 hr	23,400	28,600	38,000	29	46.4	89.5	25,200	30,900	2.5	4

[1] Alloys were extruded from 2-inch-diameter cast billets. Properties are based on average of two specimens.
[2] Bar too brittle to obtain yield point.

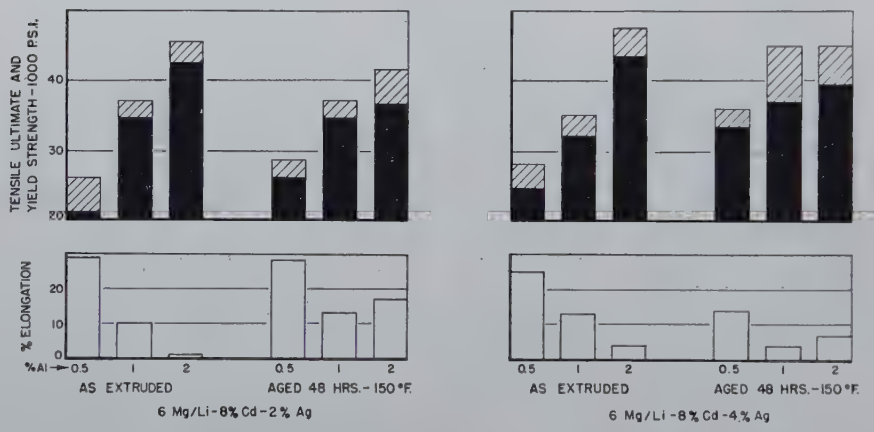

FIG 13—Effect of aluminum at two different silver levels on mechanical properties of a 6 Mg/Li-8 pct Cd base quinary alloy.

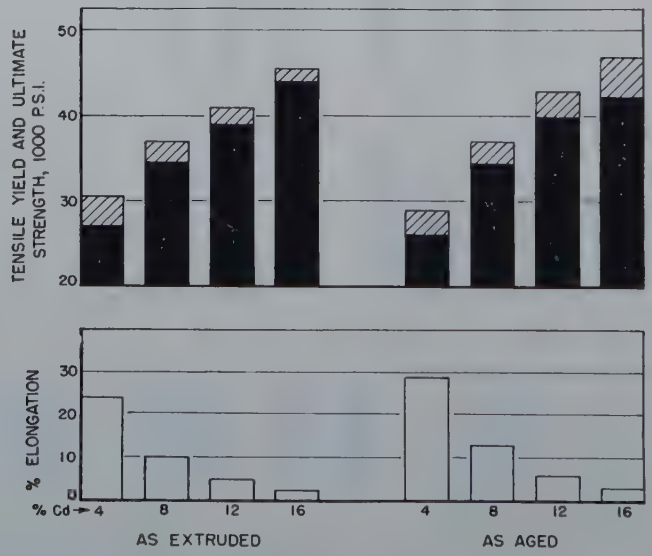

FIG 14—Effect of cadmium on mechanical properties of a 6 Mg/Li-1 pct Al-2 pct Ag alloy. (Aging treatment: 48 hr at 150°F.)

150°F aging treatment than do the alloys, listed in the table, of lower magnesium-lithium ratio.

The high-lithium, magnesium-lithium alloys were capable of dissolving cadmium in much larger amounts than the 6 pct generally added heretofore. Large amounts of cadmium, when substituted for the zinc or aluminum, not only produced high strength but enabled the alloys to retain this strength after aging at 150°F. As shown in Fig 14 and 15, the addition of 12 pct cadmium resulted in high strength which was not reduced by aging 48 hr at 150°F. However, alloys with 16 pct cadmium overaged and lost strength during the 48-hr treatment.

Continued investigation of high-cadmium-bearing alloys showed that, in the absence of zinc and aluminum, 16 pct cadmium could be added without causing overaging during the 48 hr at 150°F treatment. An alloy having the composition, 6 Mg/Li-16 pct cadmium-6 pct silver, was found to retain its high strength for over 1000 hr at 150°F. The mechanical properties of the alloy, after extruding and aging at 150°F for 48 hr, were as follows:

Tensile ultimate strength—48,000 psi
Tensile yield strength —47,000 psi
Elongation in 2 in. —2 pct

Although the ductility of this alloy was low, a slight modification of the composition to 15 pct cadmium and 5 pct silver increased the ductility considerably without seriously affecting the strength or the ability of the alloy

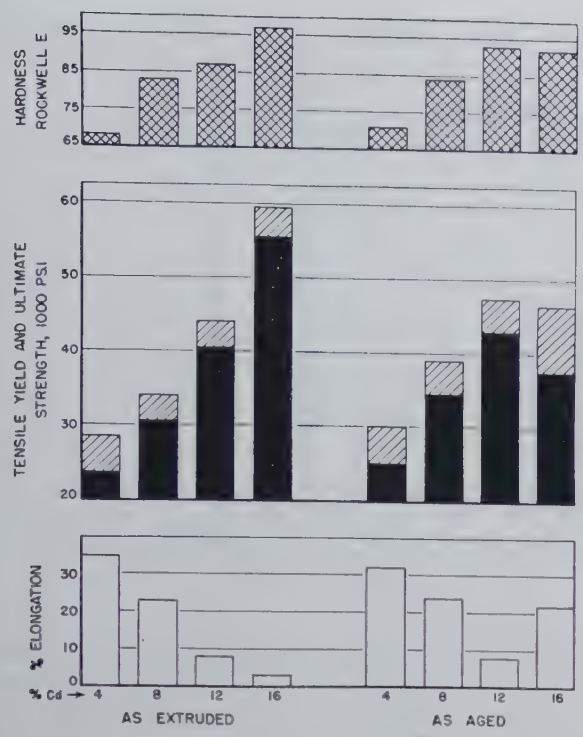

FIG 15—Effect of cadmium on mechanical properties of a 7 Mg/Li-2 pct Zn-4 pct Ag alloy. (Aging treatment: 48 hr at 150°F).

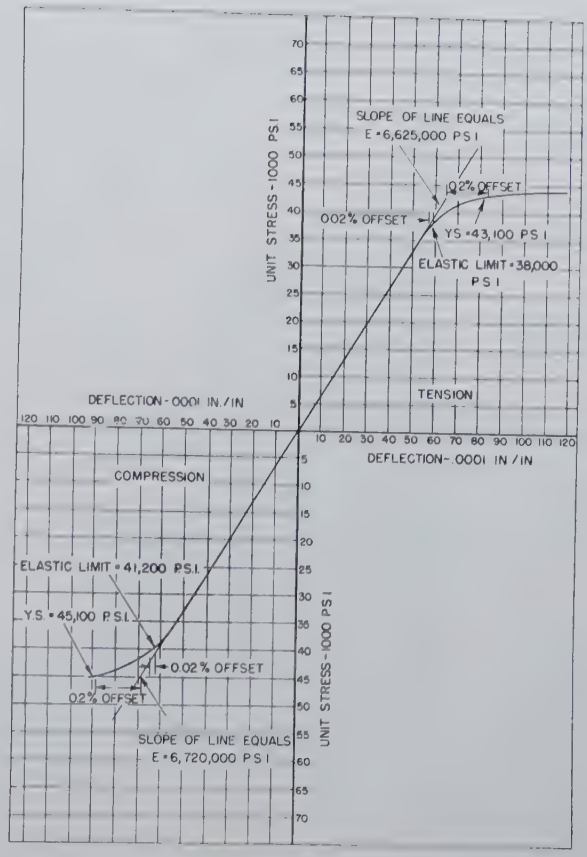

FIG 16—Tension-compression stress-strain curves for the alloy 6 Mg/Li-15 pct Cd-5 pct Ag.

to retain its strength after a prolonged treatment at 150°F.

An extensive study of the fabricating characteristics and strength properties of the 6 Mg/Li-15 pct cadmium-5 pct silver alloy was also conducted. The alloy was easily forged and rolled at 400°F, and after a solution treatment, it could be cold rolled extensively. Its mechanical properties after extruding and aging at 150°F for 24 hr were as follows:

Tensile ultimate strength	—46,000 psi
Tensile yield strength	—43,000 psi
Elongation in 2 in.	—8 pct
Reduction of area	—8 pct
Hardness, Rockwell E	—92

A stress-strain curve for the 6 Mg/Li-15 pct cadmium-5 pct silver alloy is shown in Fig 16. It is typical for the high-strength, magnesium-lithium base alloys and is characterized by a high elastic limit and a high compressive yield strength. Fig 17 and 18 show respective stress-strain curves for a commercial magnesium alloy and a commercial aluminum alloy. It will be noted that the curve for the magnesium-lithium alloy bears a greater resemblance to the curve for the aluminum alloy than it does to the curve for the magnesium alloy.

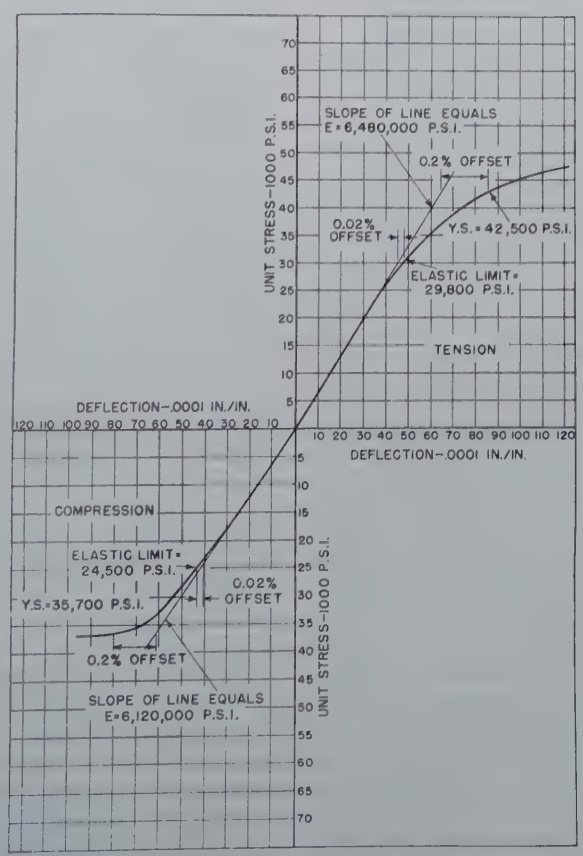

FIG 17—Tension-compression stress-strain curves for commercial magnesium alloy AZ31X.

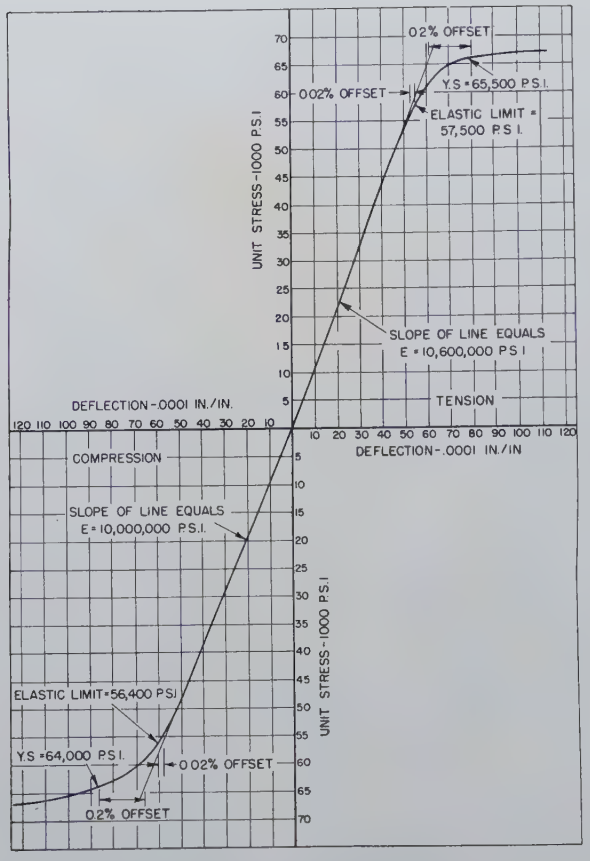

FIG 18—Tension-compression stress-strain curves for commercial aluminum alloy 14S-T.

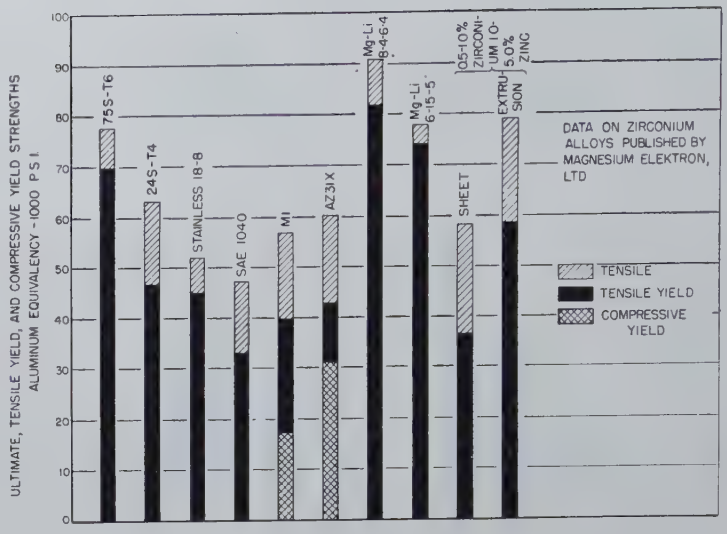

FIG 19—Comparison of strength properties of Mg-Li base alloys with those of other alloys.

COMPARISON OF STRUCTURAL CHARACTERISTICS OF MAGNESIUM-LITHIUM BASE ALLOYS WITH OTHER ENGINEERING MATERIALS

The magnesium-lithium base alloys by virtue of their low densities, 1.65 g per cc or less, have considerable advantage when compared to other structural materials on a strength-weight basis.

The strongest available commercial aluminum alloy has a yield strength of the order of 72,000 psi and a density of about 2.8 g per cc. For equivalent strength on a pound-for-pound basis, a magnesium-lithium base alloy, having a density of 1.55 g per cc, should have a yield strength, in compression and tension, of the order of 40,000 psi, while one having a density of 1.65 g per cc should possess a yield strength of about 42,500 psi. As shown in the preceding text, these yield strength values are exceeded in many magnesium-lithium base compositions.

The strength properties of two magnesium-lithium base alloys are compared with other commonly used structural alloys in Fig 19. The strength values representative of the various materials are those obtained on an equal weight basis, using the strength-weight relationship for the aluminum alloys as the basis of comparison. The alloy designated as Mg-Li 8-4-6-4 has the composition 8.1 Mg/Li-4 pct zinc-6 pct cadmium-4 pct silver. This alloy has a yield strength of 48,000 psi and an elongation of 10 pct as extruded; however, after 48 hr at 150°F, it has a yield strength of 28,500 psi and an elongation of 43 pct. The alloy designated as Mg-Li 6-15-5 has a composition of 6 Mg/Li-15 pct cadmium-5 pct silver. It has a yield strength of 43,000 psi and an elongation of about 8 pct as extruded, and these values are retained after an extended period at 150°F.

The resistance of structural materials to buckling under a compressive load is of considerable importance to designers of aircraft and other structures. F. R. Shanley[9] has suggested that a measure of the buckling resistance of wide sheet or sheet fixed on the four edges and subjected to compressive loading can be obtained from the relationship E/d^3 where E is the modulus of elasticity of the material and d is its density. The relative resistance to buckling of various materials, as determined by this relationship, is shown in Fig 20. The low density and fairly high modulus of elasticity (about 6,500,000 psi) of the magnesium-lithium base alloys make these alloys far superior, in this respect, to other structural materials.

Work-hardening Capacity and Stability of Magnesium-lithium Base Alloys

WORK-HARDENING CAPACITY

Early in the study of magnesium-lithium base alloys, it was found that most of the alloys being investigated were incapable of appreciable work hardening. There were a number of indications of the lack of work-hardening capacity, a few of which are enumerated as follows:

1. At rates of tensile loading comparable to those used for testing other materials, such as copper-base, iron-base, aluminum-base, or ordinary magnesium-base alloys, the yield strength of high-lithium, magnesium-lithium base alloys was found to be fictitiously high. The effect of the rate of loading on the yield strength of a few of the early magnesium-lithium base alloys is shown in Table 4. The first three alloys listed therein extended at a rapid rate under a tensile load near their apparent yield strength. The yield strength of the fourth alloy, which was low in lithium content, was not affected by the change in rate of loading.

2. The apparent yield strength of high-lithium, magnesium-lithium base alloys was not appreciably increased by cold stretching. The effect of a prior stretch of 5 and 10 pct on yield strength of four tensile bars is shown in Table 5.

Table 4 . . . Effect of Rate of Loading on the Tensile Yield Strength of a Series of Early Magnesium-lithium Base Alloys

Mg/Li	Composition, Pct				Yield Strength, psi	
	Mg	Li	Zn	Al	Loaded, 0.02 ipm	Loaded, 0.00004 ipm
9.7	87	9	4		25,200	21,500
9.7	87.9	9.1	2	1	25,600	23,900
8.1	87.2	10.8		2	24,200	21,500
24	94.1	3.9		2	23,000	23,000

Table 5 . . . Effect of Cold Stretching on the Tensile Yield Strength of a Series of Early Magnesium-lithium Base Alloys

Mg/Li	Composition, Pct				Yield Strength, psi		
	Mg	Li	Zn	Al	0 Pct Cold Stretch	5 Pct Cold Stretch	10 Pct Cold Stretch
9.7	87	9	4		25,200	25,600	
9.7	87.9	9.1	2	1	25,600	26,500	26,800
8.1	87.2	10.8		2	24,200	26,500	
24	94.1	3.9		2	23,000	34,100	

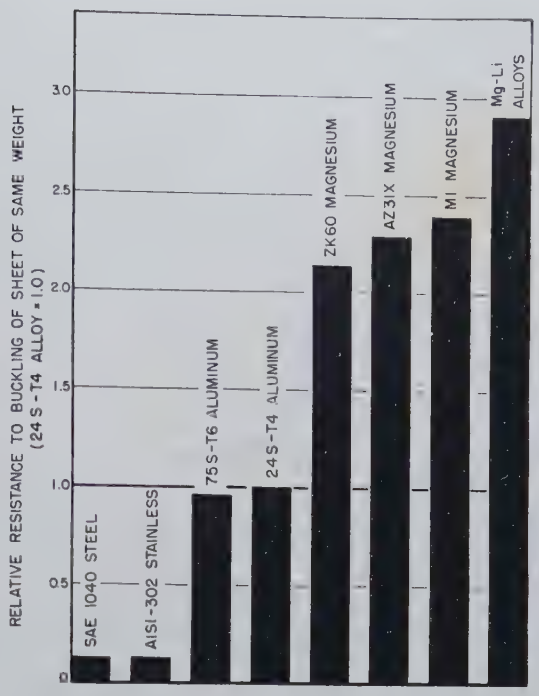

FIG 20—Relative resistance to buckling of various structural alloys compared to that of 24S-T4 aluminum alloy.

In only the low-lithium alloy was a considerable increase effected in the apparent yield strength by a 5 pct prior stretch.

3. The apparent yield strength of 26,300 psi for an extruded alloy of 87 pct magnesium-9 pct lithium-4 pct zinc was not increased by cold-drawing reductions as high as 55.5 pct.

4. The apparent yield strength of 22,500 psi for a hot-rolled alloy of 87 pct magnesium-9 pct lithium-4 pct zinc could be increased only to 24,000 psi by a 75 pct cold-rolling reduction.

Thus the inability of the first magnesium-lithium base alloys investigated to work harden satisfactorily became readily apparent. The seriousness of this was more fully appreciated when a close relationship was found between the work-hardening characteristics and the stability of the mechanical properties at moderately elevated temperatures. In order to evaluate quickly a large number of compositions and to determine the effect of various addition elements on the work-hardening characteristics of the magnesium-lithium base, a modified test to determine work-hardening capacity was devised. A schematic drawing of the testing equipment is shown in Fig 21.

In this test, the specimens are supported on rails spaced 3 in. apart and loaded in the midpoint as a simple beam. The deflections of the bars are measured at the time of loading and then at intervals over a period of a week. The bend-deflection values are plotted against the time elapsed after loading to obtain bend deflection-time curves. Such curves for alloys having good, fair, and poor work-hardening characteristics are shown in Fig 22. The total bend deflection within the 144-hr period of the test and the rate of deflection during the 120- to 144-hr period were used as a measure of the relative merit of the alloys. It will be noted from Fig 22 that deflection readings were taken for 168 hr, in order to obtain an accurate curve in the 120- to 144-hr interval.

Because the bend-deflection test procedure was used primarily to determine alloy additions which would improve work-hardening capacity, the bend tests were made, for the most part, on bars loaded in such a way that the extreme fiber stress exceeded the yield point of the material. The bend-deflection test was of little value for studying age-hardening alloys, because this type of alloy showed marked variations in behavior during the course of the test as a result of aging at room temperature.

Whereas the bend-deflection rate, as measured during the interval between 120 and 144 hr, is of interest and of value in assessing the work-hardening

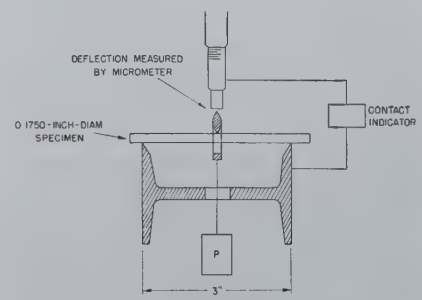

FIG 21—Bend-deflection test apparatus for determining work hardenability.

characteristics of each composition, comparisons between various alloy compositions can be made most easily by examining the total bend deflection during the 0- to 144-hr interval. Results shown in Fig 23 reveal that the ability of a material to withstand bending loads which produce an extreme fiber stress greater than the yield strength apparently depends upon the work-hardening capacity of the material and not upon the yield strength. For example, pure magnesium, with a yield strength nearly twice that of pure aluminum, deflected nearly twice as much as aluminum in 144 hr when tested at an extreme fiber stress of 21,000 psi. It is apparent, from an examination of the 9 bars at the left of the diagram, that the first lithium additions tend to increase the yield strength and to reduce the total bend

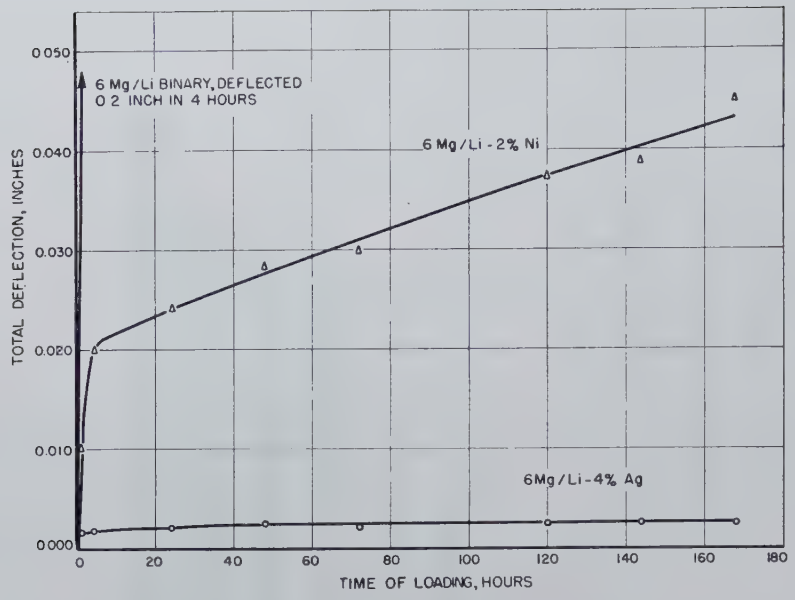

FIG 22—Typical bend-deflection rate curves.

deflection markedly. Larger additions of lithium decreased the yield strength moderately, producing some increase in total bend deflection. This trend continued until a Mg/Li of 8 was reached. At this ratio, and continuing through 6 Mg/Li, the total deflection was high. Thus, with only a slight decrease in yield strength at these high lithium contents, a deflection of 0.2 in. was obtained in 24 hr.

The additions of 4 pct and 9 pct zinc to an alloy of 8 Mg/Li base increased the yield strength to 22,000 and 31,000 psi, respectively, and reduced the total bend deflection to 0.025 in. and 0.010 in., respectively. A 0.5 pct addition of aluminum to the 8 Mg/Li base was equally as effective as a 4 pct zinc addition in raising the yield strength of the material, but was far more effective in reducing the total bend deflection. A 6 pct aluminum addition was responsible for a still more pronounced increase in yield strength. On the other hand, 6 pct aluminum was inferior to 0.5 pct aluminum in reducing the total bend deflection. It is important to note that the zinc- and aluminum-bearing alloys were of the age-hardenable type, and for this reason, strict comparisons of the work-hardening capacities of such alloys, as measured by the bend-deflection test, were not possible.

The most outstanding effect of alloy additions was observed when 4 pct silver was added to an 8 Mg/Li or 6 Mg/Li alloy. The effect of silver is shown in Fig 23.

The mechanism by which an addition such as 4 pct silver or 0.5 pct aluminum improves the work-hardening capacity of the magnesium-lithium alloy matrix is not entirely clear. It appears, however, that most additions having some solid solubility in the magnesium-lithium base at room temperature will effect some improvement in the work-hardening capacity.

In Table 6 are reported the total bend-deflection values for specimens of the four alloys previously noted in Tables 4 and 5. The total bend-deflection values of the first three alloys shown were high even though an extreme fiber stress of 21,000 psi was appreciably below the apparent yield strength of the alloys. An interesting observation made from results in Table 6 was that the second alloy, which showed some superiority in work-

Table 6 . . . Total Bend Deflection 144 Hr after Loading a Series of Early Magnesium-lithium Base Alloys

Mg/Li	Composition, Pct				Apparent Yield Strength, psi	Total Bend Deflection,[1] Inch
	Mg	Li	Zn	Al		
9.7	87	9	4		25,200	0.0085
9.7	87.9	9.1	2	1	25,600	0.0069
8.1	87.2	10.8		2	24,200	0.0092
24	94.1	3.9		2	23,000	0.0011

[1] Measured 144 hr after loading to an extreme fiber stress of 21,000 psi.

hardening capacity in Tables 4 and 5, also showed a slight superiority to the first and third alloys in resistance to bending. The bend-deflection value for the low-lithium alloy was markedly lower than the values for the three high-lithium alloys.

The bend-deflection test had certain advantages over the other possible methods for determining work-hardening capacity. It could be used to examine a large number of alloys at one time; specimen preparation was a simple matter; and perhaps of greatest importance, temperature was not a variable in the course of the test because it was readily conducted in a room kept at a constant temperature of 85°F.

The increase in hardness obtained by cold rolling a strip of the alloy to a reduction of 15 pct was also used as a measure of the effect of alloy additions on the work-hardening capacity of magnesium-lithium base compositions. It yielded some useful information and generally confirmed the results of the

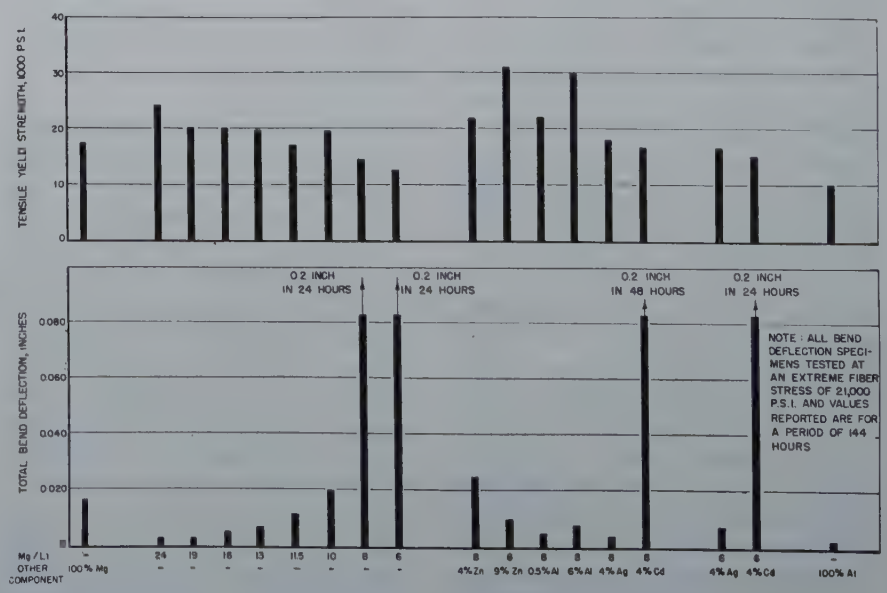

FIG 23—Total bend deflection vs. tensile yield strength for various alloys.

bend-deflection test, but was not so sensitive as the bend-deflection method for revealing the effects of alloying elements. A work-hardening test based on hardness measurements has the objection that the hardness measurement itself depends to some extent on the work-hardening capacity of the material being tested. To determine the stability of work-hardened alloys, the cold-rolled specimens were held at temperatures of 150 and 225°F and their hardness measured at periodic intervals.

The bend-deflection test was also supplemented by the use of a tensile-creep test for the latter is a more sensitive method of determining plastic flow in the region of the yield strength than is the bend creep test. The alloy additions which improved work-hardening capacity, as measured by the bend-deflection test, also improved the tensile-creep characteristics of the alloy.

STABILITY

The properties of high-strength magnesium-lithium base alloys are stable at room temperature. However at 150°F the alloys average slowly, with the magnesium strength being maintained not longer than 1000 hr. The stability is lower at higher temperatures. One of the more important objectives of the present investigation was the improvement of stability of the alloys at 150°F and higher temperatures.

It was found early in the experimental work that alloy additions which improved the bend-deflection characteristics of an alloy also improved the stability of that alloy in the age-hardened state. Silver, which was shown in Fig 22 and 23 to be markedly beneficial, had the following typical effect on stability:

Composition	As Extruded		As Aged at 150°F for 48 Hr	
	Yield Strength, psi	Elongation, Pct	Yield Strength, psi	Elongation, Pct
8.1 Mg/Li-6 pct Cd-6 pct Zn	35,800	20	24,400	36
8.1 Mg/Li-6 pct Cd-6 pct Zn-6 pct Ag	32,700	26	34,600	26.5

Other examples of the effect of silver on the stability of mechanical properties were shown in previous figures.

When it was found that silver had an important effect upon the stability characteristics of age-hardened alloys, a considerable portion of the experimental effort was directed to preparing various silver-containing alloy compositions and testing them after extruding, and after extruding and aging at 150°F for 48 hr. The mechanical properties of these alloys were discussed earlier in this paper.

One of the first alloys prepared that showed fairly good stability had the composition 7 Mg/Li-3 pct zinc-7 pct cadmium-3 pct silver. This alloy had the following properties:

	Yield Strength, psi	Tensile Strength, psi	Elongation, Pct	Reduction of Area, Pct	Hardness, Rockwell E
As extruded	37,400	40,600	20	44	87
As aged at 150°F for 48 hr	35,500	39,400	28.5	43.3	88

Age-hardening curves for this alloy, at room temperature and at 150°F, are shown in Fig 24. It is apparent from an examination of the curve for 150°F that a reasonably high hardness was maintained for only about 100 hr. Thus, the fact that the mechanical properties after aging for 48 hr at 150°F were not appreciably changed from those obtained in the as-extruded state was no indication that the alloy was stable when held for extended periods at 150°F. It became the practice with subsequent alloys to determine the aging curves, hardness vs. time at temperature, as well as the mechanical properties after various conditions of aging.

Such hardness vs. time at temperature curves showed that an increase in the amount of lithium above that required to make the alloys 100 pct beta was beneficial because it improved the stability. In most alloys investigated, maximum stability was achieved at 6 Mg/Li; therefore, a large number of compositions having a magnesium-lithium ratio of 6 were studied.

Although many elements were found which could cause precipitation in magnesium-lithium base alloys, it appeared that such precipitate-forming elements as silver, cadmium, aluminum, or zinc would be of major importance.

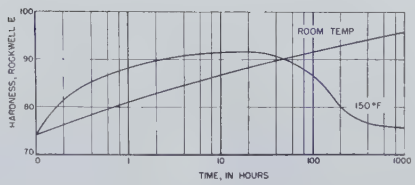

FIG 24—Age-hardening characteristics of the 7 Mg-Li-3 pct Zn-7 pct Cd-3 pct Ag alloy. (Specimens quenched from 475°F.)

Therefore, an investigation of the solubility limits of these elements in the 6 Mg/Li-base alloys was initiated. An indication of the solubility limit for an element was obtained by adding it in small but increasing increments to a magnesium-lithium base, then solution treating the alloys by quenching from 500°F, and finally determining their change in hardness with time at 150°F. The maximum hardness values obtained upon aging are plotted in Fig 25. The apparent effective solubility limits at 150°F for the four elements in the beta-phase alloys of 6 Mg/Li base were roughly 8 pct silver, 12 pct cadmium, 0.5 pct aluminum, and 1.5 pct zinc.

Investigations of this type were also conducted at other ratios of magnesium to lithium. In the beta phase, the solubility at room or at slightly elevated temperatures of almost every element increased as the lithium content increased. For example, at 8.1 Mg/Li, the maximum amount of cadmium that appeared soluble was 6 pct; at 6 Mg/Li, about 12 pct was soluble; and at 5 Mg/Li, over 16 pct was soluble. Silver seemed to be an exception. At 8.1 Mg/Li, over 12 pct silver was soluble; at 6 Mg/Li, only about 8 pct appeared to be soluble; while at 5 Mg/Li, less than 4 pct appeared to be soluble.

In order to determine their effects in age hardening, a large number of elements were added in various concentrations to a 6 Mg/Li-4 pct cadmium-6 pct silver base. The results of this study are shown in Table 7. Although many concentrations of each of the elements shown were studied, only that concentration is reported which had the greatest stabilizing effect on the alloy. It is interesting to note that many additions formed precipitates which were visible under the microscope yet did not cause age hardening.

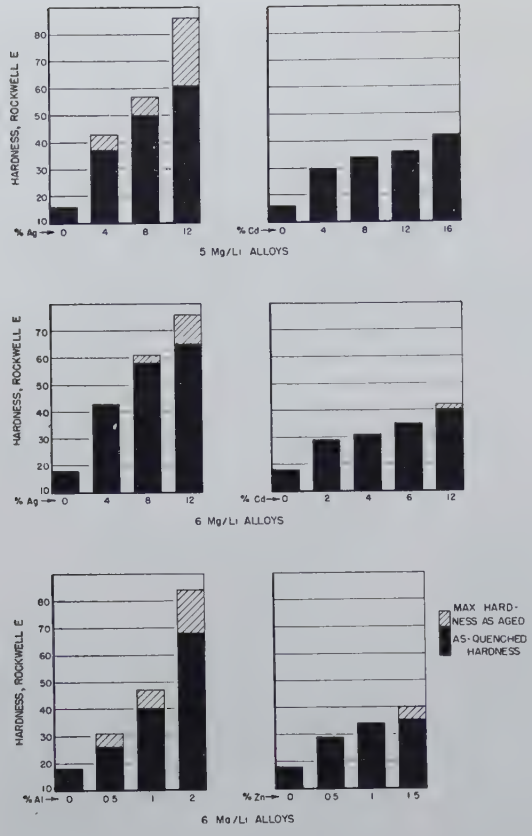

FIG 25—Age-hardening effects of various elements on magnesium-lithium base. Alloys quenched from 500°F and aged at 150°F.

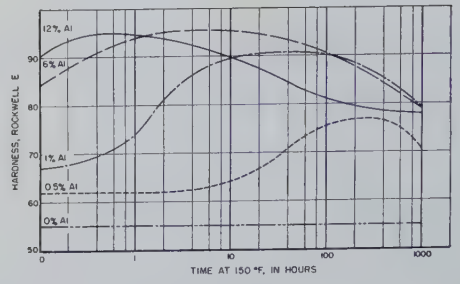

FIG 26—Effect of aluminum on 150°F aging characteristics of a 6 Mg/Li-4 pct Cd-6 pct Ag alloy. (Alloys quenched from 500°F.)

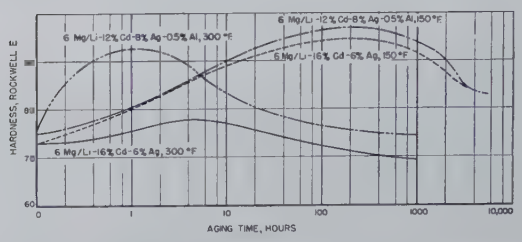

FIG 27—Aging characteristics of two high-strength magnesium-lithium base alloys. (Alloys quenched from 500°F.)

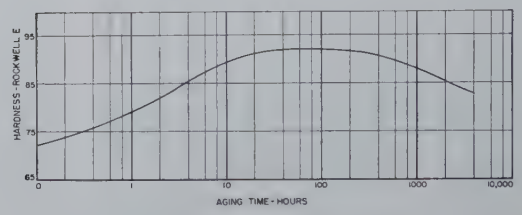

FIG 28—Aging behavior at 150°F of the 6 Mg/Li-15 pct Cd-5 pct Ag alloy following solution treatment at 500°F.

Table 7 . . . Effect of Various Elements[1] on the Age Hardening Capacity of Magnesium-lithium Base Alloys

Heat No.	Intended Composition,[1] Pct				Solution Treatment 16 Hr at °F	Aging Temperature, °F	Duration of Aging, Hr	Hardness, Rockwell E			Microscopical Examination	
	Mg/Li	Cd	Ag	Other				As Solution Treated	Maximum As Aged	At End of Test	Solid Solubility, As Quenched from Solution Temperature	Evidence of Precipitation after Aging at 300°F
1414	6	4	6		500	70		55	Did not age harden		Complete	None
						150		55	Did not age harden			
						300		55	Did not age harden			
1416	6	4	6	8 Ce	500	70		69	Did not age harden		Incomplete	Definite
						150		67	Did not age harden			
						300		66	Did not age harden			
1417	6	4	6	4 Ca[2]	500	70		63	Did not age harden		Incomplete	Definite
						150		62	Did not age harden			
						300		61	Did not age harden			
1418	6	4	6	4 Cu	500	70		68	Did not age harden		Incomplete	Definite
						150		67	Did not age harden			
						300		66	Did not age harden			
1421	6	4	6	12 Sr[2]	500	70	2500	61	69	69	Incomplete	Definite
						150		60	Did not age harden			
						300		60	Did not age harden			
1430	6	4	6	8 Tl	600	70	2000	75	87	87	Nearly complete	Definite
						150	3000	81	89	78		
						300		75	Did not age harden			
1431	6	4	6	4 Si	600	70	2000	70	86.5	86.5	Incomplete	Definite
						150		69	Did not age harden			
						300		69	Did not age harden			
1434	6	4	6	4 Ba	600	70		58	Did not age harden		Incomplete	Definite
						150		57	Did not age harden			
						300		57	Did not age harden			
1436	6	4	6	8 Sn	600	70	2000	70	88.5	88.5	Incomplete	Definite
						150		70	Did not age harden			
						300		70	Did not age harden			
1439	6	4	6	2 Pb	600	70		59	Did not age harden		Incomplete	Definite
						150		59	Did not age harden			
						300		59	Did not age harden			
1432	6	4	6	1.2 In	600	70	2000	56	81	81	Complete	Definite
						150	3000	56	65	65		
						300		56	Did not age harden			
1477	6	4	6	4 Zn	600	70	2500	73	95	95	Complete	Definite
						150	2500	72	95	80		
						300		72	Did not age harden			

[1] Other elements investigated included Te, Be, P, Bi, Mn, B, and Co, but these were not recovered in the alloys.
[2] With the exception of these elements, chemical analysis generally showed good recovery of all components.

The effects at 150°F of various quantities of aluminum on the aging characteristics of the 6 Mg/Li-4 pct cadmium-6 pct silver-base alloy, as shown in the age-hardening curves of Fig 26, were particularly interesting. As the aluminum content of the alloy was increased to 6 pct, there was a continuous increase in the maximum hardness obtained by aging. The time at maximum hardness, however, decreased as the aluminum content increased.

A large number of magnesium-lithium, high-cadmium, high-silver alloys were also studied. It was found that the alloys with 6 Mg/Li-12 pct cadmium-8 pct silver-0.5 pct aluminum, and with 6 Mg/Li-16 pct cadmium-6 pct silver, when quenched from 500°F and aged at 150°F, hardened appreciably and maintained their high hardness for a considerable length of time when held at that temperature. The aging characteristics of the two alloys are shown in Fig 27. As noted previously, neither of these alloys had as high ductility as was desired. A slight modification in composition of the alloys from 6 Mg/Li-16 pct cadmium-6 pct silver to 6 Mg/Li-15 pct cadmium-5 pct silver improved the ductility considerably. The aging curve for the latter alloy is shown in Fig 28. The alloy, solution treated to a Rockwell E hardness of about 73, is soft and ductile. Sheet of the material at this hardness can be bent several times through an angle of 180° over a sharp edge (0 radius) and straightened without cracking. The alloy can be aged at 150°F in about 48 hr to a maximum hardness of about 92 Rockwell E. At this hardness the yield strength of the material is about 43,000 psi and the elongation is about 8 pct.

Table 8 . . . Corrosion Resistance of Magnesium-lithium and Magnesium-lithium-zinc Alloys Compared with that of Commercial Alloy ASTM No. M-1

Heat No.	ASTM No.	Composition, Pct				Average Loss of Weight from Corrosion,[1] Mg per Sq Cm per Day
		Zn	Mn	Li	Mg	
251	M-1		1.26		Bal.	0.62
871				2.0	Bal.	4.92
872				4.0	Bal.	4.44
873				9.3	Bal.	0.77
874				11.0	Bal.	0.57
690		4		9.0	Bal.	2.81
875		4		10.6	Bal.	2.83

[1] Tested in cyclic immersion in 3 pct NaCl solution for 8 days. Cycle was ½ min. in the solution and 2 min. out. Solutions changed after 4 days' exposure.

The stability of magnesium-lithium base alloys may be improved by solution treatment. Alloys aged from the hot- or cold-rolled states usually contain residual stresses so that the rate of precipitation is increased and hence stability impaired.

Although the work-hardening capacity and the stability of magnesium-lithium alloys are not yet as desired, nevertheless considerable improvement has been made in these characteristics. It is of interest that the all-alpha phase magnesium-lithium alloys studied were quite capable of work hardening and their mechanical properties at ordinary temperatures were reasonably stable.

Corrosion Resistance

At the inception of the research program, it was expected that the addition of considerable percentages of lithium to magnesium would affect the corrosion resistance adversely. The experimental program was conducted on the premise that, if magnesium-lithium base alloys of satisfactory mechanical properties were developed, a method of protecting them from corrosion by cladding or by the use of paints, lacquers, and varnishes could be effected.

Early in the program, it was found that binary alloys containing about 11 pct lithium were remarkably good in their resistance to corrosion. This was demonstrated by results in Fig 29 which show the corrosive effect of alternate immersion in a 3 pct sodium chloride solution upon a series of magnesium-lithium base alloys. A specimen of ASTM No. M-1 magnesium-base alloy, the most corrosion resistant of the commercial alloys, was used for comparison. The immersion cycle was standardized at one-half minute in the solution and two minutes out, the temperature of the solution being maintained at 95°F. The corrosion rates of these alloys are given in Table 8.

It is apparent from the data that the binary magnesium-11 pct lithium alloy (Mg/Li = 8.1) is as resistant to corrosion, at least under the conditions of the test used, as the commercial alloy, ASTM No. M-1.

Results of corrosion tests on a series of magnesium-lithium-zinc-cadmium-silver alloys in a 3 pct sodium chloride solution are shown in Table 9. For comparison purposes, a magnesium-lithium binary alloy, a magnesium-lithium ternary alloy containing 4 pct zinc, and three commercial magnesium-base alloys were also tested. The resistance to corrosion of the magnesium-lithium base complex alloys decreased with an increase in the combined zinc and silver contents, as shown in Fig 30.

Preliminary tests showed that the 6 Mg/Li-15 pct cadmium-5 pct silver alloy also had poor corrosion characteristics. Its resistance to corrosion might be improved by cladding with a more corrosion-resistant material, such as the 8.1 Mg/Li binary alloy or pure aluminum. To give maximum protection, the cladding material should be anodic to the base material. Hence, solution potential measurements were made in a 3 pct sodium chloride solution on the 6 Mg/Li-15 pct cadmium-5 pct silver alloy, on the 8.1 Mg/Li binary alloy, and on 2S aluminum. The results obtained are shown in Fig 31.

Table 9 . . . Alternate Immersion, Salt-water Corrosion Resistance of Extruded Mg-Li-Zn-Cd-Ag Alloys Compared with Commercial Magnesium Alloys in Sheet Form

Heat No.	Mg/Li	Intended Composition, Pct							Average Loss of Weight from Corrosion,[1] Mg per Sq Cm per Day	Sum of Zn and Ag Contents, Pct
		Mg	Li	Zn	Cd	Ag	Al	Mn		
1091	6.0	75.4	12.6	6	0	6			18.7	12
1095	6.0	73.7	12.3	6	4	4			8.2	10
1075	6.0	72.0	12.0	6	4	6			12.6	12
1076	6.0	72.0	12.0	4	6	6			8.8	10
1092	7.0	76.1	10.9	4	4	5			6.4	9
1090	7.0	75.3	10.7	4	4	6			10.5	10
1077	7.0	75.3	10.7	4	6	4			4.7	8
1078	7.0	73.5	10.5	4	6	6			8.3	10
1093	7.0	72.6	10.4	5	6	6			10.8	11
1094	7.0	76.1	10.9	3	7	3			2.2	6
1079	8.1	73.0	9.0	6	6	6			11.1	12
874	8.1	89.0	11.0						0.5	0
875	8.1	85.4	10.6	4					2.2	4
Dow FS-1		Bal.		1			2.7	0.3	0.4	
Dow J-1		Bal.		1			6.5	0.15	0.3	
Dow M-1		Bal.						1 20	0.5	

[1] Average of triplicate specimens.

FIG 29—Specimens of magnesium-lithium alloys compared with a 1.26 pct Mn-balance Mg alloy following cyclic immersion corrosion test in 3 pct NaCl.
a. 10.6 pct Li-4 pct Zn-Balance Mg. *b*. 9 pct Li-4 pct Zn-Balance Mg. *c*. 11 pct Li-Balance Mg. *d*. 9.3 pct Li-Balance Mg. *e*. 4 pct Li-Balance Mg. *f*. 2 pct Li-Balance Mg. *g*. 1.26 pct Mn-Balance Mg (ASTM No. M-1 alloy). Reduced approximately one-third in reproduction.

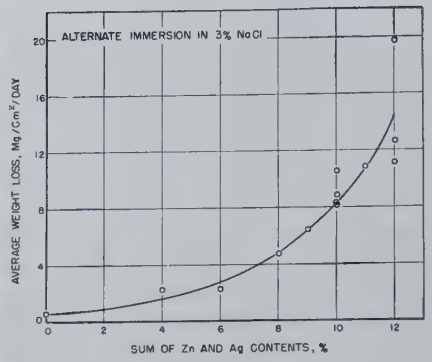

FIG 30—Effect of silver and zinc on corrosion resistance of Mg-Li alloys in salt water.

It was evident from the data that the 8.1 Mg/Li binary alloy was anodic to the high-strength alloy and, thus, would be expected to offer galvanic protection. On the other hand, 2S aluminum was found to be cathodic to the high-strength alloy and could be expected to afford only mechanical protection.

The 6 Mg/Li-15 pct cadmium-5 pct silver alloy can be clad either with the 8.1 Mg/Li binary alloy or with commercially pure aluminum. To obtain a bond between the materials used in cladding, sheets of the materials assembled in packs were tack welded at the edges and then rolled at temperatures above 600°F. Microscopical examination of the interface between the strong alloy in the core and the 8.1 Mg/Li binary alloy at the surface of the clad structure showed that actual welding had occurred in the process. On the other hand, the interface between the strong alloy in the core and 2S aluminum showed the existence of a thin layer of brittle, intermetallic compounds. For the clad structures in the as-rolled condition, these compounds were not deleterious; but after prolonged heating at 400°F, the intermetallic layer failed, causing the aluminum to separate from the magnesium-lithium base alloy.

The results of a series of corrosion tests made on the clad alloys are shown in Table 10. It appears that the corrosion resistance of the 6 Mg/Li-15 pct cadmium-5 pct silver alloy clad with the 8.1 Mg/Li binary was fairly good, although it did not quite equal that of the commercial magnesium-base alloys, AZ61X or M1. Painting of the cut edges of the clad material was especially effective in reducing corrosion in the simulated marine atmosphere. Cladding with 2S aluminum was advantageous where the edges of the core alloy were protected by paint.

In order to determine the extent of anodic protection offered by the 8.1 Mg/Li cladding on the 6 Mg/Li-15 pct cadmium-5 pct silver alloy, a number of specimens were tested on which a $\frac{1}{16}$- to $\frac{1}{4}$-in. wide strip of the cladding was removed by machining to expose the core material. These specimens were tested in aerated 3 pct sodium chloride and aerated synthetic sea water. As shown in Fig 32, the binary alloy cladding afforded protection to the exposed base alloy when a strip as wide as $\frac{1}{8}$ in. of the base alloy was exposed. These experiments were in agreement with the solution potential measurements reported in Fig 31.

Metallography

A considerable amount of work in connection with microstructural examinations and X ray diffraction studies was conducted on the magnesium-lithium base alloys. In agreement with work of other investigators, it was shown that the beta-phase solid solution had a body-centered-cubic lattice similar to that of lithium. The beta phase was obtained when additions of 10.5 pct of lithium or more were made to magnesium. No attempts were made to establish with any degree of accuracy the exact location of the boundary between the alpha plus beta and the beta-phase regions which, according to the literature, exists at about 10.3 pct lithium.

The ternary Mg-Li-Zn, Mg-Li-Cd, Mg-Li-Al, and Mg-Li-Ag alloys having sufficient lithium to consist of beta solid solution and a sufficient quantity of the third element, may contain a precipitate which has been termed theta. From X ray diffraction studies, theta has been assigned the tentative composition $MgLi \cdot LiX$ where X represents any of the elements zinc, cadmium, aluminum, silver, indium, or thallium. The lattice parameter of the theta phase has a value of about 6.92 Å in the cadmium-bearing alloys, a value of from 6.66 to 6.68 Å in the zinc-bearing alloys, a value of 6.72 Å

in the aluminum-bearing alloys, and a value of 6.78 Å in the silver-bearing alloys. The latter value is in fairly close agreement with the theoretical value of 6.81 Å calculated for MgLi · LiAg.

Partial solution of the theta phase appeared to begin in the neighborhood of 300°F, and complete solution of the theta phase in most of the experimental alloys was evident at temperatures of the order of 450 to 550°F. The experimental alloys for the most part contained relatively small amounts of theta-forming elements, and none of the alloys susceptible to aging contained excessively large amounts of theta. In the Mg-Li-Ag alloys, the lattice parameter of the theta phase was observed to change as aging progressed at 150°F. The highest experimental value obtained was 6.78 Å, but this decreased to 6.70 Å after a long time at 150°F. A similar change in the lattice parameter of the theta phase was also observed in the Mg-Li-Zn and Mg-Li-Cd alloys. Such variations in lattice parameter may indicate that the theoretical structure MgLi · LiX, heretofore assigned to theta, is a transition structure which changes on prolonged aging. Another possible explanation, discussed later in this paper, is that theta only approximates the composition MgLi · LiX and that it may have appreciable quantities of lithium in solution. Attempts to determine the cause of the changes in lattice parameters are planned for later study.

In addition to the theta phase, LiAl has been found in the Mg-Li-Al alloys. Since most of the experimental effort has been devoted to low-aluminum-bearing alloys, and since this phase appears to be more prevalent in the higher aluminum alloys, no specific information about its occurrence has been obtained. It has been observed, however, that LiAl is soluble in the matrix at high temperatures and can be precipitated at low temperatures. Its occurrence has been identified in 8.1 Mg/Li alloys containing as little as 2 pct aluminum after aging at 150°F. Moderate quantities of LiAl occur at 6 pct aluminum and large quantities at 12 pct aluminum, the quantities increasing at both aluminum contents with reduction in lithium content.

In the Mg-Li-Cd alloys, when additions of cadmium were up to 12 pct, an unidentified phase was observed. Although the phase was not identified, it was established that it was neither Mg_3Cd nor LiCd.

The occurrence of the theta phase and lithium-bearing compounds in ternary alloys is associated with a tendency toward the formation of the alpha phase. Theta and the lithium-bearing compounds appear to remove some lithium from the matrix so that alpha can form in their immediate vicinity. The association of the alpha phase with theta is shown in Fig 33, where a precipitation pattern of theta and alpha occurs in a pearlitic-like structure in the beta background. Fig 34 shows the same type of pearlitic structure after long-time aging, the white material in this case being the alpha phase. This is evidence that theta can absorb sufficient lithium from the magnesium-lithium solid solution to produce an alloy of predominantly alpha phase, and is probably best explained by considering theta to be a phase in which large quantities of lithium are soluble.

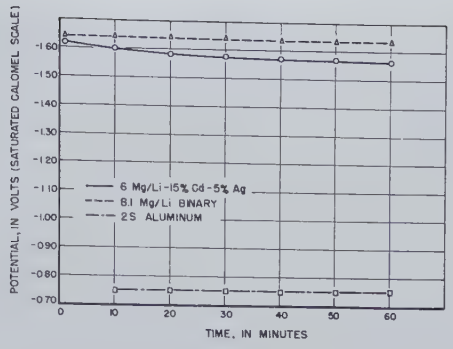

FIG 31—Time-potential values for magnesium-lithium alloys compared with aluminum, 3 pct NaCl solution at 95°F.

The mode of precipitation of the theta phase in magnesium-lithium base alloys was of interest. A Mg-Zn-Cd-Ag alloy extruded at a temperature sufficiently low to produce some cold working is shown in Fig 35. This alloy was aged 48 hr at 150°F. It is apparent from the micrograph that the precipitated theta phase is concentrated within the cold-worked grains. The same structure at a higher magnification is shown in Fig 36. The strength and ductility of alloys in which precipitation occurs

Table 10 . . . Corrosion Tests on a Clad Magnesium-lithium Base Alloy

Heat No. or Specimen No.	Specimen Description and Intended Composition, Pct	Type of Corrosion Test and Results[1]		
		1. Alternate Immersion in 3 pct NaCl at 95°F for 24 Hr. Average Weight Loss, Mg per Cm² per Day	2. Partial Immersion in Aerated Sea Water at 95°F. for 24 Hours. Average Weight Loss, Mg per Cm² per Day	3. Simulated Marine Atmosphere[2] at Room Temperature for 48 Hr. Average Weight Loss, Mg per Cm² per Day
32	6 Mg/Li-15 pct Cd-5 pct Ag alloy, clad on both sides with 8.1 Mg/Li binary	1.59	1.66	0.92
32	Same, except cut edges of core alloy were protected by paint	1.55	1.52	0.290
33	6 Mg/Li-15 pct Cd-5 pct Ag alloy, clad on both sides with 2S aluminum	50.3	48.9	1.48
33	Same, except cut edges of core alloy were protected by paint	12.7	8.97	0.045
34	6 Mg/Li-15 pct Cd-5 pct Ag alloy, clad on one side with 2S aluminum	41.9	47.5	5.3
35	6 Mg/Li-15 pct Cd-5 pct Ag alloy, clad on one side with 8.1Mg/Li binary	6.12	3.94	4.14
36	Same	5.51	3.54	5.27
2002	6 Mg/Li-15 pct Cd-5 pct Ag alloy, unclad	7.94	15.9	6.65
2003	8.1 Mg/Li binary	0.81	1.47	0.263
2S	Commercially pure aluminum	0.00	0.07	0.00
AZ61X[3]	6.5 pct Al-1.0 pct Zn-0.2 pct Mn-Balance Mg	1.21		0.11
M1[3]	1.5 pct Mn-Balance Mg	0.50		0.16

[1] The samples were cut from hot-rolled sheet material approximately 0.040 in. thick.
[2] In this test the cabinet was opened for 8 hr each week day and closed for the remainder of the time.
[3] These specimens were exposed for two weeks. Long exposures generally produce lower overall corrosion rates.
The above results are based on averages of two specimens.

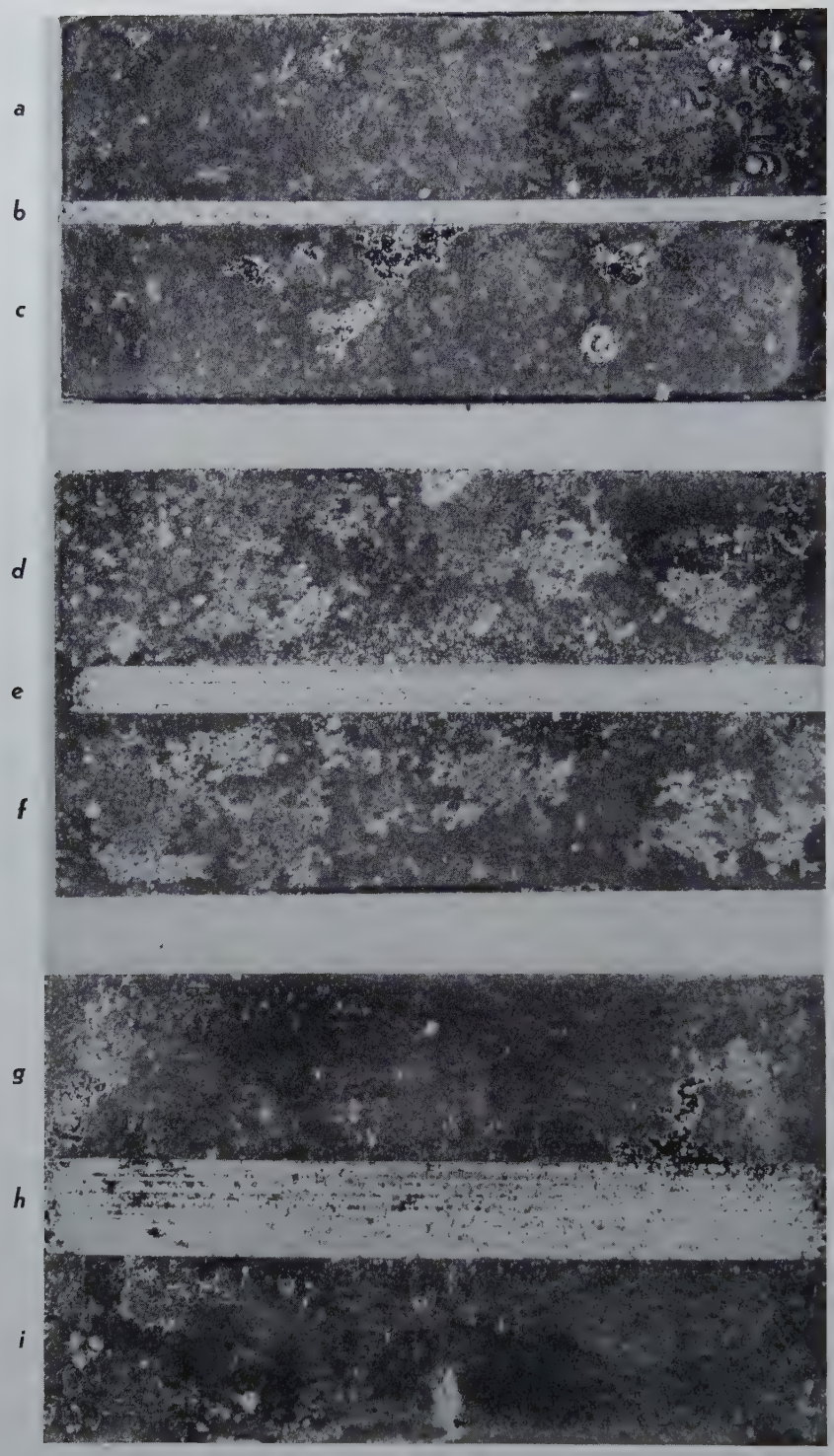

FIG 32—Experiment to show the sacrificial protection granted by the 8.1 Mg/Li binary alloy to the 6 Mg/Li-15 pct Cd-5 pct Ag base alloy. Test conditions: 48 hr immersed in aerated sea water at 95°F. (Note: The amount of cladding exposed is the same in all three experiments.)

a. Binary alloy. *b*. Exposed base alloy, $\frac{1}{16}$ in. *c*. Binary alloy. *d*. Binary alloy. *e*. Exposed base alloy, $\frac{1}{8}$ in. *f*. Binary alloy. *g*. Binary alloy. *h*. Exposed base alloy, $\frac{1}{4}$ in. *i*. Binary alloy.

in the cold-worked grains are higher than for alloys which are solution treated wherein the grains are equiaxed and where precipitation occurs only at grain boundaries.

Summary and Conclusions

The hexagonal, close-packed crystal lattice of magnesium can be converted to the body-centered-cubic lattice of lithium by an addition of about 10.3 pct by weight or more of lithium. Additions of lithium of between 5.7 and 10.3 pct produce a structure which is a mixture of lithium dissolved in alpha, hexagonal magnesium, and magnesium dissolved in beta, body-centered-cubic lithium.

The conversion of the crystal lattice from hexagonal to body-centered cubic improves many of the properties of magnesium. Some of these improvements are:

1. Increased ratio of compressive to tensile yield strength; the compressive yield strengths of beta-phase magnesium-lithium base alloys equal or surpass the tensile yield strengths.
2. Increased modulus of elasticity in compression so that the compressive modulus equals the tensile modulus.
3. Improved formability at room temperature.
4. Improved hot- and cold-rolling and extrusion characteristics.

Because of these improvements, a major portion of the experimental work was devoted to the study of the single-phase beta alloys. Considerable attention was also given to the single-phase, lithium-bearing alpha magnesium alloys and the two-phase alloys, since these alloys have certain advantages over magnesium, such as improved working characteristics, but have lower cost than the higher lithium alloys.

The melting of magnesium-lithium alloys is no more difficult than the melting of ordinary magnesium, provided certain precautions are followed. The alloys are generally melted in a steel crucible under an argon atmosphere or lithium chloride-lithium fluoride flux, or a combination of both. They can be poured in air without protection. Cast iron, or graphite ingot molds are quite satisfactory, but they should be dried before they are used.

The magnesium-lithium alloys can be hot worked with ease at temperatures of the order of 450°F. They can be cold rolled without difficulty and total reductions of 50 pct are common for most compositions. Many of the magnesium-lithium base alloys can be cold drawn. However, some difficulty is encountered when starting the cold-drawing operation because the alloys do not work harden well and tips formed on the ends of bars are not sufficiently strengthened to withstand the stresses necessary to start the bar through the die.

Magnesium-lithium base alloys hav-

ing good mechanical properties invariably possess hardnesses of the order of 85 Brinell. High-strength magnesium-lithium base alloys have been developed which have densities of the order of 1.45 to 1.65 g per cc, compared with a density of 1.8 g per cc for present magnesium-base alloys and about 2.8 for aluminum-base alloys. Since yield strengths of approximately 40,000 to 45,000 psi can be obtained with these alloys, they compare favorably on a strength-weight basis with the strongest available commercial aluminum-base alloy, 75ST.

The modulus of elasticity of magnesium-lithium base alloys varies slightly with composition; however, the alloys possess an average value of about 6,500,000 psi, which is the same in tension and compression. This value compares favorably with that for the commercial magnesium-base alloys. Because of the low density of the magnesium-lithium alloys, it can be shown that their resistance to buckling during compressive loading is better than for equivalent weights of commercial magnesium-base alloys or other available commercial structural alloys.

Two characteristics of the magnesium-lithium base alloys containing the body-centered-cubic phase which have been found to be closely interrelated are poor work-hardening capacities and lack of stability of mechanical properties in the age-hardened state. A simple bend-deflection test, in which alloy specimens were loaded above the yield stress, was developed to determine which alloy addition improved the work-hardening characteristics. This test is described in detail. Those alloy additions which were most effective in improving work-hardening characteristics were also very beneficial in improving stability of mechanical properties. The degree of stability was determined by comparing curves showing the relationship of hardness to aging time at 150°F.

By means of these tests, it was found that the addition of silver to the alloys was most effective both in improving the work-hardening capacity of the alloys and in stabilizing the mechanical properties of age-hardened alloys. However, although great progress has been made in improving these characteristics, they are not yet entirely satisfactory.

One of the best alloys developed thus far, from the standpoint of stability, has a composition of 68.5 pct magnesium, 11.5 pct lithium, 15 pct cadmium, and 5 pct silver. Its yield strength of 43,000 psi and its elongation of about 8 pct can be maintained at a temperature of 150°F for an extended period.

The corrosion resistance of most magnesium-lithium base alloys, especially those containing large quantities of zinc, silver, and/or cadmium is poor; however, it was observed that the magnesium-lithium binary alloy containing about 11 pct lithium had good corrosion resistance. This material can be used to clad and to protect anodically many of the higher strength alloys.

The magnesium-lithium base alloys containing zinc, aluminum, cadmium, and/or silver can be hardened by the precipitation of a phase, called theta, which was assigned the tentative formula MgLi · LiX where X may be any one of the elements zinc, aluminum, cadmium, or silver. The lattice parameter of theta phase varies slightly with composition and aging time. It was

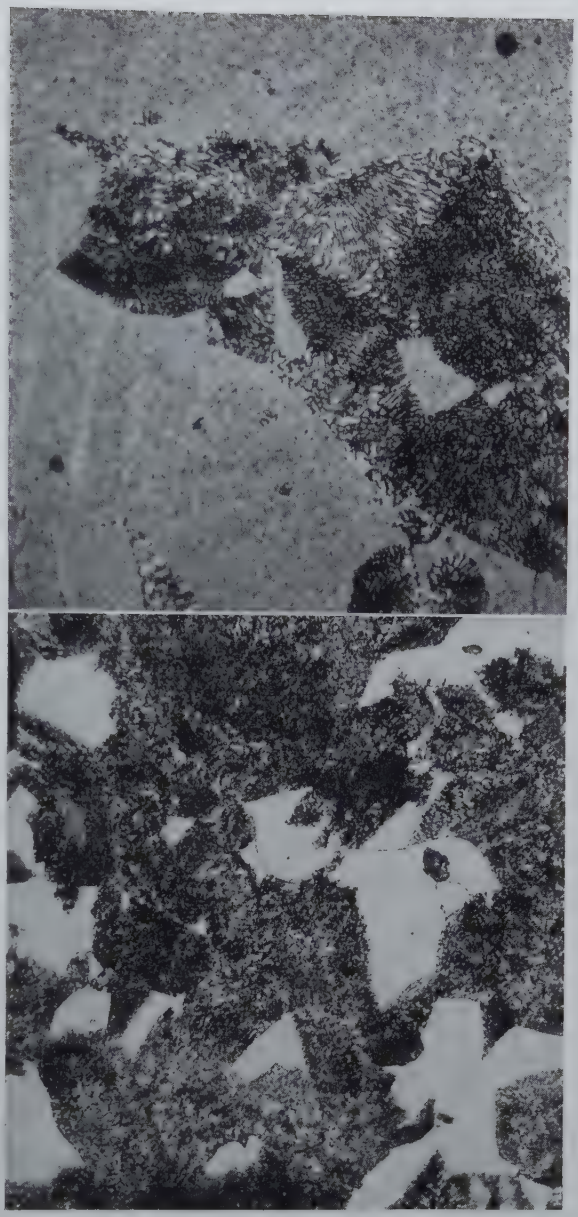

33

34

FIG 33—(Above) Pearlitic structure with beta background found in Mg-Li-Zn-Cd-Ag alloys after extruding and aging at 150°F. (Etched in 2 pct HF.) × 500.

FIG 34—(Below) Same as Fig 33 but after a prolonged aging at 150°F.
This shows a pearlitic structure with massive alpha phase. Massive alpha phase is found only when large quantities of pearlite are present. (Etched in 2 pct. HF.) × 1200.

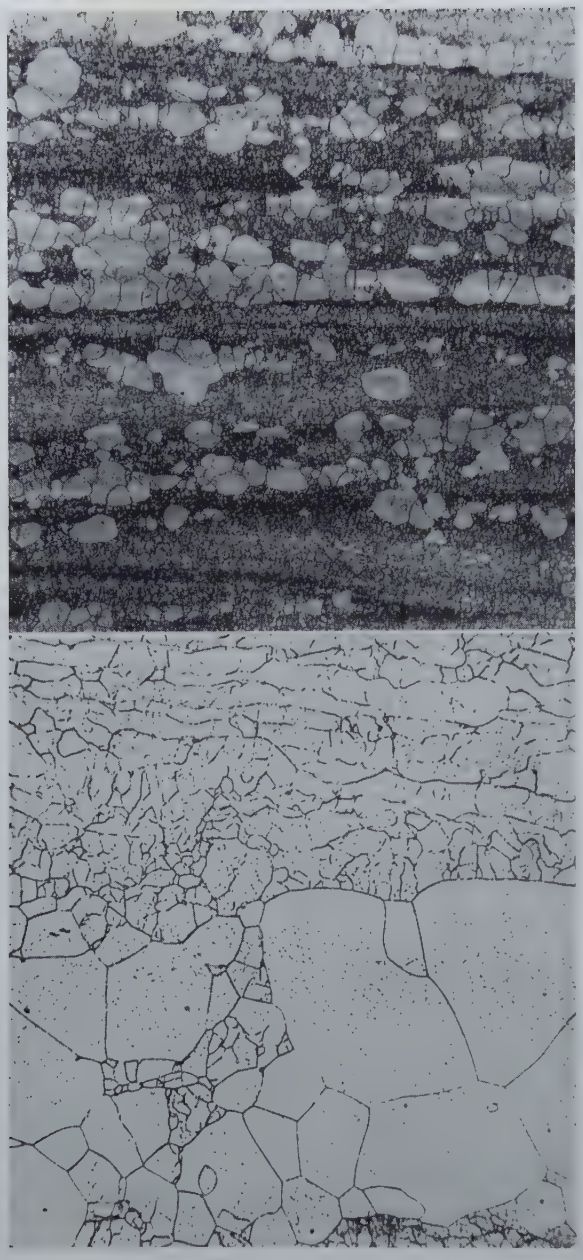

FIG 35 (Above)—Banded structure found in extruded Mg-Li-Zn-Cd-Ag alloys. (Etched in 2 pct HF.) × 100.

FIG 36 (Below)—Same as Fig 35 except at ×500. Note distorted unrecrystallized material. (Etched in 2 pct HF.)

concluded tentatively that the theta phase is a transition structure in which large quantities of lithium are soluble.

Future research on magnesium-lithium alloys will undoubtedly be concerned with improvements in stability, work-hardening capacity, and corrosion characteristics, and with efforts to employ alloying elements which are relatively inexpensive and plentiful.

Acknowledgments

The experimental work discussed herein was conducted under the sponsorship of the Mathieson Chemical Corporation and the Navy Department, Bureau of Aeronautics. Considerable assistance in planning the work was received from individuals representing the sponsors. These men included Messrs. R. E. Gage, and M. C. Taylor, from Mathieson Chemical Corporation; and Capt. J. E. Sullivan, Messrs. N. E. Promisel, and H. J. Boertzel, of the Navy.

Considerable assistance was received at Battelle from the following: Messrs. E. C. Kron and A. H. Hesse, who supervised and conducted much of the early work and made valuable discoveries and contributions; Dr. C. M. Schwartz and Mr. J. R. Doig, who conducted X ray diffraction studies; and Messrs. A. R. Elsea, and J. L. Stevens, who did the microscopical work. The assistance of Messrs. R. S. Springer, H. S. Sanders, C. R. Owens, R. V. Whittenberg, and T. C. Kronfoth, in the preparation and testing of the various melts is gratefully appreciated. Many others have made valuable contributions to the work, and while no specific acknowledgment is made to them herein, their part in this work is recognized.

References

1. R. S. Dean and C. T. Anderson: Magnesium-Base Alloy, U.S.P. No. 2,317,980 (May 4, 1943).
2. R. S. Dean and C. T. Anderson: Magnesium Alloy, U.S.P. No. 2,376,868 (May 29, 1945).
3. W. Hume-Rothery, G. V. Raynor, and E. Butchers: Equilibrium Relations and Some Properties of Magnesium-Lithium and Magnesium-Silver-Lithium Alloys. *Jnl.* Inst. Metals (1945) **71**, 589–601.
4. G. Grube, H. von Zeppelin, and H. Bumm: Das System Lithium-Magnesium, *Ztsch.* Elektrochemie (1934) **40**, 160–164.
5. O. H. Henry and H. V. Cordiano: The Lithium-Magnesium Equilibrium Diagram. *Trans.* AIME (1934), **111**, 319–332.
6. P. Sal'dau and F. Shamrai: Equilibrium Diagram of the System, Magnesium-Lithium. *Ztsch.* anorg. allgem. Chem. (1935), **224**, 388–398.
7. W. Hofmann: Solubility of Lithium in Magnesium. *Ztsch.* Metallkunde (1936) **28**, 160–163.
8. F. I. Shamrai: The Ternary System Aluminum-Magnesium-Lithium. Bull. Acad. Sci., U.S.S.R., Sect. of Chem. Sci. (1947), 605–616, (1948), 83–94.
9. F. R. Shanley: Private Communication.

Self-diffusion in Sintering of Metallic Particles

G. C. KUCZYNSKI,* Member AIME

Two particles in mutual contact form a system which is not in thermodynamical equilibrium, because its total surface free energy is not a minimum. If such a system is left for a certain period of time, the bonding of the two particles will take place in order to decrease the total surface area, even though the temperature is lower than the melting point. This phenomenon of bonding of two or more particles with the application of heat only and at temperatures below melting point of any component of the system will be called sintering, although the powder metallurgists use this term in a broader sense, including the presence of molten phase and pressure. It is the objective of this paper to study this process and the mechanisms involved in it.

This problem is of utmost importance to powder metallurgy and powder ceramics, and its technological aspects have been studied for a good many years. However, the powder metallurgical operations are too complex and include too many superimposing mechanisms, and too many variables for a direct study. It was therefore advisable for the purposes of this study to reduce the variables to a minimum. In this work the radius of the interface formed during bonding in a simple system composed of a spherical particle and a large block of the same metal was studied as a function of time and temperature. It is believed that the mechanism involved in this simple process is fundamental to any sintering operations.

Previous Work

J. Frenkel[1] was the first to make a serious attempt to develop a theory of sintering. He assumed that the process consists of a slow deformation of crystalline particles under the influence of surface tension which reduces to a viscous flow where the coefficient of viscosity η is related to the self-diffusion coefficient D by the following equation

$$\frac{1}{\eta} = \frac{D\delta}{kT} \qquad [1]$$

where δ is interatomic distance, k the Boltzman constant, and T the absolute temperature. This type of viscous flow of a crystalline substance is essentially different from the ordinary plastic flow. The latter is a specific property of crystals and cannot take place in amorphous bodies. According to Frenkel this viscous type of flow is due to the diffusion of the holes or vacancies arising in the lattice. He was able to derive an equation relating the growth of the interface between two spherical crystalline particles or between a particle and a semi-infinite crystal (Fig 1) to time t at constant temperature. This relationship can be written as follows:

$$x^2 = \frac{3}{2}\frac{a\sigma}{\eta}t \qquad [2]$$

where x is the radius of the interface assumed to be circular, a the original radius of the sphere and σ surface tension of the material. The other assumptions are that $\frac{x}{a}$ is less than 0.3 and that during the period t the original radius, a, of the metallic particle did not change appreciably.

A. J. Shaler and J. Wulff[2] followed closely the ideas of Frenkel in their theory of sintering of a mass of metallic powder. Neither Frenkel nor Shaler has validated his theoretical speculations with conclusive experimental data. Two measurements reported by

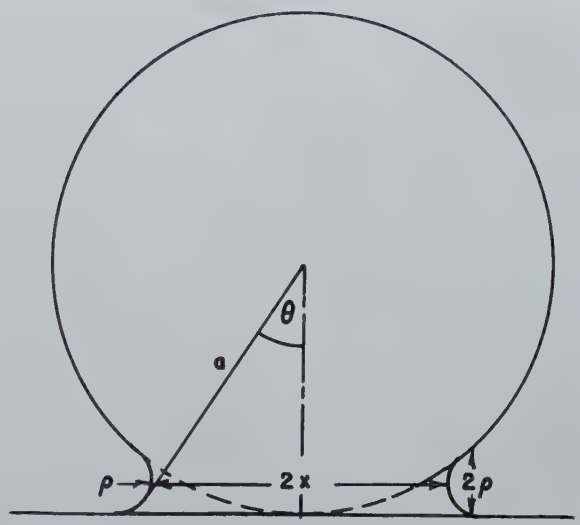

FIG 1—Schematical representation of the cross-section of a spherical particle sintered to a metallic block.

San Francisco Meeting, February 1949.

TP 2528 E. Discussion of this paper (2 copies) may be sent to *Transactions* AIME before May 15, 1949. Manuscript received November 1, 1948; revision received November 24, 1948.

* Sylvania Electric Products Inc. Bayside, N. Y.

References are at the end of the paper.

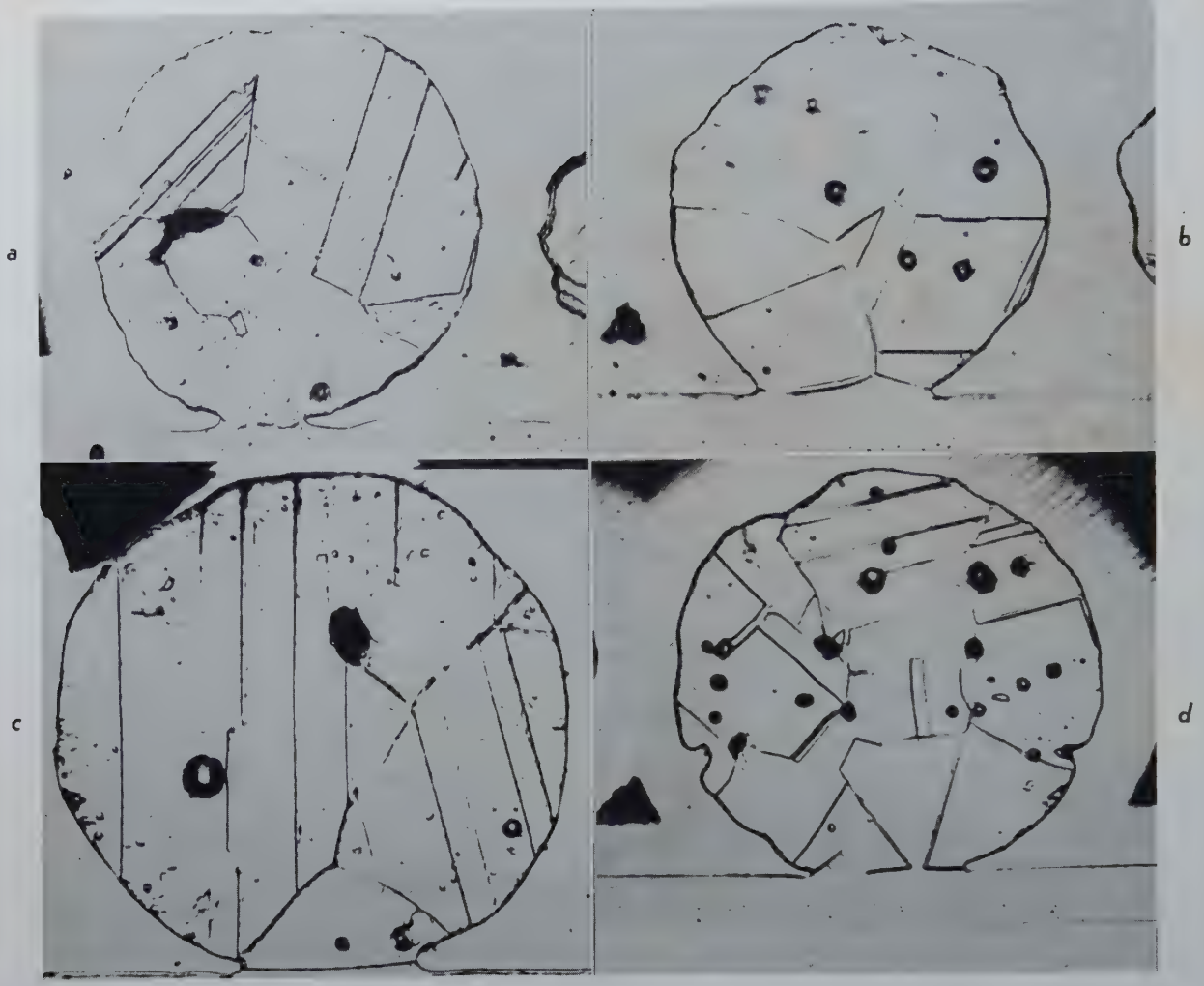

FIG 2—Copper particles sintered to copper blocks. *a*. At 700°C for 4 hr, 800 ×. *b*. At 800° for 2 hr, 900 × *c*. At 900°C for 1 hr, 1000 ×. *d*. At 1000°C for 0.5 hr, 600 ×.

Shaler for copper powder sintered at 850 and 900°C yielded a value for the heat of activation of self-diffusion in copper which was 10 pct higher than those obtained by other methods. This is by no means an adequate test of the theory. In the first place two such measurements are not sufficient for evaluating the coefficient of self-diffusion D. More important, however, is the fact that the temperature dependence is of secondary importance only. The final check of this theory will come from the experimental investigations of the time relationships such as [2] above as will be shown later.

B. Ya. Pines[3] developed a theory of sintering of the powder compacts based upon different assumptions. According to him the atoms from the surface of the compact migrate by diffusion to the internal voids filling them gradually, or, as Pines puts it, by moving the voids out from the body. This mechanism is essentially different from that postulated by Frenkel. The difference is that while Pines visualizes sintering as filling of the voids atom by atom, Frenkel envisions them filled by slow viscous creep of the crystal. The conclusions arrived at by Pines are only of qualitative nature and do not render themselves for experimental verification.

Theoretical Considerations

Formation of the common interface between two particles or a particle and a crystal block can be achieved by one, or a combination of, the following mechanisms: viscous or plastic flow, evaporation and condensation, volume diffusion and surface diffusion.

As the objective of this paper is to determine experimentally which of these mechanisms are involved in sintering of the particles it is important to discuss briefly each of these in order to find out what kind of relationships characteristic for each mechanism could be established and tested experimentally.

VISCOUS OR PLASTIC FLOW

This mechanism has already been discussed in connection with Frenkel's paper.[1] If only mechanism of viscous flow were responsible for sintering, the relationship between the radius of the interface and the time of heating at a given temperature would be expressed by Eq 2. A similar expression could be derived for plastic flow with only a different temperature dependent coefficient at variable t.

EVAPORATION AND CONDENSATION

According to the kinetic theory the rate G of evaporation of a gas from a surface above which the equilibrium pressure is p_1, and the rate of condensation on a neighboring surface of pressure p_2 is

$$G = K(p_1 - p_2) \qquad [3]$$

where K is a function of temperature only. The equilibrium pressures are related to the respective radii of curvature. In our case ρ is the radius of the area of condensation and a the radius of the area of evaporation by the well known Kelvin equation:

$$ln \frac{p_2}{p_1} = \frac{-2\sigma\delta^3}{kT}\left(\frac{1}{\rho} + \frac{1}{a}\right) \qquad [4]$$

where σ is the surface tension of the body.

As $\rho << a$, $p_2 = p_1 - \Delta p$ and $\frac{\Delta p}{p_1}$ is small, Eq 3 can be written as follows:

$$G = \frac{K'}{\rho} \qquad [5]$$

where K' is a function of temperature and p_1 only. In our problem (Fig 1) p_1 can be regarded constant because the radius of the sphere does not change appreciably. The radius of curvature ρ can be approximated as a function of x as follows: From Fig 1, it is obvious that

$$\rho = a\,(1 - \cos\theta) \text{ or } \rho = 2a \sin^2\frac{\theta}{2}$$

as θ is very small and equal to $\frac{x}{a}$,

$$\rho = \frac{x^2}{2a}$$

Introducing this value for ρ in [5] we obtain

$$G = \frac{K''}{x^2}$$

The rate of condensation G on the area A of the junction between the particle and the crystalline block should be equal to the rate of mass transport which in turn is proportional to the rate of change of volume of the junction. We can write then

$$AG = \beta \frac{dv}{dt}$$

where β is independent of time.

But $A \cong \pi \frac{x^3}{a}$ and $V \cong \pi \frac{x^4}{2a}$ so

$$\frac{K''}{2\beta} = x^2 \frac{dx}{dt}$$

and after integration

$$x^3 = \frac{3}{2}\frac{K''}{\beta} t \qquad [6]$$

In other words if the mechanism of evaporation and condensation were responsible for the formation of interface between particles, the radius of the junction should grow with such a rate that its cube would be proportional to time.

VOLUME DIFFUSION

If we assume the vacancy theory of diffusion, then the area near the interface should have higher hole concentration than the remaining body of the particle. This is due to the fact that near the interface, where the radius of curvature is small the surface energy is very high and it can be lowered by decreasing the surface area. The decrease in surface area is produced by an increase in the interface volume which is accomplished by a larger concentration of vacancies present in that region. If the interstitial atom mechanism is assumed, the junction area should be deprived of the interstitial atoms in order to decrease the total surface. This causes the flow of atoms from the other parts of our system to the junction. The third possible mechanism of diffusion known as atom exchange mechanism and sometimes considered possible[4,13] is automatically eliminated if the actual sintering is caused by diffusion because in this case no concentration gradient

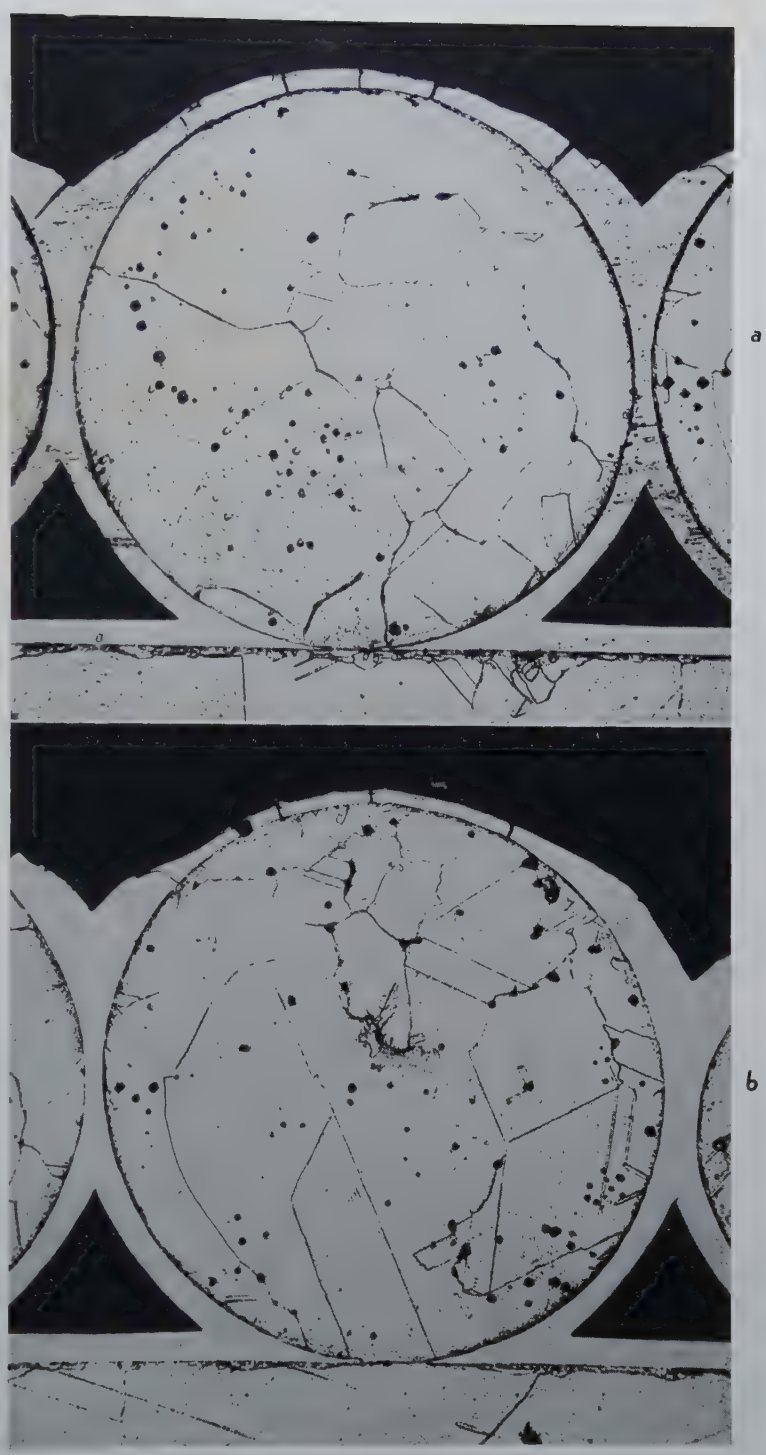

FIG 3—Silver particles sintered to silver blocks. 200 ×. *a*. (above) At 800°C for 24 hr. *b*. (below) At 900°C for 2 hr.

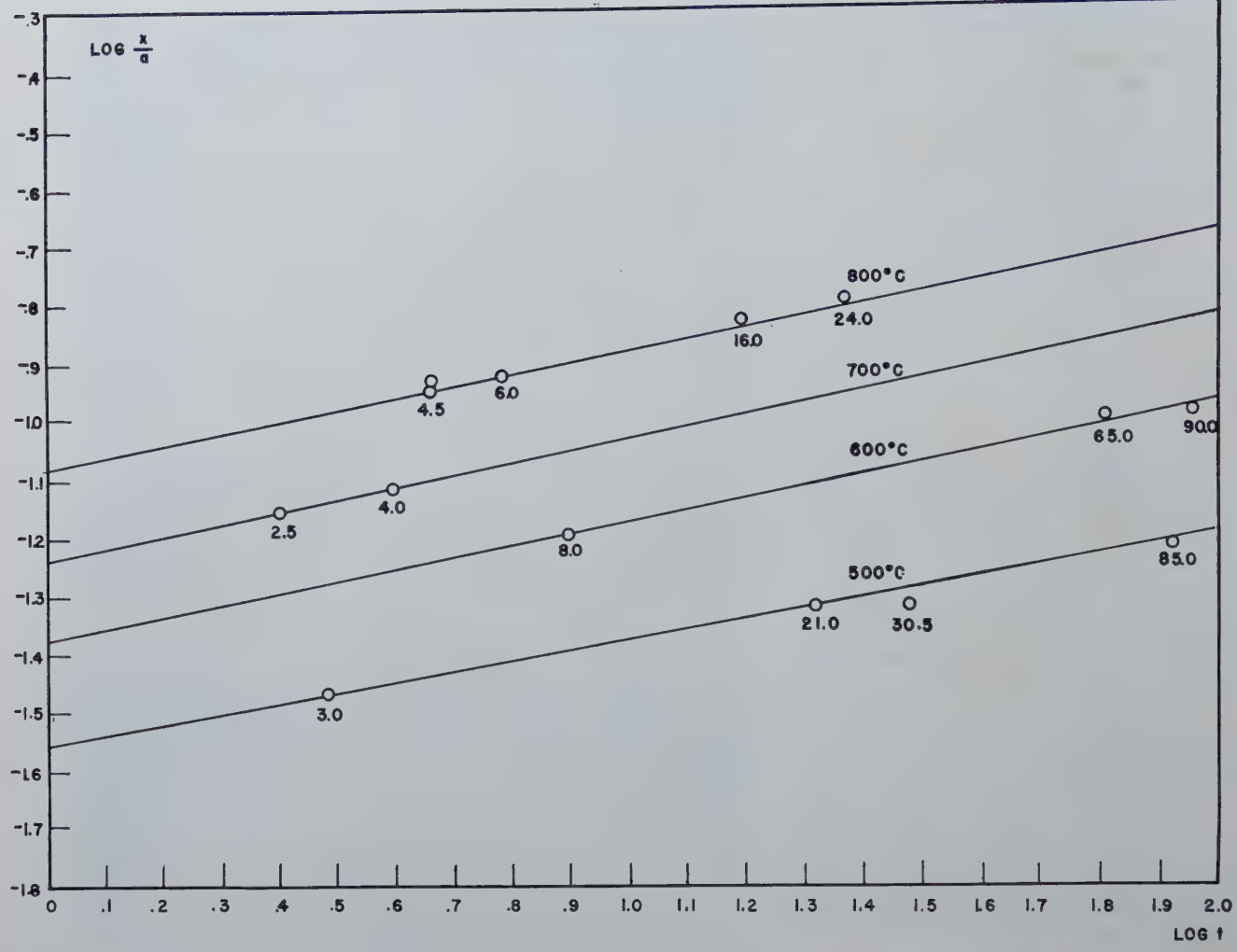

FIG 4—Logarithm of the ratio of the interface radius x to the radius of a copper particle sintered at indicated temperatures, plotted against the logarithm of sintering period t. The numbers at the points express time of heating in hours.

would be present. It is convenient to assume that the hole mechanism is the actual mechanism prevailing in self-diffusion of metals. In such a case, the surface forces tending to decrease the total surface area will build a high concentration of holes[3] underneath the surface of the junction between the particle and the crystal block. This increment of concentration ΔC can be calculated from Kelvin's Eq 4

$$\Delta C = \frac{2\sigma\delta^3}{kT}\left(\frac{1}{\rho} - \frac{1}{x}\right) C$$

where C is the equilibrium concentration of the holes equal to $e^{-\frac{E}{RT}}$, E being the energy required to produce such a hole in the lattice. As $x >> \rho$ the last equation can be written in the following form

$$\Delta C = \frac{2\delta}{\rho}\frac{\delta^3}{kT} e^{-\frac{E}{RT}}$$

As the concentration gradient is approximately equal to $\frac{\Delta C}{\rho}$, we can write the Fick's equation for our case

$$A\frac{\Delta C}{\rho} D' = \frac{dV}{dt} \qquad [7]$$

where $\rho \cong \frac{x^2}{2a}$ $A \cong \pi\frac{x^3}{a}$ and $V \cong \pi\frac{x^4}{2a}$ as before and D' the coefficient of holes diffusion which obviously fulfills the following equation $D' e^{-\frac{E}{RT}} = D_v$ where D_v is the coefficient of volume self-diffusion for a given metal. Introducing all these values into Eq 7 and integrating, we obtain

$$\frac{x^5}{a^2} = \frac{40\sigma\delta^3}{kT} D_v t \qquad [8]$$

or in other words if the mechanism of diffusion was responsible for sintering, the fifth power of the interface radius is proportional to time.

SURFACE DIFFUSION

Very similarly we shall obtain the relation between radius x and time t in case the prevailing mechanism is surface diffusion. We have to put only $A \cong 2\pi\delta$ with concentration gradient and volume rate the same as in the case of volume diffusion.

Integrating the differential equation resulting from Fick's equation we obtain

$$\frac{x^7}{a^3} = \frac{56\sigma\delta^4}{kT} D_s t \qquad [9]$$

where D_s is the coefficient of surface diffusion.

Summing up we can tabulate the relationships between radius x of the interface formed during sintering between two particles and time t. These relations are as follows:

Viscous or plastic flow	$x^2 \sim t$
Evaporation and condensation	$x^3 \sim t$
Volume diffusion	$x^5 \sim t$
Surface diffusion	$x^7 \sim t$

The experiments described in the next paragraph were carried out in order to decide which mechanism or mechanisms actually prevail during sintering.

Experimental Method

In order to study experimentally the

Table 1 . . . Copper Powder

T°C	t hr	$x \cdot 10^{-4}$ cm	$a \cdot 10^{-4}$ cm	$\frac{x}{a}$	n
700	2.0	4.0	40.2	0.100	4.5
	4.0	5.1	41.0	0.134	
	8.0	7.2	41.0	0.176	
	41.0	14.0	39.0	0.250	
800	0.5	7.0	47.0	0.145	5.0
	2.0	10.0	53.0	0.188	
	3.0	7.2	36.0	0.200	
	4.0	9.0	40.1	0.222	
	16.5	13.6	44.5	0.303	
900	0.5	12.1	41.0	0.290	5.0
	1.0	14.0	43.2	0.330	

Table 2 . . . Silver Powder

T°C	t hr	$x \cdot 10^{-4}$ cm	$a \cdot 10^{-2}$ cm	$\frac{x}{a}$	n
500	3.0	6.5	1.95	0.033	5.4
	21.0	7.9	1.68	0.047	
	30.5	9.1	1.93	0.048	
	85.0	10.2	1.79	0.060	
600	8.0	11.6	1.88	0.062	5.0
	65.0	18.8	1.87	0.100	
	90.0	17.5	1.65	0.106	
700	2.5	12.0	1.74	0.070	4.8
	4.0	14.2	1.88	0.076	
800	1.0	15.9	1.90	0.084	4.9
	4.5	20.2	1.83	0.111	
	6.0	21.5	1.81	0.119	
	16.0	25.5	1.77	0.144	
	24.0	25.0	1.55	0.162	

relationship between the radius of the interface as a function of time and temperature it is necessary to measure this radius directly if possible. This was achieved by a very simple although somewhat laborious method. The metallic particles of spherical shape were dispersed on a flat block of the same metal, heated in a controlled atmosphere (hydrogen in the case of copper, hydrogen or air in the case of silver) at different temperatures and for various periods of time. After heating, the blocks with the particles sintered to them were mounted in bakelite and cut, in order to obtain a diametral cross-section of the particle in contact with the block. This cross-section was then examined under the microscope. The diameters of the particles and their interfaces with the blocks were readily measured with the microscope eyepiece micrometer. In order to assure the greatest accuracy of these measurements, the specimens were successfully polished down and after each of such operations readings of the radius of the interface for each particle were taken until a maximum radius was obtained.

The metals used in these experiments were copper and silver. The copper was round, atomized powder obtained from Greenback Industries, Inc. The shape of the powder particles was nearly

Table 3 . . . The Volume Diffusion Coefficient D_v of Copper

T°C	t hr	$a \cdot 10^{-4}$ cm	$x \cdot 10^{-4}$ cm	$D_v \frac{cm^2}{sec}$
400	6.0	20.0	0.5	4.2×10^{-16}
		13.0	1.0	3.2×10^{-14}
		3.2	0.8	3.0×10^{-13}
500	1.0	10.0	1.0	3.8×10^{-13}
		4.0	1.0	2.3×10^{-12}
	65.0	47.5	2.0	8.2×10^{-15}
		41.5	1.9	8.3×10^{-15}
		30.0	2.0	2.1×10^{-14}
600	0.5	4.5	1.8	8.0×10^{-11}
	1.0	15.5	1.7	3.5×10^{-12}
		3.8	1.7	4.5×10^{-11}
	3.0	10.0	1.7	2.0×10^{-12}
		4.2	2.3	5.1×10^{-11}
	16.0	40.5	4.1	1.9×10^{-12}
		28.0	3.4	1.6×10^{-12}
700	0.5	4.5	2.0	1.5×10^{-10}
	1.0	3.5	1.7	5.5×10^{-11}
	2.0	40.2	4.0	1.5×10^{-11}
	4.0	47.7	6.0	4.1×10^{-11}
		41.0	5.1	2.5×10^{-11}
		33.0	4.8	2.8×10^{-11}
		26 2	3.1	5.0×10^{-11}
		16.0	3.2	1.6×10^{-11}
	8.0	43.0	7.2	6.3×10^{-11}
	11 0	39 0	14.0	4.0×10^{-10}
800	0.5	47.0	8.0	1.6×10^{-9}
		39.8	7.0	1.1×10^{-9}
		35.3	6.0	6.6×10^{-10}
		11.0	3.6	5.3×10^{-10}
	2.0	53.0	10.0	9.4×10^{-10}
	4.0	40.1	9.0	4.9×10^{-10}
	16.5	45.0	13.6	7.3×10^{-10}
900	0.5	41.0	12.1	1.8×10^{-8}
	1.0	43.2	14.0	1.6×10^{-8}
		30.5	11.0	9.8×10^{-9}
1000	0.5	47.0	15.0	4.3×10^{-8}
		40.0	14.0	4.2×10^{-8}
		37.8	14.0	4.7×10^{-8}

spherical as can be seen from Fig 2, *a*, *b*, *c*, and *d*. The diameters of these particles ranged from 4 to 100μ. The powder was fractionated by the elutriation method into three lots. The first lot contained particles greater than 35μ in diameter. The second particles between 15–35μ and the third, particles less than 15μ. The silver used was coarse atomized powder of about 350μ in diameter furnished by Stevens Institute of Technology. This powder consisted of almost perfectly spherical particles as can be ascertained from Fig 3, *a* and *b*. The copper powder contained some oxygen so it was reduced by packing it in carbon and heating in a hydrogen atmosphere at 900°C for 18–24 hr. The resulting powder developed some blow holes. The copper blocks were cast of oxygen free high conductivity copper, the silver was spectroscopically pure. Their surfaces were thoroughly polished and cleaned by etching before the powders were dispersed on them. The copper was etched with ammonium hydroxide plus hydrogen peroxide and the silver specimens with potassium dichromate. After heating, the specimens were plated with nickel in order to avoid loosening or deforming the interfaces during the subsequent metallographic operations.

Table 4 . . . The Volume Diffusion Coefficient D_v of Silver

T°C	t hr	$a \cdot 10^{-4}$ cm	$x \cdot 10^{-4}$ cm	$D_v \frac{cm^2}{sec}$
500	3.0	195.0	6.5	3.4×10^{-12}
	21.0	168.0	7.9	1.3×10^{-12}
	30.5	193.0	9.1	1.8×10^{-12}
	85.0	178.0	10.2	1.2×10^{-12}
600	8.0	188.0	11.6	2.7×10^{-11}
	65.0	187.0	18.8	3.7×10^{-11}
	90.0	165.0	17.5	2.5×10^{-11}
700	2.5	174.0	12.0	1.4×10^{-10}
	4.0	188.0	14.2	1.6×10^{-10}
800	1.0	190.0	15.9	1.3×10^{9}
	4.5	183.0	20.2	1.0×10^{-9}
	6.0	181.0	21.5	1.1×10^{-9}
	16.0	177.0	22.5	1.0×10^{-9}
	24.0	155.0	25.0	8.1×10^{-10}
900	3.5	165.0	29.5	1.2×10^{-8}

Table 5 . . . The Surface Diffusion Coefficient D_s of Copper

T°C	t hr	$a \cdot 10^{-4}$ cm	$x \cdot 10^{-4}$ cm	$D_s \frac{cm^2}{sec}$
400	6.0	13.0	1.0	7.0×10^{-12}
		3.2	0.8	1.2×10^{-11}
500	1.0	10.0	1.0	1.1×10^{-9}
		4.0	1.0	1.6×10^{-9}
600	0.5	4.5	1.0	2.3×10^{-7}
	1.0	3.8	1.7	8.8×10^{-8}
	3.0	4.2	2.3	1.8×10^{-7}

Table 6 . . . The Heat of Activation Q_v of self Diffusion and Frequency Factor D°_v for Copper as Determined by Various Investigators

Authors	Q_v cal per mol	$D^\circ_v \frac{cm^2}{sec}$
F. N. Rhines and B. F. Mehl[6]	44,000	
B. V. Rollin[7]	61,000	47.0
J. Steigman, W. Shockley, F. C. Nix[8]	57,200	0.9–11.0
C. I. Raynor, L. Thomassen, and L. J. Rouse[9]	46,800	0.3
M. S. Maier and H. R. Nelson[10]	54–61,000	0.1–0.6
This Investigation	56,000	70.0
Silver		
W. A. Johnson[11]	45,900	0.89
This Investigation	42,000	0.60

At least ten particles were measured for each temperature or time period. Some micrographs of the observed particles sintered to the metallic blocks are shown in Fig 2, *a*, *b*, *c*, and *d* and Fig 3, *a* and *b*.

Very fine copper particles (less than 10μ) in diameter were not as round as the coarse ones and consequently yielded more scattered results. Also, it was impossible to polish down these particles, in order to obtain the maximum radius of their interface. Consequently a large number of them were

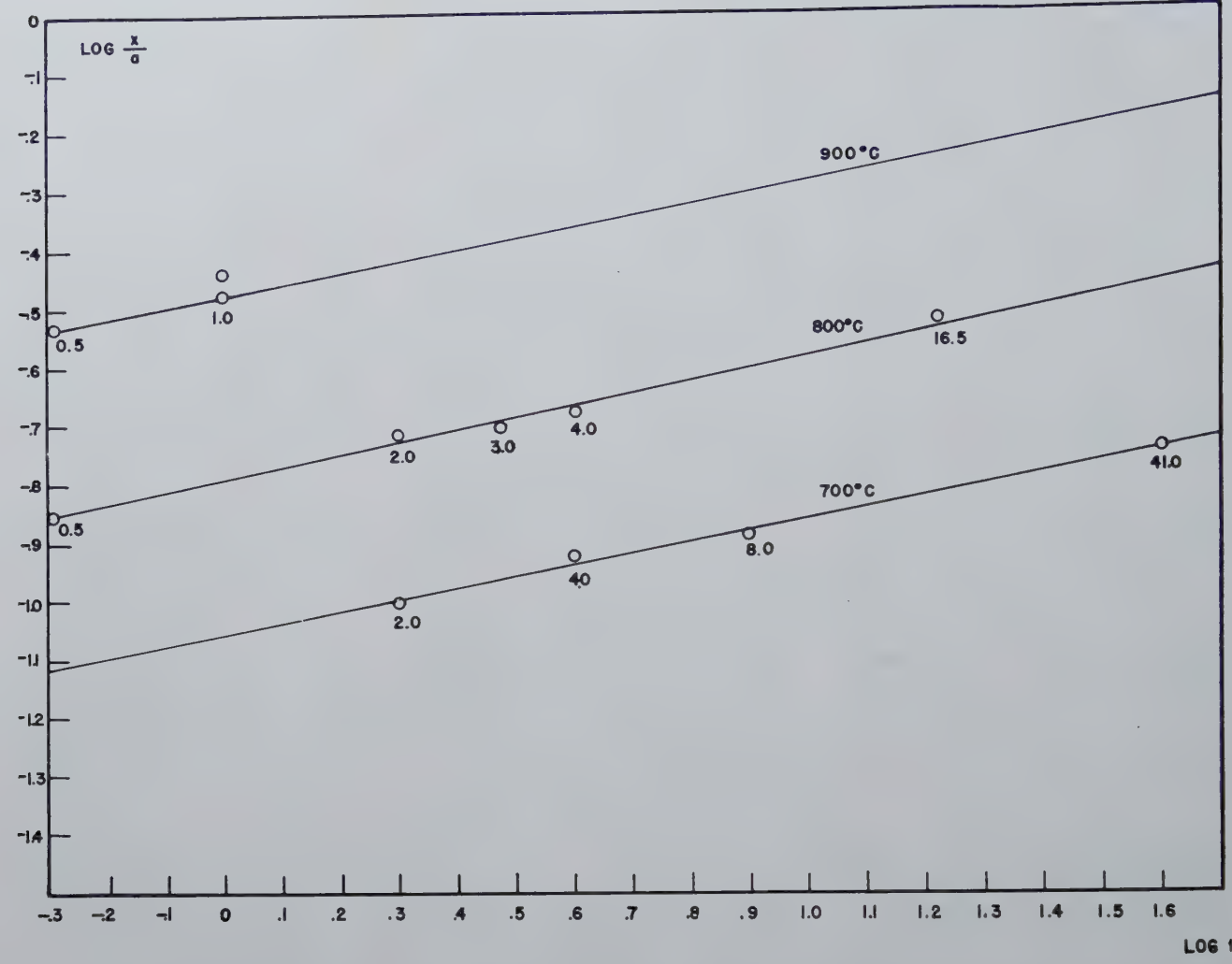

FIG 5—Logarithm of the ratio of the interface radius x to the radius a of silver particles sintered at indicated temperatures, plotted against the logarithm of sintering period t. The numbers at the points express time of heating in hours.

measured and only the largest values of radii were used for future calculations.

Results

Tables 1 and 2 contain the results obtained from measurements of the interface radii of copper and silver particles heated to different temperatures for various periods of time.

In the first and second columns of these tables, the temperature in degrees centigrade and time in hours are listed. The third and fourth column contain the observed radii of the interface and of the particle respectively (in centimeters). In the fifth column the ratios of these radii are given. The $\log \frac{x}{a}$ versus $\log t$ plots are given in Fig 4 and 5. The points fall on the straight lines whose inverse slope n is approximately equal to 5, as can be seen from the sixth volume of tables where the n values are listed.

The numbers at each point express the length of time in hours, for which a given specimen was heated.

The value 5 of the inverse slope n of the $\log \frac{x}{a}/\log t$ plot indicates that within the range of temperatures, periods of time and particle size, used in this work and listed in Tables 1 and 2, the predominant mechanism of sintering is volume diffusion in agreement with Eq 8. This last equation permits us to evaluate the coefficient of volume diffusion D_v for each temperature provided that the interface radius is known. There is uncertainty in the value of the surface tension of copper and silver as they have not been determined experimentally for solid metals. In this work the values of surface tension as measured for molten metals were adopted, based on the assumption that they should be close to those for solids. The error introduced by this choice would not change the order of magnitude of the coefficient of diffusion, calculated from Eq 8. Thus, for copper $\sigma = 1200$ ergs per cm^2 and for silver $\sigma = 1000$ ergs per cm^2 was used.[5] The values of D_v for copper and silver are listed in Tables 3 and 4 respectively, along with temperatures and periods of heating time, radii of the particles and interfaces.

D_v was plotted on the semi-logarithmic scale against $\frac{1000}{T}$. T being absolute temperature. For large particles of 40μ or more in diameter straight lines were obtained as shown in Fig 6 and 7.

The heats of activation of volume diffusion, Q_v, and frequency factors, D^0_v were determined from these graphs. Thus for copper Q_v is 56000 cal per mol and $D^0_v = 70 \frac{\text{cm}^2}{\text{sec}}$ and for silver $Q_v = 42000$ cal per mol and $D^0_v = 0.6 \frac{\text{cm}^2}{\text{sec}}$. These values are in good

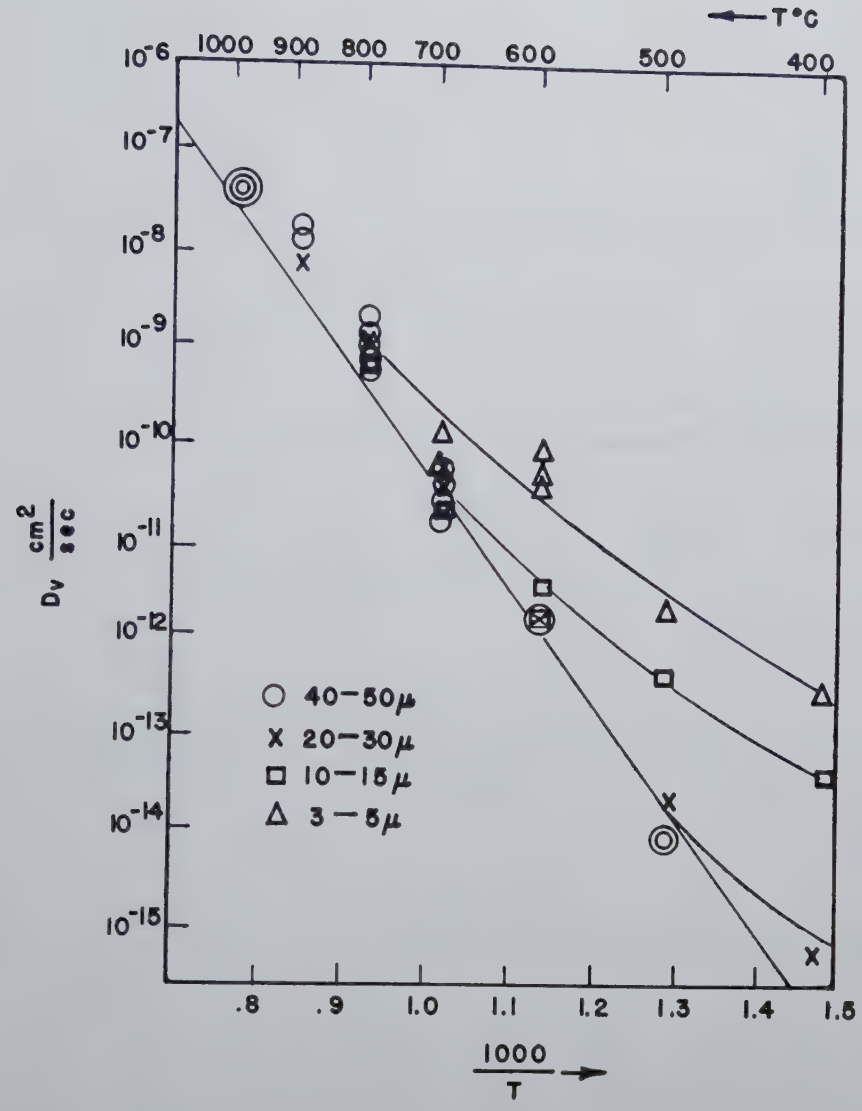

FIG 6—Variation of volume self-diffusion coefficient of copper with temperature as determined from sintering experiments. Logarithm of D_v vs. reciprocal of absolute temperatures.

agreement with those obtained by various workers who used the radioactive tracer method as is shown in Table 6. This suggests that the above described method may successfully be used for determination of the coefficient of self-diffusion of metals without using radioactive tracers. As it is difficult to get a perfectly round metallic particle it is more convenient to use wires and measure their rate of sintering to metallic blocks.*

Fig 6 shows that the coefficients of volume diffusion calculated from the rates of interface growth for small particles, (less than 30μ in diameter) when plotted on the semi-logarithmic scale versus $\frac{1}{T}$ at lower temperatures show deviations from the straight line although they fall on this line at higher temperatures; the smaller the particles the greater the deviations. These deviations are due to the surface diffusion mechanism predominant at lower temperatures and for smaller particles as will be proven later. In cases where both mechanisms, volume and surface diffusion, take place, the flow equation will be as follows:

$$\frac{dV}{dt} = nf_v + mf_s \qquad [10]$$

n and m are fractions of the overall contributing flow, functions of x and a and obviously fulfill the relationship $n + m = 1$. From Eq 8 and 9 f_v and f_s are easily calculated their values being as follows:

$$f_v = \frac{16\pi a\sigma\delta^3}{kTx} D_v$$

$$f_s = \frac{16\pi a^2\sigma\delta^4}{kTx^3} D_s$$

Substituting these values as f_v and f_s into Eq 10, we obtain

$$\frac{dx}{dt} = \frac{8a^2\sigma\delta^3}{kTx^4}\left(nD_v + m\frac{a}{x^2}D_s\right), \quad \text{since } V \cong \frac{x^4}{2a} \qquad [11]$$

When the contact area, or the radius x, is very small one should expect that the contribution of flow due to surface diffusion will be overwhelmingly greater than that due to volume diffusion especially as $D_s > D_v$. In such cases also $m \cong 1$ and Eq 11 reduces to

* The work leading toward experimental testing of this latter method is now in progress in the Sylvania Metallurgical Laboratories.

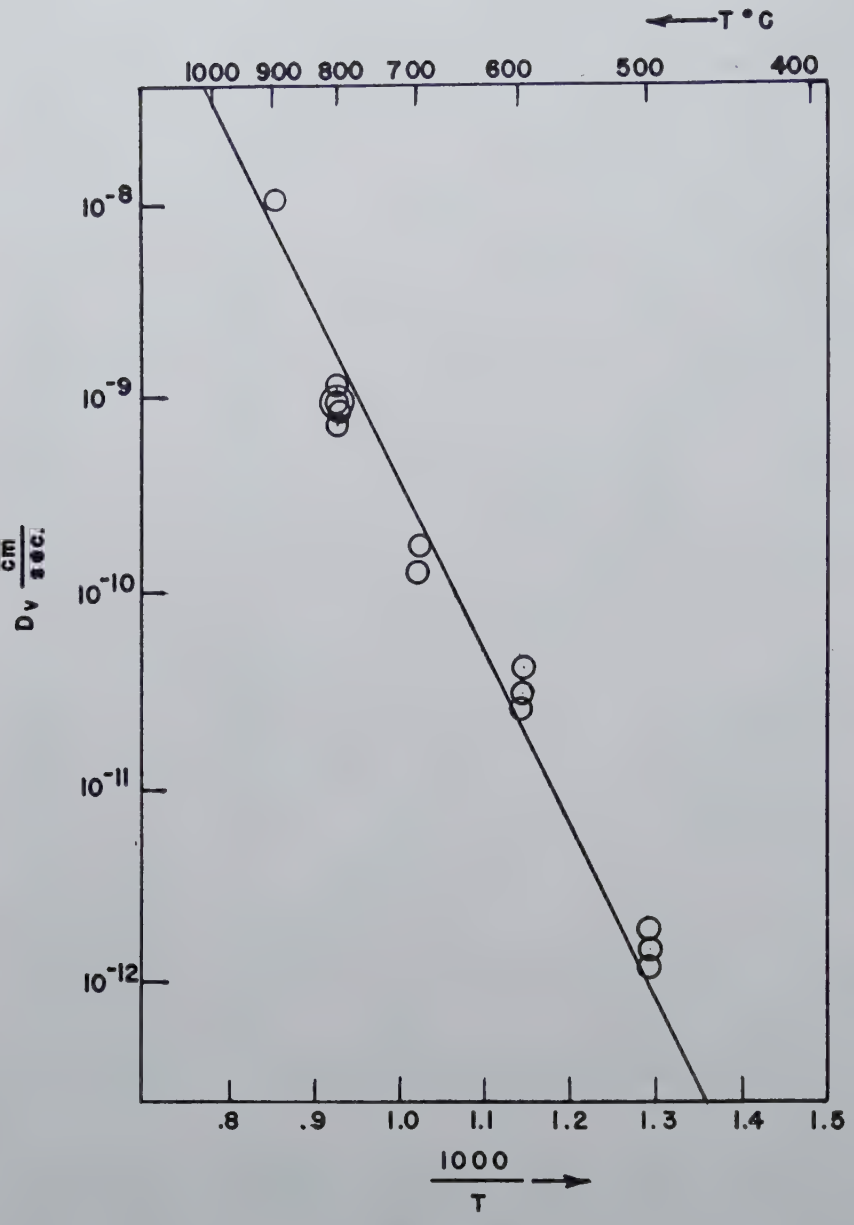

FIG 7—Variation of volume self-diffusion coefficient of silver with temperature as determined from sintering experiments. Logarithm of D_v vs. reciprocal of absolute temperature.

$$\frac{dx}{dt} = \frac{8a^3\sigma\delta^4}{kTx^6} D_s$$

which after integration gives Eq 9. The effect of surface diffusion upon sintering should be noticeable at low temperatures when D_v and x are very small, especially for small particles which have larger surface atom to volume atom ratios, and will sinter by the mechanism of surface diffusion to the longer interface radii x than the large particles. This reasoning seems to be fully substantiated by experiments as seen in Fig 6, where deviations are the larger the smaller are the particles and the lower is the sintering temperature up to about 600°C for the particles of 10μ diam or less, the volume diffusion contribution can be neglected and the problem can be treated as surface diffusion only.

In order to prove that the above discussed deviations are really due to surface diffusion, the fine (about 10μ in diam) copper powder was sintered to the copper block at 600°C for 0.5, 1, and 3 hr. The logarithm of the ratios of the radius of the interface x to the radius of the particle was plotted against log t (Fig 8) and a straight line was obtained. The inverse slope of this curve $n = 6.5$ is sufficiently close to the theoretical value 7 to indicate that the sintering mechanism in this case is predominantly surface diffusion.

Finally the experimental values of x measured at 400, 500 and 600°C allow us to estimate the surface diffusion coefficients of copper at these temperatures, from Eq 9. The calculated values of D_s are listed in Table 5 along with the values x and a. The semi-logarithmic plot of D_s vs. $\frac{1000}{T}$ is given in Fig 9. The results obtained from two sizes of particles (20 and 8μ diam) are in excellent agreement with each other. The energy of activation of surface diffusion as determined from the slope of the straight line represented in Fig 9 is $Q_s = 56{,}000$ cal per mol, the same as for volume diffusion evaluated before. The frequency factor $D_s^0 = 10^7$ $\frac{cm^2}{sec}$ is 10^5 higher than that for volume diffusion which means that although the same energy is required to change the position of an atom on the surface as inside the crystal lattice, the number of atoms possessing this activation energy is much larger on the surface than inside the crystal.

As nobody has ever before measured the coefficient of surface self-diffusion, data obtained in this work cannot be checked but the order of magnitude appears to be reasonable. The fact that energies of activation of volume and surface diffusions are nearly equal may very well be explained by Schottky's[12] mechanism of diffusion. According to him all vacancies are generated on the surface, consequently the energy of the formation of vacancy should be the same in both cases. The only difference should be expected in energies required to move an atom to the adjacent vacancy which in the case of surface migration should be lower than in the case of volume diffusion. It is believed that the greatest part of heat of diffusion is the energy required to make a vacancy on the surface. If this is true the differences in the remaining part of the energy of activation could be small enough to bar detection.

It has therefore been proven that at least for metals of low vapor pressure the rate of interface formation among sintered particles is a process controlled in the early stage by surface diffusion and in the later stage by volume diffusion. No other mechanism such as viscous flow which has been considered by Frenkel[1] and Shaler and Wulff[2] seems to be involved. The process of sintering by volume diffusion excludes the possibility of an atom exchange mechanism of diffusion[4,13,14] because in such a case no gradient

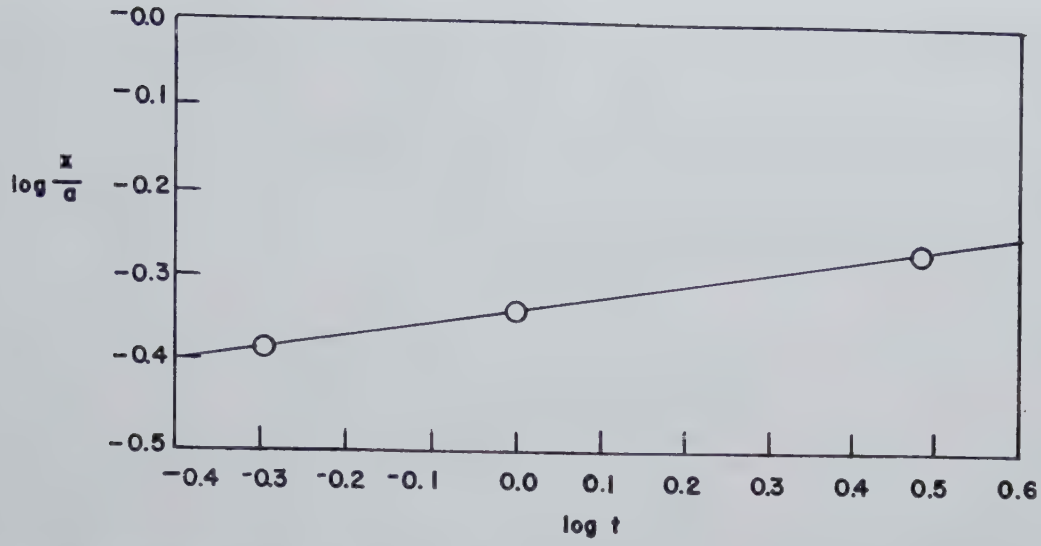

FIG 8—Logarithm of the ratio of the interface radius x to the radius a of the small copper particles (about 4μ) sintered at 600°C, plotted against the logarithm of sintering period t.

driving the atoms towards the interface, is possible. It seems to appear then that diffusion in solids proceeds through the mechanism of imperfections in the lattice such as vacancies or interstitial atoms.

Conclusions

1. It has been proven experimentally that the mechanism of sintering of two metallic particles or of a metallic particle and a flat metallic block at atmospheric pressure is predominantly that of volume diffusion for large particles and higher temperatures.
2. It is possible to measure the coefficient of self-diffusion without radioactive tracers, measuring only the rate of growth of the interface between round particles and a metallic block. The method has been checked successfully in the case of copper and silver.
3. Strong experimental evidence has been presented that at the beginning of sintering surface diffusion is operative.
4. The surface diffusion coefficient of copper has been determined.

Acknowledgment

The author wishes to express his gratitude to Mr. W. E. Kingston, Manager of Sylvania Metallurgical Laboratories, for his support of this project. Greatest indebtedness and gratitude are due to Dr. I. Zavarine of Sylvania Electric Products Inc. for his priceless suggestions and help in the experimental part of this work, and to Dr. C. Herring of Bell Telephone Research Laboratories for frequent helpful discussions of the theoretical part of this paper. The author wants to thank Mrs. L. Roth of Sylvania Electric Products Inc. for her skillful metallographic work.

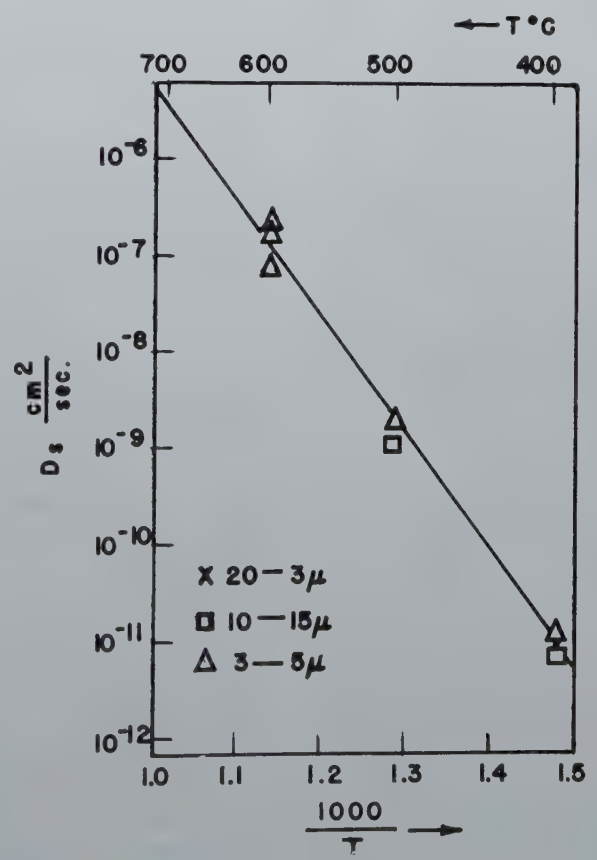

FIG 9—Variation of surface self-diffusion coefficient of copper with temperature as determined from sintering experiments of small particles. Logarithms of D_s vs. reciprocal of absolute temperature.

References

1. J. Frenkel: *Jnl. Phys.* U.S.S.R. (1945) **9**, No. 5, 385.
2. A. J. Shaler and J. Wulff: *Ind. Eng. Chem.* (1948) **40**, 838.
3. B. Ya. Pines: *Jnl. Tech. Phys.*, (1946) **16**, No. 6, 737.
4. R. F. Mehl: *Trans.* AIME (1936) **122**, 11.
5. A. Samoilovich: *Acta Physicochimica* U.S.S.R., (1946) **21**, 13.
6. F. N. Rhines and R. F. Mehl: *Trans.* AIME (1938) **128**, 285.
7. B. V. Rollin: *Phys. Rev.* (1931) **55**, 231.
8. J. Steigman, W. Shockley and F. C. Nix; *Phys. Rev.* (1939) **56**, 13.
9. C. L. Raynor, L. Thomassen and L. J. Rouse: *Trans.* Am. Soc. Met. (1942) **30**, 313.
10. M. S. Maier and H. R. Nelson: *Trans* AIME (1942) **147**, 39.
11. W. A. Johnson: *Trans.* AIME (1941) **143**, 107.
12. W. Schottky: *Ztsch.* Phys. Chem. B. (1935) **29**, 335.
13. J. Cichocki: *Jnl. de Phys.* (VII) (1938) **9**, 129.
14. F. Seitz: The Modern Theory of Solids. (1940) McGraw-Hill.

A Simple Constant Stress Creep Test

J. C. FISHER* and R. P. CARREKER*

CREEP tests are normally constant load tests. Such tests approximate some types of service conditions and therefore are justified from the engineering point of view. Coupled with this consideration is the advantage of simplicity inherent in constant load tests, as contrasted with the comparatively complex requirements of a constant stress test. It is not surprising that the vast majority of creep tests reported are of the constant load type.

Despite the enormous amount of accumulated creep test data, plastic flow is by no means completely understood. The widespread use of constant load tests is at least partly responsible for this lack of understanding. Any attempt to analyze deformation must involve the more fundamental quantity stress, rather than load. It is possible to predict constant load behavior from known constant stress data, but the reverse is much more difficult.

When a metal specimen elongates, as in a creep test, the cross section decreases, maintaining constant volume. Thus

$$\frac{A}{A_0} = \frac{l_0}{l}. \qquad [1]$$

For a constant stress test the force on the specimen must be decreased as the cross section decreases, that is, this force must be inversely proportional to the elongation of the specimen. Andrade has described three methods of obtaining the constant stress condition,[1-3] each of which is relatively complex. The most recent proposal,[3] suggests a major simplification which maintains the simplicity of the constant load test while approximating quite closely the desirable condition of constant stress. Andrade's device is admittedly more accurate but the method described below has definite advantages.

Consider a specimen in the form of a "V" supported at its ends. If a weight be applied at the vertex of the angle, the stress in each leg of the "V" is

$$S = \frac{w}{z} \cdot \sec\frac{\alpha}{z} \cdot \frac{1}{A}. \qquad [2]$$

If this stress causes an elongation Δl in each leg of the "V," the angle decreases from α_0 to a smaller angle α_1. The quantity $\sec \frac{\alpha}{z}$ thus decreases with specimen elongation while the quantity $1/A$ increases. By selecting proper initial conditions it should be possible to hold S/S_0 very nearly constant at unity.

The proper initial conditions are realized when α_0 is made equal to approximately 90°. Fig 1 compares the ratios of S/S_0 for $\alpha_0 = 85, 90, 95, 100°$, with $\alpha_0 = 0$, that is, a straight specimen, for true strains up to $\epsilon = 0.10$. It may prove convenient to measure X, the movement of the vertex, rather than the true elongation Δl. Contour lines of X/l_0 are also plotted in Fig 1.

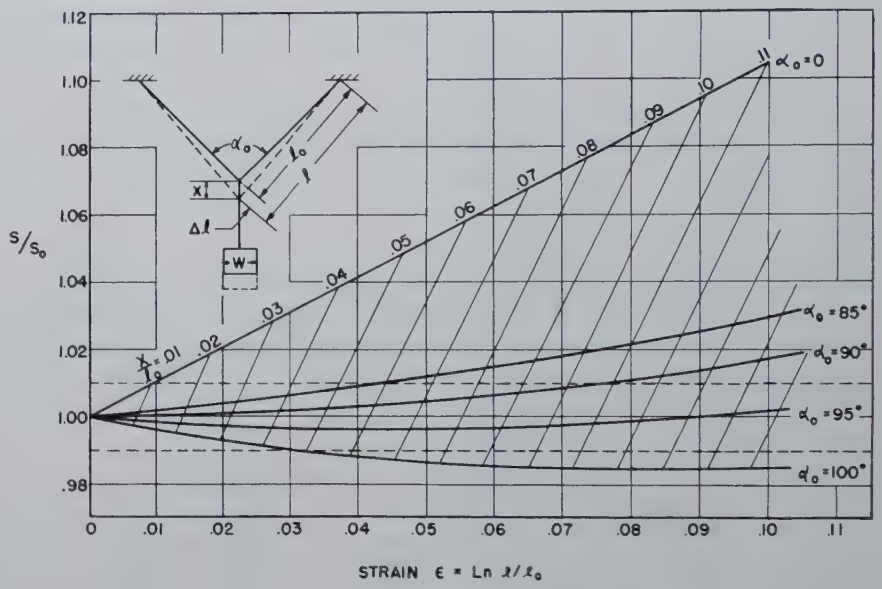

FIG 1—Variation of stress with initial angle.

The method for obtaining constant stress described above is especially suited to the testing of small wires, but may easily be extended to rods of any diameter through the use of a suitable grip which serves as the vertex joining two identical rods forming the legs of the "V."

Technical Note No. 10 E. Manuscript received October 13, 1948.

*General Electric Co., Schenectady, N. Y.

[1] References are at the end of the paper.

References

1. E. N. da C. Andrade: On the Viscous Flow in Metals, and Allied Phenomena. *Proc.* Roy. Soc., A, **84**, 1, (1910–11).
2. E. N. da C. Andrade and B. Chalmers: The Resistivity of Polycrystalline Wires in Relation to Plastic Deformation, and the Mechanism of Plastic Flow. *Proc.* Roy. Soc., A, **138**, 348, (1932).
3. E. N. da C. Andrade: A New Device for Maintaining Constant Stress in a Rod Undergoing Plastic Extension. *Proc.* Phys. Soc., **60**, (3), 304, (March, 1948).

Homogeneous Yielding of Carburized and Nitrided Single Iron Crystals

A. N. HOLDEN* and J. H. HOLLOMON,* Junior Member AIME

Introduction

INHOMOGENEOUS yielding during the early stages of plastic flow has been observed in many metals and has long been a subject of controversy.

Low carbon steel, when strained at room temperature, exhibits a distinct yield point at which the metal ceases to behave elastically and begins to flow plastically without further increase in stress,† often with an actual decrease in stress from that existing at the yield point. One manifestation of this behavior is the familiar Lüders lines. The extent of the yield point elongation (the plastic strain which results without raising the stress above that at the initial yield point) may be several percent.

Several explanations of this type of yielding in steels have appeared in the literature:[1–3]‡

1. The segregation of carbides or other constituents at the grain boundaries of ferrite forms cell-like blocks which break down at a higher stress than that at which the ferrite alone will flow.

2. The precipitation of various constituents within the ferrite itself in some way blocks initial flow until a higher stress is reached, after which a great deal of flow occurs without further increase in stress.

3. The restraining influence of neighboring, less favorably oriented grains in a polycrystal results in a storing up of energy, which on yielding is sufficient to cause the continued propagation of slip bands on the multiplicity of slip systems available in adjacent iron crystals without increase in stress.

4. Local segregation of carbon atoms increases the stress required for the initial propagation of dislocations. The stress required for further deformation is lower.[3] Such an explanation would require the presence of upper and lower yield points in single crystals.

Low and Gensamer[2] have shown that heterogeneous yielding can be eliminated by removal of carbon and nitrogen from polycrystalline steels by wet-hydrogen treatment. They also demonstrated that the re-introduction of minute amounts of carbon or nitrogen caused a return of the yield point.

Observations of the initial flow of single crystals containing small amounts of carbon and nitrogen should provide a clue to the explanation of inhomogeneous yielding. Previous tests of iron crystals[4–6] can not be considered conclusive because it is uncertain whether the carbon and nitrogen were satisfactorily removed by the decarburization technique employed.

The purpose of the experiments described herein was to determine whether single iron crystals containing either carbon or nitrogen would exhibit inhomogeneous yielding.

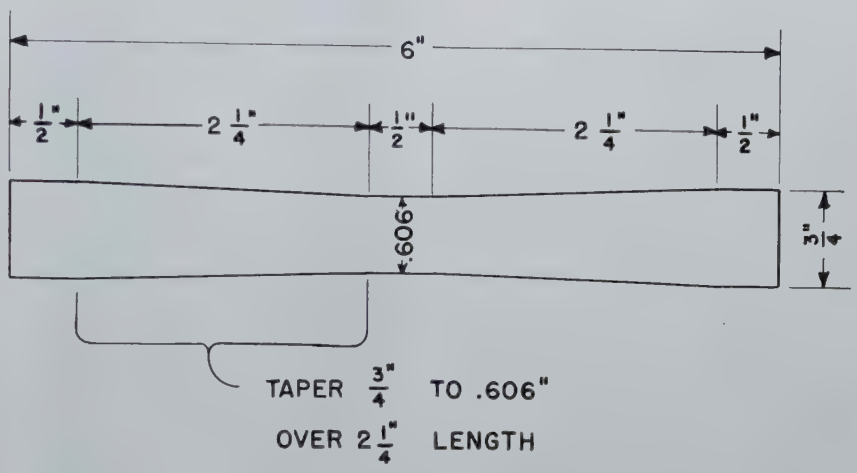

FIG 1—Shape of iron specimens.

Experimental Procedures

THE PREPARATION OF SINGLE CRYSTALS

All crystals were formed in the following way. Aluminum killed sheet material 80 mils thick was machined into specimens of the outer contour shown in Fig 1. These mildly tapered specimens were decarburized at 730°C for 16 hr in hydrogen that had been bubbled rapidly through water maintained at 70°. The resultant grain size after decarburizing was approximately ASTM 5. Several stress-strain curves were made of the decarburized mate-

San Francisco Meeting, February 1949.

TP 2521E. Discussion of this paper (2 copies) may be sent to *Transactions* AIME before May 15, 1949. Manuscript received June 2, 1948; revision received November 12, 1948.

* General Electric Research Laboratory, Schenectady, N. Y.

[1] References are at the end of the paper.

† Other types of inhomogeneous or discontinuous yielding have been observed in aluminum and other aging alloys as well as in some fairly pure metals. The terms inhomogeneous, heterogeneous, or discontinuous yielding used in this paper refer to the particular initial yielding of steel tested at room temperature.

‡ An excellent bibliography of the subject appears in Ref. 2.

rial, two of which are shown in Fig 5. The material as-wet-hydrogen treated yielded homogeneously. Nothing is known of the production history of the sheet prior to the decarburization treatment.

The material used for these specimens was analyzed before and after decarburization (carbon was determined by low pressure combustion and nitrogen by a Kjeldahl determination). The analyses were:

As-received	Pct	Wet-Hydrogen Treated	Pct
C	0.090	C	0.004
N	0.0045	N	0.003
*Al	0.09	*Al	0.09
†Si	0.05	†Si	0.05
†Mn	0.25	†Mn	0.25
Fe	balance	Fe	balance

* Total aluminum
† Spectrographic

After the wet-hydrogen treatment, the tapered specimens were strained until the change in area of the reduced section as measured with a micrometer was 2.7 to 3 pct. Subsequent annealing in pure dry hydrogen at 885°C for 72 hr converted the tapered specimens into large crystals.* Several crystals were as wide as the specimens and 4 in. in length. However, the surface of the specimens contained fine grains which had to be removed by grinding before the large crystals could be revealed by etching. It was found necessary to grind 10 mils off each flat surface with a special wheel. A photograph of a typical specimen after grinding and etching appears in Fig 2, showing the size of recrystallized grains resulting from the treatment described.

The important features of the strain-anneal method used in these experiments are the following: First, the specimens were so shaped that recrystallization was limited to a small volume of critically strained material in the narrowest region. Second, a grain formed in the critically strained region readily grew to the lesser strained regions and larger grains resulted. The lesser strained regions were not deformed sufficiently to recrystallize. Third, the specimens were placed in a hot furnace for the annealing treatments.

Tapered specimens have been employed previously,[7–10] but tapers used have been more extreme than that used in these experiments.

After forming the large grains, crystal tensile specimens were cut out with a jeweler's saw. All of the tapered specimens did not yield large enough grains from which to cut single crystal tensile specimens. Data are included for all crystals tested. The single crystal specimens had reduced sections of from $\frac{3}{4}$ in. to 2 in. in length and from $\frac{3}{16}$ in. to $\frac{5}{16}$ in. in width.

* Similar attempts have been made to obtain large single crystals of a "rimming" steel but as yet none has been successful.

FIG 2—Typical crystal size after strain annealing.

HEAT-TREATING AND TESTING OF IRON CRYSTALS

The single crystal tensile specimens were annealed in wet-hydrogen at 850°C for 16 hr. All specimens remained single crystals and it was assumed that all machining strains and any remaining carbon were removed during this treatment. Low and Gensamer[2] have found the carbon to be less than 0.003 pct after wet-hydrogen treatments. Some of the crystals were carburized by the method used by Low and Gensamer. They were annealed at 675°C for 4 hr in a mixture of butane and hydrogen. Just enough butane was bled into the furnace to color faintly the flame at the furnace door. Several polycrystals were carburized along with the single crystals to make certain that the process was effective. All of these carburized specimens were then homogenized for 5 hr at 650°C in a nitrogen atmosphere obtained by passing tank nitrogen over copper chips at 500°C and activated alumina. After this treatment, the crystals contained 0.005 pct N_2 and 0.019 pct C.

Nitriding of some of the crystals was carried out by treatments of 4 hr at 525°C in an ammonia atmosphere. The hard nitrided case was ground off to a depth where no nitrides were observable metallographically. The crystals were then stress relieved and homogenized for 5 hr at 650°C in a nitrogen atmosphere. Several polycrystalline specimens were nitrided along with the single crystals to make certain the nitriding was adequate. After treatment, the crystals contained 0.004 pct C, and 0.073 pct N_2. This nitrogen certainly exceeds the limit of solubility and probably the crystals contained a precipitated second phase even though it was not observed metallographically.

All the crystals thus far described were tested in a hydraulic tensile machine with Templin sheet grips mounted on spherical seats. Reasonable care was used in alignment. Strain was measured with a single resistance type strain gauge with a sensitivity of 2×10^{-6}. The rate of testing was the

Table 1 . . . Heat-treating and Testing of Iron Crystals

Spec. No.	Heat Treatment	Testing
12	Wet hydrogen—850°C	Templin grips—ball seat
13	Wet hydrogen—850°C	Templin grips—ball seat
23	Wet hydrogen—850°C	Templin grips—ball seat
34–2	Wet hydrogen 850°C, carburize at 675°C, homogenize at 650°C in nitrogen	Templin grips—ball seat
35	Wet hydrogen 850°C, carburize at 675°C, homogenize at 650°C in nitrogen	Templin grips—ball seat
37	Wet hydrogen 850°C, carburize at 675°C, homogenize at 650°C in nitrogen	Templin grips—ball seat
33	Wet hydrogen 850°, nitride 525°C, case ground off, homogenized at 650°C.	Templin grips—ball seat
38	Wet hydrogen 850°, nitride 525°C, case ground off, homogenized at 650°C.	Templin grips—ball seat
39	Wet hydrogen 850°, nitride 525°C, case ground off, homogenized at 650°C.	Templin grips—ball seat

same for all crystals and was such as to give 1 pct strain in 45 min. The methods of heat treating and testing are summarized in Table 1 for crystals thus far described.

It later became evident that more accurate methods of evaluating the effect of carbon and nitrogen on the strength of single crystals would be valuable. Therefore, several experiments were performed on pairs of single crystal tensile specimens cut from the same crystal.

An alternative nitriding procedure to that previously employed was used to nitride the crystal pairs. It consisted of passing hydrogen through a catalytic deoxidizer, activated alumina drier, activated charcoal tube, liquid nitrogen trap, ammonia absorber and into the nitriding furnace at 500°C. The ammonia absorber was kept at −78°C to avoid the formation of any hard nitride case which would have to be removed.

In these experiments the carburization of each of the crystals of the pairs was the same as that employed previously.

One nitrided and one carburized crystal together with their identically oriented wet-hydrogen treated counterparts were annealed in vacuum. It was intended that the temperature of the vacuum anneal would not exceed 750°C but inadvertantly it exceeded 910°C. These specimens did not remain single crystals, but became very coarsely polycrystalline.

Orientations were determined for all pairs of crystals except the specimens which became polycrystalline. These orientations are shown in Fig 3.

FIG 3—Orientation of crystal pairs (cube poles determined with optical goniometer).

The testing of crystal pairs was done in a hydraulic machine. Eight of these crystals were pulled with long flexible rods so designed that only axial loads were transmitted (see Fig 4), while the others were tested in Templin grips as previously described.

The eccentricity of the strain in the eight accurately aligned specimens was measured by the following means. Two rigid glass fibers about 6 in. in length were cemented to one side of each specimen perpendicular to the tensile axis and about ¾ to 1 in. apart. The distance between the ends of the fibers was measured with an accurate micrometer-type cathetometer sensitive to 0.001 mm. The 6-in. lever of the fibers gave a multiplication of the eccentricity of about 64. The relation between the change in readings of the cathetometer and eccentricity can be found provided the strain at the center line of the specimen is measured.* The average center line strain was measured with two resistance strain gauges cemented to the opposite flats of the specimen.

The edge strain was within 4 pct of the center line strain without any adjustment of the fixtures other than that automatically applied by the flexible tension members.

The heat treating and testing methods for the crystal pairs is summarized in Table 2.

* M = eccentricity = $\frac{e - e'}{e} = \left(\frac{w/2}{l}\right)(e - \Delta)$

e' = strain at edge of specimen
e = strain at center line of specimen
w = width of specimen
l = length of glass fibers
Δ = change in distance between fiber ends upon application of strain e.

Results

All the data are presented in the form of stress-strain curves.

Fig 5 compares the flow of polycrystalline specimens in the wet-hydrogen treated, carburized and nitrided states. These tests indicate that either carbon or nitrogen causes the return of the discontinuous yield in material which showed no discontinuity in its flow curve as wet-hydrogen treated. The nitrided polycrystals in Fig 5 contained considerable nitrogen (about 0.07 pct) which accounts for their high yield strength. The carburizing treatment on the other hand was quite mild, and the carburized polycrystals showed less increase in yield strength over the wet-hydrogen treated specimens.

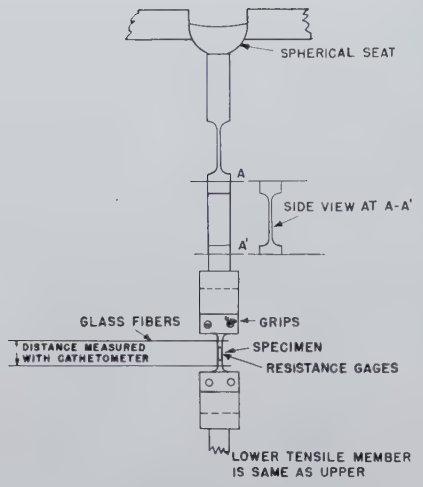

FIG 4—Flexible tensile member for axial loading of iron crystals.

Fig 6, 7, and 8 show the flow curves for nine iron crystals. The crystals whose tensile properties are those of Fig 6 were thoroughly treated in wet-hydrogen. The crystals of Fig 7 were carburized and those of Fig 8 were nitrided. None of these crystals yielded inhomogeneously. The high strength of the nitrided crystals is due to the considerable amount of nitrogen these contained.

Fig 9 and 10 show the effect of the described carburizing treatment on the flow of single iron crystals. In these two figures the flow of carburized crystals is compared with that of decarburized crystals of the same orientation. Fig 9 was obtained by testing four crystals cut from the same grain, two of which were carburized and two of which were decarburized. A scattering of the data for two identical crystals is thus obtained as well as the difference in flow strengths of the two materials. Fig 10 is the result of a test of two different pairs of crystals, one of each pair being carburized while the other was decarburized.

While the tests in Fig 9 and 10 were made in Templin grips with only moderate care in alignment, the results are significant. All crystals yielded homogeneously, and allowing for the scatter of the data, the carburized crystals were 5 to 10 pct stronger up to 0.6 to 0.7 pct strain.

Fig 11 shows the yielding of crystals 5-1 and 5-2 of identical orientation. Crystal 5-1 was nitrided under conditions which did not form a hard case. Crystal 5-2 was completely decarburized in wet hydrogen. The nitrided crystal was slightly higher in flow strength than the decarburized crystal. Both crystals yielded homogeneously.

Table 2 . . . Heat-treating and Testing Procedure for Crystal Pairs

Spec. No.	Heat Treatment	Testing
1-1	Carburized	Templin and ball seat
1-2	Carburized	Templin and ball seat
1-3	As wet hydrogen treated	Templin and ball seat
1-4	As wet hydrogen treated	Templin and ball seat
3-1	Carburized	Templin and ball seat
3-2	As wet hydrogen treated	Templin and ball seat
4-1	Carburized	Templin and ball seat
4-2	As wet hydrogen treated	Templin and ball seat
5-1	Nitrided (saturator at −78°C)	Special grips †M = 2.4 pct
5-2	As wet hydrogen treated	Special grips M = 3.7 pct
*6-1	Nitrided (−78°C)—vacuum annealed	Special grips M = 1.81 pct
*6-2	As wet hydrogen treated—vacuum annealed	Special grips M = 2.04 pct
7-1	Carburized	Special grips M = 2.3 pct
7-2	As wet hydrogen treated	Special grips M = 3.1 pct
*8-1	Carburized—vacuum annealed	Special grips M = 1.92 pct
*8-2	As wet hydrogen treated—vacuum annealed	Special grips M = 2.65 pct

* Became polycrystalline on vacuum annealing.
† Eccentricity as defined in footnote on p. 181 expressed as a percentage.

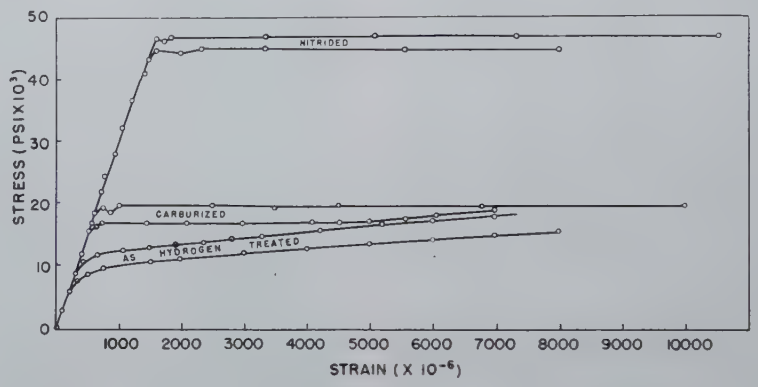

FIG 5—Yielding of polycrystalline iron.

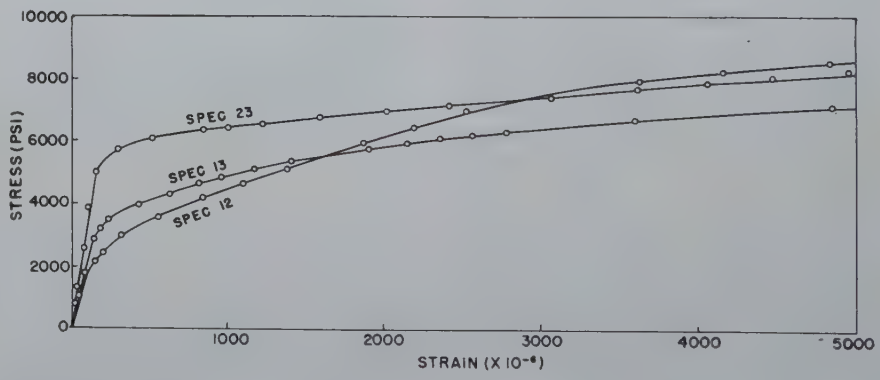

FIG 6—Wet hydrogen treated crystals of iron, random orientation, tested with single gauge in Templin grips.

Fig 12 is a plot of the flow of two identically oriented specimens. 7-1 was carburized, and 7-2 was decarburized in wet-hydrogen. The carburized crystal was considerably stronger than the decarburized crystal. Both crystals yielded homogeneously.

Fig 13 and 14 are plots of the flow characteristics of specimens which became coarsely polycrystalline during a vacuum anneal in which the temperature was inadvertantly raised too high.

Fig 13 shows the flow of a nitrided polycrystalline specimen compared to a decarburized polycrystalline specimen in which the grain size was ¼ in. or larger in diam. Fig 14 shows the deformation behavior of a carburized polycrystalline specimen in which the grain size is approximately ¼ in. in diam. The decarburized polycrystals in both instances did not yield discontinuously. The flow curve of the carburized polycrystal, however, contains a

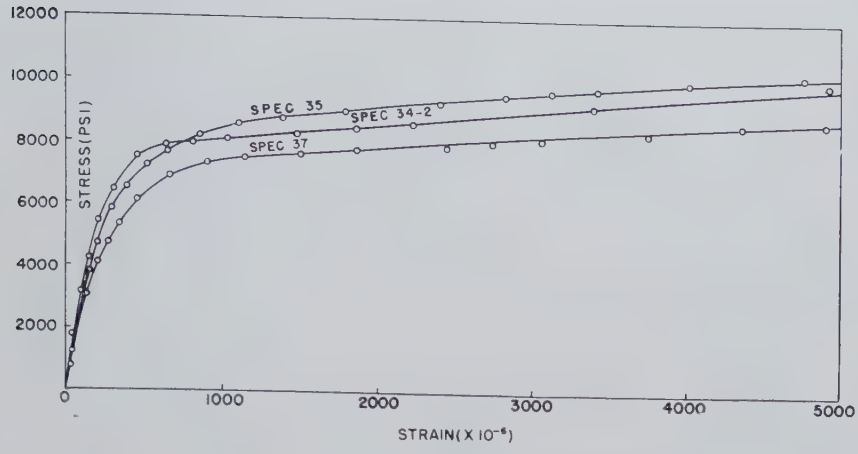

FIG 7—Carburized crystals of iron, random orientation, tested with single gauge in Templin grips.

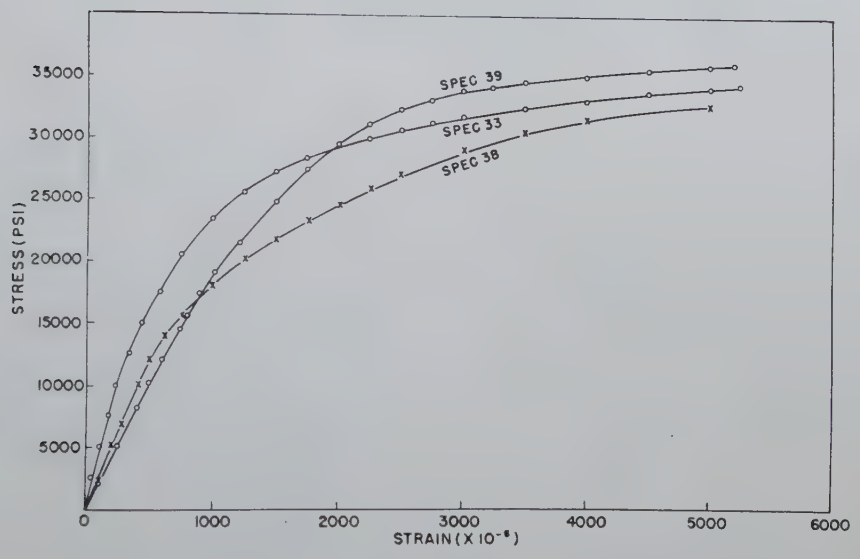

FIG 8—Nitrided crystals of iron, random orientation, tested with single gauge in Templin grips.

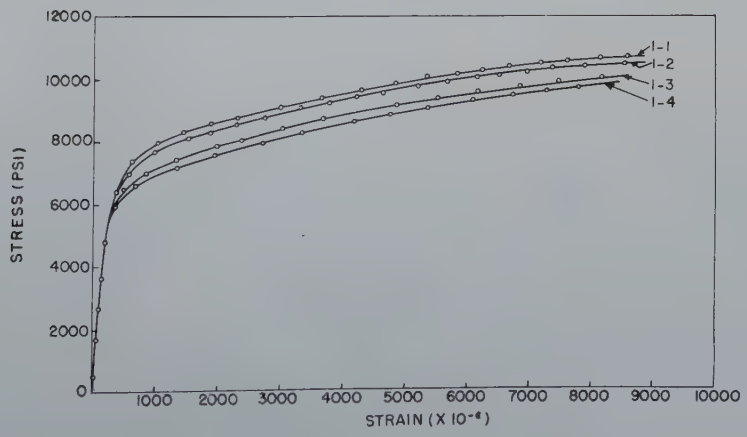

FIG 9—Yielding of four identically oriented iron crystals. 1-1 and 1-2 were carburized. 1-3 and 1-4 were decarburized. Tested with 2 averaging gauges in Templin grips.

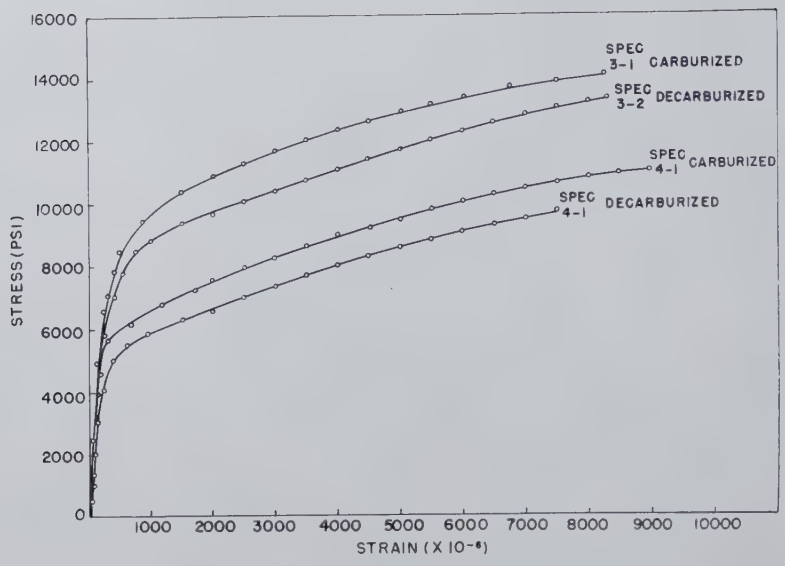

FIG 10—Yielding of iron crystal pairs showing effect of carbon on flow strength. Tested with 2 averaging gauges in Templin grips. Orientation of 4-1 and 4-2 is the same and orientation of 3-1 and 3-2 is the same.

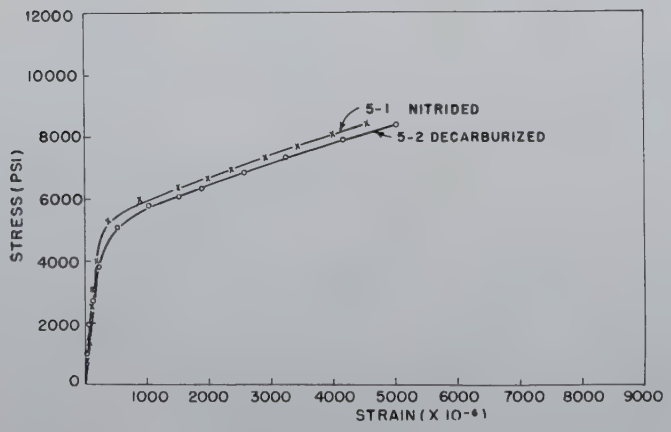

FIG 11—Yielding of identically oriented crystals showing effect of small amounts of nitrogen. Tested with less than 4 pct eccentricity.

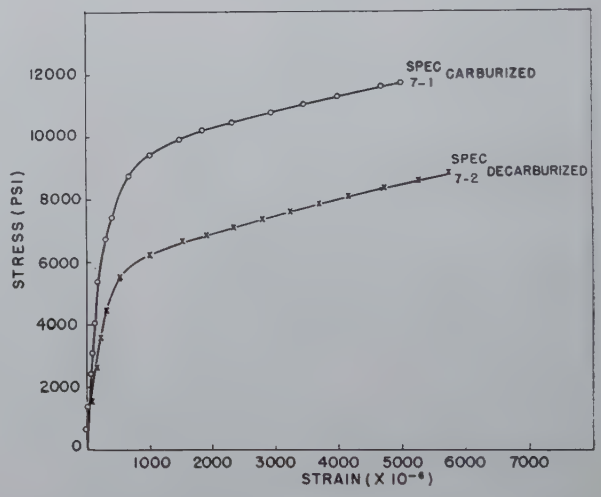

FIG 12—Yielding of identically oriented crystals showing effect of small amounts of carbon. Tested with less than 4 pct eccentricity.

slight upward concavity during initial yielding. The flow curve of the nitrided polycrystal contains no upward concavity, but it does flow at a higher stress initially and then drops to approximately the same flow stress as the decarburized polycrystal as flow progresses. Because of the large grain size it is not expected that the flow of these specimens would be greatly different from single crystals.

The original purpose of vacuum annealing was to ascertain whether the hydrogen presumably occluded in the specimens eliminated the inhomogeneous yielding. Since the vacuum annealed specimens can be considered essentially hydrogen free, the effect of the hydrogen occluded in the specimens is considered to be negligible.

In general, the data on crystal pairs show that where carbon or nitrogen has increased the flow strength, the higher strength curve remains approximately parallel to the decarburized curve, indicating that the rate of strain hardening was not affected.

The results from the tensile tests in which the specimens were more accurately aligned fail to indicate inhomogeneous yielding in single crystals of iron.

Conclusions

1. Carbon or nitrogen causes discontinuous yielding in iron polycrystals in substantiation of the findings of Low and Gensamer.

2. Carbon or nitrogen do not appear to cause discontinuous yielding in iron

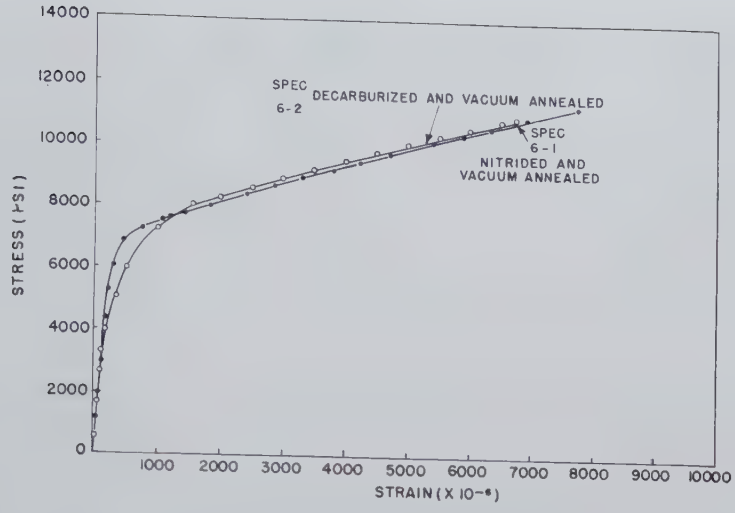

FIG 13—Yielding of extremely coarse polycrystals of iron. Tested with less than 4 pct eccentricity.

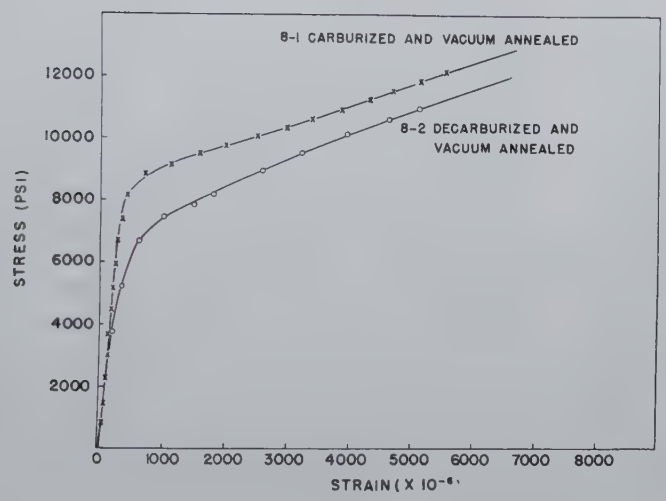

FIG 14—Yielding of extremely coarse polycrystals of iron. Tested with less than 4 pct eccentricity.

single crystals made from aluminum-killed steels. Both elements in small amounts cause an increase in the flow strengths of single crystals, but do not affect the rate of strain hardening.

References

1. A. Nadai: Plasticity. McGraw-Hill, N. Y. (1931) 86–96.
2. J. R. Low and M. Gensamer: Aging and the Yield Point in Steel. *Trans.* AIME (1944) **158,** 207.
3. A. H. Cottrell: Effect of Solute Atoms on the Behavior of Dislocations. Report of a conference on Strength of Solids. Phys. Soc., London (1948) 30.
4. C. A. Edwards and L. B. Pfeil: The Tensile Properties of Single Iron Crystals and the Influence of Crystal Size Upon the Tensile Properties of Iron. *Jnl.* Iron and Steel Inst. (1925) **112,** 79.
5. C. F. Elam and G. I. Taylor: The Distortion of Iron Crystals. *Proc.* Roy. Soc. (1926) **112,** 337.
6. L. B. Pfeil: The Deformation of Iron With Particular Reference to Single Crystals. Carnegie Scholarship Memoirs, Iron and Steel Inst. (1926) **15,** 319.
7. H. C. Carpenter and C. F. Elam: Crystal Growth and Recrystallization in Metals. *Jnl.* Inst. of Metals. (1920) **24,** 83.
8. C. Chappell: The Recrystallization of Deformed Iron. *Jnl.* Iron and Steel Inst. (1914) **89,** 460.
9. D. Hanson: Rapid Recrystallization in Deformed Non-Ferrous Metals. *Jnl.* Inst. of Metals. (1918) **20,** 141.
10. H. C. Carpenter and Tamura: Experiments on the Production of Large Copper Crystals. *Proc.* Roy. Soc. (1926) **113,** 38.

The Surface Tension of Solid Copper

H. UDIN,* A. J. SHALER,* Member, and JOHN WULFF* Member AIME

Introduction

In the study of the sintering of metal powders, we have come to the conclusion in this laboratory that further progress requires a more basic understanding of the operating mechanisms. This is emphasized in detail by Shaler.[1] He has shown that a knowledge of the exact value of the surface tension is imperative for a solution of the kinetics of sintering. This force plays a principal role in causing the density of compacts to increase.[2] Furthermore, a knowledge of the surface tension of solids is also applicable to other aspects of physical metallurgy. C. S. Smith[3] points out the relation between surface and interfacial tension and their function in determining the microstructure and resulting properties of polycrystalline and polyphase alloys.

This paper describes one group of results of an experimental program designed for the study of the surface tension in solid metals. As a by-product of this work, considerable information has been obtained on the rate and nature of the flow of a metal at temperatures approaching the melting point and under extremely low stresses, a field of mechanical behavior heretofore scarcely touched by metallurgists. The importance of this additional information to students of powder metallurgy need not be stressed.

Theoretical Considerations

Interfacial tension arises from the condition that an excess of energy exists at the interface between two phases. Gibbs[5] proves that this energy is a partial function of the interfacial area; thus:

$$\partial F/\partial s = \gamma$$

where $\partial F/\partial s$ is the rate of change of free energy of the system with changing surface area, at constant temperature, pressure and composition, and γ is the interfacial tension, or interfacial free energy per unit area.

If one of the phases is the pure liquid or solid, and the other the vapor of the substance, γ may properly be termed "surface tension," and is a characteristic of the solid or liquid.

The attempt of a body to lower its free energy by decreasing its surface gives rise to a force in the surface which is numerically equal in terms of unit length to the free energy per unit area of the surface. Thus γ may be expressed either in erg-cm^{-2} or in dyne-cm^{-1}. Similarly, surface tension may be determined either by a thermodynamic measurement of the surface energy or by a mechanical measurement of the surface force. We have chosen the latter approach.

Tammann and Boehme[4] determined the surface tension of gold by measuring the amount of shrinkage or extension of thin weighted foil at various temperatures and interpolating to zero strain. The method is of questionable accuracy because of the tendency of foil to form minute tears when heated under tension. Their assumption of $F = 2W\gamma$, where W is the width of the foil, is unsound, as the foil can decrease its surface area by transverse as well as by longitudinal shrinkage. Although their experimentation was meticulous, the paper does not include details of the sample configuration required for recalculating γ on a correct basis, even if such a calculation were possible.

In the experimental procedure chosen here, a series of small weights of increasing magnitude are suspended from a series of fine copper wires of uniform cross-section. This array is brought to a temperature at which creep is appreciable under extremely small stress. If the weight overbalances the contracting force of surface tension, the wire stretches; otherwise, it shrinks. The magnitude of the strain is determined by the amount of unbalance, so a plot of strain vs. load should cross the zero strain axis at $w = F_\gamma$. If balance is visualized as a thermodynamic equilibrium, the critical load is readily calculated. At constant temperature, an infinitesimal change in surface energy should be equal to the work done on or by the weight:

$$ds = wdl \quad [1]$$

For a cylinder, $s = 2\pi r^2 + 2\pi rl$ [2]

If the volume remains constant,

$$r = \sqrt{V/\pi l} \quad [3]$$

$$s = 2\sqrt{\pi Vl} + 2V/l \quad [4]$$

$$ds = (\sqrt{\pi V/l} - 2V/l^2)\, dl \quad [5]$$

Substituting [5] into [1] gives for the equilibrium load,

$$w = \gamma(\sqrt{\pi V/l} - 2V/l^2) \quad [6]$$

and, again expressing V in terms of r and l,

$$w = \pi r\gamma(l - 2r/l) \quad [7]$$

Here the end-effect term, $2r/l$, is neglected for thin wires in subsequent work.

Eq 7 can be confirmed by means of a stress analysis. If the x-axis is chosen along the wire, then the stress σ_x is

$$\sigma_x = \frac{2\pi r\gamma - w}{\pi r^2} \quad [8]$$

A cylinder of diameter d is equivalent to a sphere of radius r, insofar as radial surface tension effects are concerned.[3] Thus

$$\sigma_y = 2\gamma/d = \gamma/r = \sigma_z \quad [9]$$

For the case of zero strain in the x direction, the strain will also be zero in the y and z directions. Since the wire is under hydrostatic stress, Eq 8 and 9 are

San Francisco Meeting, February 1949.

TP 2530 E. Discussion of this paper (2 copies) may be sent to *Transactions* AIME before May 15, 1949. Manuscript received November 3, 1948.

* Graduate Student, Assistant Professor of Metallurgy and Professor of Metallurgy, respectively, Massachusetts Institute of Technology.

References are at the end of the paper.

equal. Thus

$$2\pi r\gamma - w = \pi r\gamma \qquad [10]$$

$$w = \pi r\gamma \qquad [11]$$

The end-correction term was again dropped, this time implicitly in Eq 9, which applies to an infinite cylinder.

With certain assumptions it is possible to calculate the strain rate under conditions of unbalance. If pure viscous flow is assumed, there should be no change in lattice energy, and all the strain energy should appear as heat. If the kinetic energy of the moving weight is neglected, the time rate of heat generation must be equal to the rate of change of potential energy and free energy of the system. The system changes its energy by changing both the position of the weight and the area of the copper surface. Thus, under isothermal conditions,

$$dQ/dt = wdl/dt - \gamma ds/dt \qquad [12]$$

where Q is the heat of viscous flow. Frenkel[6] shows that for a viscous rod under longitudinal strain, the energy dissipated in flow is given by

$$dQ/dt = (6\eta V/l^2)(dl/dt)^2 \qquad [13]$$

where η is the coefficient of viscosity. From Eq 5:

$$ds/dt = (\sqrt{\pi V}/l - 2V/l^2)\, dl/dt \qquad [14]$$

Dropping the end-effect term and combining gives:

$$dl/dt = wl^2/6\eta V - (\gamma/6\eta)\sqrt{\pi/V}\,(l)^{3/2} \qquad [15]$$

The equation can be integrated between $t = 0$ at $l = l_0$ and $t = t$, $l = l$;

$$t = 12\eta/\gamma \left\{ -\Delta r + \frac{w}{\pi\gamma} ln \left[\sqrt{\frac{l_0}{l}} \left(\frac{w\sqrt{1} - \sigma\sqrt{\pi V}}{w\sqrt{l_0} - \sigma\sqrt{\pi V}} \right) \right] \right\} \qquad [16]$$

Since $dl/dt = ld\epsilon/dt$, $w = \pi r^2\sigma$, and $V = \pi r^2 l$, ϵ and σ being strain and stress respectively, Eq 15 and 16 reduce to

$$\frac{d\epsilon}{dt} = \frac{1}{6\eta}(\sigma - \gamma/r) \qquad [15a]$$

$$t = \frac{12\eta r_0}{\gamma}\left[\frac{\epsilon}{2} + \frac{\sigma r_0}{\gamma} ln \frac{\sigma r_0^2 - \gamma r}{\sigma r_0^2 - \gamma r_0}\right] \qquad [16a]$$

where $$r = \frac{r_0}{\sqrt{\epsilon + 1}}$$

So long as cylindrical shape is conserved, Eq 16a is an exact expression, despite the presence therein of ordinary stress and strain. This is so because the equation was obtained merely by making the appropriate substitutions in Eq 16. In the actual experiments the strains measured were small enough so that the differential form, Eq 15a, could be employed throughout. It may be written as:

$$\epsilon = \frac{t}{6\eta}\left(\sigma - \frac{\gamma}{r}\right) \qquad [15b]$$

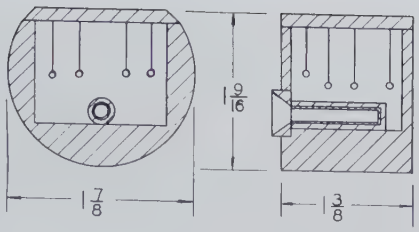

FIG 1—Copper cell with thermocouple well.

Experimental

Two series of experiments were completed, one on five mil and one on three mil copper wire. Eight specimens were used in each test, with copper weights, ranging up to about 60 dynes in the first series and 35 dynes in the second series, welded to the wires. (1 dyne is equivalent to 1.02 mg.) The wires were suspended from the lid of the copper cell, Fig 1.

The ensemble was heated in a nichrome-wound Inconel tube furnace, (Fig 2), which was maintained at a Hg pressure of 3×10^{-5} mm. The cell effectively isolated the specimens, both against contamination from furnace vapors and against loss of wire diameter by evaporation. As the experiments were conducted in a temperature range where the vapor pressure of copper was between 10^{-5} and 5×10^{-4} mm,[7] a good approximation to the isolated system "$Cu_s - Cu_g$" was attained, at least at the higher temperatures.

The furnace was constructed with three independent windings, tapered in accordance with preliminary heat-loss calculations. At any temperature within its operating limits a 6-in. zone can be held uniform to ±2°C. A Tagliabue throttling pyrometer with manual droop control was used as a constant-temperature control device. The shell of the furnace was maintained at a low vacuum with a water-aspirator to protect the highly evacuated tube against collapse.

The marking of reference points on the wire presented a difficult problem. Painting or plating the wires outside a given gauge length was considered but was abandoned as it is evident that anything which adheres to the surface lowers the surface energy. Knotting the wire at two points about 2 cm apart was found to be the simplest expedient. The gauge point is taken as the intersection of the lower loop of the knot with the straight portion of the wire, as viewed from a fixed direction with a measuring microscope. (Fig 3.)

The knotted and weighted wires were mounted and carefully straightened. They were annealed in vacuo for 2 hr at or above test temperature before measuring. A test may last from 24 to 150 hr, depending on the temperature. Initial and final lengths were measured to ±0.001 cm with a horizontal measuring microscope. Finally, the weights were detached at the lower knot and weighed, and the weight corrected by

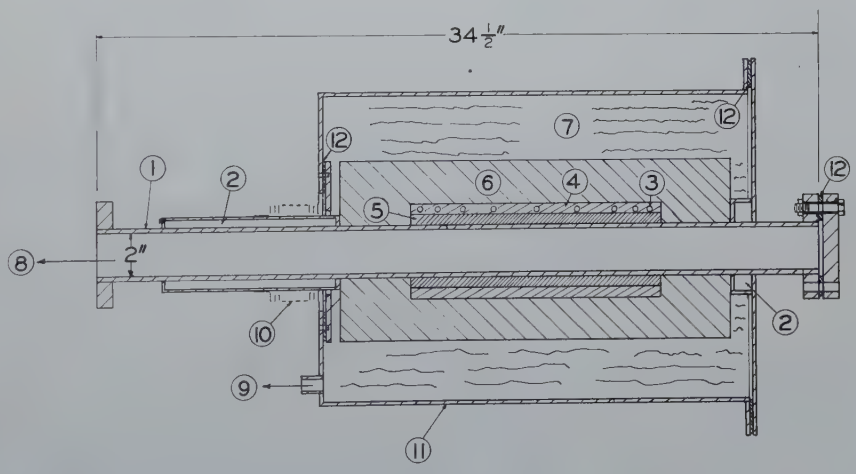

FIG 2—Vacuum furnace.

1. Inconel tube
2. Water jackets
3. Tapered nichrome resistance heater
4. Alundum cement
5. Alundum tube
6. Insulating refractory
7. Crumpled aluminum foil
8. To diffusion pump
9. To water aspirator
10. Sylphon expansion joint
11. Steel outer shell
12. Neoprene gaskets

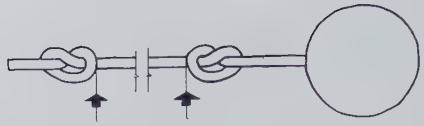

FIG 3—Typical specimen. Arrows show gauge points.

Table 1 . . . Summary of Results

Test No.			9		10		11		13		14		15		16	
Temperature, °C			1024		999		950		1049		1050		1000		950	
Time, sec × 10^{-5}			1.08		1.80		5.15		0.874		1.69		2.60		5.35	
Wire radius cm			0.0064		0.0064		0.0064		0.0064		0.0036		0.0036		0.0036	
Spec. No.	Stress Dyne/ Cm^2 × 10^{-5}	Strain × 10^3	σ	ϵ	σ	ϵ	σ	ϵ	σ	ϵ	σ	ϵ	σ	ϵ	σ	ϵ
1	0.091	−6.1	0.069	−4.4	0.076	−3.9	0.091	−4.5	0.096	−8.9	0.072	−10.7	*	†		
2	0.738	−4.5	0.076	−4.2	0.777	−2.1	0.861	−3.3	*		1.179	−5.7	1.706	−3.10		
3	1.461	−3.1	1.742	−1.8	1.774	−1.3	1.319	−2.5	2.428	−5.0	2.455	−2.1	3.508	−0.67		
4	2.368	−.6	2.350	−0.5	2.755	+1.3	2.315	−0.5	3.655	−0.8	3.393	−0.9	4.107	−0.32		
5	2.535	−0.0	2.807	+0.6	2.313	−0.6	2.865	+1.3	4.545	+3.1	3.635	−0.6	5.459	+2.00		
6	3.145	+3.7	3.180	+3.0	3.140	+1.9	2.842	2.4	5.047	4.1	4.235	+0.2	5.724	3.22		
7	3.472	4.2	3.810	2.3	3.465	2.1	3.520	3.8	*		5.540	4.6	6.682	4.89		
8	4.644	3.8	4.603	5.9	4.547	4.1	4.545	5.4	7.530	9.3	8.135	9.1	8.345	6.30		

* Specimen damaged during measurement.
† Measuring microscope accurate to ±0.0002 cm used in Test No. 16.

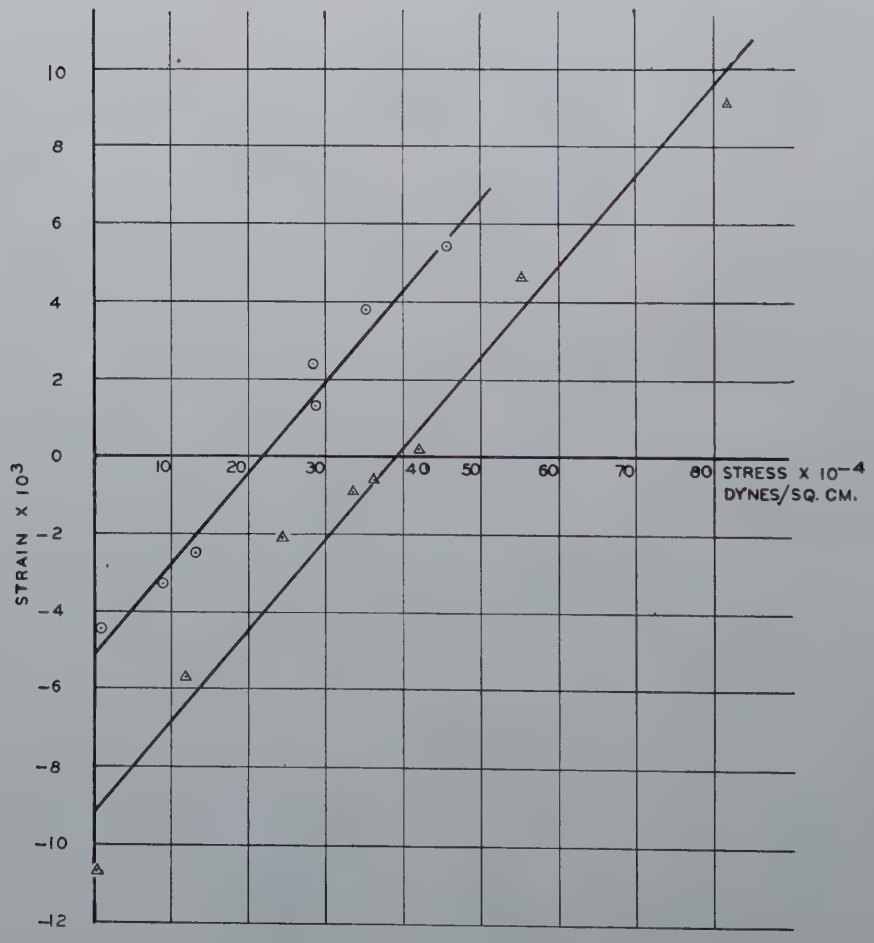

FIG 4—Stress-strain curves for test No. 15 (triangles) and test no. 13 (circles). See Table 1.

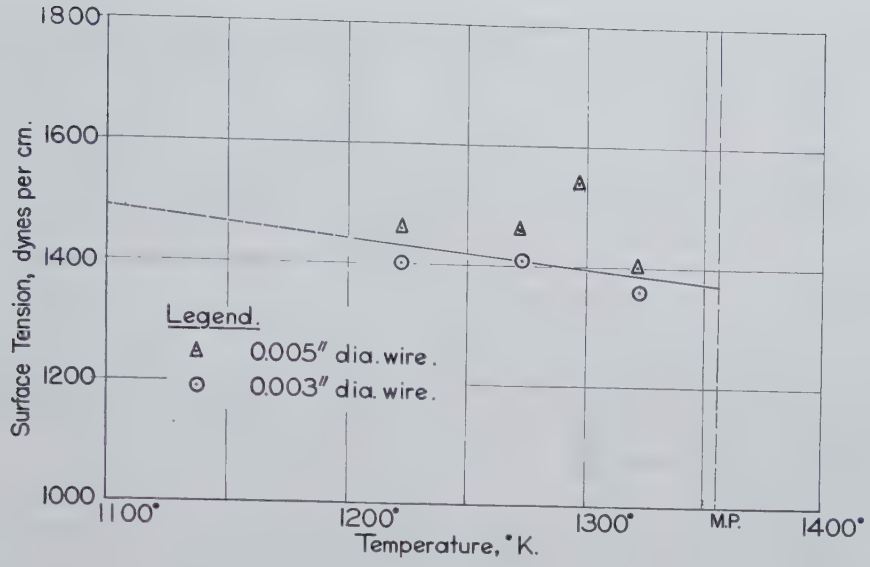

FIG 5—The temperature dependence of surface tension of solid copper.

adding one-half the weight of the gauged length of wire. Table 1 summarizes the results.

Eq 15b is assumed to hold over the range of strains in these tests, and linear least square solutions are plotted. Two such plots are shown in Fig 4. The scatter of the points is within the accuracy of the strain measurements.

Discussion of Results

SURFACE TENSION

It can be seen from Eq 15b that at zero strain the applied stress equals the stress due to surface tension, that is,

$$\gamma = \sigma_\gamma r$$

In Fig 5 the surface tensions determined from this relationship are plotted against temperature. If the anomalous point at 1298°K is ignored, a value of 1370 dynes per cm at the melting point is obtained. The temperature coefficient is -0.46 dynes cm^{-1} $°K^{-1}$, which is consistent, as is to be expected on theoretical grounds,[8] with an extrapolation to zero in the neighborhood of the critical temperature.

VISCOSITY

As indicated in the introduction, the purpose of this work was to develop an experimental method for the measurement of the surface tension of solid metals. The results on viscosity are a by-product and though interesting should be considered incomplete.

Viscous flow is defined phenomenologically as a process in which strain rate is proportional to applied shear stress. Recent theory of condensed systems includes the further criterion that the flow must be atomic as well. Steady-state creep is often termed "quasi-viscous" in that the true strain rate, while not proportional to the applied stress, is constant for a constant true stress. Kauzmann[8] points out that another mode of flow may exist in metals, which involves the motion of blocks rather than single atoms, but which is otherwise proportional to the applied shear stress, at least at low stresses.

Kauzmann's analysis of viscous flow leads to the expression

$$\eta = \frac{\lambda L k T}{2 q A l D} \qquad [17]$$

where L = spacing between flow lamellae, normal to flow direction
λ = relative motion of adjacent lamellae, per unit process of flow
q = stress concentration factor, = 1 if no part of the fluid can support shear
A = area of a unit lamella of flow
l = distance between normal and activated state of the flow unit.

D is the coefficient of self-diffusion of the material, if the mechanisms of self-diffusion and of viscous flow are identical. It is only required that the mechanisms correlate. It is not necessary that every unit involved in diffusion be also involved in viscous flow.

For an atom-wise process of self-diffusion, $\lambda = L = (A)^{1/2} = 2l$. For an atom-wise process of viscous flow under very slight shear, where the probability of a forward jump of an atom exceeds only slightly that of a reverse jump, the relationship $\lambda = 2l$ remains valid. Thus Eq 17 reduces to:

$$\eta = \frac{kT}{\lambda D} = \frac{kT}{\lambda D_0} e^{\frac{Q_D}{RT}} \qquad [17a]$$

where λ is now the interatomic spacing. If the Dushman-Langmuir value for D_0 is inserted, the expression becomes:

$$\eta = \frac{h}{\lambda^3} \frac{RT}{Q} \cdot e^{\frac{Q}{RT}} \qquad [18]$$

In our experiments the flow is viscous, at least to the extent that the data in Table 1 can be approximated by straight lines. The viscosity is given by

$$\eta = \frac{t}{6\epsilon}\left(\sigma - \frac{\gamma}{\tau}\right) \qquad [15c]$$

In Fig 6, the logarithms of the viscosities derived from Eq 15c are plotted against the reciprocal of absolute temperature. The equation of the straight line as drawn is

$$\eta = 130 e^{\frac{95000}{RT}}$$

The activation energy of 59,000 cal per mol is within the range of values reported for self-diffusion of copper.[9] The action constant, however, is 10^7 times larger than that predicted by Eq 18. The coincidence of activation energies suggests that the atom or atomic vacancy is the unit of flow, but evidently only a very small fraction of vacancies can participate in the flow.

The divergence in viscosity between the two wire sizes, (see dotted lines, Fig 6) indicates that the surface-to-

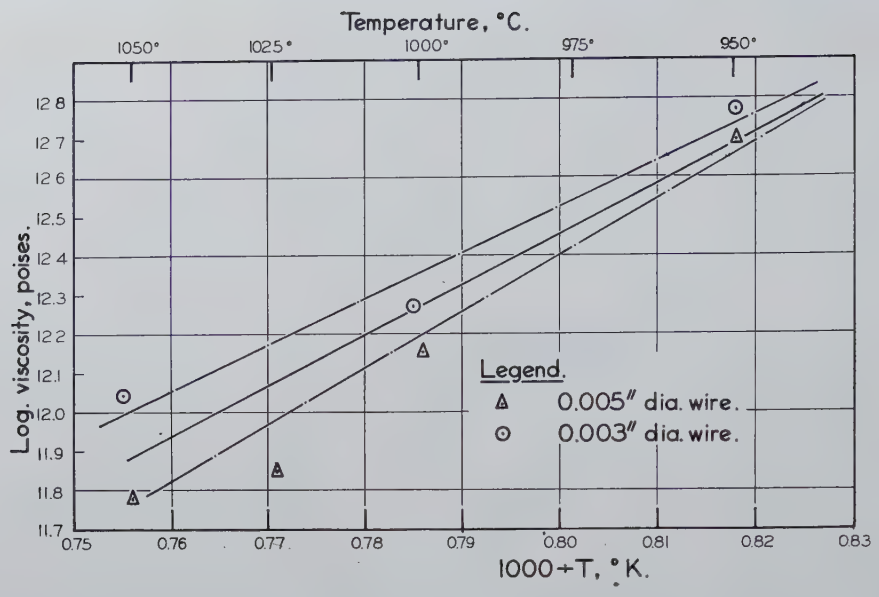

FIG 6—The temperature dependence of viscosity of solid copper.

volume ratio of the specimens may be a factor in determining the flow rate. Apparently the viscosity of the surface phase greatly exceeds that of the interior of the copper.

The mathematics of this condition has not yet been formulated, nor are the data as yet extensive enough to warrant such formulation. Nevertheless some speculation may be justified.

Surface energy owes its existence to the presence of unsatisfied atomic bonds at the surface. However, if surface tension is calculated by merely summing the energy of these broken bonds, the result is too high by roughly 10 pct[10] because the unsevered bonds in the surface layers of atoms distort in such a way as to take up some of the excess energy. These high-energy bonds might account for the strengthening of the surface layer, according to Benedicks.[11]

In fatigue testing, and in tension testing of brittle materials, failure is initiated at the surface, and the strength of the surface skin plays an important role, even in large section sizes. Benedicks and Ruben[12] investigated a quenched (untempered) carbon steel immersed in various media, and found the strength to be dependent on the surface tension of the medium.

Further experiments are planned with the purpose of determining the thickness of this surface layer, estimating the ratio of its strength to that of the interior metal, and calculating the effect such a layer will have on sintering rates.

Acknowledgment

The writers wish to acknowledge their indebtedness to the Revere Copper and Brass Co., who made the work possible through a Research Grant.

References

1. A. J. Shaler: Seminar on Kinetics of Sintering. AIME *Met. Tech.*, Dec. 1948.
2. F. N. Rhines: *Trans.* AIME (1946) **166,** 474.
3. C. S. Smith: AIME *Met. Tech.*, June 1948, TP 2387.
4. Tammann and Boehme: *Ann. Physik* (1932) **12,** 820.
5. J. W. Gibbs: Collected Works. **1,** (1931) N. Y.; Longmans, Green and Co..
6. J. Frenkel: USSR *Jnl. Phys.* (1945) **9,** 385.
7. K. K. Kelley: Contributions to the Data on Theoretical Metallurgy. (1935) USBM Bull. 383.
8. W. Kauzmann: *Trans.* AIME, (1941) **143,** 57.
9. J. Steigman, W. Shockley, and F. C. Nix: *Phys. Rev.* (1939) **56,** 13.
10. W. D. Harkins: *Jnl. Chem. Phys.* (1942) **10,** 268.
11. C. Benedicks: Pittsburgh Internat'l. Conf. on Surface Reactions, (1948) 196. Corrosion Publishing Co. Pittsburgh.
12. C. Benedicks and G. Ruben: *Jernk. Ann.* (1945) **129,** 37. (As quoted by Benedicks in Ref. 11.)

The Ionic Nature of Metallurgical Slags. Simple Oxide Systems

JOHN CHIPMAN,* Member and LO-CHING CHANG,† Junior Member AIME

Introduction

THE perennial and increasing interest in the chemical behavior of steelmaking slags has led to numerous attempts to formulate the thermodynamic properties of these solutions. The classical view is that of a solution of the component oxides in which certain acidic oxides are more or less completely held in combination with basic or metallic oxides, the nature of the interoxide compounds being derivable from the chemical behavior of the slag or from the mineralogy of a solidified specimen. The known electrical conductivity of slags has pointed to the existence of ions in the solution and a number of attempts have been made to account for the observed facts of slag behavior on the basis of a theory of complete ionization of the solution. It is the purpose of this paper to examine, in the light of ionic theory, a number of recently published series of data on slag-metal and slag-gas equilibria, with the purpose of obtaining a more complete or more satisfactory generalization than has been possible on either of the single bases of simple compound formation or complete ionization.

The attempt to formulate the ionic constitution of a complex solution is fraught with many uncertainties. An ion is not something that can be plucked from the solution and examined in detail, nor can its true formula be determined with certainty by any single experimental method. In attempting to express the composition of a slag by various ionic formulas it can be expected that alternative hypotheses of essentially equal merit will present themselves. In the present state of early development of the ionic theory of slags, it may be necessary to make some rather arbitrary choices of ionic formulas in the absence of sufficient information to yield complete certainty.

Acids and Bases

The classification of slag-forming oxides as acidic or basic apparently dates back into the days of Berzelius. It is difficult to see how the concept could have originated in the early twentieth century when it was fashionable to define an acid or a base as an aqueous solution containing hydrogen or hydroxyl ions. It is, however, entirely consistent with the modern and more general theory of acids and bases. In this theory, as originally formulated by G. N. Lewis,[1] a basic molecule is one that has an electron pair which may enter the valence shell of another atom thus binding the two together by the electron-pair bond. An acid molecule is one which is capable of receiving such an electron pair into the shell of one of its atoms. The acid, the base, and the product of neutralization may be either ions or neutral molecules. The product of such a reaction may itself be a base or an acid if it is further capable of giving or accepting an electron pair. Thus a base is a donor of electrons, an acid, an acceptor. In oxide slags the typical and ever-present base is oxide ion, 0^{--}. In behavior and in importance it is analogous to hydroxyl ion, OH^-, which is the typical base of aqueous solutions. There is nothing in the chemistry of slags which is quite analogous to the acid H_3O^+ in aqueous solutions. This is not surprising for in slag systems there is nothing which can be designated as a solvent and no ubiquitous positive ion. The chemistry of slags is in fact more complex than the chemistry of aqueous solutions and the concepts which must be evoked in its study are correspondingly broader.

In seeking a basis for a classification of slag-forming oxides as basic or acidic it must be remembered that these terms are not absolute but relative. A substance which acts as a base toward a second substance may act as an acid toward a third. This is less likely to happen among strong bases or acids than among the weak ones; there are numerous examples of weak acids which under the influence of a stronger acid behave as weak bases. Such substances are called amphoteric. A classification of the glass-forming oxides has been proposed by Sun and Silverman[2] and further developed by Sun[3] in which the oxides are arranged in order of decreasing acidity or increasing basicity, each substance being potentially capable of acting as an acid toward substances below it in the list and as a base toward those above it. It is based upon the relative strengths of the metal-to-oxygen bond as determined by the energy required to dissociate the oxide into its component atoms.[4] Data are available for computation of this energy, at least approximately, for the oxides of slags and glasses. In general those oxides from which it is most difficult to remove the positive atom are the strong acids while those in which it is most loosely held are the strong bases. It is in the latter, of course, that formation of oxide ion occurs most readily as, for example, in CaO which in solution ionizes to form the weak acid Ca^{++} and the strong base O^{--}. The order of arrangement found by Sun is shown in the first column of Table 1, to which have been added the data for

San Francisco Meeting, February 1949.

TP 2529 C. Discussion of this paper (2 copies) may be sent to *Transactions* AIME before May 15, 1949. Manuscript received November 1, 1948; revision received November 26, 1948.

* Professor of Metallurgy, Massachusetts Institute of Technology.

† Crucible Steel Co. of America, New York City.

References are at the end of the paper.

Table 1 . . . Oxides Arranged in Order of Increasing Basic Strength As Determined by Several Methods

From Relative Bond Strength[3]	From Carbonate Decomposition[5]	From Sulphate Decomposition[5]
B_2O_3	P_2O_5	
SiO_2	B_2O_3	
P_2O_5	SiO_2	
Al_2O_3	TiO_2	
Sb_2O_5		
ZrO_2		
TiO_2		BeO
BeO		Fe_2O_3
SnO_2		CuO
FeO	FeO	CoO
PbO	ZnO	NiO
MgO	CoO	ZnO
MnO	MnO	CdO
Li_2O	PbO	MnO
PbO	CdO	PbO
CaO	MgO	MgO
SrO	CaO	CaO
BaO	Li_2O	Li_2O
Na_2O	BaO	BaO

several slag oxides.

Another method of comparing basic strength of oxides is through studies of the decomposition of such compounds as carbonates and sulphates. The stronger the basic properties of an oxide, the more strongly does it hold fast to CO_2 or SO_3 and accordingly the lower is the decomposition pressure at a given temperature. Acidic oxides may be compared by their relative ability to displace CO_2 from a given carbonate. The information on relative basic strengths derived from experiments of this sort has been summarized by Flood and Förland[5] and is quoted in the second and third columns of Table 1. It is to be observed that the three columns are in very good agreement although minor discrepancies are present.

All oxide slags contain oxide ion, O^{--}, and as Stegmaier and Dietzel[6] have shown, the higher the concentration of this ion the more basic is the slag. Other basic ions such as F^- and S^{--} may also contribute to the properties which we associate with basic slags. Usually, however, the relative concentrations of these ions is small and the basicity is determined by the concentration of oxide ion. Thermodynamically a more satisfactory measure of basicity is the *activity* of oxide ion in the slag. This will be discussed in a later section.

On the basis of the Lewis theory of acids and bases the formula for oxide ion is written $:\ddot{O}:^{--}$, the pairs of dots being used to represent pairs of electrons, not statically placed as in the formula but possessing points of maximum probability which for chemical purposes are sufficiently well represented by the dots. The process of neutralization of the base O^{--} by an acid such as SiO_3^{--} consists in the transfer of a pair of electrons from the oxygen to the silicon atom where they serve as a bond to hold together the product of the reaction. The process may be shown as follows:

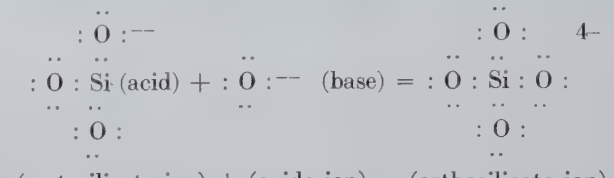

(metasilicate ion) + (oxide ion) = (orthosilicate ion)

A measure of the acidity of a slag component may thus be found in its ability to diminish the concentration of oxide ion by formation of a stable neutralization product.

SILICATES

The oxide SiO_2 has a crystal structure consisting of a multiplicity of SiO_4 groups, each silicon being surrounded by four oxygens, arranged tetrahedrally, and each oxygen being shared by two silicons. The surface layers of such a crystal might be depicted as:

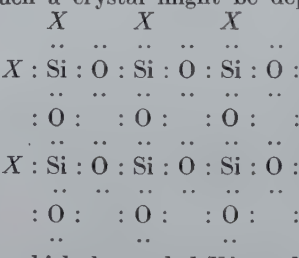

in which the symbol X is used to denote a repeating pattern of SiO_4 groups within the crystal. The tendency to form these SiO_4 groups is exceedingly strong, and they have been identified by X ray methods not only in silica but in all crystalline silicates and in glasses. There can be little doubt that the silica in slags is present in the form of some such tetrahedral groups. Consider the neutralization of a crystal of silica by oxide ions of a slag. Each silicon atom and two of its attendant oxygen atoms undergo separation from the rest of the crystal and neutralization by oxide ion to form metasilicate ion according to the equation:

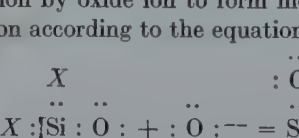

But the silicon atom has a coordination number of four and a strong tendency to surround itself by four oxygen atoms. In response to this tendency the result is a linking together of two or more ions into a chain which is characteristic of metasilicate minerals and which may be depicted by the formula:

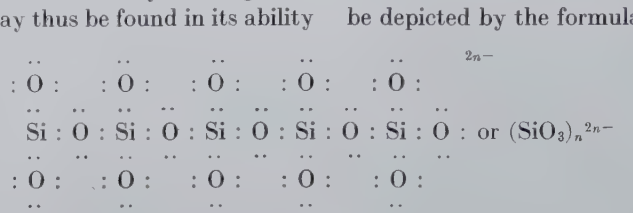

The number of silicon atoms in such a chain would undoubtedly decrease with rising temperature. The chains are strongly acidic and probably do not occur in strongly basic slags. The viscosity of an acid slag is probably dependent upon the average chain length. It is easy to imagine that a chain might, like Kekulé's snake, bite itself by the tail thus forming a closed ring, and the minimum number of silicon atoms in such a metasilicate ring would be three.

Further addition of oxide ion to a silicate melt carries the neutralization a step farther, forming pyrosilicates $[SiO_{3n+1}]^{(2n+2)-}$. To take the simplest case (and the one which is most probably significant in slags) of a pyrosilicate containing two silicon atoms, its formation is represented by:

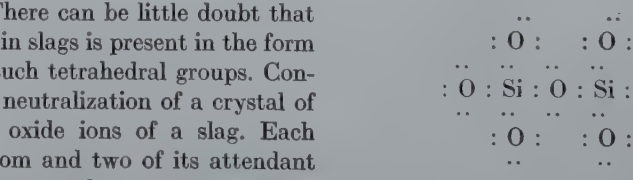

Neutralization is not yet complete until this has been converted into orthosilicate by the reaction:

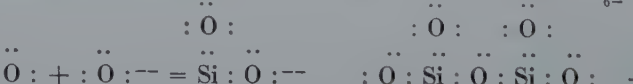

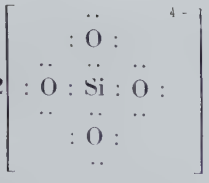

It is evident in these illustrations that the product of neutralization in one reaction may act as an acid in another. The successive steps and the relative acidity of silicon in the several forms may be represented by the following series adapted from the work of Huggins and Sun[4]:

	Acid	Decreasing Acidity			Basic
Ion	SiO_2	$Si_2O_5^{--}$	SiO_3^{--}	$Si_2O_7^{6-}$	SiO_4^{4-}
Atoms of Si per atom of O	0.50	0.40	0.333	0.286	0.250
Energy per tetrahedron K cal	3110	3123	3131	3137	3141

OTHER ACIDIC OXIDES

Phosphorus likewise has a coordination number of four and forms meta-, pyro- and orthophosphate ions whose formulas in order of neutralization are: P_2O_5 PO_3^- $P_2O_7^{4-}$ PO_4^{3-}. Similarly the other acidic oxides react with oxide ion to produce anions which become progressively less acidic as the oxygen content increases. In general the nature of these ions is less thoroughly understood than in the examples cited above, especially with respect to ionic constitution in liquid slags at steelmaking temperatures. It is sometimes possible to deduce the nature of the ion from its known chemical behavior in the slag. For example, in basic open-hearth slags the acidifying effect of one mole of Al_2O_3 is neutralized by addition of two moles of CaO. The neutralization in slags of this kind is therefore very probably represented by the equation:

$$Al_2O_3 + 2O^{--} = Al_2O_5^{4-}$$

Other oxides of similar formula may form ions of quite different type. Thus the strong acid B_2O_3 if completely neutralized gives

$$B_2O_3 + 3O^{--} = 2(BO_3)^{3-}$$

BASIC OXIDES

Any oxide which when added to the slag increases its oxide ion activity is a basic oxide. The most strongly basic oxides are those of the alkali and alkaline earth metals. In addition to oxides, the fluorides, chlorides and sulphides should be considered. Their behavior is altogether analogous to that of oxides, the negative ions F^-, Cl^- and S^{--} acting as bases.

An amphoteric oxide may function either as an acid or a base depending upon the oxide-ion activity of the solution to which it is added. As a typical example, alumina may ionize in accordance with either of the following reactions:

$$Al_2O_3 = 2Al^{3+} + 3O^{--}$$
$$Al_2O_3 + 3O^{--} = 2AlO_3^{3-}$$

It may thus increase or decrease the oxide ion activity depending upon whether the basicity of the slag to which it is added is small or great.

Ionic Solutions

Fused salts are excellent conductors of electricity and, especially in the case of the halides, have long been regarded as highly ionized. Many fused oxides, including the mixtures which we call slags, are also strong electrolytes[7] and therefore are in considerable measure dissociated into ions. Herasymenko[8] proposed that open hearth slags are completely dissociated into positive metallic ions and several kinds of negative ions including many of those mentioned in the foregoing section. He showed excellent agreement between theory and observations in many cases of slag-metal equilibrium with acid slags. The success of the theory with respect to basic slags was less noteworthy. Temkin[9] defined an ideal ionic solution and applied the concept to steelmaking slags. He defined the ion fraction of a positive or negative ion N_i^+ or N_i^- as the ratio of the amount of this ion to the total of all ions of like sign present in the solution. He treated ionic solutions as being "ideal" in the sense that the activity of each ion is equal to its ion fraction. Samarin, Temkin and Shvarzman[10] showed excellent agreement between theory and observations in the distribution of sulphur but unfortunately not for the case of oxygen distribution between slag and metal. We shall refer to the assumed equality of activity and ion fraction as "Temkin's rule."

Liquid Iron Oxide Slags

From the ionic viewpoint, the behavior of liquid iron oxide indicates clearly the presence of Fe^{++}, O^{--} and at least one other negative ion containing trivalent iron. That trivalent iron is present as an anion rather than as tripositive ferric ion is shown by the marked increase in ferric iron which attends an increase in slag basicity, other factors remaining constant. Which of a number of possible "ferrite ions" is present in basic slags cannot be decided on the basis of any evidence now available. A series of possible ions formed from ferric ion by successive neutralization with oxide ion is suggested as follows:

Fe^{+++} Fe_2O_3 FeO_2^- $Fe_2O_5^{4-}$ FeO_3^{3-}

Since the composition of the liquid may be expressed in terms of Fe^{++}, O^{--} and any one of the anions suggested, the choice of one of these becomes a matter of convenience. It will be convenient to select the formula which leads to values of activity coefficient nearest to unity, or least variable with composition. A simple calculation from the recent data of Darken and Gurry[11] showed that $Fe_2O_5^{4-}$ is the most satisfactory of the four ionic formulas suggested, from the standpoint of simplicity of calculation. The occurrence of dicalcium ferrite in solidified basic slags[12] indicates that this choice is not an unreasonable one.

Darken and Gurry[11] have established the equilibrium relationship between molten iron oxides and a gas phase containing CO and CO_2. Their data cover a temperature range from 1400 to 1600°C and compositions represented by ratios of oxygen to iron between 1.01 and 1.37. They provide as complete a set of experimental data as could be desired for thermodynamic study of these molten oxides. The data for 1600° are reproduced in Table 2 in which the first three columns are taken directly from Darken and Gurry's Table 6. The figures in the other columns will be discussed later.

In view of what has been said above with regard to the principal ions present in the solution, the principal reaction and its equilibrium constant may be written:

$$2Fe^{++} + 4O^{--} + CO_2(g) = Fe_2O_5^{4-} + CO(g) \quad [1]$$

$$K_1 = \frac{p_{CO}}{p_{CO_2}} \cdot \frac{a_{Fe_2O_5^{4-}}}{(a_{Fe^{++}})^2 \cdot (a_{O^{--}})^4}$$

In this expression the a's represent activities of the ions and it will be well at the outset to state clearly the meaning of this term. Ion activity may be defined like any other activity as

$$a = e^{\frac{\mu - \mu^\circ}{RT}}$$

where μ and μ° are the chemical potentials (free energies) of the ionic component at two concentrations, one of which, μ°, is selected as a standard for reference. The activity has no absolute value since it depends only on the difference in chemical potential; for this reason it is sometimes called the relative activity. Darken and Gurry chose as their standard state a solution in which $N_O/N_{Fe} = 1.07$ and it was on this basis that the third column of Table 2 was obtained. For our purposes it will be more convenient to adopt $N_O/N_{Fe} = 1.00$ as the standard state, corresponding to the hypothetical pure liquid FeO. Referred to this standard, the value of log a_{FeO} will differ by a constant amount from that of the third column, the new values being given in the fourth. The constant difference of 0.040 was found for each of the experimental temperatures by extrapolation to unit ion fraction of oxide ion. Corresponding values for the activity of FeO are given in the last column.

In the pure liquid FeO the activities of the ions Fe^{++} and O^{--} as well as of the component FeO will be taken as unity. These choices require that

$$a_{FeO} = a_{Fe^{++}} \cdot a_{O^{--}} \qquad [2]$$

an equation which we shall use as the definition of the activity of FeO in any slag. It should be noted specifically that nothing has been said about the degree of ionization of FeO. The definition of activity here employed* is equally useful whether the melt is completely or only infinitesimally ionized. The activity coefficient, γ, of an ion will be defined as the ratio of its activity to its ion fraction. For other ions in the solution, such as $Fe_2O_5^{4-}$ or Fe^{3+} the reference state will be the infinitely dilute solution *in FeO* in which the activity is equal to the ion fraction or $\gamma = 1$.

The equilibrium constant of Eq 1 may be obtained from the data of Darken and Gurry.[11] For slags in which the ratio of N_O/N_{Fe} is 1.15 or less and the concentration of Fe^{3+} ion is probably quite small, the calculations are shown in Table 3. The first two columns are the experimental data of Darken and Gurry's Table 6. Columns 3 and 4 are ion fractions computed from column 1 on the assumption that the liquid contains only Fe^{++}, O^{--} and $Fe_2O_5^{4-}$. Since the ion fraction of Fe^{++} is unity, the activity of O^{--} is equal to that of FeO by Eq 2. Values of a_{FeO} were shown in Table 2 for 1600° and at other temperatures may be obtained in the same manner from the experimental data. They are listed in the fifth column as $a_{O^{--}}$. It is to be noted that these experimental values of $a_{O^{--}}$ agree closely with $N_{O^{--}}$ thus making $\gamma_{O^{--}} = 1$ for these solutions.

The activity of this ion thus conforms to Temkin's rule. Now in binary solutions if one component obeys Raoult's law over a given range of composition it follows that the second component obeys Henry's law in the same range. By analogy then, since there are two negative ions, if one obeys Temkin's rule the activity of the other is proportional to concentration in the same range. It follows that in these solutions $\gamma_{Fe_2O_5^{4-}}$ (referred to the infinitely dilute solution) is unity. The values of the equilibrium constant computed from the ion fractions are given in the last column, the constancy being surprisingly good. Since deviations occur at higher ratios of oxygen to iron, the values at the lower concentrations are used to obtain the average values of K_1.

The deviations in K_1 which occur at ratios of N_O/N_{Fe} greater than 1.15 could readily be treated by imposing an activity coefficient upon any of the ion fractions involved, for example $Fe_2O_5^{4-}$. We prefer to accomplish the same purpose by the hypothesis that at higher ferric contents the concentration of the ferric ion, Fe^{3+}, becomes significant. It is likely that as the concentration of $Fe_2O_5^{4-}$ ion increases and that of O^{--} ion decreases, a significant amount of $Fe_2O_5^{4-}$ ion dissociates into Fe^{3+} and O^{--} according to some internal equilibrium which we express by the following equations:

$$Fe_2O_5^{4-} = 2Fe^{3+} + 5O^{--} \qquad [3]$$

$$K_3 = \frac{(a_{Fe^{3+}})^2 (a_{O^{--}})^5}{(a_{Fe_2O_5^{4-}})}$$

When Fe^{3+} ion is present in significant amount, it becomes no longer possible to calculate the concentration of each constituent directly from the N_O/N_{Fe} ratios without knowing the constant K_3 and the corresponding activity coefficients. However, we shall proceed to solve the problem from the Darken and Gurry data as follows:

From Eq 1 and our definition of a_{FeO}, and continuing the assumption of unit activity coefficient for oxide and ferrite ions, we may write:

$$K_1 = \frac{p_{CO}(1 - N_{O^{--}})}{p_{CO_2} \cdot (a_{FeO})^2 \cdot (N_{O^{--}})^2} \qquad [1a]$$

This expression is solved for each of the data to yield $N_{O^{--}}$ and $N_{Fe_2O_5^{4-}}$ (which

Table 2 . . . Equilibrium Gas Composition and Activity of Ferrous Oxide in Liquid Iron Oxides at 1600°C from Data of Darken and Gurry[11]

N_O/N_{Fe}	log p_{CO_2}/p_{CO}	− Log a_{FeO}	− Log a_{FeO}	a_{FeO}
(1.00)			(0.000)	(1.000)
1.012	−0.728	−0.0291	0.011	0.975
1.04	−0.371	−0.0191	0.021	0.951
1.07	−0.021	0.	0.040	0.912
1.10	+0.295	+0.0268	0.067	0.857
1.15	0.812	0.0914	0.131	0.740
1.20	1.30	0.177	0.271	0.607
1.25	1.80	0.290	0.330	0.468
1.30	2.35	0.439	0.479	0.332
1.333	2.74	0.565	0.605	0.248
1.34	2.82	0.593	0.633	0.233
1.37	3.22	0.733	0.773	0.169

Table 3 . . . Equilibrium Constant of Eq 1 at 1600, 1500 and 1400°C

N_O/N_{Fe}	p_{CO_2}/p_{CO}	$N_{O^{--}}$	$N_{Fe_2O_5^{4-}}$	$a_{O^{--}}$	K_1	
Temperature 1600°						
1.04	0.425	0.954	0.046	0.951	0.131	average 0.133
1.07	0.952	0.912	0.088	0.912	0.134	
1.10	1.97	0.857	0.143	0.857	0.135	
1.15	6.48	0.728	0.272	0.740	0.149	
Temperature 1500°						
1.04	0.384	0.954	0.046	0.954	0.145	average 0.144
1.07	0.886	0.912	0.088	0.912	0.144	
1.10	1.893	0.857	0.143	0.855	0.140	
1.15	6.60	0.728	0.272	0.731	0.147	
Temperature 1400°						
1.034	0.263	0.963	0.037	0.966	0.164	average 0.157
1.04	0.338	0.954	0.046	0.956	0.164	
1.07	0.836	0.912	0.088	0.912	0.152	
1.10	1.805	0.857	0.143	0.855	0.147	
1.117	2.82	0.819	0.181	0.815	0.143	
1.15	6.65	0.728	0.272	0.726	0.146	

* This follows the standard treatment of ion activities by Lewis and Randall; see Ref. 17, p. 326.

Table 4 . . . Calculation of Ferric-ion Activity and of K_3 in Iron Oxide Slags
Temperature 1600°, $K_1 = 0.133$

N_O/N_{Fe}	p_{CO_2}/p_{CO}	a_{FeO}	$N_{O^{--}}$	$N_{Fe_2O_5^{4-}}$	$N_{Fe^{++}}$	$a_{Fe^{++}}$	$\gamma_{Fe^{++}}$	$\gamma_{Fe^{3+}}$	$a_{Fe^{3+}}$	$K_3 \times 10^4$
1.20	20.0	0.607	0.622	0.378	0.939	0.976	1.04	0.48	0.029	2.09
1.25	63.1	0.468	0.514	0.486	0.851	0.911	1.07	0.35	0.052	2.03
1.30	223.9	0.332	0.421	0.579	0.733	0.788	1.07	0.34	0.091	1.89
1.333	549.5	0.248	0.374	0.626	0.638	0.664	1.04	0.36	0.130	2.00
1.34	668.3	0.233	0.363	0.637	0.617	0.642	1.04	0.37	0.142	1.98
1.37	1660.	0.169	0.327	0.673	0.520	0.517	0.99	0.39	0.187	1.95

is $1 - N_{O^{--}}$). The solution is shown in the first five columns of Table 4 of which the first three represent the experimental data. The fourth and fifth columns are obtained by solution of the above equation using values of K_1 from Table 3. The ion fraction of Fe^{++} is found from the stoichiometric requirements (*a*) that the ratio of the total number of atoms of the two kinds must be that of column one and (*b*) that the total positive and negative charges must be equal. From these considerations we have:

$$(N_{O^{--}} + 5N_{Fe_2O_5^{4-}})/(2N_{Fe_2O_5^{4-}} + n_{Fe^{++}} + n_{Fe^{3+}}) = N_O/N_{Fe} \quad [a]$$

$$2n_{Fe^{++}} + 3n_{Fe^{3+}} = 2N_{O^{--}} + 4N_{Fe_2O_5^{4-}} \quad [b]$$

Here N represents ion or atom fractions while n is the number of moles of ferrous and ferric ion respectively per mole of total negative ion. Simultaneous solution of Eq *a* and *b* leads to the value of $N_{Fe^{++}}$ shown in column six which in these solutions is equal to $n_{Fe^{++}}/(n_{Fe^{++}} + n_{Fe^{3+}})$.

The activity of ferrous ion in column seven is obtained by Eq 2 from the activity of FeO and the ion fraction of oxide ion which is here assumed equal to its activity. The activity coefficient shown in column eight is remarkably close to unity but the deviations are not negligible.

In order to obtain activity coefficients of Fe^{3+}, we shall assume that the activities of the two positive ions follow the same relationship as that governing the behavior of two components in a binary system. By analogy with the Gibbs-Duhem equation[17] we write:

$$\log \gamma_{Fe^{3+}} = -\int_0^N \frac{N_{Fe^{++}}}{N_{Fe^{3+}}} d \log \gamma_{Fe^{++}}$$

The integration covers the composition range extending to "pure" FeO and consequently involves a rather gross extrapolation. The uncertainty thus introduced corresponds to a constant factor in the activity and hence does not affect the relative accuracy. The resultant values of the activity coefficient and the activity of Fe^{3+} are given in Table 4. Finally the values of K_3 based upon these data are shown in the last column. The surprisingly good constancy may be due as much to the method of obtaining $\gamma_{Fe^{3+}}$ as to any other factor, but it should be noted that these values themselves do not vary greatly and a fairly constant K_3 could have been obtained using ion fractions for activities.

The Distribution of FeO between Molten Iron and Oxide Slags

PURE IRON OXIDE SLAGS

From the ionic viewpoint the distribution of FeO between molten iron and liquid iron oxide may be expressed by the following equation:

$$Fe\ (liq.) + O\ (in\ Fe) = FeO = Fe^{++} + O^{--} \quad [4]$$

$$K_4 = \frac{a_{FeO}}{\%\ O} = \frac{a_{Fe^{++}} \cdot a_{O^{--}}}{\%\ O}$$

The experimental data[13,14] on the distribution of FeO between molten iron and liquid iron oxide containing small amounts of CaO, MgO and SiO_2 are used to determine the distribution constant K_4. The most probable ion species in these slags are: Ca^{++}, Mg^{++}, Fe^{++}, O^{--}, SiO_4^{4-} and $Fe_2O_5^{4-}$. Since the concentration of ions other than Fe^{++} and O^{--} is very low, the activity coefficeint of Fe^{++} and O^{--} will be close to unity and as an approximation ion fractions may be used for activities.

A plot of log K_4 vs. $1/T$ is shown in Fig 1. The straight line is represented by the equation

$$\log K_4 = +6000/T - 2.57 \quad [4a]$$

This is essentially equivalent to the equation used by Taylor and Chipman[14] to represent the same series of data. It differs slightly because of the different standard state used here and the different method of correcting for impurities.

When the slag is in equilibrium with molten iron, it contains a small concentration of trivalent iron in the form of ferrite ion as shown by the equation

$$3Fe^{++} + 5O^{--} = Fe + Fe_2O_5^{4-} \quad [5]$$

$$K_5 = \frac{a_{Fe_2O_5^{4-}}}{(a_{Fe^{++}})^3 \cdot (a_{O^{--}})^5}$$

Values of K_5 are readily obtained from the data of Darken and Gurry. Using their limiting gas and oxide compositions, with a small correction to correspond with liquid iron, and our average values of K_1, we find at temperatures of 1600, 1500 and 1400°C that $K_5 =$ 0.0255, 0.0316 and 0.0395 respectively.

IRON OXIDE SLAGS CONTAINING LIME OR MAGNESIA

When liquid iron oxide slags containing varying amounts of lime or magnesia in solution are at equilibrium with molten iron, the concentration of

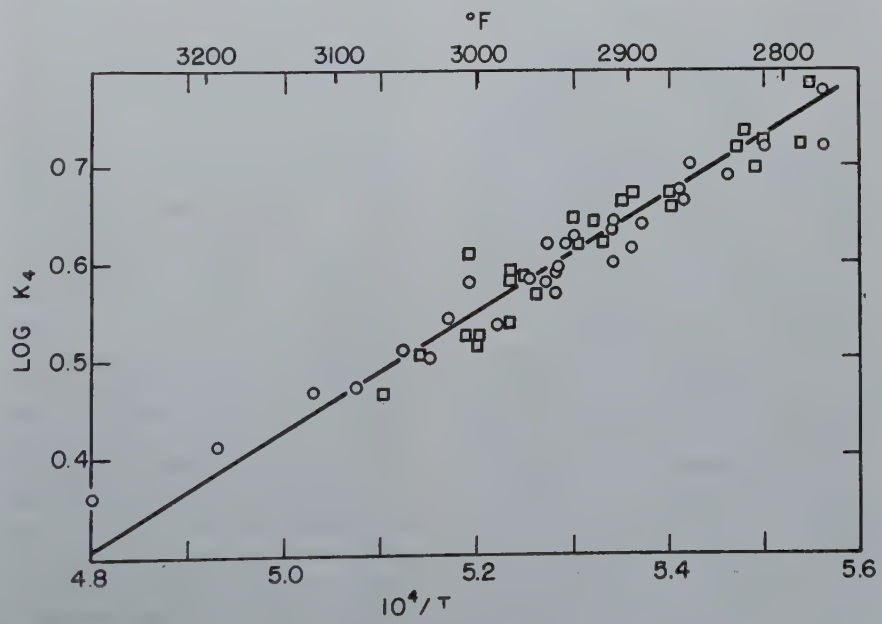

FIG 1—Temperature dependence of the ionic distribution constant for oxygen between iron and iron oxide slags. $K_4 = a_{Fe^{++}} \cdot a_{O^{--}}/\%\ O$. *Circles*, Chipman and Fetters;[13] *squares*, Taylor and Chipman.[14]

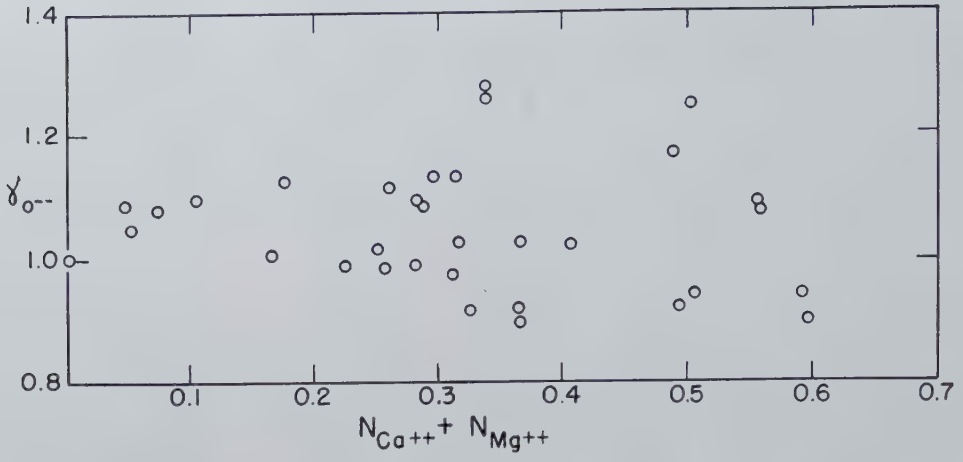

FIG 2—Activity coefficient of oxide ion in slags containing the oxides of iron, calcium and magnesium.

oxygen in the metal phase serves as a convenient measure of the activity of FeO in the slag. The concentration of ferrite ion in the slag at equilibrium with molten iron is relatively low but increases with increasing percentages of CaO or MgO. That of Fe^{3+} is entirely negligible.

Activities of Fe^{++}, Ca^{++} and Mg^{++} may be assumed equal to their ion fractions. The activity of O^{--} is obtained from that of Fe^{++}, the oxygen content of the molten iron in equilibrium with the slag, and the value of K_4 given in Eq 4a. The data of Taylor[14] and of Fetters and Chipman[15] are used in making the calculations, the results of which are shown in Fig 2. Here the value of the activity coefficient of oxide ion is plotted against the sum of the ion fractions of Ca^{++} and Mg^{++}. With a few exceptions the values of $\gamma_{O^{--}}$ fall in the range 0.9 to 1.15 and appear to be almost independent of the ratio of Ca^{++} to Fe^{++}, perhaps increasing slightly with decreasing Fe^{++}. The method of computation imposes all of the errors of experiment and of assumptions regarding activities upon the value of $\gamma_{O^{--}}$. The fact that the result lies within 10 to 15 pct of unity at all compositions indicates the usefulness of Temkin's rule in these solutions. It shows further that FeO and CaO are almost equal with respect to the amount of oxide ion that each contributes to slags of this type. This finding might reasonably be construed as evidence that both oxides are either completely ionized or not at all.

The activity of $Fe_2O_5^{4-}$ ion in these slags may be obtained from the slag compositions and values of K_5 given in the preceding section. The accuracy will be improved somewhat by combining K_5 with K_4 to obtain the following:

$$K_6 = \frac{a_{Fe_2O_5^{4-}}}{a_{Fe^{++}} \cdot (a_{O^{--}})^3 [\%\ O]^2} \quad [6]$$

Values of K_6 are given by the following equation which is based upon data previously cited for the other K''s:

$$\log K_6 = +15000/T - 8.32 \quad [6a]$$

Values of the activity coefficient of $Fe_2O_5^{4-}$ ion found from these equations and data on lime-iron oxide slags are presented in Fig 3. Here is an entirely different behavior by an activity coefficient than we have found for that of any other ion, the variation being about 100-fold within the observable concentration range. It is true that the method of calculation has piled all the errors of data and assumptions onto this coefficient; but the same data gave activity coefficients for oxide ion approximating unity. Moreover the low coefficient for $Fe_2O_5^{4-}$ ion is not related to a high concentration of this ion but is dependent upon a high concentration of the cations Ca^{++} and Mg^{++}. It is evident that these two ions exert a very different effect upon $Fe_2O_5^{4-}$ than does Fe^{++}, the effect being of the nature of an attraction between positive and negative ions. What this means in terms of the structure of the melt cannot be learned from thermodynamics alone. It may be regarded as evidence of a tendency to form complex ions or neutral compounds, or of a more pronounced close-range ordering of positive and negative ions. Flood and Förland[5] have pointed out other instances in which the stability of similar anions is markedly affected by the nature of the cation. Kheinman[16] called attention to the striking differences between melts of the compositions $2FeO \cdot SiO_2$ and $2CaO \cdot SiO_2$. The former is an excellent conductor of electricity and the conductivity is progressively diminished as the latter is added. He regards this as evidence of a change in the coordination numbers of the ions, the Ca^{++} ion being prevented from taking part in the transfer of electricity by a coating of silicate ions. The result is equivalent to the formation of "nondissociated" Ca_2SiO_4. This seems quite analogous to the case of the ferrites.

We now return to the question of what constitutes a basic oxide in slag. How can we, on the basis of ionic theory, account for the differences in behavior between the common basic oxides? That these differences are not due to different degrees of ionization of the oxides themselves has been demonstrated in the case of CaO-FeO slags where the oxide-ion activity is essentially independent of the cation. The evidence thus far presented indicates that differences in the basic strength of oxides becomes apparent only in the presence of anions other than O^{--}. And it is the ability of the cation to bind these larger anions into inactive complexes which determines the behavior of the oxide as a base. We shall not attempt a detailed discussion of the nature of these inactive complexes. They may be thought of as neutral ion-groups behaving as molecules or as regions of marked close-range order, or as parts of a network of anions in which the cations of the more strongly basic oxide become more firmly entangled. In representing them by chemical formulas we must for the present disclaim any implication as to structure.

With this understanding we may say that the stronger basic properties of CaO as compared to FeO are due

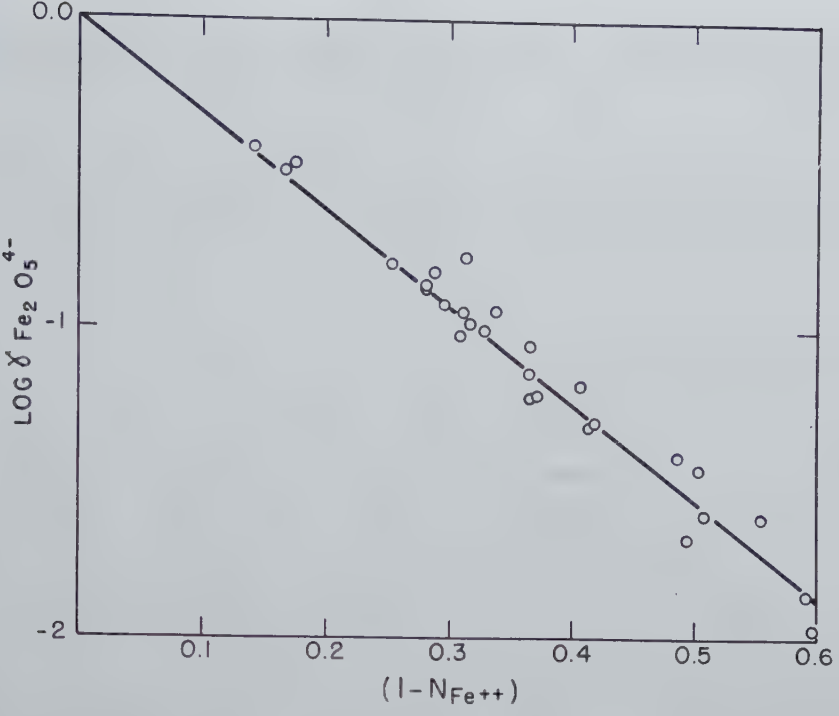

FIG 3—Activity coefficient of ferrite ion in slags containing the oxides of iron, calcium and magnesium.

to the nearer approach to completion of such reactions as: $2Ca^{++} + Fe_2O_5^{4-} = Ca_2Fe_2O_5$ than in the corresponding reaction of Fe^{++}. There is no conflict between this concept and the statement that a basic oxide is one which increases the oxide-ion activity of the slag. Addition of either CaO or FeO to a slag increases the oxide-ion concentration about equally. But the addition of CaO, by inactivating larger ions such as ferrite, increases the effective fraction of O^{--} and thereby causes a further increase in the oxide-ion activity. Kheinman[16] has shown that this concept is capable of quantitative application to silicate slags and leads to satisfactory results for oxygen and sulphur distribution in slags containing up to 30 pct silica. It is our intention to discuss such applications in more detail in a later paper.

Summary

This paper is a step toward a thermodynamic treatment of slag-metal and slag-gas reactions based upon the assumption of ionization in the slag. The Lewis theory of acids and bases is applied to slags. Basic slags contain oxide ion O^{--} which is itself a strong base. The activity of oxide ion in the slag determines its basicity and a basic oxide is one which will increase the oxide-ion activity of the slag. The step-wise neutralization of acid oxides by oxide ion is illustrated.

The theory of complete ionization of open hearth slags is discussed and it is shown that ion activities may be useful even without knowledge of the degree of ionization. Temkin's use of ion fraction as a measure of ion activity is a useful approximation; ionic solutions which are ideal in this respect may be achieved by judicious selection of ion formulas.

The data of Darken and Gurry on equilibrium of gases with liquid iron oxides are consistent with the ion formulas Fe^{++}, O^{--}, $Fe_2O_5^{4-}$ and Fe^{3+}, the last being significant only in highly oxidized slags. Thermodynamic relationships among these ions are deduced from the data.

Data on the distribution of iron oxide between metal and simple oxide slags is shown to be consistent with the same ion formulas and thermodynamic constants. In iron oxide slags the ion activity coefficients are unity. Addition of CaO or MgO has little effect on the activity of oxide ion but causes a sharp decrease in activity coefficient of $Fe_2O_5^{4-}$ ion.

The differences in basic strength of oxides in slags are ascribed to differences in the abilities of the cations to form inactive complexes with the larger anions such as $Fe_2O_5^{4-}$ and SiO_4^{4-}.

This paper is based upon part of a study of the behavior of metallurgical slags sponsored by the American Iron and Steel Institute.

References

1. G. N. Lewis: *Jnl.* Franklin Inst. (1938) **226,** 293.
2. K. H. Sun and A. Silverman: *Jnl.* Amer. Ceram. Soc. (1945) **28,** 8.
3. K. H. Sun: The Glass Industry. (1948) **29,** 73.
4. M. L. Huggins and K. H. Sun: *Jnl.* Phys. Chem. (1946) **50,** 319; (1947) **51,** 438.
5. H. Flood and T. Förland: Acta Chem. Scand. (1947) **1,** 592.
6. W. Stegmaier and A. Dietzel: *Glastech. Ber.* (1940) **18,** 297 and 353; *Ceram. Abstr.* (1941) **20,** 235.
7. J. O'M. Bockris, J. A. Kitchener, S. Ignatowicz and J. Tomlinson: The Faraday Soc. Symp. on the Phys. Chem. of Process Metallurgy (1948).
8. P. Herasymenko: *Trans.* Faraday Soc. (1938) **34,** 1234; *Archiv für das Eisenh.* (1940) **14,** 109.
9. M. Temkin: *Acta Physicochimica* U.R.S.S. (1945) **20,** 411.
10. A. Samarin, M. Temkin and L. Shvarzman: *Acta Physicochimica* U.R.S.S. (1945) **20,** 421.
11. L. S. Darken and R. W. Gurry: *Jnl.* Amer. Chem. Soc. (1947) **68,** 798.
12. E. C. Smith: *Trans.* AIME (1935) **116,** 13.
13. J. Chipman and K. L. Fetters: *Trans.* A. S. M. (1941) **29,** 953.
14. C. R. Taylor and J. Chipman: *Trans.* AIME (1943) **154,** 228.
15. K. L. Fetters and J. Chipman: *Trans.* AIME (1941) **145,** 95.
16. A. S. Kheinman: *Bull.* Acad. Sciences U.R.S.S. (1946) **10,** 1439.
17. Lewis and Randall: Thermodynamics (1923), p. 269 (McGraw-Hill).

Properties of Chromium Boride and Sintered Chromium Boride*

S. J. SINDEBAND,† Member AIME

Introduction

Prior to discussing the metallurgy of sintered chromium borides, it is pertinent to outline some of the reasoning behind this investigation and the purposes underlying the work.

This study was initiated as an approach to the ubiquitous problem of a material for service at high temperatures under oxidizing atmospheres, and it was undertaken with a view to raising the 1500°F (816°C) ceiling to 2000°F (1093°C) or better. For the reason that no small, but rather a major, lifting of the high temperature working limit was being attempted, it was felt appropriate that a completely new approach be taken to this problem.

A summary of the thinking behind this approach was published recently by Schwarzkopf.[1] In briefest terms, it was postulated that the following requirements could be set up for a material which would have high strength at high temperatures.

1. The individual crystals of the material must exhibit high strength interatomic bonds. This automatically leads to consideration of highly refractory materials, since their high energy requirements for melting are related to the strength of their atom-to-atom bonds.

2. On the polycrystalline basis, high boundary strength, superimposed on the above consideration, would also be a necessity. Since this implies control of boundary conditions, the powder metallurgy approach would hold considerable promise.

Such materials actually had been fabricated for a number of years, and the cemented carbide is the best example of these. Here a highly refractory crystal was carefully bonded and resulted in a material of extremely high strength. That this strength was maintained at high temperature is exhibited by the ability of the cemented carbide tool to hold an edge for extended periods of heavy service.

Nowick and Machlin[2,3] have analytically approached the problem of creep and stress-rupture properties at high temperature and developed procedures whereby these properties can be approximately predicted from the room temperature physical constants of a material. The most important single constant in the provision of high temperature strength and creep resistance is shown to be the Modulus of Rigidity. On this basis, they proposed that a fertile field for investigation would be that of materials similar to cemented carbides, which have Moduli of Rigidity that are among the highest recorded.

The cemented carbide, however, does not have good corrosion resistance in oxidizing atmospheres and without protection could not be used in gas turbines and similar pieces of equipment. It would be necessary then to attempt the fabrication of an allied material based upon a hard crystal which had good corrosion resistance as well.

It was upon these premises that the subject study was undertaken and at an early stage it was sponsored by the U.S. Navy, Office of Naval Research. Since then, it has been carried on under contract with this agency.

Chromium boride provided a logical starting point for such research, since it was relatively hard, exhibited good corrosion resistance, and, in addition, was commercially available, since it had found application in hard-surfacing alloys with iron and nickel. That chromium boride did not provide a material that met the ultimate aim of the study results from factors which are subsequently discussed. This, however, does not detract from the basis on which the study was conceived, nor from the value of reporting the results which follow.

San Francisco Meeting, February 1949.

TP 2519 E. Discussion of this paper (2 copies) may be sent to *Transactions* AIME before May 15, 1949. Manuscript received October 18, 1948; revision received November 26, 1948.

* This paper was also presented, in part, at The International Powder Metallurgy Congress, 1948, Graz, Austria.

† Technical Director, American Electro Metal Corporation, Yonkers, N. Y.

References are at the end of the paper.

Chromium Boride

While work on chromium boride proper dates back to Moissan,[4] there has been a dearth of literature on borides since 1906. Subsequent to Moissan, principal investigators of chromium boride were Tucker and Moody,[5] Wedekind and Fetzer,[6] du Jassoneix,[7,8,9] and Andrieux.[10]

These investigators were generally limited to studies of methods of producing chromium boride and determining its properties. Some study, however, was devoted to the chromium-boron system by du Jassoneix,[7] who did this chemically and metallographically. This system is not amenable to normal methods of analysis by virtue of the refractory nature of the alloys involved, and the difficulties of measurement and control of temperature conditions in their range. Dilatometric apparatus is nonexistent for operation at these temperatures. Du Jassoneix made use of apparent chemical differences between two phases observed under the microscope and reported the existence of two definite compounds, namely: Cr_3B_2 and CrB. These two compounds, he reported, had quite similar chemical characteristics, but were sufficiently different to enable him to separate them.

The easiest method for producing chromium boride is apparently the thermite process, first applied by Wede-

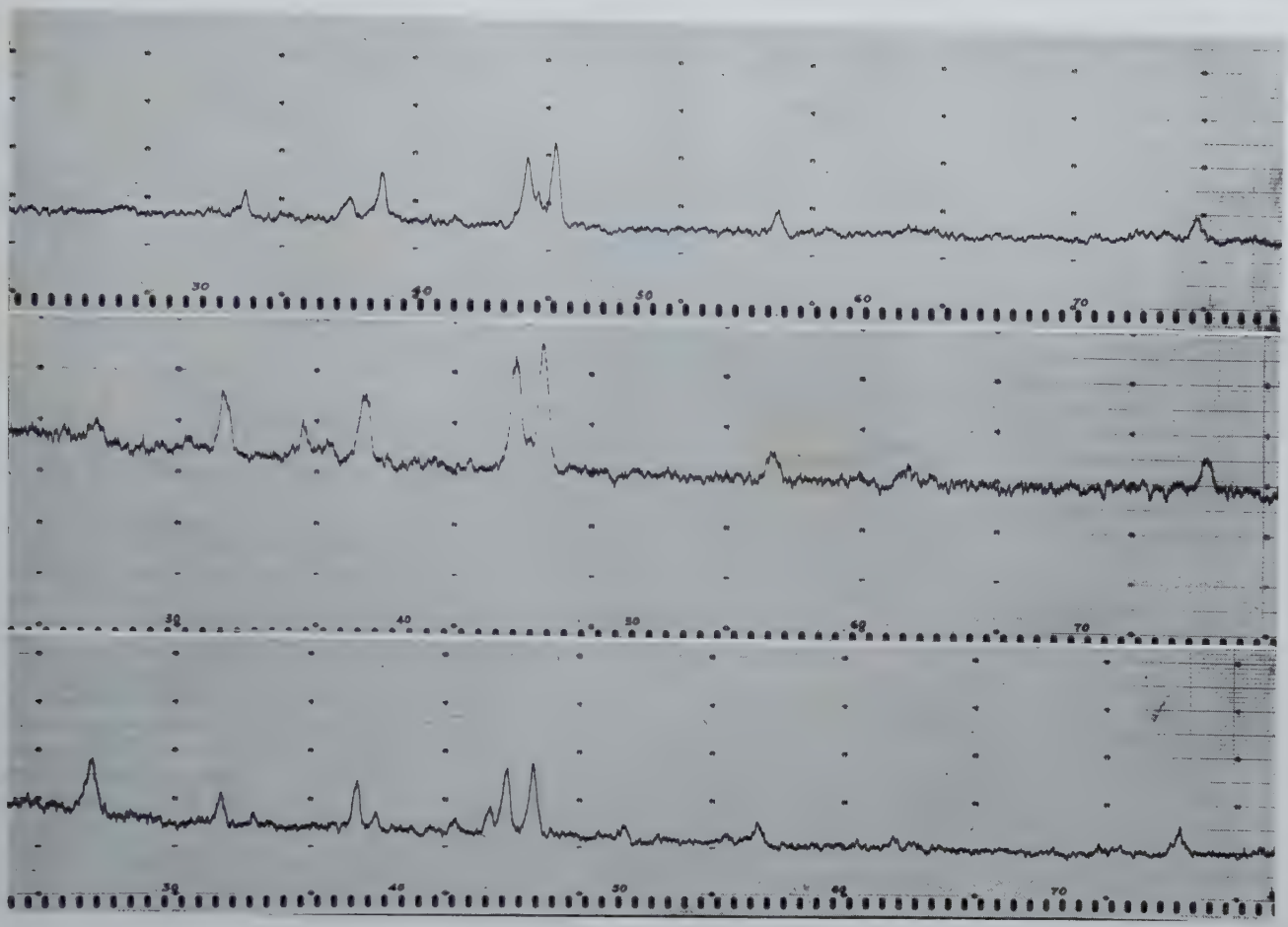

FIG 1 (top)—Chromium boride crystals. (Aluminum thermite.) Pct Boron = 18.0.
FIG 2 (center)—Chromium boride crystals. (Carbon and silicon reduction.) Pct Boron = 14.1.
FIG 3 (bottom)—Chromium boride crystals. (Electrolysis.) Pct Boron = 13.2.

kind and Fetzer.[6] The commercial product, manufactured in the United States, is also made by thermite processes,[11] involving a simultaneous reduction of boric anhydride and chromium oxide CrO_3. A purer product is obtainable by the electrolysis of fused borate baths described by Andrieux.[10]

X ray diffraction studies have been made in the present investigation of chromium borides produced by:

1. Aluminum thermite reduction of B_2O_3 and CrO_3.
2. Carbon and silicon reduction of B_2O_3, and CrO_3.
3. Electrolysis of fused borate baths.

Samples having widely different compositions were checked in the boron content range of 12 to 20 pct. This range would include both the compositions Cr_3B_2 and CrB. The X ray diffraction patterns, taken on a Philips Norelco Recorder and using Cu ($K\alpha_1$) radiation, were substantially identical over the entire range. Typical patterns are given in Fig 1, 2, and 3, and the analyses of the samples are given in the next column.

	Chromium Boride Produced by Aluminum Thermite, Pct	Chromium Boride Produced by Carbon and Silicon Reduction, Pct	Chromium Boride Produced by Electrolysis, Pct
Chromium	76.12	70.35	82.0
Boron	18.0	14.1	13.2
Iron	0.52	2.21	
Aluminum	2.14		
Carbon	0.03	1.86	1.7
Silicon	0.44	4.23	
Calcium		2.36	0.4
Magnesium		0.06	
	97.25	95.17	97.3

In Fig 3 it will be noted that a strong peak appears at 26.6° which is found relatively weaker in Fig 2. This line reflects the presence of graphite impurities.

The conclusion has been drawn that a single phase exists over this entire range, and that this is true regardless of method of fabrication. A single compound exists in this range, and its structure is maintained in adjacent nonstoichiometric compositions. This compound has, apparently, a so-called "subtractional" lattice, that is, it can lose some boron without affecting its crystal structure. This is a consequence of the small size of the boron atom relative to the chromium atom. This has led to the conclusion that there is only one compound of chromium boride, within the compositions indicated, and that it corresponds to the formula CrB.

An investigation is presently being made of the actual crystal structure of the compound CrB. This is being carried out by Mr. A. J. Frueh, Jr., at the Massachusetts Institute of Technology, and while this is not yet complete, the author, through the kindness of Mr. Frueh, is privileged to be able to present some data on this structure. The structure of CrB is orthorhombic, and its unit cell has the following dimensions:

$$a = 2.95 \text{ A.U.}$$
$$b = 7.80 \text{ A.U.}$$
$$c = 2.93 \text{ A.U.}$$

This cell contains four molecules of chromium boride, which is in accord with its measured density, as reported

in a subsequent paragraph. The four chromium atoms have the following coordinates:

x	y	z
0	0.145	0.25
0	0.855	0.75
0.5	0.645	0.25
0.5	0.355	0.75

The positions of the boron atoms have not yet been determined exactly, but this problem is presently under study and will be published by Mr. Frueh when his investigation is completed.

It is of interest at this point to recall that Hägg[12] in his study of phases of transition elements in binary systems with boron, carbon and nitrogen, drew certain general conclusions regarding the structure of such phases. He predicted that the structure could only be a relatively close-packed one if the ratio of the diameter of the transition element atom to that of the interstitial atom was in excess of 1.7. In the case of chromium boride, this ratio is between 1.6 and 1.4 in consideration of the indefinite knowledge of the diameter of the boron atom. Since the structure of chromium boride determined by Mr. Frueh is not a close-packed one, this compound apparently behaves in accordance with Hägg's rule.

Various investigators have reported that chromium boride is relatively slowly attacked by acids. Their results vary to some degree, but this is believed to be the consequence of varying impurity contents. In this investigation it was noted that hydrochloric, sulphuric, hydrofluoric and perchloric acids attack it only slowly. The only one of these capable of dissolving it completely is perchloric acid. Nitric acid attacks it almost negligibly and when dilute can be considered, effectively, to fail to attack it at all. Fused sodium peroxide dissolves it completely, as do nitrate-carbonate mixtures.

Densities varying from 5.4 to 6.7 g per cc have been reported for chromium boride. None of these investigators reported the conditions, other than temperature, under which the determination was made. Depending upon composition, the densities noted in the present study were in the range 6.15 to 6.20 g per cc at 18°C, taken in ethyl benzene by the standard pycnometric method.

The hardness of chromium boride has previously been reported to be about 8.5 on Moh's scale.[10]

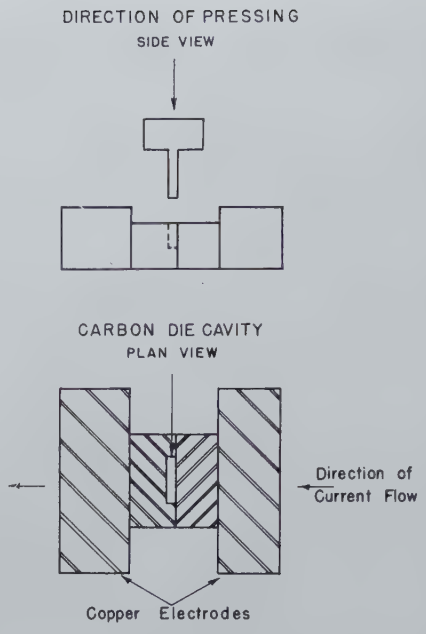

FIG 4—Schematic diagram of hot pressing.

PRESSING AND SINTERING

Attempts to cold press compacts of chromium boride and a binder when the boride content exceeded 75 pct were effectively unsuccessful. Compacts could be obtained but the resultant body, after sintering up to 1500°C in H_2, showed densities which were low and the attendant physical properties suffered. This is considered to be a direct result of the high hardness and negligible room temperature plasticity of the chromium boride. At an early stage in the work, cold pressing and sintering were abandoned in favor of hot pressing. When hot pressing was carried out at temperatures sufficiently high to melt the binder employed, highly dense bodies resulted having interesting properties.

The hot pressing method used is illustrated diagrammatically in Fig 4. A high current was passed through the graphite die proper, and the heat so generated plus heating occurring as a consequence of current passing through the work itself made it possible to raise the temperature to 1500°C in approximately 1–2 min. When the temperature was reached at which pressing was to occur, the current was stopped and pressing accomplished by hydraulic means. No provision for atmosphere was made, and the carbonaceous atmosphere within the die and the short times involved made it possible to avoid any indication of oxidation. The pressure was uniformly held at 1 tsi.

The most effective binder employed proved to be nickel, and the writer will limit himself to mixtures of 85 pct chromium boride, 15 pct nickel, for the purpose of showing the effects of certain parameters. A comparison with other binders will be made in a latter part of this paper.

The chromium boride powder used throughout the following experiments was that produced by aluminum thermite reduction, the analysis of which has already been given. The nickel powder was spectrographically analyzed to be 99.6+ pct nickel, with small impurities, as follows:

	Pct
Iron	0.22
Zinc	0.03
Copper	0.065
Lead	0.025
Sulphur	0.021

The chromium boride powder was first ball milled to a given particle size in either a stainless steel or tungsten carbide-lined mill. The latter type was employed only where the particle size desired required milling times which resulted in excessive pick-up of material from the stainless steel mill. The ball milling medium was distilled water. The balls, in each case, were of the same material as the liner. The fine powder was then ball milled again, to mix it with the binder. Water again was the medium employed. After drying the powder with alcohol, the powder mix was ready for hot pressing.

The powders were pressed into a flat bar shape 1 in. × 0.375 in. × approximately 0.200 in. thick. This shape specimen lent itself readily to transverse rupture testing where the span was $\frac{9}{16}$ in. and the load was applied at the center of the bar and span by means of a 10 mm Brinell ball. This test was the main evaluation method for room temperature properties.

The effect of particle size and temperature of pressing proved to be interrelated and interesting. For any given particle size, an optimum temperature of pressing was noted.

The optimum pressing temperature was lower with each reduction in particle size, although this effect became almost negligible once the particle size was down to 3 to 5 microns.

Optimum conditions applied when the particle size was reduced to 3 to 5 microns, and the temperature of pressing, as measured optically on the exterior of the graphite die, was 1300°C. It is estimated that this corresponded to 1550°C inside the die. Under these conditions the Modulus of Rupture was found to be circa 120,000 psi, and the hardness averaged 89 on the Rockwell A scale. Fig 5 shows the effect of temperature of pressing, under the condi-

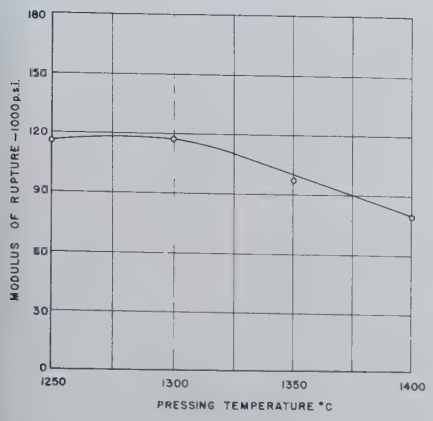

FIG 5—Effect of pressing temperature on Modulus of Rupture. 15 pct nickel binder.

tions indicated above, on the Modulus of Rupture.

Decreasing the particle size further, to a point where it fell between 1 and 2 microns resulted in increased hardness values, that is, 90–91 Rockwell A, but resulted in a decreased Modulus of Rupture optimum. This value fell to 85,000 psi.

Increasing the particle size, or the use of particle size distribution having higher average particle size, resulted in decreasing the Modulus of Rupture as well as the hardness.

The density of a cast 85/15 chromium boride/nickel alloy was measured as 6.17 g per cc and the densities obtained by hot pressing the 3–5 micron powder and 1–2 micron powder, as described above, proved to be circa 5.90 g per cc, so that densities of the order of 96 pct were achieved.

The effect of the use of binders other than nickel is best indicated by the following table, in which the optimum Modulus of Rupture obtained is indicated as well as hardness. The particle size employed was 3–5 microns in all cases, and the composition was 85 pct chromium boride, balance binder.

A typical micrograph of a nickel bound specimen is shown in Fig 6.

HIGH TEMPERATURE TESTING

The following tests have been made to indicate the behavior of this material at high temperatures:

1. Hot hardness (70 pct CrB, 30 pct Ni).
2. Stress rupture.
3. Corrosion in air.

The hot hardness tests were made in an atmosphere of N_2 in a furnace specially designed by E. C. Bishop and M. Cohen.[13] While the tests were made on a slightly different composition than is presently believed to be an optimum,

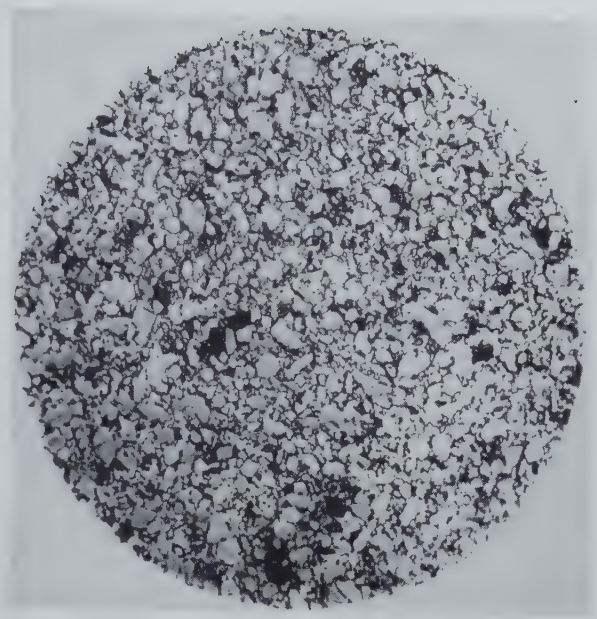

FIG 6—Chromium boride/nickel, 85/15. Etchant: 4 pct Picral. ×500

Table 1 . . . Optimum Results of Chromium Boride Sintered with Different Binders (85/15)

Binder	Modulus of Rupture (psi)	Hardness R_A
Nickel	123,000	87.4
Nickel-copper (70-30)	120,000	86.7
Nickel-chromium (60-40)	113,000	88.1
Cobalt	80,000	90.5

the effect of the use of the 85/15 would have merely translated the curve given in Fig 7 upwards about one point on the hardness scale.

Stress-rupture tests on the 85/15 composition were carried out at the Battelle Memorial Institute, and the results of the tests are given graphically in Fig 8. The hot strength, if taken at the 1000 hr point, is of the order of one

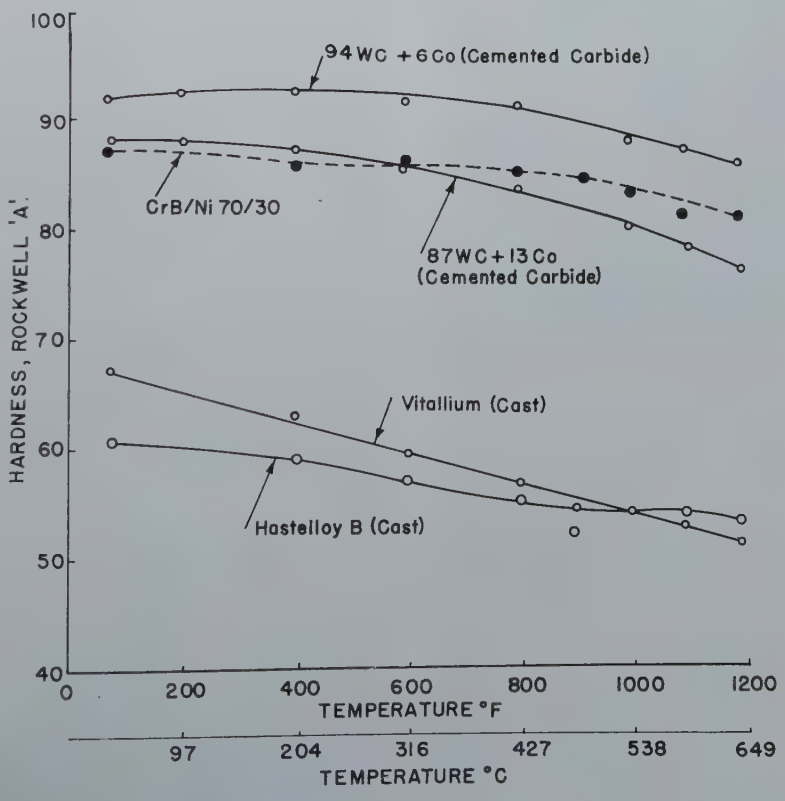

FIG 7—Hardness variation with temperature.

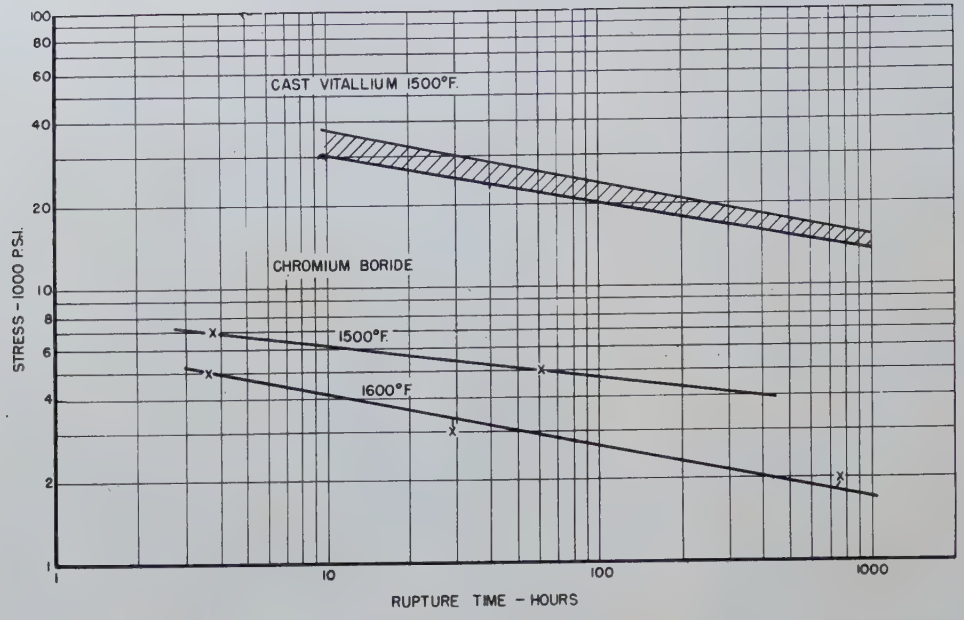

FIG 8—Stress vs. rupture time curves for nickel-bonded chromium boride.

quarter that of cast Vitallium. (Vitallium composition: 0.2 C, 28 Cr, 2.5 Ni, 62 Co, 5.5 Mo, 1 Fe.)

Table 2 gives typical results obtained when the 85/15 CrB/Ni material was tested in air for corrosion.

It was in the above corrosion tests that a serious limitation of this particular material was noted. It can be seen that there are indications of a liquid phase forming at about 1900°F (1038°C). This liquid phase is caused by the development of less refractory nickel borides and systems of these. Their formation limits the use of this material to a maximum temperature of about 1750°F (954°C). There can be no question that the formation of these lower melting point constituents also influenced the observed strength at 1500° and 1600°F (816° and 871°C). Their formation, however, indicated that further work needs to be done to fabricate a material on similar principles in which such a phenomenon will be absent. This work is in progress.

Table 2 . . . Air Corrosion Tests on Chromium Boride/Nickel 85/15

Material and Sample No.	Temperature °F	Temperature °C	Atmosphere	Time hr	Remarks
85/15 CrB-Ni					
1	1525	830	air	48	No reportable change
2	1600	871	air	48	No reportable change
3	1725	940	air	48	Slight green oxide coat
4	1850	1010	air	48	Slight green oxide coat
5	1900	1038	air	48	Initial indication of liquid phase at surface. Hardness drop from R_A 88.5 to 80. No grain size change
6	2050	1121	air	48	Dark coating formed; distortion.

Summary

It has been determined that only one chromium boride compound exists in the range 12 pct to 20 pct boron content, instead of two, as had previously been reported.

The composition of the above compound is postulated to be CrB, and its structure is reported to be orthorhombic. The dimensions of the unit cell are given as well as the coordinates of the chromium atom.

New data regarding the properties of this boride are presented.

Experimental results are given of an investigation of the pressing and sintering of chromium boride with nickel as a binder. A Modulus of Rupture of 120,000 psi is reported for such material when hot pressed.

Data are given regarding the high temperature strength and corrosion resistance of the above material. The hot strength at 1500°F (816°C) is of the order of one quarter that of cast Vitallium. The formation of a liquid phase at about 1900°F (1038°C) is noted, and a limitation of use temperature is set at 1750°F (954°C).

Acknowledgment

The writer wishes to extend his sincere thanks and appreciation to Dr. Paul Schwarzkopf for his guidance and help, to Dr. J. T. Norton for his assistance in many matters, particularly in the X ray diffraction studies, to Mr. A. J. Frueh, Jr., to Dr. Morris Cohen for the use of his Hot Hardness Testing equipment, and to Dr. H. Blumenthal and Mr. Alvin Cohan for their overall assistance throughout the above study.

References

1. P. Schwarzkopf: Powder Metallurgy Bull. I, No. 6 (Nov. 1946) p. 86.
2. A. S. Nowick and E. S. Machlin: Nat'l. Advisory Comm. for Aeronautics, Tech. Note No. 1039, April 1946.
3. E. S. Machlin and A. S. Nowick: *Met. Tech.*, Feb. 1947, TP 2137. *Trans.* AIME (1947) **172**, 386.
4. H. Moissan: C. R. Acad. Sci. Paris, **119**, 185, (1894).
5. S. A.Tucker and H. R. Moody: *Jnl.* Chem. Soc. (1902) **81**, 14–17.
6. E. Wedekind and K. Fetzer: *Ber. dtsch. chem. Ges.* (1907) **40**, 297–301.
7. Binet du Jassoneix: *Thèse.* Paris, 1909.
8. Binet du Jassoneix: C. R. Acad. Sci. Paris, (1906) **143**, 897–899.
9. Binet du Jassoneix: C. R. Acad. Sci. Paris, (1906) **143**, 1149–1151.
10. L. Andrieux: *Thèse*, Paris, 1929.
11. N. W. Cole and W. H. Edmonds: U.S. Pat. 2,088,838 (1937).
12. Gunnar Hägg: *Ztsch. Phys. Chem. Abt. B*6 (1930) 221–232.
13. E. C. Bishop and M. Cohen: *Metal Progress* **43**, Mar. 1943.

Grain Coarsening in Copper

PAUL A. BECK,* Member AIME, JOHN TOWERS, JR.,* and PHILIP R. SPERRY*

Dahl and Pawlek[1] found that electrolytic copper develops extremely coarse grains at 1000°C after about 90 pct reduction by rolling. This coarsening occurs only under conditions of penultimate grain size, deformation, and alloying which lead to the "cube" recrystallization texture.[1,2,3,5] The peculiar angular shapes and straight grain boundaries of the coarse grains were noted by several investigators.[1,4,5]

On the other hand, coarsening in Fe-containing aluminum or in Al-Mn alloys[8] does not depend on a "cube" (or any well developed) recrystallization texture. It is true that increasing deformation by rolling, and, therefore, an increasingly well developed recrystallization texture, are associated with decreasing incubation periods of coarsening.[6,7,8] Nevertheless, coarsening readily develops in aluminum even after only 30 pct reduction by rolling, where the recrystallization texture is very weak.[6,8] Also, coarsening was observed by Jeffries[9] many years ago in sintered thoriated tungsten, which presumably has no preferred orientation. In all these cases coarsening is associated with grain growth inhibition by a dispersed second phase.[8,9] The annealing temperature has to be sufficiently high to overcome the inhibition at a few locations. But if it is too high, growth starts at many points, and the resulting grain size becomes much smaller.[9] Normally, the coarse grains are more or less equiaxed, and the boundaries have a typical ragged appearance.[5,8]

Cook and Macquarie[4] demonstrated that, in addition to the texture-dependent coarsening previously found at 1000°C,[1] electrolytic tough pitch copper may also coarsen at 800°C after 50 pct reduction by cross rolling. The coarse grains formed under such conditions have rounded shapes and ragged boundaries, like those in aluminum. When the annealing temperature is higher, the tendency for their formation decreases. All these observations suggest that the coarsening at 800°C is associated with inhibition by a second phase. Actually, coarsening at 800°C after 50 pct reduction by cross rolling was observed only in tough pitch copper,[4] which contains Cu_2O particles. On the other hand, the texture-dependent 1000°C coarsening occurs in both tough pitch and oxygen-free copper;[4] it does not appear to depend on the presence of a dispersed second phase. However, the interpretation of the 800°C coarsening in Cu after 50 pct rolling as an inhibition-dependent process, similar to the coarsening in Al-Mn alloys, is somewhat weakened by the fact that this coarsening was reported[4] to occur only after cross rolling, and not after straight rolling. It was, therefore, decided to re-examine this question.

A 1 in. diam electrolytic tough pitch copper rod, No. 2 hard drawn, was annealed for 20 min at 700°C, rolled to 0.5 in., annealed 10 min at 700°C, and straight rolled to 0.064 in. It was then given a penultimate anneal of 20 min at 500°C and it was cut into four sections, which were given final reductions by straight rolling as follows:

A 30 pct reduction of area
B 50 pct reduction of area
C 70 pct reduction of area
D 90 pct reduction of area

Specimens cut from the four sections were finally annealed at 800°C in an oxidizing atmosphere. Strip *A* remained fine grained up to 10 hr, but the specimen annealed 12 hr consisted of only 2 large grains. Strip *B* had a few scattered large (½ to ¾ mm) grains after 1 min, although the balance of the specimen consisted of fine grains of about 0.02 mm. After 5 min there were several 10 to 15 mm grains present, and after 1 hr strip *B* was completely coarsened. The coarse grains had the same characteristics (see Fig 1) as those obtained by Cook and Macquarie at 800°C after cross rolling. Strip *C* had several grains of 0.05 to 1 mm after 1 min, but it was still largely fine grained after 12 hr. After 48 hr it consisted entirely of grains of about 0.5 to 4 mm, with an extraordinarily large number of twin bands. Strip *D* remained completely fine grained after 4 hr at 800°C. These results indicate that, in the deformation range of 30 to 70 pct reduction, the incubation period for coarsening as well as the rate of growth and the final size of the coarse grains decreases with increasing deformation. Similar

Technical Note 12. Manuscript received Oct. 18, 1948.

* Assistant Professor, Graduate Student, and Metallographer, respectively, Department of Metallurgy, University of Notre Dame.

[1] References are at the end of the paper.

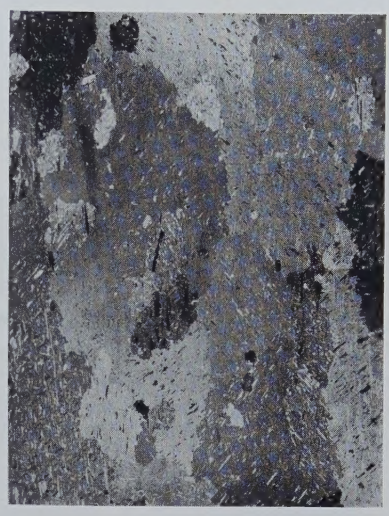

FIG 1—Tough pitch copper after final rolling of 50 pct (strip *B*) and final anneal of 1 hr at 800°C. The coarse grains have rounded shapes and ragged boundaries. Numerous small twins are entirely surrounded by coarse grains. Magnification 5 ×. (Reduced approximately one-half.)

FIG 2—Same copper as in Fig 1, after final rolling of 90 pct (strip *D*) and final anneal of 25 min at 1000°C. The appearance of this structure is dominated by the characteristically long, straight (twin) boundaries. Magnification 5 ×. (Reduced approximately one-half.)

relations were observed in the "inhibition-dependent coarsening" of Al alloys containing a dispersed phase. However, the behavior of the 90 pct rolled copper strip, which has a cube recrystallization texture, is different. Up to 4 hr it does not coarsen at all at 800°C. It coarsens at 1000°C in 3 to 6 min, in a manner typical of "texture-dependent coarsening" (Fig 2).

It may be concluded that coarsening at 800°C, after 30 to 70 pct reduction by rolling, may develop in straight rolled as well as in cross rolled tough pitch copper. This confirms the view that coarsening in Cu_2O-containing copper after 30 to 70 pct rolling is analogous to the coarsening in aluminum containing dispersed particles of a second phase.

Acknowledgment

This work was supported by the office of Naval Research, United States Navy, Contract No. N6 ori-165, T.O. No. 1.

References

1. O. Dahl and F. Pawlek: Kornordung und Kornwachstum bei Walzblechen. *Zsch. f. Metallkunde* (1936) **28,** 266.
2. G. Wassermann: Untersuchungen an Eisen-Nickellegierungen mit Wurfeltextur. *Zsch. f. Metallkunde* (1936) **28,** 262.
3. M. Cook and T. L. Richards: The Structural Changes in Copper Effected by Cold Rolling and Annealing. *Jnl.* Inst. Met. (1940) **66,** 1.
4. Maurice Cook and C. Macquarie: Development of Abnormally Large Grain Sizes in Rolled and Annealed Copper Sheet. *Trans.* AIME (1939) **133,** 142.
5. Bowles and Boas: The Effect of Crystal Arrangement on "Secondary Recrystallization" in Metals. *Jnl.* Inst. Met. (1948) **74,** 501.
6. W. Feitknecht: Crystal Growth in Recrystallized Cold Worked Metals. *Jnl.* Inst. Metals (1926) **35,** 131.
7. R. Karnop and G. Sachs: Die Grobkristallisation von Aluminum. *Metallwritschaft* (1929) **8,** 1115.
8. P. A. Beck, M. L. Holzworth and P. R. Sperry: Effect of a Dispersed Phase on Grain Growth in Aluminum-manganese Alloys. AIME TP 2475, *Metals Technology* (Sept. 1948).
9. Z. Jeffries: Grain Growth Phenomena in Metals. *Trans.* AIME (1916) **56,** 571.

Solid Nuclei in Liquid Metals

CYRIL STANLEY SMITH, Member AIME

THE partial persistence of grain size and grain shape on melting and resolidifying crystalline substances, as well as the general effects of pre-solidification and of superheating on nucleation rate, have been attributed to the presence in the liquid of crystalline impurities bearing some structural relation to the principal solid and hence capable of serving as nuclei for its crystallization. That such lattice matching does sometimes occur is well established, but it is surely improbable that a compound possessing both high-temperature stability and the requisite structural similarity should be naturally available in almost every system.

It is now suggested that a mechanism for producing appropriate nuclei exists in the crystallization of all but absolutely pure substances. Impurities can be of many kinds. Some will give rise to compounds that are less soluble in the solid crystal than in the liquid. A crystal forming from a melt or solution containing these will be supersaturated in some degree, and the foreign atoms will commence to segregate during or after solidification. They do not necessarily form pure, unstrained, crystals of the precipitating compound with its normal composition and structure. Generally—at least in the metallurgical examples that have been most studied—the first recognizable nuclei have lattice coherency with the surrounding matrix and have practically the same crystal structure and lattice spacing as the material in which they form, differing only in composition.

An extremely thin oxide layer formed under appropriate conditions on or in a solid metal will tend to be coherent with the metal lattice, and the first few atom layers of the oxide in contact with the metal will differ in both composition and structure from massive crystalline oxide. It will resemble the metal more closely than the oxide. If it did not subsequently change on melting, such an oxide film would constitute an almost perfect "template" or two-dimensional matrix to hold a few atoms of the primary metal in the exact array needed to form a nucleus for solidification.

Any precipitating material will adopt the correct spacing over a few atom diameters, and with appropriate substitution of other atoms of the correct sizes a precipitate can match the parent lattice over large areas of coherence without excessive strain. In metals, the components of a host of oxides, silicides, borides, nitrides, carbides, sulphides, and other compounds are always present in minute amounts. Some of these will be eliminated because of extreme insolubility in the liquid, while others will remain soluble in the solid; occasionally, however, particles will be formed in the solid by coherent precipitation—not of pure substances, but of whatever assortment of atoms best satisfies the joint requirements of availability, affinity, and appropriate average atom size. Of these, many will disappear on melting, but a few will persist unmelted as little rafts of complex composition, maintaining in the liquid a surface of the exact geometry needed to nucleate the solid on subsequent cooling. Their number and size distribution will determine the resulting grain size; the dimensions of the largest will determine the degree of undercooling that can occur before solidification commences.

A similar process may operate in the case of phase transformations in solids. The coherent precipitation of supersaturated minor constituents in a low-temperature phase should facilitate the nucleation of this phase on subsequent cooling after transforming into another phase at higher temperatures.

At first sight this hypothesis may seem little different from the older ones. It should therefore be emphasized that it does not depend on chance to provide the right compound to form a nucleus, but postulates that every crystal, containing minute amounts of any of a wide range of impurities, automatically engenders particles having the correct surface structure to serve as nuclei for subsequent solidification. It could operate in any system, metallic, organic, or inorganic. The suggested mechanism is closely analogous to the production of antibodies from antigens in living organisms—indeed, it was a description of the matrix theory of this process that suggested to the writer its crystalline analogue.

Technical Note No. 11. Manuscript received November 26, 1948.

* Institute for the Study of Metals, University of Chicago.

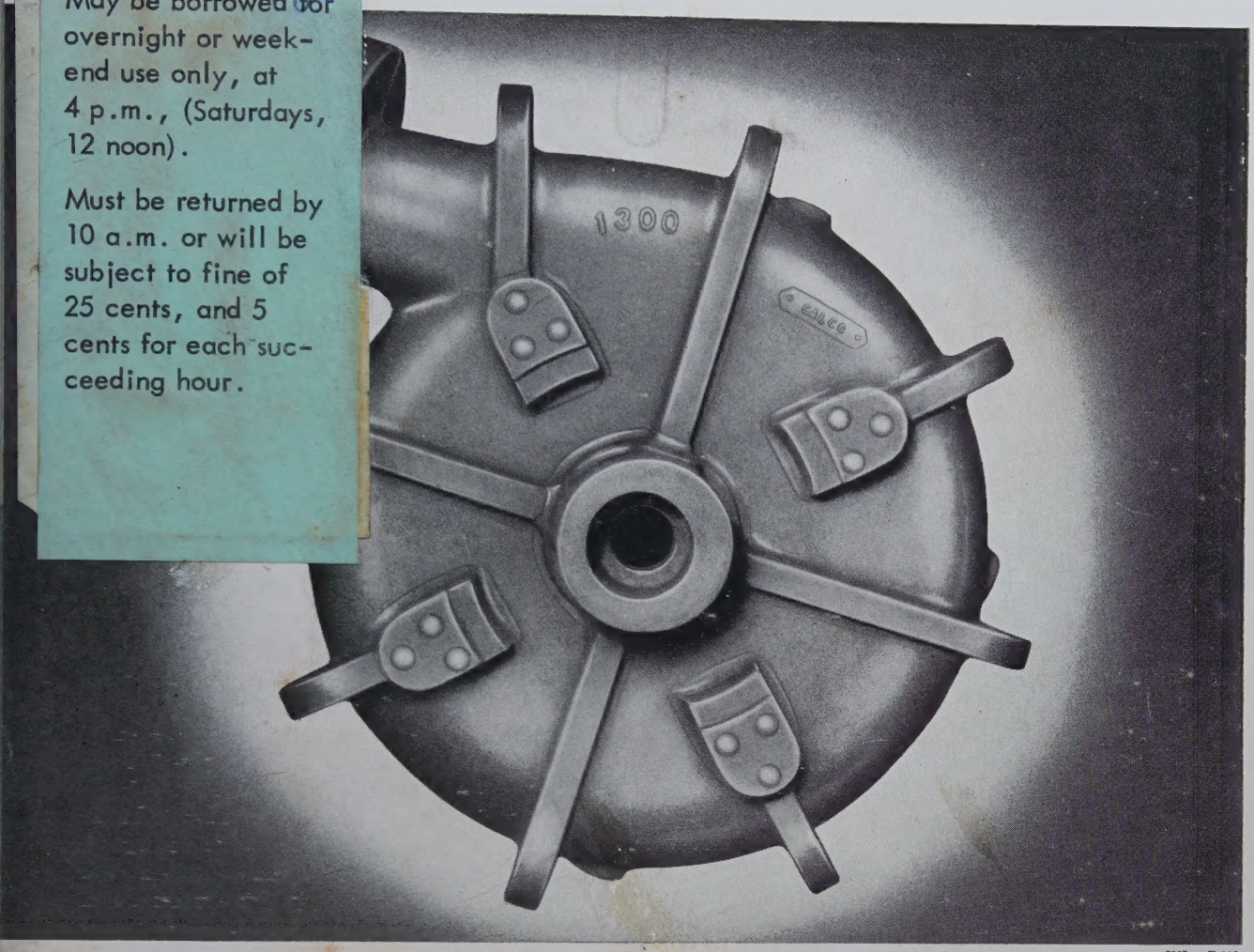

JMLco-F-110

Silicon Bronze Proves BETTER and CHEAPER!

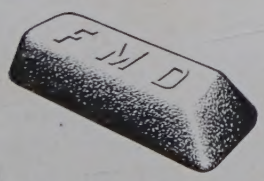

Silicon bronze was used in casting this pump casing because of its high strength, its excellent resistance to corrosion, and its price advantage over high tin bronzes.

The casing, weighing over 100 pounds, is cast by Thomas Paulson and Son, Inc., Brooklyn, New York, for the Calco Chemical Division of the American Cyanamid Company.

Practical experience proves it . . . silicon bronze does many casting jobs better and cheaper . . . with a smoother finish. It handles well in the foundry . . . is easily castable with a minimum of smoking.

Famous patented silicon bronzes offered by Federated are: Herculoy, Everdur, Olympic Bronze, and Tombasil . . . plus *all* specification alloys.

Federated's complete line of non-ferrous metals includes copper-base alloys, aluminum and magnesium alloys, bearing metals, solders, die casting alloys and fabricated lead products.

Check with your nearby Federated office for further information. Federated's metallurgical experts will be happy to help on silicon bronze or any foundry problem. Sales offices in 25 cities across the nation.

Federated first in the non ferrous field FMD

Federated METALS

ivision of American Smelting and Refining Company, 120 Broadway, New York 5, N. Y.

MOLYBDENUM-TUNGSTEN-BORON

Stocks are Maintained

A DEPENDABLE SOURCE of supply for users of Molybdenum, Tungsten and Boron, must have these materials instantly available, at convenient locations, for quick delivery, when hurry-up needs occur. Such availability the Molybdenum Corporation provides, at points here indicated. When sudden or unexpected demands arise and when your inventory is found a little short of this or that, MCA facilities may help. Correspondence on your present or anticipated requirements is invited.

AMERICAN Production, American Distribution, America Control, Completely Integrated.

Offices: Pittsburgh, New York, Chicago, Cleveland, Detroi Los Angeles, San Francisco, Seattle.

Sales Representatives: Edgar L. Fink, Detroit; Brumley-Donald son Co., Los Angeles, San Francisco, Seattle.

Subsidiaries: Cleveland-Tungsten, Inc., Cleveland, O.; Genera Tungsten Manufacturing Co., Inc., Union City, N. J.

Works: Washington, Pa.; York, Pa.

Mines: Questa, New Mexico; Urad, Colorado.

MOLYBDENUM CORPORATION OF AMERICA

GRANT BUILDING PITTSBURGH, PA.

MCA